

Dipl. Ing. Bettina MUSTER-SLAWITSCH

Thermal Energy Efficiency and Process Intensification for the Food Industry

Methodology development for breweries

DOCTORAL THESIS

For obtaining the academic degree of
Doktorin der technischen Wissenschaften

carried out at

Graz University of Technology, Austria

Supervisor:

Ao. Univ.-Prof. DI Dr. techn. Hans SCHNITZER
Institute for Process and Particle Engineering
Ao. Univ.-Prof. DI Dr. techn. Michael MURKOVIC
Institute of Biochemistry

Graz, Oktober 2014

DANKSAGUNG

Herzlicher Dank gilt meinem Betreuer Hans Schnitzer, der meine wissenschaftliche Arbeit über viele Jahre begleitet hat. Die Denkanstöße und Ratschläge aus vielen Besprechungen und Diskussionen waren sehr wichtig für das Entstehen dieser Arbeit. Ebenso herzlich möchte ich Michael Murkovic als Dissertationsbetreuer danken, für das Interesse an meinen Forschungsfragen, die Möglichkeiten am Institut das Labor für die Analytik zu nutzen, sowie die hilfreichen Besprechungen zur Interpretation der Messergebnisse.

Den Grundstein dieser Arbeit bilden die praktischen Erfahrungen in den Brauereien sowie das Projekt SOCO, die ich im Rahmen meiner Arbeit bei der AEE INTEC durchführen konnte. Bei Werner Weiß und Ewald Selvicka möchte ich mich bedanken, dass ich meine Dissertation auf Basis meiner Projektarbeit durchführen konnte. Größter Dank gilt Christoph Brunner, der als Forschungsbereichsleiter mit viel Innovation und Zielstrebigkeit zum Entstehen und der erfolgreichen Abwicklung dieser Projekte beigetragen hat. Christoph, vielen Dank für die Möglichkeit meine Dissertation durchzuführen und die unzähligen wertvollen Besprechungen und Diskussionen im Rahmen unserer langjährigen gemeinsamen Arbeit! Weiters danke ich auch herzlich meinen Kollegen Jürgen, Matthäus, Franz und Wolfgang für die Zusammenarbeit in den gemeinsamen Projekten, ihre offenen Ohren für jeglicher meiner Anliegen und die viele wissenschaftliche Inputs, die für diese Arbeit wichtig waren. Richard Heimrath, Hermann Schranzhofer, Christoph Moser und Qiang Chen möchte ich herzlich für Ihre Beiträge zur gelungenen Umsetzung von SOCO danken. Bastian Schmitt und Pierre Krummenacher danke ich für viele wertvolle Diskussionen und den wissenschaftlichen Austausch in den letzten Jahren.

Begonnen hat meine Arbeit mit Brauereien im Rahmen von regionalen und später nationalen Projekten bei der Brauerei Göss, bei der ich viele Erfahrungen aus dem praktischen Brauereibetrieb sammeln konnte. Dem Braumeister Andreas Werner und dem damaligen 2. Braumeister Harald Raidl möchte ich herzlich danken für die freundschaftliche und gute Zusammenarbeit in den Projekten, sowie ihren fachlichen Input. Besonders danken möchte ich Helmut Gahbauer, von dessen großen Erfahrungsschatz im Bereich der Energietechnik ich sehr viel lernen durfte. Die gemeinsame Auswertung und Interpretation von Messergebnissen hat mein Wissen im Bereich der Anlagentechnik und Regelung von Brauereianlagen sehr erweitert. Weiters gilt mein Dank auch der Brauerei Stiegl, insbesondere dem Braumeister Pöpperl und Hr. Siegl, sowie den Braumeistern der Brauerei Murau Günter Kecht und Christoph Lippert-Pagany. Bedanken möchte ich mich auch bei Dr. Florian Schüll des Forschungszentrums Weihenstephans sowie bei Anton Pichlmayr für die gute Betreuung während der Versuchsdurchführung im Labor des Forschungszentrums.

In dieser langjährigen Arbeit war das Vertrauen in meine Arbeit und in einen erfolgreichen Abschluss für mich sehr wichtig. Meinen Eltern möchte ich in diesem Sinne ganz herzlich für Ihre Unterstützung danken. Liebe Mama, ohne die gute Betreuung von Jakob und Simon während Auslandsaufenthalten und Bürostunden, wäre diese Arbeit nicht zustande gekommen.

Jehna Danbrook gilt ebenfalls lieber Dank für das viele Babysitten in den letzten Jahren und die sprachliche Korrektur der Arbeit als Native Speakerin.

Größter Dank gilt meinen Mann Stephan, für all die Unterstützung und Geduld und die unermüdliche Mitarbeit im Haushalt zur später Stunde, wenn ich mich wieder einmal hinter den Computer verkrochen habe. Meinen Kindern danke ich für ihren unkomplizierten Umgang mit den Tagen, an denen Mama einmal weniger Zeit hatte und ihre Lebensfreude, die mich oft Schreibsorgen vergessen ließen. Ich freue mich schon auf gemeinsame freie Wochenenden mit euch dreien!

EIDESSTÄTLICHE ERKLÄRUNG

AFFIDAVIT

Ich erkläre an Eides statt, dass ich die vorliegende Arbeit selbstständig verfasst, andere als die angegebenen Quellen/Hilfsmittel nicht benutzt, und die den benutzten Quellen wörtlich und inhaltlich entnommenen Stellen als solche kenntlich gemacht habe. Das in TUGRAZonline hochgeladene Textdokument ist mit der vorliegenden Dissertation identisch.

I declare that I have authored this thesis independently, that I have not used other than the declared sources/resources, and that I have explicitly indicated all material which has been quoted either literally or by content from the sources used. The text document uploaded to TUGRAZonline is identical to the present doctoral dissertation.

Datum / Date

Unterschrift / Signature

für Stephan

Wie herrlich für den Forschergeist,
dass man noch längst nicht alles weiß.
Er kann vergnügt sein ganzes Leben,
nach Wissen und nach Weisheit streben.
Zu hoffen bleibt, dass es gelingt,
dass es der Menschheit Gutes bringt.

Contents:

1	Summary	1
2	Introduction	4
3	Relevance of the research.....	5
4	State of the art	7
4.1	Heat Integration	7
4.1.1	The basics of pinch analysis and continuous HEN design	7
4.1.2	HEN design for batch and semi-continuous processes without consideration of heat storages	10
4.1.3	HEN design for batch and semi-continuous processes with consideration of heat storages .	12
4.1.4	Heat integration for total sites and integration of renewable energy.....	21
4.1.5	Process integration tools for variable process streams	25
4.2	Process Intensification in the food industry for sustainable processing.....	26
4.2.1	Key elements of process intensification.....	26
4.2.2	Process intensification – a methodology to identify best suited process technologies	27
4.2.3	Process Intensification for the food industry	28
4.2.4	Process intensification and its potential for low temperature heat supply	34
4.3	State of the art in the brewing industry including upcoming trends	41
4.3.1	Brewing chemistry.....	41
4.3.2	Technologies and upcoming trends in brewing	53
4.3.3	Modelling energy demand of brewing sites.....	63
5	Methodology – theoretic part.....	67
5.1	The “Brewery Model”	67
5.1.1	Model structure.....	67
5.1.2	Brewhouse section	69
5.1.3	Fermentation and filtration section	75
5.1.4	Packaging section	76
5.1.5	Water management	78
5.1.6	Energy management	78
5.1.7	General operating schedule	78

5.1.8	Modelling the thermal energy demand in breweries	82
5.1.9	Modelling effects on selected qualitative parameters	92
5.1.10	Modelling the cooling load in breweries.....	101
5.2	Optimization algorithm for heat integration based on pinch analysis and storage simulation (SOCO)	107
5.2.1	The need for heat integration tools for variable process streams.....	107
5.2.2	The pinch software SOCO.....	111
5.3	Holistic methodology to improve the potential for low temperature heat supply in the food industry via process models	119
6	Developing a new mashing technology – experimental Element.....	121
6.1	Developing mashing temperature programs for low temperature heat supply.....	122
6.1.1	Kinetic modelling of the heating profiles	122
6.1.2	Laboratory studies.....	130
6.2	Process technologies for the new mashing procedures	141
6.2.1	Limitations of the conventional mash tun for efficient energy supply	141
6.2.2	Enhanced possibilities for low temperature heat supply in conventional mash tuns	143
6.2.3	Evaluation of Oscillatory baffled reactors for mashing.....	146
7	Practical application to case studies - practical Element.....	161
7.1	Definition of brewery case studies.....	161
7.2	Thermal energy demand modelling	162
7.2.1	Benchmark data of breweries	162
7.2.2	Energy demand modelling with brewery model.....	163
7.3	Heat integration strategies for breweries.....	195
7.3.1	Applicability of the SOCO tool for heat exchanger and storage design for variable process streams.....	195
7.3.2	Heat integration and storage systems for conventional and intensified breweries	196
7.3.3	Solar heat integration and other renewable energy integration based on the result of SOCO	211
7.3.4	Discussion of heat integration scenarios.....	213
8	Conclusions	215
9	Appendix A - Brewery Model.....	218
9.1	Screenshots	218

9.2	Equation set of the Brewery model	221
9.2.1	Mass and energy balance	221
9.2.2	Variable energy demand calculations	242
9.2.3	Biochemical fermentation model.....	253
9.3	Biochemical mashing models	254
9.3.1	Biochemical mashing model – Model A	254
9.3.2	Biochemical mashing model – Model B	257
9.3.3	Biochemical mashing model – Model C	260
10	Appendix B – SOCO.....	261
11	Appendix C – New Mashing Technology	264
11.1	Experimental results.....	264
12	Appendix D –Nomenclature, references	268
12.1	Nomenclature.....	268
12.2	List of figures	275
12.3	List of tables.....	279
12.4	Literature references.....	280

1 SUMMARY

To reach the targets for the reduction in greenhouse gas emissions that have been set by the European Union, industry will have to change radically its current practices. A substantial increase in energy efficiency must be realised as well as most suitable conditions for implementing renewable energy. While over the past years the efficiency of heat generation and distribution has significantly increased in industry, radical changes in process technologies are now required to achieve the ambitious goals for minimal fossil energy consumption.

Intensification of processes for maximising process yields at minimal resources has been promoted over the past years, but the effects of these new intensified technologies on the overall production site and its energy consumption have not yet been evaluated. In the course of this thesis a methodology has been developed to identify most promising technology choices for a production system to be operated with minimal thermal energy requirement. Several processes and their interdependencies need to be taken into account in this evaluation, as well as inter- and intra-process heat integration scenarios. Two tools have been elaborated for realising the developed approach, one of which specifically for breweries for which the methodology has been applied in this thesis.

The applied methodology combines detailed process modelling including selected qualitative criteria of intermediate products with heat integration for real-life process data. For process modelling, a brewery model was developed on EES (Engineering Equation Solver) that allows the comparison of different technologies and operating conditions regarding thermal energy requirement (heating and cooling demand), hot water management and product quality. Variable process demand profiles can be generated to analyse load management. Such models identify core processes whose intensification could overcome existing bottlenecks in energy efficiency. For brewing, the mashing process has been identified as such process and a kinetic model to evaluate mash quality based on operating parameters has been implemented in the brewery model. This model allowed evaluating possible effects of new processing parameters to sweet wort production which would enhance possibilities for low temperature energy supply (suitable for integration of waste heat or renewable energy). The promising model results were verified in mashing experiments and the analytic results helped to improve the kinetic model. Based on these new mashing profiles process design calculations for a potential new mashing technology were performed.

For evaluating heat integration strategies based on the variable process demand profiles from the Brewery Model, a new heat integration tool SOCO (programmed in C#) has been developed within a project consortium of AEE INTEC and TU Graz. Algorithms for generating heat exchanger proposals based on variable process streams have been developed in the course of this thesis as well as a simulation model that allows simulating the interaction between heat exchanger and storage performances.

Finally the combined approach of process modelling and heat integration based on variable demand profiles has been evaluated for several brewing sites. These sites are fictive sites that have been set up based on the vast experience in brewery auditing. For two of these sites the implementation of the new mashing process, designed in this thesis, has been assumed.

The following results can be summarized:

- Kinetic modelling and mashing experiments show that after a first amylosis rest no further saccharification rest is necessary in infusion mashings with gradual heating at low heating rates. Fastest enzymatic action is achieved when alternating heating and cooling of the mash. Mashing profiles with 15 % less time requirement are possible.
Power demand can thus be reduced by 50% for an industrial infusion mashing process allowing low temperature heat supply of mash tuns without extensive increase of heat exchange surfaces. Oscillatory flow reactors present a suitable technology to realise continuous mashing (after a first amylosis rest) and a reasonable process design can be deduced from nomograms. Energy requirements for oscillations are however crucial and need to be further studied.
- The Brewery Model allows fast calculation of minimal thermal energy demand requirement per technology $MEDT_{Tech}$ and useful process heat requirement UPH. Parametric studies effectively help to analyse the impacts of different technologies and / or varying operating conditions. The model allows the prediction of variable process demand profiles to a satisfactory extent, however detailed knowledge on heat transfer parameters (e.g. existing heat transfer areas) and on operational practices (e.g. regulation) are required.
- The algorithms of the heat integration tool SOCO can design and optimize practical heat integration concepts. The simulation model allows the comparison of detailed design options, however manual tuning of optimization parameters is necessary. For brewhouses a promising heat integration concept combines the heat of vapour condensation and wort cooling to charge an energy storage which is discharged by wort preheating and mashing. The heat from a 2nd wort cooling stage can then be used for brew water preparation. An optimized design of this concept may cover 95 % of the thermal energy demand of these processes.
- The combined approach of process modelling and heat integration based on variable process profiles shows that by optimizing technology sets and production profiles in brewing the thermal energy demand of the main brewhouse processes can be reduced by 56 % and a 80 % reduction in power demand peaks can be reached. This refers to the comparison of a conventional brewery with 6 % evaporation rate versus an intensified brewhouse scenario (low evaporation rate in boiling, new mashing technology, optimized water management) brewing more continuously with small batches. Heat integration concepts can be effectively realised for this optimized site with 40 % less storage volume and up to 80 % smaller heat exchangers in comparison to conventional technologies.

From these results we can conclude that a continuous process can be designed for mashing after a first amylosis rest without negative effects on product quality. As the results of the thesis are based on a limited number of mashing experiments further experiments shall consolidate this conclusion. Additionally the alternating heating and cooling profiles for mashing showed that intensification of the mashing process is possible. The application of oscillatory flow reactors for mashing might additionally intensify the mashing process by increased dynamics due to the induced oscillations.

The application of process modelling tools shows that the choice of different technologies and of process profiles influences thermal energy demand and its required temperature level significantly. Hot water management is, again, proven to be a key for efficient brewhouse operations.

This work shows the significant effects of technology choices on energy efficiency, heat integration and the overall thermal energy management in industry. The combined approach of process modelling - generating variable process profiles - and heat integration analysis - allowing planning of heat exchanger and storage networks based on these profiles - enables to design optimized technology sets in industry. Detailed models of those processes posing bottlenecks to efficient thermal energy supply can reveal new processing strategies. Such models naturally need to take into account quality criteria of the products and need to be verified by experiments. Process modelling tools similar to the brewery model are recommended for different industry sectors for the identification of bottlenecks for energy efficiency and low temperature heat supply. This might stimulate new process developments for realising production sites with minimised greenhouse gas emissions.

2 INTRODUCTION

According to the “Roadmap for moving to a competitive low carbon economy in 2050” the European Union targets at a reduction of approx. 80 % of GHG emissions until 2050 (compared to 1990). These ambitious goals will clearly only be met by a holistic approach of energy efficiency measures combined with renewable energy resources. Analysing the implementation of the energy efficiency potential in industry (e.g. see energy efficiency index ODEX of the EU-27 [4]) it becomes clear that it will be vital to focus on energy efficiency solutions in each industrial energy audit to maintain a competitive European manufacturing industry.

The European food industry is a significant sector – 15 % of all employees working in producing companies are employed in the food industry . Due to increasing legislative pressure and consumer awareness the food industry is seeking solutions to create a more sustainable production. The temperature levels required in food processing make the food industry an important candidate to realize efficient low temperature heat supply over waste heat or renewable energy, such as solar heat [43].

However, the food industry faces several challenges for realizing the existing potential in increasing its thermal energy efficiency: Due to its long history, food treatment and processing are very traditional processes. In many cases the technologies applied have not changed over the decades. As many of these technologies stem from a time prior to energy efficiency or renewable energy considerations, they often pose limitations when it comes to changing the energy supply. Traditionally most of the processes are steam driven and there are a number of challenges to overcome when integrating low temperature energy (such as waste heat or renewable energy as solar heat). The widely applied stirred tank is one example of technology that poses limitations to the integration of low temperature heat due to its low heat transfer coefficient and limited heat transfer area. Traditionally large temperature gradients are applied to overcome the limitations in heat transfer. To realize low temperature heat supply however, in order to enable the required heat transfer rates, retrofit changes are necessary or new technologies need to be adopted. As quality and taste of products are key factors in processing, new process technologies need to be analyzed thoroughly for each application and there is generally a natural reluctance towards adopting new technologies. Additionally, thermal energy management can be complex, as many (traditional) processes are batch and semi-continuous processes leading to large energy demand variability over time. Heat integration on such systems requires detailed planning and the design of storage systems. These storage systems do not only influence heat integration strategies, but might also affect the overall thermal energy supply system, such as combined heat and power plants or solar process heat.

For the realisation of the existing improvement potential on thermal energy in industry, the reduction of energy demand via technological optimization and system optimization as well as the integration of renewable energy into the industrial thermal energy system needs to be further stimulated. The methodology developed by Schnitzer et al.[182] and further elaborated by Brunner et al. [48] to realise thermal energy supply in industry with minimal greenhouse gas emissions is based on a 3 step approach:

- Technological Optimization (measure to enhance energy efficiency)
- System Optimization (Pinch Analysis of a total production site)
- Integration of renewable energy (based on exergetic considerations)

While it is obvious that there must be effects of technology changes on system optimization, there are so far no tools available for the food industry allowing for a detailed analysis of these effects. The current work develops a methodology for identifying the best technology set for reaching minimal fossil thermal energy consumption. Its application allows analysing how technological changes and systematic heat integration with intelligent storage systems can reduce thermal energy consumption and improve the potential for solar process heat integration in the food industry. While the methodology is applicable to the food industry in general, focus in this work was set on breweries for which one tool has been specifically elaborated.

3 RELEVANCE OF THE RESEARCH¹

There are many recommendations and manuals on how to improve energy efficiency in brewing, such as [8, 10, 80] or [87] and several case studies have been published recently, such as [65, 71, 176, 193, 194, 196]. Energy consumption analysis based on production data acquisition systems and benchmarking have become state of the art in the brewing industry and specific tools are available [5]. The available material and the increasing environmental awareness in the sector have led to tremendous savings within the last decades [2, 63]. However, as consumption figures vary widely (national data ranging between 70.6-243.1 MJ/hl [63]) the continuing need for improvement still exists. It is often the case especially in the final steps of obtaining a completely carbon-free production site, that a detailed analysis is required. Approaches for monitoring and forecasting of energy consumption in brewing have been recently developed [32, 124].

To reach an integrated sustainable production site, it is important to analyze effects of technology changes by considering the whole energy system of the production site. Process models that allow a concise analysis of the status quo and enable parametric studies to reach an optimized technology set are therefore necessary. Process modelling for energy efficiency optimization can be done via EINSTein, a general thermal energy auditing tool for industry, which allows for technology comparison to some extent [47, 183]. Software tools, such as BATCHES, have also been applied for modelling and optimization of brewhouses [142]. There are so far no tools available dedicated for brewing which allow for analysis of energy efficiency opportunities based on detailed and holistic process modelling and parametric studies of operating conditions. The Green Brewery tool [17] was one of the initial tools used in energy balancing of brewing sites with an Excel based tool for energy balancing of brewing sites. In this work a “brewery model” is presented which allows analyzing effects of different technologies on thermal energy demand in the brewing industry.

As heat integration solutions are influenced by the implemented process technologies, the analysis of heat integration strategies for different technology sets is consequently important. The methodological

¹ Parts of this chapter have been published in the following publications by the author:

Muster-Slawitsch, B., et al., Process modelling and technology evaluation in brewing, *Chemical Engineering and Processing: Process Intensification* **84**, 98-108 (2014).

Muster-Slawitsch, B., C. Brunner, and J. Fluch, Application of an advanced Pinch Methodology for the food and drink production, *WIREs Energy Environment* **3**, (2014).

approach of the pinch analysis has proven its suitability for assisting in the design of heat integration strategies of the total site as a basis for renewable energy implementation in the past years. This has been shown for renewable energy integration at total sites [204] and specifically for solar thermal integration [48]. Recently the approach has been applied for energy efficiency and renewable energy integration in breweries [151]. However, so far only few authors have dealt with process integration approaches including storage systems. A recent review of batch process integration is given by Fernandez and co-workers [73]. Stoltze presented a combinatorial approach for searching the ideal matches of process streams and defined storages [191]. Krummenacher and Farvat presented a graphical storage pinch approach for storage design [116], while other authors worked on MILP approaches with defined superstructures for storage placement and design [54, 134]. Nement and Klemes presented a design approach for optimized temperature in a solar storage tank [154] and Atkins and coworkers worked on ideal design of a central heat storage for heat integration of batch processes in dairies [26]. Recently Walmsely et al. have shown that among various methods for selecting heat storage temperatures and heat recovery areas in indirect heat integration, the ΔT_{\min} approach leads to satisfactory solutions [209]. None of these above mentioned approaches, however, allows a system simulation of heat exchangers and storages including a storage model for stratified storages with multiple ports and connections. The design of economic process layouts to reach defined energy targets in indirect process integration will however, depend on correct choice of storage and heat exchanger design, which has also been highlighted by other authors [208]. In order to realize the energy efficiency potential of the food industry heat integration tools are required that allow the evaluation of batch and semi-continuous processes and the interaction of heat exchangers with storages. Besides process integration solutions, such tools also need to consider the possible integration of new energy supply. Especially for technologies such as CHPs, heat pumps, district heat or solar process heat the interaction of energy supply with the heat management including storages is essential. This research need has also been addressed by other authors who formulated a research need for uniform modelling tools for heat integration on total sites including more diverse energy users, including small industrial plants, integration of renewable energy and accounting for variations in energy supply and demand by tools centered around heat storage [203].

The importance of the current research can therefore be summarized as the general need for evaluating effects of new process technologies on thermal heat management and the following specific needs:

- Need for technologies in the food industry suited to low temperature heat supply and need for continuous process technologies overcoming bottlenecks of un-ideal heat- and mass transfer
- Need for strategies for heat integration taking into account the interaction of heat exchange and thermal storages and allowing an ideal placement of renewable energy supply.

To answer the core research question, whether technological changes (process intensification) and systematic heat integration with intelligent thermal storage systems can reduce energy consumption and improve the potential for solar process heat in the food industry, the following tools have been developed within this work:

- a process model for the brewing industry for evaluating different process technologies in terms of energy efficiency and selected qualitative parameters;

- an optimization algorithm for heat integration based on pinch analysis and storage simulation (integrated in the software SOCO) which allows the evaluation of heat integration solutions based on different technology sets.

4 STATE OF THE ART

4.1 Heat Integration

Heat integration has been widely applied since the early works of Hohmann and Linnhoff who introduced the concept within their theses in the 1970s [99, 128]. Heat integration has been the basis for further development of Process integration which is a more broad application of the integration concept towards general resource efficiency. The international energy agency has adopted the following definition of Process integration [195]:

"Systematic and General Methods for Designing Integrated Production Systems, ranging from Individual Processes to Total Sites, with special emphasis on the Efficient Use of Energy and reducing Environmental Effects".

In the context of thermal energy efficiency, heat integration remains the most important aspect of process integration and has developed tremendously over the past years. A comprehensive review is given by Klemes and Kravanja [113]. The main tools applied for realizing heat integration solutions are the pinch analysis and respective heat exchanger network design and mathematical programming.

Heat exchanger network design based on the pinch analysis has its foundation in the work of Linnhoff and Hindmarsh [130] who published an optimized design for continuous processes. In the following years, the concept was extended to discontinuous processes as well as to different approaches. While the pinch analysis stems from heat integration of single processes, it has proven itself as a strong tool for optimizing thermal energy management in various production processes, for single processes or based on a total site approach. Especially when the pinch analysis is applied prior to designing new energy supply systems, it is decisive to consider all hot and cold streams of the total site under consideration. In the following sections some key works of heat integration heat integration of batch and semi-continuous processes, as well as integrating on a total site basis are presented.

4.1.1 The basics of pinch analysis and continuous HEN design

The basics of the pinch analysis are best visualised within two graphical diagrams, namely the Hot and Cold Composite Curve and the Grand Composite Curve. In these diagrams the heat and cold demand of the whole production is plotted in one diagram that shows the energy (heating or cooling) demand of the processes and at which temperatures this energy is needed.

The data required for pinch analysis are all processes that have heating or cooling requirement. Processes are broken down into "streams", which are mass flows of a certain process medium that need to be heated up, cooled down or are undergoing phase change. They are defined by starting and target temperature, mass flow and specific heat capacity or enthalpy change in the case of phase change. Also streams which are not necessarily required for the process (such as waste water running to the effluent) can be included if there is the possibility that they may be used as cooling or heating agent for other streams. Each of these streams can be visualised as one vector in a temperature-enthalpy diagram. By combining the temperature enthalpy curves of all streams that have to be heated (cold composite curve)

and all streams that have to be cooled (hot composite curve) into one temperature – duty diagram the hot and cold composite curves are drawn.

Both curves are then drawn on the same plot in such a way that the cold streams are at a lower temperature than the hot streams everywhere in the diagram. This can be achieved by moving the curves along the enthalpy axis, as an enthalpy value always represents a relative and not an absolute measurement. In this way the maximum possible heat transfer becomes visible. With the help of these composite curves it is possible to determine some essential facts about the process. The curves are separated by a point of the lowest difference in temperature ΔT_{\min} that is chosen by the user as the minimal ΔT over a possible heat exchanger in the system. This ΔT_{\min} defines the temperature level in the system that can be explained as the thermodynamic bottleneck (See Figure 4-1) of the process, the so called “pinch”. The pinch temperature cuts the system into two halves: Into an area below the pinch temperature with a heat surplus that has to be removed by cooling and an area above the pinch temperature with an energy deficiency that has to be overcome by additional heating. Three important rules for heat integration are as follows:

- No external heating below the pinch temperature (enough waste heat is available, otherwise unnecessary cooling utility use is needed);
- No external cooling above the pinch temperature (cooling can be achieved by heating other process streams, otherwise unnecessary heating utility use is needed);
- No heat transfer should take place across pinch.

The overlap between the curves in Figure 4-1 shows the maximum possible heat recovery. The minimum heating demand $Q_{H,\min}$, and the minimum cooling demand $Q_{C,\min}$ can also be identified from the figure. The minimum temperature difference ΔT_{\min} is determined by economical optimization, as a lower ΔT_{\min} increases the efficiency of heat exchange, but also increases heat exchanger surfaces and costs.

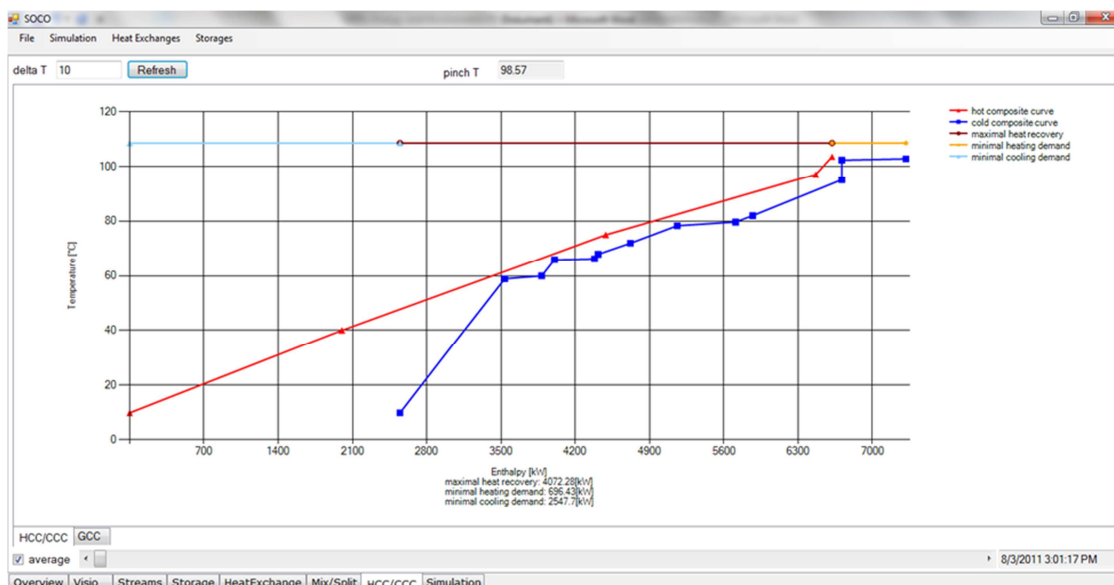


Figure 4-1: Hot and cold composite curve

A different presentation of the same data can be seen with the grand composite curve. Here the hot and cold composite curves are vertically moved towards each other by $\frac{1}{2} \Delta T_{\min}$. The difference between the heating and cooling demand (between hot and cold composite curve) are then drawn in the temperature-enthalpy diagram. In this way the heating and cooling requirement at the respective temperature levels can be clearly visualised. Areas in which there is a heat surplus at higher temperature than a corresponding demand are shown as “pockets” (highlighted in grey in the figure below) in the diagram. In these areas heat recovery can serve the heating and cooling requirements. The grand composite curve can be well used for designing heat and cold supply, as the requirements are shown at the corresponding temperature level. In this way adequate supply technologies can be chosen, such as refrigeration and deep-freezing for cooling requirements.

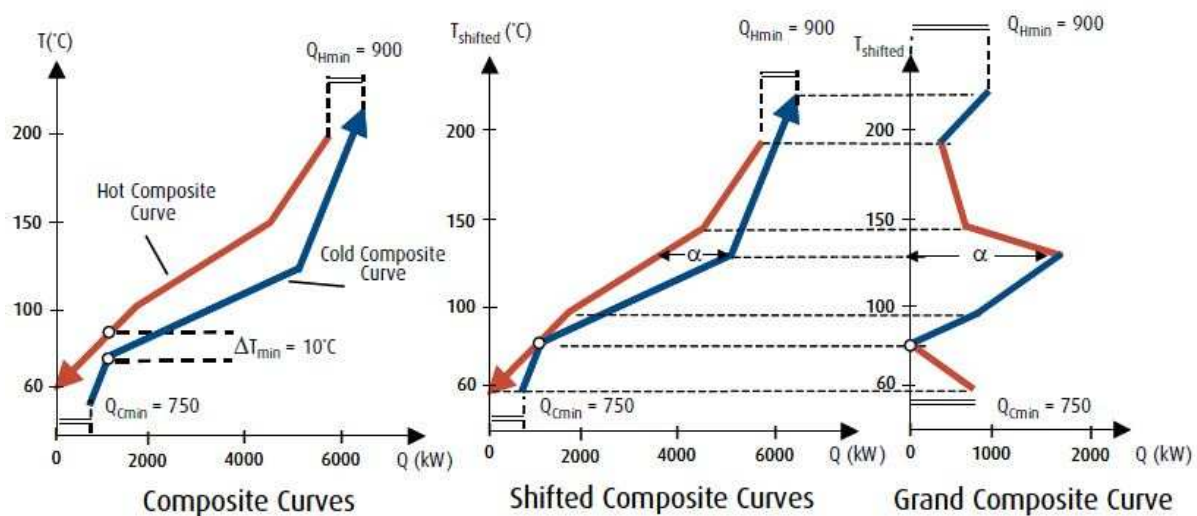


Figure 4-2: Grand composite curve [15]

Since the very early work of Linnhoff and Hindmarsh [130], the problem table or heat cascade is used as a numerical tool for locating the pinch point. In the problem table, streams are divided into temperature intervals defined by stream supply and target temperatures. The temperature intervals are also called subnetworks (SN). To ensure the possibility of heat transfer, hot streams and cold streams are separated by ΔT_{\min} . In this way feasibility of heat exchange is possible in each subnetwork and from higher subnetworks to lower subnetworks. Initially the heat input from external utilities is assumed to be zero. Then the heat flow from one subnetwork to the other is calculated, in case negative values which are not feasible occur they are set to zero. The minimum external utility on the hot side is defined as necessary input to the hottest subnetwork to make all other heat flows positive or zero. The minimum external cold utility is defined by the outflow of the coldest subnetwork. The point where the flow between subnetworks is zero represents the pinch point [130].

Based on this approach, the authors developed the pinch design method for heat exchanger networks, highlighting the fact that the problem must be divided within the areas above and below pinch and the design of the HEN must start at the pinch [130]. In order to design thermodynamically feasible matches the heat capacity flow rates of all hot streams above pinch should be smaller than those of the cold streams, while below pinch the heat capacity flow rates of the cold streams should be smaller than those of the hot streams. In this way the criterion of minimum temperature difference between hot and cold

stream is met during the complete heat exchange. In case the streams are such that these criteria cannot be obeyed, streams are split. Other basics of the HEN design are maximizing heat exchanger loads and adhering to the pinch rules (no external heating below the pinch, no external cooling above the pinch). These are the basics of the so-called “MER design”, aiming at maximum energy recovery [108].

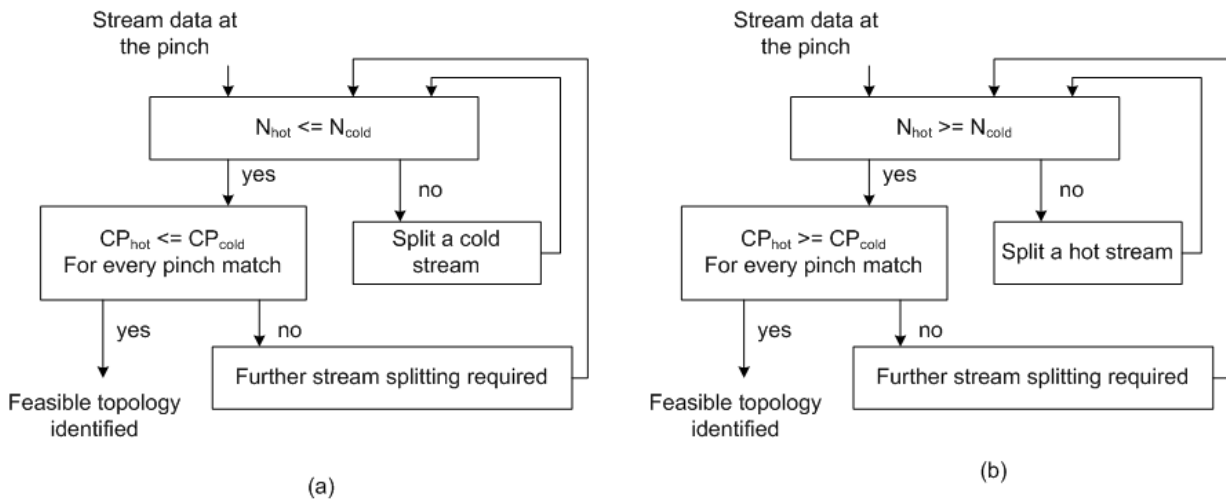


Figure 4-3: Pinch design method [130]

4.1.2 HEN design for batch and semi-continuous processes without consideration of heat storages

4.1.2.1 The time average method for batch processes

For batch processes the TAM -time average method- was proposed in the early work of Linhoff and his colleagues [129], which applies the same procedures for batch integration as for continuous processes. The TAM approach calculates time average data of all process streams without taking into account their specific operational schedules. The TAM approach is especially useful when hot and cold composite curves are drawn, as it enables a fast view of the general heat recovery potential neglecting the necessity of storage placement. For visualizing energy targets prior to detailed design however, it has proven to be a useful approach in recent food industry studies [151, 170].

The design of heat exchanger networks for batch and semi-continuous processes in a TAM approach, however, does not lead to optimal solutions [108].

4.1.2.2 The time slice model

Linhoff and his colleagues also introduced time slice models for batch heat integration [129]. In each time interval targets for hot and cold utility consumption are identified over the problem table algorithm. All utility targets are then added together to find the minimum utility during the batch period. Using this method it is only possible to identify direct heat exchangers in time intervals. The results of the analysis highlight the importance of scheduling [169].

4.1.2.3 Scheduling

For ideal process scheduling a vast number of literature is available, which will not be discussed in this review. However, the fact that good design methodologies should be able to calculate optima for a given set of operational parameters (such as schedules) and be able to handle a range of operating conditions [205] should be highlighted. These changes might also be necessary for production schedules, in the case that production schedules are not completely known or fixed or might be changed in the future.

Adonyi and co-workers include heat integration aspects while optimizing production schedules for batch plants [17]. Optimization taking solely into account ideal scheduling does not lead, per se, to simultaneous operation that enables heat exchange. Therefore the suggested approach is to search for a schedule that requires minimal external energy demand. The work does not deal with indirect heat integration, and only includes possible direct heat integration when processes run simultaneously. The S-graph approach first defines necessary linkages between process streams (e.g. start time of one process is linked to end time of another process). Then the search algorithm begins with one partial problem and all “child partial problems” are generated. After one “branching step” is finished, a “bounding step” is applied that ensures the feasibility of the partial problem and determines the utility costs.

4.1.2.4 Multiple Base Case Methodology

For targeting and design of direct integration of batch processes the multiple base case methodology has been applied considering time slices as base cases and identifying the re-use of heat exchangers in various time slices [115]. The approach of multiple base cases has been developed for flexible continuous HENs [105] and has been extended for batch processes [86, 117].

The HEN design via this methodology starts by placing matches starting from the pinch, giving priority to those matches relevant in most time slices. Heat exchanger area is calculated based on the time slice with the largest heat requirement and consequently the efficiency of the chosen heat exchanger is evaluated for the other time slices and the heat exchanger is possibly redesigned. The overall HEN is designed by merging HENs for each time slice. The approach aims at highest cost effectiveness avoiding a large number of tubes and valves [115].

4.1.2.5 Omnium Verfahren

The “Omnium Verfahren” has been developed to design HENs for discontinuous processes [92]. Contrary to classical HEN design this approach does not aim at minimal exergy consumption, the Omnium Verfahren aims at creating a simple network allowing only one heat exchanger for each match. Once a match is defined, the respective hot and cold streams cannot be connected to any other heat exchanger. To overcome the limitation that this approach does not reach the thermodynamic optimum, a repetitive application of the Omnium Verfahren has been proposed [200].

4.1.3 HEN design for batch and semi-continuous processes with consideration of heat storages

4.1.3.1 The time dependant cascade analysis and HEN design based on time slice models

In Cascade analysis [109] the problem table is extended by a time dimension. Heat can be transferred to lower temperatures over the temperature dimension of the problem table, or to other time slices over the time dimension. This way both direct and indirect heat exchanges are accounted for. Finding energy targets for batch processes includes calculation of direct heat exchange targets in each time interval, analyzing the utility demand over time (via utility-time graph) and checking for opportunities for heat storages with fixed temperature or increased ΔT_{\min} [108]. Storages that are potentially necessary to realize indirect heat transfer are, however, not designed in detail.

HEN design for batch processes with the time slice model places heat exchangers first for each time slice according to the pinch design method [130] and consequently merges the single HENs together to an overall ideal HEN. The combination of the individual designs however might not give a cost-effective design as many heat exchangers are required. The use of multi-stream and multi-purpose heat exchangers can increase cost effectiveness [108]. A MILP model for re-matching has been proposed comprising the following 3 steps for HEN design [216]:

- Initial individual design for each time interval
- Re-matching design: Application of a MILP model for adjusting matched streams and aiming to use heat exchangers commonly by matches in different time intervals considering energy and capital costs in each time interval. Rematched streams are then again designed in a HEN network (as in step 1 but now including the known restrictions from re-matching).
- Final overall design: Further opportunities to reach the most cost effective design such as analysing the area requirement for one match in different time intervals, allowing different minimum temperature differences (=multi temperature approach) etc. are evaluated heuristically.

To include heat storages in HENs based on the time slice model, heat added to a storage in one time interval is included as hot stream in the next time interval [108]. Storages have not been included in the re-matching models mentioned above.

To lower the number of HEX used in HEN design based on the heat cascade analysis, Foo et al. worked on the identification of minimum number of heat exchanger units within a batch heat exchanger network [76]. Time intervals for the hot and cold streams are defined and the equation for continuous heat exchanger networks is adapted to batch heat exchanger networks. He defined the minimum number of heat exchanger with

$$U = N_{hs} + N_{cs} - N_{ISN}$$

The design of a heat exchanger network for each time interval is done according to the time dependent heat cascade analysis. Before the network evolution is applied to make the system more complex, the target for minimum heat exchanger units can now be applied. This approach is very closely linked to the

time dependent heat cascade analysis. Real storage systems and practical issues in heat exchanger and storage planning are not included.

4.1.3.2 Problem table algorithm for time intervals

Pourali et al. [169] suggest an algorithm based on concept of “problem table algorithm”. In contrast to the concept used for continuous processes, the authors suggest combining time intervals of batch processes to maximize heat integration potential. After the time intervals are combined, the hot and cold utilities are calculated for each combination applying the problem table algorithm. To minimize overall capital costs and identify the most promising time interval combinations, cost functions for heat exchangers and storage tanks are included.

No further information is provided on how exactly storages are modelled, but it seems storage tanks are only integrated on a rough thermodynamic calculation. Additionally, the authors state that practical limitations need to be included in practice, as there might be operational and economic constraints that do not allow heat integration between time intervals.

4.1.3.3 The permutation method

The permutation method [191] features a different approach to HEN design for batch processes. It assumes that all heat exchange is happening over heat storages (heat storage units HSU). The temperatures of heat storage units are set a priori based on the process streams and a reasonable ΔT_{min} . Based on the chosen heat storage temperatures and other heuristic rules (such as decision which HSUs are matched with stream) the combinatorial algorithm searches the optimal solution. Mass balances of heat storages are included and possible splitting of process streams. The method has been extended by Mikkelsen by the so-called post-optimization which allows changes of certain parameters. The method can therefore be summarized with 3 steps [115]: 1) determination of the pinch using TAM composites; 2) simplified combinatorial search (PM); 3) post-optimization (PO) of the most interesting configurations resulting from step 2.

The result of this method is dependent on the heuristic rules [115] and the post-optimization stage is difficult to be applied in practice [116].

4.1.3.4 The storage pinch approach

The work of Kruppenacher and Favrat [116] is based on the recognition that there is a linkage between the schedule of process streams and the minimum number of intermediate heat storages which can be identified over a time-slice model. Their work focuses on indirect heat exchange in any case, not matter whether there is an overlap between heat availability and heat demand or not.

The basic approach is to integrate a storage composite curve between the hot and the cold composite curves. An example is shown in Figure 4-4 with 4 storage unit. Storages have constant temperature and variable mass flow and heat can only flow from one storage tank to an adjacent one. Adjacent storages are defined as storage-sub-systems (see Figure 4-4).

The degrees of freedom in the design represent the amount of heat recovery, the number of storage tanks, the temperature and mass flow of the storage fluids, heat contribution of each stream to each

storage sub-system, re-scheduling of streams and possible re-use of heat exchangers in similar conditions.

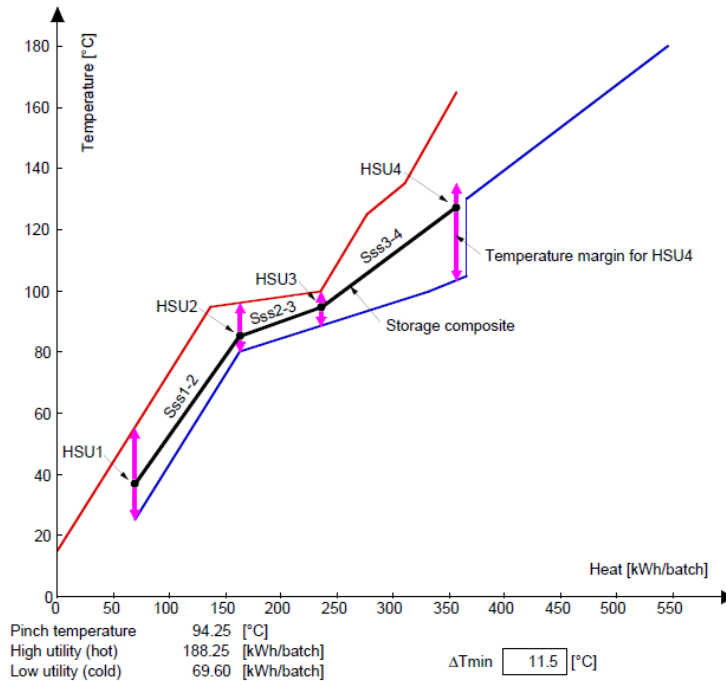


Figure 4-4 : Hot and cold composite curves (TAM approach) and storage composite curve [116]

Firstly, the graphic procedure includes drawing the “limiting supply temperatures profiles”. The authors formulate a procedure to identify the minimum number of storages that are required reach the heat recovery possible based on the time average approach.

For defining the indirect heat integration concept, the authors use a cost minimization approach. For a small heat recovery (first defined only vertically between hot and cold composite curve) and low number of storages the total costs are calculated and subsequently the heat recovery is continuously increased. The authors find that the cost curves decrease until they reach a minimum and then increase sharply. This sharp increase is caused by a heat storage unit and its corresponding temperature (defined as shown above) - the authors refer to it as the “storage pinch”.

After the cost target has been identified, the assumptions (such as vertical heat transfer only) can be relaxed. The authors discuss that the heuristic targeting methodology presented needs to be verified by applying genetic algorithms for design and optimization of indirect heat integration systems.

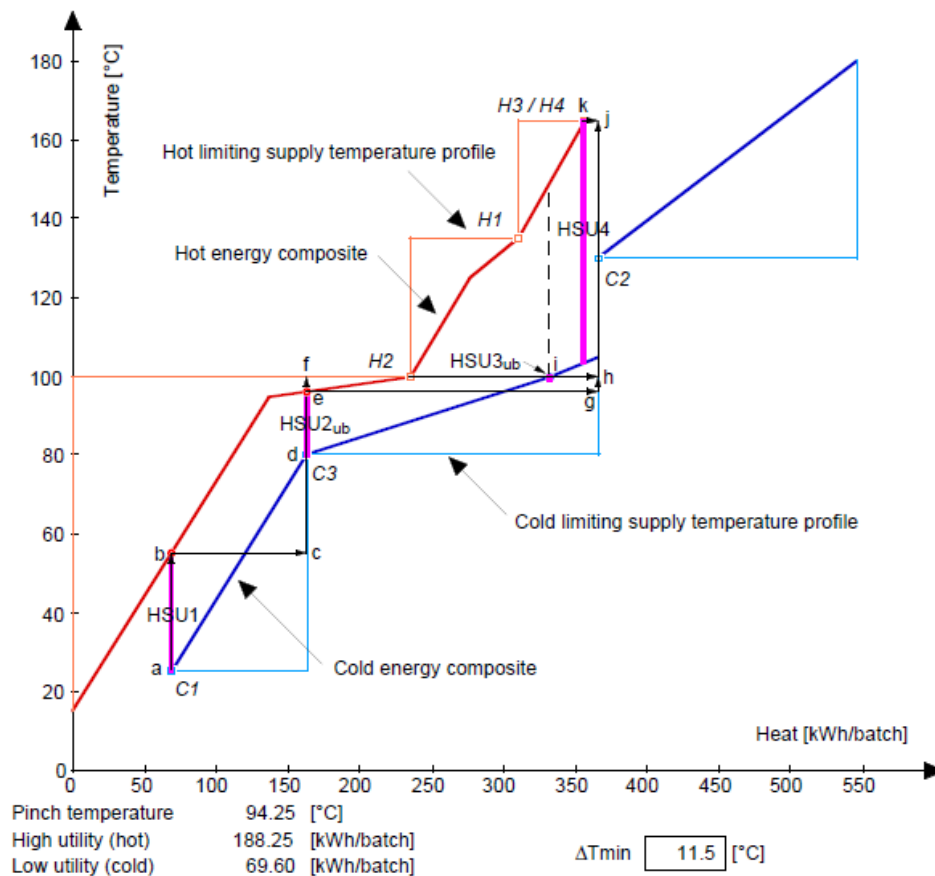


Figure 4-5: Limiting supply temperature profiles [116]

For designing HENs Kruppenacher [115] developed algorithms based on the Struggle genetic algorithm that identify heat exchanger networks for indirect heat integration (over storages) and for direct batch integration (aiming at best utilization of heat exchangers) with minimal costs. The work on direct batch integration is based on the multiple base case methodology as shown above (see 4.1.2.4), while the work for indirect heat integration is based on the storage pinch approach. The genetic algorithm searches for the most suitable temperatures of heat storages and amount of heat exchanged between processes and storages based on a defined superstructure and a user-defined number of heat storages. The superstructure only allows indirect heat integration, the hot streams charging various storages which are discharged via the cold process streams. Within the superstructure process streams can only have constant heat capacity flowrates and heat losses of the storage systems are neglected [115].

4.1.3.5 Heat recovery loops for integrating batch processes

Atkins and his colleagues [26] demonstrate the use of heat integration over storage with a practical example from a dairy. Having several non-continuous streams within the plant, they show that the time slice model is not appropriate to identify the best heat exchanger matches. Their model includes one stratified storage tank which takes over all heat integration tasks. The ideal temperature of the storage tank can be derived from adapted pinch curves, where the schedules of streams have to be taken into account.

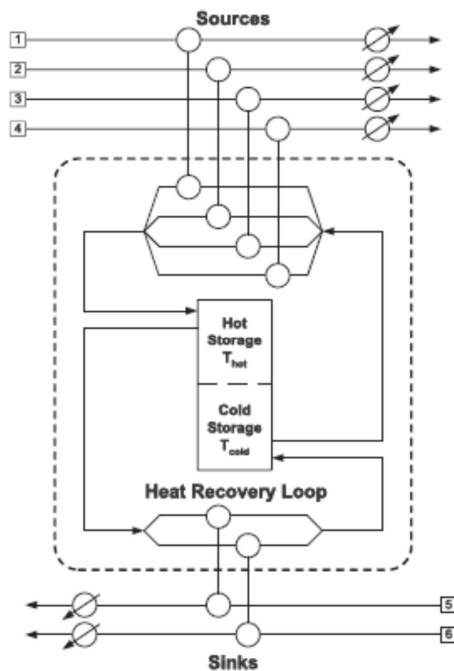


Figure 4-6: Schematic of the heat recovery loop [26]

In a further work Atkins applied such central heat recovery loops to integrating individual plants within a large factory. A spreadsheet algorithm is proposed for evaluating which streams are included in the heat recovery loops and in order to calculate the storage needs [27].

Walmsely et al. have recently shown that among various methods for selecting heat storage temperatures and heat recovery areas in heat recovery loops, the ΔT_{\min} approach leads to satisfactory solutions for storage temperature selection and heat exchange areas can be well designed based on time-average heat capacity flowrates [209]. They suggest the use of time-average data during processing time.

4.1.3.6 EINSTEIN – HEN algorithm for processes that are variable in time

The heat exchanger network design implemented in Einstein is partly drawn from the pinch algorithm [130] and based on the general concepts of the combinatorial algorithm implemented in PE² (see 4.1.3.9) [149]. It was developed within the European project EINSTEIN. During the selection of heat exchangers, the operational schedules of streams are not considered, which might not lead to an ideal situation after the heat exchangers are truly simulated taking into account their true operational schedules. HEN design is conducted separately for the above/below pinch region and the sequence of steps to define the best matches of sinks and sources is organized in the following order.

- Set an initial ΔC_p (allowable difference for heat capacity flowrates between hot and cold stream; this is automatically set from 10 %-100 %)
- Select hot stream with highest heat capacity flowrate C_p
- Run through all cold streams (loop)
 - Calculate heat capacity flowrate C_p of each cold stream
 - Check whether difference in C_p is smaller than allowable difference

- $|C_{p_{hs}} - C_{p_{cs}}| < \Delta C_p$
- Calculate the temperature range in which hot and cold stream overlap
 - $T_{low_cold} = \text{Max}(T_{start_cs}, T_{end_hs})$
 - $T_{high_cold} = \text{Min}(T_{end_cs}, T_{start_hs})$
 - $\Delta T_{cold} = T_{high_cold} - T_{low_cold}$
- Recalculate the same temperature range ΔT_{cold_old} for cold stream which proves to be the best, in which hot and cold stream overlap (in case no cold stream has been selected before (first run through loop of cold streams), ΔT_{cold_old} is set to zero.
- The maximum transferable power is calculated between the hot and cold streams once this is done for the actual cold stream: $m_{cs} * c_{p_{cs}} * \Delta T_{cold}$
 once this is done for the so far best cold stream $m_{cs_old} * c_{p_{cs_old}} * \Delta T_{cold_old}$
 In case the actual cold stream can transfer more heat than the so far best one, it is selected and set to the “best match” for this heat exchanger
- The loop re-starts for the next cold stream
- Once the best cold match has been selected for this hot stream, the required mass flow of the hot stream for the heat exchange is calculated. In case only a certain mass flow percentage is necessary $percent_{hs}$, a second hot stream is created with the same attributes, however with a mass flow percentage $1 - percent_{hs}$. If this remaining mass flow is still larger than 20 % of the total mass flow, this hot stream is added to the sorted list of hot streams in the above pinch region and is considered in the next runs of the HEN algorithm.
- Once the match over the heat exchanger has been defined, the heat exchange is calculated and a necessary storage size for a storage buffering the hot stream for later re-use is approximated. The HEN design procedure then re-starts by selecting the next hot stream.
- The calculation is stopped once all cold streams are matched, or when the maximum length of calculation loops is reached, which is set to 10 times the number of hot streams.

4.1.3.7 Optimization of schedules to reach minimum energy storage

Majozi's work [134] deals with determination of the ideal production schedule that “results in minimum energy use or maximum profit”. Based on the basic information of current production schedules, hot and cold duties and temperatures of heat sources and heat sinks, available storage size and utility cost information, the author suggests a mixed integer linear programming (MILP) approach to solve the above mentioned problem. The basic “superstructure” that determines the possible interconnections between heat sources and heat sinks, is based on the idea that only process fluids are pumped, whereas the heat storage medium always remains within the storage tank.

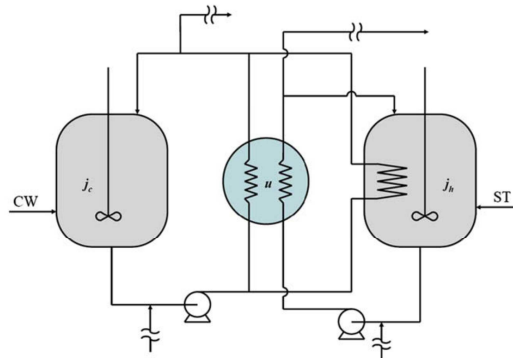


Figure 4-7: Superstructure of the mathematical model [134]

Besides thermodynamic necessary constraints in the model, several operational constraints are integrated in the algorithm, such as

- Direct heat integration can only involve one pair of units (one source and one sink)
- If there is no heat integration between a process unit and the storage tank, the storage temperature remains constant
- Only one unit can be integrated with the storage tank at any given point in time.
- If a process unit is heat integrated with another process unit, it cannot be simultaneously integrated with the heat storage.

These operational constraints make it impossible to model some important practical aspects, such as temperature losses in storage tanks, stratified storages, mixing of process media, storage tanks with several in- and outlets possibly operating at the same time, parallel operation of direct heat integration, and storage tank loading/unloading.

4.1.3.8 Indirect energy storage system optimization over MILP

The aim of the proposed algorithm by Chen and Ciou [54] is to develop a heat exchanger network for batch plants including thermal storages to reach minimum external energy demand. In contrast to other authors, Chen et al. propose a simultaneous (and not sequential) optimization of heat integration and storage system.

The superstructure, which considers the possible configurations of indirect heat exchange network, includes serial and parallel connections of heat exchangers. Surplus heat is taken by the heat transfer medium (absorption) which can later supply heat where needed (heat rejection).

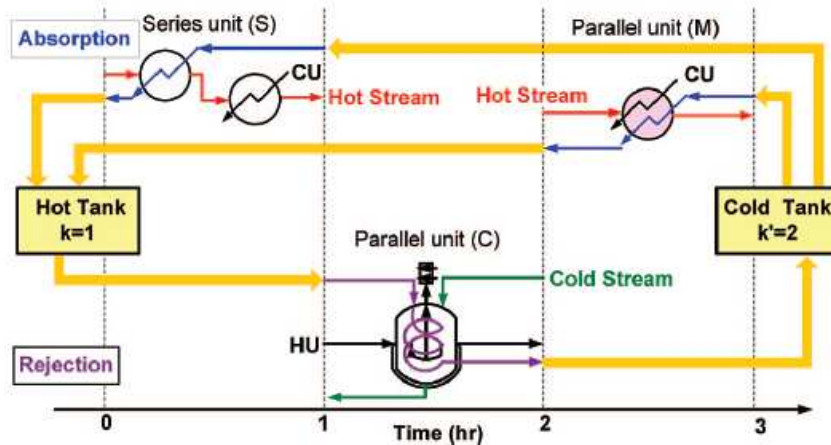


Figure 4-8: Conceptual structure of an indirect network (2 hot streams, 1 cold stream and one heat transfer medium) [54]

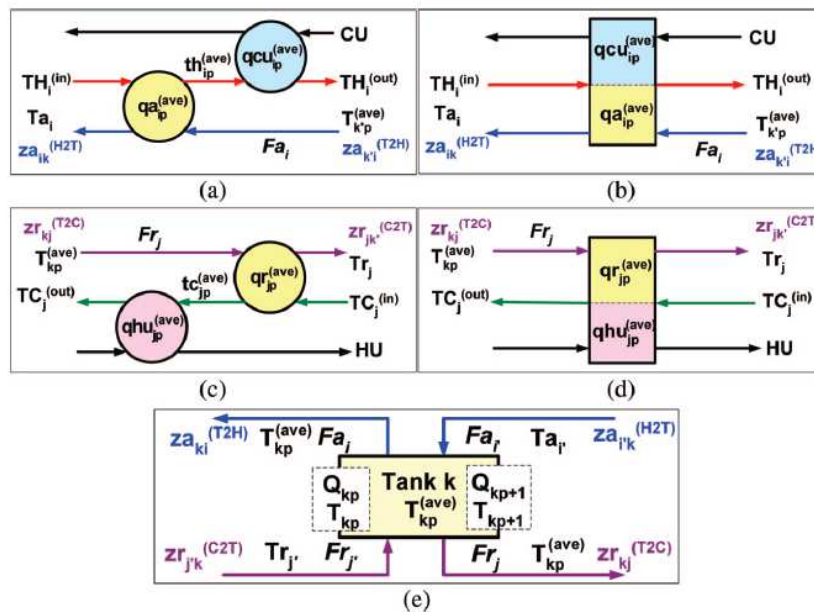


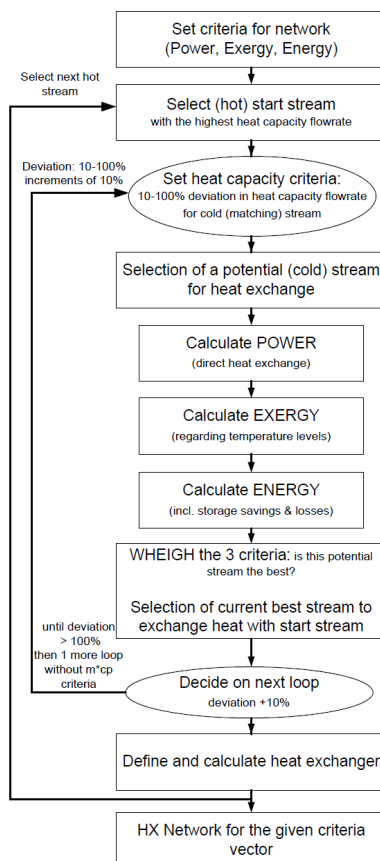
Figure 4-9: Possible configurations of heat exchange units: serial absorption (a), parallel absorption (b), serial rejection (c), parallel rejection (d), heat storage (e) [54]

The model includes heat balances over the different process streams and units, such as the heat transfer medium, serial heat exchangers and parallel heat exchangers. It also takes into account the temperature driving force and a maximal number of tanks (to be entered by the user). Storage tanks are ordered by temperature and multiple tanks are necessary for storing the heat transfer medium at various temperatures. Remaining energy in the tanks is calculated and the minimum tank size is defined. On heat exchange rates constraints are also included by defining an upper and lower limit of heat exchange rate. Finally, only one inlet and outlet connection is allowed for each heat exchanger that uses the heat transfer medium. Most importantly, it must be noted that it is assumed that all heat integration takes place over the heat transfer medium (no direct heat exchange between processes). For the optimization

two objectives are defined, one minimizing the external energy demand and the other minimizing storage tank sizes.

In their further work, Chen und Ciou extended their model to variable temperature storages via linking their MINLP GAMS model to a Matlab program for temperature simulation [53]. The outcome of the Matlab simulation is embedded in the model via one variable to allow for a simplified temperature calculation within the MILP model.

4.1.3.9 Combinatorial approach to design HEN for batch processes – PE2



Muster-Slawitsch and colleagues have developed a combinatorial approach to design HENs for discontinuous and continuous processes. The main steps used in the developed heat exchanger network design algorithm are shown in Figure 1, some of which have been explained in chapter 4.1.3.6, as the PE2 algorithm has been used as a basis for Einstein. Three criteria

- power of heat exchange,
- transferable energy – if necessary over storage - and
- exergy

define the combination of different streams within the system in order to design the heat exchanger network. The weight of these criteria runs from 0-100. The best ranked heat exchanger network (based on its energy saving potential) is then finally chosen.

The algorithm works with an adapted time slice model to calculate the energy transferred over heat storage when the processes are not running continuously. Storage calculations, limited to hot buffers, are an integral part of the heat exchanger network design to calculate the transferable energy.

Figure 4-10: Algorithm for heat exchanger network design with batch processes [149]

4.1.3.10 Time level grand composite curves

For targeting heat integration in batch processes a graphical approach has recently been proposed by Chaturvedi and Bandyopadhyay [50]. Based on the grand composite curve the authors suggest modified grand composite curves by shifting source and sink segments by $\frac{1}{2} \Delta T_{\min}$ in order to account for potential heat storages. These modified grand composite curves are drawn for each time slice. Then time level grand composite are generated by adding the pinch source segments of the previous interval to the

modified grand composite curve of the current time interval. Via problem table algorithm the overall utility requirements can be targeted.

The same authors have developed a minimum storage algorithm for batch processes in water pinch analysis via a time interval approach that considers availability and demand in each time interval [51]. The application of a few rules limits storage so that it does not become oversized. Finally, the summation of single storage requirements leads to the total storage requirement. The approach is basically similar to the approach for single storages within the calculation module “Define Massflow and Energy in a potential storage” within SOCO as presented in chapter 5.2.

4.1.3.11 Heat duty time diagrams for HEN design including batch processes

Heat duty – time diagrams have recently been presented as a tool for targeting heat integration featuring batch streams and identifying the basic structure of heat exchanger networks [210]. All process streams are drawn in a heat duty – temperature diagram sorted by supply temperature. Hot streams are shown with a negative slope, while cold streams show a positive slope. The graphical approach helps to quickly visualise the variance of process streams within time slices. Indirect heat exchange can be accounted for by temperature degradation of the hot streams to a potential storage medium. The authors state that the basic structure of a heat exchanger network can easily be identified via the heat duty – time diagrams and pinch analysis, however, this will mainly hold true for simple projects using this solely graphical approach. Storage design, temperature stratification and losses are not considered.

4.1.4 Heat integration for total sites and integration of renewable energy

The grand composite curve is usually the graph on which basis energy supply alternatives are evaluated. While it can be drawn based on the information of processes, it is also possible to draw it based on the information of the existing supply equipment. In this way exergy losses are visualised and optimized new energy supply equipment can be designed [137]. For identifying the most promising energy supply alternatives, the heat demand of an overall production site has to be taken into account, instead of the consideration of single processes. This is called total site analysis.

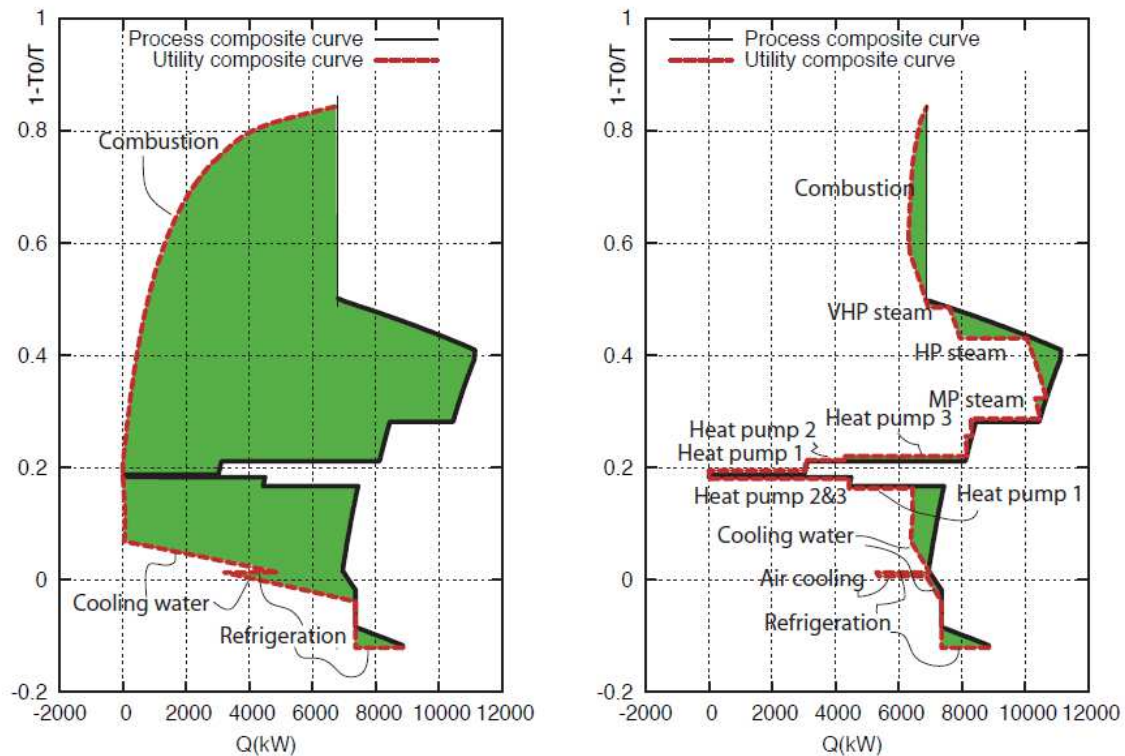


Figure 4-11: Process and utility grand composite curves [137]

Early work on total site integration focuses on the possibility of transferring heat from one plant to another plant via the existing steam mains [61, 112]. Bagajewicz extended the concept and introduced additional heat transfer circuits for indirect heat integration between multiple plants [30], [31] similar to the concept of heat recovery loops (see also 4.1.3.5).

The basic idea of total site analysis can be described via the construction of the site source and site sink profiles. Based on the grand composite curves for each process the remaining energy availability (site source curve) and energy demand (site sink curve) is extracted. To account for inter-plant heat recovery potential zones of heat recovery (pockets) are first eliminated from the grand composite curves. The parallel representation of the site source and site sink profile allows for analysis of whether or not the available heat is at high enough temperatures to deliver steam (at various temperatures) into the steam mains for supplying the remaining energy demand [61].

4.1.4.1 Total site integration including renewable energy

Perry and co-workers extended the concept of total site integration for larger regions and included renewable energy supply [165].

Varbanov and Klemes suggested a targeting procedure for integrating renewables in total sites, taking into account the time variability of the renewable energy [203, 204]. In their approach site profiles and site composite curves are drawn for each defined time slice, for which heat recovery (if necessary over storage) is maximised. The degrees of freedom in the analysis include the type of renewable energy which is to be taken into account, the processes to be included in the total site (e.g. demand of

neighbouring facilities) and the possibility of storing excess heat for later reuse. The steps to identify the targets for total site integration include obtaining the integration targets for each process unit in each time slice and further obtaining the utility targets via the total site profiles and total site heat cascade. Targets for energy storage for each utility are obtained by analysing the flows between time slices within the total site heat cascade [203].

An example of the site source and sink profiles including the design of renewable energy (e.g. solar heat) is given in the following figure for one time slice. Similar curves are drawn for all time slices [204].

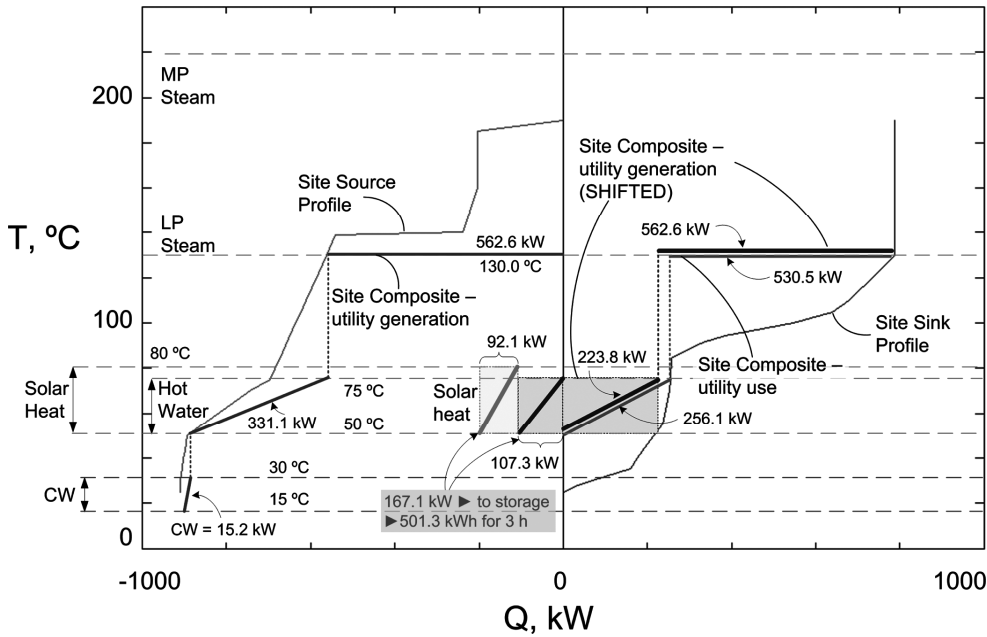


Figure 4-12: Site targets for solar capture and storage in one time slice [204]

While the approach shows a good targeting procedure, there is no possibility for heat exchanger and storage design for practical applications.

Nemet and Klemes propose a graphical approach based on the pinch curves to determine the minimum necessary temperature of heat storage for a solar thermal system [154]. The process as shown in Figure 4-13 is graphically represented in hot and cold composite curves. Two additional curves are being added – the minimal capture temperature curve and the captured solar energy curve.

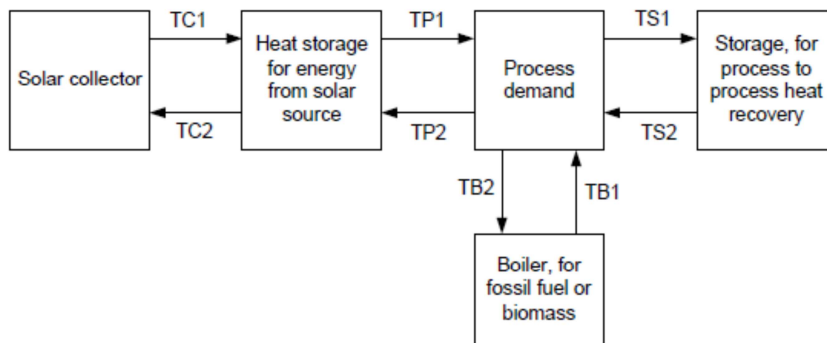


Figure 4-13: Process scheme for heat storage design for solar thermal system [154]

The minimal capture temperature curve (MCTC) is based on the part of the CCC which needs external heating. Shifting the curve in temperature results in two parts of the minimal capture temperature curve – the temperature region in which the heat has to be captured and brought to the storage and the temperature region in which the storage transfers the heat to the processes [154].

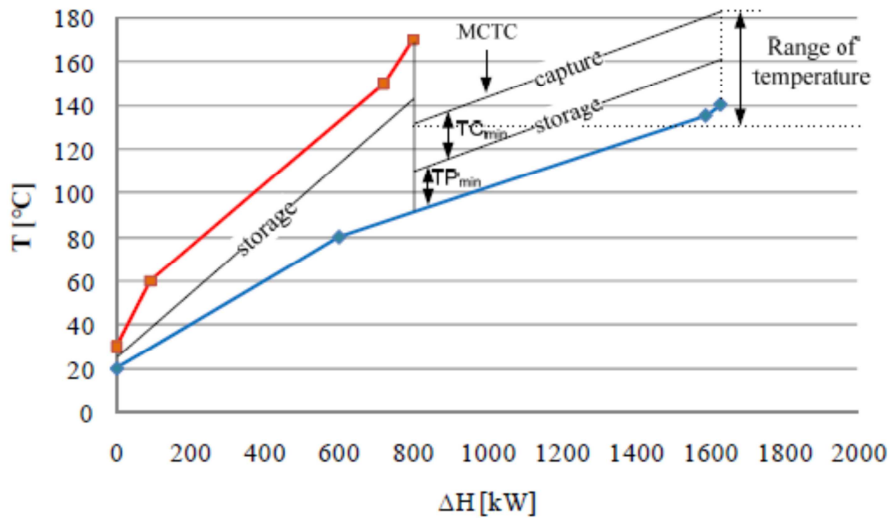


Figure 4-14: Generation of the minimal capture temperature curve [154]

The new 2nd curve, the captured solar energy curve (CSEC) is determined by the solar heat that can be brought into the system. It is calculated by multiplying the solar irradiation, the efficiency of the solar thermal system and the available area. The intersection of CSEC and MCTC represents “a minimal feasible temperature of the capture”. Also the maximum amount of solar energy to be brought into the system is defined [154].

Outlook is given in the paper to consider the two storages in the system in a combined way.

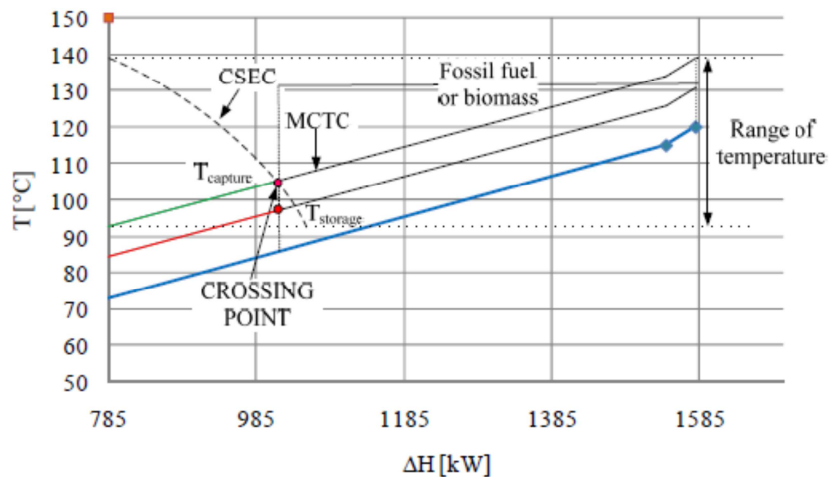


Figure 4-15: Intersecting the captured solar energy curve with the minimal capture temperature curve [154]

4.1.4.2 Integrating solar process heat

It is obvious from the above cited works that the integration of solar heat in the graphical analysis of the pinch analysis is problematic due to the time variability of the solar heat supply. For non-continuous processes time average representations of the grand composite curve can be applied, but design needs to be more detailed and evaluate several scenarios. This has been shown for dairies by Atkins et al. [25] and Quijera and Labidi [170] who proposed a combined evaluation of pinch analysis and exergy analysis for designing solar thermal plants in industrial environments.

In addition to the challenge of time variability the solar heating system's efficiency is depending on the chosen system concepts, the collector type, operating temperatures and storage size. These facts have been highlighted within Task 33 on Solar Heat for industrial Processes and is currently again under focus in Task 49 on Solar Process Heat for Industrial Applications.

The basics of integrating solar process heat in industry have been summarized and defined in the Integration Guideline of IEA Task 49 [150]. A system of different integration concepts has been elaborated [181], which basically differs between

- Integration on process level and
- Integration on supply level.

Integration on process level means integrating solar heat as heat supply unit for one or several processes with a direct link to the process heat exchange unit. Supply level integration, on the other hand, embraces all integration concepts where solar heat is integrated in the general heat supply network of the company (e.g. boiler feed water, condensate runback etc.).

There are several possibilities to identify the most suitable integration points for solar heat. Pinch analysis is a very good basic tool for this identification. A comparison of different approaches based on the pinch analysis has been carried out in this work (see chapter 5.2.1) and published in [150].

Based on the selection of possible candidates for integration points in industry, a ranking matrix was suggested by Ben-Hassine [150] to identify the best integration points for which detailed design studies are then performed.

4.1.5 Process integration tools for variable process streams

Within IEA Task 49 several tools have been evaluated on their potential use for variable process streams [118]. The well known tools such as ASPEN Energy Analyser, SuperTarget and HEAT-int stem from process integration analysis for continuous processes and allow optimization of heat exchanger networks for new design and retrofit projects. However, they do not include storage networks for discontinuous processes. This holds also true for Optimal Heat and INTEGRATION. Over the past years a number of tools are being developed for the holistic design of heat integration and renewable energy implementation. These are notably EINSTEIN, OSMOSE and CERES. PinCH, SOCO and OBI are finally process integration tools with emphasis on discontinuous or variable process streams. However, beside SOCO, the tool developed in this work, no tool currently allows for heat integration on the basis of dynamic process streams including storage simulations [118]. An overview of available tools and their features regarding solar heat integration is currently under publication within the B1 deliverable of IEA Task 49 on Process Integration Tools. Details on several process integration tools can also be found in [9].

4.2 Process Intensification in the food industry for sustainable processing

A large number of optimization approaches and new technological developments can be summarized by the umbrella term “Process Intensification”. Process Intensification leads to substantially smaller, safer and cleaner processes with significant improvement in process efficiency by radical process changes [85, 172, 202]. Process Intensification (PI) as defined by the Research Agenda for Process Intensification [83] is: “A set of often radically innovative principles (“paradigm shift”) in process and equipment design”.

Process Intensification aims to optimize production processes based on its core functions. The first step towards an intensified process is to raise the question: What is (are) the key function(s) that my process needs to achieve? Based on a methodological analysis of the process in question, it is possible to determine whether Process Intensification technologies can achieve these key functions and can overcome the existing bottlenecks at the same time. This essentially will lead to an enhancement in process efficiency. Depending on the necessities and parameters of the plant, the solutions will integrate one or more possible benefits of PI. These can be summarized by a few key elements.

4.2.1 Key elements of process intensification

The main benefits of process intensification come about by the following approaches:

- Minimize the size – Combine functions
- Make your process faster/more efficient – Overcome transfer limitations (heat and mass)
- Make your process controllable – change from batch to continuous processes

Minimize the size

The size reduction of processing units is characteristic in PI. The approach itself targets and develops technology which increases the driving forces of processes, integrates functions and equipment [131]. It is where PI really differs from other optimization techniques. Whereas cleaner production or process integration can boost up your energy efficiency; using heat sink recuperation, pinch analysis or consultant specific methodology analysis, PI - if applied thoroughly and the process is adequate - can make radical changes in the equipment and process layout with a several fold size reduction and cost improvement.

Synergy is sought for on a molecular scale, in energy transfer, and in processing units [202]. In “conventional” processes one is used to having one piece of equipment for each function. The PI approach tends to avoid such design, integrating several functions into one piece of equipment. A very typical example is the multifunctional reactor, which may combine a separation process or heat exchanging step with the chemical reaction. Such intensified designs are smaller and more compact, while maintaining the product production rate [202].

Make your process faster/more efficient

One of the pillars of PI is optimization of heat and mass transfer [173, 202]. In any chemical reaction the slowest step is the rate determining step, and in many cases it is limited by heat or mass transfer. These are the bottlenecks that PI targets in order to obtain a faster, more efficient and continuous process.

Some examples are:

- In large batch tanks the energy transfer from the tank walls to the medium can be rate determining and a continuous system with improved heat transfer can reduce equipment size and process time several fold.
- Selective heating of one substance in a mixture or a solid sheath reduces heating requirement, as all energy input for heating the surrounding is saved.
- In processes where certain compounds are taken out by evaporation, selective mass transfer processes (e.g. over a membrane) can reduce energy requirement substantially.
- With a better understanding of the energy levels of molecules involved in the chemical and physical processes, it is possible to design equipment that will provide the most efficient form and transfer mechanism.

There are numerous examples of technological solutions to overcome heat and mass transfer limitations, either by active or passive intensification strategies [173].

Make your process controllable / Change from batch to continuous

The change from batch to continuous is a very important aspect of PI in process and equipment design. It is linked to one of the principles of PI to “give each molecule the same processing experience”, thus to avoid large residence time or temperature distribution in stirred tanks [202]. The increase in process control and reduction in operation time when considering single-purpose equipment makes continuous processes more effective and efficient [18]. In the cases where the reaction permits such a change it is possible to obtain an increase in the process rate, avoiding formation of unwanted by-products and avoiding unnecessary energy losses [202].

For batch operation, the time during which the maximum energy is generated is only a fraction of the batch cycle time. In order to control the reaction, it is necessary to be able to cope with the maximum likely heat evolution so as to prevent runaway. On the other hand, the continuous process running at the same production rate requires a considerably smaller reactor and heat exchanger due to the uniformly distributed time load [18].

4.2.2 Process intensification – a methodology to identify best suited process technologies

The methodology of selecting intensified technologies has been well defined by other authors. Figure 4-16 shows the basic steps according to [173] p. 456-461. To reach “intensified” processes first bottlenecks of crucial processes need to be analysed and on this basis new solutions for overcoming these limitations need to be developed.



Figure 4-16: The PI tower - steps towards an intensified process (steps acc. to [173])

To account for the difference between intensification of single process steps and optimizing the complete production system, a new definition of PI has recently been suggested by Ponce-Ortega et al.[168]: Intensification of unit operations and intensification on plant level. “Unit intensification” aims at intensifying one unit operation without considering the effects on the rest of the plant, which will result in higher yields due to increase in selectivity or reduced equipment size at constant yield. “Plant intensification” on the other hand aims at increasing the overall yield of the production system by reducing inventory, reducing raw materials and by-products. This is linked to the aim of process intensification to achieve sustainable processing as defined by the European Research Agenda of PI [83].

Especially for heat integration in the food industry, the inter-dependence between new technologies and overall energy optimization is an important factor. This is highlighted in the 3-step approach by Schnitzer et al.[182] and further elaborated by Brunner et al. [48] to realise thermal energy supply in industry with minimal greenhouse gas emissions:

- Technological Optimization (measure to enhance energy efficiency)
- System Optimization (Pinch Analysis of a total production site)
- Integration of renewable energy (based on exergetic considerations)

However, a holistic methodology for process intensification for sustainable processing has so far not been defined in literature.

4.2.3 Process Intensification for the food industry

Several innovative technologies for process intensification have been developed in recent years that increase process efficiency, product quality and/or energy consumption [173]. In the food industry many of the developed technologies are still not implemented for several reasons. Firstly, the applicability is a central issue, solutions might be different according to the industry and scale. A generalization is not always possible due to technical differences or due to different process constraints. Secondly, the developments may face scale-up challenges and little pilot plants and practical experiences exist. Investment costs and the fear of a negative influence on product quality are additional factors that do

not trigger the integration of new technologies. Due to these factors, there is a natural reluctance to the adoption of new techniques [144].

When considering energy and water efficiency, a few operations can be identified within the production chain of food products that are important candidates for improvement and worth an analysis for process intensification possibilities. This list does not claim to embrace all potential PI strategies that have been applied in the food industry.

1. Dewatering (Drying/Evaporation) – one of the main energy intensive processes (from a thermal energy perspective)
2. Pasteurisation – one of the most common processes in the food industry, also largely contributing to the energy demand
3. Mixing

Drying, evaporation, pasteurization etc. are thermally driven and highly energy intensive. The basic function of the process however is not heating up the product: It is removing water, destroying molecules or eliminating biological activity [43]. Besides these crucial operations two more general topics are decisive when speaking about process intensification for the food industry:

4. From batch to continuous – many inefficiencies result due to the fact that food processing is done largely in batch processes
5. Heat transfer – a general hot topic in process intensification, in the food industry relevant also for solid biomass

These above mentioned problems have been formulated within the milestone “Low cost small scale processing technologies” of the Research of Process Intensification for the Food Industry [43].

4.2.3.1 Intensification examples for heat transfer

The following tables summarize some intensification examples for heat transfer with respect to food processing. While Table 4-1 links the technologies to selected unit operations, Table 4-2 gives an overview of application examples and research status for each technologies based on selected books and reviews.

As described earlier, current process technologies in the food industry are often the bottleneck when it comes to integrating low temperature heat, such as waste heat and/or solar heat that would lead to sustainable energy supply. As this work deals with the consideration of changing processes for enhancing the integration of low temperature heat supply, more focus will be dedicated on this topic in the next chapter.

Table 4-1: Selected intensification examples for heat transfer applied in or researched for operations in the food industry

<i>Technology / Unit Operation</i>	<i>pasteurization</i>	<i>Sterilization</i>	<i>cooking</i>	<i>heating/reaction</i>
HEX reactors				
compact HX (plate HX; extended surface HX)	x	x		x
inserts (offset strip fins; metallic foams; vortex generators)				x
microchannel reactors	x	x		x
static mixers in shell and tube HX				x
Spinning disc				x
ultrasound	x	x	x	x
PDX			x	x
oscillatory flow reactors				x
direct electroheating / ohmic heating	x	x		x
indirect electroheating/microwave heating	x	x	x	x
indirect electroheating/IR heating	x			
indirect electroheating/RF heating	x	x	x	x
UV irradiation/Pulsed Light	x	x		
Pulsed Electric Field	x	x		
High Hydrostatic Pressure	x	x		

Table 4-2: Intensification examples for heat transfer in the food industry²

Technology	application examples		intensification	challenges	sources
HEX reactors					
<i>compact HX (plate HX; extended surface HX)</i>	widespread use in industry; e.g. flash pasteurization	applied	thermal intensification/heat transfer	fouling	[22]
<i>inserts (offset strip fins; metallic foams; vortex generators)</i>	chemical reactions (e.g. catalytic reactions)	applied	flow intensification/mixing	fouling	[22]
microchannel reactors	chemical industry	applied	flow intensification and thermal intensification	fouling	[22]
static mixers in shell and tube HX		applied	flow intensification (plug flow at low Re number), thermal intensification --> greater heat transfer rates		[22]
Spinning disc	chemical industry (polymer processing): condensation reactions, devolatilization, radical reactions	early	flow intensification; high heat and mass transfer rates	short residence time	[173]
ultrasound	cooking; pasteurization (in combination with heat pressure or both; low temperature pasteurization (50°C) with US promising); depolymerization; US can inactivate or increase enzyme activities	early; research for each application needed	less heat treatment à less negative impacts on food quality; higher sensitivity of micro-organisms due to mechanical/physical/chemical effects in acoustic cavitation; enhanced heat transfer through cavitation or acoustic streaming; chemical reactions with radicals produced from cavitation;	faster inactivation of enzymes when ultrasound is not used as pretreatment	[163], [28], [52]

² Parts of this table are waiting to be published in:

Muster B., Brunner C., *Process Intensification and Solar Process Heat*, In Galluci (Ed.), *Process Intensification for Sustainable Energy Conversion*, Wiley Ltd.

Technology	application examples		intensification	challenges	sources
PDX	mixing and heating in supersonic region; e.g. wort heating in breweries	small number of commercial applications	flow intensification and thermal intensification		[14]
oscillatory flow reactors	heating single fluids; ester hydrolysis reaction; aroma compound production; protein refolding; flocculation; crystallization;	small number of commercial applications	heat transfer rates decoupled from flow velocity, enhanced heat transfer rates; uniform mixing behaviour; enhanced mass transfer due to small bubbles (suspensions; gas liquid contacting)		[22], [155], [173], Nitech Solution
direct electroheating / ohmic heating	sterilization, pasteurization of pumpable foods; blanching of vegetable purees;	limited commercial applications (3-6t/h)	heat transfer decoupled from heat transfer coefficients; uniform heating based on electrical conductivity; very fast change in temperature; microbial inactivation due to thermal effects and electric field	faster inactivation of enzymes; fouling (proteins) and corrosion (mainly at low frequencies); temperature runaway possible; material with non-conductive parts; precise temperature/mass flow control required;	[102, 103, 187]
indirect electroheating/microwave heating	drying (incl MW-freeze drying and MW vacuum drying), cooking, blanching, concentration, pasteurization, thawing, tempering, roasting and baking; products: meat, fish, dairy products, potatoes, pasta, grains, fruits, vegetable and juices etc.	limited commercial applications	thermal intensification, reduction in pasteurization and cooking time; rapid heating; high potential for hybrid processing (with hot air; vacuum, ormotoc, freezing, IR/RF)	non-uniform heating (design of oven); dielectric properties of material change during treatment - effects must be well understood;	[201]
indirect electroheating/IR heating	pasteurization		bacterial deactivation possible at low temperature (e.g. 40°C)		[135]
indirect electroheating/RF heating	meat cooking, packaged ham pasteurization; disinfestation of fruits; liquid food heating (starch solutions, guar solutions)and pastuerization (milk,fruit juices)		thermal intensification (ionic depolarization induces thermal effect); reduction in pasteurization and cooking time; rapid heating	uniformity of temperature in solid food (outside vs. inside); liquid food: temperature distribution and penetration depth analysis on larger scale; lack of information regarding impact on quality; missing dielectric property data; scale-up;	[138]

Technology	application examples		intensification	challenges	sources
UV irradiation /Pulsed Light	pasteurization/sterilization (e.g. sterilizing films of packaging material)		non thermal technique; inactivation of microorganisms without chemicals	poor penetrating power of light	[164]
Pulsed Electric Field	preservation of pumpable fluid or semi-fluid foods (e.g. milk, liquid whole egg; vegetable soup, fruit juice)	commercial application for fruit juice	inactivation of microorganisms without chemicals & heat but via high voltage pulses; combination with mild heat treatment potentially interesting	research need (e.g. efficiency of PEF treatment; equipment design; effect on food properties); non-uniformity of electric field strength may lead to over-processing and deteriorate quality	[164]
High Hydrostatic Pressure	cooked meats, seafood and fish, vegetables and fruit juices	82 commercial applications in 2005	minimal heat impact; uniformity; little energy input; packaged food can be treated (aseptic processing)	limitation in killing spores; products are chilled; mainly used for acid foods (inhibits bacterial growth)	[164]

4.2.4 Process intensification and its potential for low temperature heat supply³

When we speak of intensifying an industrial process, we usually aim at higher productivity with smaller reactor equipment. This increase in yield of products, while maintaining the raw materials and decreasing byproducts and maintaining or decreasing energy input is, in many cases, achieved by an increase in mass and/or heat transfer. Often these phenomena are interlinked with each other, as in processes with heat transfer as limiting step, mass transfer can also be enhanced once the heat transfer limitation is overcome. On the other hand, an increase of mass transfer rates induced by physical change of the process design (e.g. change from evaporation to a membrane based process) can allow processes to run at different temperatures and might change the possibility of integrating different energy supply. Naturally, all intensification strategies that affect heat transfer rates and/or change the heat supply to the processes might positively or negatively affect the potential for integrating new heat supply technologies. Another important aspect for the integration of new energy supply is the continuity of process energy demand. In many cases it is actually the change from a batch reactor to a continuous reactor which will lead to mass and heat transfer improvements. A continuous energy demand profile may additionally be in better coincidence with e.g. the solar availability.

Below, some examples are given of the aforementioned intensification strategies. There are several strategies to overcome heat transfer limitations, such as:

- increase of heat transfer area,
- increase of heat transfer coefficient ,
- increase of temperature gradients, or
- change to energy supply without thermal gradients

These changes may or may not affect the basic reactor set-up of the existing plant, as they can - at least to some extent - usually be integrated into an existing plant by adaptations. Retrofit changes are naturally limited by existing space and existing construction and regulation. A change in technology will of course improve enhancements possibilities further.

Changing the physical process phenomenon on the other hand, clearly requires a technology change and replacement of the existing equipment. Considering changes that affect the integration of energy supply possibilities, such as solar heat, we specifically need to look at

- increase in selectivity of separation processes (e.g. change from atmospheric evaporation to membrane assisted processes)
- electromagnetic action on molecules and microorganisms (e.g. change from thermal inactivation of microorganisms to non-thermal techniques, such as microwave or pulsed electric field)

Finally, the change from batch to continuous processes must be examined. Due to the elimination of peaks in heating/cooling demand this has a large effect on energy supply and its design.

³ Parts of this chapter are waiting to be published in:

Muster B., Brunner C., *Process Intensification and Solar Process Heat*, In Galluci (Ed.), *Process Intensification for Sustainable Energy Conversion*, Wiley Ltd.

4.2.4.1 Increase of heat transfer area

As low temperature heat supply often leads to lower temperature differences between heat supply and process temperatures, an increase in either heat transfer area or an increase in heat transfer coefficient is beneficial for the integration efficiency. This is also important for low temperature solar heat production in flat plate or evacuated tube collectors. In many cases, as will be shown, a combined enhancement of heat transfer coefficients and larger heat transfer area is applied for enabling low temperature heat supply.

The increase of heat transfer area is a very basic enhancement strategy. By increasing the heat transfer area, it is possible to lower the temperature gradient between energy supply and process (when maintaining the same heat transfer coefficient). This makes it possible for existing processes to quite simply be retrofitted for new low temperature energy supply, such as district heat or low temperature solar heat. It depends on the current process layout, however, if there are limits to adding new heat transfer area.

Basically, a “simple” addition of HX area without additional intensification would contradict the PI goal to reduce equipment sizes. It is, however, still a viable solution for integration of low temperature heat supply. However, in most cases the addition of new heat transfer area accompanies the enhancement of heat transfer coefficients. Figure 4 shows a design of a new mash tun retrofitted with additional heat exchange area (including improvement of heat transfer) for enabling the heating of the mash tun with solar process heat. This system has recently been introduced in a Heineken brewing plant in the European funded project SOLARBREW, designed by AEE INTEC and GEA Brewing Systems [140]. The new heating plates have a special surface layout for enhancing heat transfer coefficients and the application of heat supply with lower temperature should also lead to less fouling. The plates are designed in a specific manner to enable integration with the existing vessel with positive effects on mixing and cleaning possibilities.



Figure 4-17: Mash tuns (schematic figure and real plant) supplied by steam (source: AEE INTEC)

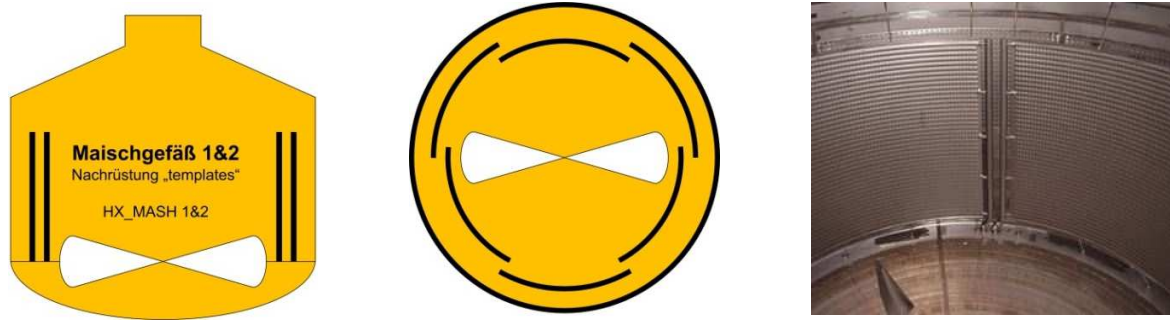


Figure 4-18: Heating plates on the inside of the mash tuns for low temperature heat supply (source: AEE INTEC and GEA Brewery Systems GmbH)

When speaking of heat transfer increase in process intensification, one immediately thinks of compact heat exchangers. Compact heat exchangers integrate maximum heat transfer areas in small and compact equipment. The degree of compactness is described by the term HX compactness factor which shows the ratio of heat transfer surface over the equipment volume [m^2/m^3]. The large heat transfer areas and the usually high heat transfer coefficients would enable integration of solar heat and any low temperature heat supply very well. Compact heat exchangers with extended surfaces have a specific area of $800 \text{ m}^2/\text{m}^3$ [74].

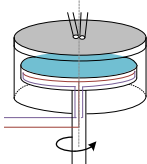

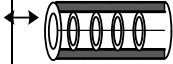

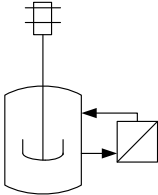
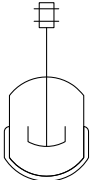
4.2.4.2 Increase of heat transfer coefficient

There are several means employed to increase heat transfer coefficients. In many processes in industry heat transfer coefficients are limited by the heat transfer coefficient (α) on the process fluid side. Intensification strategies therefore mainly aim to overcome this limitation.

Heat transfer coefficient limitation is especially pronounced in stirred tanks, where the velocity inside the tank is comparably small and α -values on the process fluid's side are therefore low. Enhancements of heat transfer coefficients in stirred tanks can be achieved by improved mixing (e.g. via optimized baffle design for the respective application) leading to a more uniform temperature distribution and higher turbulence. Some processes in which pumping of process fluid is not critical will allow placing heat exchangers outside the process bath, thus increasing the design flexibility and enabling the integration of low temperature heat supply more easily. In external heat exchangers the possibilities for increasing convective flow (and therefore Nu values) on the process and on the supply side is usually much larger than in internal heat exchangers placed in process vessels. Limitations may arise due to limits in process fluid velocity to reduce shear stress on the product or due to limits in temperature increase of the process fluid in processes where temperature must be kept in very precise ranges (e.g. galvanic baths).

Increasing heat transfer coefficients in heat exchangers has been researched quite extensively, recently reviewed by [22]. Plate heat exchangers performance can be improved by different surface effects (corrugation), extended surfaces (e.g. plate-fin HX) or inserts (e.g. foams). This last class of heat exchangers with inserts (plate reactors) can be efficiently used as reactors, as the inserts not only enable increased heat transfer, but as well better mixing behaviour [22].

Table 4-3: Figure 12: Increase in heat transfer efficiency from batch stirred tanks to intensified heat exchangers ([a] own data, [b] own calculations based on comparison with batch stirred tank (base data [189]), [c] estimated based on tubular heat exchanger)

Heat exchanger /reactor	spinning disc	compact multifunctional heat exchanger (offset strip fins)	plate heat exchanger	oscillatory flow reactor	tubular exchanger reactor	batch reactor with external HX	batch reactor with double jacket
Scheme							
heat transfer coefficient W/m ² K	15000 [173]	5000 [75]	2000-4000 [a]	1500-2500 [4a]	500 [197]	1000 [197]	400-800 [152, 197]
specific area m ² /m ³		800 [75]		400 [4b]	400 [197]	10 [197]	2,5 [197]
magnituded of residence times	seconds	seconds - minutes	seconds - minutes	minutes - hours	seconds - minutes	minutes - hours	minutes - hours

In addition to the intensification of classical heat exchanger concepts already mentioned, there are also different reactors for intensified heat transfer. Reay et al. have classified the enhancement strategies for heat transfer into passive and active enhancement strategies [173]. While the strategies thus far mentioned for intensifying heat exchangers are mainly passive (extended surfaces, inserts etc), new reactor concepts for intensified heat transfer mainly rely on active enhancement strategies. Examples are rotational reactors (e.g. spinning discs), fluidized bed (membrane) reactors or oscillatory flow reactors. Another interesting approach is the active intensification of heat transfer rates in heat exchangers over ultrasound [173].

4.2.4.3 Increase of temperature gradients

For the increase of temperature gradients two approaches are obvious for processes which are indirectly heated: either increasing the temperature of the energy supply medium or lowering the process temperature. For the integration of solar process heat the aim will be to lower the process temperature as an increase in supply temperature will not favour the efficiency of the low temperature heating system. This holds true for integration of low temperature heat supply such as waste heat.

Generally, we can conclude that the integration of low temperature heat will actually lead to a decrease in temperature gradients. This decrease must be balanced by a corresponding increase in heat transfer surface and/or coefficient. We could argue that a decrease in temperature gradients does not fall under the basic idea of intensification, however in most cases intensification of heat exchangers aims at an increase in heat transfer coefficient [22], thereby allowing for low temperature gradients. Additionally, if a measure serves the sustainability of the process while maintaining its efficiency, it is a valid and sustainable approach for the process system design.

Lower process temperatures

Regarding *increasing* temperature gradients in processes with low temperature (solar) heat supply the process temperature must be lowered. Lower process temperatures can be reached by changing the chemical pathway of a process: This happens in the textile industry with the use of low temperature detergents. Similarly, it takes place in the metal surface industry specifically because degreasing and washing baths are aimed to be operated at low temperature. The main aim is to reduce heat transfer losses from these large, usually uncovered baths. Such approaches enhance the potential for low temperature heat supply.

Runback temperatures can obviously be lowered when process temperatures are lower and are largely influenced by the heat exchanger design. In a counter-current plate heat exchanger the runback temperature approaches the temperature at the inlet of the process medium. In such designs the heat transfer coefficient is so high that temperature gradients can be low. This is in line with the common intensification strategy to change from vessel operation to more structured plug flow reactors [202].

Technologies which lead to lower process temperatures are often also membrane based processes. This is further discussed below. Another important approach which is related to this discussion is the decrease of process heating rates for low temperature heat supply. In this case however, strictly speaking, the temperature gradients are not lowered, but the heating profile of the process is changed. Obvious examples of this approach can be found when changing from a batch process to a continuous process, eliminating peaks in heating demand.

4.2.4.4 Gradientless process energy supply

An important aspect in eliminating heat transfer limitations and intensifying processes is the shift towards gradientless processes, in which driving forces do no longer depend on temperatures of product/process medium and supply medium. Gradientless processes are no longer thermally driven, but rather they are driven by electrical energy. There are a number of very promising processes in which this intensification approach has been realized [164, 188].

Microwave heating is a very promising example as the heat is generated exactly where it is needed and there is no heat for convective/conductive heat transfer to the particles [201]. A typical thermal process in which microwave application has been widely studied is drying, however there are also a number of other application examples in which an intensification of mass transfer is often realised in accompaniment with heat transfer enhancement [188].

Microwave heating, as well as other electromagnetic induced heating such as IR or RF have no potential for being heated with low temperature heat. However, in some cases the combination of an electromagnetic intensified process with low temperature heat could be envisioned.

4.2.4.5 Increase in selectivity of separation processes

Membrane processes increase selectivity and efficiency in transporting specific components and can thus improve the performance of reaction (e.g. by shifting the equilibrium of a certain reaction). Due to these facts membrane processes may intensify energy intensive processes [64]. This intensification of transport and reaction efficiency may enable lower process temperatures, which can be exemplary shown for membrane distillation or pervaporation.

Membrane distillation is a promising alternative in comparison with conventional evaporation. In membrane distillation the targeted evaporation runs at a much lower temperature than in conventional evaporation due to the difference in vapor pressure over the membrane. An aqueous feed solution is heated on one side of a hydrophobic microporous membrane which does not allow aqueous molecules to penetrate. Only volatile substances will pass the membrane and are collected on the permeate side. The low operating temperature, due to the fact that the liquid does not need to be heated above its boiling point, is only one of the advantages of membrane distillation in addition to reduced fouling and low operating pressure. Condensation of the volatile substances on the permeate side can be achieved via several means (aqueous solution; cooled air gap, seep gas transportation to a condenser or vacuum). For further details the reader is referred to specific literature [64].

Low temperature energy, such as solar heat, could be used in membrane distillation to preheat the feed solution prior to entering the membrane module. Figure 4-19 shows a possible process scheme, which has been studied by Brunner et al. [46]. The feed solution is pumped through a first heat exchanger in which the waste heat of the hot retentate preheats the incoming feed stream. The feed is then further heated with solar energy and (if necessary) heated to its target temperature in a final heating unit. When the feed is only circulated once over the membrane, the temperature difference between incoming feed stream and target temperature will be sufficient for efficient operation of the solar system. In such plant designs the collectors can operate at target temperatures close to (or even below in case of preheating only) the process temperatures.

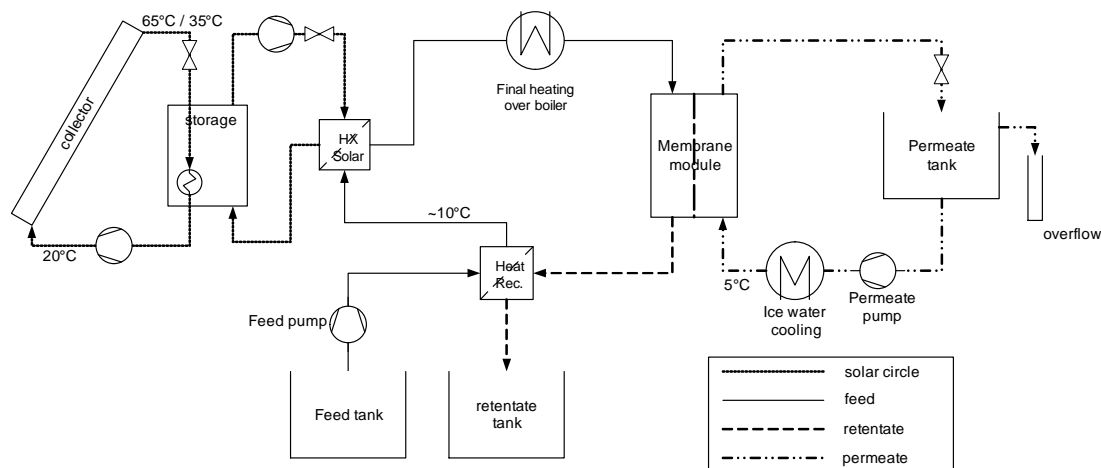


Figure 4-19: Basic scheme of a membrane distillation unit heated by solar thermal energy over an energy storage tank [46]

A similar example of a promising application of low temperature heat for intensified process systems is pervaporation. In pervaporation a selective membrane is used as a barrier between two phases, the liquid feed and the vapour permeate. The process depends on the sorption equilibrium and the mobility of the components through the membrane and is fairly independent of the vapour liquid equilibrium. The desired component which is in liquid form in the feed permeates through the membrane and evaporates while passing the membrane, because the partial pressure of the permeating component is kept lower than the equilibrium vapour pressure [211]. Permeabilities depend on the solubility and diffusion rates through the membrane.

Pervaporation units have promising potential to be used in combination with conventional distillation columns to overcome azeotropes in distillation [64]. Feed temperatures are often in the range between 20-90°C, showing a potential for low temperature heat supply or solar heat integration even with non-concentrating collectors.

4.2.4.6 Electromagnetic action on microorganisms

When speaking of intensifying thermal processes, the electromagnetic action on microorganisms is an important field of research. In the food industry it is studied as an alternative to thermal pasteurization and sterilization techniques. Table 4-2 includes also different electric processes currently studied as alternatives to thermal processes in the food industry based on selected review papers. These technologies clearly will not lead to an increase of energy supply with low temperature heat, however until now, rapid pasteurization and sterilization processes have also not been highly important applications for solar process heat due to the fast required heating rates and high potential for heat recovery.

4.2.4.7 Changing from batch to continuous processes

In various subsections above, it has become clear that a major impact on the potential for low temperature heat integration is the required temperature profile of the process itself. The intensification strategy from batch-processes to continuous processes is a perfect example of changing the temperature

profile to more continuous gradual heating rates, which positively enhances the performance of the solar loop.

The general advantages of a continuous process can be summarized as follows:

- High process efficiency, small residence time distribution, structured processes
- Good process controllability
- Low energy intensity (no peaks in heating/cooling demand)
- Low cleaning requirements
- Flexible processes
- Decreased energy distribution losses due to continuous heat demand

Figure shows the flow characteristics in a typical stirred tank versus a plug flow reactor. While the motion of an incoming particle is hardly defined in a stirred tank, the flow is much better predictable in structured plug flow reactors [202]. This fact shows that reactions in plug flow reactors are much better controllable due to the small residence time distribution which is again linked to advantages in terms of energy efficiency and supply.

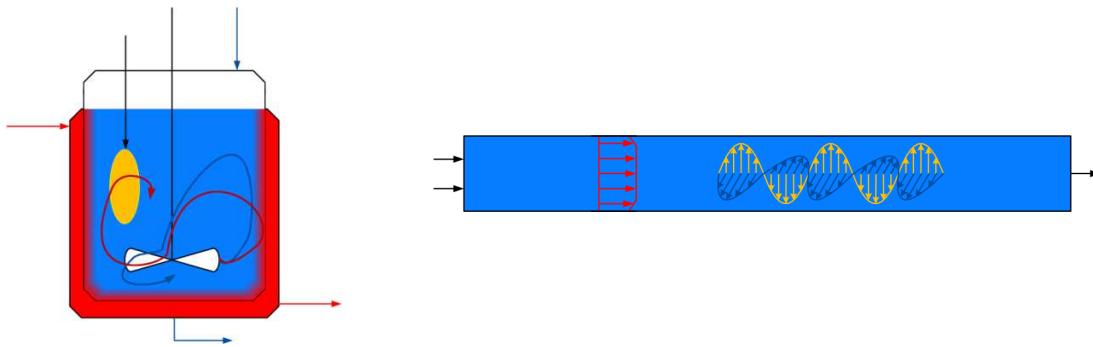


Figure 4-20: Flow characteristics in stirred tanks versus plug flow reactors [202]

4.3 State of the art in the brewing industry including upcoming trends

4.3.1 Brewing chemistry

4.3.1.1 Malting chemistry

The aim of malting is the modification of the barley grains which is important for the formation of enzymes [120] p. 161 and cell wall degradation, leading to chemical reactions and physical modification of the grain [59] p.18. Additional aims of malting are the development of distinctive colour and aroma while eliminating undesired aroma compounds [90] p.189.

In malting, firstly, malt is hydrated and swelled by adding steep-water at a temperature of 16-18 °C [59], p.17. During “steeping” which lasts about 2 days [34] steep water is periodically drained and fresh water added. When water is drained humid air can be blown through the grain. Such “downward ventilation” assists in drainage, provides oxygen and removes CO₂ and heat [59] p.17. Enzyme formation which is activated in a process called germination starts at a water content of 30 %. Once the rootlet appears at

the base of each germinated grain, germination starts and the grain might be transferred to a germination vessel [59] p.17. The germination process takes 2-5 days at temperatures of 16-20 °C and typically at moisture contents of 43-46 % [34]. Temperature profiles might vary between germination with increasing temperature, germination at constant temperature or germination at decreasing temperature [90]. Germination requires aerobic conditions which makes good aeration necessary [120] p. 163, [59] p.17. Cooling of the grain beds by moist air flow is a difficult task as the air flow must inhibit water loss during germination, which will naturally occur as the air warms up and absorbs water [90]. The most important enzymes for brewing are amylases which degrade the starch present in the malt [120] p. 163, however also a number of other enzymes are released such as hemicellulases, proteolytic enzymes and phosphatases [90] p. 192. Some of these catalyse the physical modification of malt [59] p.18 in which the cell wall is dissolved. Initially, the degradation of cell wall of proteins sets the pentosan structure free. Then xylanases degrade organic acids and pentosanases and finally glucanases start the degradation of β -glucan and open the cell membrane [120] p. 165. The proteins of the cell are then degraded partially and starch granules are broken [59] p.18, [90] p. 192.

Malt modification has influence on many later stages in brewing [126] p. 80-89:

In mashing it affects extract recovery by the formation of amylase enzymes and by increasing malt friability, so that the starch granules can be easily attacked by enzymatic breakdown. Enzymatic action of α - and β -amylases during malting is minimal [90] p. 193.

Malt modification affects fermentability, not only via the extract recovery, but also via the breakdown of cell wall proteins leading to an increase of available nitrogen for yeast metabolism.

Many flavour compounds are formed during fermentation, therefore, way malt modification also influences beer flavour. S-methylmethionine (SSM), the pre-cursor for the unwanted dimethylsulphide (DMS) is also formed during malting. SSM is very heat sensitive, quickly forming DMS which is then readily evaporated, and therefore values are minimal in high temperature kilning (ale malts). When SSM is released to the wort it will form DMS during wort boiling, however again evaporation during boiling ensures the quick release of the compound. However, in whirlpools standing times at high temperature can lead to formation of DMS which is not released and can negatively affect beer flavour.

An important degradation mechanism of malting is the breakdown of β -glucan by glucanases. Dissolved β -glucan leads to highly viscous wort and beer, having a negative impact on lautering and beer filtration performance.

Finally, foam stability is also affected in malting by ensuring an appropriate number of proteins remain in the malt. Over-modification can lead to less foam stability.

In general important enzymatic activity, excluding amylases, which contribute to malt modification takes place during malting and their action in the later mashing process is minimal [126].

The following factors influence the building of enzymes [120] p. 164, [90] p. 192:

- content of amylases in raw material
- size of corn (large germs form more amylases)
- water content (higher water content in green malt increases amylases content)

- Temperature (cold germination favours formation of amylases, high temperatures fasten start of enzyme formation, but leads to reduced yields)
- Oxygen content

For the degradation of cell walls (lyses of the germs) the right germination time is important. Germs should be fully lysed to avoid a possible negative impact on saccharification in mashing; however over-cytolyses may lead to losses. It is also aimed to fully degrade β -glucanes to avoid possible negative impacts on beer viscosity and filtration [120] p. 164.

After the appropriate germination time, enzyme formation and physical modification of malt is stopped in the kilning process when hot air is blown through a ca. 1m deep bed of grains [59] p.19. The grain is initially dried in a low temperature air flow. After passing the humid grain the air leaves the bed moist and cooled by the evaporation of water. Once the drying zone reaches the bed's surface the temperature of the air leaving the bed increases and its moisture decreases. At this point the airflow is reduced and the temperature is gradually increased to the required curing temperature, usually 80-100 °C [59] p. 19-20. In the curing mode a progressively larger air stream is recirculated to reduce the energy required for hot air production. Most enzymes are destroyed at the elevated temperatures reached in kilning. In pale malt production when malt is dried a low temperature to a low moisture content some enzymes might survive. In coloured and special malts where the temperature is increased when the grain is still wet enzyme destruction is almost (or might be even) complete [59] p.20. After kilning the moisture content of the malt is reduced from 41-50 % to 3.5-4 % for pale malt and 1.5-2 % for dark malt [90].

Because of the costs of kilning, the use of unkilned malt, or rather, green malt, has been tried. As green malt is not chemically stable, it has to be used as soon as it is produced. Green malt is very rich in enzymes and yields highly fermentable wort with good extract. However, it is said to give beer an unpleasant flavour. Due to this reason and because of its instability, it has been used only seldom. A compromise would be to dry malts at low temperature to 7-8 % moisture. Such material does not seem to give unpleasant flavour and kilning would use less energy and be less cost intensive. *"Despite these advantages such malt is apparently not in use"* [59] p.29.

4.3.1.2 Mashing Chemistry

The main aim of mashing is to convert the carbohydrates in the malt to fermentable sugars, to be later fermented by yeast to ethanol during fermentation. This happens by adding water to the grist, typically 3-4hl/100 kg beer depending whether dark or pale beers are produced [90] p. 198 and heating this mash in a certain time-temperature programme. 91-92 % of the solids in the wort are said to be carbohydrates, mainly sugars and dextrins [59] p.89, [114, 162]. The carbohydrates present in malt include mainly starch (~ 85 %) and free sugars (mainly sucrose) [59] p.125, [89]. The conversion of starch granules is one of the most important steps because of the abundance of starch in malt.

Starch consists mainly of amylose and amylopectin (also some protein, lipids and ash are present in starch), both being polysaccharides with long chains of glucose monomers. In amylose the monomers are linearly bound together (over α -1,4-linkages), whereas in amylopectin the chains are branched (α -1,4-linkages and α -1,6-linkages) [59] p.130.

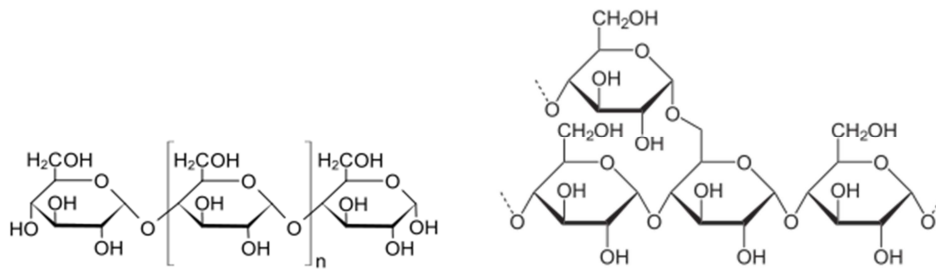


Figure 4-21: Amylose (left) and Amylopectin (right)

In order to enable a relatively fast enzymatic attack to break down amylose and amylopectin, the starch granules need to be gelatinized. Gelatinization means dissolution of the starch granules, when starch is hydrolysed in the presence of water and heat. Gelatinization temperatures vary depending on the starch type and the amount of water present. For typical starch present in barley malt the gelatinization temperature is in the range of 60-67 °C [59] p. 40, [67, 132] (61,2 °C for barley). For smaller granules the gelatinization temperature might be higher, with values given from 51-92 °C. Studies on starch gelatinization suggest that gelatinization already starts at low temperatures and is not a sudden transition [171]. Below gelatinization temperature starch can also be broken down however the process runs much slower [59] p. 109, [132]. Gelatinization temperature is a characteristic of the starch and its origin and is not influenced by the degree of gelatinization. On the other hand, the degree of gelatinization has a large influence on its degradation [132]. Gelatinization enthalpy for barley is in the range of 14,1-15,9 J/g starch studied for raw material and isolated granules respectively [132].

The enzymes active in starch degradation are a mixture of several enzymes, which are together called diastase [59] p. 131. In diastase, the enzymes mainly responsible for starch depolymerisation are α - and β -amylases. α -Amylase breaks the α -1,4-linkages of amylose and amylopectin and releases oligosaccharides, sugars (glucose and maltose) and dextrans. Linkages at chain ends are broken less intensively by α -amylase and the enzymatic attack stops near the α -1,6-branch points [59] p. 131, [49]. β -Amylase breaks the α -1,4-linkages of dextrans (which have been released by α -amylase) and releases glucose and mainly maltose, but also limit-dextrans which will not be broken down further, because the activity of β -amylase also stops near the α -1,6-branch points [59] p. 133-135.

Furthermore, a debranching enzyme (limit dextrinase) is active, responsible for breaking down the α -1,6-linkages and releasing amylose and other products (maltose, maltotriose) without α -1,6-linkages from branched oligosaccharides. Glucosidase is also active during mashing, an enzyme which mainly produces glucose and maltose from maltose, maltotriose, isomaltose and dextrans. The glucosidase can hydrolyse native starch and act synergistically to α -amylase. However, in comparison to the other three enzymes of the diastase the glucosidase has been not as extensively investigated [37].

The degradation of starch is thus a combined action of several enzymes acting simultaneously. For enzymes, as selective biological catalysts, the environment is decisive for its activity [126]. Often the enzymatic activity is inhibited due to enzyme destruction rather than the lack of substrate [59] p. 134-135. One important aspect in enzyme destruction is temperature, as enzymes, just as all proteins, are all sensitive to heat [126]. Of the enzymes in diastase α -amylase is most resistant to heat with a temperature optimum at 65-70 °C [59] p. 77. β -amylase has a temperature optimum in the range of 55 °C [145]. Similar or even better thermostability is attributed to limit-dextrinase [59]. Glucosidase is

very sensitive to temperature with the highest activity at 40-45 °C [59] p. 163, [146] and its activity is therefore not relevant in mash procedures which begin close to gelatinization temperature [161].

Enzyme activity is often stated as diastatic power (DP) which describes the activity of α - and β -amylases, limit dextrinase and glucosidase collectively. This standard measure on which brewers mainly rely in terms of enzyme activity [126] measures the amount of starch liquefied by the diastase present in 1g of enzyme preparation [214]. The activity of β -amylase can be correlated well with diastatic power (DP) [69, 110, 127, 133], according to the equation [178]

$$DP [WK] = 0.365 \times Act_{\beta - Amylase} [U/g] + 65.7$$

Malt analysis according to EBC includes the measurement of α -amylase activity in ASBC units [23]. ASBC units are correlated to Ceralpha Units (CU) according to [1]

$$Act_{\alpha - Amylase} [U/g] = 0.23 \times CU + 0.61$$

Due to the fact that only β -amylase is well correlated to diastatic power, a more transparent analysis has been proposed to measure the single activities of α -amylase, β -amylase and limit dextrinase in combination with β -amylase thermostability in order to better predict the fermentability of different malt samples [68-70].

Influencing factors in mash processing:

Generally, all catalytic reaction rates can be increased with increasing temperature, however higher temperatures also increase the rate of enzyme deactivation as was shown above. All enzymes are heat labile, α -amylase being the most heat resistant up to temperatures of > 70 °C. β -Amylase is heat sensitive and begins to reduce its activity at lower temperatures which also holds true for limit dextrinase and glucosidase. Because of the close linkage of temperature and enzymatic activity, the rests in a mashing program are chosen to optimize certain reactions. Low temperature rests are needed when breakdown of proteins and β -glucans are needed which is the case in under-modified malts. The rests at 65 °C should maximise starch conversion and the production of fermentable sugars [59]. It is important to note that extract recovery can be high when high mash temperatures are chosen (e.g. 80°C), however because of the limited activity of β -amylase the fermentability is low, which means many un-fermentable dextrans have been produced, but little fermentable sugars such as maltose have been produced.

The influence of heating rates has not been studied extensively in literature. Tse and co-workers [199] analysed the effects of heating rates on viscosity while analysing the effects of agitation in mashing. High heating rates showed a sharp peak in mash viscosity, which was explained by the fact that gelatinization of starch leads to viscosity peak at fast heating rates. High heating rates gelatinize more starch to large polymers, but enzymatic reaction is slower. At lower heating rates (0.5-1 K/min) enzymatic processes seem to predominate according to their findings.

The influencing factors of enzyme activity are, however, not limited to temperature only, but also include [59]:

- **Inhibition by products from enzymatic activity** (e.g. proteins, sugars, reduced availability of water)
- **pH**
- **finest of grist**

Kühbeck and his colleagues [119] found a trend towards lower β -glucan values for fine grist (hammer milling). First the β -glucan is released faster in fine grist and the glucanase is not able to rapidly degrade it, leading to higher β -glucan concentrations. In this stage the enzyme concentration is the limiting factor for the degradation and degradation lags behind the release of β -glucan. However, at higher temperatures when the glucanase becomes inactive, less β -glucan is left to be released, so in absolute figures lower final β -glucan levels can be expected.

For FAN concentrations it was found that finer grist leads to a more intensive proteolysis and the FAN concentrations are higher after mashing in (30 mg/100 ml vs. ~18 mg/100ml). However, for coarse grist comparable levels are reached after some time (~28 mg/100ml after ~40 min [temperature increase from 45-62 °C after ~30 min with 1 °C/min heating rate]), so it can be concluded that longer mash stands can compensate the slower proteolysis in coarse grist [119].

Variations of milling procedures did not have an effect on extract recovery according to these authors. Additional studies suggest that using very fine grist accelerates the mashing process and higher extract yields are obtained [59, 126] p. 129.

- **presence of water (gravity)**

The influence of mash thickness or gravity is controversial in literature, however the studies may differ in the liquor to grist ratios which are applied.

According to Tse et al. [199] the reaction rates catalysed by α - and β -amylases are following a Michaelis Menten model, meaning that limitations to the reaction rate come from a lack of substrate or from a lack of enzyme. They found that in high gravity mashing (mash to liquor ratio of 1:3 or 1:2,5) the enzymes are at all times saturated with substrate and no mass transfer limitations need to be overcome, so it can be concluded that high gravity mashing does not have a negative impact. In fact, the authors found larger maltose concentrations in higher concentrated mashes. The limiting factor in mashing appeared to be enzyme saturation. However, taking into account the dilution effect, the results show that in concentrated mash (1:3) 467 g maltose were released per kg mash whereas in the thin mash (1:5) 600 g maltose per kg mash. (This would support Briggs and colleagues that in high concentrated mashes the amylase is inhibited).

According to the studies compiled by Briggs and co-workers [59] it has to be noted that mash thickness has a considerable effect on mashing when very concentrated mashes are produced. Mashes with a very low liquor/grist ratio (liquor/grist ratio of <2 ml/g) can have reduced extract recoveries, slower starch degradation, higher amounts of total soluble nitrogen (TSN) and FAN etc. Enzyme stability is enhanced in concentrated mashes, so at *high temperatures* concentrated mashes can give higher fermentability. At *normal mash temperatures* a weaker mash (with higher liquor-to-grist ratio) seems to give higher fermentable worts, as high concentrations of sugars and dextrins can act as inhibitors to amylase activity. In general the fermentability of mashes is lower when mashing is done at higher temperatures, due to the inactivation of β -amylase.

Kühbeck et al. [119] studied the effect of extract concentration in upward and isothermal mashing for mash concentrations of 1:4 and 1:5. In these range of concentrations the difference in extract found was only due to dilution. The same was true for FAN values of the mashes and β -glucan levels.

- **Type of malt**

Malt modification is an important factor, as poorly modified malt will release much more β -glucan than well modified malt [119].

- **Duration of mash stands**

For a temperature programmed mashing process (45 °C, 62 °C, 70 °C, heating rate 1 °C/min) mash stands of 20 min seem to be enough for reaching desired FAN concentrations of ~ 30 mg/100ml. Longer stands reached slightly higher values of 32-35 mg/100 ml in the studies of Kühbeck and his colleagues [119]. For poorly modified malts desired FAN concentrations could not be reached even after elongated mash stands, so longer mash stands can only partly compensate low mash quality. The same temperature programmed mashing showed that when using poorly modified malt β -glucan levels increased when longer mash stands were applied. For well modified malt mash stand duration had no significant influence and β -glucan concentrations stayed very low. For extract recovery the same authors could show that the process is mainly dependent on when a temperature of 57 °C was reached, independent on mash stand duration. Even shortest mash stands of 20 min reached a maximum extract yield [119].

Evaluation of mash quality:

The parameters indicating mash quality can be grouped into three main groups: cytolytic parameters, amylolytic parameters and proteolytic parameters. Important parameters for each group have been listed and described by Dickel in his work [62]:

Cytolytic parameters: viscosity, friability, Carlsberg Test, β -glucan

Proteolytic parameters: raw protein content, soluble nitrogen, free amino nitrogen (FAN)

Amylolytic parameters: extract, diastatic power, α -amylase activity, final attenuation, photometric iodine test

The importance of these analysis groups is shown by the discussion of one parameter per group:

- **FAN (Free Amino Nitrogen):** FAN levels (measure for amino acids necessary for yeast metabolism) are important to enable good yeast growth and therefore rapid fermentation. The total nitrogen content is also important for the foam characteristics in beer [59] p. 148. The FAN levels are related to the proteolysis in the mash, the degradation of proteins. Desired values are in the range of 300-350 mg/l [119], with lowest acceptable values of 100-140mg/l [59] p. 148. FAN levels are influenced by malt modification, fineness of grist and mashing temperature (activity of proteolysis highest at around 50 °C). Generally, low temperature rest increase FAN levels, as well as finer grist which causes a more intensive proteolysis [119]. However, studies have found that overall mashing parameters (temperature, grist fineness) only influence FAN levels to a minor extent compared to malt modification [119].
- **β -glucan:** As mentioned previously (see 4.3.1.1) low β -glucan levels are desired, as β -glucan is associated with slow wort separation, slow filtration and high wort viscosity. β -glucan is released from malt and needs to be degraded by the action of β -glucanase which is very heat labile and therefore active only at low temperatures (<50 °C). However, malt modification reduces the amount of β -glucan release to such an extent, that duration of low temperature mash stands

does not influence the β -glucan levels anymore and these stands are no longer necessary. Well modified malt gives low β -glucan levels, regardless of the temperature profile applied [119].

- Fermentable extract: Extract gained from starch hydrolysis in mashing is not completely fermentable. Fermentable carbohydrates formed in mashing are glucose, maltose, maltotriose, fructose and sucrose. Dextrins are the major group of non-fermentable carbohydrates [59] p. 124-127. Extract is mainly produced by the activity of amylases. To produce a high fermentability the activity of β -amylase is important, which is a major contributor of dextrin degradation to fermentable sugars [59] p. 136-138. 64-77 % of extract are commonly fermentable [59] p. 127.

Modelling of the mashing process:

Several researchers have been studying kinetic models for the mashing process. In addition to some well-known studies for starch degradation and sugar formation of Marc and Engasser [136], Koljonen and colleagues [114] and Brandam and co-workers [44], stochastic models have been proposed [39] and fast assessment models have been elaborated for high temperature mashes [145].

Marc and Engasser developed a kinetic model for starch hydrolysis and production of fermentable sugars in 1983 [136]. The reaction pathways described in this model are also recorded in more recent books and studies [59, 114]. Marc and Engasser's model embraces the following points:

- The gelatinization of starch is seen as an instantaneous process, which alters the kinetic hydrolysis constants of α -amylase for dextrin production before/after the gelatinization temperature.
- Dissolution of carbohydrates already present in the malt, occurring in the first minutes of the mashing process, is modelled as zero order reaction.
- The dissolution of α - and β -amylase from malt is influenced by the transport coefficient and the concentration difference between enzyme in the malt and enzyme in the liquid.
- α -amylase is active to produce dextrins and maltotriose, modelled as first order reaction.
- β -amylase is responsible for further converting the dextrins released by α -amylase to glucose, maltose, maltotriose and limit dextrins. The reactions are modelled as first order reaction, however the formation of maltose from dextrins is modelled as Michaelis Menton reaction.
- Sucrose hydrolysis to glucose and fructose by invertase is modelled as first order reaction below 55 °C (assuming invertase to be completely denatured above this temperature).
- Enzyme denaturation is modelled as first order reaction.
- All enzyme hydrolysis reactions as well as enzyme denaturation are influenced by temperature over Arrhenius relationships.

Koljonen and co-workers developed a very similar model, however neglecting the dissolution rate of carbohydrates already present in the malt, but rather assuming a sudden dissolution. Gelatinization, however, is modelled as a continuous process between two temperatures. No production of maltotriose by dextrins is described [114]. The model was applied for dynamic optimization studies and new model parameters have been developed [66, 67]

Both models allow modelling the mashing process at different temperature levels and different stand durations. The effects of finest of the grist and gravity are not analysed. Glucan hydrolysis was not taken into account in either of the two models above, however it is presented by Kettunen [111] and re-visited by Durand and co-workers [67].

Brandam et al. [44] developed a model for the hydrolysis of starch during mashes which requires malt specification and temperature profile of the mashing process to predict enzyme activity and dextrin and fermentable carbohydrate formation. The reaction scheme that forms the basis of the model differs from other authors in that favours α -amylase as the key enzyme for the formation of maltotriose, glucose and dextrans; maltose is formed by the action of both α - and β -amylase. Enzymes act only on gelatinized starch. Gelatinization is modelled as first order reaction, however with different activation energies depending on whether it occurs above or below the threshold temperature for starch gelatinization (60 °C for the malt used in their studies). The difference in gelatinisation of amorphous and crystalline starch is seen as reason for this discontinuity.

Enzyme activity is modelled by taking into account temperature denaturation and increasing enzymatic activity over temperature effect. Denaturation is modelled as first order reaction, whereas the temperature dependent activity of the enzymes is modelled by polynomial laws (two different laws for α - and β -amylase depending on the temperature range). In contrast to Muller [145] the relative specific activity of β -amylase reduces linearly at higher temperatures.

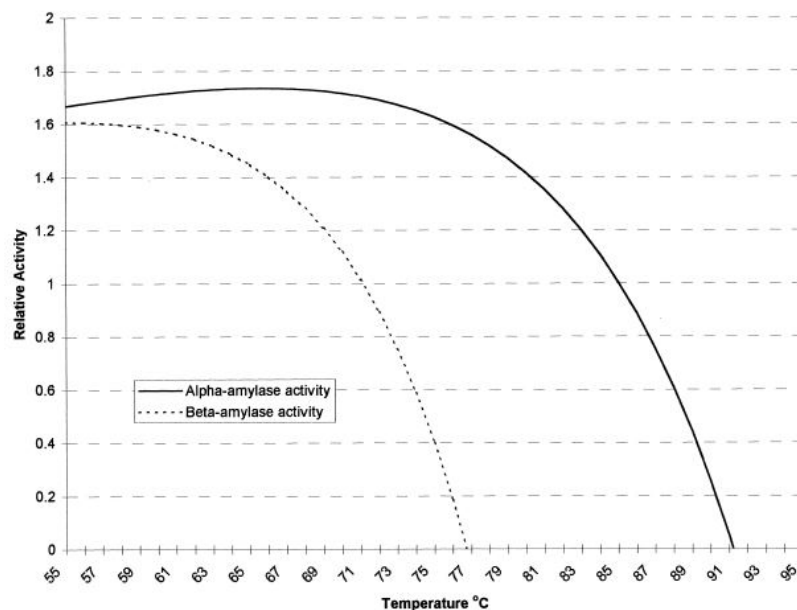


Figure 4-22: Relative activity of amylases activity as a function of temperature acc. to [145]

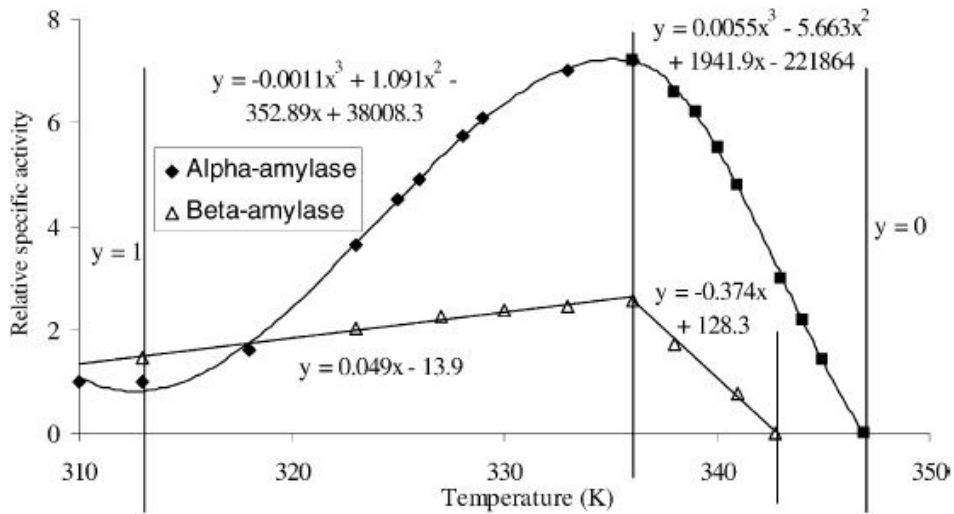
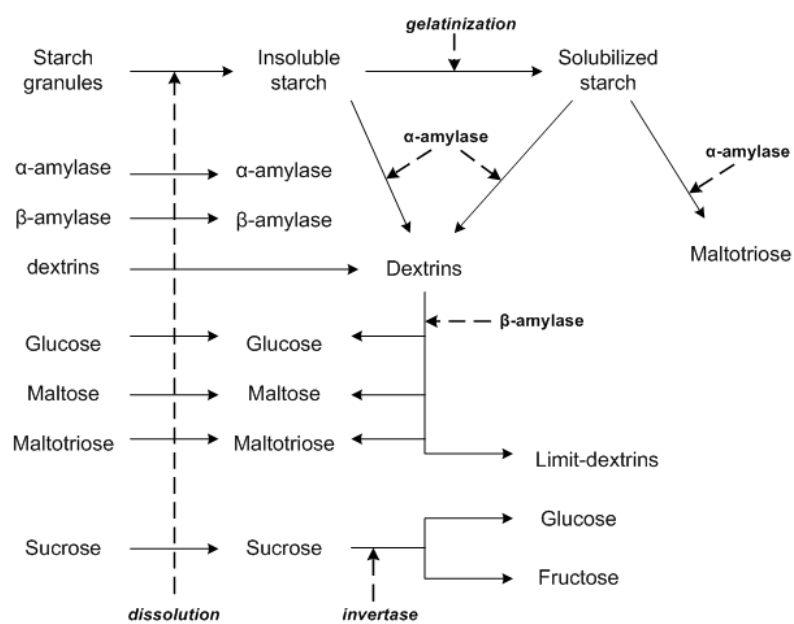


Figure 4-23: Polynomials describing the specific activity of amylases during mashing acc. to [44]

Starch and dextrin hydrolysis is modelled as second order reaction, depending on the substrate and the enzymatic activity. The influence of temperature on the reaction rates of starch and dextrin hydrolysis and carbohydrate formation is not modelled by applying Arrhenius law, but is rather only taken into account via the temperature depending enzyme activities (polynomial laws). Input parameters of the model are starch composition (starch concentration and amylase potential) and operating conditions (temperature profile during the process). The model manages to reach the real mashing results with good accuracy, despite the fact that it does not take into account the grain size variation of the starch. Small granules have higher gelatinisation temperatures and the model results therefore show a complete gelatinization of starch in contrast to the experimental results. However, the authors conclude that the effort of considering the effect of grain size is not justified, as the model is only slightly improved.



a)

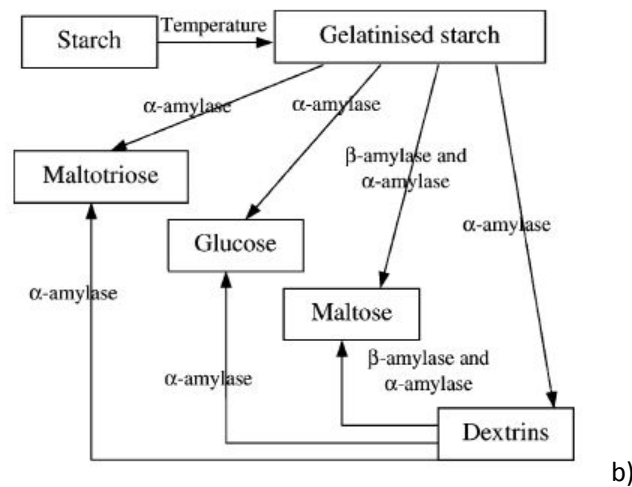


Figure 4-24: Comparison of the hydrolysis schemes a) Marc and Engasser, 1983 [136] b) Brandam et al., 2003 [44]

A significant difference to the early work of Marc and Engasser lies in enzyme dissolution. According to the findings by Brandam et al., “*amylases and initial carbohydrates can be considered immediately dissolved in liquid phase*” [44]. Marc and Engasser modelled enzyme dissolution that takes place in the first 20 minutes during mashing [136].

4.3.1.3 Chemistry in wort boiling

The wort boiling process has a number of objectives which have been summarized and discussed by numerous authors [156, 213], [125] p. 417, [19] p.221, [59] p. 308. The European Brewery Convention has published a “Manual of good practice – Wort Boiling and Clarification” which lists wort boiling objectives as follows [58]:

1. Malt enzyme inactivation
2. Wort sterilization
3. Extraction and isomerization of hop compounds
4. Protein coagulation
5. Formation of protein/polyphenol complexes
6. Formation of flavour and colour complexes
7. Formation of reducing substances
8. Fall in wort pH
9. Evaporation of water for concentration of wort gravity
10. Evaporation of volatile compounds derived from mashing
11. Evaporation of volatile compounds derived from hops.

As most of these functions such as isomerization, enzyme inactivation and sterilization are only affected by temperature and time, only volatile removal and wort concentration require some form of evaporation. The removal of volatile substances however does not necessarily correlate with the evaporation of water, which is of rather low interest to most breweries [19] p. 221. An important aspect

in volatile removal is the state of the liquid wort with which the vapours are in thermodynamic equilibrium. Hertel and colleagues demonstrated the difference in efficiency of volatile removal between open cooking systems and vacuum evaporation systems. In vacuum evaporation the liquid wort is flashed and the amount of vapours formed depends on the system pressure. The vapours are now in chemical equilibrium with the flashed wort at different temperature and pressure which has significant effects on volatile removal [96]. Based on these considerations, the authors show that rectification systems can reach highest volatile removal.

An important volatile derived from malt is dimethylsulphide (DMS). DMS is a product of the thermal degradation of S-methylmethionine (SMM). SMM has a half life of 35 minutes at 100 °C, which increases by a factor 2 with every 6°C decrease in temperature. The level of DMS should stay below 40-60 ppb, below which no negative effects on beer flavour occur. DMS is rapidly lost during evaporation, however SMM continues to break down at high temperatures. It is therefore important to cool the wort down as soon as possible after boiling, so little SMM degrades into DMS that cannot be evaporated [59] p. 335, [126].

There are another few decisive reaction pathways during wort boiling: First, it is the isomerization of hop acids. Hops are added during boiling to achieve a desired bitter taste component, measured in Germany in BE (Bittereinheiten) which is due to the hop bitter acids. The bitter taste primarily comes from the α -acids of hop oils which are extracted during boiling [120] p. 387. During isomerization insoluble α -acids are converted to their soluble forms (iso- α -acids) [156]. The rate of the isomerization reaction is temperature dependant and shows relatively fast kinetics at conventional boiling temperatures. Usually 90% of the wort bitterness can be produced within the first 30 minutes of the boil [156]. Hops can be added in various forms, as natural hops, in form of powders or pellets. Also hop extracts are available. Pre-isomerized hop products have the advantage that the hops do not need to be isomerised during boiling and thus a shorter boiling time is possible. However, they are not allowed when brewing is done according to the German purity law (Reinheitsgebot). The different products vary in their content of hop α -acids and the achievable yield. In general, the yield of bitter compounds is about 30 %, so roughly three times the amount of bitter substances in form of hop α -acids need to be added to the beer to reach the desired amount of bitter units [120] p. 387.

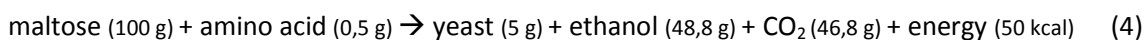
During boiling wort changes in colour due to the Maillard reaction. This non-enzymatic reaction between amines, or amino acids, and carbonyl compounds is an important and well-studied reaction during the brewing processes. It occurs partly during malting and continues during boiling. While certain colour formation is wanted, an over-production of decomposition products from the Maillard reaction is not desirable. HMF (5-hydroxymethylfurfural) is one substance formed from the Amadori compounds of the Maillard reaction that can lead to stale beer flavour [59] p. 327-329.

Another important function of wort boiling is protein coagulation. During boiling the pH of wort drops by 0.1-0.2 units due to the addition of hop acids, the formation of acidic Maillard products. The pH of wort, that drops 0.1-0.2 units during boiling due to the addition of hop acids or the formation of Maillard products, influences protein coagulation. Proteins denature at high temperature, become insoluble and coagulate. The precipitated material is referred to as hot break or hot trub. The importance of protein coagulation is due to the possible negative effects of these high molecular substances in fermentation, where they might affect the accessibility of yeast to the medium by membrane blocking. Proteins which survive into the final beer can lead to clarification problems and affect taste [59] p. 325-326.

4.3.1.4 Basics of Fermentation

The most important route of the yeast metabolism is the conversion of fermentable sugars to alcohol and carbon dioxide under anaerobic conditions. The yeast metabolism is quite complex and depends on various factors such as yeast strain and initial cell number, initial wort gravity and composition, temperature, pressure and initial oxygen concentration. In the presence of too much oxygen further oxidation reactions occur and water and CO₂ are left as main products. Therefore the initial concentration of oxygen is highly important, to provide just enough oxygen to enable the yeast to synthesis necessary membrane components such as unsaturated fatty acids or sterols.

Basically, the biochemical equation of beer fermentation can be stated in the following simplified way [35]:



Similarly, this relation is defined within the Balling Formula [120] p. 913.

Of course a variety of other products, which are especially important for the flavor of the beer, are also generated during fermentation, however they are less decisive when it comes to model the cooling requirement during fermentation.

For beer fermentation it is important to know the initial concentration of fermentable sugars in the wort, as these are converted by the yeast to alcohol and carbon dioxide as main products. Wort gravity is traditionally measured in °Plato. 1 °Plato is equivalent to 1 g sucrose/100 g water. Therefore lager wort with a specific gravity of 12 °Plato (equivalent to a gravity of 1046 kg/m³) contains approximately 12.6 g extract/100 ml wort. Approximately 75 % of these sugars will be fermentable and are actually converted to ethanol [59] p. 102-114. During fermentation, cooling needs to be applied to make up for the heat generated in the exothermic processes. The heat released can be assessed as difference of internal energy of glucose (2880 kJ/mole glucose) and alcohol (2620 kJ/mole glucose). A certain amount of the energy difference is stored by the yeast as 2 ATPs (61 kJ/mole) [59]. The heat of reaction is therefore roughly 100 kJ/mole glucose (556 kJ/kg extract).

DMS levels can be influenced during fermentation as yeast strains are (to varying extent) capable to reduce DMSO to DMS. This reaction is positively influenced by low temperature, nitrogen limitation, higher pH and higher gravity. Depending on the shape of the vessel, the formed DMS can be efficiently volatilized with the produced CO₂ [126] p. 127.

4.3.2 Technologies and upcoming trends in brewing

Brewing beer is an old tradition and many breweries rely on traditional beer production technologies. In the last years, however, there have been several innovative approaches to wort production and some of the most important technological trends are outlined below. Packaging technologies are only briefly described as they are not focus of this study and filtration techniques are not included in this review. Design guidelines of plant technologies for various technologies are available in standard literature and have been published as doctoral thesis [207].

4.3.2.1 Mashing

In mashing one can basically differ between infusion and decoction mashing. In decoction mashing typically a part of the mash is transferred to a separate vessel and is cooked (decoction mash). The remaining main mash rests or undergoes gradual heating. Mixing the decoction mash with the main mash increases the temperature of the whole mashing system. Decoction mashing often operates with 1-2 decoction mashes [59] p. 93. Mashing with a three mash decoction procedure may be applied in case malt is not well-modified and mashing in occurs at low temperatures [59] p. 93. Decoction mashes are heated slightly below boiling temperature with some intermediate rests [90] p. 198. Figure 4-25 shows a possible temperature-time diagram in decoction mashing. The main mash undergoes saccharification rests similar to infusion mashing. Typically, decoction mashing requires 20-50% more energy than infusion mashing, with a typical value for single decoction mashing at 11 MJ/hl [59] p.203.

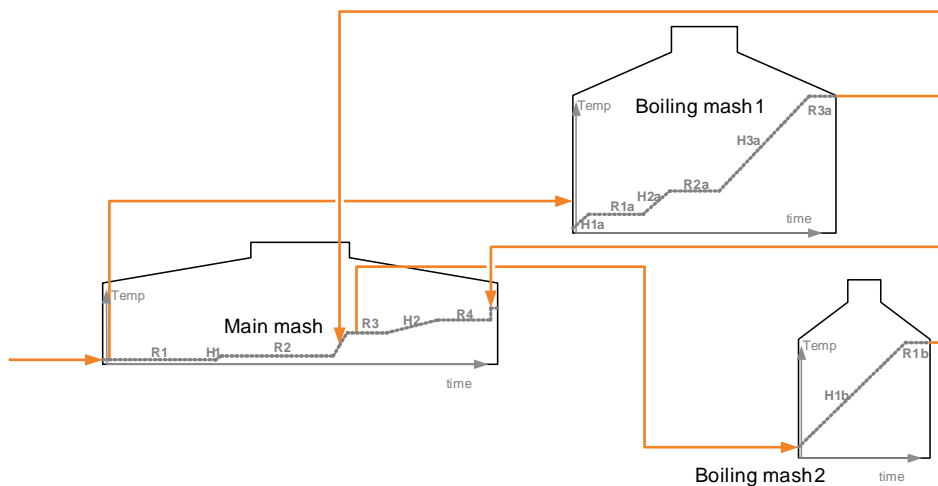


Figure 4-25: Example of a decoction procedure with 2 decoction mashes

In infusion mashing the whole mash system is treated in one vessel. Figure 4-26 shows a traditional temperature profile of a temperature-programmed infusion mash (temperature profile A) [59] p. 110. The first rest at around 50-55 °C is dedicated to proteolysis. In case well modified malt is used in mashing, mashing-in can be performed at higher temperatures if the malt quality does not require high proteolytic activity in mashing. Saccharification rests at around 65 °C and enables starch conversion and ensures the production of sugars to reach fermentable wort. In most infusion programs two rests are performed for efficient amylase activity, one at 60-65 °C to allow the heat labile β -glucanase to react, while a second rest at 72 °C gives opportunity for some final α -amylases [59]. In current literature, only very few alternative mash programs report a single saccharification rest (see temperature profile B) [59] p. 125. In both temperature profiles A and B saccharification rest(s) last(s) for 60-65 minutes. A final rest stops enzyme reactions and reduces the viscosity to aid filtration [19]. Optimization of mashing procedures based on dynamic simulations have suggested longer expositions of the mash at lower temperatures at the expense of stand times at higher temperatures favors minimal polysaccharide concentration in the mash [67]. Kühbeck and co-workers have shown that variations of mash stands

between 20-40 minutes for mash stands at 45, 60 and 70 °C do not show significant qualitative effects for well modified malt [119].

In both mashing techniques one or several stirred tanks are applied for the mashing process. The vessel is heated from the outside with welded steam coils, in the past double walls have been used [59] p. 203. Heating zones are mounted at the base and on the side of the vessel [59] p. 203. A large impeller ensures a well mixed environment. It is important to mix the mash gently and to avoid shear which may break particles and lead to negative effects in filtration. Maximum tip-speed of 3.8 m/s is advised. Modern mixers manage to mix the mash efficiently, which ensures high heat transfer by sweeping the mash over the heat exchange surfaces [59] p. 203-204. Heating rates have traditionally been around 1 K/min [59] p. 96 and have been applied as such in studies on mashing parameters [119]. More recently this policy changed slightly and lower heating rates have been successfully employed. In some breweries heating rates are also lower in practice in comparison to their initial design. Heat transfer plates have also been developed (see 4.2.4) which enable high heat transfer coefficients thus allowing for lower temperature gradients in heating. This fact enables heating the mash tun with low temperature heat sources. When maintaining traditional heating rates large heat transfer areas are required which make a complex retrofit necessary. The required heat transfer area can obviously be reduced with lower heating rates in mashing. An alternative to heating the mash via indirect heat transfer is heating infusion mashes via steam injection. Steam injection can assist in mixing the mash and induces no risks of fouling but requires high purity steam and care to inhibit local overheating [59] p. 203.

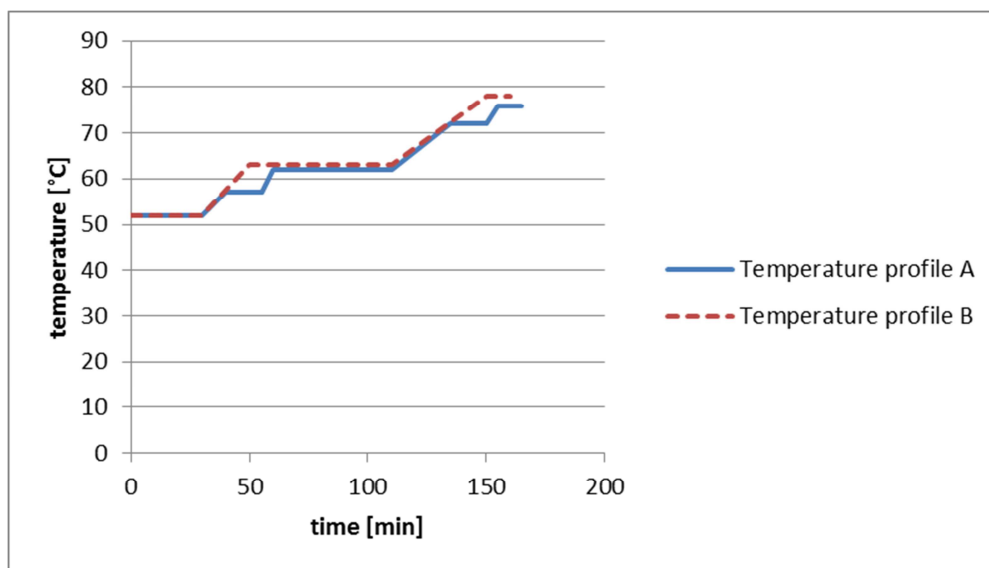


Figure 4-26: Temperature profiles in temperature programmed infusion mashes

4.3.2.2 Mash separation

The classical brewing equipment includes a lauter tun for mash separation. The lauter tun is a large vessel with a low height to diameter ratio [19]. It consists of a false bottom on top of the real bottom. The mash is introduced gently to minimize shear, splashing and oxidation. Within the lauter tun the husks settle on the false bottom, while the clear wort filters through and is collected via various pipes from the real bottom [19]. Knives, of which various types are available [59] p. 208, are installed which can cut through the filter bed to ensure a good permeability of the bed [19]. Lauter tuns require long

stand-times of typically 3 hours [19]. For the first minutes wort is usually re-circulated until the filter bed layer is dense enough and clear wort is drained and collection is started. Various rinses drain out the extract from the spent grains [59] p. 211. A typical profile of rinses during lautering is shown in Figure 4-27. Wort collection is stopped once the extract of the wort has fallen to a defined value. Finally spent grains are withdrawn. Some breweries use the liquid from the washing and drainings, which still contain low values of poorly fermentable extract, for the subsequent mash [59] p. 212. The operation of lautering is fully automated with continuous improvement.

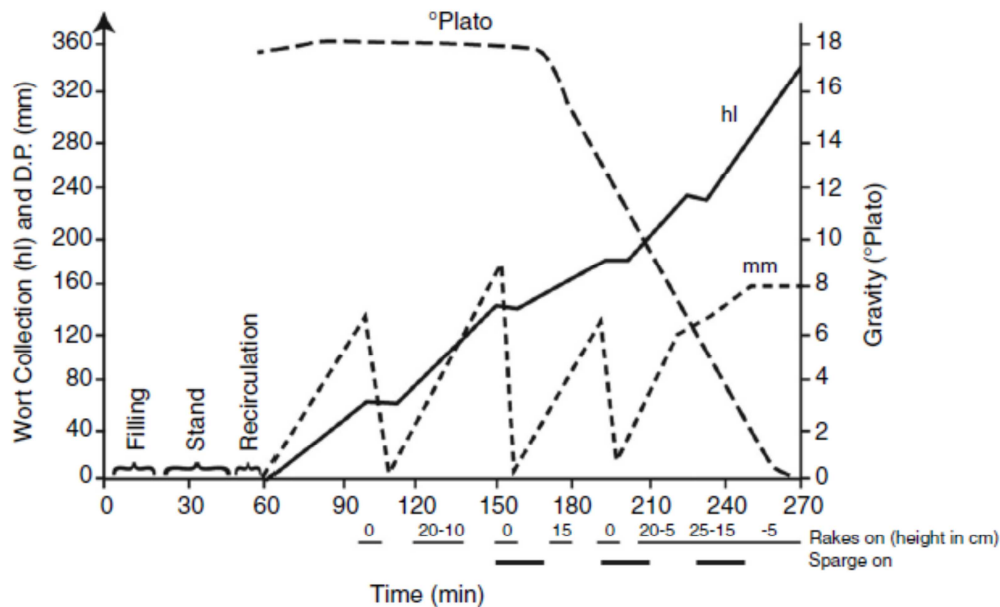


Figure 4-27: Profile of wort collection and rinses during lautering [125]

An alternative to lautering is mash filtration where husks and wort are separated by filter cloths. Mash filtration enables shorter cycle times (105 minutes) and allows for 14 cycles per day, however is less flexible to different loadings [19]. The chamber filter consists of various chambers which are each equipped with one membrane and one filter cloth. The mash enters from below and the clear wort is withdrawn through the rapidly increasing filter bed and the cloth. The membranes are then inflated with air, so the filter cake is pressed against the cloth and strong wort can be withdrawn. After deflation, sparging liquor enters through the mash ports, and the filtration and inflation cycle starts over. At the end, the chambers open and the spent grains fall onto a conveyor with which they are withdrawn. Usually mash filters are used with very finely ground grist [19] p. 219-220. Mash filters are perfectly suitable for high gravity brewing, because only little sparging water is necessary [90]. The Belgian plant engineering company Meura has recently refined their well known Meura 2001 filter with optimized design of the filter chambers [11].

The increasing efficiency of modern lautering and mash filters has outdated the Strainmaster technology, which is still in place in several breweries for mash separation as a simple and rather fast separation technique. The vessel of a Strainmaster is rectangular with a conical shape at the bottom where perforated sieve pipes are arranged. Spent grains have to be wet when they are withdrawn which is the main reason that lower extract yields are achieved with Strainmasters [90] p. 199.

4.3.2.3 Wort boiling

Wort boiling is one of the core processes in brewing. The classic technology is a stirred tank heated via steam coils at the bottom and at the side. In the past, Wort boiling was the most energy intensive unit operation in brewing, because traditionally evaporation rates were around 8-10% per hour [90, 157]. Modern wort boiling techniques produce high quality wort with 2-5% evaporation rate depending on the technology as has been shown and summarized by numerous authors, such as [20, 98, 104, 141, 157]. Technological differences in wort boiling embrace different placement of heat exchangers (inside vs. outside), differences in wort flow (natural vs. forced circulation), pressure and temperature profile during wort treatment. Comparisons of different technologies are available in several studies and articles [104, 107, 141, 157, 213].

Decisive parameters in heating the wort are the temperature of the heating surfaces, which may lead to fouling and heat stress, and the homogenous mixing of the wort to achieve a vigor boiling without mechanical stress [107, 157], [59] p.339. Internal boilers are realized as tube bundles in the center of the wort kettle, and the wort circulates via natural convection. Over the last decades internal boilers have been designed with low heating gradients and efficient mixing behaviour [88]. Achieving steady operation of internal boilers without forced wort flow is a challenge to the operators. The disadvantage of pulsation of wort flow can be overcome by realising the wort flow with a small pump [107]. Wort spreaders are often in use to allow a homogenous mixing. It has also been shown that submerged flow of wort after exiting the internal boiler leads to enhanced wort quality [29]. External boilers are placed outside the wort kettle and wort is continuously withdrawn to be heated and re-enters the kettle with a temperature around 103-105 °C [59] p. 341. External heaters are usually designed as shell and tube heat exchangers with the wort passing through the tubes (3-4 circulations per hour) or as plate heat exchangers (7-10 circulations per hour) [125] p. 424. External boilers may be heated with lower steam pressures due to their larger heating surfaces. This is an advantage to wort boiling as it leads to a more gentle heating of the wort which has qualitatively positive effects and reducing cleaning requirements [107], [19] p. 223. Another advantage of external heaters is that they may be used for wort preheating as soon as wort enters the kettle [125] p. 424.

Some of the modern wort boiling variations of boiling at normal or light overpressure with internal or external boiler include dynamic low pressure boiling, high temperature wort boiling and rectification. Boiling at slightly elevated pressures has the advantage of reducing boiling time by roughly 20 % in comparison to unpressurized systems [59] p. 344, [107].

Dynamic low pressure boiling is usually realised with internal heat exchangers. During boiling the pressure is alternated. After a phase of slight overpressure the pressure is released and evaporation occurs. Such pressure changes are performed six times per hour, leading to enhanced evaporation of volatiles in comparison to conventional low pressure boiling at around 1.1-1.2 bar. Evaporation rates are in the range of 4-5 % [88]. In case an internal boiler without forced wort flow is used for dynamic low pressure boiling, care has to be taken to avoid reduced stripping behaviour and increased fouling which may occur due to unideal flow behaviour [107].

Very high evaporation efficiency for boiling with internal or external boilers can be achieved via rectification systems [95, 98]. To overcome the limitations in evaporation efficiency a rectification column is connected to the wort kettle through which wort vapours pass from below and a side-stream

of wort from the bottom of the kettle enters on top of the column. The concentration difference between the vapours and the wort lead to an efficient mass transfer of volatiles into the vapour stream. Evaporation rates can be reduced to 2-3 % [95, 98]. The system proves to have the highest evaporation efficiency in comparison to other modern boiling technologies [97].

Based on the idea that many of the wort boiling objectives, other than volatile removal and water evaporation, do not require wort evaporation, boiling processes have been developed that separate the boiling process into two steps:

One of these boiling processes is the “Schonkochverfahren”. In the first phase the wort is heated to 97-98 °C and is held at this temperature level. The duration of this rest during which the wort is homogenized was initially 50-70 minutes, but can be reduced to 30-45 minutes [40], [41], [21]. This induces an evaporation of 0.3-1 %. After hot trub separation, the subsequent vacuum stripping at 300 mbar enables efficient evaporation of volatiles. The wort cools down to evaporation temperature (in case of 260 mbar vacuum the wort cools to around 63 °C) during stripping and is further cooled via wort cooling [40, 41]. The hot water produced in the wort cooler after the Schoko process reaches around 60 °C which is still high enough to serve brew water for mashing [41]. Studies have shown that the energy requirement for heating brew water rinses and increased pumping demand for vacuum production are smaller than the thermal energy savings of the boiling process [21].

Vacuum evaporation systems are also propagated as add-on systems to existing wort boiling kettles [107]. It is important to avoid foaming which is too intense (frothing over) to enable efficient volatilisation. For a good thermal energy management, the warm water produced after vapour condensation should be of good use and not be wasted [107]. Qualitatively, aroma compounds are evaporated less efficiently in vacuum evaporation systems, because the vapours are in equilibrium with the liquid wort and not with the incoming feed, as it is the case in conventional boiling systems [96].

Steam strippers are an alternative concept for efficient removal of volatiles [12]. After whirlpool stand the wort enters a stripping column in which steam (0.5-2 %) of the wort volume [125] p. 428 is driven counter-currently. Column packaging ensure a high mass transfer area and evaporation rates of 1-2 % are sufficient for effective volatilisation [19] p. 241, [125] p. 428. A wort boiling process including steam stripping comprises a holding step of the wort of 30-50 minutes without evaporation, hot trub removal in a whirlpool and finally stripping the wort with maximal 2 % evaporation rate [12].

Similarly, stripping with strip gas, such as N₂, CO₂ or air is possible. Evaporation of the precedent boiling process can be reduced, as volatile removal is performed with high efficiency in the stripper. Regulation of the stripping process is possible via the amount of strip gas used [72].

The Merlin system, which uses a thin film evaporator for boiling, realises heating and boiling the wort via circulation between the whirlpool and the thin film evaporator. After the heating and boiling phase and a whirlpool rest, a stripping phase is performed within the Merlin vessel [59] p.343. However, it has been discovered that oxidation of wort and colour formation might negatively affect beer quality [125] p.427.

Continuous high temperature boiling is another process which relies on the two-step approach of heating and evaporation. In this process, the hot holding period only lasts 150-180 seconds at a temperature of 130-140°C [90], [59] p. 344. At such high temperature the reaction rates of hop isomerization and coagulation of nitrogen compounds is enhanced. Wort is heated in 3 stages to the

target temperature and the vapour energy is recovered to serve parts of this heating process. The wort is evaporated in a separator which is operated at lower pressure [157]. Due to some qualitative problems and high fouling due to the high temperatures, high temperature wort boiling has had limited success so far [59] p. 344.

Two wort boiling technologies that are different from ones mentioned so far in terms of kettle heating, is the combined mash and wort boiling kettle “Triton” and the PDX approach:

The combined mash and wort boiling kettle Triton, developed by Krones, is heated with dimple plates from the side and wort is circulated by a pump over the wort spreader. The wort is heated gently evaporation can be reduced by wort stripping which can be realised within the same vessel. The flexible system is especially designed for small and medium sized breweries [13].

A completely different approach is the PDX heater for wort boiling. In this system the wort is heated via direct steam injection. Next to overcoming fouling problems and avoiding thermal losses in heat transfer, enhanced volatile removal is claimed for the process. A case study shows successful brewing with 30 minutes boiling at 2.5 % evaporation [14].

Other boiling processes at even lower temperatures have thus far only been studied in scientific works. Mezger showed in his thesis that the holding temperature of 90 °C is a lower limit for reaching high quality worts. A new vacuum boiling process was developed based on the Schoko process with holding and evaporation temperature of 90 °C [141].

Heat recovery for boiling vapours

In addition to these technological differences, there are also various approaches to vapour recovery during wort boiling. Mechanical vapour compression is widely implemented. It reduces external energy requirement during boiling to the start-up phase where the wort is heated to boiling temperature and first vapours are being produced. Afterwards the vapours released from the evaporation process are re-compressed over a mechanical compressor and the hot vapours are used to heat the wort in the kettle. Instead of a mechanical pump driving the compression process, thermal vapour compression may be implemented. Here, high pressure steam is injected through an injector nozzle and mixed with the vapours [19] p.242.

Another widely implemented solution for energy recovery is the “energy storage tank”: The heat released by vapour condensation of the vapours released in boiling is stored in a thermal storage tank. The heat is used in the next brew in order to pre-heat the incoming wort prior to boiling. At an evaporation rate of 4.5 % the heat requirement of wort heating is typically balanced [88, 106]. The use of hot water as a heat transfer media for wort preheating has benefits, because in addition to energy recovery the wort can be gently heated which has positive qualitative effects [106]. The energy stored in the storage tank can also be used for other processes [6, 147, 148, 151]. Hot water production is one alternative, however, in a brewery without extensive hot water requirements for packaging and CIP plants, hot water (in addition to hot water produced via wort cooling) is not usually in high demand [151]. Breweries producing hot water from vapour energy with the Schoko process might have an overproduction of hot water depending on the evaporation rate [107].

The energy of the hot wort is usually re-used via wort coolers for brew water production. The idea to recover this heat for other processes, such as preheating incoming wort to boiling is not new [157]. The

use of this energy for wort preheating and mashing is also suggested by heat recovery algorithms such as the pinch analysis [151]. Such heat recovery system is on the market as Equitherm system by the company Krones [81].

Some breweries apply heat recovery from hot wort before the wort enters the whirlpool. In that way wort is cooled below 90 °C and the thermal degradation of SMM to DMS is limited [55].

4.3.2.4 Continuous wort production

Over the past decades continuous wort production has gained more and more attraction. While there are still critical remarks on its benefits [36], the potential of continuous processing to increase quality, limiting energy peaks and reducing equipment size has led to commercial availability of technological solutions [12]. Over the past decades a number of patents have been published on continuous wort processing.

Due to the long extraction process of fermentable extract from malt, a continuous process layout for mashing is a challenge. While solutions based on plug flow reactors have been patented [206], [60], Meura commercially sells a combined system of plug flow reactors and resting tanks to ensure complete enzymatic action [12]. However, so far no true continuous process is implemented for mashing as the applied heating profiles and enzymatic reaction times make tubular reactors very long and cost intensive. Mash filtration is a state-of-the-art continuous process solution for lautering [12]. A series of mini-lauter tuns have also been suggested and patented [60]. Continuous boiling is usually realised with stripping columns [12, 60, 206] or distillation columns [98].

The following (non-exhaustive) list gives an overview of patents for continuous wort production:

- | | |
|------|---|
| 1974 | Method of mashing for the production of wort and the apparatus for the implementation of this process; <i>Moll, Bastin and Peters, France, US Patent No. 3,398,848</i> |
| 1983 | Apparatus for the continuous cooking of wort: preheating, holding tank at high pressure (6 bar, 140°C), subsequent two stage lowering of pressure for evaporation; <i>Kraftanlagen AG, Germany, US Patent No. 4,388,857</i> |
| 1985 | Continuous wort boiling with distillation column, as sweep gas live steam, vapours from boiling or nitrogen or oxygen is used; <i>Holstein und Kappert GmbH, US Patent No. 4,550,029</i> |
| 1992 | Method of hydrolyzing starch to produce saccharified mash (continuous stirred tanks); <i>Vogelbusch GmbH, US Patent No. 5,114,491</i> |
| 1992 | Process for continuous preparation of wort: continuous enzymatic conversion of malt in rotating disc contactor and separation of spent grain; <i>Heineken NL, US Patent No. 5,536,650</i> |
| 2000 | Process for continuous boiling of wort: Continuous wort preparation at atmospheric conditions incl. mashing in plug flow reactors (rotating disc contactor), wort boiling in |

distillation type stripping column with >5 trays, steam being used as stripping medium; *Heineken NL, US Patent No. 6,017,568*

2010 Continuous brewing process: Continuous wort preparation with low temperature energy medium incl. mashing in plug flow reactors (heated/non-heated pipes), lautering with mini lauter tuns wort boiling in column with several heating surfaces; *Krones AG, US Patent No. 2010/0291261*

4.3.2.5 Wort cooling

Wort cooling is usually realized in plate heat exchangers. 1-Stage wort coolers cool down the wort in one heat exchanger with one cooling medium. In most cases this is cold brew water which may have been chilled already depending on the temperature of its availability. Also the “pitching” temperature at which the cold wort is sent to the fermentation cellar is important, as it determines the required temperature of the cooling medium. While water coming from rivers usually doesn’t require cooling, water from deep wells is often too warm to be used without cooling. 2-Stage wort coolers use two cooling media to cool down the wort. This might be sensible if the temperature of a storage tank should be boosted with the energy from the hot wort and cold water is only used for cooling the remaining heat of the wort. Such a system has been implemented for several years in an Austrian brewery [78, 212] and is currently advertised by Krones AG [6].

4.3.2.6 Fermentation and Maturation

Fermentation is commonly realized in chilled fermentation tanks. The process usually lasts 7-10 days. Yeast converts the fermentable sugars in wort to ethanol and CO₂ and produces the flavour compounds of the beer. Heat released in the exothermic fermentation process needs to be dissipated via cooling of the fermentation tanks. At the end of the fermentation process yeast is harvested, cooled and stored to be later used for subsequent fermentations.

A common technology is cylindrical-conical fermentation vessels. These vessels are chilled via cooling jackets on the cylinder walls. In some breweries fermentation vessels are cooled with cooling water (indirect cooling) while in others a cooling agent (e.g. ammonia) is directly evaporated within the cooling jackets (direct cooling) [59] p. 519. Direct cooling has the advantage of direct heat exchange, however the performance of cold production of the whole plant may be low due to losses within the large cooling medium system. The fermentation process itself may be performed as “top fermentation” or “bottom fermentation” depending on the yeast strain used. Top fermented beer is fermented at 12-25 °C and the yeast stays on top of the fermented beer, whereas bottom fermentation is performed at 1-10 °C and used yeast sinks to the bottom of the fermentation vessels [90].

There have been many studies regarding continuous fermentation on immobilized cells and there is ongoing research on the topic. An overview of beer production using immobilized cells is given in [153]. However, in terms of energy demand the large number of parallel batch fermentations can be seen as a continuous process with variable energy demand.

The product from primary fermentation is called ‘green beer’. Green beer subsequently undergoes maturation or lagering. During this process secondary fermentation may occur where remaining yeast uses little amount of remaining carbohydrates in beer. Maturation takes place in closed tanks and

produced CO₂ dissolves in the beer. An important aspect of maturation is the removal of haze-forming materials. This is also referred to as stabilization and increases the shelf life of beer. The maturation process is traditionally a long process for bottom fermented beers, however modern practices allow for accelerated maturation within a few weeks [59] p. 519.

4.3.2.7 Pasteurization

Beer is shipped to the customer either in kegs, or in non-returnable or returnable bottles or cans. Depending on the type of packaging cleaning, pasteurization and filling technologies vary.

Pasteurization technologies are mainly influenced by a few factors including the time of pasteurization, whether the beer is pasteurized before being filled, or whether the filled package is being pasteurized.

Pasteurization prior to filling: Kegged beer, and in many cases also beer bottled in returnable bottles, is usually pasteurized before it is filled. This allows for the use of a flash pasteurizer, a plate heat exchanger with a large heat recovery section in which the incoming beer is heated by the hot beer that has just reached pasteurization temperature. The external energy demand is reduced to heating the beer a few Kelvin, which may be – depending on the efficiency of the heat recovery section, in the range of 2-5 K. The possible heat exchange depends mainly on the reachable temperature difference at the cold end – how far the pasteurized beer can be cooled down prior to filling by the incoming cold beer from the cellar. For kegs the remaining heat demand after heat recovery is very small, as the beer can be cooled down to low temperature before filling it into the kegs. For bottles, filling temperature should not be too low to ensure the bottles do not break due to the fast temperature change after bottle-washing. Typically the beer in flash pasteurizers is being pasteurized for 20 seconds at 75 °C (corresponding to 50 pasteurisation units (PU)) [59] p. 774. An alternative to pasteurization is sterile filtration in which microorganisms are retained via filtration [59] p. 774. Sterile filtration and flash pasteurization is only possible in combination with aseptic filling.

Pasteurization of filled beer: In case beer is filled into the packaging units before, a tunnel pasteurization is used to pasteurize the filled packs. Typically the beer bottles are being pasteurized for 20 minutes at 60°C (corresponding to 20 pasteurisation units (PU)) [59] p. 774. Tunnel pasteurization is by far more energy intensive than flash pasteurization [71, 151]. On the one hand the packaging unit has to be heated as well and additionally heat recovery can only take place indirectly over recirculating water flows.

Novel trends in processing suggest steam injection or non-thermal pasteurization techniques, such as UV or microwave [164].

4.3.2.8 Overview of intensification approaches in brewing

Table 4-4 summarizes the intensification approaches that have been discussed in the chapter above.

Table 4-4: Intensification approaches of selected process steps in brewing

Process step	Intensification
Brew house/fermentation	High gravity brewing
Mashing	Addition of glucanase and pentosanases to complete the cell wall digestion and release starch
Wort separation	Membrane mash filters

	(useful for extract recovery in high gravity brewing)
Wort boiling	Limited evaporation; Stripping/rectification
Wort boiling	Continuous wort boiling
Hop isomerisation	Pre-isomerisation
Oxygenation of wort prior to fermentation	Static mixers/centrifugal mixers
Fermentation	Continuous fermentation on immobilized cells
Dearation for de-oxygenated water	Rotating packed beds
Filtration	Cross flow filtration for main beer filtration
Filtration	Sterile filtration with membranes
CO ₂ addition and deoxygenation [12, 16]	Hydrophobic gas membranes
Pasteurization	Steam injection, UV, Microwave

4.3.3 Modelling energy demand of brewing sites

Brewing is often said to be an energy intensive process [158] with energy costs in the range of 3-8 % of the production costs [8]. A recent survey shows that European breweries consume on average 116.8 MJ/hl total energy, of which 5.3 % currently comes from renewable resources. 9.6 % of the consumed electricity in European breweries is generated over CHP plants [63]. The range of national data between 70.6-243.1 MJ/hl already shows the importance and the potential of energy efficiency in brewing. In economic terms thermal energy costs for German breweries were ranging from 2 to over 10 Euros per hl in 2012 [179]. The specific energy demand of brewing may range from 65-180 MJ/hl thermal energy demand and 6.8-20 kWh/hl electrical energy demand as can be seen from Table 4-5 which summarizes a few figures from various studies. Values for these figures are heavily depending on implemented process technologies and on production capacity. Not only the yearly production capacity is decisive, but also how well real production fits to the existing capacities. Breweries brewing only a few batches per week will remain much more inefficient than breweries aiming at maximising their weekly brewing capacity [122].

Table 4-5: Specific energy consumption figures of breweries

Literature reference	Specific energy demand figures	Production capacity
Global Brewery Survey 2012 [7]	207 MJ/hl (thermal and electrical)	
European Brewery Survey 2010 [63]	116.8 MJ/hl (total direct energy) National data ranges from 70.6-234.1 MJ/hl	
Brauunion Sustainability report [45]	65,8 MJ/hl thermal 6,8 kWh/hl electrical	~ 1 Mio. hl
Article from plant engineers [122]	104-212 MJ/hl thermal	~ 1 Mio. hl, value range for breweries between 5-8,000 hl/week and 17-20,000 hl/week

Natural Resources Canada, Manual for energy efficiency[8]	150 MJ/hl thermal 8-12 kWh/hl electrical	
British brewing industry [2]	146 MJ/hl (thermal and electrical)	
Reference Document on Best Available Techniques in Food, Drink and Milk Industries [16]	118.7 MJ/hl thermal 10.5 kWh/hl electrical	German breweries with > 20 employees, data from 2000
Energy efficiency manual GEA Brewery Systems [87]	90-150 MJ/hl thermal 7-12 kWh/hl electrical	300-500,000 hl/a
Case Studies		
[71]	261.63 MJ/hl, 41 % elect, 59 % thermal	1.7 Mio. hl/a
[194]	205-240 MJ/hl total 160-180 MJ/hl thermal 45-60 MJ/hl electrical	250.000 hl/a
[151]	60 MJ/hl	1 Mio hl/a
[124]	68 MJ/hl thermal 8.5 kWh/hl electrical	

Specific figures for single production steps also vary in literature, as these are also heavily influenced by the technologies applied in the brewhouse and by the packaging units. An extensive overview is given in [87].

There are many recommendations and manuals on how to improve energy efficiency in brewing, such as [8, 10, 80] or [87] and several case studies have been recently published, such as [65, 71, 176, 193, 194, 196, 215]. The available material and the increasing environmental awareness in the sector have led to tremendous savings within the last decades. In the UK, breweries cut energy consumption by 54 % from 1976 - 2006 and reduced CO₂ emissions by 63 % [2].

However, as consumption figures vary widely, there is still the continuing need for improvement, and often especially in the last final steps of obtaining a completely carbon-free production site, a detailed analysis is required. So far there are no tools available dedicated to brewing which allow for analysis of energy efficiency opportunities based on detailed process modelling. While several works have been dedicated to simulating specific production areas (such as fermentation or packaging), no holistic process model for brewing has been developed. The Green Brewery tool [151] was the beginning of this work with an Excel based tool for energy balancing of brewing sites. In the following a short list of available tools linked to energy demand modelling and energy efficiency are listed which are specifically targeted towards breweries:

4.3.3.1 Energy Saver

The Energy Saver Tool is a benchmarking tool developed from Campden BRI and KWA Business Consultants [5]. Based on the production data, energy bills and consumption figures, it allows the user to allocate the energy demand to different processes. In case no measurement data is available it allows

the user to calculate energy demand figures based on installed load, load factor (average load of equipment) and operating hours. Based on this energy balance a benchmark comparison is carried out for specific demand figures of each production unit. Further certain energy saving measures can be selected by the user from a list and the general saving potential is shown for each measure. The Energy Saver is a powerful benchmarking tool and gives fast indication of improvement potential. If not on measurements, the energy balance is however not relying on energy calculations based on temperatures and mass balances and therefore does not take into account technology specific data. As with every benchmarking tool the user can evaluate the performance of unit operations, but the reason for the high consumption cannot be evaluated. Also no variations of energy demand can be evaluated.

4.3.3.2 Einstein

EINSTEIN has been developed in two European projects as a fast energy audit tool for industry and large scale buildings [183]. Based on a process model, the user has the possibility of calculating energy demand figures per process and together with data on overall energy consumption, an energy balance is drawn by the tool. With the definition of process schedules Einstein also allows calculation and visualisation of energy demand variabilities. The tool is aimed to be open to all industry sectors and includes modules to assess design options and saving potential of various renewable energy technologies. Einstein is a powerful tool for evaluating thermal energy management of a production site and its potential towards renewable energies. It is however not dedicated to brewing and does not allow comparison of different brewing technologies.

4.3.3.3 Information system for monitoring and targeting

Production data acquisition systems are used widely in breweries to monitor operating parameters. An example of such a monitoring system has been published for the Brewery Sofia, which shows how data is being metered and allocated to reports and figures for evaluation[24]. The management approach “monitoring and targeting (M&T)” has claimed to allow for 11 % of savings in electricity consumption and 13 % in fuel consumption.

4.3.3.4 Monitoring and forecasting of energy consumption

An interesting approach for monitoring and forecasting of energy consumption has been presented for Foster’s brewery in Yatala, Australia [124]. A real-time utilities consumption model was developed that combines simulation of energy consumption with measured values. In case no meters exist, the real time model allows calculation of energy consumption of certain areas by knowing the overall energy consumption and energy demand figures of other areas. The model seems powerful for the monitoring and forecasting of energy consumption data.

Recently Bai and co-workers have published a methodology to predict energy consumption of the beer brewing process [32]. Their methods include data envelopment analysis, a comparison method used in economics, for analysing and functional neural networks for modelling the energy consumption. Their work promises effective modelling of the energy consumption; however the method seems to be difficult to apply in practice.

4.3.3.5 Modeling and optimizing brewhouses with Batches

An interesting model for optimizing energy demand profiles in brewing has been set up with “Batches”, a software designed to model batch and semi-continuous processes. A model has been designed for four brewhouses of an industrial brewery which can analyse utilization rates of equipment as well as energy demand profiles. The model shows that required production equipment could be potentially reduced by 1/3 without affecting production flexibility and yield. By optimizing production planning and limiting available steam consumption, the analysis also revealed that peak energy demands could be reduced significantly without negative effects on production [142].

The objective of modelling energy demand profiles and analysing the optimization potential is similar to the Brewery Model described in this thesis. The model based on Batches however does not allow for a detailed analysis on energy efficiency measures in single production steps and cannot model heat integration possibilities.

5 METHODOLOGY – THEORETIC PART

In order to evaluate industrial processes for their sustainability in terms of thermal energy efficiency, a two step methodology has been developed. Firstly, a process model for breweries evaluates different technology sets on thermal energy demand and selected qualitative parameters. This model allows for the comparison of technologies for their applicability for energy optimized food production systems. Parametric studies can be performed to evaluate the effects of operating parameters. The tool allows the calculation of variable energy demand profiles over time, as well as variable energy availability profiles. The subsequent analysis of these time dependent profiles can be performed in a newly developed advanced pinch and storage management tool which allows simulation of thermal energy flows in industry and proposes the placement of heat exchangers and storages. Based on the information of remaining energy demand at different temperature levels energy supply systems can be efficiently designed.

The combination of these two approaches gives a holistic methodology to evaluate process systems in the food industry via process models (brewery model) including technological changes and systematic heat integration. The process model is set up for brewing processes only, however the basic principles can be extended to other industry sectors. The pinch analysis tool can be applied for any production process.

5.1 The “Brewery Model”

A “Brewery Model” has been developed on EES (Engineering Equation Solver) to generate a holistic energy balance of a brewing facility. The calculation tool performs thermal energy demand calculations based on user-provided data. Further time-variable energy demand per process as a basis for subsequent pinch analysis can be calculated. Visio flowsheets are used for visualization of basic brewing flowsheets in EES where data can be entered. Various technologies can be chosen for mashing, boiling, wort cooling and packaging, including different heat integration options. Energy and mass balances are performed in order to calculate energy flows of each product stream. Results are presented in energy per hectolitre of brewed beer (for brewhouse and fermentation cellar) or packaged beer (for the packaging area). Parametric studies allow the comparison of different technology sets and/or production parameters. The model has been established based on the experience of energy auditing in various international brewing sites and is thus applicable to various breweries with different site specifications.

5.1.1 Model structure

The Brewery Model is structured based on a brewing flowsheet with three main sections: The main brewhouse section comprises all process steps until the cold wort is sent to the fermentation cellar. Fermentation and filtration is then considered in a separate section and finally packaging constitutes the last section of the model. Additionally the water management and energy management sections give an overview of water and energy flows on site. The main page of the model (see Figure 5-1) only shows selected result figures and allows no data entry.

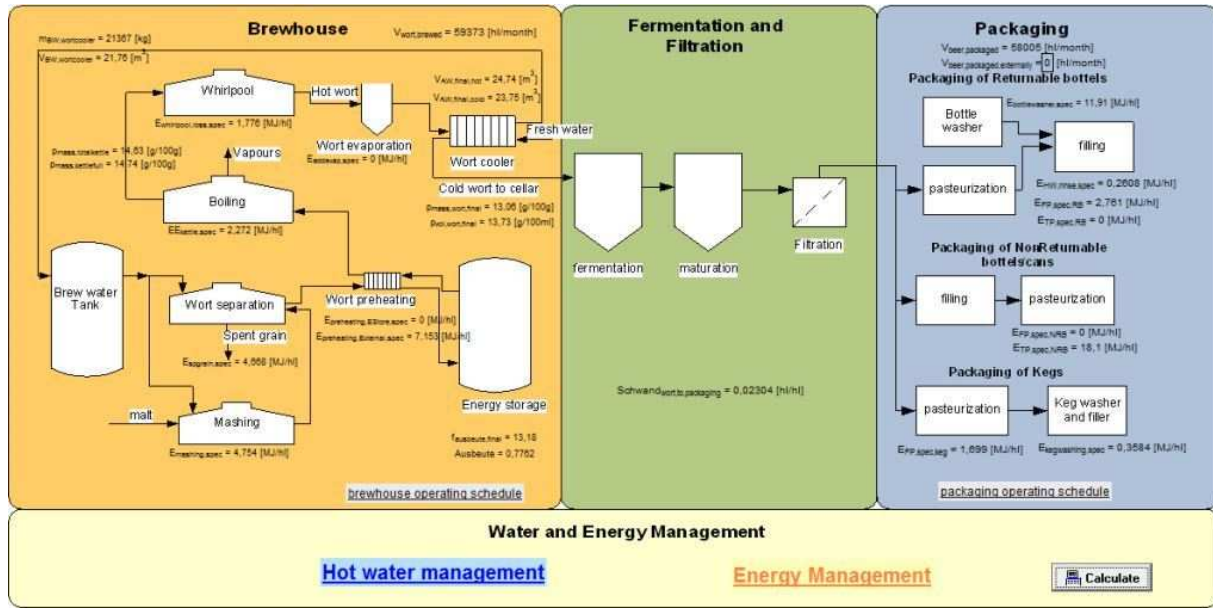


Figure 5-1: Start page of the Brewery Model

From this main page the “section overview tabs” can be selected which give a more detailed flowsheet of the respective processing steps. Here, the user defines the overall production parameters and operating conditions. For some selected processes or heat recovery options “technology tabs” can be activated, in which detailed operating data is defined (such as time-temperature profiles) and different technologies can be chosen for one process. Here, o heat transfer data such as heat exchanger size and heat transfer coefficients are also defined.

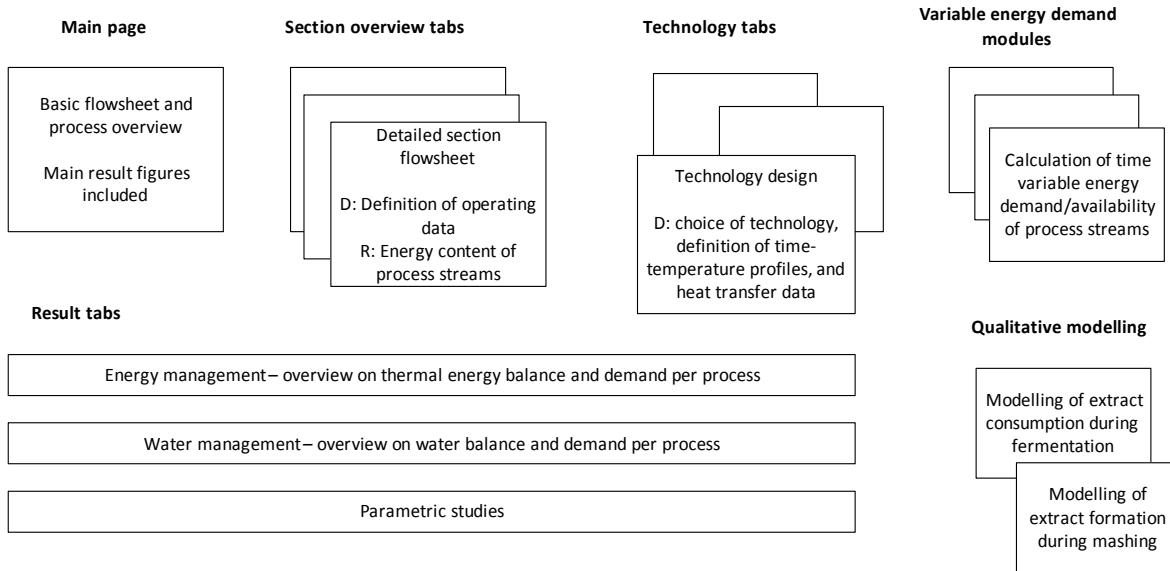


Figure 5-2: Overview of the Brewery Model

The mass and energy balances implemented in the EES program are described in section 5.1.8. Cooling demand modelling is described in 5.1.10.

Based on the data defined in the technology tabs, calculation modules can be accessed to calculate the respective energy demand and availability of the process streams over time. These calculation modules are separate EES files and are further described under 5.1.8.3.

For qualitative modelling two further modules are available: Based on a given starch composition a kinetic mashing model is included to calculate extract formation during the mashing process and similarly, a kinetic model allows for the calculation of extract consumption during fermentation. These modules will be described in section 5.1.9.

5.1.2 Brewhouse section

Figure 5-3 shows the section overview tab for the brewhouse section. It shows the main process steps mashing, lautering, wort preheating, wort boiling, trub separation in the whirlpool and wort cooling. Heat recovery from wort coolers to a hot water storage tank which is standard in breweries is assumed. Based on this process, flow sheet data can be entered for all processes. In the section overview tab the main data is specified, such as mass of process fluids used and temperature of incoming and outgoing process media in a process, which together with fluid parameters give the overall energy requirement. Heat recovery options for vapour recovery are also chosen in this tab as they affect the main flowsheet. The following heat recovery options for vapour heat recovery can be chosen:

- Energy storage for wort preheating
- Mechanical vapour compression
- Thermal vapour compression
- Energy storage for hot water preparation
- Energy storage for general energy supply (various processes)

5.1.2.1 Mashing

While only the amount of malt and brew water used for the mashing process in combination with the start and end temperature of the process are given in the section overview tab, all other details in the process are defined in the mashing technology tab. Table 5-1 summarizes the technology, heat supply and heat recovery options that can be chosen.

Table 5-1: Technology, heat supply and heat recovery options in the brewery model for mashing

Process	Technology options	Heat supply options	Heat recovery options
Mashing	Infusion mashing Decoction mashing	jacket heating (outside) heating plates (inside) steam injection <i>(heating medium specified by temperature and pressure)</i>	Heat recovery from hot wort over energy storage

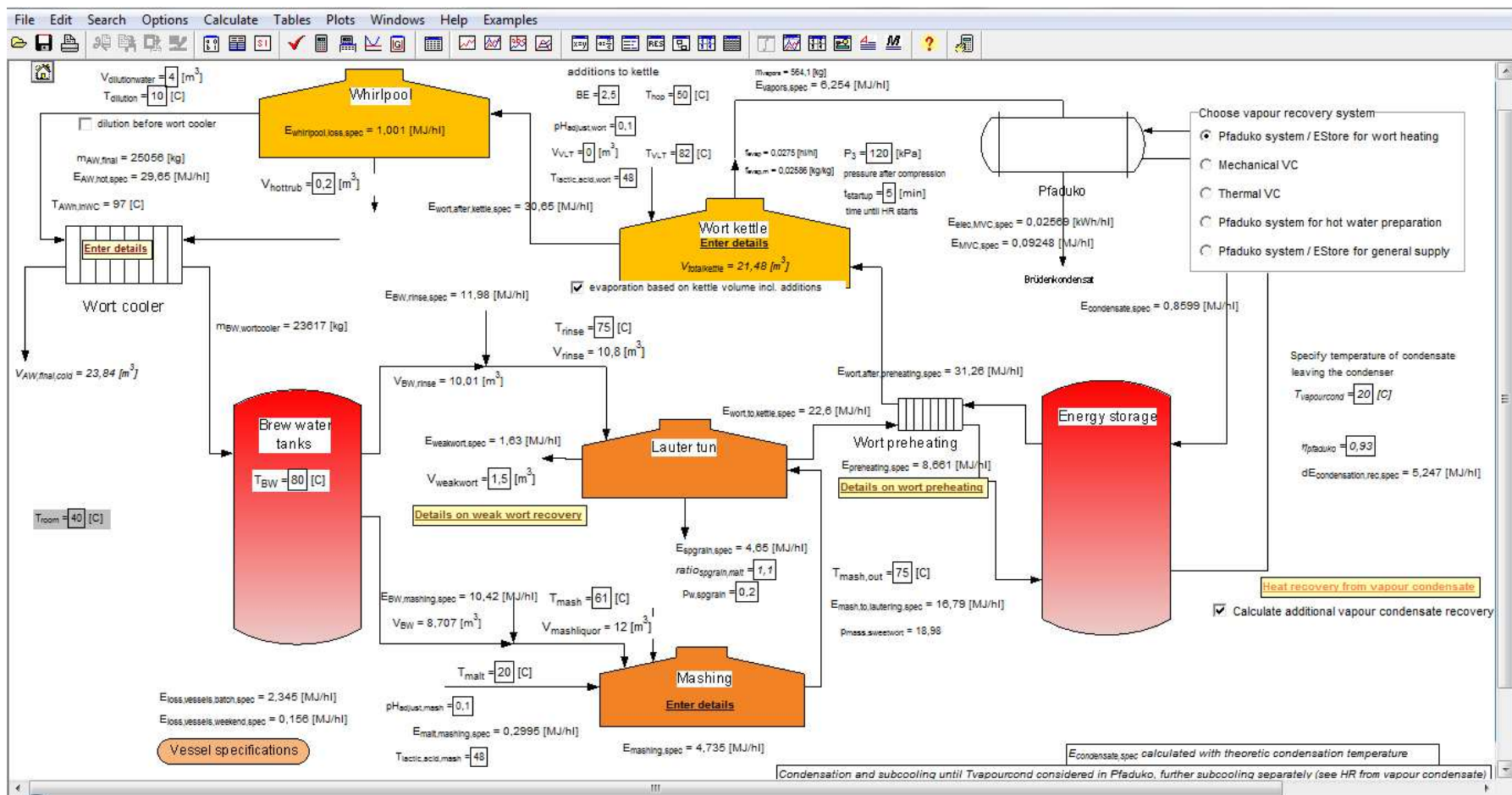
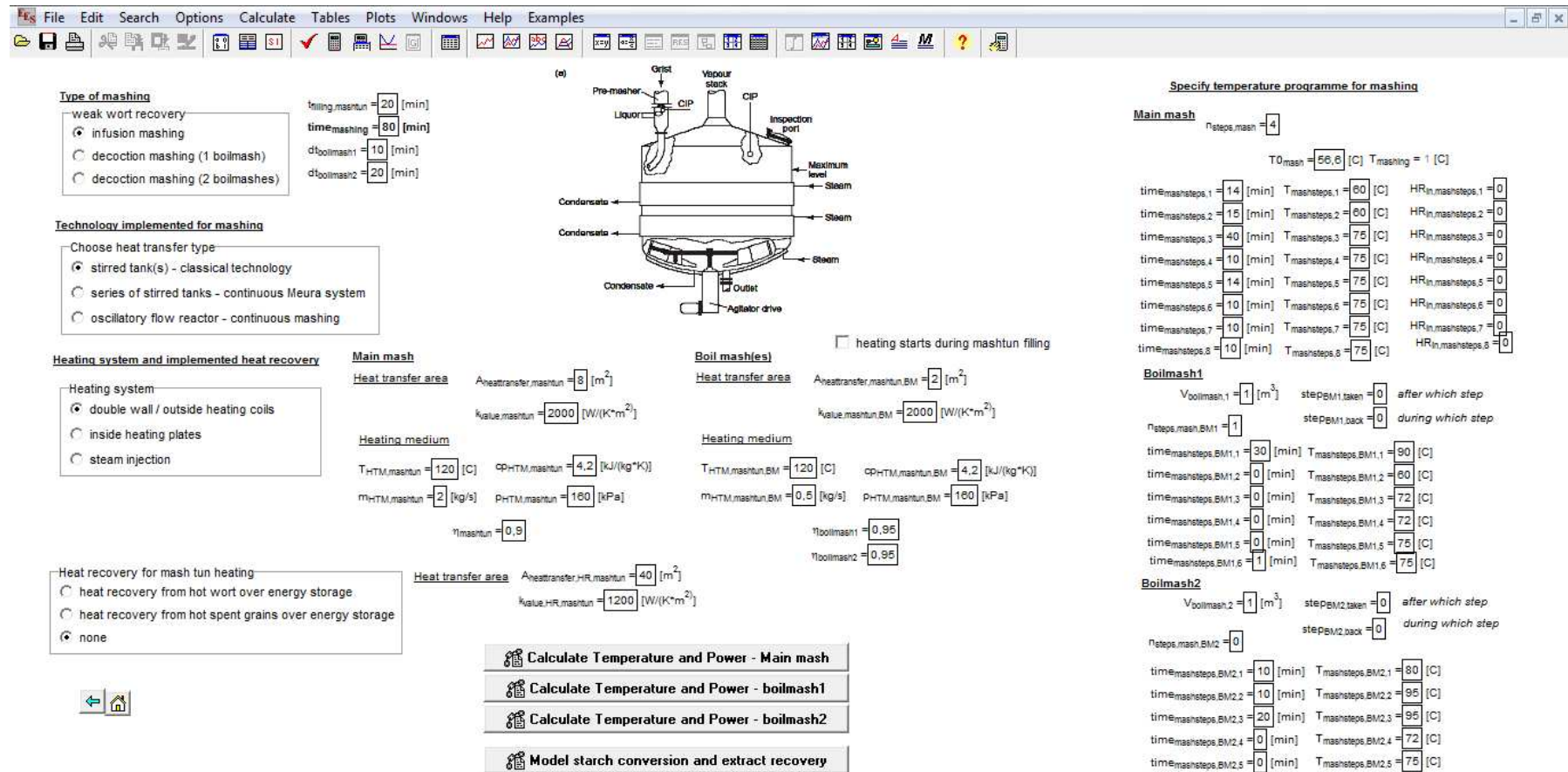


Figure 5-3: Brewhouse section of the Brewery Model



Type of mashing

- weak wort recovery
- infusion mashing
- decoction mashing (1 boilmash)
- decoction mashing (2 boilmashes)

$t_{filling, mashtun} = 20$ [min]
 $time_{mashing} = 80$ [min]
 $d_{boilmash1} = 10$ [min]
 $d_{boilmash2} = 20$ [min]

Technology implemented for mashing

- stirred tank(s) - classical technology
- series of stirred tanks - continuous Meura system
- oscillatory flow reactor - continuous mashing

Heating system and implemented heat recovery

Heating system

- double wall / outside heating coils
- inside heating plates
- steam injection

Heat recovery for mash tun heating

- heat recovery from hot wort over energy storage
- heat recovery from hot spent grains over energy storage
- none

Main mash

Heat transfer area: $A_{heattransfer, mashtun} = 8$ [m²]
 $k_{value, mashtun} = 2000$ [W/(K*m²)]

Heating medium: $T_{HTM, mashtun} = 120$ [C], $CP_{HTM, mashtun} = 4.2$ [kJ/(kg*K)]
 $m_{HTM, mashtun} = 2$ [kg/s], $P_{HTM, mashtun} = 160$ [kPa]
 $\eta_{mashtun} = 0.9$

Boil mash(es)

Heat transfer area: $A_{heattransfer, mashtun, BM} = 2$ [m²]
 $k_{value, mashtun, BM} = 2000$ [W/(K*m²)]

Heating medium: $T_{HTM, mashtun, BM} = 120$ [C], $CP_{HTM, mashtun, BM} = 4.2$ [kJ/(kg*K)]
 $m_{HTM, mashtun, BM} = 0.6$ [kg/s], $P_{HTM, mashtun, BM} = 160$ [kPa]
 $\eta_{boilmash1} = 0.95$
 $\eta_{boilmash2} = 0.95$

heating starts during mashtun filling

Specify temperature programme for mashing

Main mash: $n_{steps, mash} = 4$
 $T_{0, mash} = 56.6$ [C], $T_{mashing} = 1$ [C]

Step	Time [min]	Temperature [C]	HR _{in} [0]
1	14	60	0
2	15	60	0
3	40	75	0
4	10	75	0
5	14	75	0
6	10	75	0
7	10	75	0
8	10	75	0

Boilmash1

$V_{ool, mash, 1} = 1$ [m³], $step_{BM1, taken} = 0$ after which step
 $n_{steps, mash, BM1} = 1$, $step_{BM1, back} = 0$ during which step

Step	Time [min]	Temperature [C]
BM1.1	30	90
BM1.2	0	60
BM1.3	0	72
BM1.4	0	72
BM1.5	0	75
BM1.6	1	75

Boilmash2

$V_{ool, mash, 2} = 1$ [m³], $step_{BM2, taken} = 0$ after which step
 $n_{steps, mash, BM2} = 0$, $step_{BM2, back} = 0$ during which step

Step	Time [min]	Temperature [C]
BM2.1	10	80
BM2.2	10	95
BM2.3	20	95
BM2.4	0	72
BM2.5	0	75
BM2.6	1	75

Buttons:

- Calculate Temperature and Power - Main mash
- Calculate Temperature and Power - boilmash1
- Calculate Temperature and Power - boilmash2
- Model starch conversion and extract recovery

Figure 5-4: Technology tab for mashing

Figure 5-4 shows the technology tab for the mashing process. It is possible to define temperature programmes for infusion mashing or decoction mashing with up to 2 decoction mashes. Temperature programmes are defined with a starting temperature and subsequent mash steps for which time and target temperature are given. Thus, for rests, the target temperature remains the same as the initial temperature and only the rest time is defined. For heating steps, the target temperature is the final temperature of the current heating step and the time required is based on the respective heating rate.

Heat supply is basically defined via heat transfer coefficients and the heat transfer area. For the heating medium the heat capacity, operating temperature and pressure are defined, as well as the maximum flow through the heat exchanger. The boxes for selecting the technology and heat supply options should only give a brief overview.

As lautering is only thermally relevant in terms of rinsing water requirement, there is no specific technology tab for wort separation. For the lautering process the amount of water for rinsing is specified in the brewhouse section as well as potential re-use of weak wort for the mashing process of the subsequent brew. The relative amount of spent grains (based on the initial grist used in mashing) defines the mass balance of malt husks and extracts:

$$\begin{aligned}
 m_{malt} + \frac{m_{extract;ww}}{m_{weakwort}} * m_{weakwort;rec;mash} \\
 = m_{extract} + m_{extract;ww} + m_{spgrain} * (1 - p_{water;spgrain})
 \end{aligned}
 \tag{5-1}$$

5.1.2.2 Wort preheating

Wort preheating is realised over external or internal heat exchangers of the wort kettle or over dedicated wort preheaters. In many breweries wort preheating is at least partly covered over heat recovery. Therefore, the technology tab for wort preheating specifies the heat supply media and defines the heat exchange parameters. In case wort preheating is realised within the boiling kettle, the heat transfer parameters of the kettle have to be specified. Figure 9-2 in Annex 9.1 shows the technology tab of wort preheating.

5.1.2.3 Wort boiling

Although certain wort boiling objectives should be met in each boil (see 4.3.1.3), the design possibilities for the wort boiling process are quite extensive (see 4.3.2.3). While in the section overview window only the additions to the kettle are specified, all details are defined in the respective technology tab for wort boiling. Specification via definition of time, temperature and pressure over the boiling duration enables modelling of most boiling techniques. The technology tab for wort boiling therefore offers the possibility to define 10 boiling steps defined via time, temperature (change) and pressure during the boil. Additionally, it can be defined if energy is supplied to the boiling steps and whether the vapours generated in this step are used for heat recovery (in the specified heat recovery system). Heat transfer parameters can be defined via heat transfer area, estimated heat transfer coefficient and the heating medium, for which temperature, pressure and maximum mass flow are the decisive parameters.

It is also possible to state whether additional wort treatment, such as vacuum evaporation or stripping, occurs after the boil. Parameters for these processes are defined in the technology tab of wort boiling and there is another sub-window for vapour heat recovery from this additional wort treatment. For calculating time-variable energy demand profiles, however, the definition of these

phenomena is done via an additional boiling step. In case such a treatment is performed after the whirlpool rest, the whirlpool rest itself must also be defined as a boiling step to calculate the time schedule of the process correctly.

Table 5-2: Technology, heat supply and heat recovery options in the brewery model for wort boiling

Process	Technology options	Heat supply options	Heat recovery options
Boiling	<i>Specification via definition of time, temperature and pressure over the boiling duration enables modelling of most boiling techniques, such as:</i> <ul style="list-style-type: none"> - Conventional boiling with natural or forced flow - Dynamic low pressure boiling - Rectification - High temperature boiling - Schoko - Varioboil 	Internal boiler External boiler Steam injection <i>(heating medium specified by temperature and pressure)</i>	Energy storage for wort preheating Energy storage for hot water production Energy storage for general energy supply to other processes Mechanical vapour compression Thermal vapour compression

File Edit Search Options Calculate Tables Plots Windows Help Examples

Kochsysteme

- conventional internal/external boiler
- internal/external boiler with forced flow (Stromboli, SmartBoil)
- Dynamic low pressure boiling (Jetstar)
- Rectifikation (Hertel)
- high temperature boiling
- PDX
- Schonkochverfahren
- vacuum evaporation Varioboil

temperature with which wort enters kettle $T_{wort,External} = 95 [C]$

$t_{filling,kettle} = 10 [min]$

$t_{boiling} = 60 [min]$ p in kettle at boiling start

$P_2 = 101 [kPa]$

Choose heat transfer type

- internal boiler
- external boiler
- heating coils
- direct steam injection

Heat transfer in kettle

$A_{heattransfer,kettle} = 24 [m^2]$

$k_{value,kettle} = 6000 [W/(K \cdot m^2)]$

$\eta_{kettle} = 0.85$

Heating medium

$m_{HTM,kettle} = 3 [kg/s]$

$P_{HTM,kettle} = 400 [kPa]$

$T_{HTM,kettle} = 150 [C]$

$T_{HTM,kettle,out} = 90 [C]$

additional boiling equipment after trub separation

- wort stripping
- vacuum evaporation
- none

$t_{soo,evap} = 30 [min]$

$P_4 = 101 [kPa]$ p before evaporation

$P_5 = 101 [kPa]$ p during evaporation

for steam stripping $PERC_{steam,stripping} = 0.015$

$P_{steam,stripping} = 400 [kPa]$

$T_{steam,stripping} = 150 [C]$

$f_{soo,evap} = 1 [hl/hl]$ additional evaporation (vol%)

$T_{sat,s} = 99,91 [C]$ temperature of wort after evaporation

Details - vapour recovery from additional evaporation

$n_{steps,boiling} = 4$

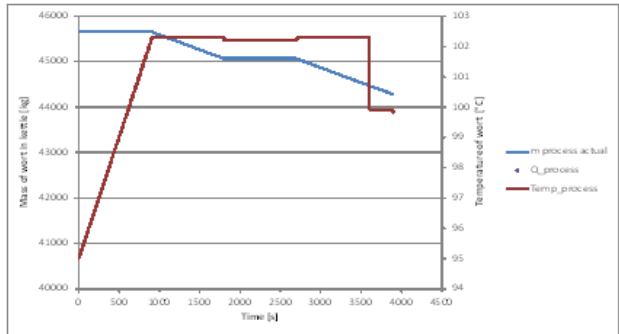
heating starts during kettle filling

time _{boilingsteps}	P _{wort,boiling}	T _{wort,boiling}	E _{in,boilingsteps}	HR _{in,boilingsteps}
1	101 [kPa]	99,5 [C]	1 [kJ]	0
2	110 [kPa]	103 [C]	1 [kJ]	0
3	110 [kPa]	103 [C]	1 [kJ]	0
4	101 [kPa]	100 [C]	0 [kJ]	0
5	130 [kPa]	108 [C]	1 [kJ]	0
6	101 [kPa]	100 [C]	0 [kJ]	0
7	130 [kPa]	108 [C]	1 [kJ]	0
8	101 [kPa]	101 [C]	0 [kJ]	0
9	130 [kPa]	108 [C]	1 [kJ]	0
10	101 [kPa]	101 [C]	0 [kJ]	0

check sensible input data (p,T), that wort is not in superheated state

define additional evaporation after trub separation as one of the boiling steps

checkS = ok



Specification on air parameters in kettle

$T_{air,kettle} = 90 [C]$

$h_{air,kettle} = 1 [m]$

$\phi_{air,kettle} = 0.5$

Calc Temperature and Power during boiling

Figure 5-5: Technology tab for wort boiling

The thermal relevance of the whirlpool is restricted to the withdrawal of the hot trub and the cooling of the wort during the whirlpool rest. Parameters for these events are specified in the section overview of the brewhouse.

5.1.2.4 Wort cooling

As wort cooling is a central process, in terms of heat integration in the brewhouse, a separate technology tab for wort cooling is also available. Here, definitions of cooling stages and cooling media are possible in order to correctly calculate the amount of energy recovered for hot water generation or for heat integration to other processes.

Table 5-3: Technology, heat supply and heat recovery options in the brewery model for thermal brewhouse operations

Process	Technology options	Heat supply options	Heat recovery options
Wort cooling	1-stage wort cooler 2-stage wort cooler	<i>(cooling media specified by temperature)</i>	Brew water preparation Heat recovery for process heating and brew water preparation

5.1.3 Fermentation and filtration section

There is no significant thermal energy demand in the fermentation or filtration cellar. Only cleaning (if not carried out as cold CIP) adds to the thermal energy demand, however its demand is insignificant in comparison to the CIP systems in packaging and in the brewhouse. Therefore, the energy demand modelling of the Brewery Model is restricted to the hot water demand for cleaning, which can be specified within the section overview.

Cooling on the other hand, is a decisive process also in terms of potential heat recovery from cooling compressors, so a cooling load calculation has been included in the Brewery Model. Cooling is mainly required in the temperature range between -1 and 12°C. Electricity demand for cold production is in the range of 1-2 kWh/hl beer. For Austrian breweries this translates to an annual consumption of 15 Mio. kWh electricity for cold production, which corresponds to a primary energy demand of almost 40 Mio. kWh.

To account for all major processes with cold demand the following processes are modelled: brew water cooling, fermentation tanks, beer cooler, yeast tanks and maturation tanks. Figure 5-6 shows a flowsheet of these processes.

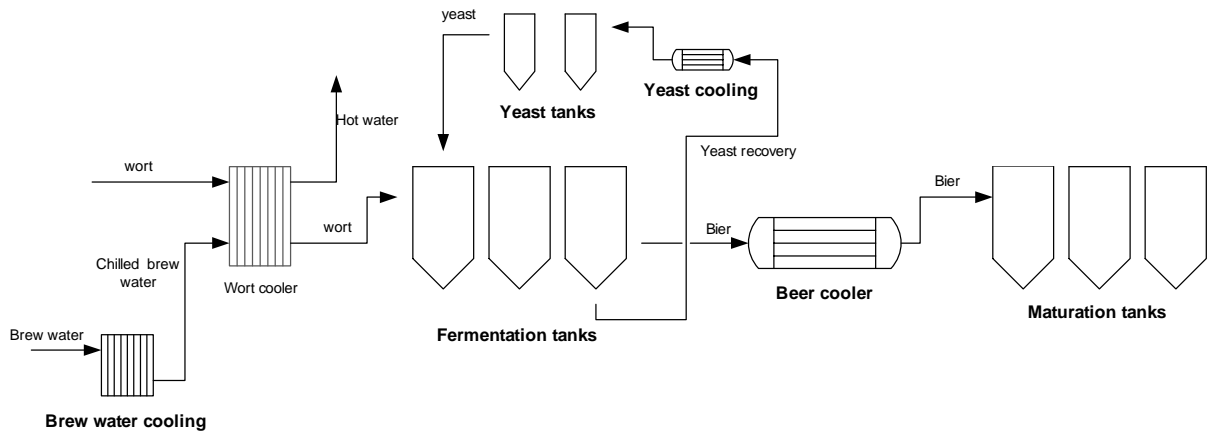


Figure 5-6: Flowsheet of cooling processes in breweries

The basic cooling load of each process based on the production parameters is calculated via the parameters defined in the “fermentation and filtration section overview”. For the fermentation tanks a more detailed model has been integrated which is simulated in a separate EES file that can be accessed via the section overview window. A screenshot of the section overview is given in Figure 9-3 in the appendix.

Similar to the calculation of varying energy demand over time, the cooling demand profiles are calculated based on the data of the Brewery Model in a linked Excel file.

5.1.4 Packaging section

The packaging section is divided into three sub-areas: packaging for returnable bottles, for non-returnable bottles or cans and keg packaging. In each section thermal energy demand for cleaning, pasteurization and filling is calculated based on user-defined data.

The following processes are implemented depending on the kind of packaging:

- Non-returnable bottles and cans: flash pasteurization, tunnel pasteurization and chamber pasteurization.
- Returnable bottles: Bottle washing, filling and flash and tunnel pasteurization.
- Kegs: combined keg washer and filler

For bottle washing and pasteurization technology tabs are available in which heat transfer parameters are specified. These are later used for the modelling of energy demand profiles.

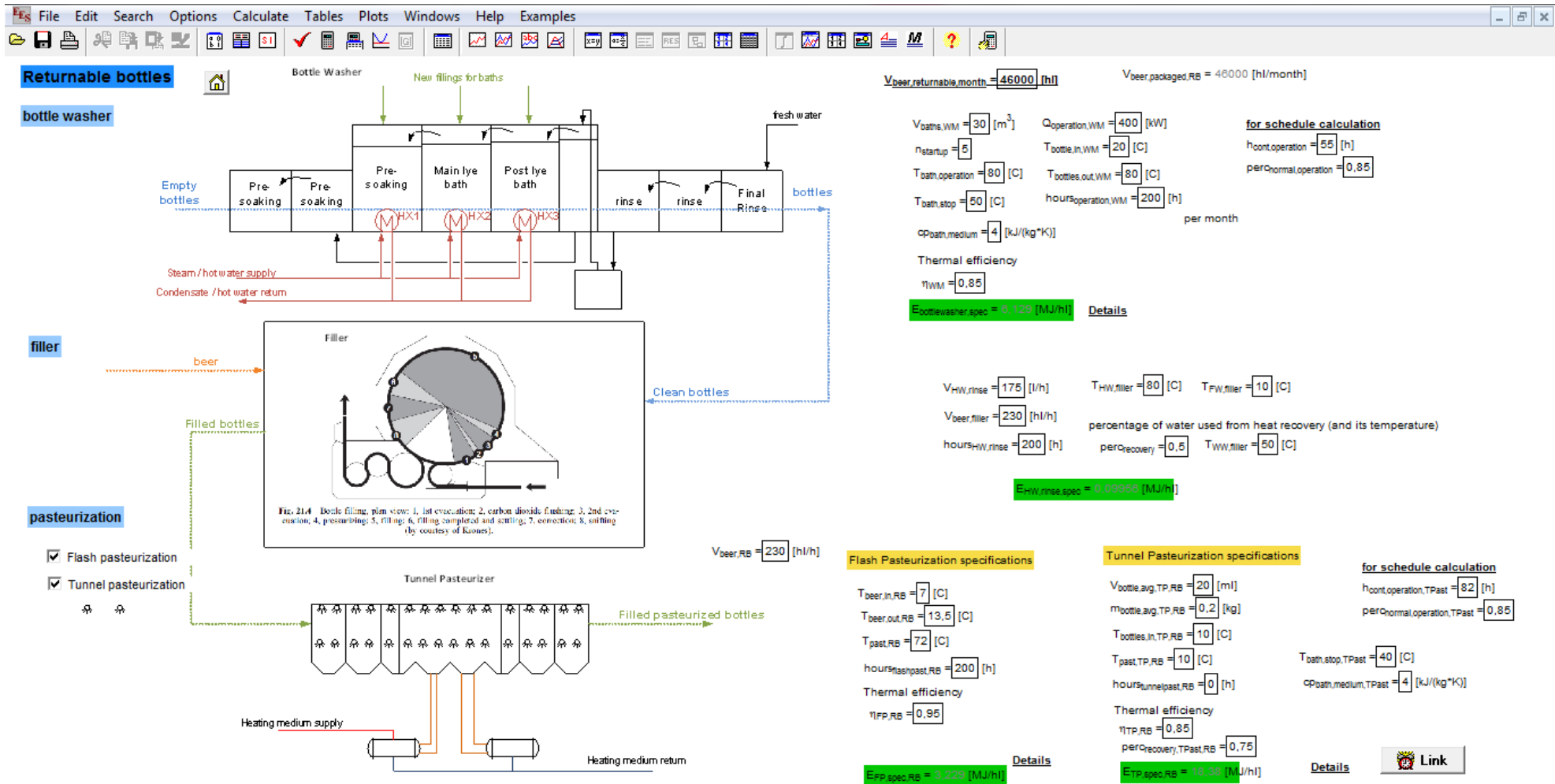


Figure 5-7: Section overview for returnable bottle washing

5.1.5 Water management

The water management section shows a hot water balance of the brewery and indicates whether there is a surplus or demand of hot water (see Figure 5-9) and whether there is a respective energy requirement. Graphs are included to visualize the balance. Available hot water is calculated via brew water generated over wort cooling heat recovery and hot water possibly generated by vapour condensation or vapour condensate subcooling from vapours formed in the kettle or from vapours of additional wort treatment steps. All these values are already defined in other technology tabs and their information is just summarized in the water management section. Additionally, the user can specify in this section whether hot water is generated via steam condensate cooling. This is done in some breweries that would otherwise lose this energy in badly insulated open condensate systems. On the demand side process hot water demand is specified in other tabs and summarized in this section. The water management section is also the place to define the amount and temperature of hot water required for cleaning and CIP systems and for other general uses. The overall energy requirement for hot water preparation is given by

$$\begin{aligned}
 E_{HW,externalheating} & \hspace{15em} 5-2 \\
 & + (E_{BW,wortcooler} + E_{HW,rec} + E_{HW,vapourcondenser} \\
 & + E_{HW,addevap} + E_{WW,addevap}) * N_{brews,week} \\
 & + E_{HW,steam;condensate} \\
 & = E_{CIP,brewhouse} + E_{CIP,packaging} + (E_{BW,mashing} + E_{BW,rinse}) \\
 & * N_{brews,week} + E_{HW,keg} + E_{HW,filler} + E_{HW,general,needs}
 \end{aligned}$$

5.1.6 Energy management

In the energy management section (see Figure 5-10), the main results of thermal energy requirement is given for each section and the energy flows in terms of specific energy in MJ/hl are available as a basis for a Sankey diagramm.

5.1.7 General operating schedule

In this section the general operating schedule must be defined by the user. Date and time of start of brewhouse operation must be entered, as well as the number of days per week on which the brewhouse is in operation. Additionally, the average number of brews per week and the time between brews must be entered, as well as the general brew duration and volume. For the brewhouse processes more detailed information is questioned, which is relevant for calculation of time-variable energy demand profiles, as well as for calculating radiation losses from vessels.

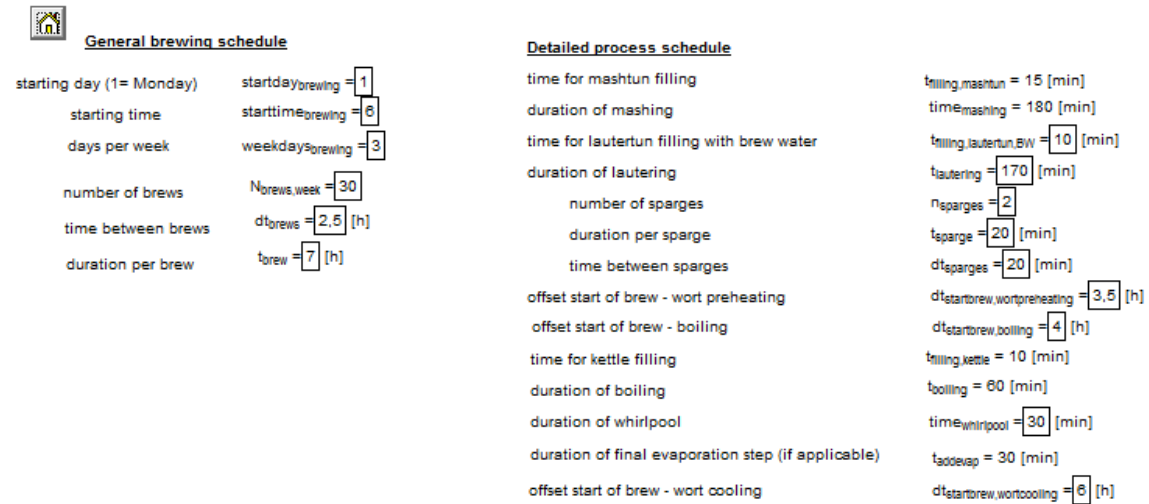


Figure 5-8: Input of brewing operating schedule in the Brewery Model

File Edit Search Options Calculate Tables Plots Windows Help Examples

Hot water management

Hot water consumers

Brew water for mashing	$V_{BW} = 21,77 \text{ [m}^3\text{]}$	per brew	$T_{BW} = 80 \text{ [C]}$
Brew water for wort separation	$V_{BW,rinse} = 23,18 \text{ [m}^3\text{]}$	per brew	
Hot water for CIP (in brewhouse)	$V_{CIP,brewhouse} = 220 \text{ [m}^3\text{]}$	per week	$T_{CIP,brewhouse} = 80$
Hot water for CIP (packaging)	$V_{CIP,packaging} = 60 \text{ [m}^3\text{]}$	per week	$T_{CIP,packaging} = 80$
Hot water for rinsing in bottle filling	$V_{HW,filler} = 8,14 \text{ [m}^3\text{]}$	per week	$T_{HW,filler} = 80 \text{ [C]}$
Water demand for keg washing (relevant when hot water being used)			
	$V_{FW,kegwasher} = 6,797E-16 \text{ [m}^3\text{/per week]}$		$T_{FW,keg} = 10 \text{ [C]}$
Other HW demand for keg packaging	$V_{HW,keg} = 0 \text{ [m}^3\text{]}$		$T_{HW,keg} = 80 \text{ [C]}$
General other hot water consumption	$V_{HW,general,needs} = 250 \text{ [m}^3\text{]}$	per week	$T_{HW,general,needs} = 70 \text{ [C]}$

$T_{FW} = 10 \text{ [C]}$ $V_{HW,consumption,per,week} = 1877 \text{ [m}^3\text{]}$

Hot water produced by

Brew water produced from wort cooling	$V_{BW,wortcooler} = 51,36 \text{ [m}^3\text{]}$	per brew	$T_{BW} = 80 \text{ [C]}$
Hot water generation by vapour condensation	$m_{HW,ptaduko} = 0 \text{ [kg]}$	per brew	$T_{hotwater,ptaduko} = 80 \text{ [C]}$
Hot water generation by vapor condensate recovery	$m_{HW,rec} = 0 \text{ [kg]}$	per brew	$T_{WHot} = 80 \text{ [C]}$
Hot water generation by steam condensate	$m_{HW,steam,condensate} = 0 \text{ [kg]}$	per week	$T_{HW,steam,condensate} = 80 \text{ [C]}$
Hot water generation by vapour condensation (additional evap.)	$V_{HW,addevap} = -5,603E-16 \text{ [m}^3\text{]}$	per brew	$T_{HW,addevap} = 80 \text{ [C]}$
Hot water generation by vapor condensate recovery (additional evap)	$V_{WW,addevap} = 4,483E-16 \text{ [m}^3\text{]}$	per brew	$T_{WW,addevap} = 50 \text{ [C]}$

$V_{HW,production,per,week} = 1541 \text{ [m}^3\text{]}$

water balance per week

need to produce hot water from external energy sources

$V_{HW,externalheating} = 335,7 \text{ [m}^3\text{]}$ (negative value signifies over-production of hot water)

$E_{HW,externalheating} = 8,647E+07 \text{ [kJ]}$

$E_{HW,externalheating,spec} = 6,355 \text{ [MJ/hl]}$ (based on brewed wort volume; hl cold cast wort)

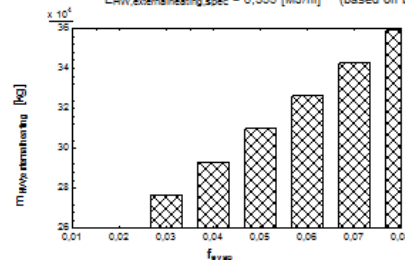


Figure 5-9: Hot water management analysis within the Brewery Model

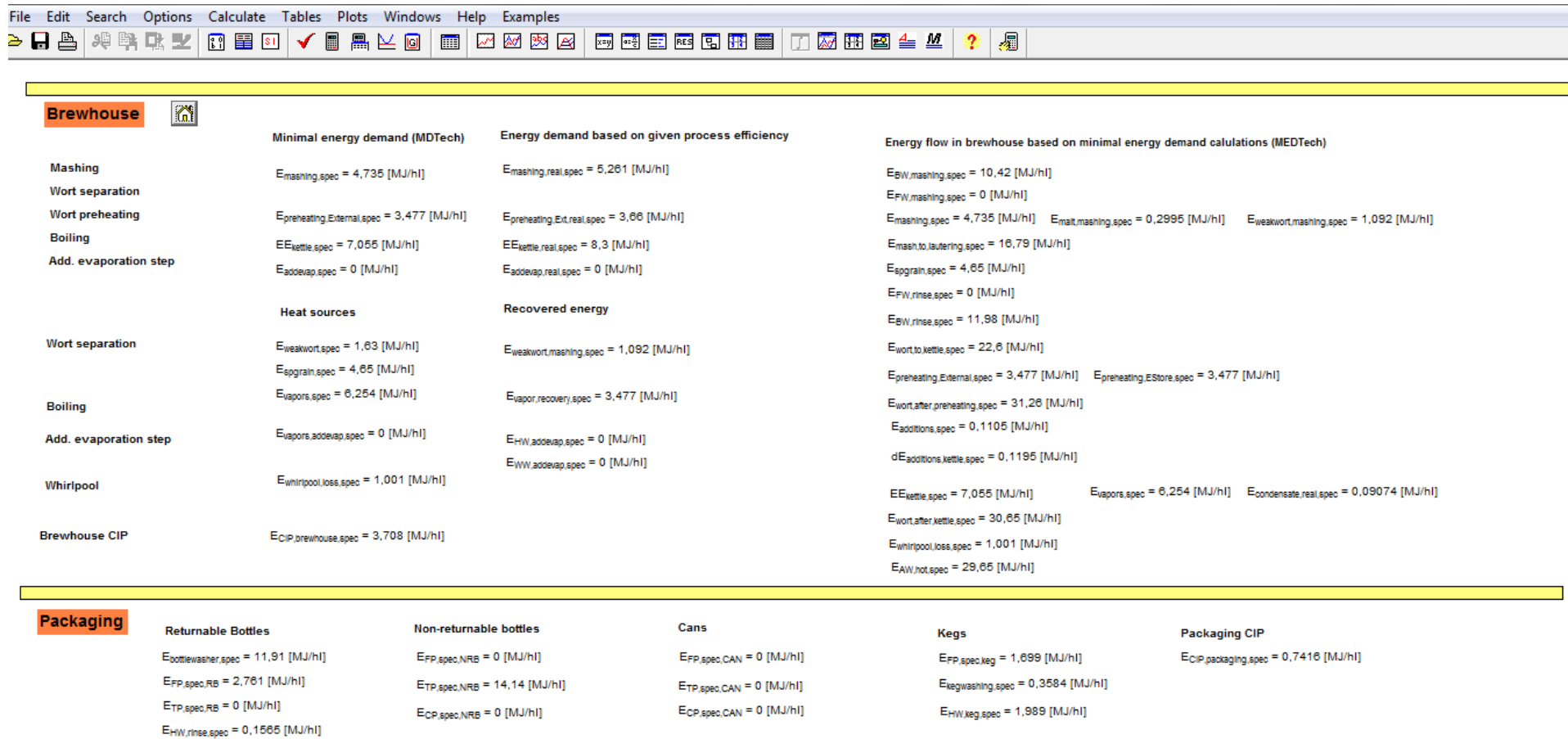


Figure 5-10: Summary of energy demand figures within the Brewery Model

5.1.8 Modelling the thermal energy demand in breweries

5.1.8.1 Minimal thermal energy demand

The brewery model calculates the minimal thermal energy demand for a brewery based on its site-specific operating parameters and implemented technologies. This “minimal thermal energy demand per technology – $MEDT_{Tech}$ ” has been shown to be of importance to operators, as it is the ultimate target for energy demand reduction for the given process parameters and therefore can stimulate enhancements in efficiency. Below an example for the MEDT for a mashtun, processing an infusion mash, is shown.

$$\begin{aligned}
 MEDT_{mashtun, \frac{kJ}{brew}} &= V_{mashing \text{ liquor}} * \rho_{mashing \text{ liquor}} * (T_{final} - T_{mash;in}) \\
 &+ m_{malt} * c_{p \text{ malt}} * (T_{final} - T_{malt})
 \end{aligned}
 \tag{5-3}$$

In reality the process and distribution efficiency will add to the $MEDT_{Tech}$ in order to result in the useful supply heat USH which is the heat generated in the boiler or by other heat supply equipment necessary to cover the energy demand of the production [151]. The conversion efficiencies of the energy supply technologies will then influence the relation between the useful supply heat and the final thermal energy demand FET [183].

$$USH = \sum_{j=1}^k (m_j * H_{uj}) * \eta_{conversion} + FET_{districtheat} + FET_{CHP} * \eta_{thermal}
 \tag{5-4}$$

$$USH * \eta_{conversion} * \eta_{process} = \sum_{i=1}^n MEDT_{tech;i}
 \tag{5-5}$$

The brewery model calculates the $MEDT_{Tech}$ for each process based on the defined parameters and technologies. In addition, the process efficiency is questioned for each process in the brewery model, so the useful process heat demand is shown.

$$USH * \eta_{distribution} = UPH = \sum_{i=1}^n MEDT_{tech;i} / \eta_{process}
 \tag{5-6}$$

This can be compared with thermal energy demand measurements per process to show whether the real process efficiency is in the estimated range. Such measurements, combined with the knowledge of the $MEDT_{Tech}$, can also be used to determine the real process efficiency.

In most breweries thermal energy demand measurements per process are not implemented, but at least the useful supply heat is known. The comparison of the calculated energy demand, based on $MEDT_{Tech}$ and estimated (or partly measured) process efficiencies, to the useful supply heat shows the thermal energy losses occurring in the distribution system. Here, leaking valves or steam traps and open condensate tanks may contribute to the losses, as well as badly insulated pipings. In most breweries the deviation between calculated useful supply heat demand and actual consumption of useful supply heat is in the range of 15-20 % for steam-based systems. In one brewery running on hot water as energy transfer medium the deviation was in the range of 5-10 %. This shows well that thermal energy distribution based on steam does require sensible care of operators. Additionally it is interesting to compare the calculated make-up water demand for boiler feed water with the actual

input of make-up water per week or per month. In most breweries the actual demand is much higher than the expected figure based on processes requiring direct steam. All these analyses in comparison to the calculated values, which can be quickly determined in the Brewery model, add to the accuracy of the thermal energy balance of a brewery.

While the $MEDT_{Tech}$ is based on a specified technology, the aim of the brewery model is also to compare different technologies to evaluate their effects on the overall energy demand. In this way, the technologies that eventually lead to the overall minimal thermal energy demand can be chosen. The brewery model allows for such comparisons by calculating the $MEDT_{Techs}$ for different technology scenarios. For each run of the brewery model, the complete brewery is calculated, and the effects of one technology change on the water and energy management can be easily identified.

5.1.8.2 Energy and mass balances

Energy and mass balances are performed in the Brewery Model in order to calculate energy flows of each product stream. Results are presented in energy per hectolitre of brewed beer (for brewhouse and fermentation cellar) or packaged beer (for the packaging area).

The following equations show calculation examples for some selected processes. The full equation set is presented in the appendix.

Mashing:

At first, the amount of hot brew water for the mashing process is calculated over the mass and energy balance:

$$m_{BW} + m_{FW} = m_{mash} \quad 5-7$$

$$m_{BW} * cp_{BW} * T_{BW} + m_{FW} * cp_{FW} * T_{FW} = m_{mash} * cp_{mash} * T_{mash} \quad 5-8$$

The energy input in the mashing process via the hot brew water is calculated based on a selected reference temperature (defined within the Brewery Model) and the specific energy demand is defined in the brewhouse section in the units MJ per hl of cold cast wort.

$$E_{BW;mashing} = m_{BW} * cp_{BW} * (T_{BW} - T_{ref}) \quad 5-9$$

$$E_{BW;mashing;spec} = \frac{E_{BW;mashing} * \left(\frac{0001 MJ}{kJ}\right)}{V_{AW;cold} * \left(10 \frac{hl}{m^3}\right)} \quad 5-10$$

Possible weakwort recovery is also considered.

$$m_{mash;total} = m_{mash} + m_{weakwort;rec;mash} \quad 5-11$$

$$\begin{aligned} m_{weakwort;rec;mash} * cp_{weakwort} * T_{rinse} + m_{mash} * cp_{mash} * T_{mash} \\ = m_{mash;total} * cp_{mash} * T_{mash;total} \end{aligned} \quad 5-12$$

$$\begin{aligned} m_{mashing} * cp_{mashing} * T_{mashing} \\ = m_{mash;total} * cp_{mash} * T_{mash;total} + m_{malt} * cp_{malt} * T_{malt} \end{aligned} \quad 5-13$$

The energy demand is calculated per mash step in the time-temperature profile of the mashing process. One mash step is defined by two temperatures and the time required for the respective heating or holding.

$$E_{mainmash}[j] = V_{mashing;mainmash}[j] * \rho_{mashing} * c_{p,mashing} * (T_{mashsteps}[j] - T_{mashsteps_afterBMMix}[j - 1]) \quad 5-14$$

with $T_{mashsteps}$ defining the temperature which is reached at the end of the current mashing step and $T_{mashsteps_afterBMMix}$ taking into account whether a boil mash has been mixed to the main mash prior to this mash step. $T_{mashsteps_afterBMMix}$ is then calculated according to formula 5-15.

$$T_{mashsteps;afterBMMix;j} = \frac{(V_{mashing;mainMash;j} * \rho_{mashing} * c_{p,mashing} * T_{mashsteps;j} + V_{boilmash;j} * \rho_{mashing} * c_{p,mashing} * T_{boilmash})}{(V_{mashing;mainMash;j+1}) * \rho_{mashing} * c_{p,mashing}} \quad 5-15$$

$V_{mashing;mainMash}$ gives the current mashing volume, again accounting for the possibility that a certain amount of mash is currently treated in a separate boil mash.

The energy content of the hot mash entering the lautering process is given by

$$E_{mash;to;lautering} = m_{mash;total} * c_{p,mash} * (T_{mash;out} - T_{ref}) + m_{malt} * c_{p,malt} * (T_{mash;out} - T_{ref}) \quad 5-16$$

Lautering

For lautering the mass and energy balance again define the amount of cold and hot brew water used for the rinses:

$$m_{BW;rinse} + m_{FW;rinse} = m_{rinse} \quad 5-17$$

$$m_{BW;rinse} * c_{p,BW} * T_{BW} + m_{FW;rinse} * c_{p,FW} * T_{FW} = m_{rinse} * c_{p,rinse} * T_{rinse} \quad 5-18$$

In addition to energy balances for single processes, overall mass and component balances are integrated to take into account the interdependences within the brewing process. For calculating the amount of extract in the wort and the amount of spent grains mass and component balance of malt husks and extract are included:

$$m_{spgrain} * m_{kettlefull} + m_{weakwort} = m_{mash;total} + m_{rinse} * m_{malt} \quad 5-19$$

$$m_{malt} + \frac{m_{extract;ww}}{m_{weakwort}} * m_{weakwort;rec;mash} = m_{extract} + m_{extract;ww} + m_{spgrain} * p_{w;spgrain} \quad 5-20$$

With the amount of spent grains defined via the known ratio of spent grains over malt input:

$$\frac{m_{spgrain}}{m_{malt}} = ratio_{spgrain,malt} \quad 5-21$$

An approximate value is assumed for extract content of weak wort, as given in the literature [120].

$$\frac{m_{extract;ww}}{m_{weakwort}} = 0.02 \quad 5-22$$

The extract content of any process stream is important for the calculation of the correct heat capacity and density. For the wort collected after lautering to the kettle, mass percentage of extract in wort [g/100g] is given by

$$p_{mass;kettlefull} = \frac{m_{extract}}{m_{kettlefull}} * 100 \quad 5-23$$

which is the basis for density according to the Plato-tables [120] which are included as lookup files in the Brewery Model. The heat capacity is also calculated based on the extract content of the wort:

$$cp_{wort} = cp \left[water; T = \frac{T_1 + T_2}{2}; P = P_1 \right] * (1 - p_{mass}) + cp_{malt} * p_{mass} \quad 5-24$$

Wort Preheating

Once the mass of wort entering the kettle is known ($m_{kettlefull}$), the energy demand to heat the wort from lautering to the target temperature of wort preheating can be calculated. This “target” temperature is generally the boiling temperature at the specified pressure, however in case a wort preheater heats the wort prior to the entrance to the kettle, the target temperature might be the final temperature with which the wort leaves the wort preheater.

In the wort preheating technology tab the user can choose whether heat recovery over an energy storage is used to preheat the incoming wort in the boiling process. If this is the case, the energy demand calculations take into account whether the energy was delivered by heat recovery or via an additional preheating system heated with external resources.

$$E_{preheating;EStore} = m_{kettlefull} * cp_{wort} * (T_{wort;EStore} - T_{rinse}) \quad 5-25$$

$$E_{preheating;External} = m_{kettlefull} * cp_{wort} * (T_{wort;External} - T_{wort;EStore}) \quad 5-26$$

Boiling

In boiling, initially additions to the kettle are defined and the mass of wort and its extract content is updated. Several boiling technologies are implemented in the Brewery Model. However, details on boiling and evaporation profiles r mainly affect the energy demand profiles (see 5.1.8.3). The overall energy demand is mainly influenced by the evaporation rate. The enthalpy of the vapours at saturation are calculated with temperatures slightly above and/or below saturation temperature.

$$E_{evaporation} = m_{vapors} * h_1 \quad 5-27$$

$$h_1 = h(water; T = T_{sat;2} + 0.5; P = P_2) - h(water; T = T_{sat;2} - 0.5; P = P_2) \quad 5-28$$

The energy content of the vapours based on the reference temperature is calculated as

$$\begin{aligned}
 E_{vapors} &= m_{vapors} \\
 &\quad * (h(\text{water}; T = T_{vapourcond;theory} + 1; P \\
 &\quad = P_{vapourcond}) \\
 &\quad - h(\text{water}; T = T_{ref}; P = P_{vapourcond}))
 \end{aligned}
 \tag{5-29}$$

With the temperature of the vapours assumed 1 Kelvin above the saturated water temperature at the given pressure

$$T_{vapourcond;theory} = T_{sat}(\text{water}; P = P_{vapourcond}) \tag{5-30}$$

For calculating the heat recovery potential, it is important to distinguish between the energy content of condensation and of subcooling to a specified condensation temperature, which defined the enthalpy of the vapour condensate:

$$h_{condensate} = h(\text{water}; T = T_{vapourcond}; P = P_{vapourcond}) \tag{5-31}$$

For mechanical and thermal vapour compression, the compression work is calculated via the isentropic and polytropic enthalpy changes during compression from pressure P_1 to pressure P_2 :

$$T_{sat;1} = T_{sat}(\text{water}; P = P_1) \tag{5-32}$$

$$s_1 = s(\text{water}; T = T_{sat;1} + 0.1; P = P_1) \tag{5-33}$$

$$h_1 = h(\text{water}; T = T_{sat;1} + 0.1; P = P_1) \tag{5-34}$$

$$h_2 = h(\text{water}; s = s_1; P = P_2) \tag{5-35}$$

$$dh_{isen} = h_2 - h_1 \tag{5-36}$$

$$h_{poly} = h_1 + \frac{1}{\frac{\eta_{isen}}{h_2 - h_1}} \tag{5-37}$$

$$dh_{poly} = h_{poly} - h_1 \tag{5-38}$$

Whirlpool and additional evaporation

While the amount of hot trub is a user defined value, the extract content of the hot trub is taken from literature. With these parameters the final amount of cast wort and its extract content can be calculated. Energy losses during whirlpool operation are calculated as temperature difference between the temperature of the wort after boiling and the temperature of the hot wort which is specified by the user.

$$m_{extract;AW;final} = m_{extract} - m_{extract;hottrub} \tag{5-39}$$

$$m_{AW;final} = m_{AW} - m_{hottrub} + m_{dilutionwater} \tag{5-40}$$

$$\begin{aligned}
 E_{whirlpool,loss} &= m_{AW,whirlpool} * cp_{AW,whirlpool} * (T_{to,whirlpool} \\
 &\quad - T_{AW,h,whirlpool})
 \end{aligned}
 \tag{5-41}$$

In some breweries an additional evaporation step is performed after trub separation. In the brewery model, two technologies are included: vacuum evaporation and steam stripping. The amount of vapours that evaporate can be calculated via the difference in enthalpy of the wort before and after this step. In case of steam stripping this is defined via the amount of steam used; in the case of vacuum evaporation the energy is defined via the pressure release in the system. The amount of vapours in vacuum evaporation are calculated based on the flash gas ratio at the given pressure.

Vacuum evaporation:

$$h_{VE,in} = h(\text{water}; T = T_{VE,in} - 0.1; P = P_{VE,in}) \quad 5-42$$

$$y_{VE} = \text{Quality}(\text{water}; T = T_{VE}; h = h_{VE,in}) \quad 5-43$$

$$m_{vapors,VE} = y_{VE} * m_{wort} \quad 5-44$$

Steam stripping

$$dE_{evap,SS} = m_{steam,add} * [h(\text{water}; T = T_{steam,SS} + 0.1; P = P_{steam,SS}) - h(\text{water}; T = T_{sat,SS} + 0.1; P = P_{SS})] \quad 5-45$$

$$m_{vapors,SS} = \frac{dE_{evap,SS}}{h_{evap}(\text{water}; T = T_{sat,SS})} \quad 5-46$$

The mass of cast wort must be re-calculated taking into account the vapours formed in the additional evaporation step and, in case of steam stripping, the input of steam. In case of dilution prior to wort cooling, water being added to the cast wort, the mass of the wort is updated accordingly.

$$m_{AW;addevap} = m_{AW,whirlpool} - m_{vapors,add} + m_{steam,add} \quad 5-47$$

$$m_{AW;final} = m_{AW;addevap} + m_{dilutionwater} \quad 5-48$$

Wort cooling

Finally, the cooling of the wort according to the user-defined pitching temperature provides the amount of hot brew water that can be produced for the subsequent brews. This applies for a 1 stage wort cooler.

$$m_{BW;wortcooler} = \left[\frac{m_{AW;final} * cp_{AW;final} * (T_{AWh,inWC} - T_{AWc}) * \eta_{wortcooler;1}}{Cp(\text{water}; T = \frac{T_{BW} + T_{CW}}{2}; P = P_1) * (T_{BW} - T_{CW})} \right] \quad 5-49$$

$$E_{BW;wortcooler} = m_{BW;final} * cp_{AW;wortcooler} * cp \left[\text{water}; T = \frac{T_{BW} + T_{ref}}{2}; P = P_1 \right] * (T_{BW} - T_{ref}) \quad 5-50$$

For 2 stage wort coolers, the calculations are adapted. Here, an example for heating a heat transfer medium in the first stage and producing brew water in a second stage is given:

$$m_{HTM;wortcooler} = \left[\frac{m_{AW;final} * cp_{AW;final} * (T_{AWh,inWC} - T_{AWc,stage1}) * \eta_{wortcooler;1}}{Cp(water; T = \frac{T_{HTM,out} + T_{HTM,in}}{2}; P = P_1) * (T_{HTM,out} - T_{HTM,in})} \right] \quad 5-51$$

$$m_{BW;wortcooler} = \left[\frac{m_{AW;final} * cp_{AW;final} * (T_{AWc,stage1} - T_{AWc}) * \eta_{wortcooler;2}}{Cp(water; T = \frac{T_{BW} + T_{CW}}{2}; P = P_1) * (T_{BW} - T_{CW})} \right] \quad 5-52$$

The contraction factor, which is usually 0.96, is also calculated:

$$contraction = \left[\frac{h(water; T = T_{AWh}; P = P_1)}{h(water; T = T_{AWc}; P = P_1)} \right] \quad 5-53$$

Packaging:

When packaging beer into returnable bottles, non-returnable bottles, kegs and cans there are a few core processes which are relevant in terms of thermal energy demand: bottle washing, pasteurization and keg washing and filling. Besides cleaning-in-place (CIP) systems are considerable consumers of energy.

Energy demand of bottle washing is defined by the size of the water volume to be heated at start-up as well as the continuous heat load required for keeping the washing machine in operation.

$$E_{startup,WM} = V_{baths,WM} * \rho_w * cp_w * (T_{bath,operation} - T_{bath,stop}) * n_{startup} \quad 5-54$$

$$E_{operation} = Q_{operation} * h_{operation} \quad 5-55$$

Thermal energy demand of flash pasteurization is calculated via the beer flow in the pasteurizers, while tunnel pasteurization is defined via the amount of bottles being pasteurized. Over the required thermal power and the operation hours the energy demand is specified.

$$Q_{flashpast} = V_{beer} * \rho_{beer} * cp_{BEER} * [(T_{past} - T_{beer,in}) - (T_{past} - T_{beer,in})] / \eta_{FP} \quad 5-56$$

In tunnel pasteurization the theoretic energy demand to heat the filled bottle to pasteurization temperature does not represent the actual energy demand of tunnel pasteurizers as a considerable percentage of the required energy is recovered via the water system that heats the bottles. This is taken into account via the parameter perc_recovery_TP.

$$Q_{tunnelpast} = (m_{beer} * cp_{beer} + m_{bottle} * cp_{bottle}) * [(T_{past} - T_{bottles,in}) * (1 - perc_{recovery;TP})] / \eta_{FP} \quad 5-57$$

While most beer is treated in flash or tunnel pasteurization, there are also small pasteurization units for specific products, which might be filled in kegs, cans or bottles. In these pasteurizers a pasteurization chamber is heated to the defined pasteurization temperature and then the temperature is held for the specified time to reach the required pasteurization units. In the Brewery

Model we refer to these small units as chamber pasteurization or pallet pasteurization. Energy demand of one charge being pasteurized in a pasteurizer for pallets is given by the energy demand for heating the chamber and the energy demand for maintaining the temperature.

A standard keg washer and filler consists of several washing compartments for which hot water baths exists. These baths must be heated and energy demand is defined via fresh water being added to the baths and maintaining the heat which is lost via spraying the hot water onto the kegs.

$$Q_{bath} = m_{spray,bath} * cp_w * (T_{bath} - T_{keg,in}) + m_{FW,bath} * cp_w * (T_{bath} - T_{FW}) + S_{bath} * U * (T_{bath} - T_{room}) \quad 5-58$$

Additionally, steam is used for sterilizing the kegs. The aim of the sterilization is to heat the kegs to the programmed sterilization temperature. Steam input is calculated roughly by assuming the double steam input that would be theoretically necessary to heat the kegs to sterilization temperature.

$$Q_{steam} = \frac{m_{keg}}{t_{sterilisation}} * cp_{keg} * (T_{steril} - T_{bath}) * 2 \quad 5-59$$

Energy demand for CIP systems are heavily influenced by the amount of fresh hot water which is required for cleaning. The main water flow is recycled and energy demand for maintaining this flow on the operating temperature is calculated with a known factor of required energy per m³ of fresh water [78].

In addition to these processes, the packaging hall requires water to be at a temperature between 60-80°C for the bottle fillers and for manual washing of the floors. The latter may require a substantial amount of energy depending on the water temperature and the operational practice of the personnel. Both are included in the calculations of the Brewery Model.

5.1.8.3 Calculation of energy demand profiles

As brewing is a batch process, thermal energy demand varies significantly over time. Therefore equations for calculating time-dependent energy demand were integrated for batch processes which are thermally relevant such as mashing, wort preheating, wort boiling, wort cooling and fermentation. Based on the existing (user-defined) energy supply and the given heat transfer area, the energy demand profile is calculated over time

$$T = T_{initial} + \int_{t_{start}}^{t_{end}} \left[\frac{Q_{process}}{m_{process} \cdot cp_{process}} \right] dT \quad 5-60$$

The following flowsheet shows the overall calculation procedure for mashing.

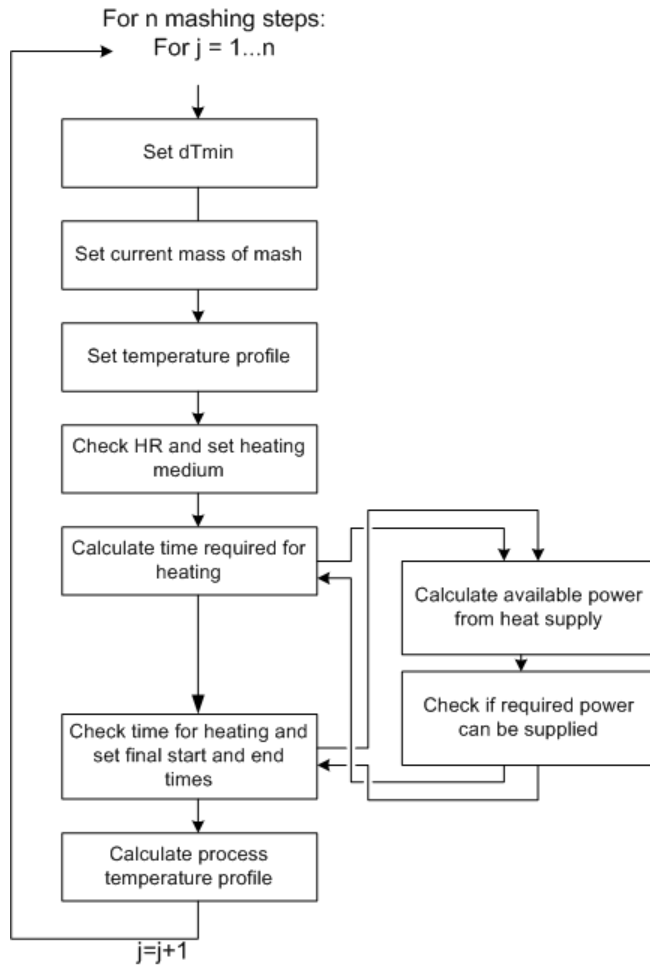


Figure 5-11: Calculation procedure for energy variability in mashing

The basic calculation of the energy demand profile is based on the definition of process steps, which define the temperature-time program. An example of process steps for a mashing process is given in Table 5-4 below. For each process step, the real temperature increase and energy input is calculated based on the targets and the existing heat transfer framework, such as available heating medium and heat transfer area. The possible heat duty delivered via the heating medium and transferred over the existing heat transfer area is defined by:

$$Q_{HM} = \dot{m}_{heating} * (h_{1, HM} - h_{2, HM}) \quad 5-61$$

$$h_{HM} = h(\text{water}; T = T_{HM}; P = P_{HM}) \quad 5-62$$

$$Q_{test} = k * A * \Delta T \quad 5-63$$

The transferable heat duty is thus given as the minimum of Q_{HM} and Q_{test} . The required heating time based on the process heat requirement is given over the process medium and the targeted temperature increase.

$$E_{process} = m_{process} * cp_{process} * (T_{process} - T_{init}) \quad 5-64$$

$$Q_{process} = \frac{E_{process}}{t_{heatingup}} \quad 5-65$$

Table 5-4: Example of process steps in mashing

Process step	Start temperature [°C]	End temperature [°C]	time of process step [°C]
1	58	62	15
2	62	62	30
3	62	72	20
4	72	72	15
5	72	75	10
6	75	75	15

Similar procedures have been developed for the other thermally relevant processes. In boiling, the vapour formation is calculated additionally as is the respective change of process medium. Evaporation is calculated based on the specifications of the respective boiling step as subcooled evaporation, flash evaporation or as continuous evaporation during the process duration:

Subcooled evaporation is modelled over diffusion of water in the air based on the temperature and pressure during the current boiling step and taking into account the surface area of the wort in the kettle.

$$m_{vapors,step} = \left[-D_{w,in,air} * \frac{MM_w}{R * T_{step}} * \frac{p_{step}}{h_{air}} * \ln \left(\frac{p_{step} - p_{sat}}{p_{step} - p_{air}} \right) \right] * d^2 * \frac{\eta}{4} \quad 5-66$$

For the evaporation occurring due to pressure release, the vapors formed during flash evaporation are calculated based on the enthalpy of the wort and the flash gas ratio at the given temperature and pressure:

$$y_{step} = Quality(water; p = p_{step}; h = h_{process,step-1}) \quad 5-67$$

$$m_{vapors,step} = y_{step} * m_{process} \quad 5-68$$

Other evaporation processes are modelled based on time ratio of boiling steps with vapour formation:

$$m_{vapors,step} = m_{vapors} * \left(\frac{t_{step}}{t_{boiling}} \right) \quad 5-69$$

The results of the energy demand profiles are stored for each process step and then summarized in Excel where in combination with the information on the operation schedules a demand profile for one week is calculated. A screen of the Excel-tool for the mashing process is shown in Figure 9-1 in appendix A and an example of the result visualisation is shown in Figure 5-12.

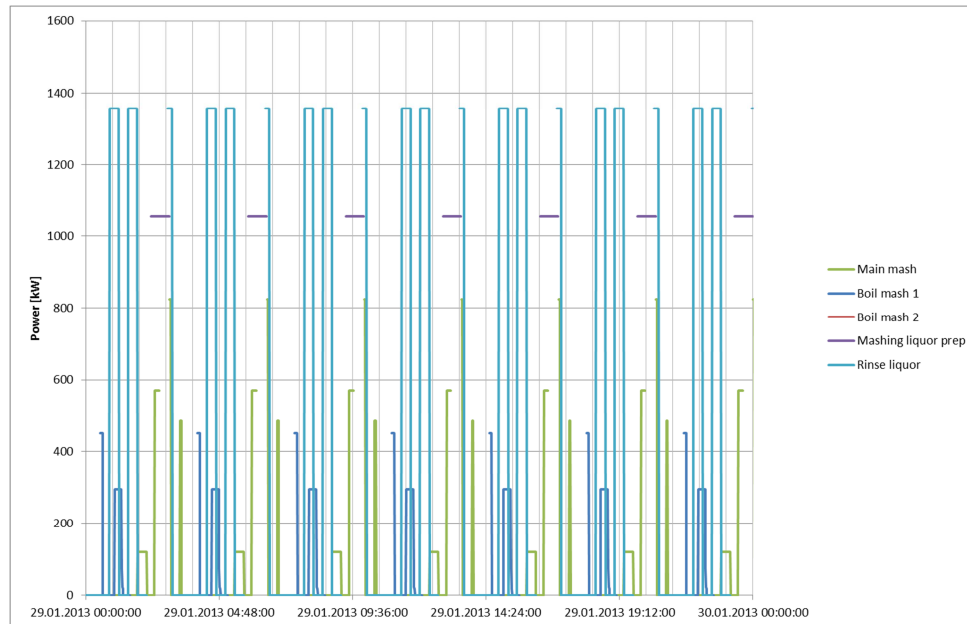


Figure 5-12: Visualisation of an energy demand profile for the mashing process

5.1.9 Modelling effects on selected qualitative parameters

5.1.9.1 Modelling effects of process parameters in mashing

To analyse the effects of temperature gradients and temperature profiles in the mashing process kinetic models for the mashing process were implemented into the brewery model. Based on the available models (see chapter 4.3.1.2) the following two models were chosen:

Model A: Model A is based on the work of Marc and Engasser [136] and of Koljonen and co-workers [114]. As the work of Koljonen built upon the basic model of Marc and Engasser, the setup of these two models is quite similar. The main difference is a difference in kinetic parameters, due to the fact that enzyme concentration is specified in g/l in the model by Marc and Engasser, while Koljonen and co-workers need the enzyme activity in U/l as input parameter. A combined model “model A” was implemented in EES. The kinetic mashing model assumes instantaneous dissolution of carbohydrates already present in the malt and gradual gelatinization according to the findings of Koljonen et al. The degradation of native starch to dextrans is modelled via the activity of α -amylase while subsequent degradation to maltose and other fermentable sugars is modelled primarily over the action of β -amylase. Model parameters have been taken from Marc and Engasser.

Model B: Model B is an implementation of Brandam’s work [44]. As in Model A, it models starch degradation over the action of α - and β -amylase. Input parameters are starch composition and enzymatic activities of the malt (U/g malt). In comparison to Model A the reaction pathways are modelled differently, as more degradation paths (e.g. release of maltose) are attributed to the action of α -amylase in comparison to β -amylase (see also chapter 4.3.1.2 for basics on the kinetic models in literature).

The following results are available for each model:

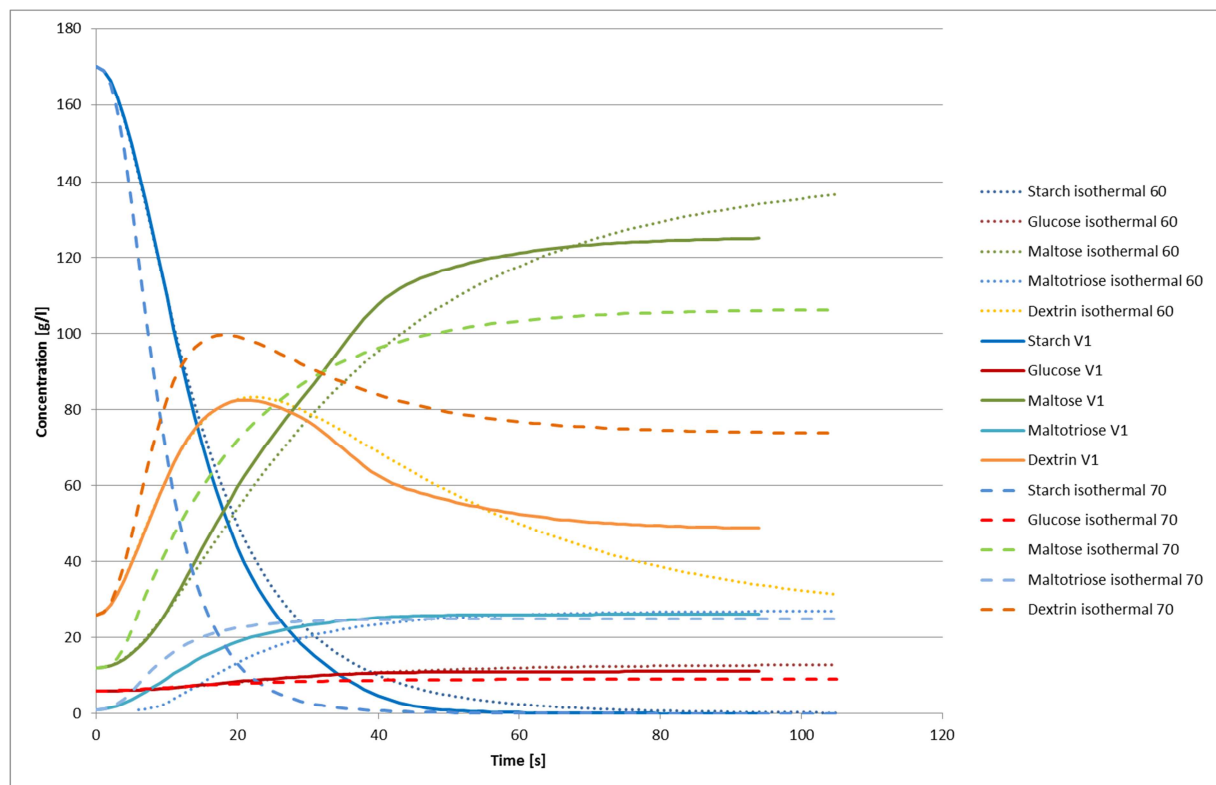
- Profiles of enzyme activities

- Concentration of fermentable and non-fermentable carbohydrates over the mashing time

The aim of including a kinetic mashing model in the Brewery model was twofold:

1. To allow the user to evaluate the effects of different temperature programs on fermentable sugar formation
2. To develop new potential mashing temperatures programs suitable for low temperature heat transfer to be later evaluated in laboratory experiments.

These main aims are met with models that allow the relative comparison between different temperature programs while the absolute results per temperature program are less important. The temperature sensitivity of the model is clearly a decisive aspect. The models were therefore evaluated based on their suitability to compare different temperature programs for infusion mashes. Formation of fermentable sugars and enzyme concentration was modelled over the course of several mashings. Both models show sensitivity to different temperature profiles. Figure 5-13 shows the results of implementing three different mashing profiles for both models: a standard industrial temperature program and two isothermal mashings at 60 and 70 °C. All mashings start at a mashing-in temperature of 58 °C. The standard industrial program then heats the mash to 62 °C, rests for 15 minutes at this temperature before further heating to 72 °C. After a 2nd rest at 72 °C final heating is performed up to 75 °C where the temperature is held in a last rest for 25 minutes. The isothermal mashing heat the mash to the target temperature within 5 minutes and hold the defined temperature for 100 min.



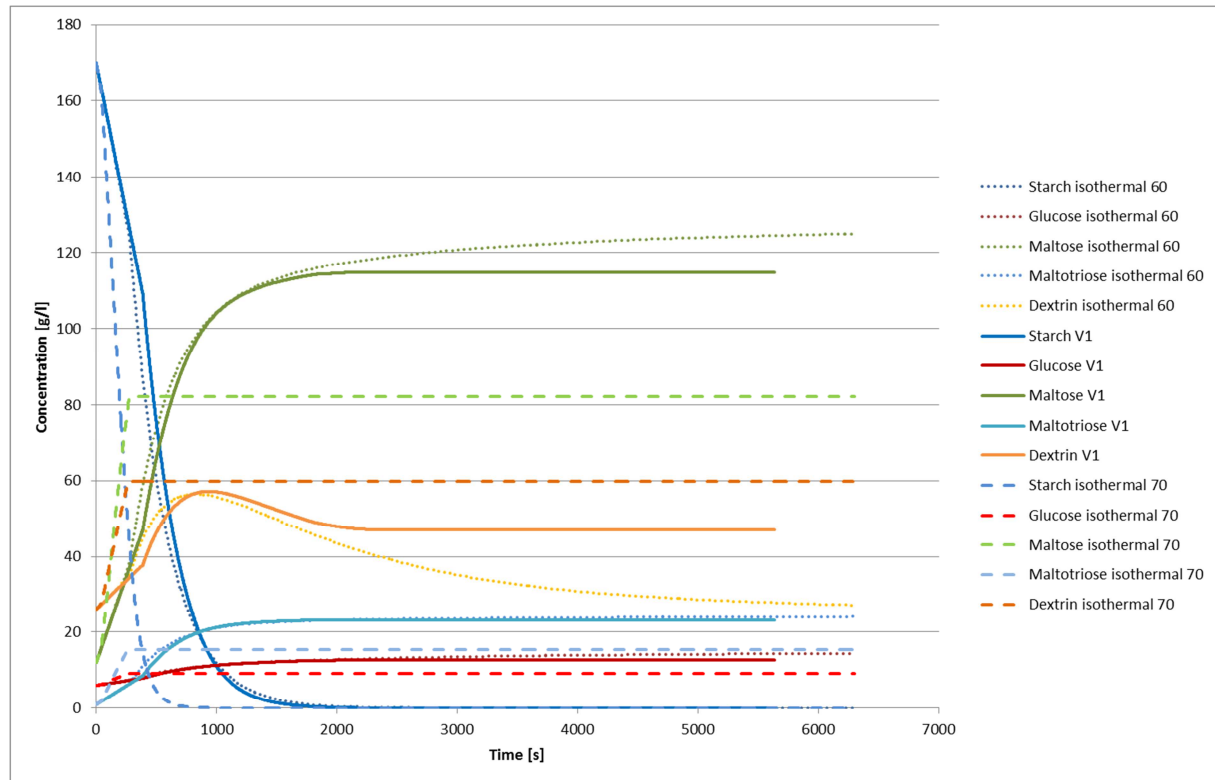


Figure 5-13: Temperature sensitivity of the implemented kinetic mashing models (top: Model A, bottom: Model B)

The modelling shown in Figure 5-13 was done based on the enzyme activities stated in each of the reference papers on which the models are based [44, 136]. Therefore the formation of fermentable sugars cannot be compared on absolute terms, due to the different enzyme activities. In Model A reference enzyme activity of α - and β -amylase are identical, whereas in Model B β -amylase activity is significantly higher than α -amylase activity. However, similar trends can still be observed in Figure 5-13. Highest maltose concentrations are reached at isothermal mashing at 60 °C, as β -amylase activity is still high at this low temperature. In contrast lowest fermentability is reached with isothermal mashing at 70 °C where dextrin concentration remains high, as the heat sensitive β -amylase is not able to degrade dextrans to maltose. The standard industrial mashing program reaches values close to mashing isothermally at 60 °C, while still enabling the mash to heat to lautering temperature and inactivating enzyme activity at the end of the process to reach a stable mash quality.

In addition to different reference enzyme activities, there are even more distinct differences between Model A and Model B. Two important differences are the difference in modelled starch degradation pathways and the different enzyme dissolution modelling (see 4.3.1.2). While Model A relates α -amylase activity primarily to degradation of native starch to dextrans and models further degradation of dextrans to sugars via β -amylase activity, Model B models the formation of sugars from dextrin over α - and β -amylase activity. Another major difference is that Model B assumes an immediate dissolution of enzymes into the liquid phase, while model A includes modelling their dissolution within the first time of the mash procedure.

Both of these differences show the fact that starch hydrolysis and formation of fermentable sugars is modelled faster in Model B. The difference in enzyme dissolution becomes clear when the relative enzyme activity is calculated over the mashing time. Figure 5-14 shows a recalculation of the solubilized enzyme concentration of Model A (related to enzyme activity) and the enzyme activity modelled in Model B to relative enzyme activities in order to compare the two models. Relative enzyme activity of each enzyme ($Act_{rel,i}$) is simple calculated over the current activity of each enzyme (Act_i) based on its maximum activity during the course of mashing ($Act_{max,i}$).

$$Act_{rel,i} = \frac{Act_i}{Act_{max,i}}$$

5-70

It becomes clear that the enzyme activities in Model A lag behind those modelled in Model B. Denaturation is additionally modelled stronger and at lower temperatures in model B.

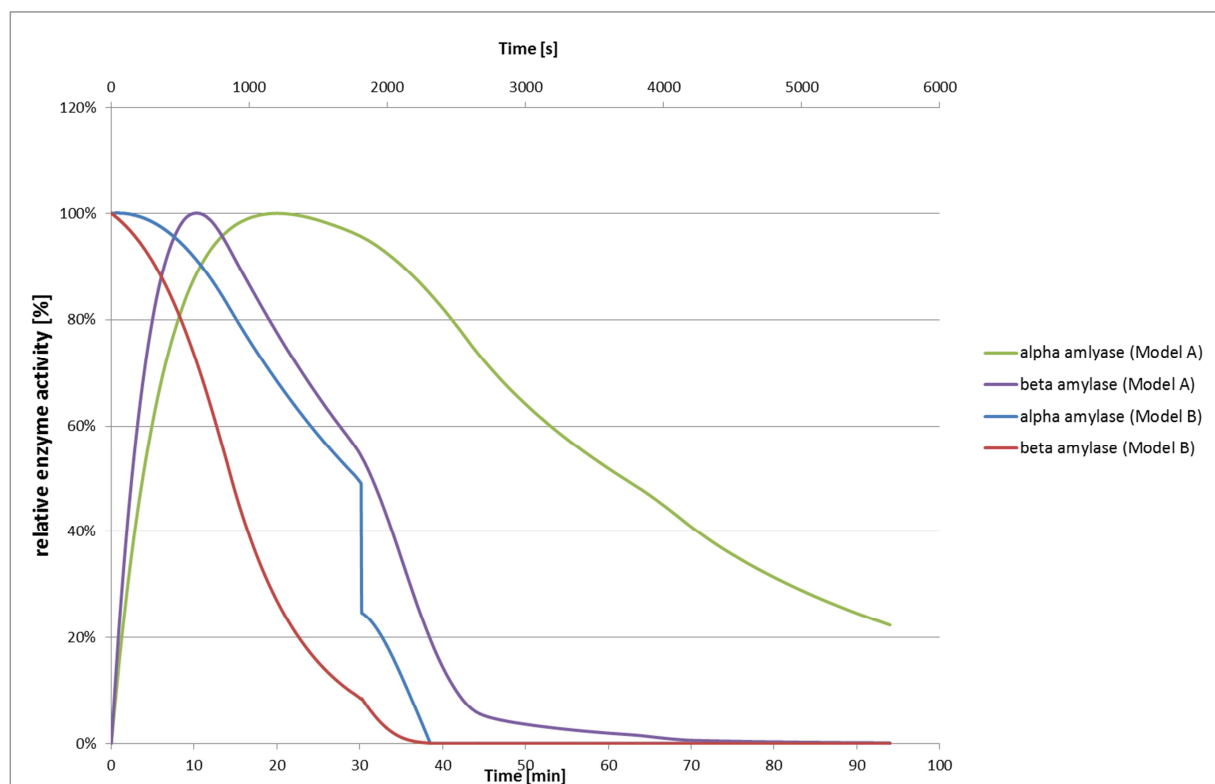


Figure 5-14: Relative enzyme activity over time modelled for an industrial temperature programmed mashing

Figure 5-15 and Figure 5-16 directly compare the formation of sugars in an industrial temperature programmed infusion mash modelled by Model A and B. For easier comparison similar ratios of enzyme activities have been chosen in both models. Enzyme activities in Model B were taken according to the reference literature [44] and the enzyme concentrations in Model A were adapted: First β -amylase was taken as stated in the reference literature [136] and α -amylase was recalculated with the activity ratio of Model B. Then α -amylase was taken as stated in the reference literature and β -amylase was recalculated with the activity ratio of Model B. Input parameters are given in Table 5-5.

Table 5-5: Input parameters for modelling starch degradation with similar enzyme activity ratios

	Run 1	Run 2		Run 1 and 2
Model A			Model B	
α -amylase	4.8 mg/l	12 mg/l	α -amylase	200 U/g
β -amylase	12 mg/l	30 mg/l	β -amylase	500 U/g
Ratio	2.5	2.5		2.5

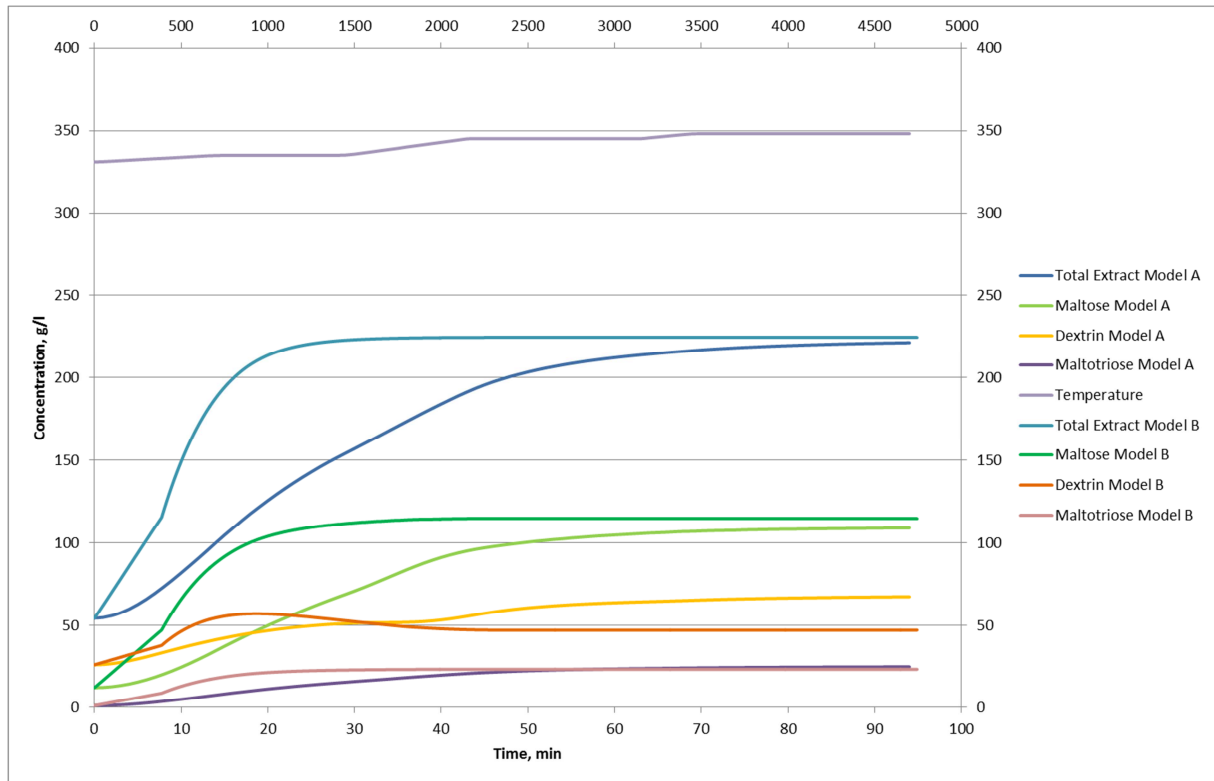


Figure 5-15: Run 1: Starch degradation modelled in Model A and B with same enzyme activity ratios

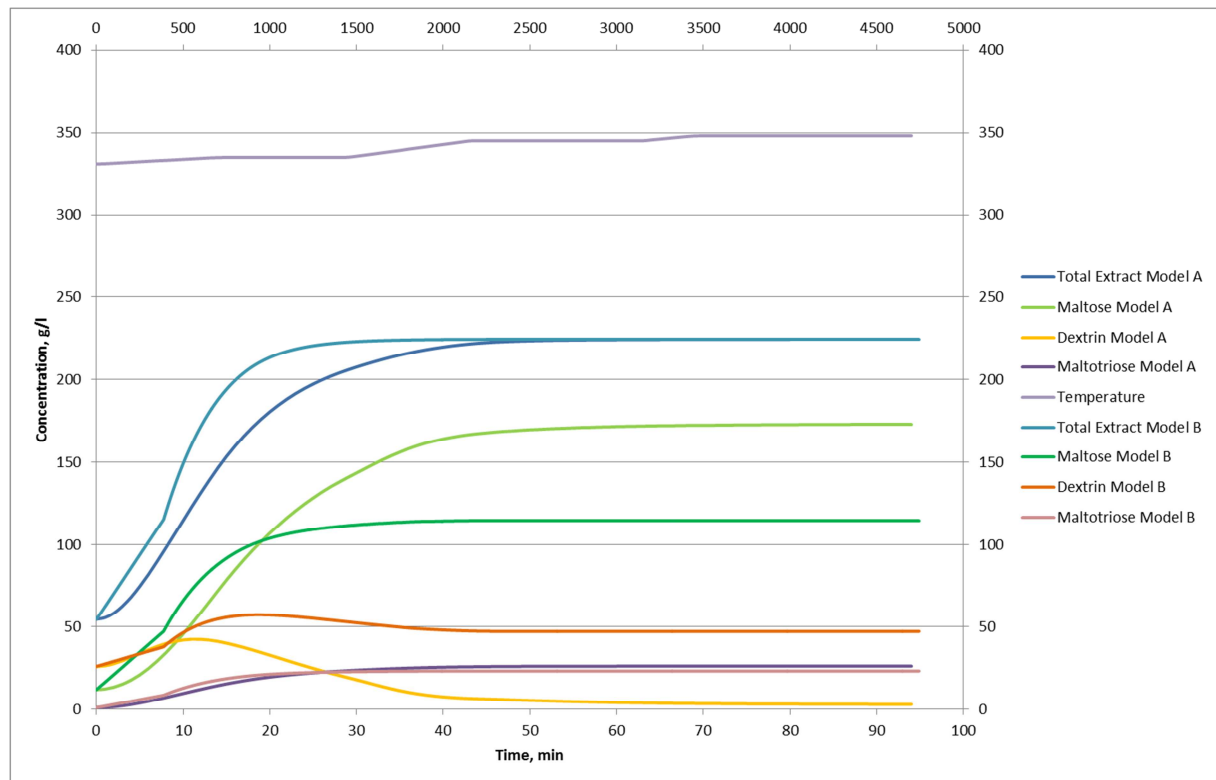


Figure 5-16: Run 2: Starch degradation modelled in Model A and B with same enzyme activity ratios

The comparison in Figure 5-15 shows the evidence that in Model A the formation of sugars occurs slower due to the fact that all starch has to be degraded first by α -amylase in order to be transformed to maltose by β -amylase. In Run 1 the concentration of α -amylase is minimal and therefore reaction takes time. In Run 2 the hydrolysis of Model A is much faster due to higher availability of α -amylase, however the increased concentration of β -amylase leads to the fact that dextrins are almost completely degraded to maltose and other sugars. Therefore the maltose concentration is much higher compared to the findings of Model B.

Due to their differences it was decided that both models in the Brewery Model would be initially implemented, while own mashing trials should confirm the accuracy of the models. One major limitation of Model A is the required input of enzyme concentration in g/l. This is usually not available as the standard measurement for enzyme activities is U/g of malt.

The implementation of both models in separate EES programs is accessible via the mashing technology tab in the Brewery Model. The complete equation set of the model is presented in appendix 9.3. The applied models are deliberately created to be simple and not to take into account all aspects of mashing, due to the following arguments:

Glucan hydrolysis was not taken into account in the models, because it was not presented in the literature from either of the two models [136], however it is presented by Kettunen et al., 1996 and re-visited by Durand et al., 2009 [67]. The laboratory tests finally confirmed the hypothesis that in mashes with high malt quality there is no need for glucan hydrolysis modelling for evaluating different temperature profiles.

Enzymatic action for sucrose and fructose formation was not modelled, as the temperature profiles considered in this work all start at a mashing-in temperature of > 55 °C.

Both models do not allow the analysis of the effects of finest of the grist. Based on the findings of Brandam et al., it can be concluded that the efforts to take into account grist finest in modelling the formation of fermentable sugars are not worth considering for model improvement [44].

The amount of grist and water added to the grist are input parameters to Model A, so this model could potentially show the effect of mashings for worts with different gravity. In Model B these parameters are not taken into account. However, all model parameters have to be adapted to correctly represent gravity. The parameters taken from Marc and Engasser are suitable for worts with a gravity of 12 °Plato.

The initial model implementations were verified with literature values for the mashing process and later-on verified with analysis results from 20 practical tests performed in laboratory scale. Results are shown in chapter 6.

5.1.9.2 Modelling gravity decrease during fermentation

For beer fermentation it is important to be aware that the initial concentration of fermentable sugars are in the wort, as these are converted by the yeast to alcohol and carbon dioxide as main products. Wort gravity is traditionally measured in °Plato. 1 °Plato is equivalent to 1 g sucrose/100 g water. Therefore a lager wort with a specific gravity of 12 °Plato (equivalent to a gravity of 1046 kg/m³) contains approximately 12.6 g extract/100 ml wort. Approximately 75 % to 85 % of these sugars will be fermentable and are actually converted to ethanol [59].

For the thermal energy balance of a brewing site the heat released during fermentation is a decisive aspect. Therefore a simple fermentation model was sought to be included into the Brewery model. Several models from literature [56, 57, 93, 198] were evaluated to show the uptake of sugars and conversion to alcohol over time. The biochemical model proposed by Trelea et al. [198] can be used for the assessment of sugar consumption during the course of fermentation. It actually describes the production of CO₂ and relates it to sugar consumption, reduction of wort density and ethanol production. The produced CO₂ C_{prod} is calculated via Treleas model taking into account substrate limitation via the Monod constant K_s and inhibition by ethanol accounted for by the constant K_i. The model is shown in appendix 9.2.3.

$$C_p = \int_0^{t_{\text{total}}} \left[\left(v_{\text{max}} \cdot \left[\frac{S}{K_s + S} \right] \cdot \left[\frac{1}{1 + K_i \cdot E^2} \right] \right) \cdot (C_p + C_0 \cdot X_0) \right] dt \quad 5-71$$

$$S = S_0 - Y_S \cdot C_p \quad 5-72$$

$$E = Y_{E;g} \cdot C_p \quad 5-73$$

$$D = D_0 - Y_D \cdot C_p \quad 5-74$$

The maximum reaction rate v_{max} in this model is dependent only on operating conditions temperature, pressure and yeast concentration.

The model was built upon data taken from pilot scale experiments at a constant fermentation temperature. Fermentations have been performed between 10 and 15 °C. Thus, the comparison with literature data cannot be done on an exact basis as not only operating conditions such as

temperature and pressure influence the results as well as the wort composition and the specific yeast strain used [198]. The model was simulated with EES (Engineering Equation Solver) and the outcome compared with the sugar consumption or wort density reduction rates stated in other literature [56, 59, 159].

To reproduce the expected fermentation rates and CO₂ and ethanol concentrations, two factors of the model have been adapted. The yield coefficient of CO₂ based on density Y_D was adapted to account for a correct balance between sugar consumption and density decrease. The factor K_i accounting for the ethanol inhibition effect was also adapted to reach realistic ethanol concentrations. The fermentation profile reached via these changes corresponds to the findings of other authors [59, 159]. As the minimum temperature in Trelea's model is defined with 10 °C, the fermentation profiles at lower temperatures are less accurate, as data for these have not been validated during model development. However, as most industrial (bottom) fermentations predominantly take place at 10-13 °C, a lower accuracy at temperatures below 10 °C does not substantially affect the usability of the model.

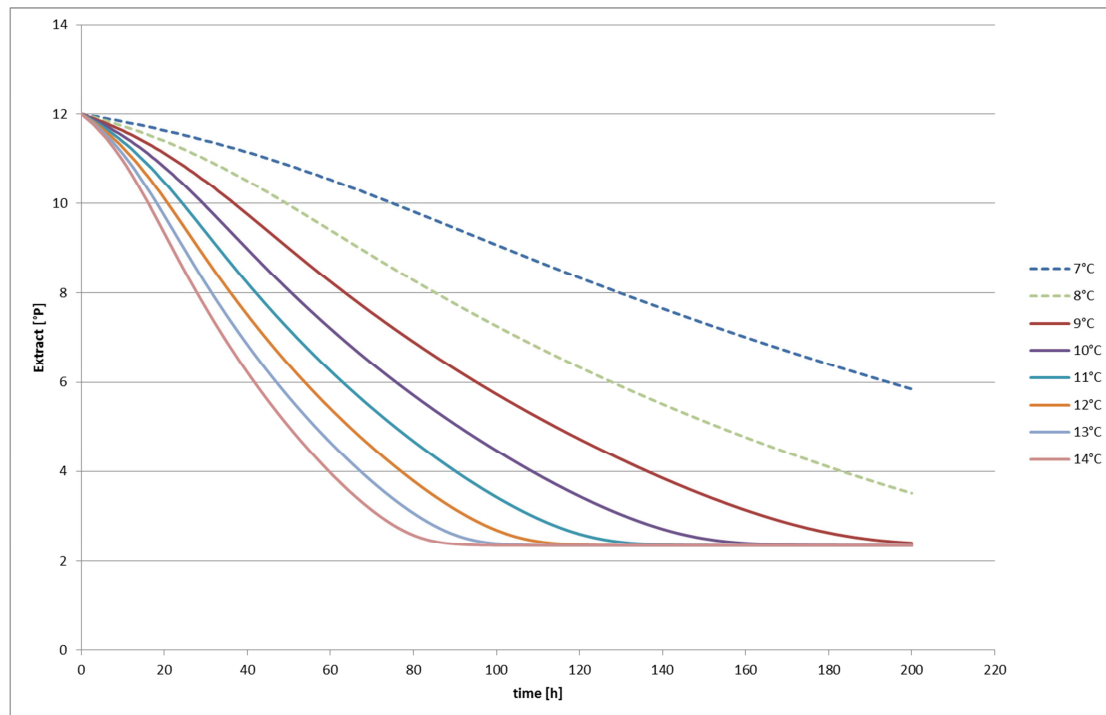


Figure 5-17: Reduction of wort gravity over fermentation time for various fermentation temperatures (initial wort gravity 12° Plato)

The fermentation model was linked to the brewery model over the fermentation section. The initial concentration of fermentable sugars in the wort modelled in the brewhouse section of the brewery model is the starting point for the model. Gravity given in g extract/100 g wort is converted to g/100 ml according to the Plato tables [120]. Based on the data entries on wort fermentability, pressure and temperature in the fermentation section of the brewery model, the model can be calculated. Data can be exported to and visualized in Excel. The model implementation in EES was extended to model the fermentation profiles based on a defined temperature profile during fermentation. Based on user specifications and typical temperature profiles [56] the temperature profile is calculated and the actual fermentation profile is checked in each time step during modelling. An example of the formation of ethanol and CO₂ is shown in Figure 5-18, for wort with

initial gravity of 12 °Plato with pitching temperature of 9 °C and main fermentation temperature of 12 °C.

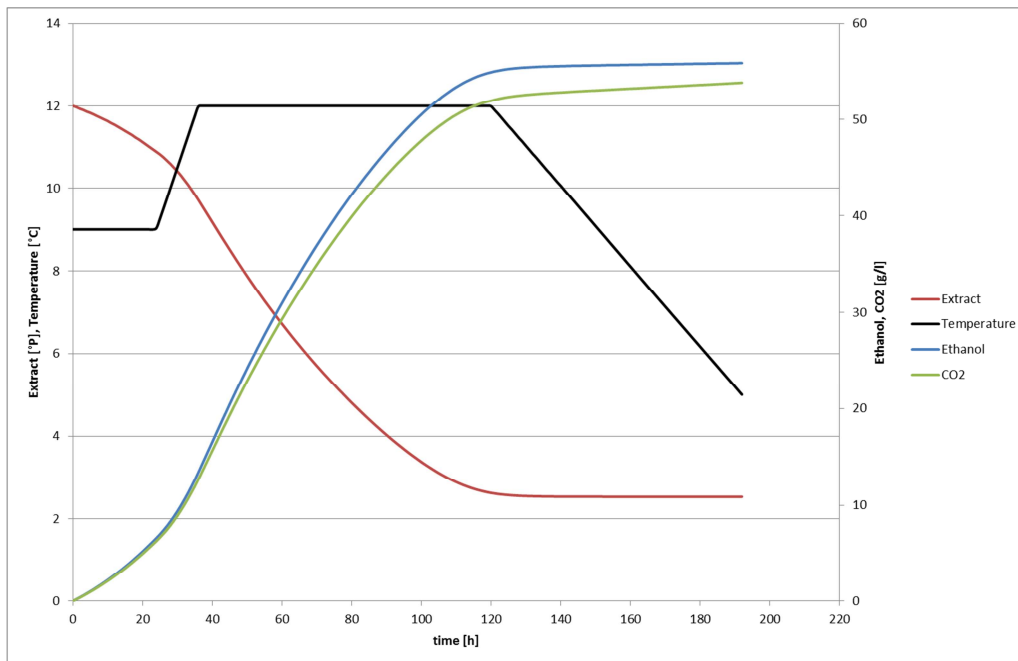


Figure 5-18: Formation of ethanol and CO₂ based on the biochemical model (initial gravity of 12°Plato; pitching temperature of 9°C and main fermentation temperature of 12°C)

Furthermore a comparison was performed between the effects of the implemented EES model on initial wort gravity (see Figure 5-19) and the effects published earlier. The main result was that the fermentation time only increases slightly with higher wort gravity and this can be proved with the model. It must be stated that the differences between earlier published experiments and the outcome of this model are probably a result of different operating conditions.

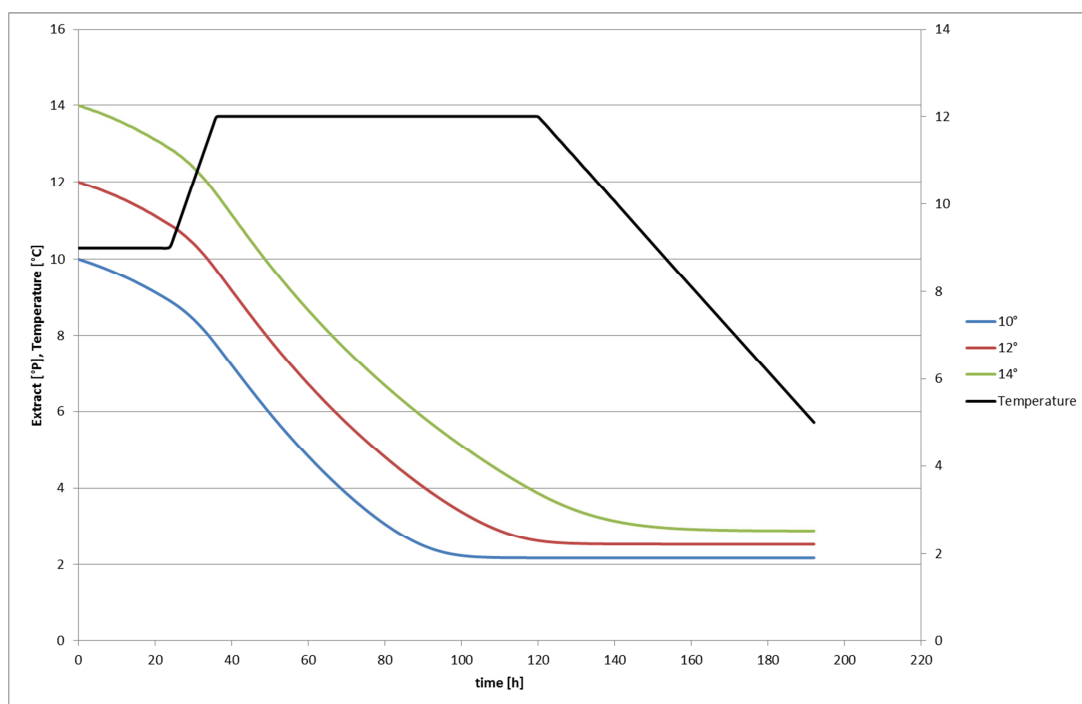


Figure 5-19: Reduction of wort gravity as a function of initial wort gravity acc. to the biochemical model (initial yeast cells 10 x 10⁶ cells/ml; saturated oxygen)

Due to its simplicity, the implemented model will not reproduce an exact reduction in wort gravity. However it seems to represent similar fermentation profiles as presented in literature for similar operating conditions. The model was primarily implemented to calculate the cold demand based on the fermentation profile, which can be done with satisfying accuracy (see chapter 5.1.10).

5.1.10 Modelling the cooling load in breweries

5.1.10.1 Parameters influencing cold demand profiles in breweries

Figure 5-20 shows the specific electricity demand for cold production of three breweries from the years 2008-2010. The breweries have the following characteristics:

- Brewery 1: NH₃- direct evaporation (in most plants) and water-based re-cooling, evaporation temperatures -3 °C to -6 °C
- Brewery 2: NH₃ and R404a evaporators und glycol as cold transfer medium, dry re-cooling, evaporation temperature -10 °C
- Brewery 3: R22 and R404a evaporators und glycol as cold transfer medium, dry re-cooling, evaporation temperature -7 °C to -9,5 °C

All breweries have cylindroconical fermentation tanks with jacket-cooling.

For all breweries we can dedect an increase in specific electricity demand for cold production in the summer months. In Brewery 2 and 3 also higher demand occurs in october and november. The comparison between demand in the summer months from May to September with demand in the winter months from January to April shows an increase in specific electricity demand for cold production by 29 % (Brewery 1) to 46 % (Brewery 3). It is important to note that Brewery 3 also cools an administrative building in the summer time.

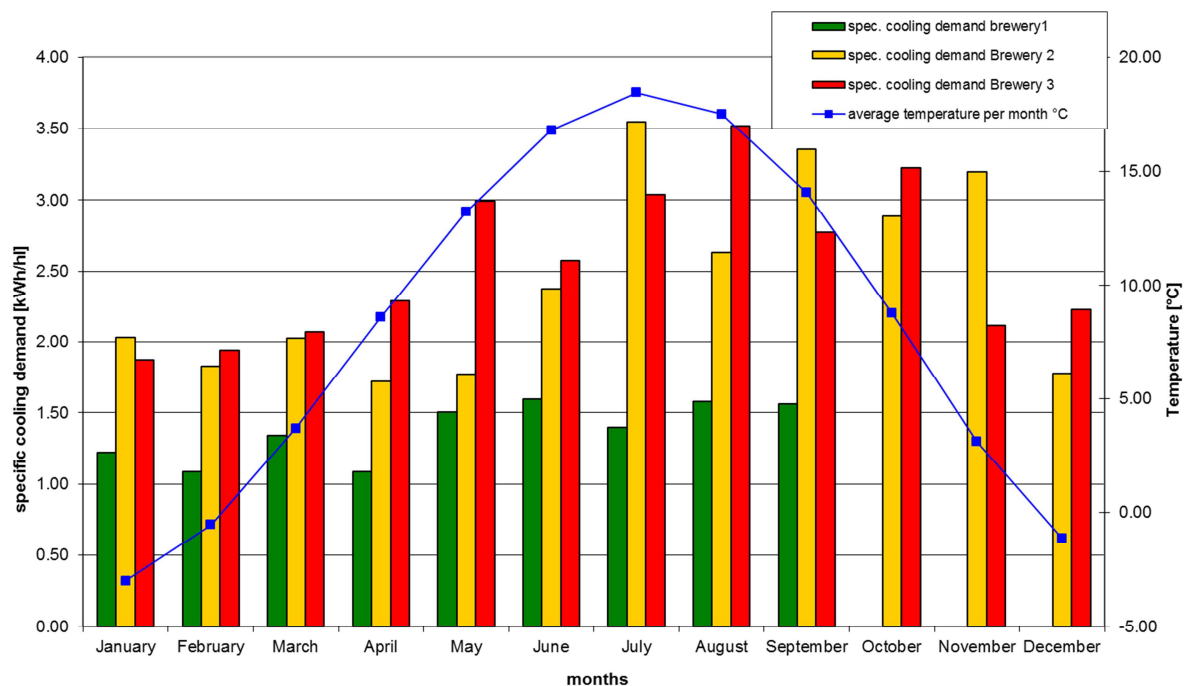


Figure 5-20: Electricity demand for cold production from 3 breweries (Brewery 1 data from 2008, Brewery 2 data from 2010 and Brewery 3 data from 2009) in comparison with the average ambient temperature per months in 2008 at the site of Brewery 1

An important reason for this increase is the reduction of EER of cooling compressors at higher condensation temperature in summer. For ammonia evaporators the theoretic EER of a cooling machine at typical evaporation temperatures reduces by 12-13% when the condensation temperature decreases by 4 °C at constant evaporation temperature (siehe Figure 5-21). This effect of increasing condensation temperatures is much more significant at breweries with dry re-cooling in comparison to sites with water based re-cooling systems. For modelling the process cooling demand, however, this effect does not have any influence.

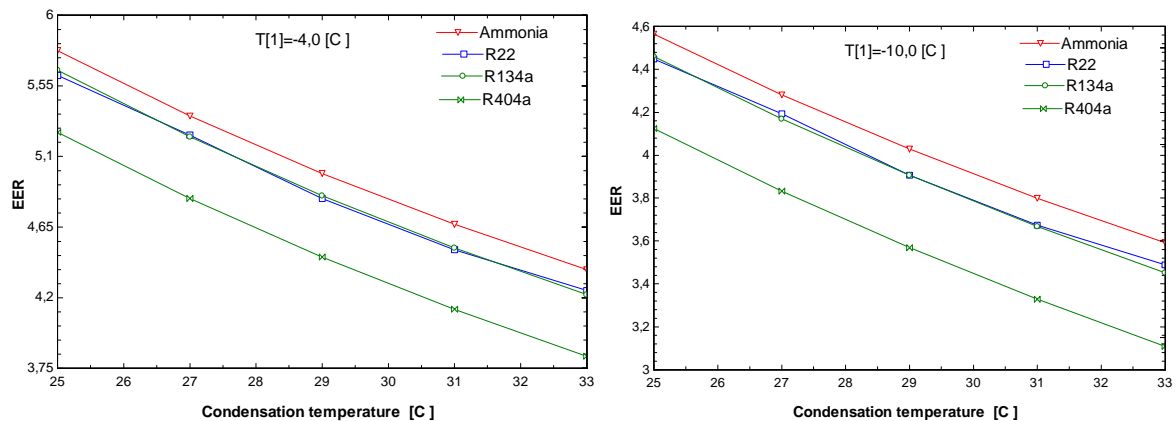


Figure 5-21: Influence of evaporation (T₁) and condensation temperature on the EER of a single-stage cooling compressor

Another reason for the higher cooling demand in summer is the brew water cooler that delivers chilled water for wort cooling. In the winter months the available cold water is often sufficient or only requires minimal cooling. In the summer months this cooling demand increases. An increase of fresh water temperature by 4 K leads to an increase of 9.5% of the overall cold demand and respectively to an increase of 9.5% of electricity demand for cold production. The increase of fresh water temperature is linked to the increase of the ambient temperature, so there is a direct link between ambient temperature and process cold demand.

Based on these two reasons an increase of 10-30% of electricity production can be explained, depending on the site-specific increase of fresh water temperature and condensation temperature in the summer months.

Based on this analysis it can be concluded that an additional effect of ambient temperature to the process cooling demand is in the range of 10%. The ambient temperature also influences, depending on the construction, the radiation losses of the cellar buildings where fermentation and maturation is carried out. The assumption that ambient temperature only has minor effects to the process cooling demand (besides the factors stated above) is confirmed in a detailed analysis of the cooling demand of one brewery over one month with comparison of ambient temperatures (see Figure 5-22).

It can therefore be concluded that the ambient temperature influences the process cooling demand mainly based on two factors:

1. Increase of fresh water temperature (effect on brew water cooler) and
2. Increase of radiation losses of the buildings.

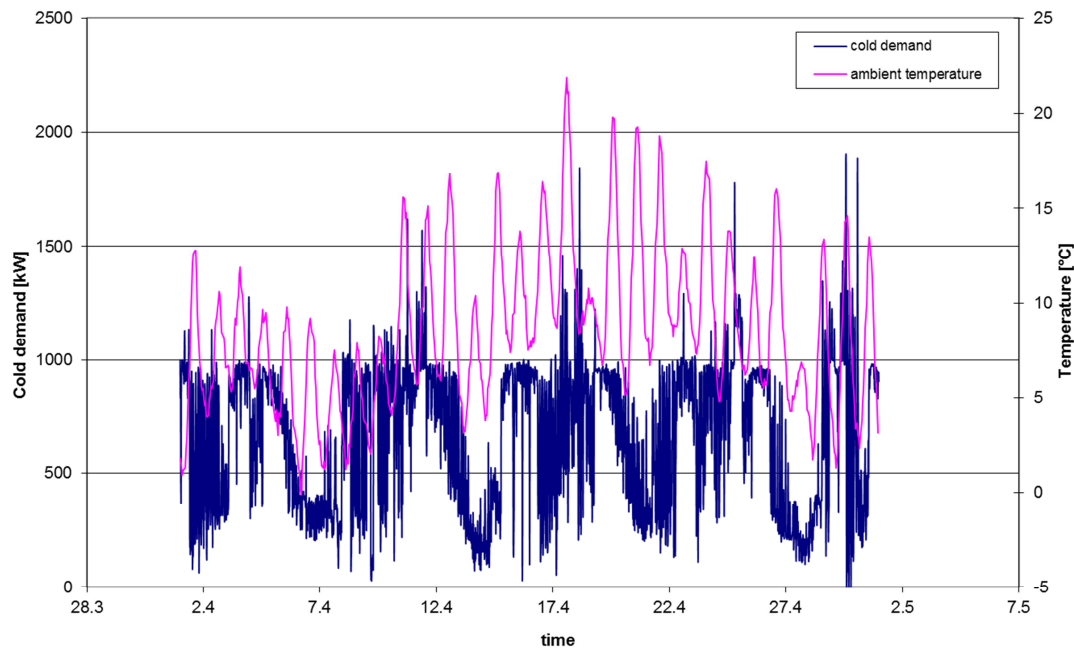


Figure 5-22: Effect of ambient temperature of the cold demand of one brewery (measured data)

5.1.10.2 Calculation of cold demand profile

A few general parameters are essential in order to correctly calculate the variations of processes with cold demand. These conform to the general parameters defined in the Brewery Model (see 5.1.7). Below the most important equations for calculating the cold demand are shown. As stated above (5.1.3) several processes are responsible for the cold demand in breweries. While the fermentation model is calculated in EES, the cold demand of all other processes and the overall cooling demand profiles are combined in an Excel tool linked to the Brewery Model.

Brew water cooling

The brew water cooler is calculated based on the water and beer flow capacity and the water temperatures defined by the user:

$$Q_{BWC} = \frac{\text{capacity}_{BWC} * \rho_w * cp_w * (T_{FW} - T_{CW})}{\eta_{BWC}} \quad 5-75$$

As discussed above, the variations in fresh water temperature can significantly influence the cold demand of the brew water cooler. Calculations are based on a typical fresh water temperature or on user-defined minimal and maximal fresh water temperatures. The influence of these temperature variations over the year is taken into account via a parabolic equation. A direct coupling of fresh water temperature to ambient temperature has not been integrated, as the fresh water temperature may depend more or less on ambient temperature based on its source (river water, spring water etc.).

Fermentation

For modelling of the cooling requirement it is necessary to take into account the varying cooling rate which is heavily influenced by the fermentation rate of the beer, as fermentation is a major contributor to cold demand in breweries. During fermentation, cooling needs to be applied to make

up for the heat generated in the exothermic processes. The heat released can be assessed as difference of internal energy of glucose (2880 kJ/mole glucose) and alcohol (2740 kJ/mole glucose). A certain amount of the energy difference is stored by the yeast as 2 ATPs (61 kJ/mole)[59]. The heat of reaction is therefore roughly 100 kJ/mole glucose (556 kJ/kg extract).

Based on the model and the resulting wort gravity the cold demand is calculated based on the reaction heat (see 4.3.1.4) and the amount of extract that is fermented in the respective time step. The initial concentration of fermentable sugars in the wort modelled in the brewhouse section of the brewery model is the starting point for the fermentation model. Fermentation temperature and rate must also to be defined.

$$Q_{ferm} = \frac{(E_{ferm,i} - E_{ferm,i-1}) * q_{ferm} * V_{tank} * Convert(hl, l)}{\eta_{ferm,tanks}} \quad 5-76$$

Modelling of the demand profiles takes into account the number of fermentation tanks and the typical tank volume. These parameters are crucial to determine when fermentation tanks are filled with wort and when fermentation begins. Lastly, the duration of main fermentation and the information regarding whether the wort is further cooled after main fermentation within the fermentation tanks are required. Based on these parameters the cold demand profiles of the fermentation tanks can finally be calculated.

The continuous variations of the cold demand profile are only correctly modelled after some time, as the model needs some time until all tanks are filled and in operation. Therefore, the first weeks of modelling show a strong increase in demand, until the demand profile settles at the expected variations.

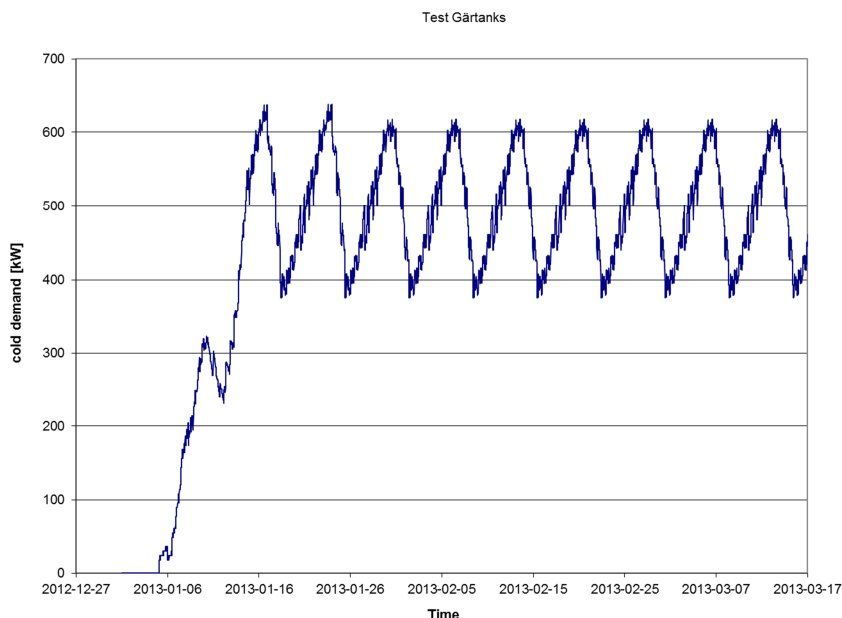


Figure 5-23: Demand profile of cooling requirement for the fermentation tanks

Beer cooler:

The beer cooler is calculated based on the water and beer flow capacities and the operation temperature which was defined by the user. The times when tanks are filled and emptied are known from the fermentation profiles and therefore the operation times of the beer cooler is also defined.

$$Q_{BC} = \frac{\text{capacity}_{BC} * \rho_{beer} * cp_{beer} * (T_{final,ferm} - T_{BC,out})}{\eta_{BC}} \quad 5-77$$

Yeast harvesting and storage

After harvesting yeast, it is cooled to the storage temperature to minimize its biological activity. This temperature is in the range of 2-4 °C. The yeast tanks, in which the yeast is stored and a minimal fermentation of the nutrients occurs, are also cooled.

$$Q_{YC} = \frac{\dot{V}_{yeastflow} * \rho_{yeast} * cp_{yeast} * (T_{yeast,in} - T_{yeast,out})}{\eta_{YC}} \quad 5-78$$

Maturation tanks

The required heat removal in maturation tanks is modelled similar to fermentation tanks over extract consumption and specific heat of reaction. However in most cases heat removal in maturation tanks is negligible, as fermentation is almost complete and cooling is usually done before the beer enters the maturation tanks. Therefore, no detailed load profile is calculated and the overall required heat removal is equally distributed over the maturation time.

$$Q_{mat} = \frac{1}{\eta_{mat} * t_{mat}} * [V_{mat,tank} * x_{ferm,mat} * q_{ferm} + V_{mat,tank} * \text{Convert}(hl, l) * \rho_{beer} * cp_{beer} * (T_{BC,out} - T_{mat})] \quad 5-79$$

The overall cold demand can finally be visualised and the demand profile can be taken as basis for further considerations on compressor operation and waste heat removal.

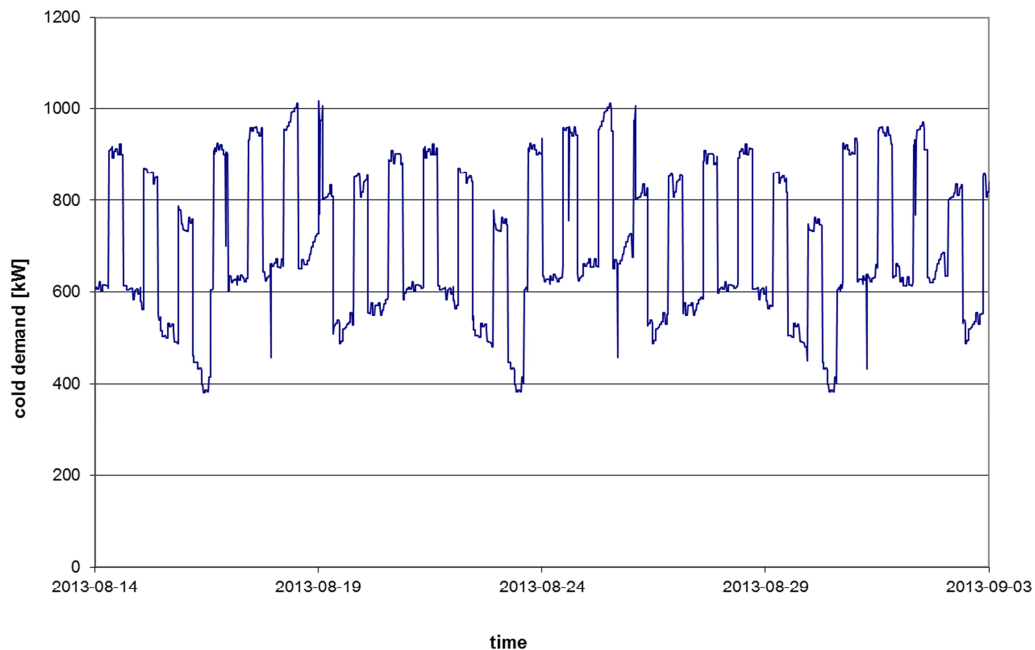


Figure 5-24: Modelled profile of cooling demand over several weeks in a 1 Mio. hl brewery

Influence of ambient temperature on the cooling load

Based on the analysis presented above (see 5.1.10.1) we can conclude that the influence of ambient temperature on the cooling load of breweries is rather small. The user has the possibility to enter his expert judgment on how much % ambient temperature influences the cold demand of the respective brewery. 10 % is given as an indicative value.

Based on the temperature variation over the year a parabolic approximate equation is generated. The integral of this equation is the cold demand which has to be allocated in addition to the process cold demand. Based on the integral values per month, a monthly factor is generated which shows the increase in cold demand due to the ambient temperature.

5.2 Optimization algorithm for heat integration based on pinch analysis and storage simulation (SOCO)

While modelling tools, such as the Brewery Model, allow the identification of material and energy flows based on chosen technologies, as well as comparing the effects of production parameters and implemented process technologies, a systematic approach for identification of heat integration potential and placement of renewable heat sources is still required. For this reason, a tool has been developed based on the pinch analysis which allows generation of heat exchanger networks and storage networks and the simulation of respective energy flows. The tool SOCO has been developed at AEE INTEC in a project consortium together with the Technical University of Graz. The implemented storage model and the algorithm for proposing new storages has been elaborated at the Institute of Thermal Engineering, while other algorithms have been developed at AEE INTEC by myself with scientific inputs of Jürgen Fluch and Christoph Brunner. The company Bongfish was responsible for the software development.

5.2.1 The need for heat integration tools for variable process streams⁴

For analysing heat integration options in processes that feature variable demand profiles, it is essential to take into account storages and their effects on heat transfer. This is required for batch processes, such as breweries, as well as for integration solar process heat. The need for such tools, in comparison to the graphical analysis available from pinch analysis, is shown in the following. Solar heat integration is discussed here as an example, however most of the facts also hold true for waste heat flows that are varying in temperature and time.

5.2.1.1 Identifying integration points based on graphical tools from pinch analysis

When it comes to integrating heat into thermal energy systems of a production site, the question of choosing the most suitable integration point, in terms of technical and economic aspects, has to be tackled. Solar heat, for instance, can be integrated to a specific unit operation (“on process level”) or in the utility system (“on supply level”) as e.g. heating of make-up water of the steam system. The integration point is defined as the interface between the solar plant (including solar heat storage) and the heat sink side (materialized by a heat exchanger transferring solar heat to the heat sink, or a valve / pipe connection if the heat sink media flows in the collector as well).

Solar heat has several unique features in comparison to other utilities: independent of any resources and free of costs, its availability and intensity are determined by the solar radiation and cannot be guaranteed. Additionally the efficiency of a solar collector is dependent on the collector inlet and outlet temperatures, so the choice of the integration point is important for the achievable solar heat gains. To address the integration of solar heat in Pinch Analysis, there are two main challenges: 1) the time dependency of the solar heat availability needs to be reflected in the analysis and 2) the solar heat gains will not be known in detail until the solar process heat system concept and especially the mean collector temperature is defined.

⁴ Parts of this chapter have been published in the following publication by the author:

Krummenacher P., Muster-Slawitsch B., Methodologies and software tools for integrating solar heat into industrial processes. 13th International Conference on Sustainable Energy technologies SET2014- E10049. Geneva, 2014.

Identification of minimum possible operating temperature and maximum heat rate of solar based on GCC

For the integration of solar heat into processes, the process GCC (for integration on process level) as well as the utility GCC (for integration on supply level) are relevant.

The process GCC (and total site profiles, in case total sites are analysed) shows the heat requirement per temperature level of the process(es) and therefore easily allows the identification whether heat supply at a temperature level appropriate for solar collectors is possible. As pointed out above, the GCC implicitly assumes full exploitation of the internal heat integration potential which is not always possible due to various limitations (in such a case the set of streams making up the GCC should be modified accordingly, changing the conditions for solar process heat supply). A GCC represents a heat balance of several hot streams and several cold streams within temperature intervals, so heating and cooling requirements of several unit operations are included or even of several processes in total site analysis. Therefore several unit operations often compose the heat requirement per temperature level depicted in the curve. If a solar plant is designed based on the process GCC, one assumes that it can supply several unit operations, some of which possibly only partially (e.g. preheating). In practice, this might be well possible, but experience has shown that this is not always economic in case the existing heat supply infrastructure has to be changed. In addition, different supply and return temperatures (different temperature gradients for heat transfer) might be necessary/possible for solar heat supply depending on the technical layout of the single unit operations. This has an important implication on the solar system, as return temperatures influence the efficiency of the solar plant to a large extent. Therefore, the selection of 1-2 unit operations is often sensible, which can be best supplied by solar heat.

The utility GCC, on the other hand, shows the temperature levels at which the process heating and cooling requirements are actually supplied. Based on this curve, the analysis of solar integration on supply level is well possible. Obviously we constrain ourselves by the existing utility network, likely resulting in higher exergy losses and less solar yield, depending on the location. But new utilities may be considered as well, in which case the constraint of the existing supply lines will be overcome.

As for all graphical curves in Pinch Analysis, there is a challenge to consider variable process streams (in terms of temperature and heat duty). Design considerations are therefore usually done based on time average representations (i.e. data averaged over time, considering time variable process streams as if they were continuous) or based on time slices [21]. For the latter, different curves in different time slices can be used as a basis to evaluate how the pinch point changes over time and whether this might influence the decision for the integration of solar heat.

For a food packaging line example process [118], the GCC is represented on Figure 5-25 (left) highlighting the possible placement of solar heat operated between 85 and 100 °C. This heat demand is composed of several processes. The curves as drawn assume full exploitation of the thermodynamic heat integration potential with all other streams. In case these heat recovery opportunities will not be followed, the GCC has to be re-drawn after the respective streams have been eliminated, as shown in Figure 5-25 (right). The GCC then looks very different. The process features a heat sink starting as low as 15 °C (corresponding to 20 °C for heat supply) and any supply of solar heat above this temperature will be thermodynamically sensible.

Once the maximum heat rate for solar heat is identified from the GCC, it needs to be analysed whether this heating requirement is composed of several streams. If so, the designer can either opt for supply line integration (usually a more flexible solution) or for process level integration of solar

process heat. If possible the designer might opt to integrate solar heat into the return line of the existing supply line (e.g. preheating the condensate prior to the boiler). However, this might be at a higher temperature in comparison to the process temperatures depending on the pressure of the existing steam supply, which is not visible in the process GCC. In case the designer wants to integrate solar heat at a temperature level around 80 °C, he will have to decide whether several processes will be (partially) supplied by solar or whether it is more economic to choose one process with the full share of heat demand in the respective temperature range.

While we have so far only considered grand composite curves, the same analysis can be done on the basis of total site profiles that have been suggested for designing heat supply for overall production sites. A total site profile is based on the data from several grand composite curves. The grand composite curves have been drawn per process and the information of all processes is then summarized in the total site profiles. In these profiles, as for GCCs, only the remaining heat demand is shown and a full exploitation of the heat recovery potential is assumed. In general, total site profiles provide the same information as a grand composite curve which has been drawn for several processes and all aspects discussed above are therefore valid.

The idea to use all waste heat in a central heat recovery loop to supply various processes might be viable especially if several processes require heat demand on similar temperature levels. In such cases the integration of solar heat can occur quite easily on supply level by integrating it into this central heat recovery loop. The economic viability of whether a process will be connected to this central loop will depend on the economic effort of integration and the percentage of its heat demand that is covered via heat integration. Heat recovery loops can be designed based on the hot and cold composite curve, however, limitations of temporal process variations in terms of temperature and heat duty have to again be considered.

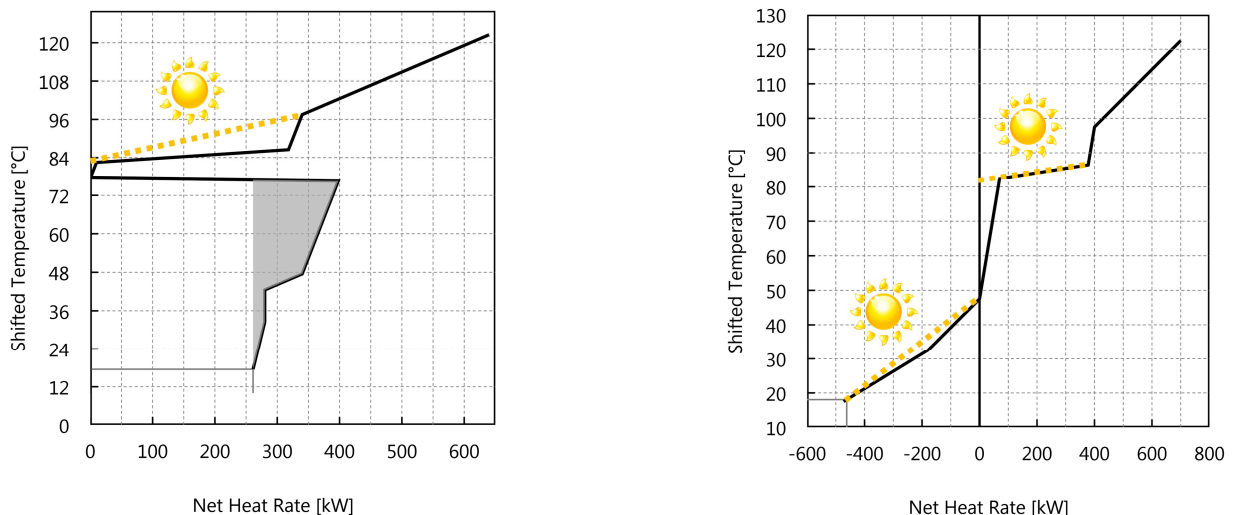


Figure 5-25: GCC of the food packaging line including all streams (left) , and GCC excluding several heat recovery options (right) at $\Delta T_{\min}=5^{\circ}\text{C}$. [116]

Drafting of the list of possible integration points of solar heat based on CCs

After the utilities (including solar heat) have been drafted based on the GCC, the hot utility streams can be added to the hot CC. For solar, the actual temperature and heat load will not be known until the integration point and the “solar process heat system concept” (the technical layout including all necessary components of the solar thermal system including storage, as well as the integration

concept) are defined (this is because the efficiency varies according to the technical layout and to the supply and return temperatures, which will be optimized based on the integration point(s)). In spite of this limitation, the addition of a “solar stream” to the CCs visualises the potential for solar heat integration quite well.

Again, since both hot CC and cold CC consist of several, partly superposed streams, design heuristics or computerised algorithms for placing heat exchangers are necessary to identify the most promising integration point. For solar process heat, such algorithms require the consideration of the time aspect (see below). But it is a challenge to consider the time aspect in CCs. Hot and cold CCs can show data on a full time average approach (average data over complete time cycle), on a time average approach taking into account operating hours (average data during operation hours in the time cycle) or single data in different time steps. To visualize the real variations of solar heat these time steps should be less than 1 hour. Other process variabilities (e.g. in start-up phases, batch processes) might require even smaller time steps. In this case the visualization of CCs can only be done with an interactive scroll bar over time. First design considerations will naturally be done based on time average representations. For solar heat, summer data should be applied to avoid a heat surplus in the summer time.

Figure 5-26 shows how the hot CC changes when adding the solar hot streams. It can be seen that the drafted heat rate corresponds to the maximum solar heat contribution which can be supplied for the selected temperature range. If the heat rate would be increased beyond these values, the cold CC should be moved to the right to maintain the ΔT_{\min} at the economic optimum, hence increasing the hot and cold utility consumptions correspondingly.

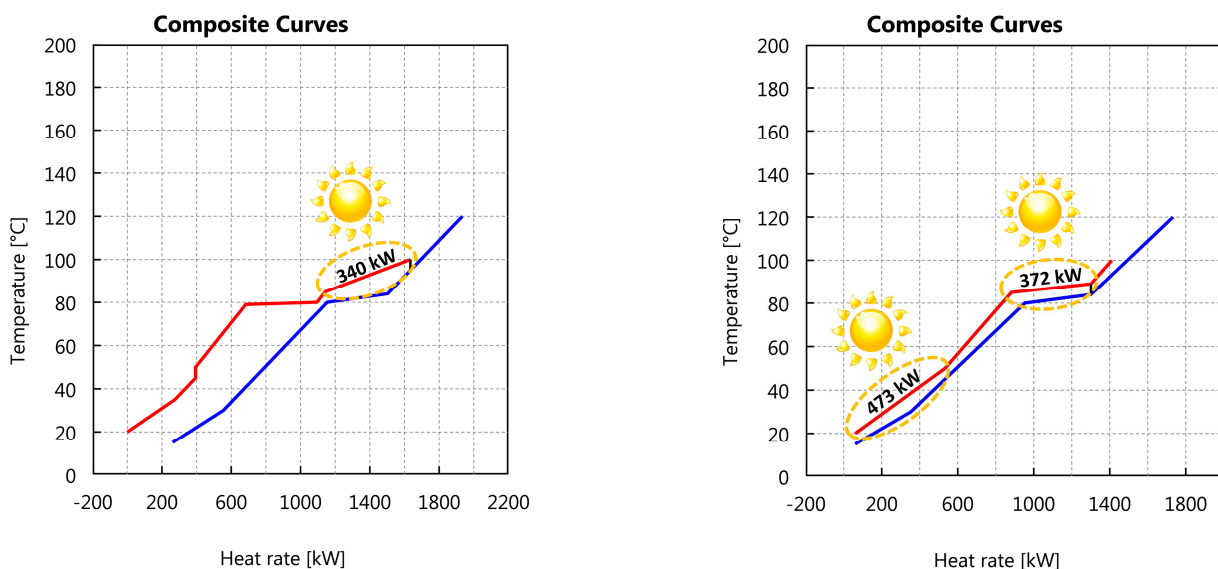


Figure 5-26: CCs after introducing solar heat as a hot utility stream (selected and sized with the GCCs from Figure 5-25); $\Delta T_{\min}=5^{\circ}\text{C}$. [116]

Practice relevant proposal of HESN and improvement by system flowsheet simulation

The GCC and CCs provide preliminary insight into the appropriate integration of solar heat and direct the analysis in the right direction, however there are limitations. One important limitation, which also holds true for batch processing in general, is that the graphical tools do not include time variability. As heat storage is extremely important for solar heat integration and the efficiency of the

solar process heat plant, this issue needs to be addressed. Obviously this holds true for all discontinuous process profiles. In processes with highly variable heat demand the practical measures (placing of heat exchangers, integration of solar heat to a specific integration point) may not be identifiable solely based on the graphical analysis.

From the discussion above it becomes clear that the tools offered by pinch analysis are powerful for first considerations of heat integration for variable process streams, however for planning the practical design it is necessary to consider temporal variations and possible thermal storage in detail. Here, the designer has to advance from the pure graphical representation to an optimization based approach. One possible way to do so is to

- design a heat exchanger and storage network for waste heat integration with an algorithm considering the aspect of time,
- analyse the remaining heat demand and subsequently
- re-design this network due to new utility integration (such as solar process heat).

For solar heat, this re-design can integrate solar heat as an additional heat source to certain processes and/or storages based on considerations done via the GCC or CC as discussed above. Alternatively algorithms for heat exchanger and storage network (HESN) design can propose most promising integration points.

Therefore heat exchanger and heat storage network design algorithms for variable process streams are required to identifying and compare process integration measures, and finally translate the thermodynamic potential to practical solutions. Based on such combined proposals of heat recovery, solar integration and storage placement, simple system simulations with adequate tools should deliver more precise information with only slightly more effort in comparison with the graphical analysis.

Due to the lack of programs allowing for such an analysis, SOCO has been developed.

5.2.2 The pinch software SOCO⁵

The newly developed pinch analysis tool “SOCO” allows the analysis of time-dependent energy demand curves (which may be generated by the brewery model). The SOCO tool, programmed in C#, allows the design of heat exchanger and storage networks (HESN) leading to minimal energy consumption of the total site. Below a short outline of the programme is given, mainly focussed on the calculation methodology. A manual for the software is available, to which the reader is referred for further details.

Data entry

The energy demand of process streams is defined over mass flows, heat capacities and temperatures, which can vary over time. An Excel template is provided for entering time-varying stream information. The duration of each time step can be chosen by the user, based on the available data (e.g. 1 second, 10 seconds, 1 minute, 1 hour etc). Heat exchangers and storages can be defined in

⁵ *Parts of this chapter have been published in the following publication by the author:*

Muster-Slawitsch, B., C. Brunner, and J. Fluch, Application of an advanced Pinch Methodology for the food and drink production, WIREs Energy Environment 3, (2014).

SOCO as components specified by the parameters shown in Annex B. Additional components include several types of splitters and mixers.

Pinch analysis

On the basis of the process streams a pinch analysis is carried out. The hot and cold composite curves, showing the cumulative enthalpy-temperature curves for hot and cold streams respectively, can be shown for each time step or in a time-average approach.

Simulation of the thermal energy system

Energy flow simulation in heat exchangers and storages can be conducted based on a user-defined Visio drawing of the thermal energy system. An iteratively working calculation solver has been developed and integrated which solves the (in case of storages non)-linear energy balance. The solver algorithm checks which component is defined and solves the problem in steps. In case of dependencies between two components, the components are calculated several times. A matrix gives an overview of the systems inter-dependencies and its solve-ability. This solver-matrix is shown in Figure 5-27 for a simple example of hot water preparation. A hot stream is stored in a storage tank and is later on used for heating the water requirement (cold stream).

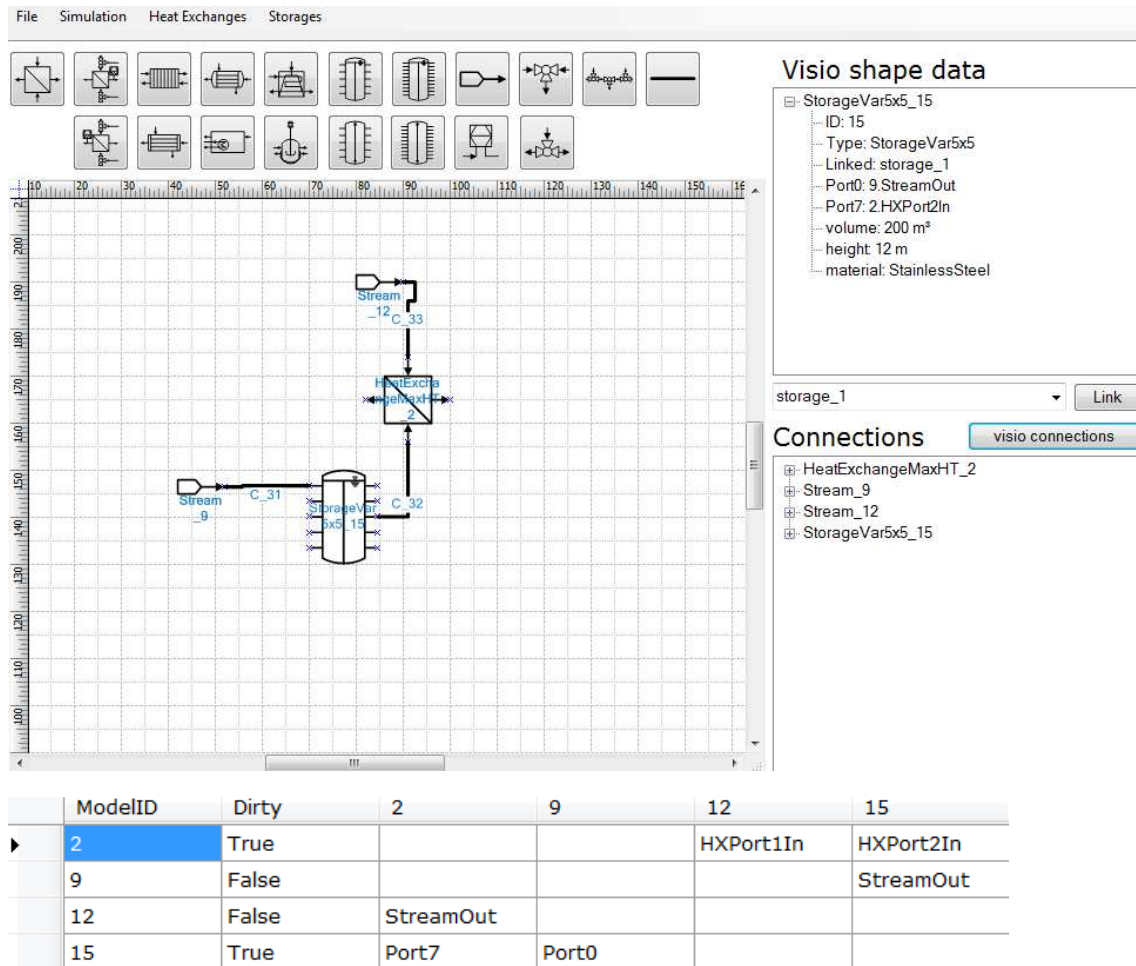


Figure 5-27: Solve-ability matrix of SOCO simulation algorithm

Each component is given a unique ID. As this ID stems from the internal Visio ID it seems to be a random number. Usually the order of drawing is reflected in the order of the IDs. The solver matrix now shows all connections between the components. Based on the solve-ability criteria of each

component the solver can assign whether the variable requires calculation (dirty = true) or whether the component is defined (dirty = false). For example the data of given heat sources and heat sinks (streams) are per se defined and are not changed during calculation. Therefore the components 9 and 12 show “false” in the list of components. The heat exchanger and the storage on the other hand show “dirty” as they are not yet defined according to their component requirement. Basic requirements defining whether components are solve-able or not and results of each component calculation are as follows:

- heat exchangers: input streams (mass flows and temperatures) are required; transferred energy and heat exchange is calculated as well as remaining energy demand and availability. In case of a heat exchanger being placed after a storage tank with varying level, the ideal outflow of the storage for the subsequent heat exchange is calculated.
- storages: mass flows and temperatures of input streams as well as mass flows of output streams are required; temperatures of outgoing streams at specified port heights as well as temperature stratification within the storage and losses are calculated. The integrated storage model has been developed at the TU Graz [143].
- mixers: two input streams are required (mass flows and temperatures); outgoing stream is calculated
- temperature defined mixer: output stream is required; SOCO calculates the mass flow of the input streams based on the defined mass flow and temperature of the output stream.
- splitter with known splitting rate: requires 1 known stream (either input or output)
- splitter with unknown splitting rate requires 2 known streams (either input or output); the 3rd stream connected to the splitter is calculated. In this splitter type the splitting ratio may vary in each time step.

Once a component is solved the solver-matrix is updated with new information. Some components will be solve-able, while others might have been influenced by the prior calculation and will need to be solved again. In case no component is solve-able, the calculation starts the “init-mode”. Only HX calculations can be started with “init-streams”. The result of these calculations reveals new streams with which the other components are solved. In this “init-mode” the following priorities are valid for calculations:

1. All heat exchangers are calculated

- Rules for init streams:
 - i. The “init stream” is taken from closest known stream or measurement equipment in the process layout (visio drawing)
 - ii. in case two HX need the same init streams and these two HX are not connected with each other, the init stream is used for one HX and the remaining energy of this stream is used as init stream for next HX.
 - iii. in case two HX need the same init streams and these two HX are connected with each other, the same init stream is taken for both HXs
 - iv. for HX with mixers between init streams and the heat exchangers, the mixed stream of the streams is used as “init stream” for this heat exchanger
- Order rules:
 - i. Heat exchangers are solved by ID number
 - ii. Heat exchangers with mixers between init stream and HX are calculated last
- Result:

- i. input stream to HX
- ii. transferred energy over time
- iii. remaining energy demand and availability

- Convergence:

- i. The calculated input stream to the HX is checked for convergence

2. all components are calculated based on the solve-ability rules and the solver-matrix

- Init streams:

- i. No additional init streams, output of each component calculation is integrated in solver-matrix

- Order rule:

- i. according to solve-ability definition (see above)
- ii. components are solved by ID number

- Result:

- i. Depending on component (see above)

- Convergence:

- i. Calculation continues as long as components are influenced by any calculation until convergence is reached
- ii. The calculated input stream to the HX is checked for convergence

Results can be viewed as diagrams and data can also be exported to Excel for further processing. The effect of changes in the system configurations can be analysed by changing the Visio drawing and the respective settings of the equipment (heat exchangers, storages, splitter or mixers).

Simulation of heat exchangers and storages with varying level

Looking at the simple example of hot water preparation shown above, one could argue that practically often the heat transfer happens first and the prepared hot water is then stored for later use. SOCO is able to simulate both options. In case of hot mass transferring storages with subsequent heat exchange however (as shown above), SOCO is able to optimize the mass flow leaving the storage for best suitability for the following heat exchange (calculation module "Define Massflow and Energy in a potential storage"). This mass flow is defined over a potential heat exchange calculation in each time step. Based on the difference between energy demand (cold streams – cs) and availability (hot streams – hs) dE , the possible store-able energy $dE_{storeable}$ is calculated.

$$dE = E_{hs} - E_{cs} \quad \text{5-80}$$

$$\text{If } dE_{storeable}[i + 1] > 0: dE_{storeable}[i] = dE[i] \quad \text{5-81}$$

$$\begin{aligned} \text{If } dE_{storeable}[i + 1] < 0: dE_{storeable}[i] \\ = dE_{storeable}[i + 1] + dE[i] \end{aligned}$$

As $dE_{storeable}$ specifies how much energy is available at the respective time step, it is now possible to define how much energy of the hot stream in each time step is required for overall maximum energy transfer. The amount of energy required from the hot stream $E_{HX,hs}$ is:

$$\text{If } dE_{storeable}[i] < 0: E_{HX,hs}[i] = E_{hs}[i] \quad \text{5-82}$$

$$\text{If } dE_{storeable}[i] > 0: E_{HX,hs}[i] = E_{hs}[i] - dE_{storeable}[i]$$

Finally it can be derived how much energy of the hot stream per time step can be used for direct heat exchange $E_{HX_hs_direct}$ and how much is sent to the storage $E_{HX_hs_indirect}$.

Simulation of heat exchangers and storages with fixed level

Fixed level storages are basically energy storages which are loaded and unloaded via heat exchangers. The implemented model [143] allows maximum 20 port connections, which is equivalent to 10 loading or unloading heat exchangers. In order to simulate the interaction between heat exchangers and storages, the heat exchange module initialises a calculation which defines the mass flow of the storage medium. The initialisation of this calculation is based on a hypothetical heat exchange calculation between all hot streams loading the storage and all cold streams unloading the storage. In this hypothetical calculation, a similar approach as presented above (calculation module “Define Massflow and Energy in a potential storage”) is used for calculating the required heat transfer to the storage per loading heat exchanger in each time step as well as the possible heat transfer per unloading heat exchanger in each time step from the storage. Within the subsequent procedure an iterative routine between storage model and heat exchange calculation for each heat exchanger is activated.

In the heat exchange calculation, first the mass flow of the storage medium (m_{sm}) is defined over the known enthalpy required to load the storage in this time-step. The general aim is to load the storage to high temperatures or unload the storage to very low temperatures. The mass flow definitions are therefore as follows:

$$m_{sm} = \frac{QH_X}{cp_{sm} * [(T_{hs,in} - \Delta T_{HX}) - T_{sm,in}]} \quad 5-83$$

$$m_{sm} = \frac{QH_X}{cp_{sm} * [T_{sm,in} - (T_{cs,in} + \Delta T_{HX})]} \quad 5-84$$

Depending on the port diameter to which the heat exchanger is connected, a maximum flow velocity which must not be exceeded is defined. In this case the mass flow of the storage medium is reduced. The user also has the possibility of defining a minimum and maximum mass flow of the storage medium. These checks are also performed in the heat exchange calculation. Finally, checks include temperature limits as well as whether enough heat transfer area is available.

With the known storage medium flow and its temperatures entering the storage (leaving the heat exchanger respectively T_{sm_out}), the storage model is activated and calculates the temperatures of the storage medium leaving the storage to the heat exchangers T_{sm_in} . As T_{sm_in} is a required input parameter to the HX calculation an iterative calculation is necessary until T_{sm_in} and T_{sm_out} converge .

HX and Storage Proposal

This module suggests the placement of heat exchangers and storages on the basis of defined process streams. The optimization algorithm proposes the setting of heat exchangers based on the three criteria transferable energy, heat duty (power of heat exchange) and the so-called exergy criteria which is the temperature difference on the hot side of the heat exchange (heat source temperature vs. temperature of the cold stream after heat exchange). The weight of these criteria can be adjusted by the user. Additionally the user can set several parameters for heat exchanger and storage calculation in the optimization algorithm. For heat exchangers these include, among others, minimal

power of heat exchange (to exclude very small heat exchangers), minimal energy transfer as percentage of total energy transfer, ΔT_{\min} and approximate k-value for heat exchange area calculation (see Figure 5-28).

HX and Storage Proposal Simulation

Detailed simulation settings

stream name	Criteria settings	HX settings	Storage settings
<input checked="" type="checkbox"/> steam conden...	Energy 0.5	Min. Power 20 kW	Min. volume 0.5 m ³
<input checked="" type="checkbox"/> wort	Power 0.2	Min. Energy transfer (based on total energy requirement) 5 %	Max. volume 200 m ³
<input checked="" type="checkbox"/> waste heat co...	Exergy 0.3	Load in HX should not exceed average load by 20 times	Possible Storage mode <input type="text"/>
<input checked="" type="checkbox"/> mashing	Sum 1	k-value 4000 W/m ² K	Temperature levels of +/- 5 K will be integrated in one storage
<input checked="" type="checkbox"/> BottleWashing	Pinch delta T 0 K	dT 2 K	Minimum mass flow for creation of new storage 10 %
<input checked="" type="checkbox"/> Pasteurisation			
<input checked="" type="checkbox"/> HotWater			

After separating streams for HX Proposal in Above/Below Pinch Region only streams with > 15 % energetic value of the initial stream will be considered in proposal generation

After HX generation, remaining streams with > 3 % energetic value of the initial stream will be considered in proposal generation

Figure 5-28: Detailed settings for the heat exchange and storage proposal algorithm

Based on the selection of heat recovery matches, the potential heat exchange and the three corresponding criteria are calculated in each time step, assuming a potential storage (calculation module “Define Massflow and Energy in a potential storage”). In each time step the required heat exchange area is calculated. As heat exchange area influences the temperatures of the streams and consequently has impact on the temperature stratification in the storage, the user can define whether the heat transfer area should be limited by user-defined multiplication factor of the on average required area. To this degree, the load in the heat exchanger will not exceed the average load by a certain factor, which hinders the proposal to suggest huge areas which are only necessary in very few time steps. Minimum and maximum storage size can be defined for storages. A storage is finally designed based on the potential heat exchange.

The algorithm that has been recently published [149] takes into account the time variability of the process streams and if necessary suggests a potential energy storage for each heat exchange. Figure 5-29 shows a concise flowsheet of the combinatorial approach being used. The proposed heat exchanger network is shown in SOCO as a list of proposed heat exchangers and storages. For each heat exchanger overall parameters are given, as shown in Figure 5-30. The user can integrate the proposed equipment in a Visio drawing of the thermal energy system and run a system simulation. After the system simulation details on heat exchange performance can be accessed by double-clicking on each heat exchanger (see Figure 5-31) or heat storage.

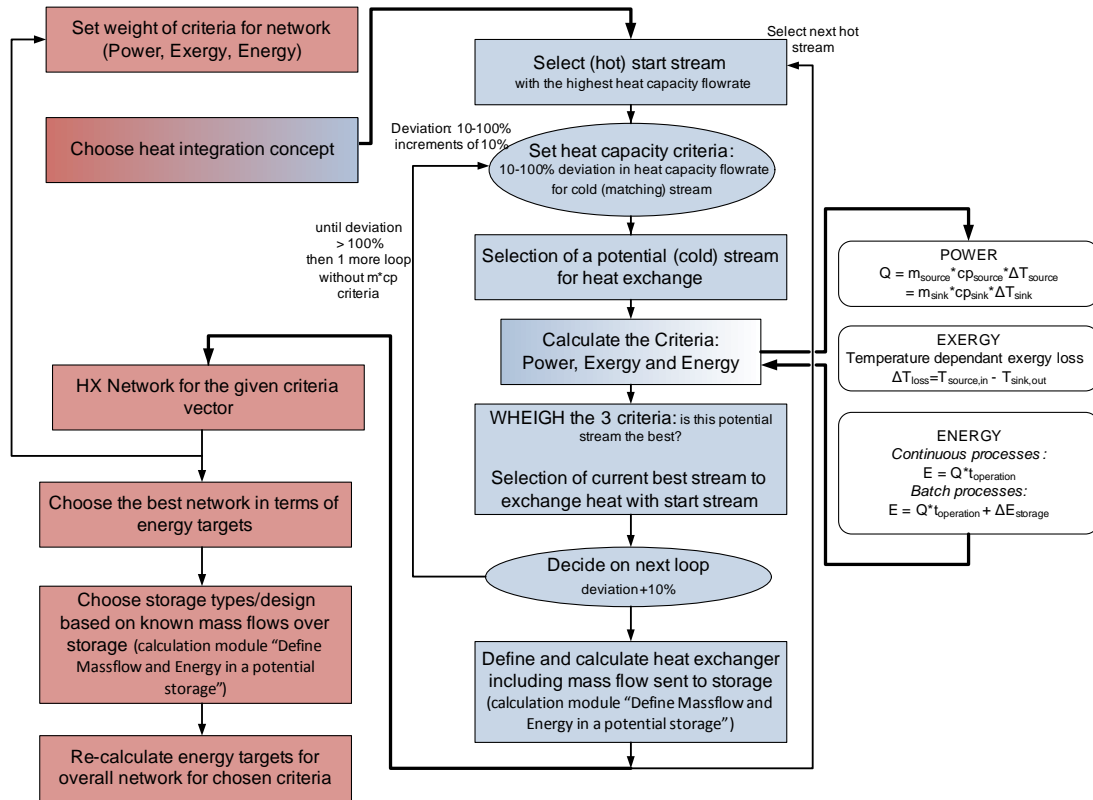


Figure 5-29: Algorithmic steps of the heat integration proposal

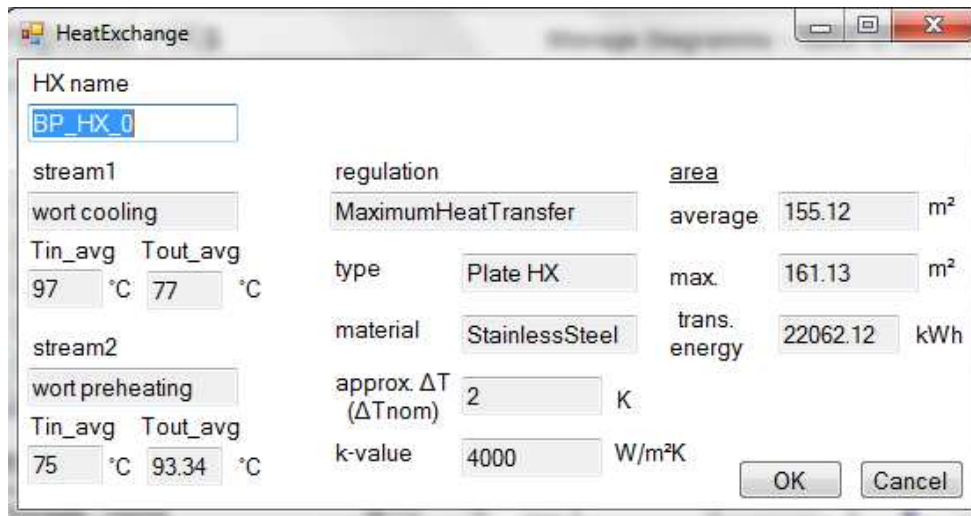


Figure 5-30: Presentation of one proposed heat exchanger in SOCO (example)

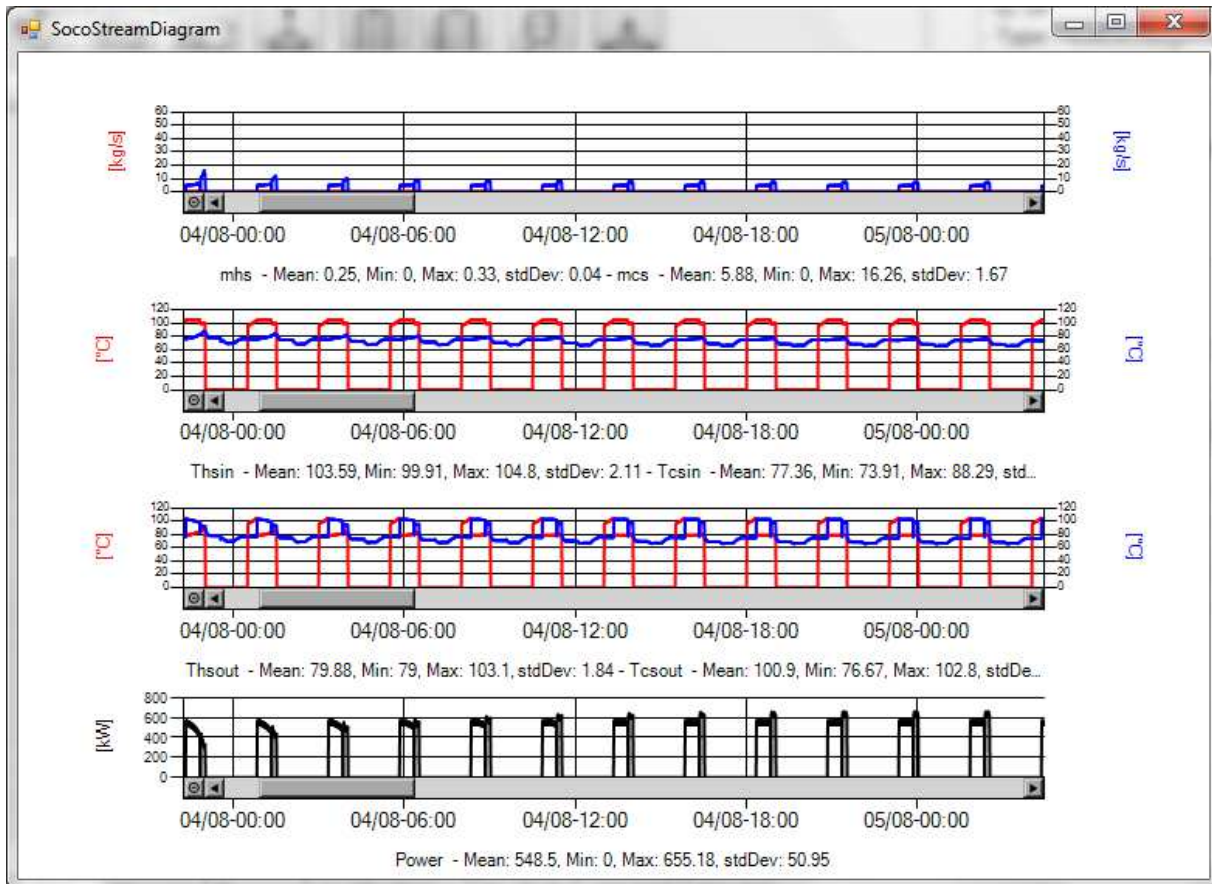


Figure 5-31: Presentation of heat exchange performance results in SOCO (example)

5.3 Holistic methodology to improve the potential for low temperature heat supply in the food industry via process models

Sustainable and efficient food production systems must have the following key features:

- High product quality,
- High process efficiency in terms of productivity and process yields,
- High energy efficiency in terms of heat transfer from the supply equipment to the processes,
- Use available low temperature heat sources for process heat requirements (waste heat or other low temperature heat supply).

How can we develop such intensified process systems that allow for low temperature heat supply? With the tools presented above the following methodology has been developed for this analysis (see Figure 5-32).

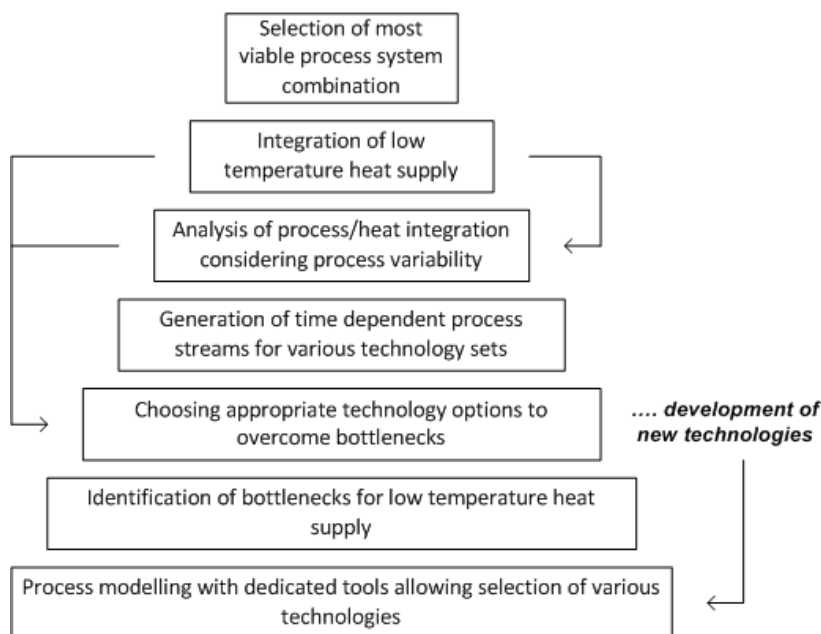


Figure 5-32: Holistic methodology for developing intensified food production systems for low temperature heat supply

Process modelling with dedicated tools allowing selection of various technologies is the starting point to evaluate energy efficiency of different technology sets. Additionally, bottlenecks for low temperature heat supply will become obvious due to existing heat transfer areas, necessary heating rates etc. In case no appropriate technology options are available to overcome these bottlenecks, this fact might stimulate new developments. Once process variability over time can be modelled for various technology sets, these process streams can be analysed for heat integration opportunities. Here, time variability is a decisive aspect and appropriate tools need to be applied. Based on the heat integration studies, consideration of low temperature heat supply can follow. Iterations might be necessary as integration of low temperature heat supply and waste heat from processes must be sensibly linked and holistic solutions must be simulated. Finally, studies for several technology sets can be compared and evaluated based on the targeted key factors, which will in most cases be the factors energy efficiency and costs.

In this work, the two tools that have been presented cover this methodology for the brewing industry. The Brewery model generates variable process streams for several technology options and SOCO evaluates the integration potential for waste heat and other low temperature heat supply.

Additionally the development of a new process technology for mashing has been stimulated, due to the fact that mashing is a very good candidate for low temperature heat supply in terms of its process heat demand; however the existing stirred tanks and applied heating rates make retrofit difficult.

6 DEVELOPING A NEW MASHING TECHNOLOGY – EXPERIMENTAL ELEMENT

When implementing the methodology described above (see Figure 5-32) in breweries, one quickly comes to the conclusion that mashing is a decisive process candidate for low temperature heat supply [140, 147, 148, 151]. However, the existing process technology poses limitations when changing the energy supply for the mashing process. Additionally, mashing is the slowest process in the brewhouse when mash filtration is applied for wort separation. There are therefore several good reasons for studying new mashing technology options that would overcome these bottlenecks.

Based on the known kinetics of extract recovery and sugar formation during the mashing process, as discussed in chapter 4.3.1, the following hypotheses were established:

- lower kilning temperature enhances malt quality;
- starch hydrolysis might be enhanced via oscillations;
- better enzymatic action can be achieved in mashing when heating is carried out with low temperature energy supply as high temperature gradients (in high temperature energy supply) lead to increased enzyme inactivation;
- a continuous mashing process with low heating rates could be possible (with intensified starch hydrolysis) and low temperature heating: 2nd rest in infusion programmes can be replaced by slow gradual heating.

Kilning is an important process in terms of thermal energy intensity and it has a high potential to integrate renewable energy [140]. The development of a kilning process at lower temperatures would enhance integration possibilities of low temperature heat sources such as solar process heat. The focus of this thesis was on brewhouse processing rather than on malting, therefore no further research activities have been taken towards realising this potential.

The intensification potential for starch hydrolysis was also not studied in detail in this thesis. A short literature review on starch hydrolysis via ultrasound proved the hypothesis that starch swelling and enzyme activity could be improved via ultrasonic treatment, although early studies claim a decrease in enzyme activity. Based on these results especially for non-energy intensive ultrasonic treatment [38, 121, 184, 217], it seems that hydrolysis might be intensified via oscillations. For several reasons, as will be discussed later on in this paper oscillatory flow reactors would be an interesting alternative to the traditional mashing process in stirred tanks. Future studies will reveal to which extent oscillations induced in such reactors influence starch hydrolysis.

The main focus of the current work was the development of a (continuous) mashing process with low heating rates that enables better integration of low temperature heat supply. To validate the hypotheses stated above the following steps were taken in the thesis:

1. The influence of the temperature gradient of the heating medium in the mash tun on the temperature distribution in the tun was analysed. For this analysis the temperature and the width of the boundary layer was calculated to assess the influence on enzyme activity.
2. The influence of temperature profiles was tested with the kinetic mashing models introduced in chapter 5.1.9.1. Mashing profiles with different heating gradients and temperature rests

based on the hypothesis of mash heating with low heating rates were composed and the results of extract recovery and sugar composition was modelled.

3. Lastly, the influence on the enzymatic action in low temperature heated tuns (low temperature gradient & low-medium heating rates) was tested in laboratory tests to further proof the hypothesis and the model results.
4. Oscillatory flow reactors were chosen as potential technology to realise the newly developed mashing process on industrial scale. Basic design calculations have been performed as a starting point for further research in pilot scale.

6.1 Developing mashing temperature programs for low temperature heat supply

For the evaluation of temperature programmes for mashing with low temperature heating gradients, temperature profiles were chosen with the following criteria:

- Low heating rates
- Reduced mashing time
- Potential for continuous process treatment
- Enhanced enzyme activities
- Avoidance of retrogradation

The chosen temperature profiles are shown in Table 6-2. The focus of the analysis was the hypothesis that the 2nd rest in mashing (saccharification rest) could be replaced by continuous heating with low temperature heating rates. A standard infusion mash program from industry was taken as reference for the analysis (test 1). Starting from a mashing-in temperature of 58 °C the mash is heated with a heating rate of 0.3 K/min to 62 °C where the amylase rest is performed for 15 min. The mash is then heated further to 72 °C with a heating rate of 0.7 K/min and held for 20 min at 72 °C for the sugar formation. Finally the mash is heated to 75 °C with a heating rate of 0.5 K/min. The temperature of 75 °C is held for 25 min to ensure the inactivation of the enzymatic activities.

In test 2 this heating program is generally copied, however instead of the rest for sugar formation at 72 °C the mash is heated continuously from 62 °C to 75 °C within 40 min, which is also the total time taken in test 1 to come from 62 °C to 75 °C. Test 3 and test 4 are variations of test 2 with heating times of 30 and 50 minutes respectively for the heating phase from 62 °C to 75 °C. In test 5 the amylase rest at 62 °C is also shortened from 15 minutes to 5 minutes. Finally test 9 has the same heating profile as test 4; however final temperature is 72 °C instead of 75 °C.

Test 6-8 are “dynamic” temperature profiles in which heating and cooling phases alternate. In setting up these schedules attention was paid to avoid retrogradation. When amylose retrogrades, it crystallizes and separates from solution which makes it resistant to enzyme activities. This effect can occur when cooling the solution below its gelatinization temperature once hydrolysis has already started [59] (p. 130).

6.1.1 Kinetic modelling of the heating profiles

Initially these new heating programmes for mashing were modelled with the kinetic models A and B, as introduced in chapter 5.1.9.1. Results for an initial starch concentration of 170 g/l and initial sugar contents as given in Table 6-1 generally show a high potential for gradual slow heating of mashes without saccharification rest. The models were applied for a mash with 15.5 g/100ml gravity and

with enzyme activities as stated in reference literature [44, 136]. The findings are compiled in Table 6-3 and visualised in Figure 6-1 and Figure 6-2.

Table 6-1: Initial starch composition for modelling mashing temperature profiles

Enzyme activities	
α -amylase in malt	
Model A	0.012 g/l
Model B	200 U/g
β -amylase in malt	
Model A	0.012 g/l
Model B	500 U/g
Initial carbohydrate concentration in mash	[g/l]
starch	170.00
glucose	6.00
maltose	12.00
maltotriose	1.00
dextrin	26.00
limitdextrin	-
sucrose	7.50
fructose	2.00

Table 6-2: Selected Temperature profiles applied to analyse the effects of temperature profiles on sugar composition with the kinetic mashing model

	Test 1		Test 2		Test 3		Test 4		Test 5		Test 9	
	Mashing in temperature 58°C											
	time	target temp.	time	target temp.	time	target temp.	time	target temp.	time	target temp.	time	target temp.
	[min]	[°C]	[min]	[°C]	[min]	[°C]	[min]	[°C]	[min]	[°C]	[min]	[°C]
Heating	14	62	14	62	14	62	14	62	14	62	14	62
Rest	15	62	15	62	15	62	15	62	5	62	15	62
Heating	14	72	40	75	30	75	50	75	30	75	50	72
Rest	20	72	25	75	25	75	10	75	25	75	10	72
Heating	6	75										
Rest	25	75										

	Test 6		Test 7		Test 8	
	Mashing in temperature 58°C					
	time	target temp.	time	target temp.	time	target temp.
	[min]	[°C]	[min]	[°C]	[min]	[°C]
Heating	14	63	10	64	12	63
Cooling	15	61	5	61	5	61
Heating	40	75	8	66	8	65
Rest	25	75				
Cooling			6	62	6	62
Heating			10	68	12	68
Cooling			5	65	5	66
Heating			10	72	30	75
Cooling			7	67		
Heating			20	74		

Table 6-3: Model results for mashing programs with low temperature heating gradients

		starch		glucose	maltose	maltotriose	dextrin	limitdextrin	saccharose	fructose
MODEL A										
final concentrations										
basic conditions V1	[g/l]	0.01	[g/l]	11.10	125.10	26.11	48.82	11.32	7.50	2.00
deviation of test results based on basic conditions (V1)										
V2	[g/l]	0.01	[%]	2.20%	2.11%	0.53%	-7.87%	4.79%	0.00%	0.00%
V3	[g/l]	0.02	[%]	1.16%	0.71%	0.27%	-2.91%	2.50%	0.00%	0.00%
V4	[g/l]	0.02	[%]	2.89%	2.80%	0.72%	-10.60%	6.29%	0.00%	0.00%
V5	[g/l]	0.03	[%]	-3.64%	-3.47%	-0.85%	9.78%	-8.22%	0.00%	0.00%
V9	[g/l]	0.04	[%]	3.81%	3.62%	0.91%	-14.33%	7.97%	0.00%	0.00%
V6	[g/l]	0.01	[%]	2.12%	2.11%	0.50%	-7.72%	4.55%	0.00%	0.00%
V8	[g/l]	0.06	[%]	0.27%	0.71%	0.04%	-2.26%	0.61%	0.00%	0.00%
MODEL B										
final concentrations										
basic conditions V1	[g/l]	0.00	[g/l]	12.64	114.80	23.21	47.15	-	7.50	2.00
deviation of test results based on basic conditions (V1)										
V2	[g/l]	0.00	[%]	1.33%	0.69%	0.43%	-3.72%	0.00%	0.00%	0.00%
V3	[g/l]	0.00	[%]	1.02%	0.52%	0.30%	1.77%	0.00%	0.00%	0.00%
V4	[g/l]	0.00	[%]	2.02%	1.03%	0.60%	-2.84%	0.00%	0.00%	0.00%
V5	[g/l]	0.00	[%]	-3.27%	-1.59%	-0.91%	13.47%	0.00%	0.00%	0.00%
V9	[g/l]	0.00	[%]	2.69%	1.37%	0.81%	-4.38%	0.00%	0.00%	0.00%
V6	[g/l]	0.00	[%]	1.71%	0.61%	0.43%	-2.84%	0.00%	0.00%	0.00%
V8	[g/l]	0.00	[%]	0.24%	-0.35%	0.09%	8.64%	0.00%	0.00%	0.00%

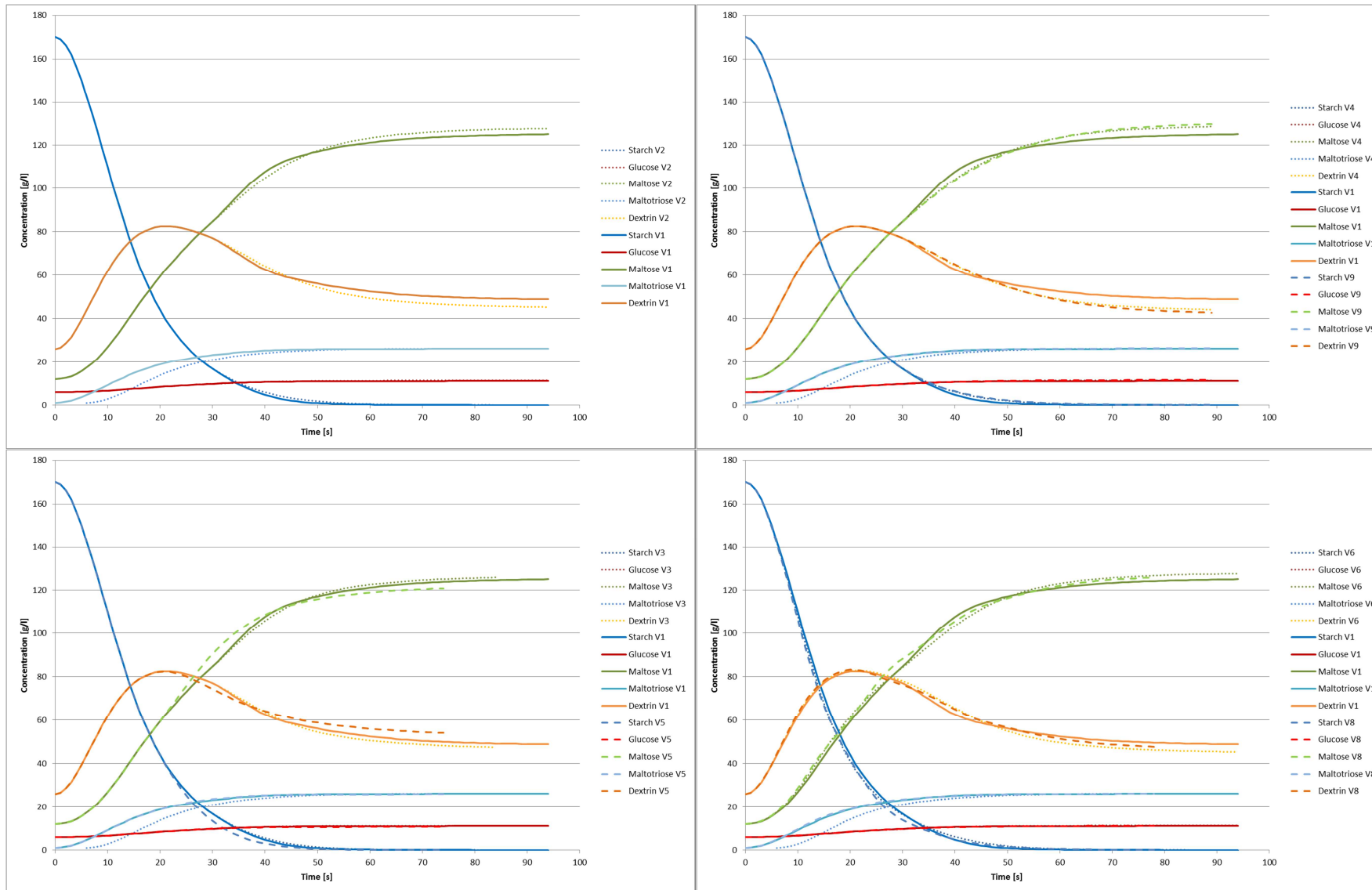


Figure 6-1: Model results for temperature profiles 1-8 simulated with Model A (a-d)

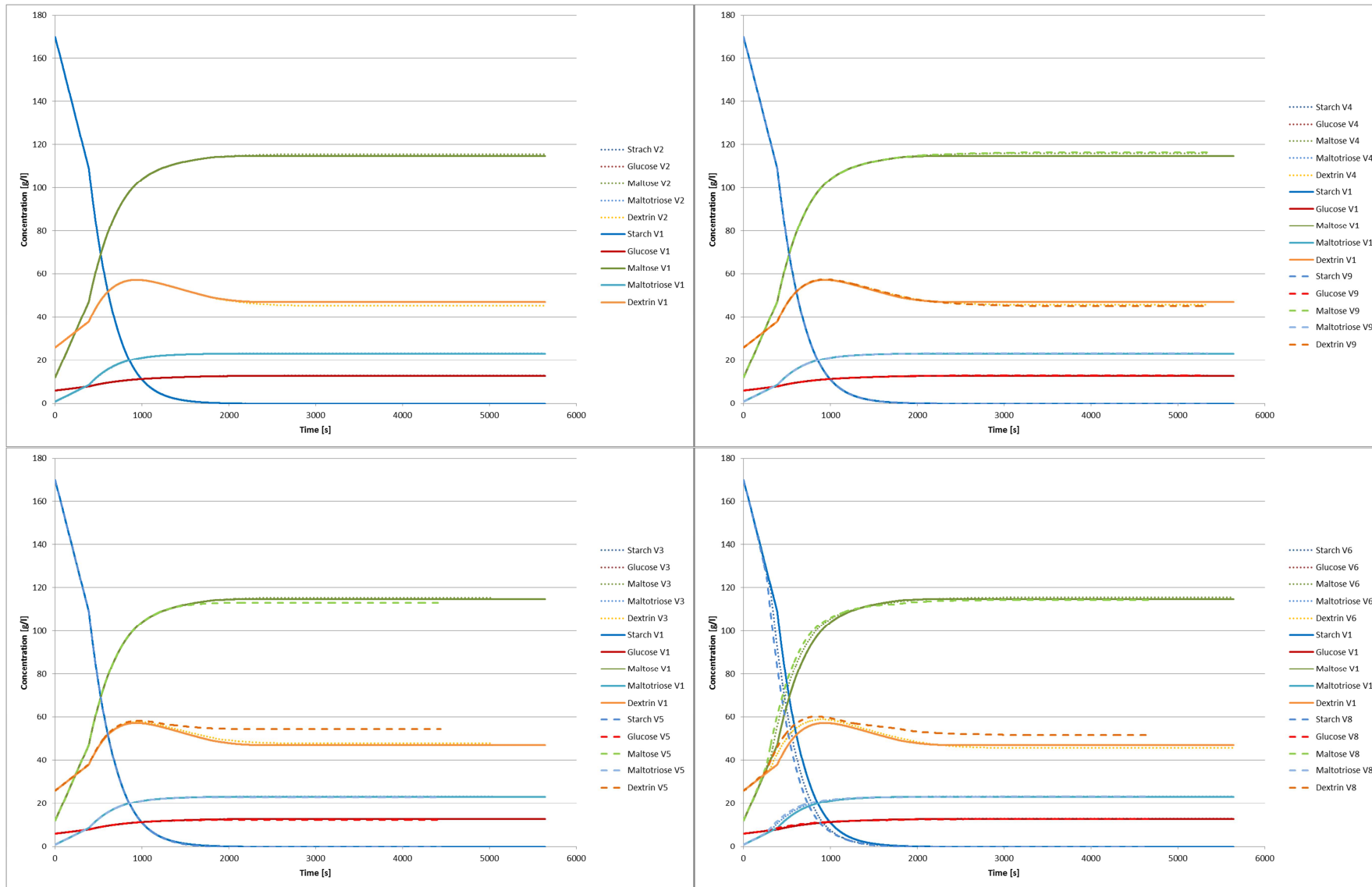


Figure 6-2: Model results for temperature profiles 1-8 simulated with Model B (a-d)

Although both models are sensitive to temperature changes (see also 5.1.9.1), the chosen temperature profiles only lead to minor deviations in sugar concentrations. This holds true for almost all temperature profiles and for both models, although the absolute results and profiles differ between Model A and B. While the peak in dextrin formation is much more pronounced in Model A, hydrolysis is taking place much faster in Model B. Both effects can be explained by the different enzyme activity ratios between α -amylase and β -amylase used in these runs. While in model A the activities of α - and β -amylase are identical, in Model B β -amylase has a much higher activity than α -amylase. For this reason, β -amylase degrades dextrin produced by α -amylase very quickly, leading to fast hydrolysis and a minor peak in dextrin formation due to the rapid ongoing reactions.

There is a mass balance inaccuracy in both models between starch degradation and extract formation. Total extract values TE have therefore been corrected by the cumulated difference between starch degradation ST and the sum of all extract compounds E:

$$TE_{corr,t} = TE_t - \sum_{i=0}^t \left[\Delta \left(\sum_{j=1}^n E_{n,i} - \sum_{j=1}^n E_{n,i-1} \right) + \Delta(ST_i - ST_{i-1}) \right] \quad 6-1$$

While too little sugars are formed in model B, Model A over estimates extract formation and leads to more extract than degraded starch. This is also the reason for the fairly high difference between the model results of absolute maltose concentration in Test 1.

Additionally, in both models the mass balance between dextrin and sugar formation is not exact, so the decrease in dextrans does not exactly equal the increase in sugar production. In model A deviations up to 0.4 g/l or 0.16 % (based on total extract) occur, while deviations in Model B are up to 4.9 g/l or 2.32 % respectively.

In Table 6-3, deviations are shown based on the single sugar values (e.g. change in maltose concentration based on maltose concentration of Test1), so the percentages cannot be concluded.

In plot a) of Figure 6-1 and Figure 6-2 the comparison of test 1 and test 2 are shown. Test 2 does not include a second saccharification rest at 72 °C but gradually heats the mash to its final temperature with a low heating rate of 0.33 K/min. Deviations are minor and below 2.2 % for the modelled sugars. Dextrin production is reduced and more sugars are formed, so fermentability of the mash is slightly increased. Starch is degraded to the same extent as in Test 1.

The results of Test 4 and Test 9 in comparison to Test 1 are plotted in plot b) of the figures. In these tests a similar profile as in Test 2 is applied, but the heating rate is even lower at 0.26 K/min. Additionally, the final rest at 75 °C is shortened to 10 min. While Test 4 heats the mash to 75 °C, Test 9 only heats up to 72 °C. Deviations for Test 4 are similar to Test 2. Again, fermentability is increased and dextrin formation reduced. Starch is again degraded completely in Model B, Model A gives a remaining concentration of 0.02 g/l. In test 9 these results are even more pronounced which is probably due to the higher activity of β -amylase at lower temperature. However Model A results in 0.04 g/l remaining starch degradation.

The comparison of Test 3 and Test 5 to the standard profile (test 1) is shown in plot c). Test 3 is similar to Test 2 and 4, with a slightly higher heating rate at 0.43 K/min. Model A again shows the same trend as in Test 2 and Test 4, but less pronounced which would indicate that the higher heating

rate does not allow β -amylase to act as efficient as in the former Tests. Model B shows conflicting results with a small increase in both sugar production and dextrin formation.

Test 5 is the only test in which the first rest is shortened to 5 min instead of 15 min. The models immediately react by showing a less fermentable wort, confirming the knowledge that the amylases require time at lower temperatures to act efficiently on starch degradation and extract formation. While model B still shows complete starch degradation, model A results in 0.03 g/l remaining starch concentration. In this tests both models show the strongest imbalance between dextrin and sugar production.

Test 6, shown in plot d) of Figure 6-1 and Figure 6-2 is a slight variation of Test 2 in which little cooling is applied during the saccharification rest. The model results show no effect on this change in temperature profile, and the results reflect those reached in Test 2.

In Test 8 more heating and cooling sequences are applied. Although the total mashing time is considerably reduced in this profile, Model A shows the lowest deviations for this test in comparison to the standard profile of Test 1. However, remaining starch concentration is increased to 0.06 g/l which is still a very small value. Model B also shows insignificant changes in sugar formation, however an increase in dextrin concentration.

According to the model applications the hypothesis that heating with slow heating rates would not affect mash quality negatively and that “dynamic” temperature profiles could potentially reduce mashing time considerably was strengthened.

6.1.2 Laboratory studies

6.1.2.1 Laboratory set-up and analyses methods

To prove the potential of new mashing profiles lab tests were performed at the University Weihenstephan in Germany. The studies were financed by AEE INTEC. Batch tests were performed with 1500 g malt and 6 l water in an electrically heated stirred tank. Two profiles, namely Test 1 and Test 4 were additionally carried out at higher gravity with 1900 g malt. Standard Pilsner malt (from BESTMALZ AG) was used and milled to 0.8 mm. Once the mashing-in temperature of 58 °C was reached, malt was added. Malt addition took approximately 1 minute and lowered the temperature to about 55 °C. Heating to 58 °C was then performed within 4-5 minutes and subsequently the defined temperature profiles were applied. Practically achieved heating rates might deviate from the defined ones, as heating rates could not be automated in the set-up, but required manual tuning of the electrical heating coils.



Figure 6-3: Experimental set-up

Several samples were taken during the tests. This was done over a probing tube over which a volume of about 200 ml of mash was taken out. The mash was then filtered over a Macherey Nagle filter paper (MN 514 ¼) before the continuous phase was further analysed. Three main parameters were chosen to evaluate mash quality: Extract and sugar formation; FAN (free amino nitrogen) and β -glucan.

While FAN and β -glucan were only evaluated at the end of the tests, total extract and selected sugars were measured during the course of the mashing. Analyses of total extract, FAN and β -glucan were conducted by the laboratory in Weihenstephan according to MEBAK II 2.10, MEBAK II 2.5.2 and MEBAK II 2.8.4.1 respectively. Sugar analysis was performed at TU Graz. Maltose, sucrose and glucose were analysed enzymatically using a test kit from Megazyme (K-MASUG) and oligomeric carbohydrates by HPLC analysis (Carbohydrate analyzer, Dionex PA200). *The enzymatic K-MASUG test kit for sugar analysis requires determination of absorbance units for all sugars, for the combined sugars sucrose and glucose and for free glucose by itself. Thus, in general it would be necessary to evaluate all three tests for one sample. As sucrose concentration changed only insignificantly during the course of the mashings in Test 1 and Test 2, only the first and last sample were analysed for the*

combination of sucrose and glucose for the other tests. To calculate the correct maltose concentration, the average absorbance value of these two measurements was then subtracted from the absorbance value of all sugars to give the pure maltose concentration. This procedure might lead to some inaccuracy, however as the change in sucrose concentration is the range of 0.5-3 g/l the effect will be minor.

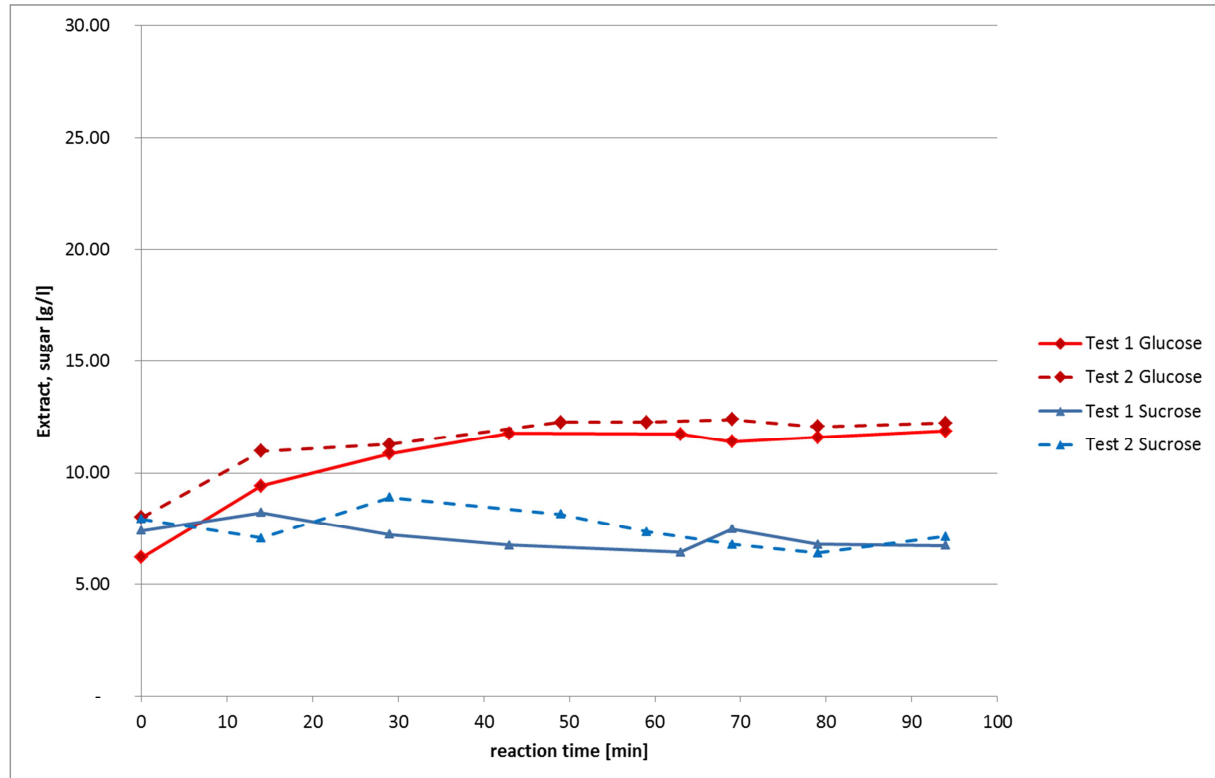


Figure 6-4: Sucrose concentration during the course of mashing

Malt was analysed for α -amylase activity (Rohstoffb. 3.1.4.7), β -amylase activity via diastase power (Rohstoffb. 3.1.4.6), water content (Rohstoffb. 3.1.4.1), extract (Rohstoffb. 3.1.4.2) and gelatinization temperature (Rohstoffb. 2.7). Starch content of malt was measured with the Megazyme test kit for total starch (K-TSTA).

6.1.2.2 Results and discussion

Table 11-1 in Annex 10 shows the result of the malt analyses. The results for sugar analysis, FAN, β -glucan and pH are summarized in Table 11-2 in Annex 10.

The laboratory experiments proved the hypothesis that the newly proposed mashing profiles do not influence the mash quality. The tests even showed a fermentability that was better than expected by the model. Total extract gain is only slightly increased by the newly proposed mashing profiles (in all profiles except test 3), and rather stays constant over the tests whereas fermentability is slightly increased based on the analysis results as more fermentable sugars are formed (see Table 6-4).

Detailed data was gained during the mashing experiments for maltose, glucose and sucrose evolution during the course of the mashing process. For maltotriose HPLC analysis was performed, however only the final samples of selected tests have been analysed. HPLC analysis of sugars confirms that there were also no significant difference of maltotriose content in the new profiles (shown for test 8) in comparison to a standard infusion mashing profile (test 1).

Table 6-4: Results of extract and selected fermentable sugars in the final wort after mashing

		Total extract	glucose	maltose	sucrose
final concentrations					
basic conditions V1	[g/l]	175.00	11.87	89.05	6.75
V2	[g/l]	178.60	12.24	90.06	7.15
V3	[g/l]	174.25	12.02	90.71	6.65
V4	[g/l]	177.05	12.98	95.08	6.18
V9	[g/l]	175.90	12.94	93.70	6.41
V6	[g/l]	177.15	12.26	94.91	6.46
V8	[g/l]	177.05	12.88	93.92	7.16

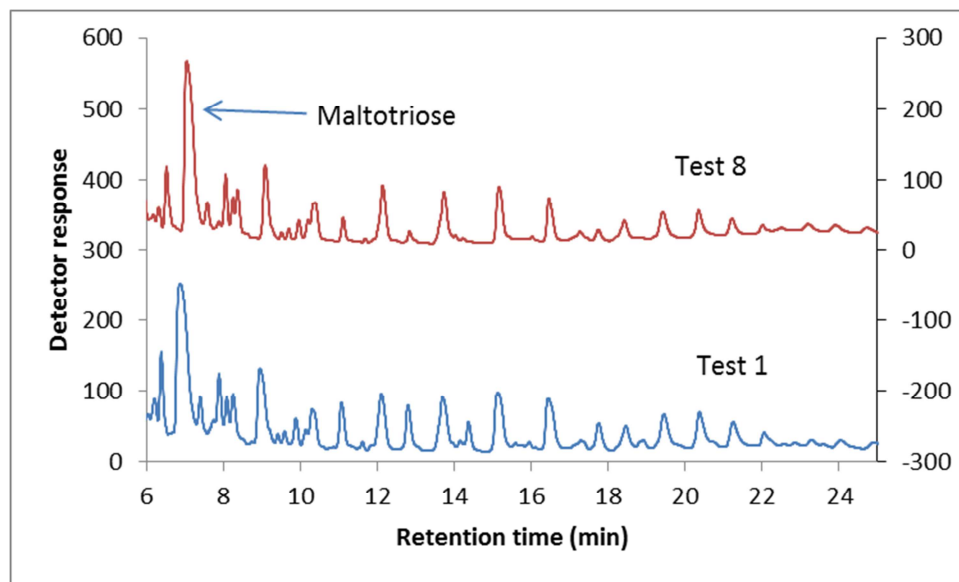


Figure 6-5: Sugar analysis of maltotriose and higher oligomers

The next figures summarize the result of the sugar analysis in diagrams. The solid lines represent the results for the standard process (Test 1), whereas the dashed and dotted lines represent the results for the new temperature profiles. The comparison of Test 1 with Test 2 and Test 3 (Figure 6-6 and Figure 6-7) shows no significant change, neither in extract formation nor in formation of maltose or glucose during the mashing process. This proves the hypothesis that - after a first amylosis rest - no further saccharification rest is necessary in mashing. This is an important result: firstly because the heating rates during mashing can be reduced and the thermal power requirement can be reduced by more than 50 %. This reduces the necessary peak in heat demand which occurs in breweries when mashing and wort boiling is performed at the same time. Secondly, mashing times can be reduced as shown with Test 3, where the mashing process lasts only 84 minutes in comparison to 94 minutes in the standard profile.

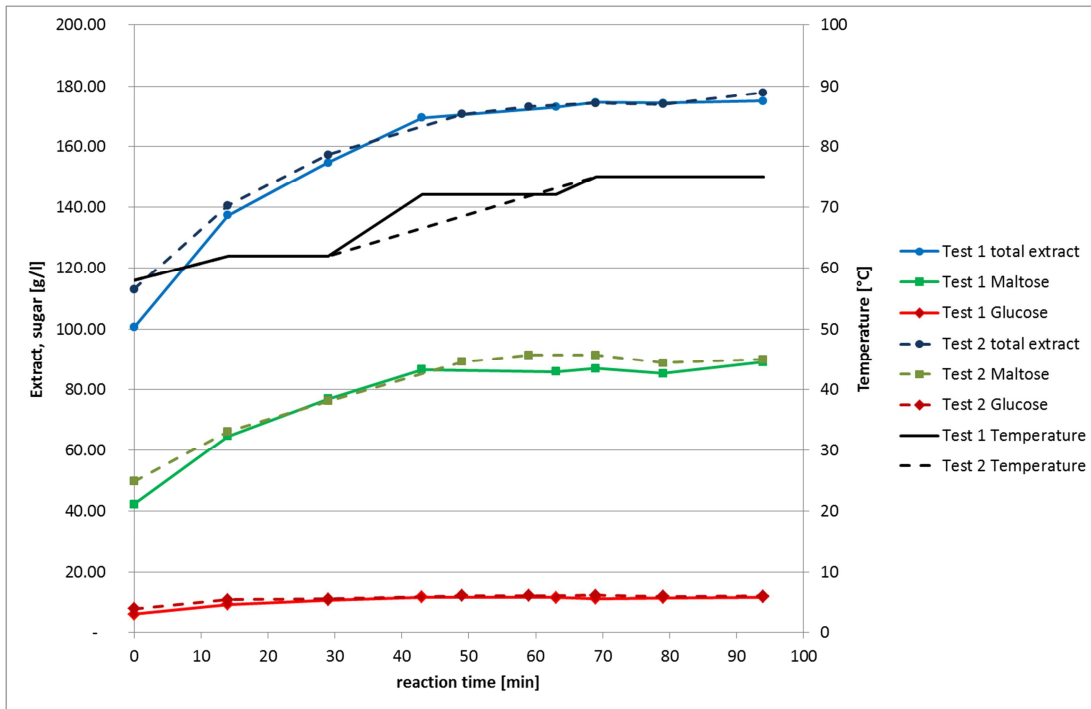


Figure 6-6: Evolution of total extract, maltose and glucose during mashing - comparison of the standard temperature profile (Test 1) to Test 2

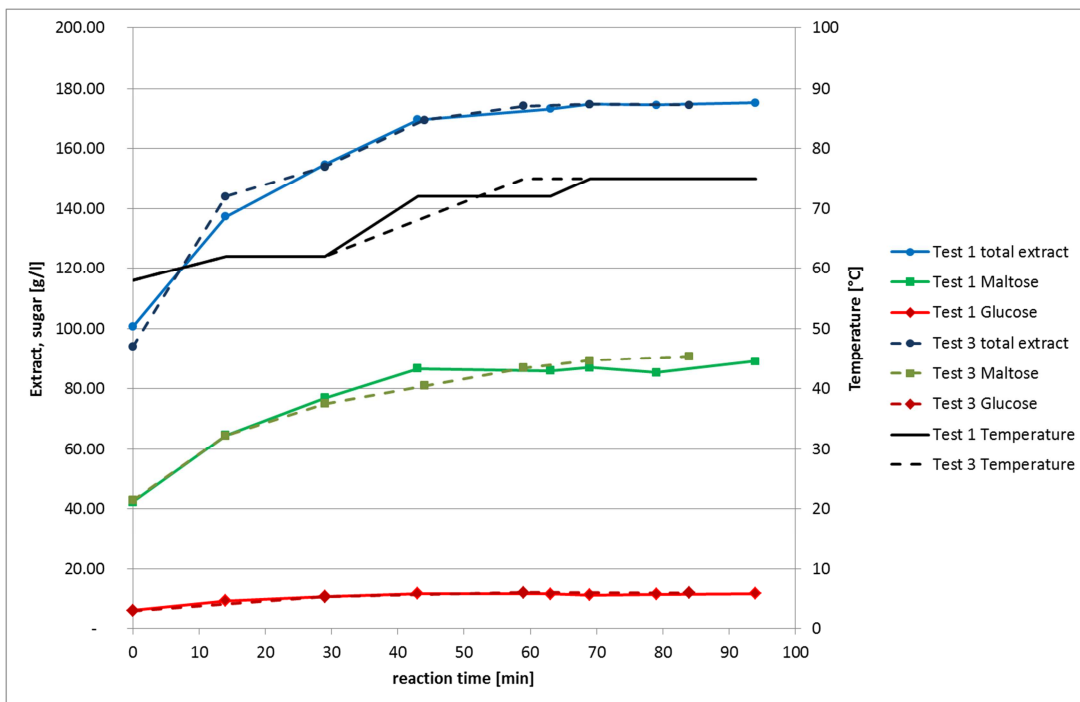


Figure 6-7: Evolution of total extract, maltose and glucose during mashing - comparison of the standard temperature profile (Test 1) to Test 3

Heating the mash even more gently at heating rates of 0.26 K/min as shown in Test 4, increases the absolute amount of maltose formation and its production rate is also slightly enhanced. The rate of total extract formation however remains similar to Test 1. Similar final values are also observed when the final target temperature is reduced to 72 °C instead of 75 °C (Test 9). The results of these tests are visualized in Figure 6-8.

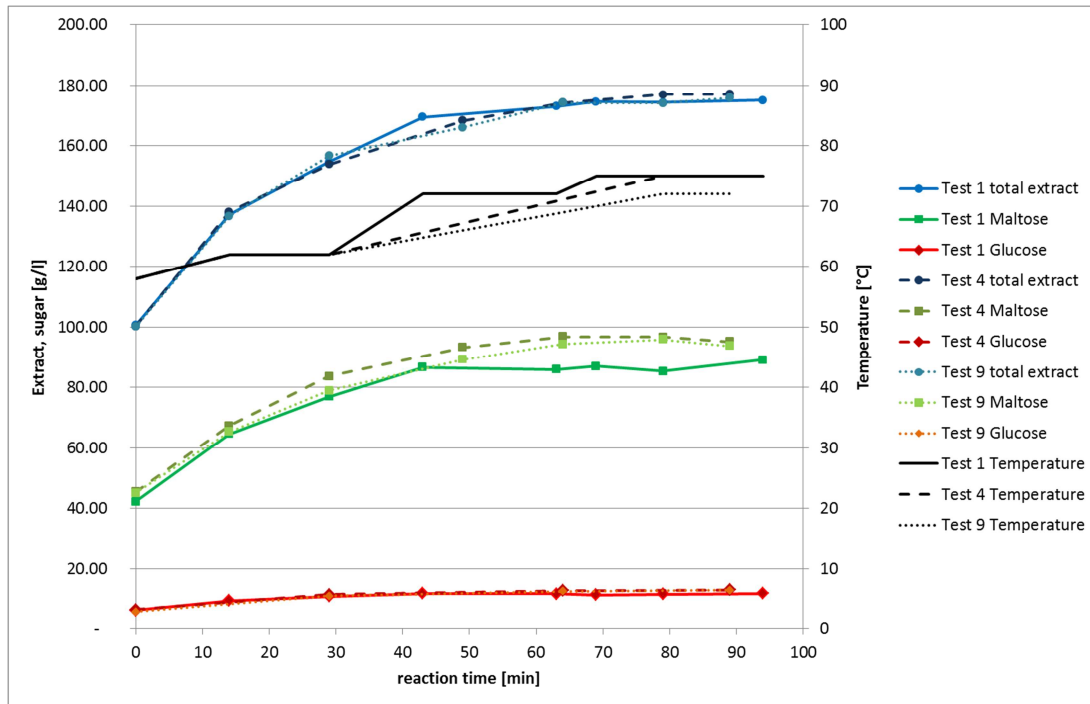


Figure 6-8: Evolution of total extract, maltose and glucose during mashing - comparison of the standard temperature profile (Test 1) to Test 4 and Test 9

Figure 6-9 shows the result of the “dynamic” profiles. Here, for the first time, a significant improvement of the production rate of total extract and maltose can be observed. Thus the dynamic performance seems to have intensified the enzymatic reactions.

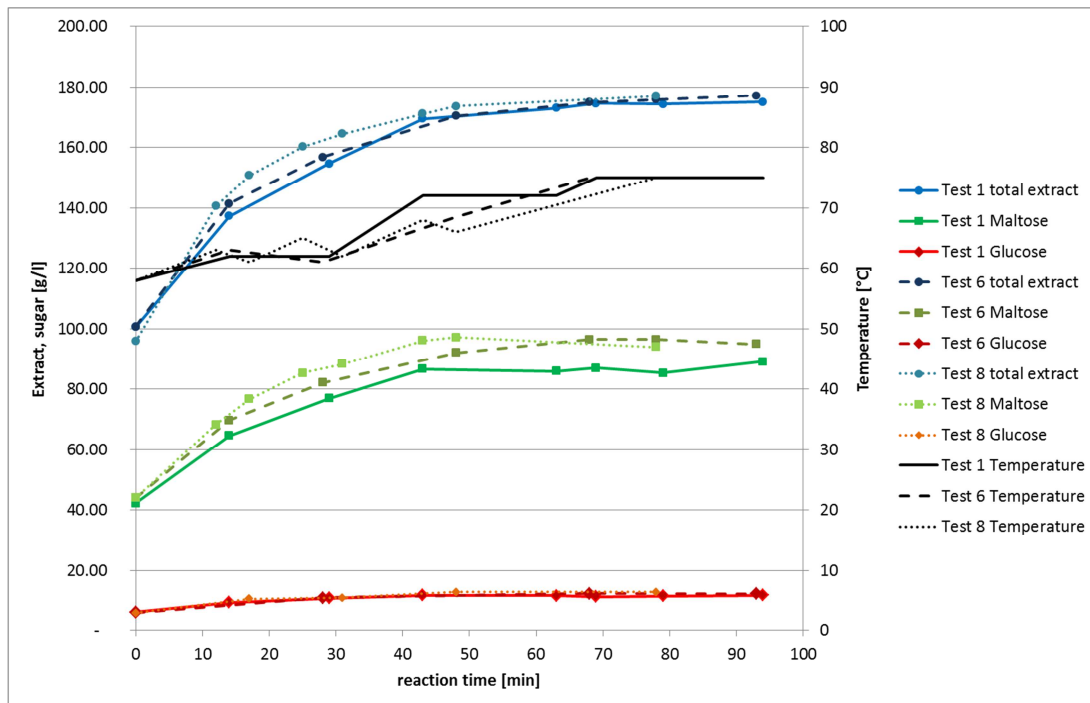


Figure 6-9: Evolution of total extract, maltose and glucose during mashing - comparison of the standard temperature profile (Test 1) to Test 6 and Test 8

The effect is pronounced in the beginning when the mash was heated to 63 °C and then cooled to 61 °C instead of keeping it constant at 62 °C. Another considerable effect is noticeable when the

mash is then heated again to 65 °C and cooled to 62 °C in Test 8 (dotted lines). Here, more tests with different dynamic profiles would show further improvement potential. In test 8 the final maltose concentration of Test 1 was already reached after 30 minutes. However, the increase in total extract is not as pronounced. Further tests need to validate the overall wort quality after 30 minutes of dynamic mashing. Such short mashing procedures would radically change the conventional processing. Most importantly however is that new process technologies that allow for heating and cooling of the mash, preferably via heat exchange in a continuous reactor would be necessary (see 6.2.3.1). Obviously enzyme deactivation must be subsequently ensured which could be done during wort preheating before boiling. Wort separation also has to be performed prior to wort boiling. These two targets could be realized via a continuous mash filtration and subsequent wort preheating. The results generally lead to a new hypothesis that mashing could be performed dynamically in a continuous reactor with subsequent wort separation at low temperature in mash filters and rapid heating in wort preheaters to boiling temperature. A possible flowsheet is presented in 6.2.3.1. Enzyme deactivation will probably be less important in continuous (fast) mashing, when the mash is continuously separated from grist and immediately heated to boiling temperature.

Finally, tests at higher gravity again proved that absolute wort composition after mashing will not be affected negatively with a mashing profile with low heating rates (Test 4), however no increase in production rate was found. The results are summarized in Figure 6-10.

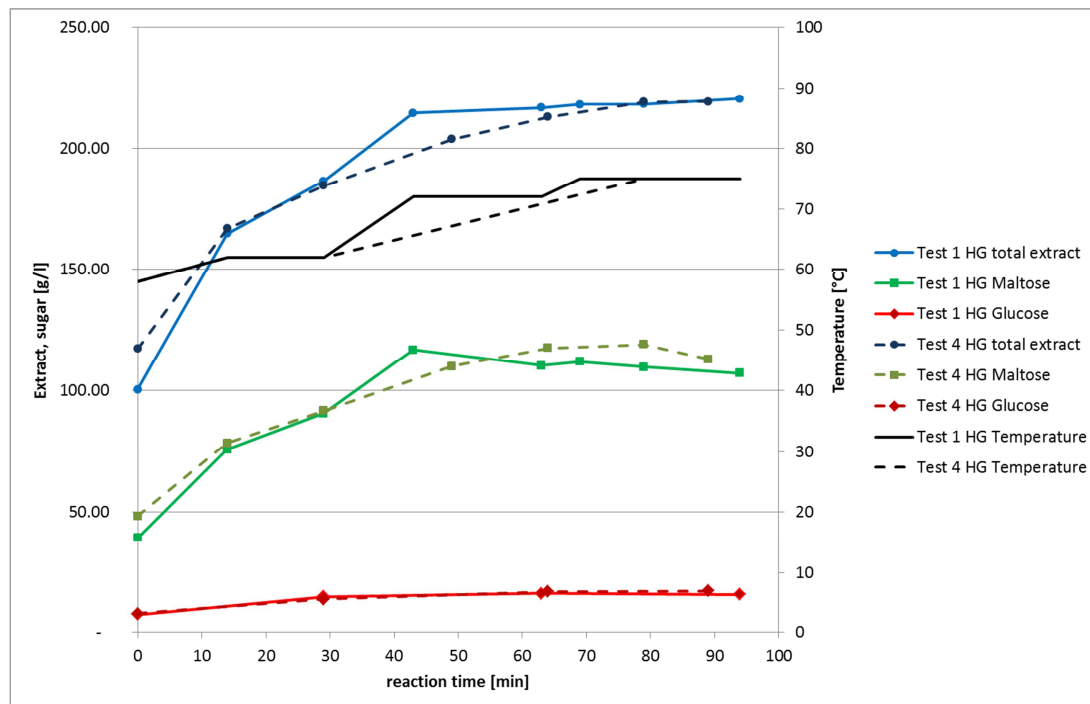


Figure 6-10: Evolution of total extract, maltose and glucose during mashing - comparison of the standard temperature profile (Test 1) to Test 4 at higher gravity

In Figure 6-11 the effect of new profiles on FAN and β -glucan levels is presented. It can be seen that FAN and β -glucan are basically uninfluenced by the temperature profiles during mashing if well modified malt is used, a fact that has already been stated by other authors [59, 119].

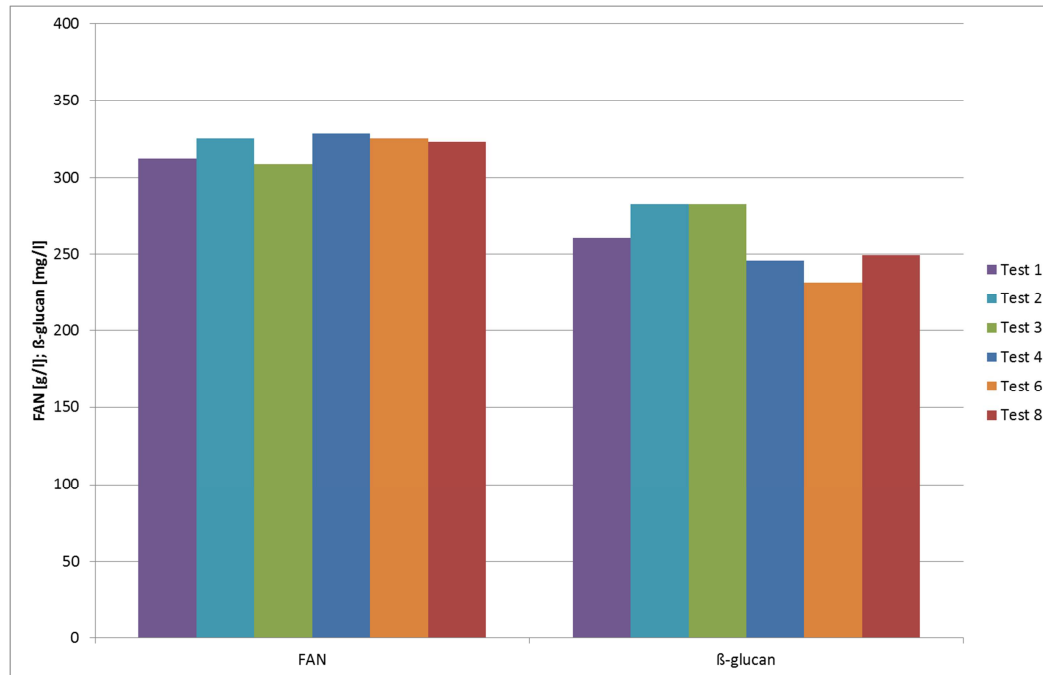


Figure 6-11: FAN and β -glucan analysis for the test runs

The newly developed mashing profiles in this study are different to optimized profiles reported by Durand et al. [67] based on dynamic simulations, because in their study optimization was carried out for temperature and duration of mash stands while defining the number of mash stands to 3-5 stands and the total mashing time to 115 min. This is significantly longer than the total mash duration chosen in the profiles in this work. Mashing-in temperatures were also significantly lower. However, their findings include two optimized profiles with mash stands only at low to moderate temperatures (~ 42 - 64 °C), which to some extent, is in line with the findings in this study. The authors do not consider enzyme deactivation. A significant difference to the mashing profiles presented in this work is the very high heating rates in the simulation based optimization [67].

6.1.2.3 Adaptation of kinetic models to test results and discussion

Although the laboratory experiments confirmed the hypothesis developed with the kinetic models A and B, the absolute values and time profiles of the model were not exactly reproduced in the experiments. This is due to several reasons: Firstly, malt specifications were different and secondly the temperature profiles achieved in the experiments deviate slightly from the defined ones due to the significant temperature drop after mashing in and also due to the manual tuning of the temperature in the technical set-up.

However, even when the malt specifications were changed, the fast hydrolysis shown by the experiments could not be reproduced in the kinetic models. Therefore the models were slightly adapted.

At first, the malt analysis data was extended from the values given in literature in order to have a reasonable value for detailed composition of the malt. Barley consists of starch, sugars, proteins and non-starch polysaccharides such as β -glucan, of which about 2/3 are non-soluble [100]. Starch content in different barley varieties has been widely analysed and lies in the range of 58-68 % [59,

100, 120, 190]⁶. During malting starch content reduces by approximately 5 % [120], so malt has a starch content of about 53-63 %. For modelling the compounds present in wort after mashing, we are most interested in the soluble compounds of malt, which are in addition to starch, sugars, proteins and soluble non-starch polysaccharides including pentosans and glucans.

Sugar content of malt is in the range of 8-9 % with the main sugars being glucose and fructose [59, 120]⁷. For modelling the fermentable extract composition an assessment of the initial sugar contents is important. This was conducted according to the recalculation of Briggs based on the values published by Hall and co-workers [59]. Sucrose concentration was increased according to the findings in the experiments. Table 6-5 summarizes the malt composition used in the models.

Table 6-5: Malt composition assessment

Malt composition	
Starch	56%
Glucose	2.9%
Fructose	0.5%
Sucrose	3.5%
Maltose	0.7%
maltotriose	0.4%
Glucans and pentosans	2.3%

Starch hydrolysis was modelled with the known malt parameters. For Model A, the bases of modelling on the enzyme concentration in g enzyme per l wort, a reasonable conversion factor for U/g enzyme (based on the analysis of U/g malt) was found before model adaptation by varying α -amylase concentration and fixing β -amylase with the known ratio from the analysis of enzyme activity. The best data fit was found at the conversion factor $13,00 \cdot E6$ U/g enzyme.

The same temperature profile as in the experimental tests was applied, considering the temperature drop after adding the grist to about 55.5 °C and the subsequent heating to 58 °C within 5 minutes. This was then taken as the starting point for the comparison to the analysis results, as the first sample was drawn once the temperature had reached 58 °C.

Figure 6-12 shows the result for the standard mashing profile (Test 1). While Model A shows a slower hydrolysis, Model B slightly overestimates the hydrolysis rate. Total extract formation is modelled especially faster. The difference between both models has already been highlighted in chapter 5.1.9.1. It was shown that one major difference is that Model B assumes an immediate dissolution of enzymes into the liquid phase, while model A includes modelling their dissolution within the first time of the mash procedure. This seems to be main reason for the slow hydrolysis found within Model A. The slope of the curve for total extract formation and maltose formation of Model A is actually more similar to the experimental data than the steep slope of the curves of Model B.

Model A was therefore adapted to exclude the dissolution of enzymes, so that an immediate dissolution is assumed. Additionally the activation energy for denaturation of β -amylase and the reaction constant for glucose hydrolysis were slightly changed (see Table 4-3).

⁶ Kunze, p. 169; Briggs, p.125

⁷ Kunze, p. 169; Briggs, p.125

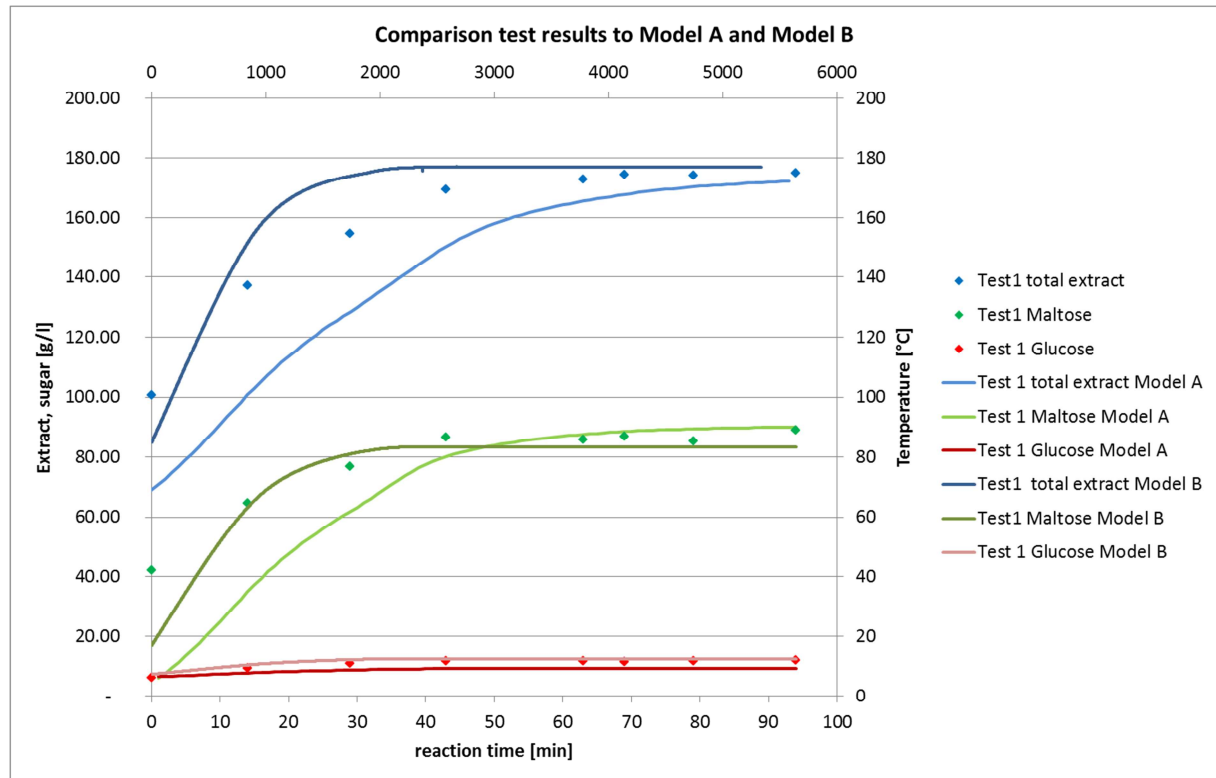


Figure 6-12: Comparison of experimental test result to starch hydrolysis models

Table 6-6: Parameter adaptation for Model A

Parameter	Model A	Model A - adapted
B_{glucose}	$9 \text{ [l/(g*min)]} * 10^{(12)}$	$12,5 \text{ [l/(g*min)]} * 10^{(12)}$
$E_{\text{denat,}\beta\text{-amylase}}$	$4,5 * 4,185 \text{ [J/mol]} * 10^4$	$4,488 * 4,185 \text{ [J/mol]} * 10^{(4)}$

Figure 6-13 shows the comparison of the experimental data of Test 1 to the modelled values. The model now fits very well to the data. We can therefore conclude that the basic modelling of Marc and Engasser provides hydrolysis schemes that are acceptably accurate [136], and the assumptions by other authors [44, 114] to neglect dissolution modelling of sugars and enzymes present in starch is valid. For better usability of the model the parameters can be adapted to allow for directly using standard activity measurement of α - and β -amylase.

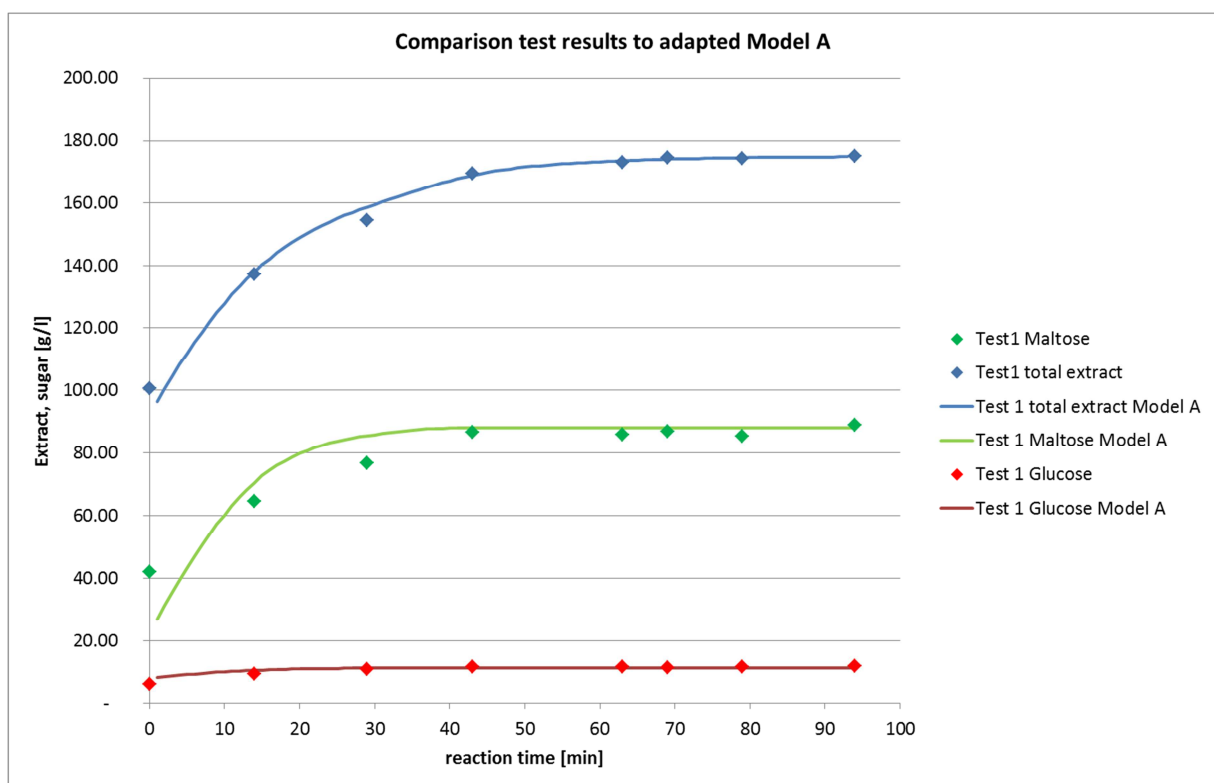
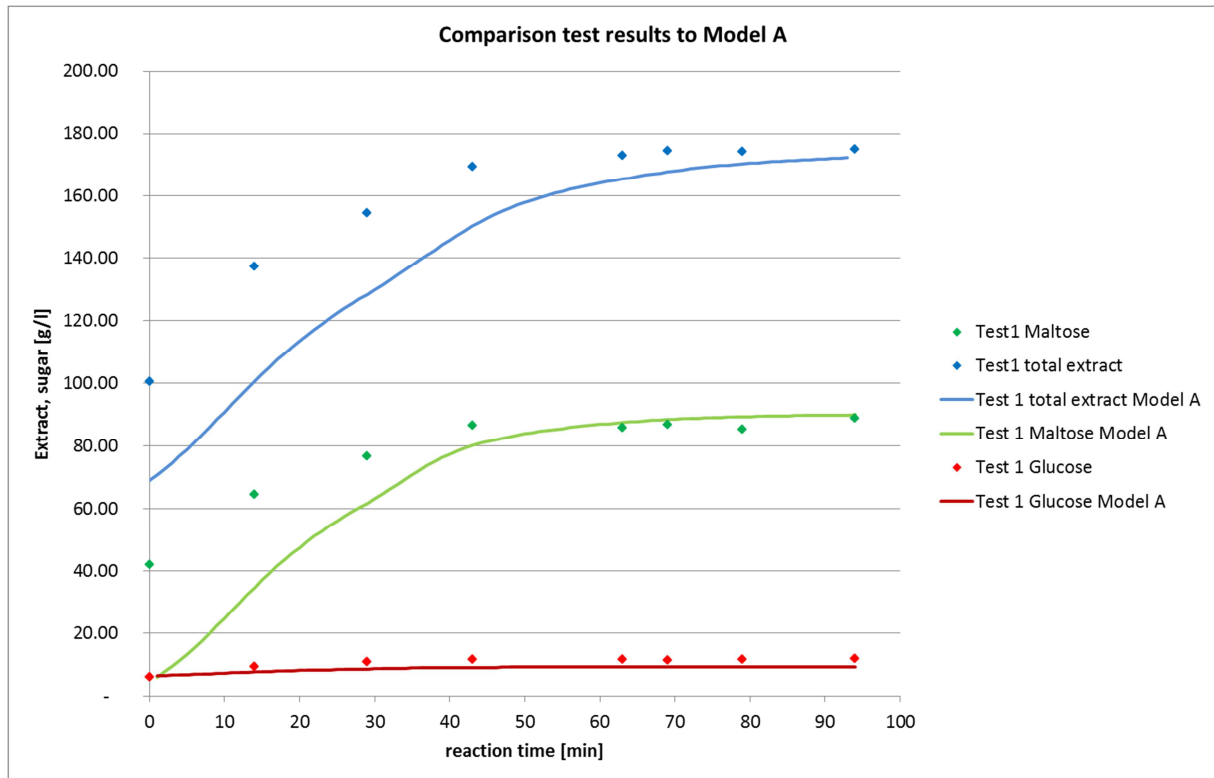


Figure 6-13: Comparison of experimental data to Model A (top) and to the adapted Model A (bottom)

Interestingly, the results of Model A with the given specifications of the malt used in the laboratory, shows a different pattern in comparison to the model results showed in 6.1.1. This is mainly due to the different amylase activities of the two different malts. With equal activities of α - and β -amylase in 6.1.1 an increase of dextrin formation is shown after the first 20 minutes of mashing. The malt

used in the laboratory has significant higher β -amylase activity. With this malt a decrease in dextrin formation is shown (see Figure 6-14). This can be explained by the rapid dextrin decomposition by the abundant β -amylase, while the formation of dextrins by α -amylase lacks behind to level it off. At higher temperatures, when β -amylase denatures, the action of α -amylase becomes visible. This is shown in Figure 6-15, where relative enzyme activity is calculated as actual enzyme activity based on the maximum activity of each enzyme as given in 5.1.9.1.

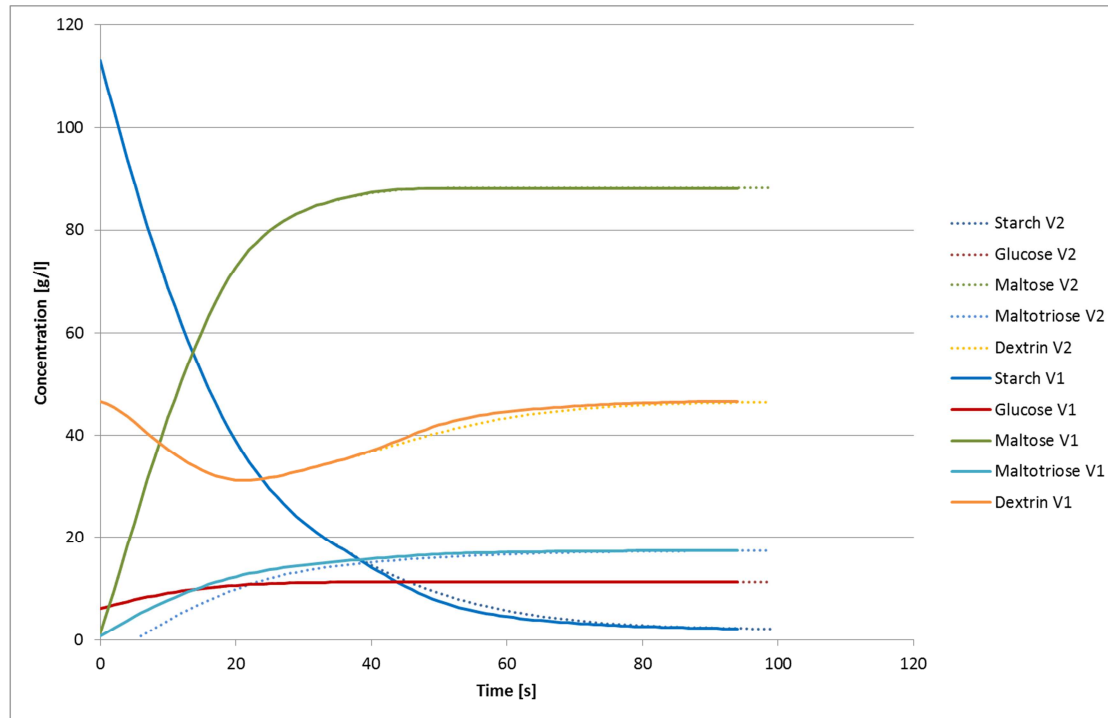


Figure 6-14: Results of the adapted Model A for Test 1 and Test 2

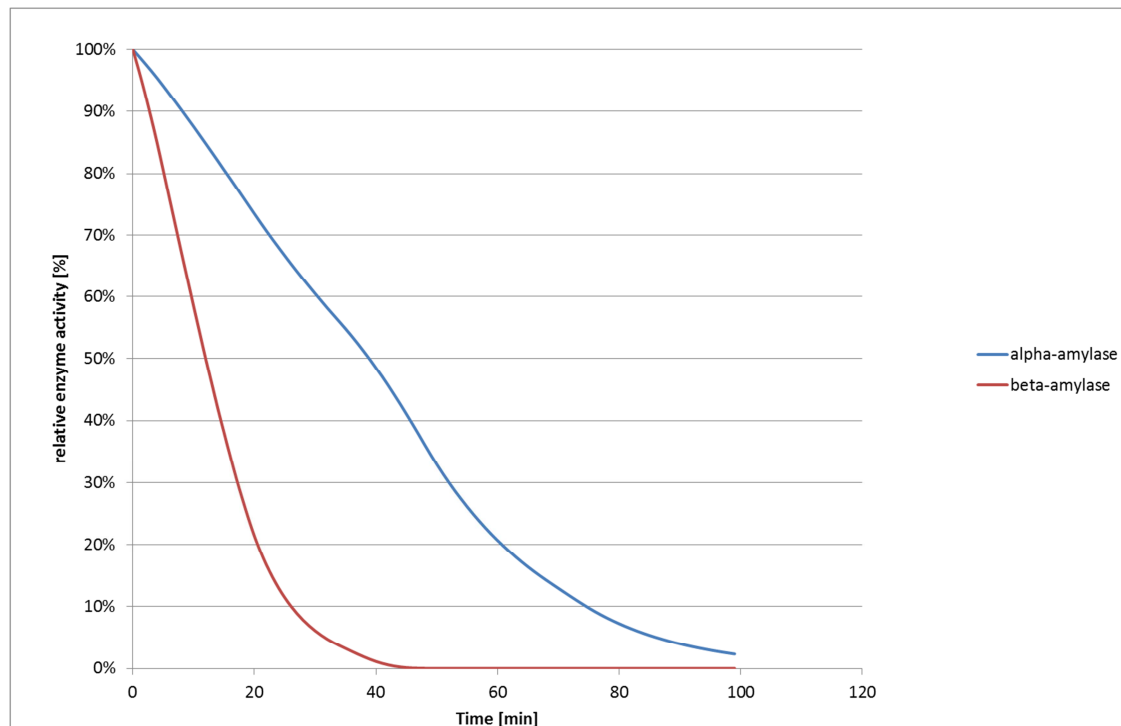


Figure 6-15: Relative enzyme activity modelled by the adapted Model A for Test 1

6.2 Process technologies for the new mashing procedures

6.2.1 Limitations of the conventional mash tun for efficient energy supply

Heating of conventional mash tuns usually takes place from the outside, via double walls or welded tubes through which steam is flowing as a heat carrier in most cases. This type of heating results in a low heat transfer coefficient: the mash is agitated at low velocity to avoid shear stress and therefore the heat convection at the inside of the tank is limited.

Figure 6-16 shows an example of the overall heat transfer coefficients in a stirred tank with a high viscosity process medium with stirrer tip speeds of 1-7 m/s. When assuming a heat transfer coefficient α -value 4,000 W/m²K on the supply side, k-values are one order of magnitude below, so clearly the α -value of the process fluid side in the stirred tank is the limiting factor in heat transfer. In addition to the low α -value of the process fluid side fouling on the inside of the tank may additionally pose limitations to heat transfer. Assuming a k-value of 350 W/(m²K) a fouling layer of 0.5 mm with a heat conductivity of 1 W/(m²K) the overall k-value is reduced by 15 %.

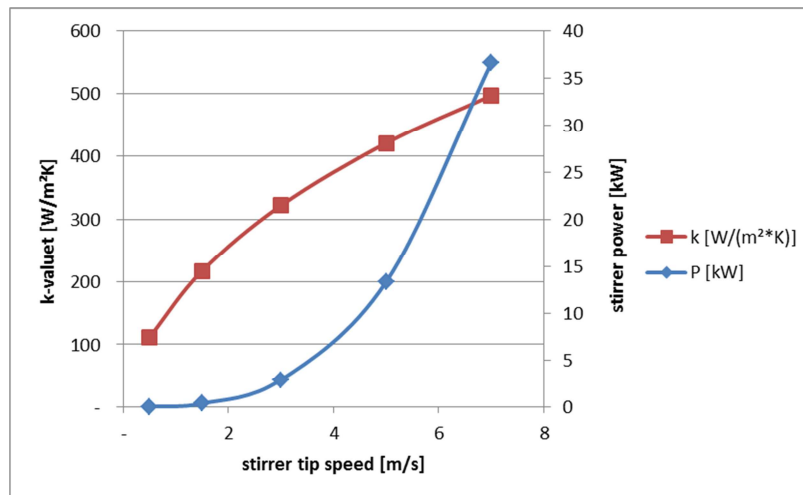


Figure 6-16: Exemplary data for heat transfer coefficients and stirrer power for a high viscosity process medium in a batch stirred tank with heating jackets

Heat transfer coefficients can be increased via increasing stirrer speeds, however at higher costs with more powerful motors. Additionally in food treatment, and especially in mashing, the gentle treatment of the process medium is vital to avoid negative effects of shear stress. Secondly, heat transfer might be increased via increasing heat supply temperature leading to a higher temperature gradient. However, in mashing it is known that high wall temperatures lead to increased fouling which again negatively affects heat transfer and requires intensive cleaning of the vessels.

In mash tuns, k-values are typically in the range of 350-900 W/m²K for water heated/cooled vessels [177]. These values are too low to allow a simple retrofit to low temperature heat supply systems (integration of renewable energy and waste heat). Heat transfer areas that are required to realise such heat supply with current heat transfer coefficients are much larger than the existing transfer areas. This holds true for the process heating rates commonly applied in practice and will be further shown in 6.2.2. For retrofit, therefore, additional heat transfer plates have to be installed. Heating plates mounted inside the stirred tank are a sensible solution and recent developments in dimple plate design enable efficient heat transfer (e.g. BUCO Wärmeaustauscher International GmbH), leading also to better heat transfer coefficients in comparison to double walls or welded tubes.

As has been summarized in Table 4-3 stirred tanks do generally not perform well compared to other technologies in terms of heat transfer due to their wide residence time distribution and their low heat transfer coefficients.

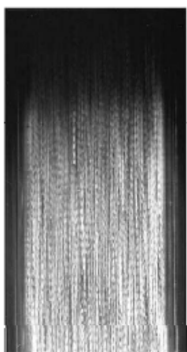
Mashing also faces the problems common to other batch process in terms of energy efficiency. In discontinuous processing energy demand might increase due to additional heat input necessary to heat up vessels to operating temperature. For this reason operators might seek to minimize breaks between batches. When the brewhouse is operating, vessels are usually in operation every 2-3 hours. Some breweries tend to brew several days (e.g. Monday – Wednesday) 24 hours per day rather than brewing each weekday. In this case there is only one long operation break after which the vessels have to be brought to operating temperature. While short breaks minimize heat losses, care has to be taken with leaking steam valves and fittings during stand-by operation. It has been observed several times in practice that during breaks processes without heating requirements still show a constant heat demand. Such “constant” heat consumers might lead to substantial energy losses. Approaches towards more continuous processing are here beneficial for minimizing energy losses.

It is common practice to implement alternatives to stirred tank reactors for higher process efficiency. In many cases it is state-of-the-art to use more efficient technologies, such as flash pasteurizers for continuous pasteurization. In comparison to chamber pasteurization, in which solid products are pasteurized, continuous flash pasteurization requires only 1/10 of the energy demand, as high k -values and large heat exchanger areas allow internal heat recovery.

The research of Özkan and co-authors [160] and the research agenda for process intensification [84] have demonstrated that processes performed in plug flow can enhance the reaction rate substantially due to a more structured process layout. The stirred tank is a classic example of a process technology which does not reach such conditions, but rather shows wide residence time distribution and low mass transfer rates.

However, there are certain processes, classically done in stirred tank reactors, that cannot be performed in plug flow reactors:

- processes with long residence times (minutes - hours)
- small plants in which several process steps (including processes with slow intrinsic kinetics) are performed in the same vessel
- processes, for which good mixing behavior is essential.



For processes with long residence times the current available plug flow reactors are not a sensible alternative, as long material and cost intensive reactors would be required. The velocity of the process media in such reactors would be so low that heat transfer coefficients would be low and low temperature heat supply could not be realized. Neither plate - nor tube reactors enable efficient mixing of process fluids.

Figure 6-17: Visualisation of flow behaviour in plug flow reactors [154]

Due to the listed reasons, mashing cannot be performed efficiently in classical tubular reactors.

To allow efficient low temperature heat supply in mashing, there are therefore two main options:

- new temperature profiles during mashing that allow for better integration of low temperature heat supply in mash tuns without affecting the product quality
- develop new mashing technologies, based on new reactor concepts and continuous processing

These options will be discussed within the next chapters.

6.2.2 Enhanced possibilities for low temperature heat supply in conventional mash tuns

The above developed new temperature programmes for mashing allows for the development of a low temperature heat supply much easier in comparison to the classic profiles. In the following discussion, this is shown for the conventional mashing profile Test 1 compared to newly developed profiles such as Test 2 and Test 4. With the new profiles here opening the pathways for more unconventional temperature profiles, heat transfer requirements might be even more reduced with future research.

Heat transfer into a stirred tank can be calculated according to [77] assuming constant supply temperature of the heat transfer medium $T_{hs,in}$ and varying runback temperature:

$$\frac{T_{hs,in} - T_{mash}(t)}{T_{hs,in} - T_{mash,in}} = \exp \left[- \left(\frac{\dot{m}_{hs} * c_{p,hs}}{m_{mash} * c_{p,mash}} \right) * \left\{ 1 - \exp \left(\frac{-k * A}{\dot{m}_{hs} * c_{p,hs}} \right) \right\} * t \right] \quad 6-2$$

with

$$\frac{1}{k} = \frac{1}{\alpha_{hs}} + \frac{s_w}{\lambda_w} + \frac{s_f}{\lambda_f} + \frac{1}{\alpha_{pm}} \quad 6-3$$

based on the heat transfer coefficients α on the heat supply side (hs) and process medium side (pm) and on the thickness and heat conductivity of the wall (w) and fouling layer (f).

To account for the varying mass flow of the heat supply medium based on its varying runback temperature $T_{hs,out}$, and to take into account the effects of the runback temperature on heat transfer, the transferred heat was also calculated based on:

$$Q = k * A * \Delta T \quad 6-4$$

ΔT is calculated based on the temperature gradients at the start and the end of each heating step:

$$\Delta T = \frac{\Delta T_{start} - \Delta T_{end}}{\ln \left(\frac{\Delta T_{start}}{\Delta T_{end}} \right)} \quad 6-5$$

$$\Delta T_{start} = \frac{(T_{hs,out} - T_{mash,start}) - (T_{hs,in} - T_{mash,start})}{\ln \left(\frac{(T_{hs,out} - T_{mash,start})}{(T_{hs,in} - T_{mash,start})} \right)} \quad 6-6$$

$$\Delta T_{end} = \frac{(T_{hs,out} - T_{mash,end}) - (T_{hs,in} - T_{mash,end})}{\ln \left(\frac{(T_{hs,out} - T_{mash,end})}{(T_{hs,in} - T_{mash,end})} \right)} \quad 6-7$$

The mass flow of the heat supply medium was then calculated based on a targeted runback temperature:

$$\dot{m}_{hs} = \frac{Q}{(T_{hs,in} - T_{hs,out}) * c_{p,hs}} \quad \text{6-8}$$

We assume a mash process processing of about 180 hl mash with a liquor to grist ratio of 3.5 hl/100 kg malt. Based on typical design criteria [207], a mash tun for carrying out an infusion mashing for this size should have the volume of

$$V_{mash\ tun}[hl] = V_{mash} * [(100\% + f_{ST})/100\%] = 243 \text{ hl}$$

based on an assumed factor for additional volume (Steigraum) f_{ST} of 35 %. With a D:H ratio of 1:1 [207], height and diameter equal to 3.14 m. In a typical mash tun in practice, this tun would be equipped with a heating area of about 6 m² on the bottom of the vessel and another 4-6 m² on the side. This heat exchange area would be sufficient for heating the vessel with hot water at 135 °C, with a k-value of 828 W/m²K based on the parameters given in Table 6-7 and a standard industrial infusing mash with a temperature profile of Test 1.

Table 6-7: Parameters for calculating heat transfer coefficient in a hot water heated mash tun (welded tubes)

α_{hs}	λ_w	s_w	s_f	λ_f	$\alpha_{pm} [180]$
[W/m ² K]	[W/mK]	[m]	[m]	[W/mK]	[W/m ² K]
2000	15	0.0015	0.0002	1	2451

Table 6-8 shows which percentage of the required heat input could be supplied. Percentages higher than 100% mean that heat transfer with the given parameters is possible. Due to the fact that usually one heating step is limiting, other heating steps might show a percentage well above 100%. In practice lower heat supply medium flows are necessary for these heating steps.

Table 6-8: Heat transfer in a conventional hot water heated mash tun

conventional water heated mash tun (hot water boiler; temperature profile acc. to Test 1)							
	$T_{mash,in}$	$T_{mash,out}$	heating rate	$T_{hs,in}$	$T_{hs,out}$	A	possible energy input based on requirement
	[°C]	[°C]	[K/min]	[°C]	[°C]	[m ²]	[%]
STEP 1	58	62	0.29	133.5	100	11.0	313.06%
STEP 2	62	72	0.71	133.5	100	11.0	103.79%
STEP 3	72	75	0.50	133.5	100	11.0	115.25%

If the same vessel should now be used for low temperature heating with a supply temperature of 90 °C (runback 80 °C), the possible heat transfer has to be re-calculated. In case steam is used as a heat carrier in the existing system, the usability of the installed heat exchanger surface for water as a heat carrier has to be checked additionally. The new heat transfer coefficient will be higher, assuming a decrease in fouling layer by 50 % due to the lower temperature of the wall. This results in a heat transfer coefficient of 902 W/m²K. With these new boundary conditions, the required heat cannot be supplied to the system with the given 11 m² of heat exchange area. Instead 30 m² would

be necessary. The limiting factor is the high heating rate in the current temperature profile of the mashing process. In case a temperature profile in mashing is used with lower heating rates, such as the developed profiles in Test 2 or Test 4, required transfer areas result in 11 and 9 m² respectively. This shows that the newly developed temperature profiles for mashing make low temperature heat supply possible without retrofit of heat exchange area.

Table 6-9: Heat transfer in mash tuns via welded tubes heated with low temperature heating medium for different mashing programs

conventional water heated mash tun (low temperature water supply; temperature profile acc. to Test 1)							
	T _{mash,in}	T _{mash,out}	heating rate	T _{hs,in}	T _{hs,out}	A	possible energy input based on requirement
	[°C]	[°C]	[K/min]	[°C]	[°C]	[m ²]	[%]
STEP 1	58	62	0.71	90	80	30	506.23%
STEP 2	62	72	0.50	90	80	30	139.66%
STEP 3	72	75	0.00	90	80	30	101.63%
water heated mash tun with new heating profile (low temperature water supply; temperature profile acc. to Test 2)							
	T _{mash,in}	T _{mash,out}	heating rate	T _{hs,in}	T _{hs,out}	A	possible energy input based on requirement
	[°C]	[°C]	[K/min]	[°C]	[°C]	[m ²]	[%]
STEP 1	58	62	0,29	90	80	11	245,94%
STEP 2	62	75	0,33	90	80	11	101,09%
water heated mash tun with new heating profile (low temperature water supply; temperature profile acc. to Test 4)							
	T _{mash,in}	T _{mash,out}	heating rate	T _{hs,in}	T _{hs,out}	A	possible energy input based on requirement
	[°C]	[°C]	[K/min]	[°C]	[°C]	[m ²]	[%]
STEP 1	58	62	0.29	90	80	9	207.67%
STEP 2	62	75	0.26	90	80	9	102.72%

In case old welded tubes are not usable, because they are designed for steam heating, the new temperature profiles still substantially reduce the effort and costs of a retrofit. For retrofit, therefore, additional heat transfer plates have to be installed. Heating plates mounted inside the stirred tank are a sensible solution and recent developments in plate design enable efficient heat transfer, also leading to better heat transfer coefficients in comparison to double walls or welded tubes. Heat transfer coefficients of such plates are in the range of 1000-2000 W/m²K. Assuming a k-value of 1458 W/m²K based on the parameters in Table 6-10, necessary heat exchange area can be substantially reduced with the newly proposed mashing temperature programs.

Table 6-10: Parameters for calculating heat transfer coefficient in a low temperature heated mash tun (internal heating plates)

α_{hs}	λ_w	s_w	s_f	λ_f	α_{pm}
[W/m ² K]	[W/mK]	[m]	[m]	[W/mK]	[W/m ² K]
5000	15	0.0015	0.0001	1	3500

While 19 m² heat transfer area would be required for heating a standard temperature programmed infusion mash, only 5.5-7 m² heat transfer areas are necessary for the new temperature profiles. Results of the heat transfer calculation are summarized in Table 6-11.

Table 6-11: Heat transfer in mash tuns via internal heating plates heated with low temperature heating medium for different mashing programs

conventional water heated mash tun (low temperature water supply; temperature profile acc. to Test 1)							
	$T_{mash.in}$	$T_{mash.out}$	heating rate	$T_{hs.in}$	$T_{hs.out}$	A	possible energy input based on requirement
	[°C]	[°C]	[K/min]	[°C]	[°C]	[m ²]	[%]
STEP 1	58	62	0.29	90	80	19	513.03%
STEP 2	62	72	0.71	90	80	19	141.91%
STEP 3	72	75	0.50	90	80	19	103.78%
water heated mash tun with new heating profile (low temperature water supply; temperature profile acc. to Test 2)							
	$T_{mash.in}$	$T_{mash.out}$	heating rate	$T_{hs.in}$	$T_{hs.out}$	A	possible energy input based on requirement
	[°C]	[°C]	[K/min]	[°C]	[°C]	[m ²]	[%]
STEP 1	58	62	0.29	90	80	7	251.66%
STEP 2	62	75	0.33	90	80	7	103.12%
water heated mash tun with new heating profile (low temperature water supply; temperature profile acc. to Test 4)							
	$T_{mash.in}$	$T_{mash.out}$	heating rate	$T_{hs.in}$	$T_{hs.out}$	A	possible energy input based on requirement
	[°C]	[°C]	[K/min]	[°C]	[°C]	[m ²]	[%]
STEP 1	58	62	0.29	90	80	5.5	205.43%
STEP 2	62	75	0.26	90	80	5.5	101.80%

6.2.3 Evaluation of Oscillatory baffled reactors for mashing

Oscillatory baffled reactors have been researched by numerous researchers in the past years mainly for chemical applications. A core characteristic of OBRs is their ability to decouple flow velocity and

residence time. This is achieved via oscillations inducing turbulent flow of process media (typically Re 1000-2000) between baffles while the net flow velocity remains in the laminar regime (Re 50-200). Oscillating reactors are thus perfectly suited for processes in which long residence times are necessary and high mixing performance is essential. Oscillations are induced into the fluid via a piston, the reactor itself remains stationary. The area between the baffles is highly turbulent and ideally mixed. Very high mass and heat transfer coefficients can be reached in this way.

Figure 6-19 shows that Nusselt number, as dimensionless parameter for heat transfer, can be significantly increased in oscillating reactors especially at slow net flow of the process medium resulting in a low Reynolds number of the process medium flow. In comparison to stirred tanks, OBRs in principle show better mass transfer rates, an effect that is even more pronounced at higher power densities [155].

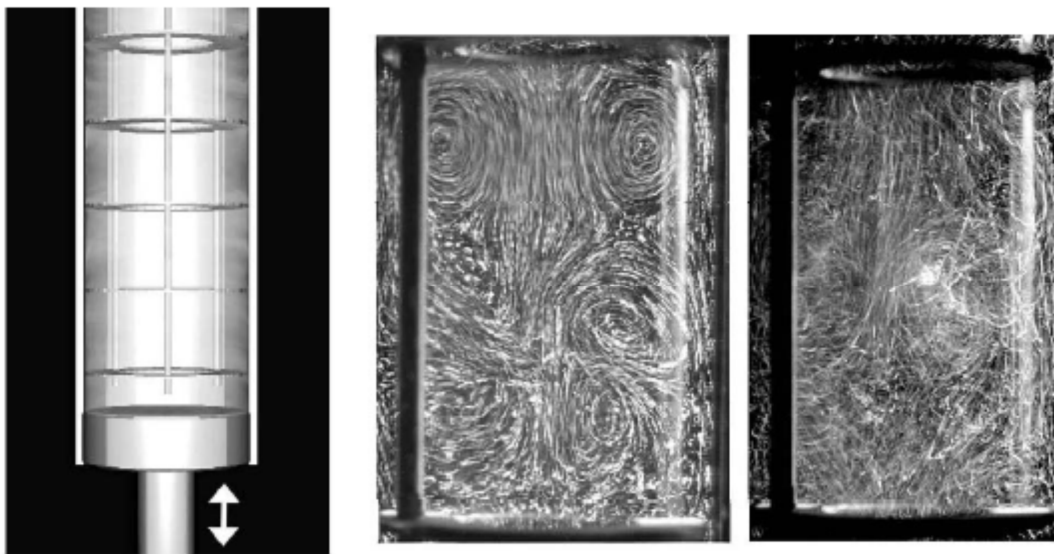


Figure 6-18: Visualisation of fluid flow in an oscillatory baffled reactor [154]

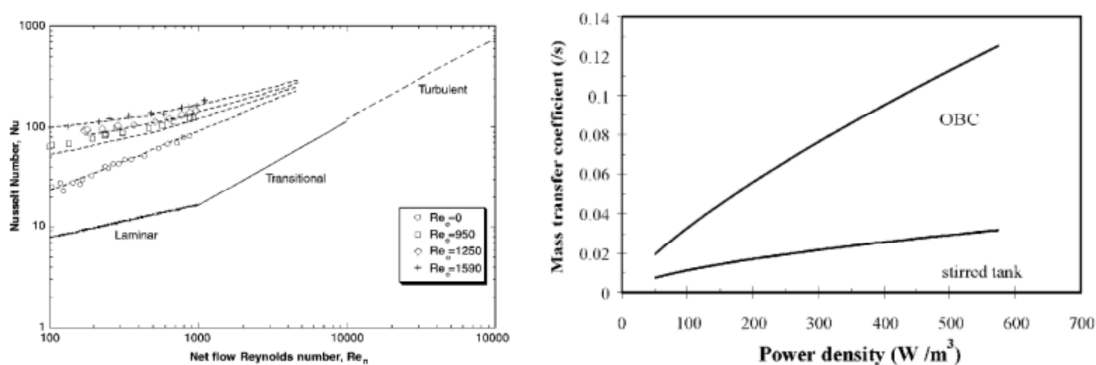


Figure 6-19: Increase in heat and mass transfer in oscillating reactors [155, 192]

Due to improved process conditions reaction times may be significantly reduced and heating and cooling processes can be enhanced. The following table shows some selected research studies in the chemical industry.

Table 6-12: Examples of OBR implementation in research studies

application	Effects on reaction time, mass transfer, heat transfer and flow regime	source
methylester (biodiesel) production	Reduction of the reaction time by 75-90% in comparison with a stirred tank with equal yield	[167]
Gas-liquid contacting (air in glycerol)	Increase in mass transfer by two orders of magnitude in comparison to bubble columns	[174]
Fluid mixing (water and ink)	High degree of plug flow; narrow residence time distribution at laminar flow	[175]
Spiral baffles for fluid mixing	Increase of Nu by a factor of 4 in comparison to a stationary tubular reactor	[186]
bio-butanol production	Increase in productivity by 38%	[139]
Protein Refolding	Equal product yield in OBR and stirred tank at considerable lower Reynolds numbers (1/3)	[123]
Bio-polymer production	Considerable increase in polysaccharide productivity and reduction of reaction time in OBR by 50% in comparison to stirred tanks	[79]

It can be proved that the implementation of OBRs can lead to a significant improvement potential in chemical processing with increase in productivity of 30-40%, shortening of reaction times of 50-90 % and an increase of heat transfer up to a factor of 4. NiTech Solutions Limited (<http://www.nitechsolutions.co.uk>), as well as AM Technology (<http://www.amtechuk.com>) from the UK sell OBRs for a number of applications (crystallization, extraction, polymerization, heterogeneous catalysis and reactions) on industrial scale. So far, OBRs have not been tested and implemented in food processing.

As discussed above the technology readiness is proved in certain applications, however there are a number of research projects still dealing with the detailed rheology with complex process media in oscillatory flow reactors. The use of an OBR technology for mashing as first application in the food industry therefore has high innovative characters. There are a number of reasons why the OBR technology will have to be specifically adapted for mashing:

- Mash is a non-Newtonian fluid whose viscosity is considerably higher than water and changes during processing. The viscosity of mash is influenced by the liquor to grist ratio and the fineness of the grist. The work of Tse et al. [199] and Herrmann [94] have shown the varying behaviour of the viscosity of the mash during processing. A large viscosity peak occurs during swelling and gelatinization of starch until the large polymers are further degraded into sugar by enzymatic action. The quicker the heating rate, the more pronounced is the peak in viscosity [199]. Herrmann also showed in his work that viscosity is affected first by gelatinization until subsequent dissolution reaction lead to further changes in viscosity. Viscosity measurements showed values in the range of 80-297 mPas for coarse grist (0.8 mm

roller distance) and 20-37 mPas for fine grist (0.2 mm roller distance) for a liquor to grist ratio of 1:2.8. Mashing profiles were comparable to our standard profile (Test 1) with an amyloysis rest at 62°C and a saccharification rest at 72°C before heating to 78°C at the end of the process. However, mashing-in was performed at 40°C with a first proteolysis/cytolysis rest at 50°C. At the end of the amyloysis rest at 62°C viscosity was found to be <129 mPas for coarse grist and < 25mPas for fine grist. After husk separation the viscosity of the wort was in the range of 1-2 mPas [94]. As viscosity has a significant influence on the operating parameters of oscillatory flow reactors, the operation of such reactors must be tuned to these high viscous and non-Newtonian fluids. Inconventional reactors these fluid characteristics are also a challenge due to high energy input via stirring and low heat transfer coefficients. A development of OBRs for such fluids could lead to a significant leap in technology.

- For process media in the food industry gentle treatment is decisive for food quality. Here, thermal stress is important as well as mechanical stress due to shear forces. Due to the improved heat transfer and shorter reaction times in OBRs, thermal stress should be reduced. Regarding mechanical stress, OBRs should also have positive effects as shear forces from gentle oscillations should be lower in comparison with stirrers or pumps (in case of external heat exchangers). The operation of OBRs in the food industry will require such parameters that minimize thermal and mechanical stress.
- The biological activity of food stuff leads to the fact that media tend to build up biological films on layers (fouling). This hinders heat transfer and increases cleaning demand. Based on the oscillating flow fouling should be reduced in comparison to conventional technologies. Again, this will be a decisive aspect for operating conditions of OBRs for food stuff.
- The viscosity and fouling characteristics of process media also has impact of the baffle design. In the chemical industry perforated plates are commonly used and advanced baffle geometries are currently under research. For food stuffs with emulsions and/or particle loading ideal geometries need to be found for the different application requirements. For mashing, helix baffles seem to be most promising, as they avoid clogging of particles. Additionally their use seems to have positive effects on narrow residence time distribution [186].

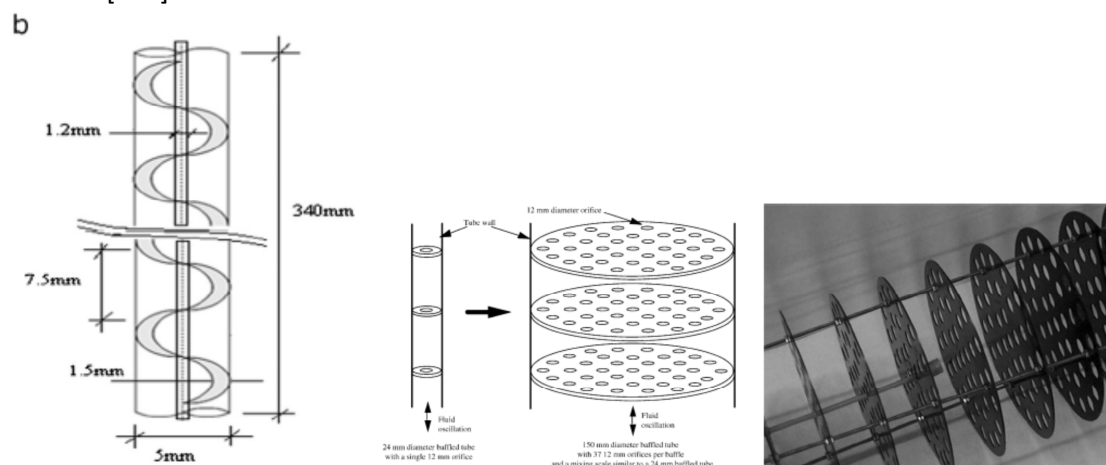


Abbildung 1: Examples of helix and perforated plate baffles for oscillating reactors [185, 186]

6.2.3.1 Design of an OBR for mashing

In the design of oscillatory flow reactors, there are a few decisive design parameters [192]. Two key figures are the oscillatory Reynolds number Re_o and the net Reynolds number Re_{net} . While Re_{net}

describes the flow profile of the medium in the tubular reactor without oscillations, Re_o gives the Reynolds number of the oscillating flow. This oscillatory Reynolds number is calculated based on the frequency and the oscillation amplitude.

$$Re_{net} = \frac{\rho * u * d}{\eta} \quad 6-9$$

$$Re_o = \frac{x * \omega * d * \rho}{\eta} \quad 6-10$$

$$St = \frac{d}{4 * \pi * x} \quad 6-11$$

$$\psi = \frac{Re_o}{Re_{net}} \quad 6-12$$

The velocity ratio defines the increase of Re_o based on Re_{net} . Typical values are 2-6 for achieving good plug flow [192], while for meso-scale reactors at lower Re_{net} velocity ratios are recommended at 4-10 [166].

The Strouhal number describes the frequency for vortex shedding. Its definition for oscillatory flow reactors is given in Formula 6-12, it relates the pipe diameter to the chosen oscillation amplitude. For most technical application $St = 0.2$ is a standard value [42, 218]. In Figure 6-20 the Strouhal number is plotted over the pipe diameter for different oscillation amplitude. The blue area marks the feasible operating region for Strouhal numbers close to 0.2. According to research experience of oscillatory flow reactors values should be below 0.4 to achieve good flow regimes [91]. Very low Strouhal numbers, at high amplitudes and Reynolds numbers, are critical as their corresponding critical velocity for instable flow is also very low [218].

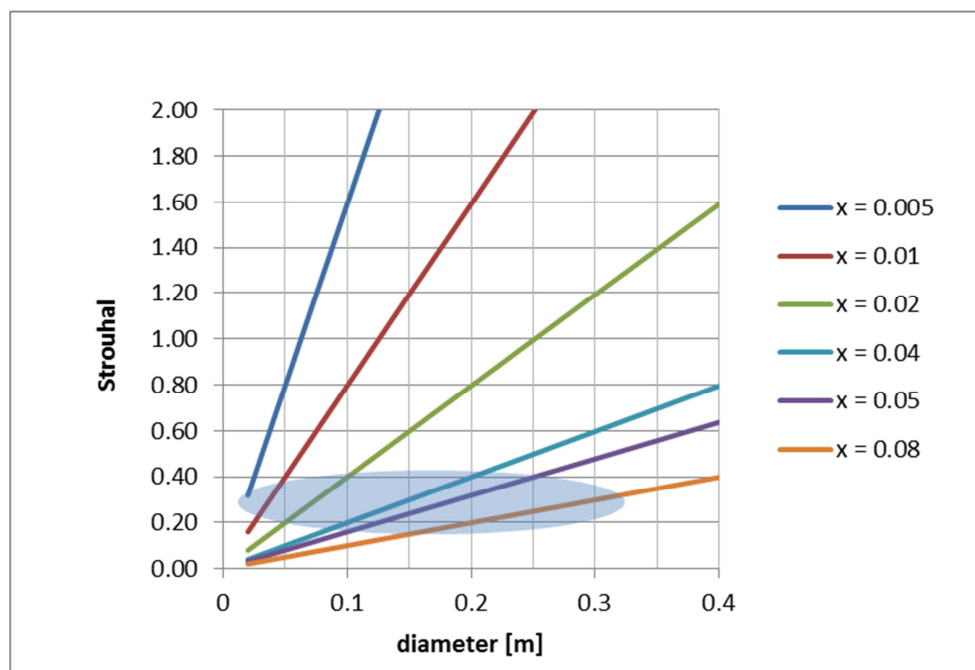


Figure 6-20: Strouhal number for different oscillation amplitudes

Additionally there are two important geometric ratios which should be kept constant [192] which are the baffle spacing L and the baffle orifice open area S . The optimized baffle spacing is

$$L = 1.5 * d \quad \mathbf{6-13}$$

S which is defined as

$$S = \frac{d_0^2}{d^2} \quad \mathbf{6-14}$$

is normally in the range of 0.2-0.4, with 0.25 being a typical value [192].

Based on the dimensionless parameters a design-nomogram has been developed for a process medium with given viscosity and density and for oscillations at a defined frequency. It consists of 3 diagrams which are linked to each other:

- Diagram 1 plots Re_o over the pipe diameter for different oscillation amplitudes. It further relates Re_o to Re_n over the velocity ratio.
- Diagram 2 shows the relation of Re_n to the superficial velocity in the reactor based on the chosen diameter. The dependence of the production volume to the superficial velocity is also shown on the secondary axis.
- Finally, diagram 3 relates the superficial velocity to the reactor length over the chosen residence time.

Based on the diagram for the Strouhal number (see Figure 6-20), a feasible oscillation amplitude can be selected for a chosen diameter. Knowing the diameter and the oscillation amplitude, Re_o can be calculated in diagram 1 and Re_{net} is defined over the choice of a velocity ratio. Once Re_{net} is known we can move to the upper diagram 2 where the superficial velocity v is given via the chosen diameter. The superficial velocity is linked to the production volume Q according to

$$Q = \frac{d^2 * \pi * u}{4} \left[\frac{m^3}{s} \right] \quad \mathbf{6-15}$$

With the definition of the residence time the required length of the tubular reactor can be read from diagram 3.

The design nomogram can also be used for choosing a feasible design for a required production volume. In that case the production volume is first chosen in diagram 2 and the superficial velocity is known via the choice of the pipe's diameter. Diagram 2 visualizes the feasible diameters: when the vertical line from the production volume intersects with the dashed lines representing the relation between superficial velocity and production volume for a given diameter. Via the known superficial velocity the net Reynolds number is defined for the given diameter. In diagram 1 the chosen pipe diameter and a feasible oscillation amplitude (for Strouhal ~ 0.2) define the oscillatory Reynolds number and the velocity ratio is calculated via the known Re_{net} from diagram 2.

In order to be applicable to mashing, two nomogramms have been developed for the different viscosity ranges of mashes depending on milling size. Based on Herrmann's work [94], a viscosity of 130 mPas was defined for a coarse grist mash, while a viscosity of 20 mPas was defined for a finely ground grist used in mashing. Mash density was set to 1090 kg/m³. Frequency was set to 2 Hz.

The design nomograms show that viscosity is a decisive parameter and the design values change considerably based on its value. In Figure 6-21 (for viscosity 130 mPas) and Figure 6-22 (for viscosity 20 mPas) several possible design configurations are shown. In the design configurations residence time was chosen at 30 minutes. This short residence time was chosen, as the new temperature profiles have shown the potential for considerably faster mashing procedures and an intensification of mass transfer could be further expected by the use of OBRs. The nomograms are however set up in a way that a different residence time only affects the result of the required reactor length in diagram 3. Due to this fact the general designs are also valid for longer residence times when the reactor length is adapted.

Figure 6-21 shows two feasible configurations for high viscosity mash for a pipe diameter of 150 mm and 200 mm with the straight and dashed lines. The pipe diameters were chosen at these values as smaller diameters lead to lower oscillatory Reynolds numbers. For Strouhal to be approximately 0.2, the oscillation amplitude should be rather high at 4-8 cm for these tube sizes according to Figure 6-20. 8 cm was chosen for $d = 200$ mm, while 4 cm oscillation amplitude was chosen for $d = 150$ mm. The resulting Reynolds numbers Re_o are 1,686 and 632 respectively. With a velocity ratio of 6 net Reynolds numbers are defined with 279.5 and 104.8. The straight lines visualize the further design criteria for $d = 200$ mm. The superficial velocity results to 0.17 m/s and a volume of approximately 200 hl/h can be produced. Diagramme 3 reveals that a tube length of approximately 300 m is necessary for 30 minutes residence time. With $d = 150$ mm and Re_{net} is 104.8, the superficial velocity is 0.083 m/s, as visualized with the dashed red lines in the nomogram. Production volume results to slightly above 50 hl/h, while 150 m tubing is required for 30 minutes residence time.

In case a higher production volume should be achieved, a larger pipe diameter is required. The red dotted design lines in the diagram represent an additional design for 620 hl/h production capacity. 350 mm pipe diameter is chosen and the superficial velocity is 0.18 m/s. The tube should be 320 m long for a residence time of 30 minutes. Re_{net} is 521. This time, no velocity ratio is chosen, but the velocity ratio is calculated based on the known Re_{net} and the Re_o resulting from choosing a feasible oscillation amplitude (8 cm) to the predefined pipe diameter. Re_o is 2,950 and the velocity ratio is 5.64.

Similarly, some design options are depicted in Figure 6-22 for low viscosity mash. The straight and dashed lines show two configurations for tube diameters of 200 mm and 150 mm. For $d = 150$ mm again 4 cm oscillation amplitude is chosen, as in one of the designs for the highly viscous mash. However, while the higher viscosity has resulted in an oscillatory Reynolds number of 632, Re_o is now 4,109. With a velocity ratio of 6 the net Reynolds number is 681 and the superficial velocity again results in 0.083 with a production capacity of slightly above 50 hl/h. 150 m tubing is necessary for 30 min residence time. The comparison with the design presented earlier for mash at higher viscosity for the same diameter size, demonstrates the influence of viscosity on the oscillatory Reynolds number. While an oscillation amplitude of 4 cm reaches an oscillatory Reynolds number 632 for the high viscous mash (130 mPas), the low viscous mash (20 mPas) results in an increase of oscillatory Reynolds number by a factor of 6.5.

This also becomes obvious when looking at the design for $d = 200$ mm at low viscosity (straight lines in Figure 6-22): An oscillation amplitude was chosen at 5 cm, as higher amplitudes would result in a value of Re_o above 10,000. In this case Strouhal results to 0.32 and Re_o to 6,848. Aiming at a similar net Reynolds number the velocity ratio would be 10 and Re_{net} results to 666. With a tube length of 110 m for 30 min residence time the production capacity results in 70 hl/h.

More design configurations are shown for a larger capacity requirement at 200 hl/h. Two options are shown in the nomogramm (dotted and dashed/dotted lines), one for a pipe diameter of 200 mm and one with 300 mm. For the 200 mm diameter the required length is above 300 m. Re_{net} is almost 2000. As the oscillation amplitude must not be too low for Strouhal to be in the feasible operating range, the velocity ratio is rather low at less than 4 (see dotted lines). In case the diameter is chosen at 300 mm, the net Reynolds number is lower; however, the oscillatory Reynolds number is higher due to the fact that a high oscillation amplitude is required to keep Strouhal in the range of 0.2. In the diagram the oscillation amplitude x is set to 0.4 and the resulting velocity ratio is 6.5.

Table 6-13 summarizes the design examples shown in the nomogramms. For designing oscillatory baffled reactors, the number of baffles is defined with the baffle spacing L . Based on equation 6-13, the number of baffles is in the range of 311 to 1038 in the design examples.

The comparison of the oscillatory Reynolds number (achieved in a stirred tank), is important for the calculation of the Nusselt number and heat transfer considerations and also gives an indication of the improvement potential in heat transfer. We can see that much higher Reynolds numbers can be achieved in OBRs due to the oscillations, especially at low viscosity.

The power requirement, however, for achieving oscillation is obviously much higher for the viscous fluid at high amplitude. For considerations regarding whether OBRs can be sensibly designed for the mashing process, power density calculations were done to assess the power requirement of OBRs versus conventional stirred tank reactors. Power density calculations were conducted according to Baird and Stonestreet [33] given in the design methodology for OBRs of Stonestreet and Harvey [192]. For $St < 0.2$ the quasi-steady model is applied and for $St > 0.2$ the Eddy Enhancement Model is used. For the empirical eddy mixing length the recommended value from [192] was used. Table 6-13 summarized the results for the basic designs shown in the nomogramms for residence times of 30 minutes and 60 minutes. The large difference between the designs is mainly due to the power requirement for the net flow through the longer tube at higher residence times. The baffle orifice open area obviously influences the pressure drop calculations and the required power respectively.

To assess the comparable power input in conventional stirred tank mash tuns, a power density of 0.2 W/kg was taken, based on the data of a local brewery. The comparable mash tun size was calculated based on the hourly production capacity of the OBR designs and a residence time of 95 minutes, the same as in standard mashings.

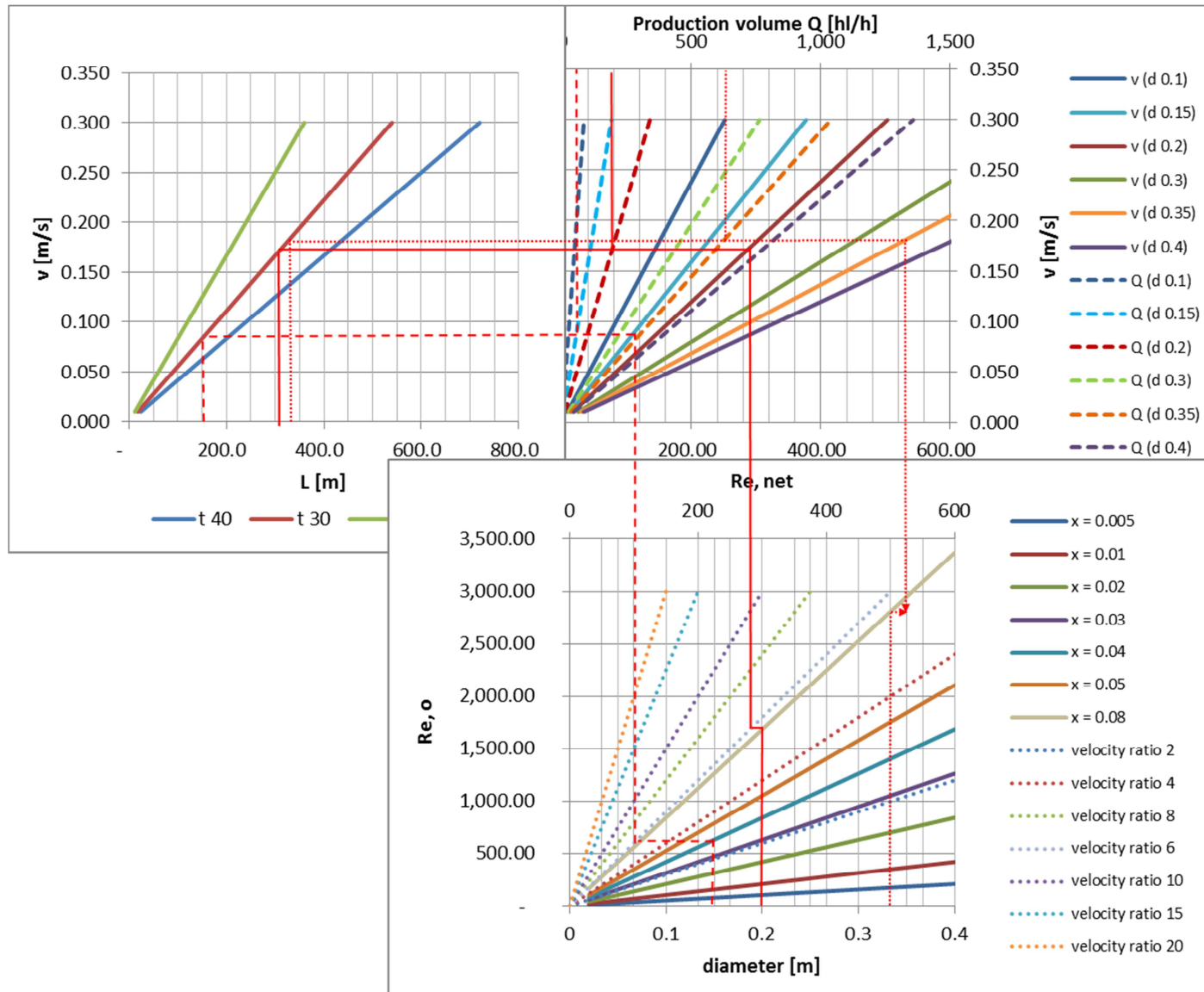


Figure 6-21: Design diagram for OBR design for a mash with coarse grist (viscosity 130 mPas)

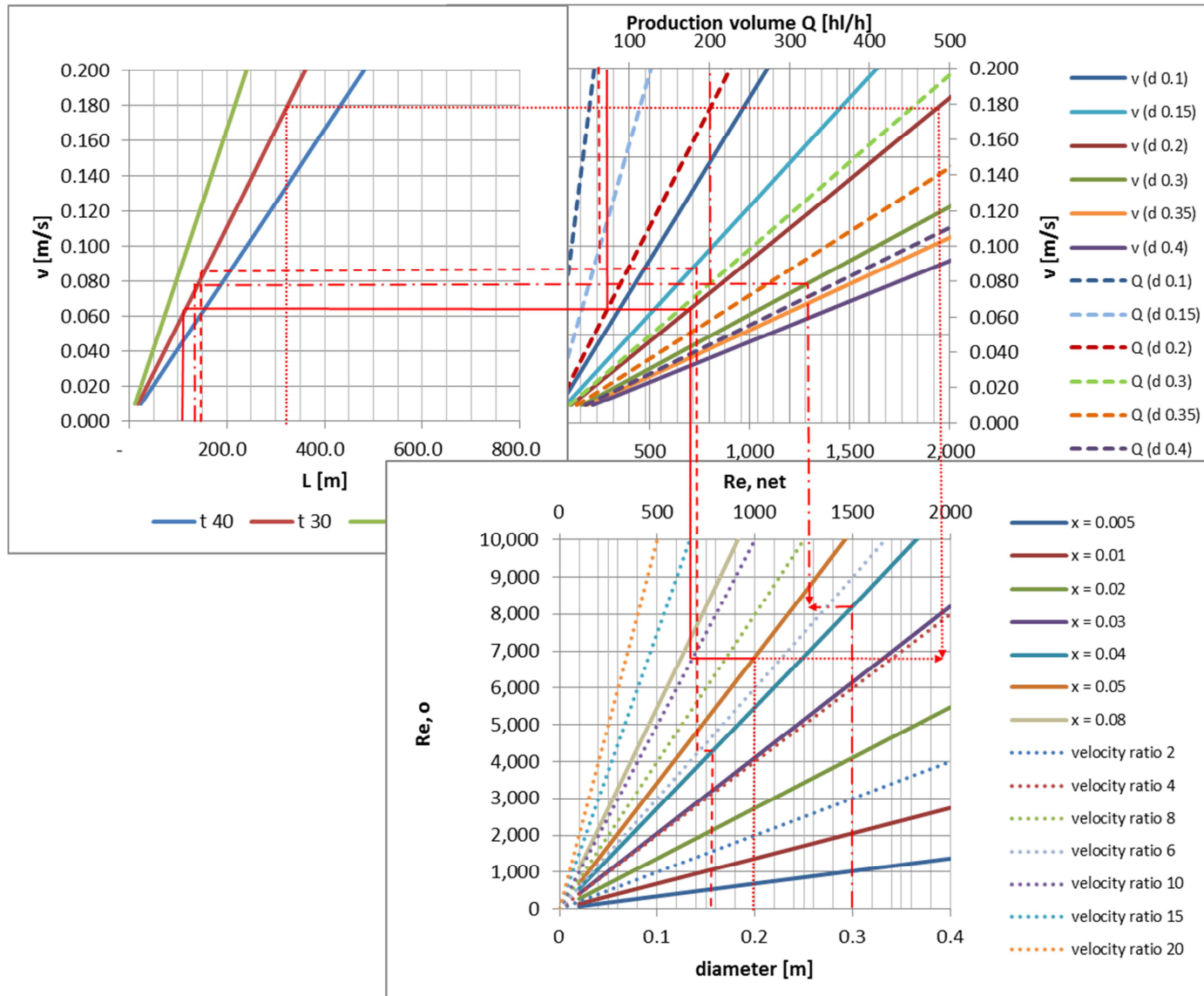


Figure 6-22: Design diagram for OBR design for a mash with fine grist (viscosity 20 mPas)

Table 6-13: Summary of design examples for OBRs for mashing

	diameter d m	superficial velocity. u m/s	reactor length. z m	produc tion rate. Q hl/h	Re.o	Re.net	velocity ratio	x0. oscillation amplitude	Strouhal number	total power density W/m ³	required power kW	stirrer power conventional kW	comparable mash tun size hl
$\eta = 130$ mPas, residence time = 30 min													
Design 1	0.15	0.08	150	53	632	105	6.0	0.04	0.30	1931	5.1	1.8	84
Design 2	0.2	0.17	305	192	1686	284	5.9	0.08	0.20	34311	328.8	6.6	303
Design 2 a	0.2	0.17	305	192	1580	284	5.6	0.075	0.21	5946	57.0	6.6	303
Design 3	0.35	0.18	320	616	2950	522	5.7	0.08	0.35	3899	120.0	21.3	975
residence time = 60 min													
Design 1	0.15	0.08	300	53	632	105	6.0	0.04	0.30	1931	10.2	1.8	84
Design 2	0.2	0.17	610	192	1686	284	5.9	0.08	0.20	34311	657.5	6.6	303
Design 2 a	0.2	0.17	610	192	1580	284	5.6	0.075	0.21	5946	114.0	6.6	303
Design 3	0.35	0.18	640	616	2950	522	5.7	0.08	0.35	3899	240.1	21.3	975
$\eta = 20$ mPas, residence time = 30 min													
Design 1	0.15	0.08	150	53	4109	681	6.0	0.04	0.30	1931	5.1	1.8	84
Design 2	0.2	0.06	110	69	6849	666	10.3	0.05	0.32	2082	7.2	2.4	109
Design 3	0.3	0.08	140	198	8218	1272	6.5	0.04	0.60	948	9.4	6.8	313
Design 4	0.2	0.18	325	204	6849	1968	3.5	0.05	0.32	3136	32.0	7.0	323
residence time = 60 min													
Design 1	0.15	0.08	300	53	4109	681	6.0	0.04	0.30	1931	10.2	1.8	84
Design 2	0.2	0.06	220	69	6849	666	10.3	0.05	0.32	2082	14.4	2.4	109
Design 3	0.3	0.08	280	198	8218	1272	6.5	0.04	0.60	948	18.8	6.8	313
Design 4	0.2	0.18	650	204	6849	1968	3.5	0.05	0.32	3136	64.0	7.0	323

Power requirements for the low viscosity mash are in the range of 5-9 kW for 50-200 hl/h for 30 minutes residence time (design 1-3). Increasing the residence time by a factor 2 results in doubling of the required power input. Design 4 shows a considerably higher power requirement, with the same production capacity as in Design 3, but a smaller diameter and longer reactor length. It is known that the larger the ratio of the reactor length over the diameter (z/d) the higher is the required power density for tubular reactors and also for OBRs [192]. This fact is confirmed by the results: While z/D is 933 for design 3, it results to 3,250 for design 4. Thus, the z/D ratio is a crucial factor for designing reasonable OBRs.

For the high viscosity mash, power requirements are substantially higher for the examples presented. However, power requirement is not a function of viscosity. This is shown in design 1 which is comparable to the first design of the low viscosity mash: required power input is also 5.1 kW. Factors influencing power requirement for the net medium flow are mainly velocity ratio and reactor length, while power requirement for oscillation is dependent on oscillation amplitude, frequency, fractional open area and reactor length.

Design example 2 in high viscosity mashing delivers approximately 190 hl/h with a diameter of 200 mm. Here, the Strouhal number results in 0.199 in which case the pressure drop calculation for $St < 0.2$ becomes valid [192]. Power requirement is then over 300 kW which is an infeasible design. By decreasing the oscillation amplitude (design 2a) Strouhal becomes 0.21 and the power requirement results to 57 kW. In reviewing the results for the low viscosity mash, one could increase the diameter in this design to 0.3 m by decreasing the reactor length to 135 m. This would again result in the same production capacity, however with a power requirement of 33.8 kW. Thus, there is still potential for optimizing OBR design based on the consideration of power requirement. The fact that power requirement doubles by doubling the reactor length, can be observed again in these design examples.

In comparison to the conventional stirred tank all OBR designs show an increase in power requirement. For low viscosity mash the difference can be reduced to a few kW and fine tuning of the design could even go below the requirements for conventional agitation. However, in this case Strouhal numbers are in the range of 0.4-0.6. Table 6-14 summarizes design options for a mash of 200 hl/h for high and low viscosity mash. With fixed diameter and tube length, velocity ratio, Strouhal number and power requirements are constant for the different viscosities, but the absolute values of Re_o and Re_{net} change considerably.

It is important to note that the Reynolds number achieved in conventional mash tuns is in the range of 500. With comparable amount of power requirements it is possible to increase this number substantially in OBRs, especially for low viscosity mash. For high viscosity mash Re_o could be increased by a factor of ~ 2.5 at comparable power input, while in low viscosity mash the factor would be 18. This increase will result in a better Nusselt number and increase of heat transfer coefficient. The surface area of the reactor tube in Table 6-14 is 10 m² which should be sufficient for heat transfer, as shown in chapter 6.2.2.

Table 6-14: OBR design for 200 hl/h production

	d m	u m/s	z m	Q hl/h	Re,o	Re,net	velocity ratio	x	Strouhal number	number of baffles	total power density W/m ³	required power kW	stirr er pow er conv enti onal kW	compar able mash tun size hl	z/d
n = 130 mPas, residence time = 30 min															
Design 6	0.33	0.06	116.9	200	1391	180	7.7	0.04	0.66	236	829	8.3	6.9	317	354
Design 7	0.33	0.06	116.9	200	2782	180	15.5	0.08	0.33	236	3169	31.7	6.9	317	354
n = 20 mPas, residence time = 30 min															
Design 6	0.33	0.06	116.9	200	9040	1168	7.7	0.04	0.66	236	829	8.3	6.9	317	354
Design 7	0.33	0.06	116.9	200	18080	1168	15.5	0.08	0.33	236	3169	31.7	6.9	317	354

6.2.3.2 Discussion of OBRs for mashing

It becomes clear from the results above that viscosity of the mash has a decisive impact on the flow regimes within OBRs. Operating a reactor with the same operating conditions (oscillation amplitude, velocity ratio) will result to very different Reynolds numbers of the net flow, as well as of the oscillating flow.

It is known that the larger the ratio of the reactor length over the diameter (z/d) the higher is the required power density for tubular reactors and also for OBRs [192]. This results to the fact that residence times are limited to avoid too long reactors with infeasible power requirement. In OBRs additionally power requirement is (among others) also a function of oscillation amplitude. From the results above it seems that oscillation amplitudes will have to be chosen below 4 cm to enable an operation at reasonable power input. In general, it needs to be stated that the choice of the empirical mixing length largely influences the results of the power dissipation calculations. According to Baird and Stonestreet, the mixing length should be in the same order of magnitude as the orifice diameter [139]. Only lab-scale testing will allow better to predict the real range of required power density and validate the use of the correct eddy mixing length.

Summarizing, there are a number of open questions in using OBRs for mashing that have to be dealt with.

At first, only residence times in the range of 40 minutes will be reasonable, otherwise power requirements will be too high. Therefore, mass transfer intensification in OBRs will have to be tested on pilot scale, whether reaction rates can be increased so that lower residence times will be possible. It has already been presented in section 6.1.2 that dynamic processing in terms of dynamic heating and cooling seems to intensify the hydrolysis reactions. Another option would be to perform the first amylosis rest in a (continuous) stirred tank and then use the OBR only for heating the mash at a low temperature gradient to its target temperature. It was possible in this work to successfully show that no further saccharification rest is necessary. The stirred tank for the first amylosis rest could be operated continuously without heating the reactor, which would allow a continuous mash processing. Figure 6-23 shows a possible flowsheet.

Furthermore, the choice of feasible baffles for the mash will be crucial. Husks should not be affected to avoid any negative effect on subsequent wort separation. Shear stress must be kept to a minimum, which also has to be proven on pilot scale.

In the reactor design the separation between process medium and oscillating piston e.g. via membranes is important, to allow for aseptic processing.

Most importantly, any negative effect on quality must be eliminated and pilot tests will have to prove the reasonable performance of OBRs for mashing.

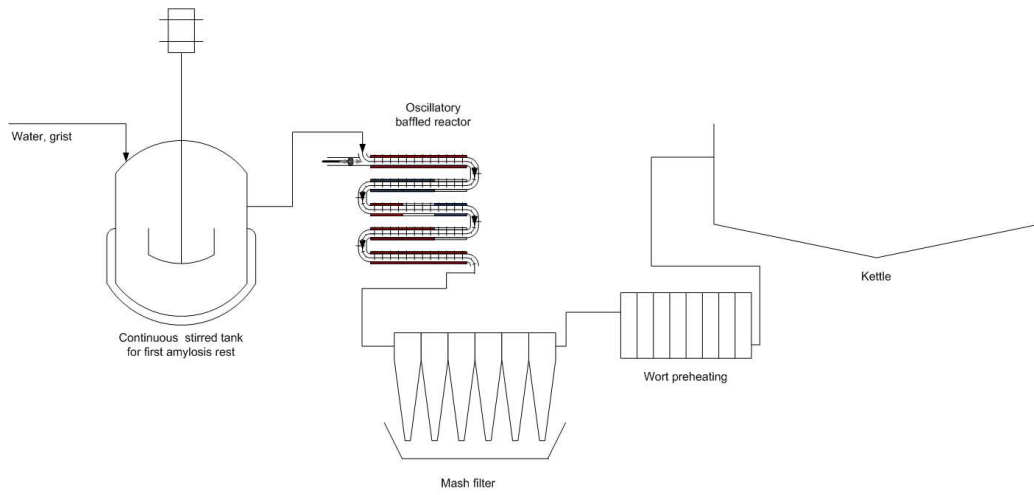


Figure 6-23: Scheme for mashing with an oscillatory reactor

7 PRACTICAL APPLICATION TO CASE STUDIES - PRACTICAL ELEMENT

This chapter shows the application of the above developed methodologies (Brewery Model, SOCO and new mashing technology) within case studies. At first five fictive brewery sites (two including the new mashing technology) are analysed via the Brewery Model. The analysis proved the potential of the holistic consideration of all process technologies in terms of thermal energy management. For two of these sites heat integration concepts are developed with the software SOCO and the remaining energy demand as basis for solar heat supply considerations is shown. Specific solar design studies are out of the scope of this work.

7.1 Definition of brewery case studies

Three fictive breweries (site 1, site 2 and site 3) based on vast practical experiences in brewery auditing as well as on conventional brewing technologies and inspired by real brewery data have been chosen as test cases for the brewery model and the evaluation of SOCO. To analyse the effects of technology change, two more breweries (site 4 and site 5) were defined for which the implemented brewing technologies were changed to more innovative process technologies - mostly recent state-of-the-art technologies. The data for the fictive case studies was based on the experience in brewery auditing.

In the conventional production system in site 1 - site 3 a standard operational profile of 30 brews per week (10-12 batches per day [19]) is assumed. Technologies in the conventional production system of site 1 comprise an infusion mashing system, wort preheating over an energy storage loaded by the vapours from boiling, dynamic low pressure boiling with 6 % evaporation, hot clarification in a whirlpool (incl. a few Kelvin of temperature losses due to addition of chemicals at this stage of the brewing process) and a one stage wort cooler. Brew water preparation is performed over heat recovery with wort cooling, as in any standard brewery. The beer is brewed at 12 ° Plato without addition of dilution water. A tunnel pasteurizer is used in packaging for non-returnable bottle filling (~28 % of produced beer) and a flash pasteurizer for returnable bottle filling (~72 % of produced beer).

At site 2 mashing is conducted with two decoction mashes and boiling is performed with an internal boiler with 2.8 % evaporation. The vapour condensers loads the energy storage for wort preheating. Whirlpool losses are negligible. Hot water of 78 % degrees is recovered over the 1-stage wort cooler. The brewery bottles 66 % of its production capacity, the remaining 34 % are filled in kegs. Production capacity is 950,000 hl per annum.

Site 3 has a smaller production capacity of 400,000 hl/a. For mashing a 1-decoction mash is used. Boiling is done at traditionally high evaporation rates of 8.6 %. Vapour energy is recovered by mechanical vapour compression which supplies the boiling process. Wort is preheated via steam in the external boiler. At site 2 and site 3 beer is also brewed at roughly 12 ° Plato, and no dilution water is added before fermentation. Site 3 bottles 57 % of the produced beer, while the remaining 43 % are sold in kegs.

The fourth brewery which was considered (site 4) has roughly the same beer output as site 1, however its brewing schedule is different as it is operating a smaller production line. Thus 60 brews per week are

produced in 6 days, keeping the available time for weekend cleaning down to approx. 24 hours. The brewery is brewing beer at higher gravity (16 ° Plato) and later adding dilution water in order to reach the required beer quality. This results in the use of less water within the brewing process itself. For mashing a new infusion mashing profile with low heating rates is assumed based on the results of chapter 6. The temperature profile of Test 4 in chapter 6 has been chosen. For boiling, a rectification column is applied bringing evaporation down to 2,7 %. Whirlpool operation is improved leading to less temperature losses in wort cooling. Finally a non thermal pasteurisation technology for non-returnables is assumed. Packaging in site 4 is performed on 60 % of bottles. 40 % of the brewed volume is packaged into kegs with a specific hot water demand of roughly 6 l/keg.

Site 5 has the same specifications as site 4, but applies a boiling procedure similar to the Schonkoch-Verfahren. In the kettle the wort is held at 98 °C for 50 minutes. During this period 0.6 % of the wort evaporates, which is in the range stated in reference literature [40], [41]. After trub separation vacuum evaporation is performed at 30 kPa inducing an evaporation of 4.6 %. The cast wort is withdrawn to the wort cooler at 69.1 °C. While at all other sites the brew water tank has a temperature of 80-82 °C, the temperature of the tank in site 5 is 62 °C.

7.2 Thermal energy demand modelling

7.2.1 Benchmark data of breweries

Benchmarking is a classical approach to identify energy efficiency potential in the industry. Over the course of several studies and projects benchmarks were collected. An example of a benchmark-comparison of a 1 Mio. hl brewery is given in Figure 7-1.

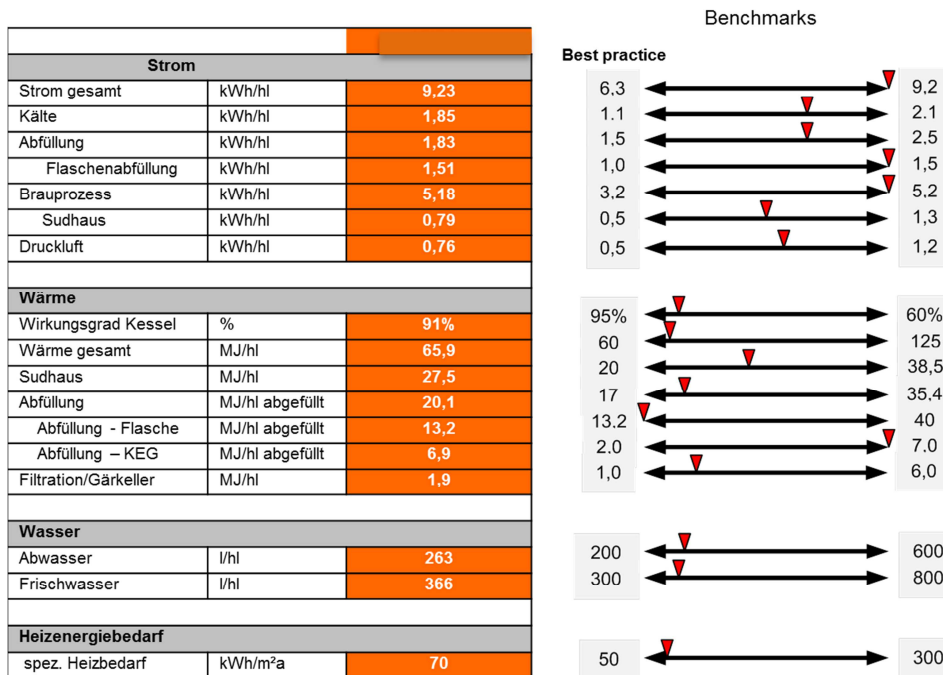


Figure 7-1: Benchmark comparison for a brewery (production capacity ~ 1 Mio. hl)

A major drawback of benchmarking however is that no detailed information is provided as to which measures will actually overcome the present inefficiencies, as the area for improvement is analysed (e.g. high electricity demand in packaging) but not the detailed source. In addition, no details regarding technological differences are shown in a benchmark comparison. This makes the comparison of different production sites difficult, as site specific framework conditions cannot be considered.

7.2.2 Energy demand modelling with brewery model⁸

The brewery model calculates energy demand figures based on the minimal thermal energy demand per technology $MEDT_{tech}$ (see chapter 0). This energy demand, calculated based on the site-specific production data and implemented technologies shows the ultimate target for energy demand reduction for the given framework (operating parameters and technologies). Additionally, the process heat demand is calculated over a user-defined process efficiency. Before discussing the results of the energy demand figures calculated by the model for the five case studies, the verification of the model with measurements is shown.

7.2.2.1 Verification of the model with data from measurements

As the Brewery Model was developed over the course of several brewery audits, the comparison of calculated data with measured data was possible. Energy demand analysis with the brewery model proved to simulate the real energy demand profiles with acceptable accuracy. The comparison of the modelled energy demand with the real energy demand profile of industrial brewhouses shows that the model accounts for 80 – 90 % of the real energy demand. This difference is mainly due to energy losses occurring on real sites as the model performs a calculation of minimal energy demand figures only considering defined (known) process inefficiencies. It was shown that the model comes closer to reaching real energy demand figures for a brewery operating on hot water boilers in comparison with breweries that use steam boilers as energy supply. The calculated in comparison to the measured energy demand of the brewhouse accounts for 90 % of the used thermal energy. In breweries with steam boilers with open condensate systems larger energy losses are expected. In one brewery that was analyzed the deviation between calculated energy demand, again including known process efficiencies which have been identified by measurements and detailed analysis, and real energy demand amounts to 83 %. Early works have suggested an overall efficiency from steam raising to heating of cooper kettles of 65-70 %, with the majority of losses (~20 %) being due to steam raising [101].

The verification of the data produced by the model was most possible for the brewhouse energy demand in one brewery (brewery S) operating with hot water as a heat transfer medium. It was possible to measure the energy demand of the complete brewhouse operations with ultrasonic flow meters and temperature measurements over the course of one week. Figure 7-2 shows the results of 4 hours of measurement. The pattern of the different brews is visible.

⁸ *Parts of this chapter have been published in the following publication by the author:*

Muster-Slawitsch, B., et al., Process modelling and technology evaluation in brewing, *Chemical Engineering and Processing: Process Intensification* **84**, 98-108 (2014).

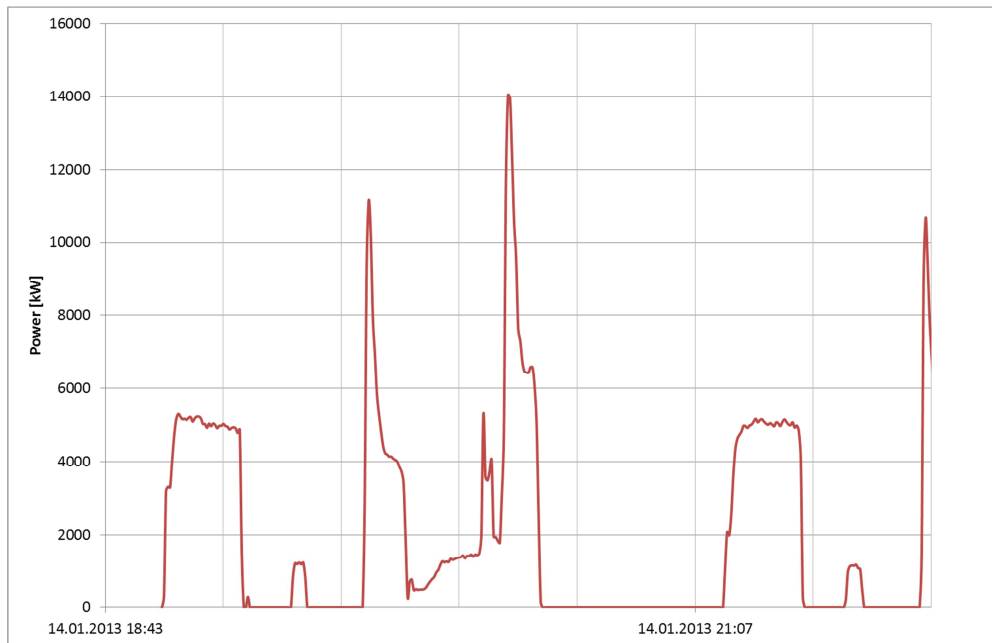


Figure 7-2: Measured thermal energy demand of the brewhouse over 4 hours

During the course of the measurement 31 brews were brewed. Based on the average brew size of 629 hl, this corresponds to a total wort production of 19,499 hl. The measurement showed an energy consumption of 151,074 kWh during this production period. The specific energy demand required for the brewhouse was therefore 27.9 MJ/hl cast wort.

As shown in chapter 5.1.8 the brewery model calculates the energy and mass balance over each process step in the brewhouse and provides all the data necessary to visualize the energy flow of the produced wort in the brewhouse. The results for the brewery S are shown in Table 7-1 and are visualized in Figure 7-3.

Table 7-1: Calculated energy flows in the brewhouse S for model verification

INPUT	MJ/hl CW	OUTPUT	MJ/hl CW
MASHING			
Brew water	13.79	losses	0.50
Cold water	0.00	to lauter tun	19.94
Additions	0.40		
Malt	0.14		
energy	6.08		
IN total	20.45	OUT total	20.45
WORT SEPARATION			
From mash tun	19.94	Spent grain	5.47
Brew water for rinses	12.92	Weak wort	1.91
Cold water for rinses	0.00	Wort from lauter tun	25.49
IN total	32.87	OUT total	32.87
WORT PREHEATING			
	0.00		

Wort from lauter tun	25.49	Wort to kettle	36.07
Energy from energy storage	6.66		
Energy from boiler	3.92		
IN total	36.07	OUT total	36.07
WORT KETTLE	0.00		
Wort to kettle	36.07	vapours	7.81
Energy for starting the boil	0.22	Vapours from start-up	0.25
Energy during boiling	6.80	Wort from kettle	37.12
additions	1.37		
Heating of additions	0.72		
IN total	45.18	OUT total	45.18
WHIRLPOOL	0.00		
Wort from kettle	37.12	Hot trub	0.18
	0.00	losses Whirlpool (balanced)	0.83
	0.00	To wort cooler	36.11
IN total	37.12	OUT total	37.12

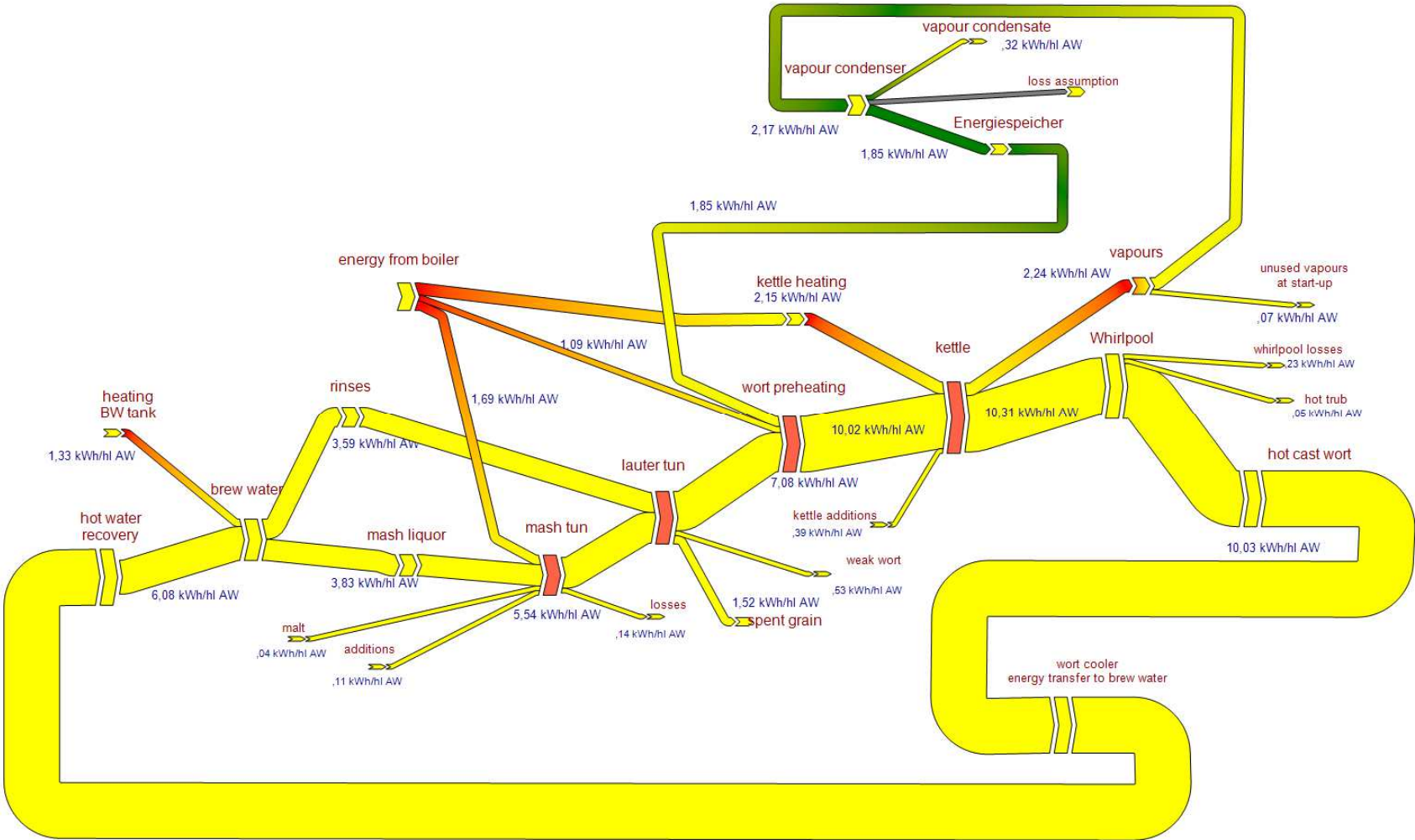


Figure 7-3: Sankey of energy flows in the brewhouse of brewery S, used for model verification

Practical Element – Application to case studies

The calculated energy demand for the brewing processes is 17.75 MJ/hl. The supply line heating the brewhouse also heats up all hot water which is necessary for brewing and packaging. The majority of hot water required at the production site is recovered over wort cooling, however – at the time of the analysis - still 8.1 MJ/hl of hot water need to be heated for brewing, packaging and CIP. Additionally the brewhouse CIP is heated with the same supply line during operation, which results in an energy demand of 0.61 MJ/hl. In total the calculated energy demand supplied by the measured supply line to the brewhouse therefore results in a measurement of 26.46 MJ/hl. In comparison to the measured energy demand of 27.9 MJ/hl, the calculation amounts to 94.8 % of the measurement. This signifies an efficiency of heat transfer of roughly 95 %. Keeping in mind the batch operation of brewing and the corresponding heat losses of heating vessels, this efficiency is better than might be expected. As this brewery is using hot water as an energy transfer medium, all losses usually linked to open condensate systems in steam systems are avoided. Additionally the brewhouse has been rebuilt within the last decade and all heat transfer systems are in very good condition. Finally, there might be small deviations between the reported average process parameters, which are the basis for the calculation, and the real brewing conditions of single brews. It can therefore be concluded that the calculated energy demand is in realistic correspondence to the measurement. This is further supported when comparing the results to benchmarks [87].

Comparison between calculated data from the model and real measurements were also done for energy demand variability. The energy demand variability was calculated with the variable energy demand modules of the Brewery Model (see Figure 5-2). It was shown that energy demand variations can be modelled to a satisfactory accuracy when energy supply parameters (heat transfer area, strategies for process regulation) are well known. Figure 7-4 shows the calculated energy demand profile of mashing, boiling and wort preheating of brewery S in comparison to the measured energy demand. The brewery applies a two - decoction mashing program and recovers vapour energy over energy storage for wort preheating. The overall power peaks of 11 and 14 MW - when all three processes require energy - are not reproduced in the model, as the defined heating rates would lead to lower peak demands. It becomes clear that slight deviations between defined process times and heating rates to real practice can substantially affect the energy demand profile. As discussed above, some additional energy demand is used for warm water preparation which is stored in the warm water tanks to be later used as brew water. In general, this demand is minor and mainly required at the beginning of the week. However, the heat exchanger for warm water preparation might start at single moments during the week, which can additionally lead to higher overall peak demands in real practice in comparison to the model.

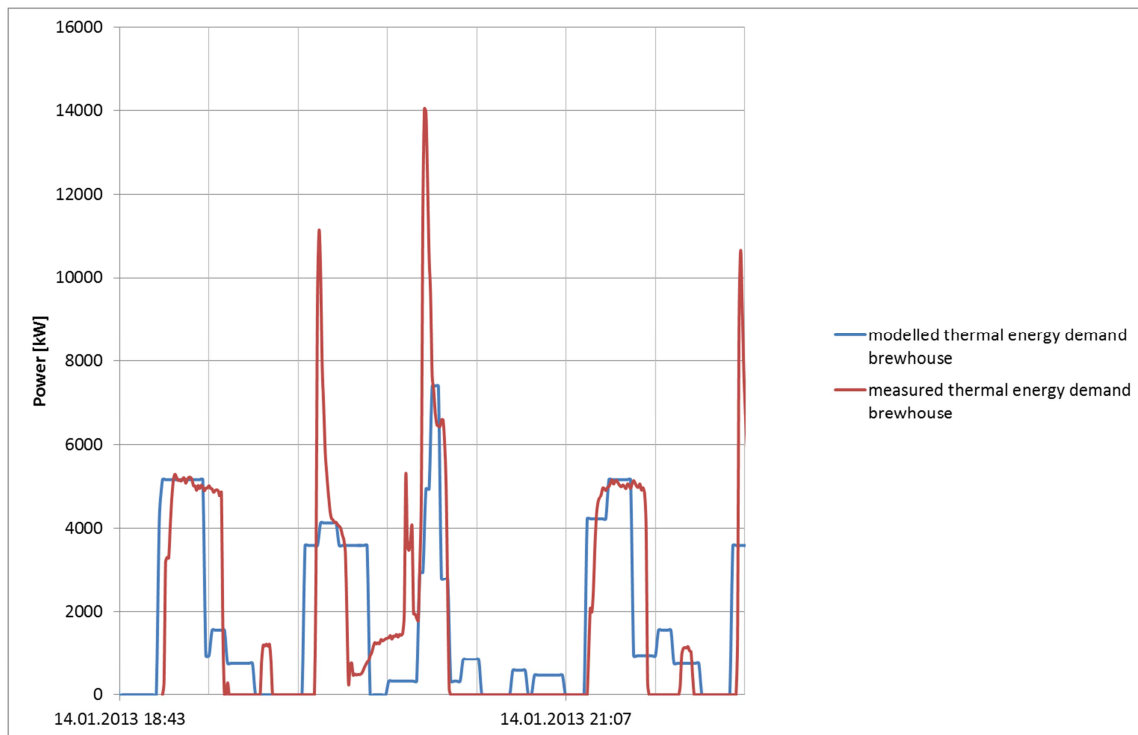


Figure 7-4: Calculated versus measured energy demand profile

The calculation of cooling demand was done based on the fermentation model and further calculations as explained in section 5.1.10. Cooling demand curves were compared with real data from an industrial brewing site. The model outcome slightly overestimates (106 %) the required energy demand. It must be stated that the effect of outside temperature is included with 10 % of the overall cooling load. As shown in Figure 7-5 the modelled cooling load variations follow the real profile quite well, although a shift of the maxima can be observed. These shifts occurring are a result of the user definitions of the fermentation time profile in the model calculation as well as the fact that the fermentation model does not describe the real profiles in detail. Cooling load variations are also not modelled exactly as in reality; however, this is mostly due to the control of the real plants.

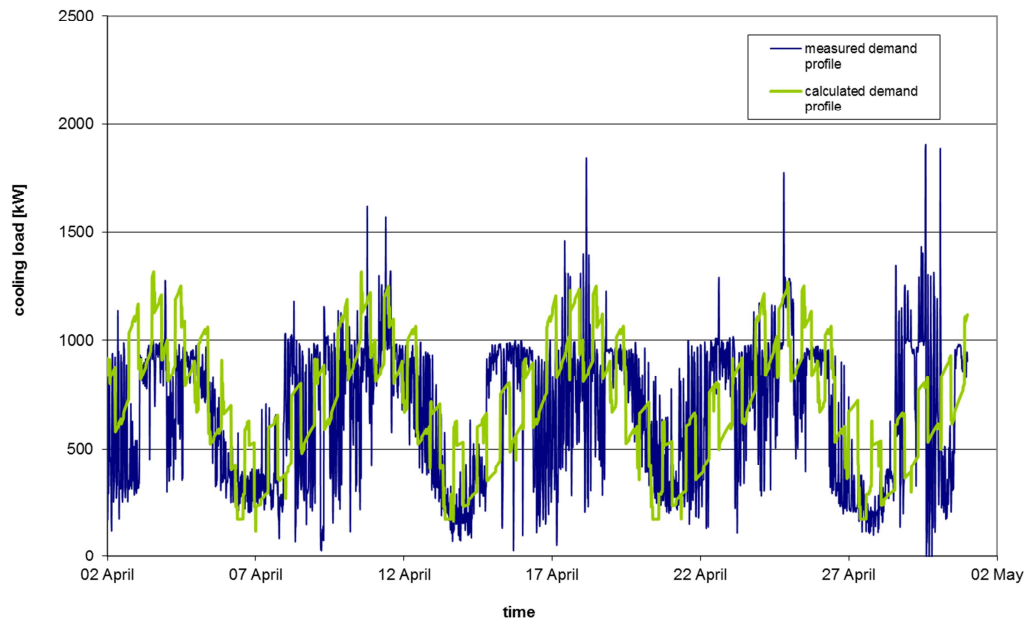


Figure 7-5: Calculated versus measured cooling load profile

7.2.2.2 Model results for the case studies and discussion

Table 7-2 shows the key brewhouse parameters for the five case studies. The comparison of the case studies shows that the model can analyse the specific conditions of each brewery. The first three sites show common brewing practices for the capacity ranges from 300,000 hl to 1 Million hl per year. The operation with 30 brews per week is often found in industry and the technologies in mashing, mash separation and boiling, are also commonly applied. The breweries were deliberately chosen with different evaporation rates in wort boiling, showing the range from 2.8 % - 8.6 % that can be found in industrial practice. Many breweries nowadays operate with vapour recovery systems which are assumed in site 1 and site 2, but also mechanical vapour compression, as in site 3, is often used. Site 4 and site 5 combine more recent state-of-the-art technologies with low wort evaporation and minimized losses in comparison to site 1. Brewing is also accomplished at higher gravity with addition of 40 hl dilution water prior to fermentation. Wort gravity prior to fermentation is still higher at site 4 and site 5, so final attenuation will be 2 % higher in comparison to site 3 to reach the same final alcohol content in beer. This difference allows the analysis of the cooling demand at different attenuation rates. The major difference of site 4 and site 5 is that more brews are being assumed in smaller batch sizes. The fact that a similar brewing capacity as in site 1 can be achieved is due to the assumption that 60 brews are possible within a week which is made possible with the use of a mash filter with reduced mash separation time as in comparison to lauter tuns.

It is essential to evaluate technologies with a holistic view on the overall production site. Each technology influences energy demand profiles and/or the water management of the brewery which is also influenced by brewing capacity and packaging types. The EES model allows a quick comparison of specific energy and water demand figures taking into account all processes on site.

Table 7-2: Description of breweries

	brewing capacity	packaging capacity		brewing technology					Brew volume		
		bottles	kegs	mashing	mash separation	kettle	Evap. rate	vapour recovery	cold wort	cast	brews /week
	[hl]	[%]	[%]						hl/brew		[g/100ml]
site 1	659979	100%	0%	infusion	lauter tun	Dynamic low pressure boiling	6%	energy storage + wort preheating	454	30	13.7
site 2	915195	66%	34%	decoction	lauter tun	internal heater	2.8%	energy storage + wort preheating	629	30	12.8
site 3	327713	57%	43%	decoction	lauter tun	external heater	8.6%	mechanical vapour compression	223	30	12.6
site 4	695890	60%	40%	infusion	mash filter	internal heater	2.8%	energy storage + wort preheating	238	60	13.7
Site 5	696113	60%	40%	infusion	mash filter	Schonkochverfahren	5.2%	warm water generation	238	60	13.7

Practical Element – Application to case studies

Table 7-4 shows the specific hot water consumption figures. Figures are based on the brewed wort volume in hl cold cast wort. Hot water consumption describes the overall hot water requirement on site, which is partly generated over heat recovery (hot water recovery) and partly heated by the existing energy supply (hot water demand). The latter two are the sum of the overall requirement which ranges from 1.07 to 1.55 hl/hl for the five case studies. At site 1-4 hot water temperature is in the range of 80 °C, while site 5 recovers water at 62 °C only, because of the implemented vacuum evaporation achieving a final temperature of the hot cast wort of about 69 °C.

74 – 100 % of the overall hot requirement can be recovered with the implemented heat recovery, basically by the wort cooler in these case studies. Warm water generation by heat recovery is additionally done by vapour condensation only at site 5. At this site 22.2 m³ per brew can be generated over the wort cooler and 4.6 m³ via vapour condensation during vacuum evaporation.

Brew water demand describes the warm water demand for the brewing liquor in mashing and wort separation. It is in the range of 0.79-1.02 hl/hl brewed wort volume. Liquor-to-grist ratios range from 2.86 hl/100 kg at sites 4 and 5 to 3.77 hl/100 kg at site 2. For sparging, brew water requirements are ranging from 2.6-3 hl/100 kg with the lowest values used in the breweries that use mash filters for wort separation. Other requirements are stated for brewhouse CIP, and the hot water demand in packaging. Usually not all single water consuming processes are measured, so there is a substantial amount of hot water requirement for “other” uses.

The comparison shows that site 3 has the largest demand of hot water generation by external resources. This is due to the rather high specific consumption figure for brewhouse CIP which is partly influenced by its smaller production capacity, as hot water demand for brewhouse CIP is largely influenced by existing vessel sizes and piping dimensions. While site 4 requires the least brew water demand due to the beer gravity during brewing, specific warm water recovery figures are also low. Based on its efficient warm water consumption in the packaging area however, hot water demand and recovery are almost balanced. Because site 5 has two heat recovery processes installed for hot water generation, it can produce all required brew water over heat recovery. The higher specific brew water demand for brewing is due to the temperature of the hot water: With 62 °C hot water in the hot water tank, the brew water demand for mashing liquor and rinses in wort separation equal the overall water input in these processes. Usually the amount of water taken from the hot water tanks at 80 °C is less and the overall water input is achieved by mixing with cold water.

Table 7-5 summarizes the minimal energy demand requirement (MED_{Tech}) per brewery in selected processes in the brewhouse. Mashing, wort preheating, boiling and hot water generation have been chosen as the most important processes in the brewhouse. In Table 7-6 these figures are shown including assumed process efficiency factors in the range of 0.8 to 0.95, depending on the vessel being used or the heat exchanger. For wort preheating, if applicable in the case study, the use of an energy storage with a user-defined efficiency of the recovery system is included in the demand figures. The specific demand figures are in the expected range based on the known benchmarks for the implemented technologies [87], however at the lower end, as no further energy losses are included.

Table 7-3: Assumed process efficiency in key brewing processes

	Assumed process efficiency			
	hot water generation	Mashing	wort preheating	boiling
site 1	0.95	0.85	0.95	0.85
site 2	0.95	0.9	0.95	0.9
site 3	0.95	0.8	0.85	0.85
site 4	0.95	0.9	0.95	0.85
site 5	0.95	0.85	0.95	0.88

MED_{Tech} figures for mashing vary between 4.75 and 5.87 MJ/hl. The lower energy requirements result from the infusion mashings at low heating rates. Figures in wort preheating and boiling vary largely from 2.26 – 9.88 MJ/hl for wort preheating and from 2.2 – 17.34 MJ/hl for wort boiling. This depends largely on the heat recovery scheme which is implemented. Wort preheating has its lowest energy demand at site 1, as the rather high evaporation rate of 6 % leads to sufficient energy supply by the vapour condenser. In theory energy demand for wort preheating could be fully covered, however it is assumed that not the full potential is being tapped and the wort is preheated only to 90 °C which saves 7.5 MJ/hl. Thermal energy demand for wort boiling is highest at site 1 and lowest at sites 3 and 5. At site 3 the mechanical vapour compression system shifts the energy demand from wort boiling to wort preheating. At site 5 the low temperature boiling process and vacuum evaporation after trub separation shifts the energy demand to hot water generation.

Table 7-5 and Table 7-6 also show the energy demand required for hot water generation. Based on the specific hot water demand figures site 3 has the largest energy requirement for hot water production and site 4 shows the least requirement. The importance of hot water management becomes obvious when considering the range of figures from 3.53 to 7.65 MJ/hl (MED_{Tech}). For all sites a process efficiency of 0.95 has been assumed for hot water generation. In real practice this might be less depending on the state of the heat exchanger. In some cases this is placed at a location which is not easily or often accessed, so losses are not quickly identified. The low hot water requirements at site 4 lead to minimal energy demand for overall hot water production and consequently brew water production. At site 5 minimal energy requirements for hot water production is 4.65 MJ/hl which is in the same range as at site 2. This results from the fact that the hot water consumers such as CIP and packaging processes require water at 80 °C, while it is recovered at 62 °C. Additionally hot water for rinses in wort separation requires 2.53 MJ/hl additional heating to its target temperature of 72 °C.

With these site specific differences the energy demand per temperature level changes based on the technology sets chosen in the brewhouse. Table 7-5 and Table 7-6 show the energy demand on 4 different temperature levels for mashing, wort preheating and wort boiling. Results are summarized in Figure 7-6 based on the UPH figures (Table 7-5). Site 3 and Site 5 show a similar pattern due to

Practical Element – Application to case studies

requirement of wort preheating, while site 2 and site 4 cover this demand – with different efficiency - to some extent over the vapour condenser. Energy demand of these sites is more or less shifted to higher temperatures to cover the boiling energy demand. Site 1 is similar to site 2 and 4 however with a more pronounced pattern, as wort preheating energy requirement is minimal and boiling requirement high due to the higher evaporation rate of 6% in comparison to 2.8% at sites 2 and 4. The energy requirement of wort preheating is influenced by the temperature of the wort after wort separation which depends on the temperature of the brew water rinses in wort separation which is again usually linked to the final temperature of the wort after mashing. In all sites mashing is done until a target temperature of 75 °C and sparging in wort separation is done at the same temperature level. Only site 3 employs a decoction mashing until 78 °C and sparge water is also applied at 78 °C. Secondly, the wort is preheated to a temperature between 90 °C and its saturation temperature prior to the kettle, depending on the boiling technology and whether the final heating to boiling temperature is done in the kettle. At site 3 for example the external boiler is used for wort preheating and for the boiling start-up, leading to the fact that wort preheating is modelled until its saturation temperature. In most other sites with an energy storage system for wort preheating, wort is preheated to 90-95 °C over the preheating system and then heated further within the kettle.

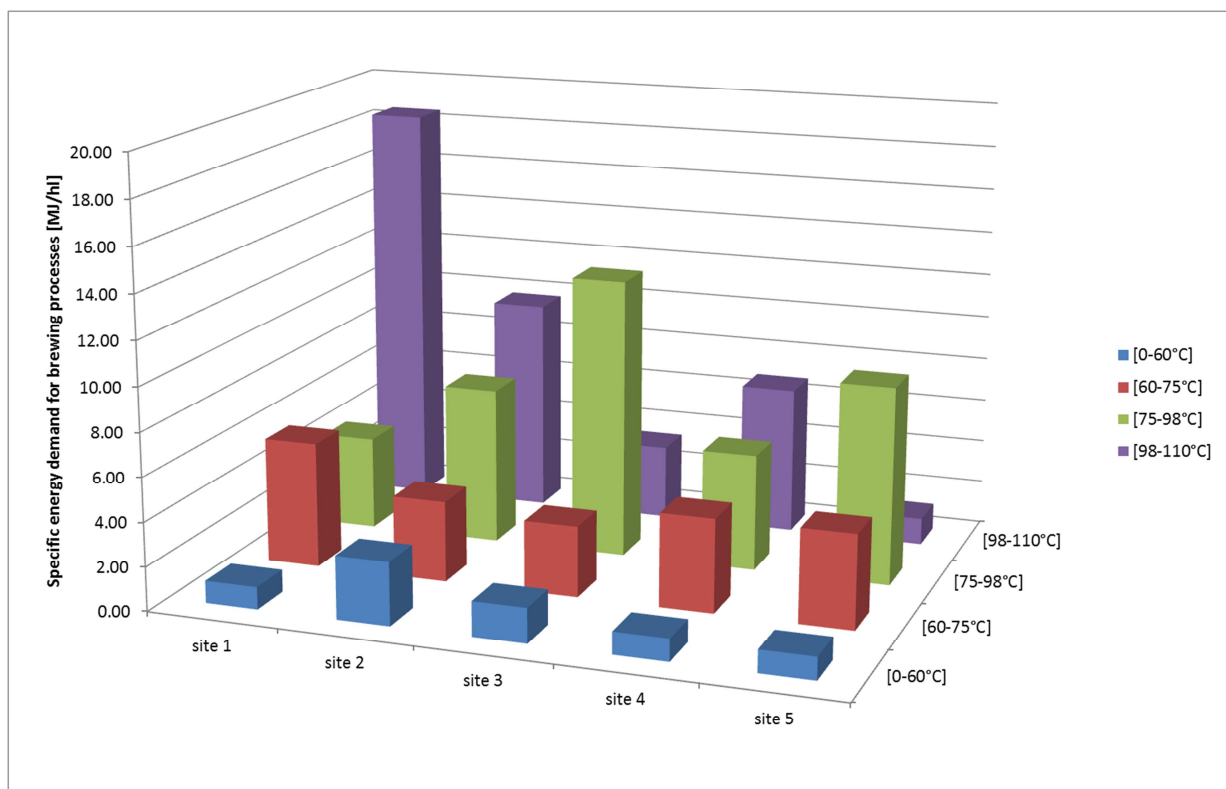


Figure 7-6: Specific energy demand for key brewing processes on different temperature levels

When the energy demand for hot water preparation is included, the energy demand distribution by temperature gives a different picture. The energy demand in the lower temperature level is obviously increased the most at site 3 due to its large specific demand for hot water preparation. At site 1, 2 and 5 the increase is similar as the energy demand for hot water generation is in a narrow range from 4.65 to

6.35 MJ/hl for all these sites. At site 5 however, the increase between 60-75 °C is larger because at this site it is necessary to heat the brew water further to lautering temperature or for packaging requirement.

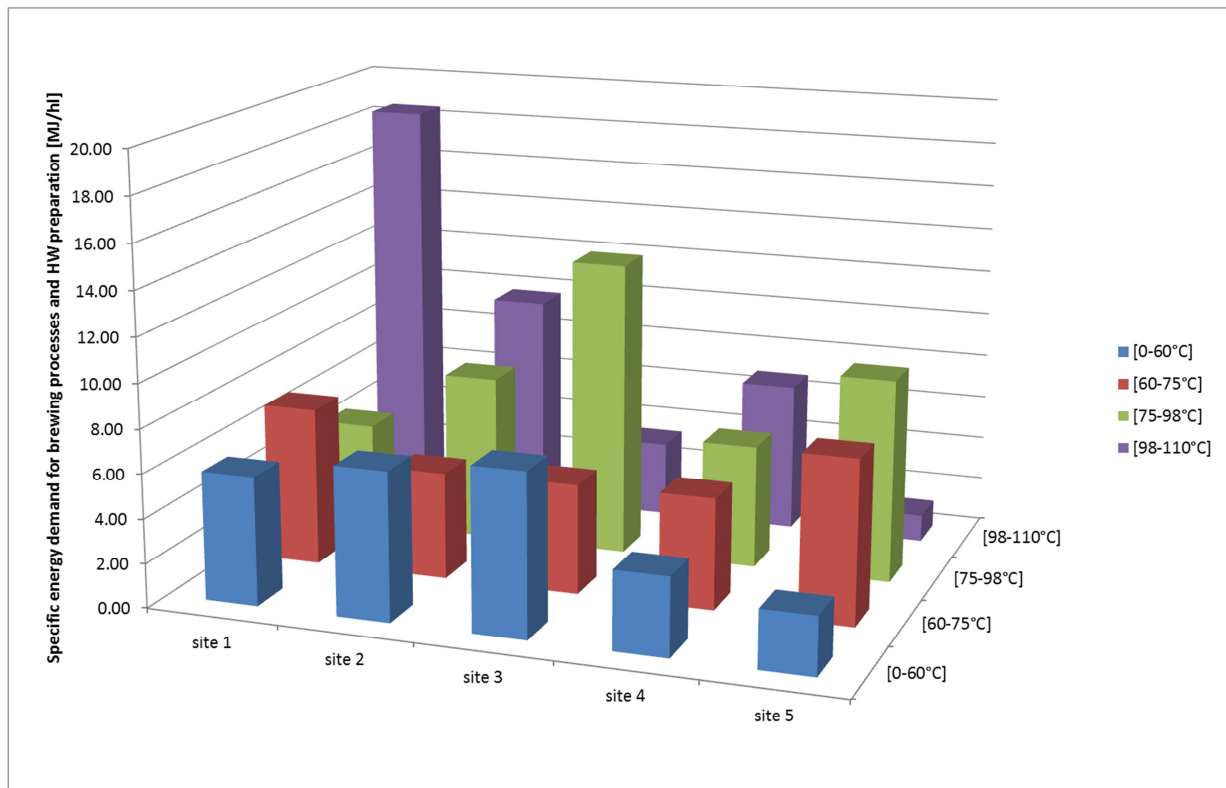


Figure 7-7: Specific energy demand for key brewing processes and hot water preparation on different temperature levels

Waste heat of selected processes is shown in Table 7-7 for the different sites. Obviously the largest heat flows are the vapours from wort boiling of which a large share is recovered via the implemented heat recovery schemes. Within the five selected case studies, the largest recovery rate is achieved at site 3 via the mechanical vapour compression. Here, only vapour losses in the start-up phase of the boiling process are considered. Lowest recovery is realised at site 1 with an inefficient heat transfer from the energy storage to the wort. At the same time energy contained in the vapours is higher than the demand in wort preheating due to the rather high evaporation rate of 6 %. In the other breweries with energy storages for wort preheating (site 2 and site 4) recovery rates are about 50 %. Recovery rate of vapour energy can be maximized through good regulation of the vapour condenser and the heat transfer medium flow carrying the heat to the energy storage. In most boiling processes vapour formation is not a steady state process and the operation of the vapour condenser must therefore be tuned to the process schedule. Obviously the efficiency of the vapour condenser and the energy storage also influence the recovery rate. Weekend losses and corresponding temperature drop in the energy storage must be considered. Heat recovery rate of vapour energy is also rather high at site 5 (~ 73 %). Here, evaporation during maintaining the wort at low temperature in the kettle is not included in the heat recovery scheme, which accounts for 0.6 % corresponding to an energy value of 1.40 MJ/hl. The subsequent vapour energy

Practical Element – Application to case studies

realised during vacuum evaporation, 11.1 MJ/hl, are recovered as hot water with high efficiency (0.95). The production of warm water at lower temperature from vapour condensate is not considered, as it is in none of the other sites (site 1 - site 4).

The second largest waste heat flow in the brewhouse is usually the heat contained in the spent grains. This accounts to 4-5 MJ/hl. However, it is difficult to tap into this potential for heat recovery due to the nature of the spent grains. While still pumpable at 70-80 % of water content, the medium would hinder heat transfer in conventional heat exchangers due to clogging and fouling. Tube-in-tube heat exchangers, similar to black water heat exchangers, could be a possibility. Heat transfer could potentially be intensified via oscillating tube-in-tube heat exchangers. This hypothesis has not been verified within the scope of this study.

Another rather large waste heat stream is waste water from brewhouse CIP with an energy content of roughly 3 MJ/hl. At site 3 waste water from brewhouse CIP even contains 6.6 MJ/hl, because of the large specific water demand for brewhouse CIP on this site (see above). It's worth considering waste water from brewhouse CIP separately from other waste water streams, as it has the highest temperature and therefore the largest potential for heat recovery. According to the experience from actual plants, waste water temperature of 65 °C has been assumed for all production sites. In case there is a demand for warm water on site, or for preheating cold water for hot water generation, a heat exchanger could be installed for preheating water and storing it in a designated warm water tank for further purposes.

Other significant thermal energy losses may occur in the whirlpool in case the hot wort cools down significantly. While in some breweries such cooling is done deliberately for heat recovery purposes (wort precooling), unwanted temperature drop should be avoided. At the chosen production sites, site 1 shows an extreme case of temperature drop within the whirlpool to 88 °C. Losses rise up to 5 MJ/hl in this case. Generally losses are lower; within the range of 0.8-1 MJ/hl.

Finally, thermal energy is required to heat the mass of the vessels to process temperature. This is required at the beginning of the week, but also in between brews when vessels cool down during breaks. The four major vessels (mashtun, lauter-tun, kettle and whirlpool) have been considered, while other equipment such as vacuum evaporator or boilermash kettles have been neglected. The amount of energy lost for vessel heating depends on the time between brews, the temperature and surface area of the vessel and the brew volume. As the surface to volume ratio is larger for small batches, higher losses occur for smaller batch volumes. Site 3 has the lowest batch volume and reaches a specific heat loss of 4.01 MJ/hl, while site 2 has the largest. Its specific heat loss is 1.85 MJ/hl. Lowest losses (1.61 MJ/hl) are realized at site 5, with lowest temperature in the boiling kettle.

Table 7-8 lists a few specific energy demand figures for packaging processes. Data for the case studies have been estimated based on measurements from real plants. Clearly flash pasteurization, used in most of the case studies, requires little energy in comparison to tunnel pasteurization. Bottle washing has a specific energy demand in the range of 6-7.5 MJ/hl, however in one case study it results to 22 MJ/hl. For this case study very high stand-by losses have been defined, similar to the data which have been found in one brewery audit in a real brewery. Details on the evaluation of packaging processes will not be discussed within this chapter, but can be easily evaluated by the Brewery Model.

Table 7-4: Specific hot water consumption and recovery figures

	Overall hot water consumption and recovery figures			Hot water consumption figures in specific production areas				
	HW consumption	HW recovery	HW demand	BW demand	Brewhouse CIP	Bottle packaging	Keg packaging	others
	[hl/hl]	[hl/hl]	[hl/hl]	[hl/hl]	[hl/hl]	[hl/hl]	[hl/hl]	[hl/hl]
site 1	1.38	1.13	0.25	0.99	0.16	0.04		0.18
site 2	1.36	1.20	0.16	0.96	0.13	(incl. in others)	0.11	0.16
site 3	1.53	1.14	0.40	1.01	0.29	0.02	0.07	0.14
site 4	1.15	1.02	0.14	0.79	0.13	0.03	0.07	0.14
Site 5	1.33	1.35	0.00	0.97	0.13	0.03	0.07	0.14

Table 7-5: Specific energy demand figures (MEDT_{Tech}) in the brewhouse

	Energy demand per temperature level (main brewing processes only)				Energy demand in selected processes				
	[60-75°C]	[60-75°C]	[75-98°C]	[98-110°C]	hot water demand	mashing	wort preheating	boiling	SUM (of these 4 selected processes)
	[MJ/hl]	[MJ/hl]	[MJ/hl]	[MJ/hl]	[MJ/hl]	[MJ/hl]	[MJ/hl]	[MJ/hl]	[MJ/hl]
site 1	5.40	6.27	4.12	15.88	6.35	5.72	2.26	17.34	31.67
site 2	6.20	4.37	6.81	8.75	5.09	5.87	6.83	8.33	26.12
site 3	6.78	4.32	11.19	2.83	7.65	5.39	9.88	2.19	25.11
site 4	3.29	4.48	4.96	6.01	3.35	4.735	3.477	7.17	18.73
site 5	2.45	6.91	8.47	1.11	4.65	4.75	7.153	2.39	18.94

Table 7-6: Specific energy demand figures including process efficiencies (UPH) in the brewhouse

	Energy demand per temperature level (main brewing processes only)				Energy demand in selected processes			
	[60-75°C]	[60-75°C]	[75-98°C]	[98-110°C]	hot water demand	mashing	wort preheating	boiling
	[MJ/hl]	[MJ/hl]	[MJ/hl]	[MJ/hl]	[MJ/hl]	[MJ/hl]	[MJ/hl]	[MJ/hl]
site 1	5.78	7.15	4.75	18.51	6.68	6.73	2.38	20.41
site 2	6.68	4.81	7.57	9.76	5.36	6.52	7.19	9.76
site 3	7.33	4.94	13.34	3.40	8.05	6.74	11.62	2.59
site 4	3.53	5.00	5.57	6.78	3.53	5.26	3.66	8.44
site 5	2.61	7.40	9.20	1.21	4.89	5.28	7.53	2.72

Table 7-7: Waste heat in selected processes in the brewhouse

	waste heat in selected processes				
	spent grain	Vapours	whirlpool losses	Waste water Brewhouse CIP	Batch operation of vessels
	[MJ/hl]	[MJ/hl]	[MJ/hl]	[MJ/hl]	[MJ/hl]
site 1	4.83	17.54 (6.77 recovered)	5.03	3.73	2.71
site 2	5.37	8.05 (4 recovered)	0.78	3.06	1.85
site 3	4.45	24.4 (21 recovered)	0.89	6.62	4.01
site 4	4.65	6.25 (3.47 recovered)	1	3.00	2.51
Site 5	4.65	12.49 (9.18 recovered)	1.78	3.00	1.61

Table 7-8: Specific energy demand figures in packaging

	Energy demand in selected processes					Keg – Flash pasteurization	Keg washing and filling
	NRB - Flash pasteurization	Bottle Washer	Tunnel pasteurization	Chamber pasteurization			
	[MJ/hl]	[MJ/hl]	[MJ/hl]	[MJ/hl]	[MJ/hl]		
site 1	2.76	7.15	19.23				
site 2	5.0	6.0			2.5	4.0	
site 3	1.8	22			1.6	5.5 + 7.6 WW	
site 4 and site 5	2.68	6.43			1.7	2.35	

The Sankey diagrams, given below for sites 1, 4 and 5 (see Figure 7-8, Figure 7-9, Figure 7-10), show the data in a more transparent way. The efficiency of existing heat recovery can be quickly analyzed. At site 1 and site 4 for example, the potential to heat the wort prior to kettle would be higher than what is actually reached in practice. While the efficiency of the vapour condenser is user defined, the user can also enter the temperature to which the wort can be heated in practice in case not all vapours are being condensed and the full potential of vapour condensation is not tapped. At site 4 for example, the brewery has been defined heating the wort to 85 °C which is lower than the maximum possible temperature (91 °C) that could be reached when all energy can be transferred over the storage tank.

The energy flow diagrams show well the effect of wort preparation to the overall energy management. This clearly effects the water management and the shift in energy demand from kettle heating to wort preheating is well shown.

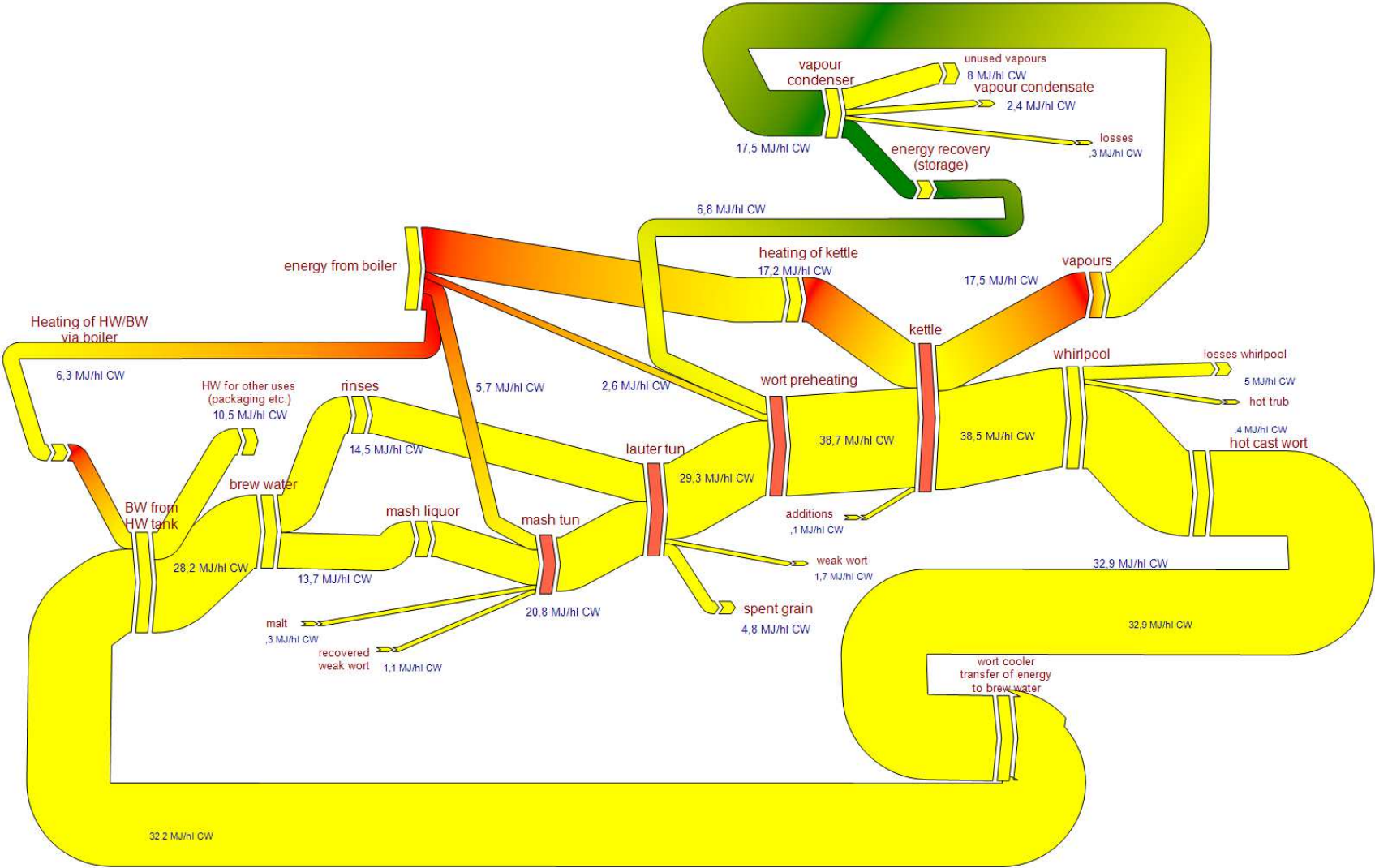


Figure 7-8: Sankey diagramm of brewhouse energy flows of site 1

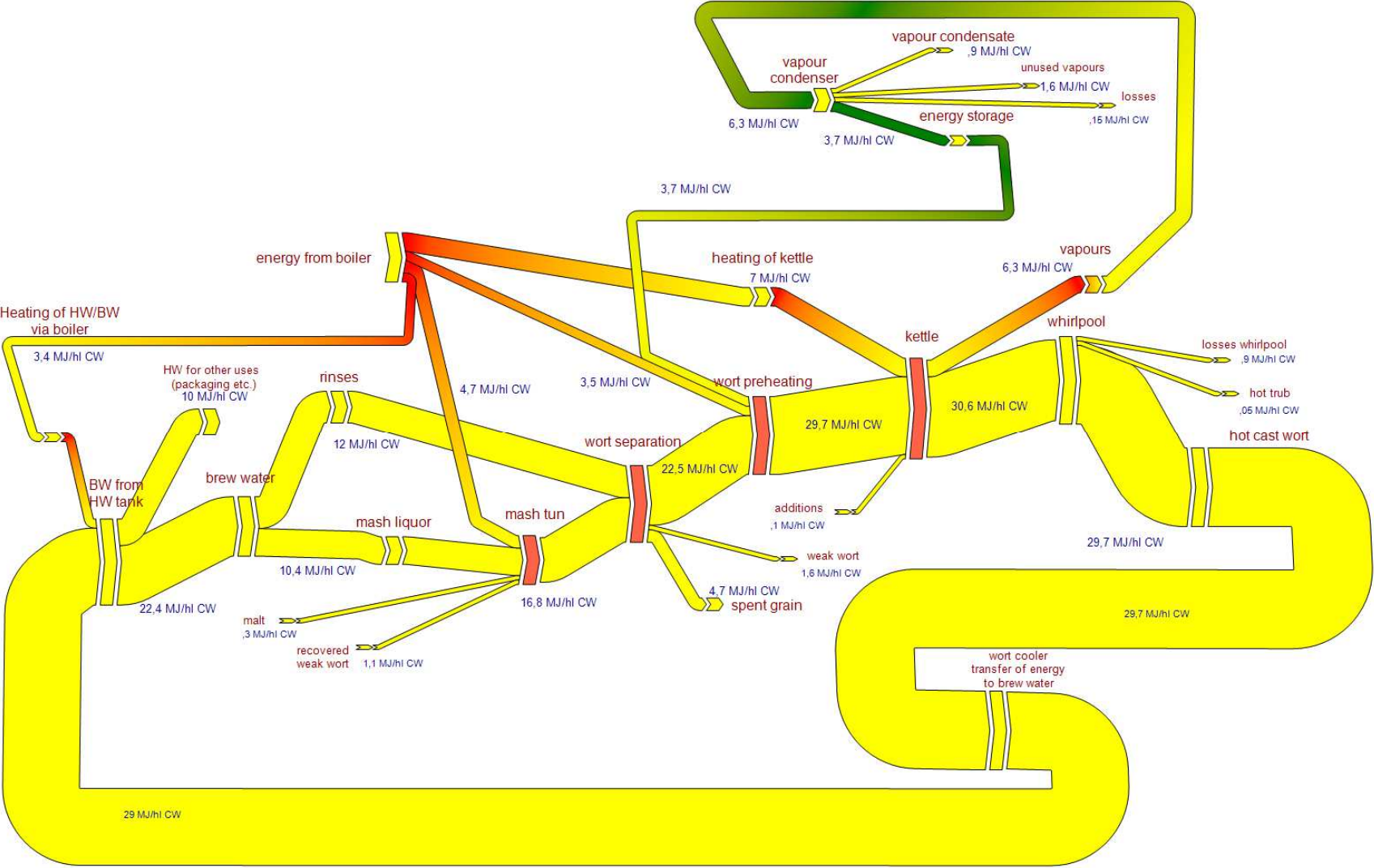


Figure 7-9: Sankey diagramm of brewhouse energy flows of site 4

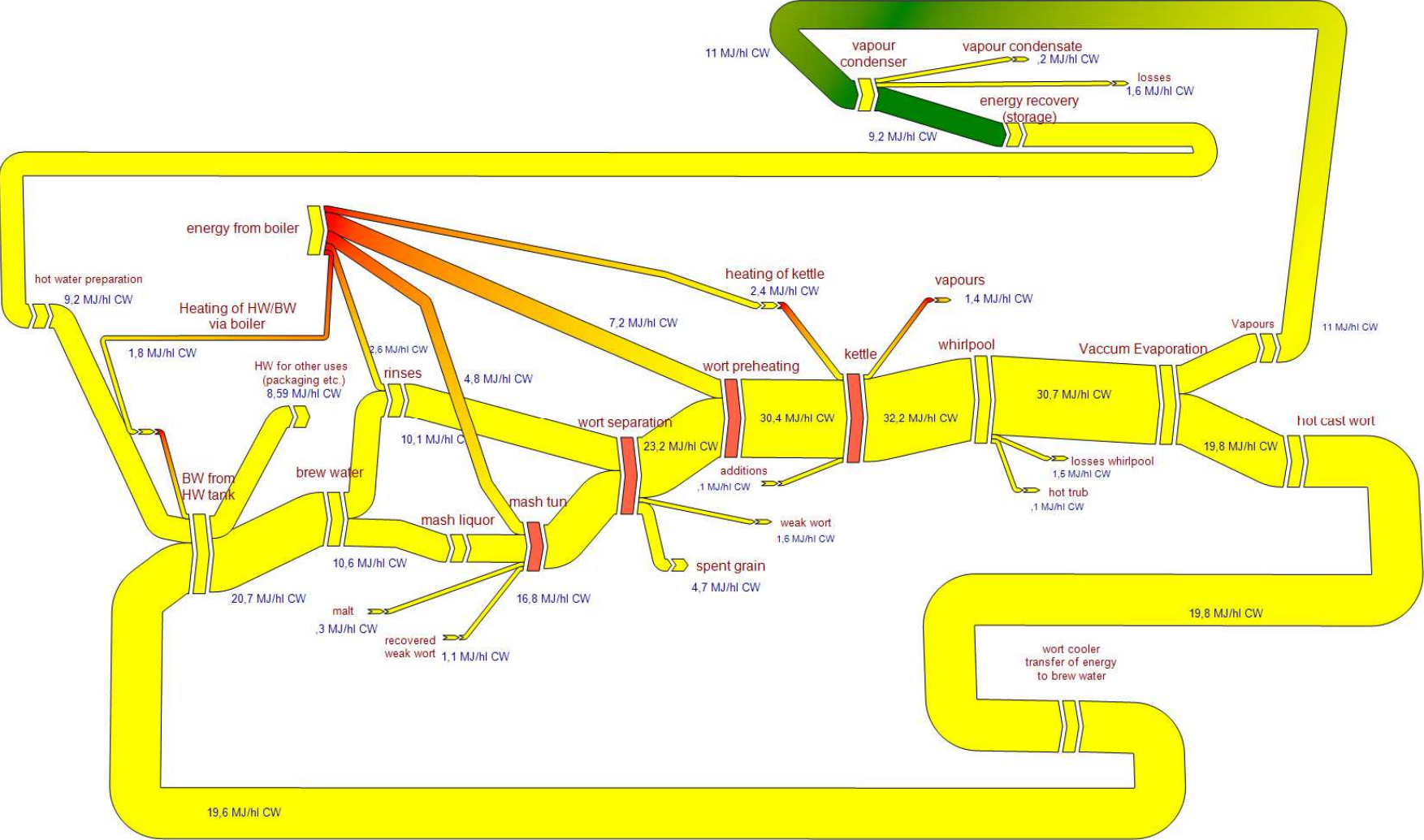


Figure 7-10: Sankey diagramm of brewhouse energy flows of site 5

Besides the evaluation of overall energy demand figures, the brewery model allows the calculation of energy demand profiles. Heat demand variability of site 1 (conventional production) and site 4 (optimized production) is shown in Figure 7-11 including packaging processes. Overall thermal energy demand of the selected processes (Hot water generation including brew water, mashing, wort preheating, boiling, bottle washing, flash pasteurization and tunnel pasteurization) is 26 % lower in brewery 4 compared to brewery 1 due to the process improvements shown in chapter 7.1. However, the major difference can be seen in energy demand variability. Brewery 4 clearly shows a more even energy demand profile and fewer peaks in thermal energy demand.

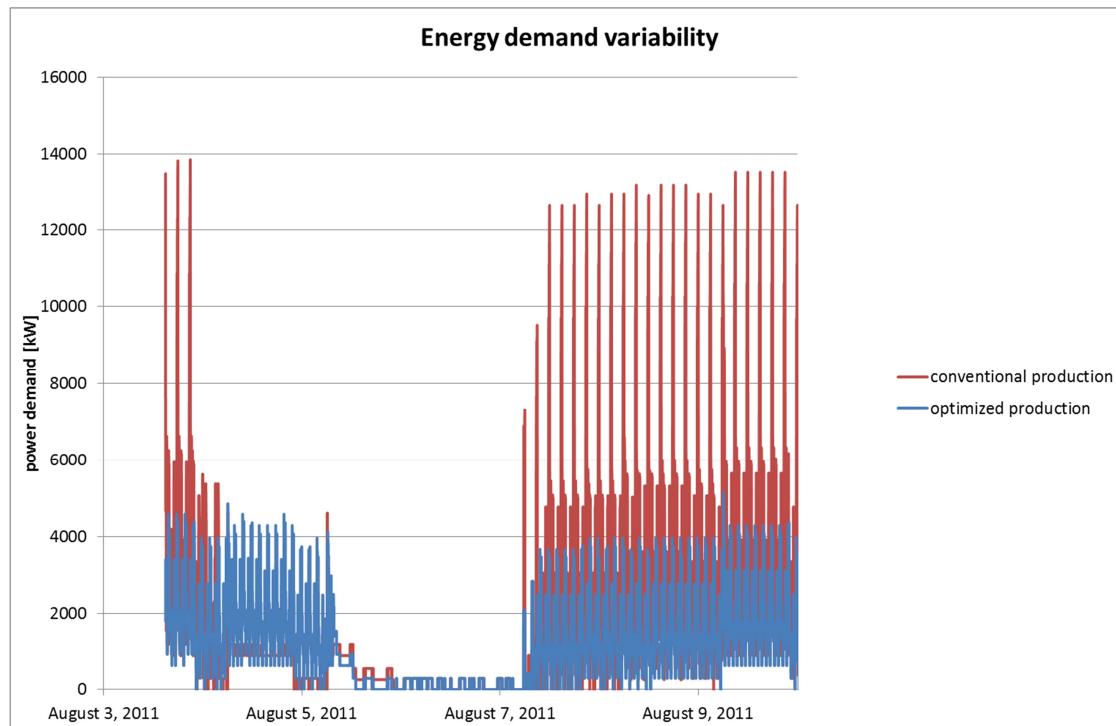


Figure 7-11: Energy demand variability for the brewery case studies 1 and 4

In Figure 7-12 the energy demand profiles between the brewhouse technology sets of all brewery sites are compared. Results are shown as specific energy demand in kW/hl over time. Most importantly, energy demand profiles vary significantly between the brewhouses. This proves the importance of evaluating energy demand profiles over time for heat integration considerations and/or design of new energy supply technologies. Such energy demand profiles are not only influenced by basic technology choices, but also by existing heat transfer area and heat supply management. In most breweries a large peak in energy demand occurs when boiling and mashing the subsequent brew are performed at the same time. As energy supply equipment is designed to cover this peak demand, the boiler is often operating at part load. A reduction in energy intensity in these processes will therefore lead to the possibility of designing heat supply equipment at lower capacity avoiding losses in part load operation.

At site 1 the peaks in energy demand are especially pronounced due to the rather high evaporation rate of 6 % in comparison to the other sites. When wort boiling coincides with mashing of the subsequent brew, energy demand peaks to 11,2 kW/hl or 5,400 kW. Site 2 shows high demand peaks up to 12 kW/hl or 7,400 kW when mashing co-incides with wort boiling of the precedent brew. At site 3 the evaporation rate of 8 % only effects the thermal energy requirement in boiling to a minor

extent due to the use of mechanical vapour compression. At this site the power peaks are due to the overlap of energy demand in mashing with either wort preheating or the first minutes of wort boiling before the start of the mechanical vapour compressor. Peak demands are in the range of 7 kW/hl or 1,600 kW. Site 4 has the most even demand profile. This is due to the fact that 60 brews are being brewed in smaller batches, but also due to the mashing temperature programme with low heating rates that is implemented in this brewery. Wort preheating is largely achieved through heat recovery. Energy peaks, when mashing and remaining energy demand for wort preheating coincide, are in the range of 4.6 kW/hl or 1,100 kW. Compared to site 1 which produces an equivalent amount of beer with a different technology set, this is a reduction in energy peaks by 79.8 %. This further proves that the technology change proposed in this work for mashing can add to the energy efficiency of brewing sites. Site 5 needs to account for energy demand for wort preheating from external resources only, as heat recovery is used for warm water production. Peak demand is in the range of 7 kW/hl or 1,700 kW. Compared to site 1 the reduction in peak power requirement is 68.7 %. Wort preheating is achieved within less than 30 minutes in this brewery. As there are other time limiting production steps, a slower heating of the wort would realize a smoother demand profile. This also holds true for the other breweries and shows a potential for optimization of energy demand profiles.

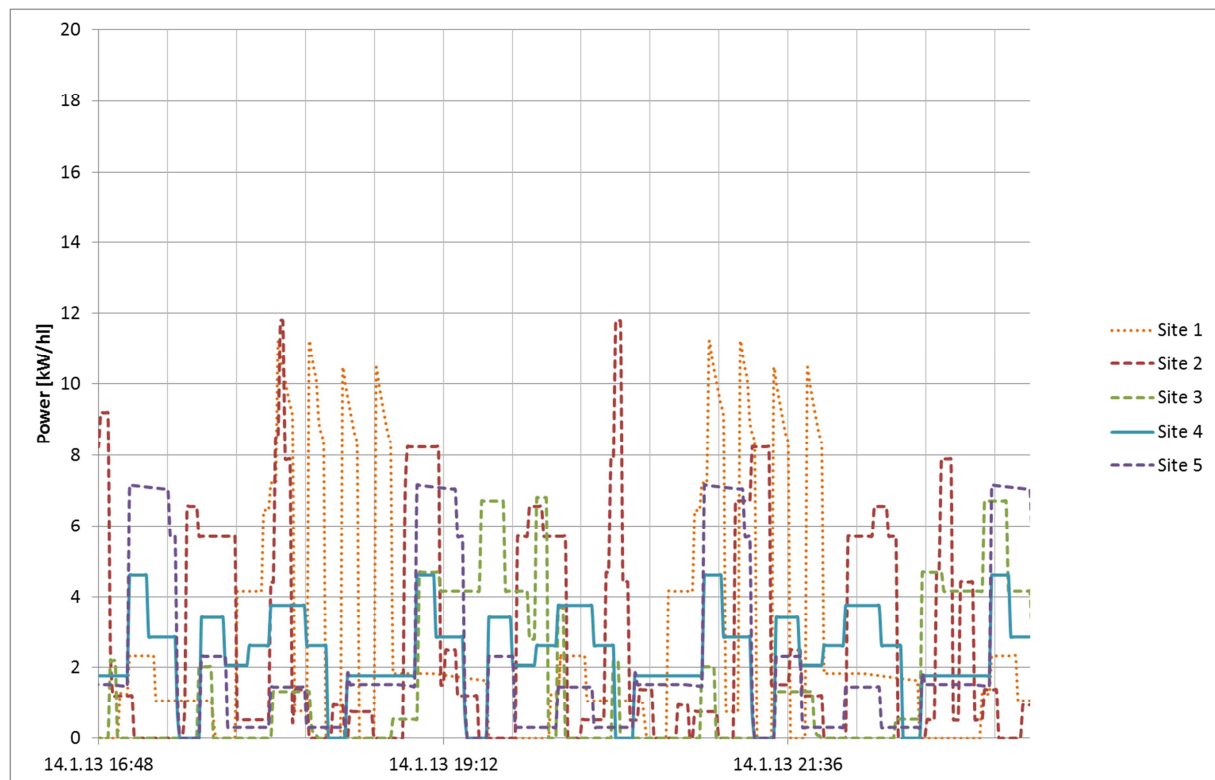


Figure 7-12: Energy demand profiles of the five breweries with different technology sets

7.2.2.3 Parametric studies with the brewery model on key brewing parameters

When applying the brewery model to industrial case studies, the effects of parameter or technology change on the energy demand can be evaluated. This has been shown in the comparison of the different brewing sites based on selected key parameters in the last chapter.

Further, parametric studies can be performed by varying a few key brewing parameters and selecting the output parameters which are of interest. The effects are displayed in a summary table which allows a quick overview on the results. Below a few examples are presented and discussed.

Evaluation of heat recovery technologies for different evaporation rates

The parametric studies can be used for the evaluation of different technologies for one case study via the selection of technological solutions for single process steps. Figure 7-13 shows an evaluation of specific energy demand figures for wort preheating and boiling for two vapour recovery options for brewery site 3: vapour compression versus vapour condensation and energy storage for wort preheating for a brewery at different evaporation rates. Depending on the efficiency of the vapour condensation system, vapour compression may be a sensible choice especially at higher evaporation rates when operated without additional steam requirement during vapour compression, which can be found in older plants. The efficiency of vapour condensation, energy storage and transfer to hot wort is also decisive in this comparison. Measurements have been conducted in one brewery, showing an efficiency of 84 % in a modern brewhouse. In this graphic, vapour condensation is only considered for wort preheating leading to the fact that at higher evaporation rates, vapours cannot be fully used for recovery. In such situations additional recovery for hot water production or heat integration for other process heating is a sensible option.

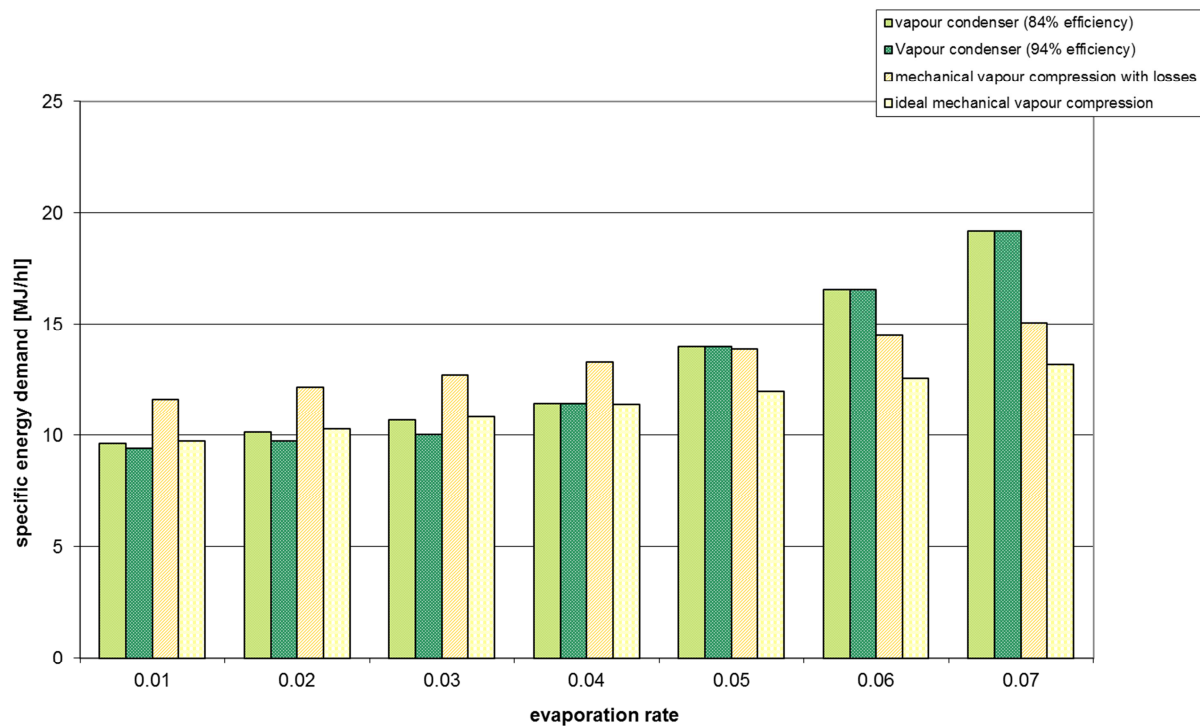


Figure 7-13: Comparison of specific energy demand of wort preheating and boiling for two vapour recovery options for brewery 3: mechanical vapour compression versus vapour condensation for wort preheating

Evaluation of hot water heating requirement for different evaporation rates

An important factor for breweries is the balance of the warm water demand which is influenced by a number of factors, as we have seen in chapter 7.2.2.2. The following analysis shows the necessity of

hot water preparation for different evaporation rates based on the technology sets of site 4 and site 5.

Based on a constant input of brew water and malt, Figure 7-14 shows the specific minimal energy demand for hot water preparation for site 4 and site 5 at different evaporation rates. It has to be highlighted that, according to their definition, both sites require hot water for CIP and other packaging processes at 80 °C. Warm water for general uses (200 m³ per week) is required at 70 °C.

While at site 4, the evaporation rate during boiling is changed due to the vigour of the boil, at site 5 the pressure of the vacuum evaporation system is varied between 30 and 60 kPa. The evaporation in the kettle is fixed at 1 % for this parametric study. (As shown earlier actually 0.6 % of wort evaporate during holding the wort at 95 °C in the kettle at site 5. Depending on the air parameters above the wort surface, the vapour formation within the kettle can be calculated as evaporation in subcooled state based on water diffusion.)

Site 4 shows a linear increase in demand for hot water preparation which is due to the decrease of recovered brew water at high evaporation rates due to lower cast wort volume. At site 5 the evaporation pressure directly influences the temperature of the cast wort and consequently the brew water temperature. In this analysis a 7 K temperature drop between saturation temperature of the vacuum pressure and brew water temperature has been assumed. The higher the evaporation rate, the lower is the pressure during vacuum evaporation and thus the recovered water temperature. The four evaporation rates modelled here correspond to an evaporation pressure of 30, 40, 50 and 60 kPa. At 30 kPa, and an evaporation rate of 5.6 respectively, energy for hot water preparation is highest. At this pressure the wort cools to 69 °C in vacuum evaporation. The high evaporation rate leads to a large production rate of hot water at 62 °C which slightly exceeds the hot water demand. However, hot water is required at 80 °C for CIP and packaging processes at site 5 and sparge water also requires heating to 75 °C. This results in a substantial heat demand for heating the hot water to the required temperature. At 40 kPa (corresponding to an evaporation rate of 4.4) the energy requirement for hot water preparation drops significantly. The corresponding saturation temperature is 76 °C, allowing for a brew water temperature of 69 °C. This increase in brew water temperature reduces the heating requirement substantially. Hot water production is now less than hot water demand, although the vapour energy from vacuum evaporation is used for hot water generation. However, due to the cast wort temperature of 73 °C (assuming 3 K temperature drop from saturation temperature to real cast wort temperature) 9.5 % less hot brew water can be generated at a hot water temperature of 69 °C, in comparison to site 4 with a cast wort temperature of 97 °C and a brew water (hot water) temperature of 80 °C. At the same time 23 % more hot water per hl wort is required as brew water at site 5.

While at higher evaporation pressures the *temperature* of brew water that can be recovered over the wort cooler increases, the *amount* of brew water that can be recovered decreases. The heat demand for generating brew water and for heating recovered brew water to its target temperature thus compete against each other. At a certain evaporation pressure the sum of these heating requirements give a minimum. At site 5 this is the case at 50 kPa and 74 °C brew water temperature.

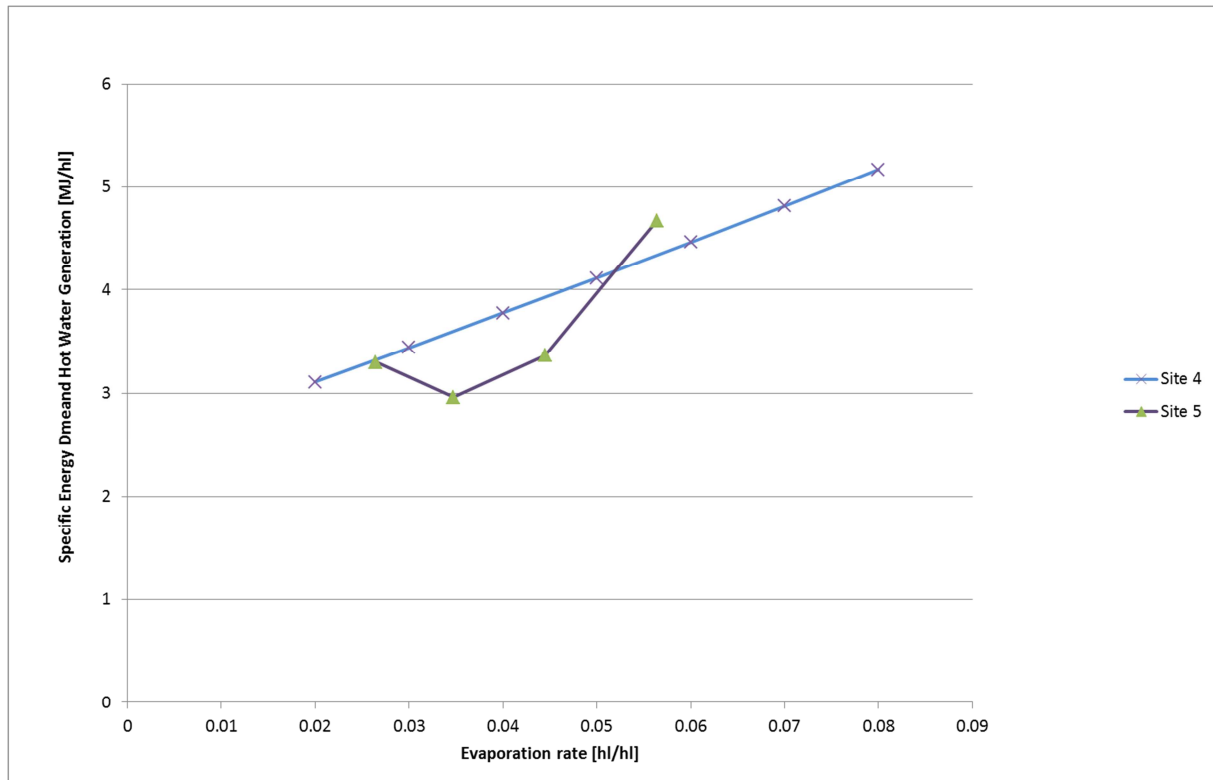


Figure 7-14: Specific energy demand for Hot Water Preparation at different evaporation rates for site 4 and site 5

The overall thermal energy requirement for mashing, wort preheating and wort boiling in combination with the energy demand for hot water preparation is shown in Figure 7-15. We can see that MED_{Tech} values for both sites are very similar with a slight increase in energy demand for site 5 at lower evaporation rates and for site 4 at higher evaporation rates. For site 4, the increase at higher evaporation rates is due to the fact that the use of the energy from vapour condensation is modelled for wort preheating (up to 98 °C) only. With increasing vapour formation the energy from vapour condensation is higher than the energy demand for wort preheating and the vapours cannot be recovered. For evaporation rates above 4 % the additional production of hot water over the vapour condenser is therefore advisable for site 4. The efficiency of the vapour condenser is assumed with 84 % leading to minimal wort preheating requirement of 0.35 MJ/hl at 4 %, while at 2 % evaporation still 4.15 MJ/hl have to be supplied to preheat the wort to 98 °C.

For site 5 a minimum energy demand of brewing processes and hot water preparation can be found at 3.5 % evaporation, similar to the findings for hot water preparation only. As vapour recovery is only linked to hot water preparation this is expected. As mentioned above the temperature difference (losses in heat exchange) between wort temperature in vacuum evaporation (saturation temperature at vacuum pressure) and brew water temperature was assumed with 7 K. In case this can be lowered with efficient heat exchangers, energy demand can be reduced. This effect is shown in Figure 7-16.

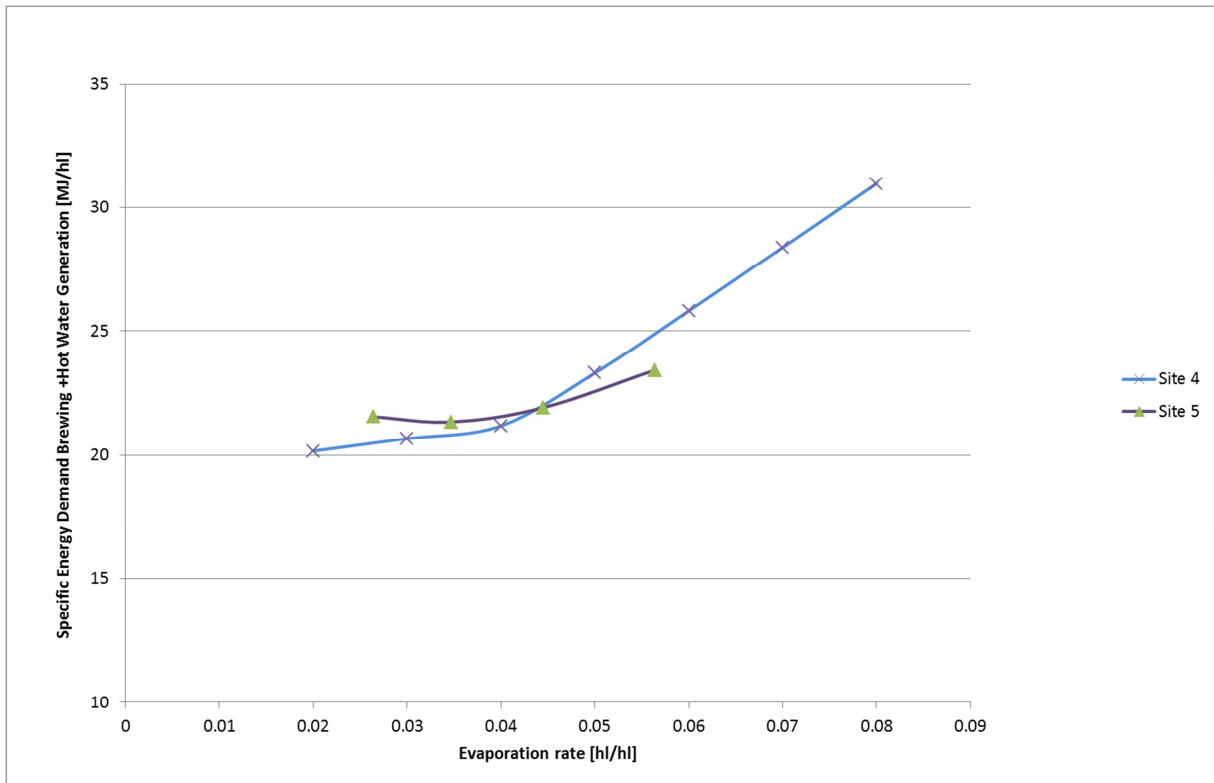


Figure 7-15: Specific energy demand for Brewing Processes and Hot Water Preparation at different evaporation rates for site 4 and site 5

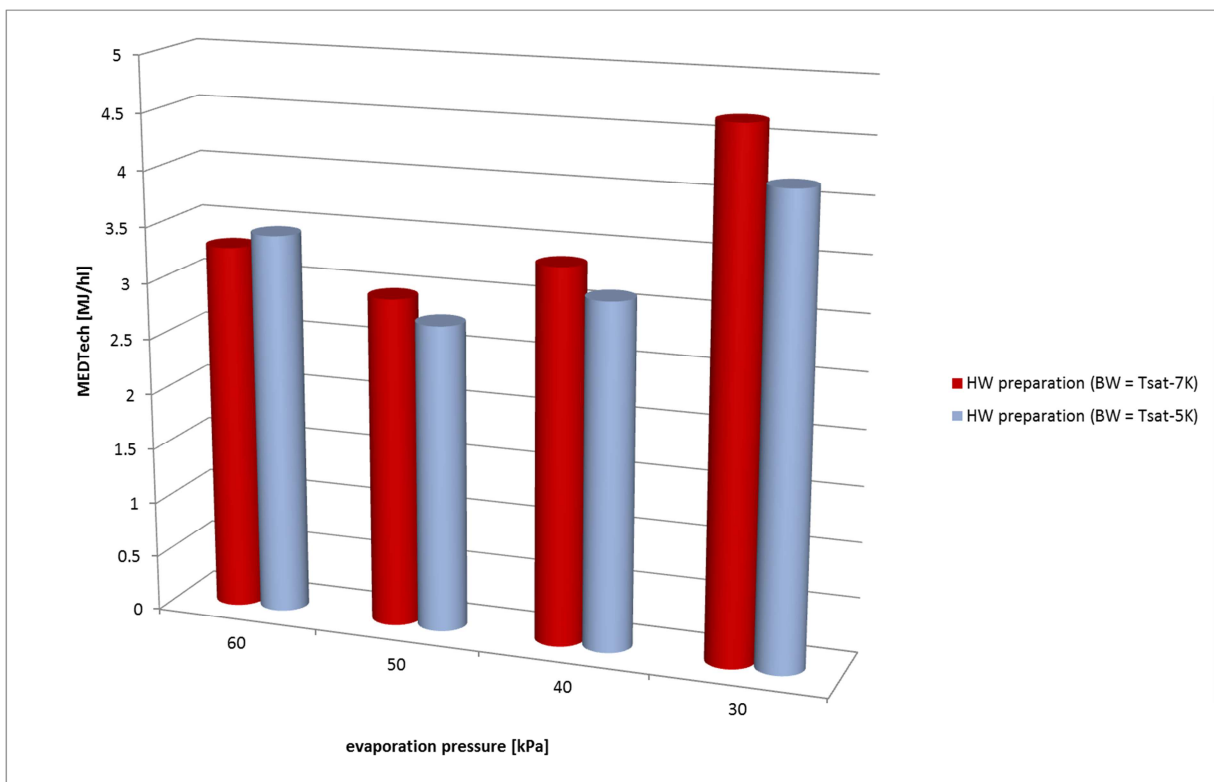


Figure 7-16: Specific energy demand for hot water preparation at site 5 with different efficiency of brew water recovery

Evaluation of water heating requirement for hot water temperatures

As stated above the required hot water temperature is an important influencing factor in this analysis. When the hot water temperature is changed in the EES Model, the effect of its temperature on the energy demand for hot water preparation can be analyzed. This is done in the following, while keeping the cast wort temperature fixed (97 °C for site 4 and 66 °C for site 5).

This is shown in Figure 7-17 for site 4 and site 5 with 3 % evaporation. At site 4 the hot water temperature requirement in packaging and for CIP was linked to the brew water temperature, thus the temperature in the hot brew water tank was changed according to the temperature requirement of the processes. Temperature requirements for hot brew water for mashing and wort separation remained unchanged. Depending on the amount of water that needs to be heated in addition to the installed heat recovery, energy demand for hot water preparation has its minimum at a certain hot water (and brew water) temperature. For site 4, minimum energy requirement was found at a temperature range of 75 °C where enough hot water is generated for all processes and yet there is no demand of rinse water.

At site 5 the temperature of the brew water tank is fixed around 62 °C, as the temperature of the hot cast wort is defined at 66 °C, close to the saturation temperature of the evaporation pressure in vacuum evaporation. Still, changes in temperature requirement for CIP and packaging processes are obvious: The closer these temperatures are to the brew water temperature, the smaller the heating requirement for hot water.

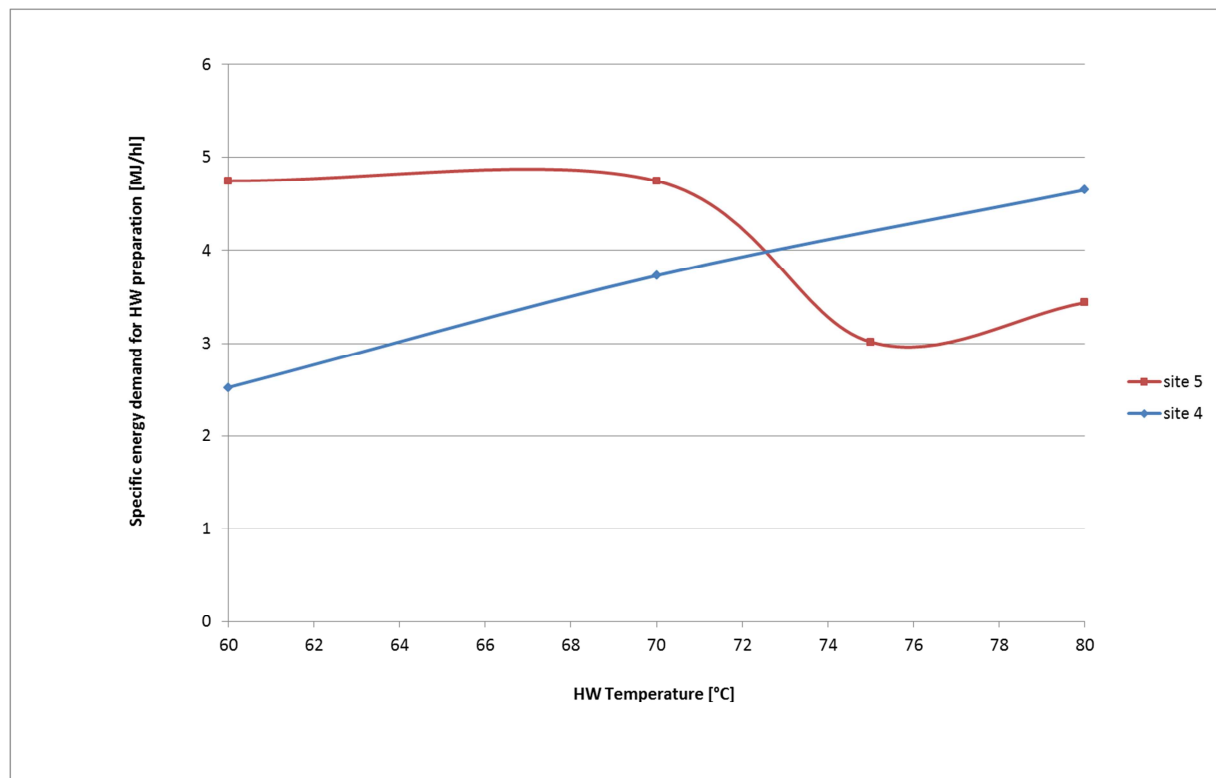


Figure 7-17: Influence of hot water temperature on the energy demand for hot water preparation for site 4 and site 5

Evaluation of energy demand for different gravities

The reduction of energy demand due to high gravity brewing is a known fact in breweries [120] p.614. The Brewery Model easily allows for parametric studies on the effects of wort gravity. Wort gravity can be changed simply by adapting the input parameters of mashing and rinse liquor and/or malt input.

The chosen case studies have different wort gravities of the final cast wort. Although site 4 and site 5 add dilution water, they still have a higher wort gravity. In order to reach the same gravity in sales beer as the other breweries, the required attenuation will be higher. This effect is visible in the fermentation profile of the brewery, as shown in a comparison between site 2 and site 4 in Figure 7-18. With the chosen parameters (5 days main fermentation at 12 °C, subsequent cooling within the tanks to 5 °C within 3 days) the remaining extract is almost identical, but site 4 shows a slightly higher attenuation and a higher production of CO₂ and Ethanol. This difference in attenuation obviously leads to a higher cooling demand for fermentation at site 4. Table 7-9 summarizes the cooling demand for fermentation for all production sites. For all sites the same fermentation parameters have been assumed (identical yeast concentration, 5 days main fermentation at 12 °C, subsequent cooling within the tanks to 5 °C within 3 days). Pitching temperature varies between 8.5 °C (site 2) and 10 °C (site 1 and site 4/5). As expected, cooling demand increases with higher gravity linked to the amount of extract that is fermented. While for the chosen production sites, cooling demand increases only up to 0.5 MJ/hl, this figure might be higher at other breweries that brew at higher gravities. These increases in energy demand need to be taken into account when evaluating energy savings for high gravity brewing.

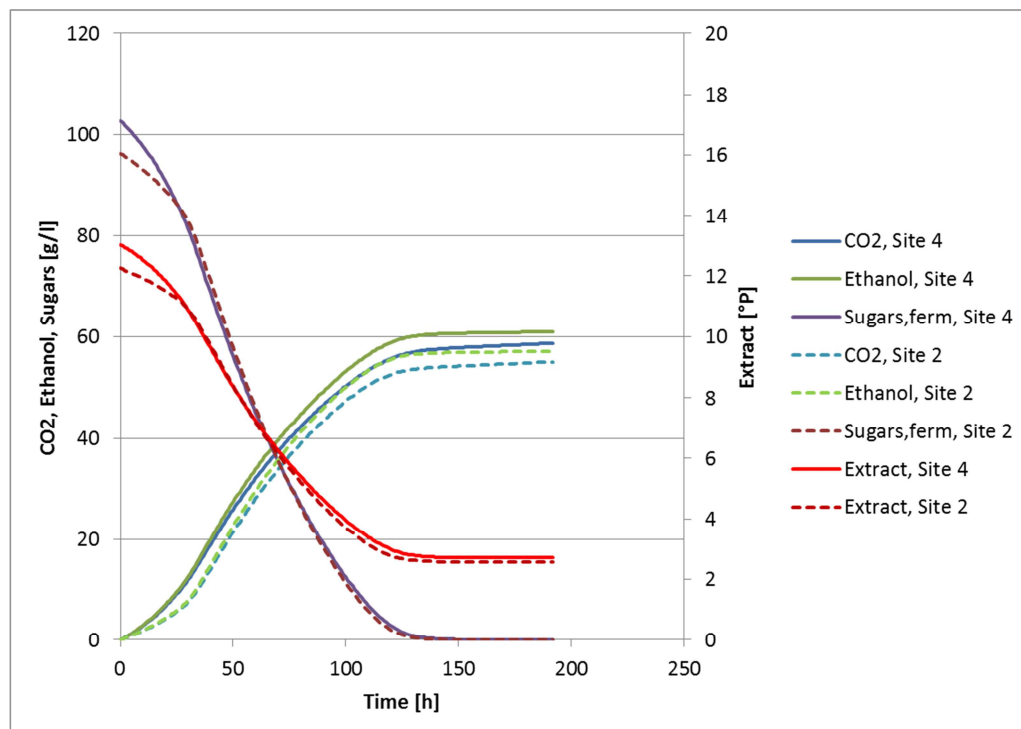


Figure 7-18: Results of the fermentation model for site 2 and site 4 (5 days mainfermentation at 12°C)

Table 7-9: Cooling demand for fermentation at the different production sites

	gravity	final gravity	attenuation	cooling demand fermentation	cooling demand fermentation & cooling within tanks
	[g/100g]	[g/100g]		[MJ/hl]	[MJ/hl]
site 1	12.67	2.651	0.791	6.19	9.41
site 2	12.25	2.578	0.789	5.97	9.19
site 3	12	2.536	0.789	5.85	9.06
site 4 and site 5	13.03	2.713	0.792	6.37	9.59

When we evaluate brewhouse energy demand, energy requirement slightly increases at higher gravities based on the brewed volume. This is due to higher energy demand in mashing due to more malt input at constant mash liquor. Additionally, energy demand for hot water preparation increases as lower heat capacity of the wort leads to less brew water that can be produced over the wort cooler. Overall energy demand, however, is reduced per hl produced beer, as dilution water increases the produced volume after the brewing processes. This dependence is shown for brewery 4 and brewery 5 in the following pages.

First, the changes in specific energy demand by adding more dilution water is shown. On the left the so far modelled situation is shown with addition of 40 hl dilution water prior to fermentation. This number is then increased to 50 hl and 75 hl. Extract content decreases respectively and pitched wort volume increases. In these graphs, however, energy requirement for producing the dilution water in the required water quality is not included (see Figure 7-19).

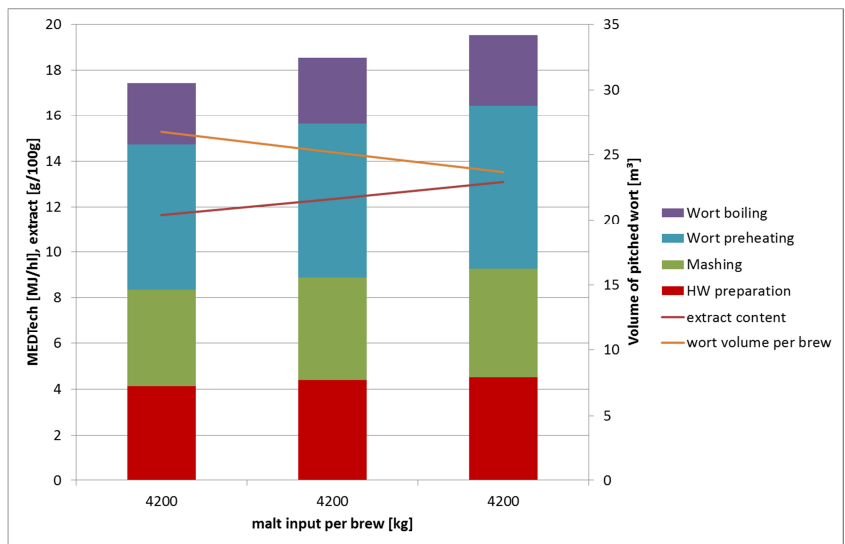
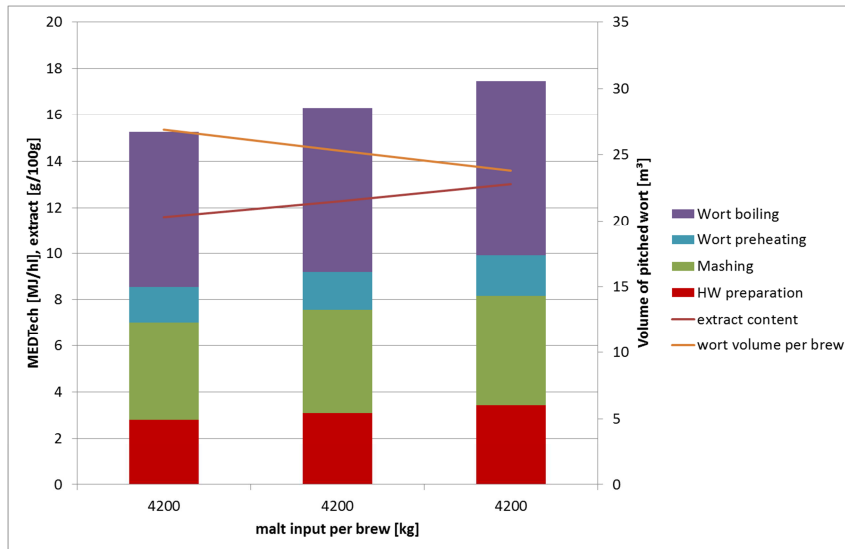


Figure 7-19: Minimal specific thermal energy demand in selected brewhouse processes for varying addition of dilution water (above: site 4; below: site 5)

Figure 7-20 shows the variation in specific energy demand for selected processes with increasing malt input for constant brew water input and 40 hl dilution water. Obviously extract content is increasing and wort volume per brew is roughly constant. Changes in energy demand are most obvious for hot water preparation. As stated above, this is related to the lower brew water yield over the wort cooler.

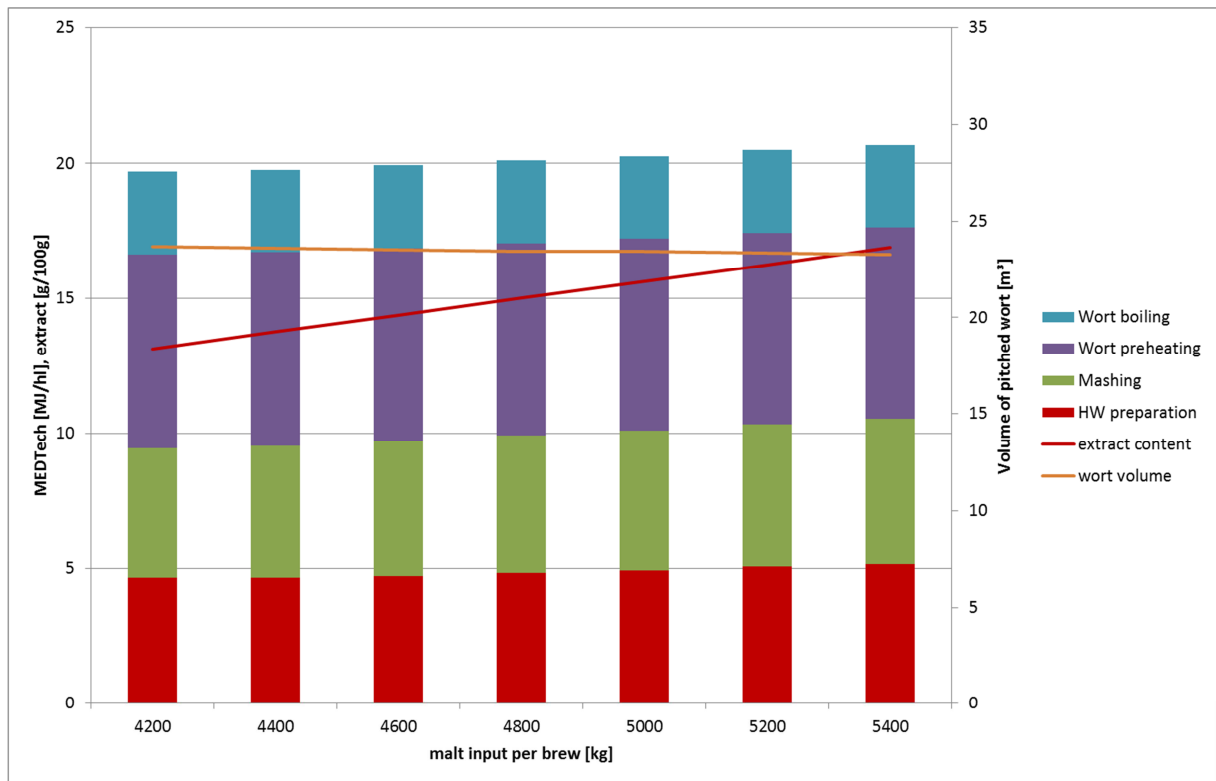
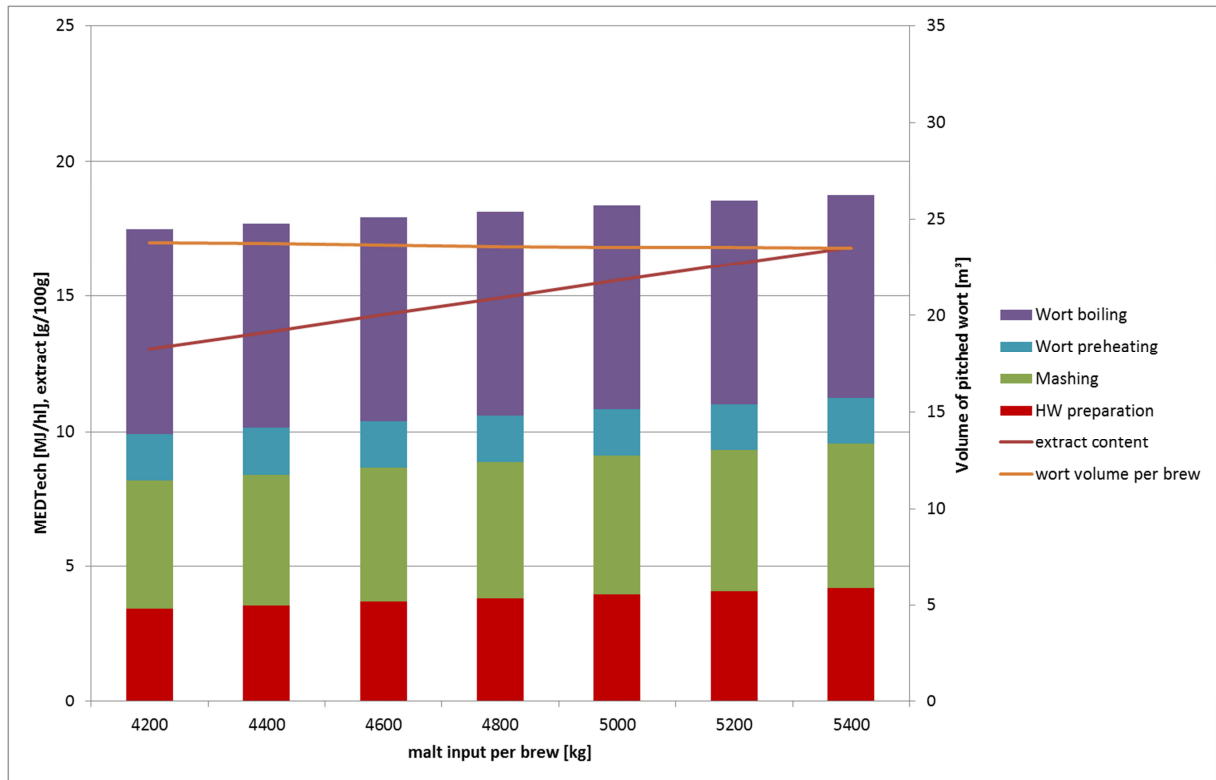


Figure 7-20: Minimal specific thermal energy demand for selected processes with increasing malt input and constant brew water input (above: site 4; below: site 5)

Finally, Figure 7-21 shows evolution of energy demand for increasing malt input, however with corresponding increase in dilution water. Thus, in this graph the wort is brewed at higher gravity due to the higher malt input, but the extract content of the final wort remains the same due to the

addition of more dilution water prior to fermentation. Wort volume per brew increases which is the main reason for the decrease in specific energy demand.

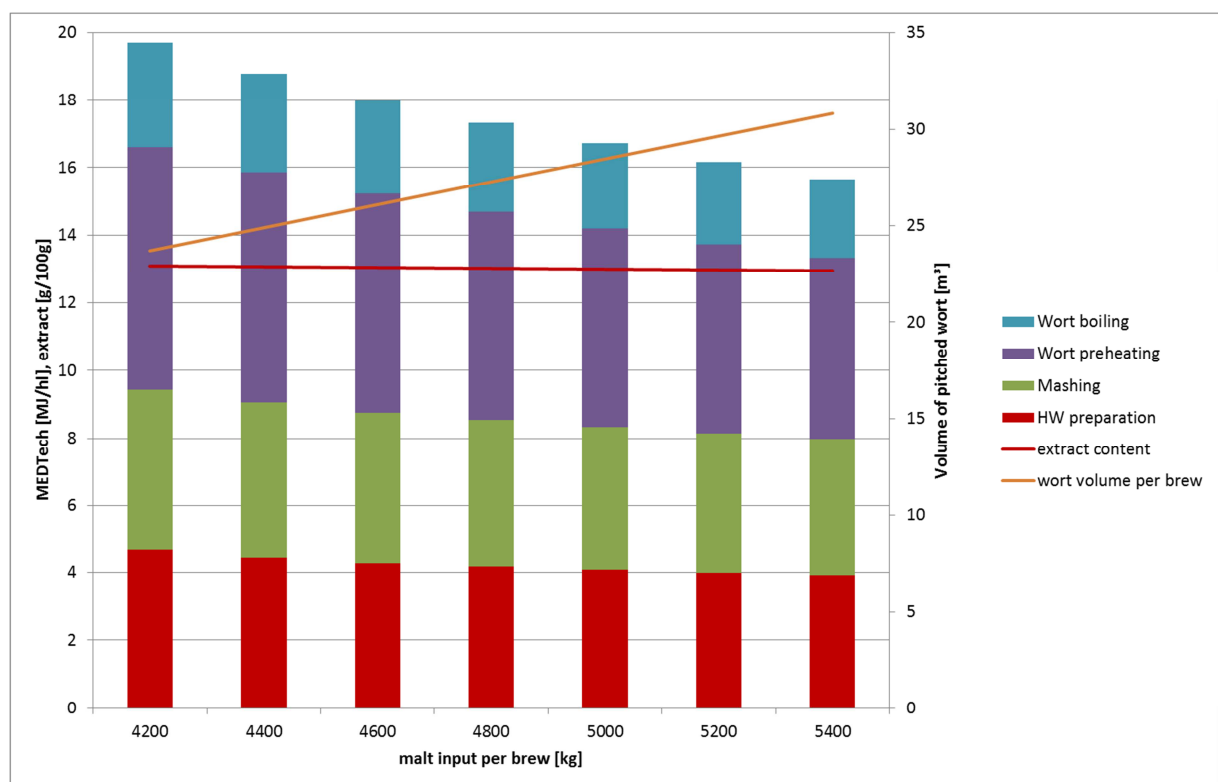
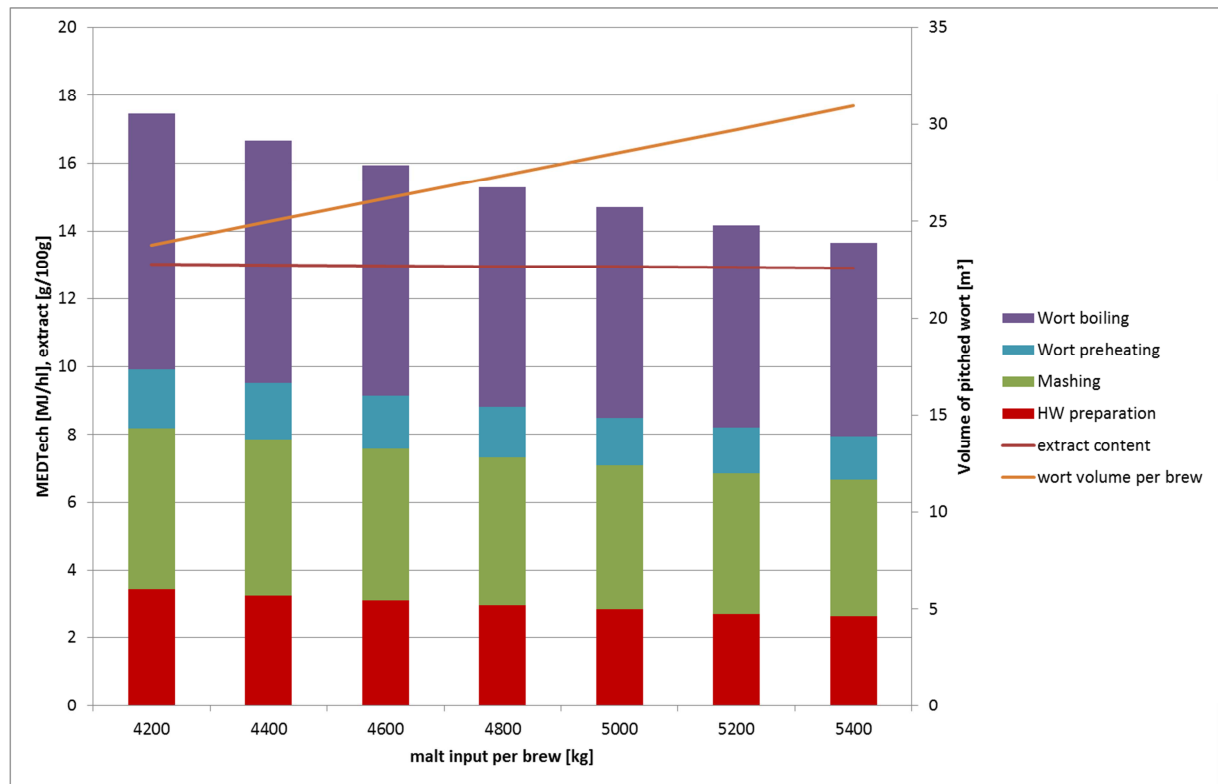


Figure 7-21: Minimal specific thermal energy demand for selected processes with increasing malt input and corresponding increase in dilution water (above: site 4; below: site 5)

7.3 Heat integration strategies for breweries

7.3.1 Applicability of the SOCO tool for heat exchanger and storage design for variable process streams

The applicability of SOCO for developing and designing heat integration strategies for variable process streams has been tested within a diploma thesis at AEE – Institute of Sustainable Technologies [82]. Plausibility verification has been done with three case studies that were investigated with SOCO. For each case study, a proposal was generated and a heat integration network designed and simulated. These case studies were also simulated with two other tools, namely Heat-Int and PinCh. Additionally functionality verification has been performed with a list of 37 functions and features that were all tested.

This functionality test revealed two major functional constraints, namely the size of the proposed storages and proposed port heights. This problem could be quite fast resolved; the code had called a wrong matrix as a basis for calculating the necessary storage size. 5 items of the functionality test initially foreseen are still inactive, and the remaining 87% are active or show minor constrains. These 7 items with minor constrains include for example the user-definition of maximum and minimum storage size. To the user, this seems to work inaccurate. The root of the problem is that this check is performed based on the required storage volume not yet including additional volumes for port heights.

Plausibility verification confirmed that – after correction of proposed storage sizes – SOCO proposes profitable heat exchanger networks including the required storages. The heat exchanger proposal algorithm taps the big potentials and its proposal can be easily converted to practical solutions by the expert. Profitability calculation, which have to be performed by external tools as economic performance assessment is not included in SOCO, showed similar pay-back times which were achieved with the other tools. SOCO however is the only tool that can simulate real-life data. The developed solver matrix allows system simulations of combined heat exchanger and storage flowsheets. However, it reaches its limits in very complex flowsheets, especially when stream splitters are included were mass flows should be defined via the target temperatures.

In summary, SOCO proves to fill the gap for a pinch-tool that can work based on real-life data. The proposal algorithm for network proposals and the solver matrix for solving system simulations work satisfactory. Heat exchanger performance and energy distribution within storages over time can be well simulated and analysed. By varying parameters such as port heights of storages studies can be performed for optimal design configurations.

In the following the application of SOCO for brewery sites 1 and 4 is shown.

7.3.2 Heat integration and storage systems for conventional and intensified breweries⁹

Heat integration strategies for brewery cases 1 and 4 are analysed with SOCO in this chapter. First, a pinch analysis is performed and proposal for heat exchanger and storage networks (HESN) are generated with SOCO which are then translated to practical heat integration strategies. In the following, these strategies are simulated with SOCO analysing the effects of energy flow variability on heat integration performance and storage stratification. Similar results have been presented in [147], however in this chapter the data have been actualised to represent the brewery cases as described 7.2. For site 4, however only packaging into bottles is assumed for site 4 to allow for better comparison to site 1. The use of flash pasteurization and tunnel pasteurization for returnable and non-returnable bottles is also considered for both sites. “Brew water” preparation and “hot water” preparation are calculated as separate water demand profiles. “Brew water” includes the water required for mashing and sparging liquor, while all other hot water requirements (brewhouse CIP, packaging, general needs) are included in “hot water” demand. To account for the importance of hot water and brew water management, the initial case studies a) were adapted to versions b) with lower brew water temperature and lower hot water requirement and versions c) with additionally lower hot water temperature. In version b) it is assumed that brewhouse CIP can be performed with 30% less water, while overall 36% of hot water demand can be reduced. This is an ambitious assessment, in line with the challenging targets the brew industry currently sets itself for lowering general water consumption down to less than 3.5 hl/hl. As more continuous process profiles will require less water for cleaning and in most areas including cleaning of vessels and CIP cold make up water is used, the target of ~80 m³ hot water demand for general needs per week is set for this assessment on optimized heat integration scenarios. An overview of the versions that have been simulated with SOCO are outlined in the following table.

Table 7-10: Overview of case study versions simulated with SOCO

Brewery cases	a)	b)	c)
Site 1	Data as presented in 7.2 BW demand at 80°C HW demand at 80°C	BW demand at 75°C HW demand lowered: Brewhouse CIP: 0.1 hl/hl Packaging 0.03 hl/hl General needs: 0.06 hl/hl	HW demand as in b) at temperature of 75°C
Site 4	Data as presented in 7.2; only packaging into bottles BW demand at 80°C HW demand at 80°C	BW demand at 75°C HW demand lowered: Brewhouse CIP: 0.1 hl/hl Packaging 0.03 hl/hl General needs: 0.06 hl/hl	HW demand as in b) at temperature of 75°C

⁹ Parts of this chapter have been published in the following publication by the author:

Muster-Slawitsch, B., C. Brunner, and J. Fluch, Application of an advanced Pinch Methodology for the food and drink production *WIREs Energy Environment* **3**, (2014).

7.3.2.1 Pinch Analysis and HESN proposal by SOCO

Figure 7-22 and Figure 7-23 show the hot and cold composite curves for the brewery cases 1 and 4 on a time average approach. In SOCO time average is usually calculated as time average data during process operation to allow for better comparability of batch and semi-continuous processes. For both sites, versions a) and c) are shown.

Table 10-1 provides an overview of the stream data sets. Variable process stream data sets, shown in Figure 7-11, have been composed with the Brewery Model and imported into SOCO. The considered time span is roughly 1 week. All corresponding energy values are therefore given in kWh/time span. These demand profiles include known process efficiencies and are based on the UPH values (see 7.2.2.2). It is important to note that vapour condensation and subcooling to 75 °C has been modelled as one hot stream, with an averaged specific heat capacity based on the enthalpy and temperature difference of the vapours and the vapour condensate at 75 °C. This simplification does not have negative effects on the further heat integration analysis, as the energy from the vapours is always assumed to be integrated over vapour condenser into an energy storage over a heat transfer medium. The heat uptake of this heat transfer medium is modelled correctly and not influenced by this simplification.

Due to the fact that in some processes large vessels are gradually being heated over time, average heat capacity flow rates are high while average temperature differences over time between process start and process end are small.

The hot and cold composite curves are shown for a minimal temperature difference ΔT_{\min} of 10 Kelvin. Due to the vast heat recovery possibility in breweries between wort cooling and brew water preparation, both HCC/CCC curves for site 1 and site 4 show a large heat recovery potential.

While at site 1 the pinch temperature is 94 °C and basically all heat exchange occurs below pinch with rather large temperature gradients, the pinch temperature of site 4 is at 64 °C and temperature gradients are significantly lower between heat sources and heat sinks. The conventional brewery (site 1) has the quantitatively larger heat recovery potential due to the higher amount of waste heat, linked to the larger vapour formation in boiling. However, due to the differences in operation schedules a deeper analysis including storages is necessary to reveal the real heat recovery potential.

The effect of changes in hot water management between version a and c of the sites, is not well visible based on the graphical analysis. Lower hot water demand at lower temperatures result to lower heating requirements, but also maximal heat recovery potential is decreased and minimal cooling demand is increased. This would signify that the heat sources cannot be tapped to their full potential.

However, as it has been stated earlier, the pure graphical analysis for variable process profiles might lead to misleading conclusions. The further analysis with SOCO will reveal the effects of changes of process technologies (site 1 versus site 4) and changes in hot water management (version a versus version b) to real heat integration schemes.

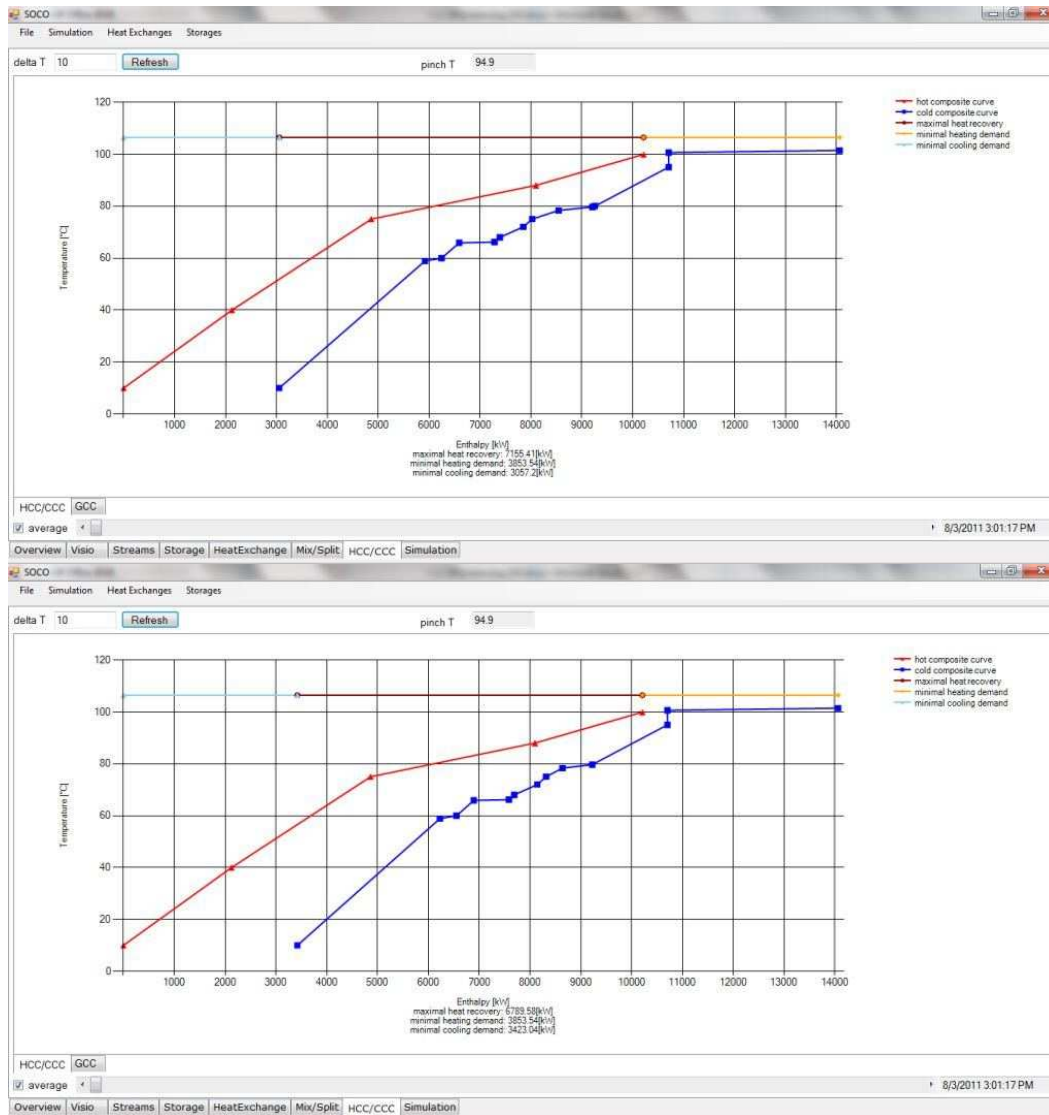


Figure 7-22: Hot and cold composite curves of the brewery site 1 (above a; below c)

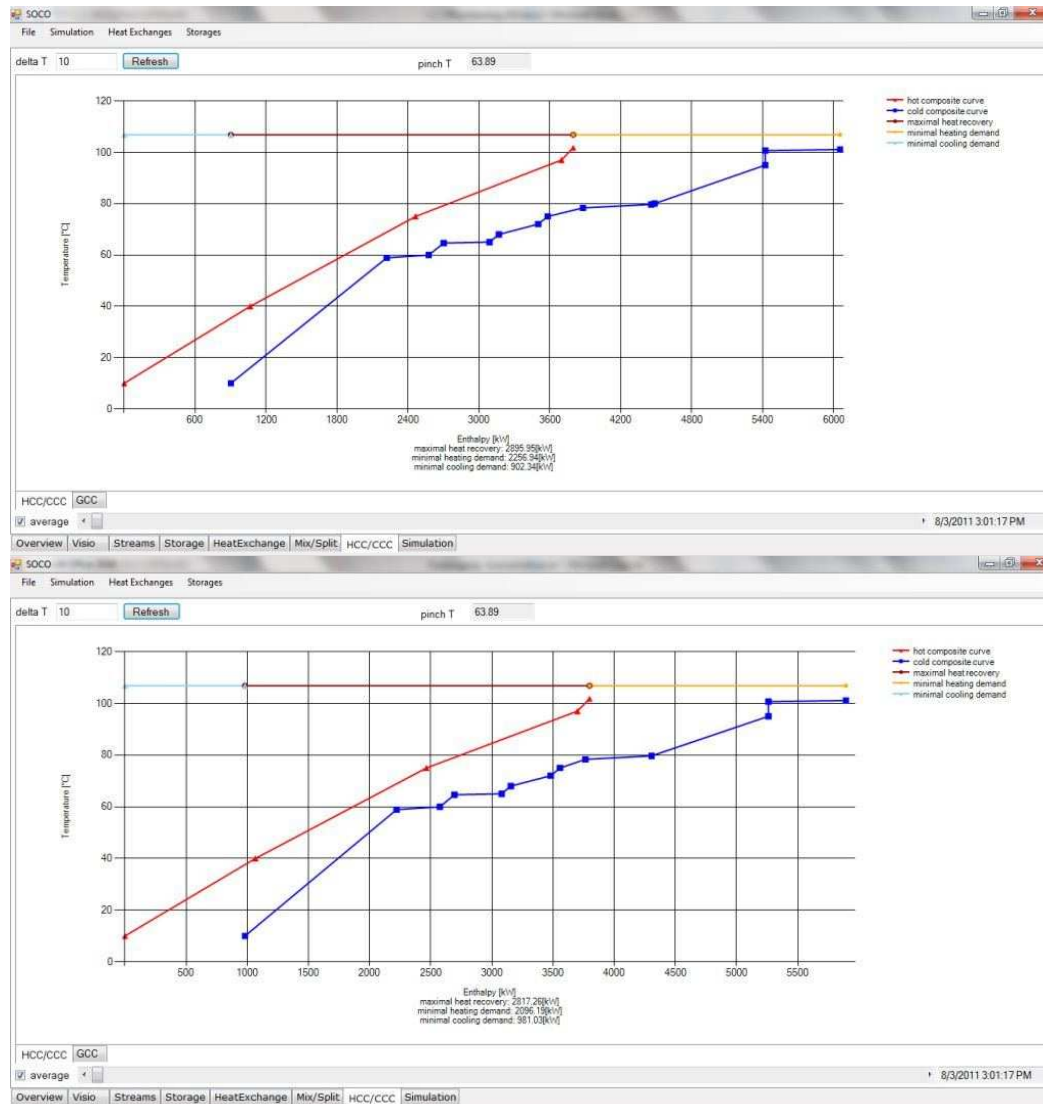


Figure 7-23: Hot and cold composite curves of the brewery site 4 (above a; below c)

The heat exchanger proposal suggested by SOCO is to a large extent influenced by the criteria settings (energy, power and exergy). Especially the factor “exergy” is an important parameter and influences the proposal outcome significantly. As explained in 5.2.2 it ensures that high value (high temperature) energy is not converted to low grade (low temperature) energy. For the purposes of this study, the following settings have been chosen:

- Power 0.1
- Exergy 0.6
- Energy 0.3

Aiming at an optimized heat integration scheme a very low temperature difference for heat exchange (3 Kelvin) was chosen for the proposal generation. All settings for the heat exchanger proposal algorithm are given in Figure 10-2.

The outcome of SOCO’s proposal for heat exchanger and storages is summarized in Table 7-11 and Table 7-12. Heat exchanger proposals with energy savings of less than 2,500 kWh/week have been excluded from the proposal.

Table 7-11: Heat exchanger and storage network proposal by SOCO for Brewery Site 1

Site 1, version A						
HX	heat source	T [°C]	heat sink	T[°C]	transferred energy [kWh/week]	Storage Size [m ³]
1	Vapour Cond.	99.9-75	Brew water	10-65	50759	7
2	wort cooling	88-13	Hot water	10-65	32571	144
3	wort cooling	88-78	Wort preheating	75-78	4240	24
4	wort cooling	78-62	Pasteurization	58.9-59.4	8380	76
5	wort cooling	88-69	Mashing	65.9-66	7380	4
6	chillers	75-63	pasteurization	59.4-59.7	6260	69

Site 1, Version B						
HX	heat source	T [°C]	heat sink	T[°C]	transferred energy [kWh/week]	Storage Size [m ³]
1	Vapour Cond.	99.9-75	Brew water	10-61	50759	7
2	Wort cooling	88-78	Wort preheating	75-79	6357	24
3	Wort cooling	78-69	Mashing	65.9-66	6717	74
4	Wort cooling	69-13	Hot water	10-64	17058	138
5	Wort cooling	88-81.3	Bottle washing	78.3-78.6	3918	> 200
6	Wort cooling	81.3-61.9	Pasteurization	58.9-59.5	11089	75
7	Vapour Cond.	99.9-75	Mashing	66-66.1	2629	-
8	chillers	75-71	Flash Past.	68-69	4099	> 200
9	chillers	71-62.5	Pasteurization	59.5-59.8	4349	115

Site 1, Version C						
HX	heat source	T [°C]	heat sink	T[°C]	transferred energy [kWh/week]	Storage Size [m ³]
1	Vapour Cond.	99.9-75	Brew water	10-61	50759	7
2	Wort cooling	88-78	Wort preheating	75-79	6357	24
3	Wort cooling	78-69	Mashing	65.9-66	6717	74
4	Wort cooling	69-13	Hot water	10-65	17343	144
5	Wort cooling	88-81.3	Bottle washing	78.3-78.6	3918	> 200
6	Wort cooling	81.3-61.9	Pasteurization	58.9-59.5	11089	75
7	Vapour Cond.	99.9-75	Mashing	66-66.1	2629	-
8	chillers	75-71	Flash Past.	68-70	4099	> 200
9	chillers	71-62.5	Pasteurization	59.5-59.8	4349	115

Table 7-12: Heat exchanger and storage network proposal by SOCO for Brewery Site 4

Site 4, Version A						
HX	heat source	T [°C]	heat sink	T[°C]	transferred energy [kWh/week]	Storage Size [m ³]
ABOVE PINCH						
1	Wort cooling	97-78	Wort preheating	75-93	21078	28
2	Wort cooling	78-62	Pasteurization	59-60	18018	167
3	Vapour Cond.	101.8-75	Brew water	59-78.5	19144	2
4	chillers	75-62	Hot water	59-70	5561	26
BELOW PINCH						
5	Wort cooling	61-13	Brew water	10-57	48518	58
6	Wort cooling	60.5-13	Hot water	10-28	6929	13
7	chillers	60-40	Hot water	28-48	11361	55

Site 4, Version B						
HX	heat source	T [°C]	heat sink	T[°C]	transferred energy [kWh/week]	Storage Size [m ³]
ABOVE PINCH						
1	Wort cooling	97-78	Wort preheating	75-93	21078	3.7
2	Wort cooling	78-62	Pasteurization	59-60	18018	167
3	Vapour Cond.	101.8-75	Brew water	59-74.5	17121	1.6
4	chillers	75-62	Hot water	59-71.5	4026	5.9
BELOW PINCH						
5	Wort cooling	61-13	Brew water	10-57	52305	62.4
6	Wort cooling	60.5-13	Hot water	10-28	3837	8.4
7	chillers	61-40	Hot water	28-48	10502	30.7

Site 4, Version C						
HX	heat source	T [°C]	heat sink	T[°C]	transferred energy [kWh/week]	Storage Size [m ³]
ABOVE PINCH						
1	Wort cooling	97-78	Wort preheating	75-93	21078	28
2	Wort cooling	78-62	Pasteurization	59-60	18018	167
3	Vapour Cond.	101.8-75	Brew water	59-74.5	17121	1.6
4	chillers	75-62	Hot water	59-71.8	4129	5.9
BELOW PINCH						
5	Wort cooling	61-13	Brew water	10-57	52305	62.4
6	Wort cooling	60.5-13	Hot water	10-27	3837	8.4
7	chillers	61-40	Hot water	27-55	10502	30.7

The HESN proposals between the two brewery case studies do deviate, but also show consistent trends to integrate the energy of vapour condensation, wort cooling and the waste heat of cooling compressors (chillers) for the processes brew water, hot water, wort preheating, mashing and pasteurization. It is important to highlight that the heat exchanger proposal starts its algorithm based on the hot process with the largest heat capacity flow rate, which is vapour condensation in case of site 1, and wort cooling in case of site 4. Also, the proposal is optimized purely on the basis of energy recovery, without taking into account costs. The proposal calculates an approximate storage size which is required for each heat exchanger, however no real system simulation between heat exchanger and storage unit is run during the proposal generation.

At site 1 the use of the energy from vapour condensation is suggested for generating brew water, and to a minor extent to heat the mashing process. In version A with high hot water demand for CIP and packaging, the energy of the wort cooler is primarily used for hot water preparation. Further wort cooling energy is suggested for wort preheating, pasteurization and mashing. At lower hot water demand (Versions B and C), the use of wort cooling is first integrated with wort preheating and mashing, before it is used for hot water preparation and finally also integrated partly with the packaging processes. The integration with packaging processes requires large storage sizes which reveals that integrating brewhouse processes first (usually also located close together) is advisable. Lowering the brew water temperature to 75 °C (while increasing its mass to fulfill the requirements of mashing and sparging) does not have any positive effect on heat integration based on the proposal result.

At site 4, the proposal result is divided into a part “above pinch” and “below pinch”, as SOCO adheres to the pinch rule that no heat transfer should be transferred across pinch. Therefore the HESN proposal generation is done separately for the regions above and below pinch. For site 4 all versions A-C give the same HESN proposal. The energy of wort cooling is first integrated with the energy demand of wort preheating. Subsequently its energy is for tunnel pasteurization however requiring a large storage unit. Above pinch, vapour condensation is used for brew water generation, while below pinch brew water is generated over the energy of wort cooling. Hot water is preheated by the wort cooler below pinch, then further heated over the waste heat of chillers.

A basic result of the heat exchanger proposal with high relevance on the exergy criteria is to use the hot wort and wort cooling not only for brew water preparation, but to take first advantage of the high temperatures for preheating the incoming wort prior to boiling. Similar results have already been suggested in earlier works [151].

As in brewery 1 vapour condensation energy is much higher due to the higher evaporation rate and wort cooling energy is slightly lower due to whirlpool losses, vapour condensation energy is suggested for brew water preparation. The remaining energy demand for brew water preparation is covered by wort cooling. Wort cooling is then further used for hot water preparation, mashing and packaging processes (mainly tunnel pasteurization). In brewery 4, on the other hand, wort cooling above pinch is integrated to wort preheating and pasteurization and only below pinch it is used for brew water and hot water generation. Considering the potential of using the energy of wort cooling and vapour condensation above pinch for other processes than wort preheating, the mashing process might be a more promising alternative to tunnel pasteurization due to its location close to these heat sources. Evaluating heat recover options for a brewery site without tunnel pasteurization the integration of the mashing process has also been suggested by SOCO [151].

It can be basically summarized that a thermodynamic optimized heat recovery proposals suggests the use of wort cooling and vapour condensation for wort preheating, mashing and brew water preparation. Remaining heat availability is suggested to be further integrated into the heating of the tunnel pasteurization process and bottle washing. Conventional heat recovery systems in breweries apply wort coolers for brew water preparation and energy storages loaded by vapour condensation for wort preheating. The novel approach of SOCO suggests a more integrated scheme to basically use both heat flows for both heat sinks and to further include the heating of the mash tun. Integration of waste heat or any other low temperature energy supply into mash tun heating requires retrofit of conventional mash tuns, as current heat transfer coefficients and existing heat transfer areas are too low. Successful retrofit possibilities have been shown by [140] in a recent project on solar process heat integration in mash tuns. Minimal temperature difference may then be reduced to roughly 15K. As it has been suggested in this work (see chapter 6), an optimized mashing process with an oscillatory reactor as new mashing technology could potentially further reduce the minimal temperature difference requirement to <math><10\text{ K}</math>, thus allowing easier integration of low temperature heat sources.

7.3.2.2 Simulation of a new energy storage design

When the proposed heat exchangers are re-mapped into a practical heat exchanger network, the resulting possible energy storage design is presented in Figure 7-24. Vapours and wort cooling load an energy storage, and the remaining hot wort is further cooled down over brew water preparation including a 2nd storage with varying levels. The energy storage delivers energy to wort preheating and additionally to the mashing process. The integration of the waste heat of chillers and the energy demand for hot water preparation are not yet included.

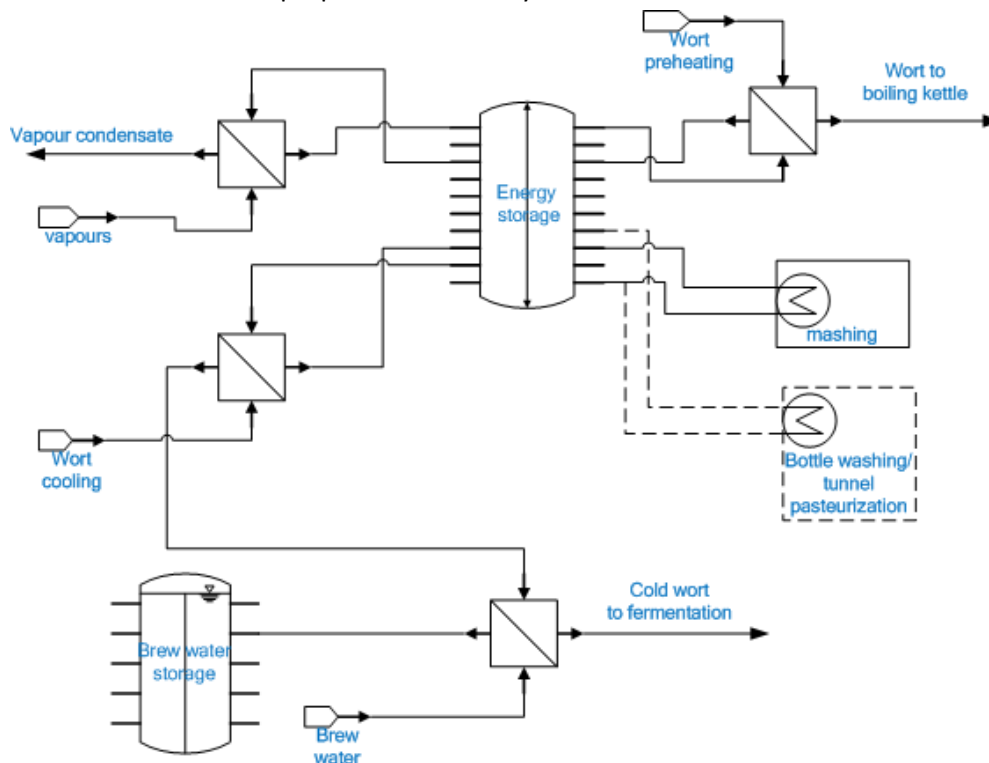


Figure 7-24: Scheme of the heat exchanger network proposed by SOCO

After drawing the practical heat exchanger and storage network (HESN) as visio drawing in SOCO and setting the parameters for system simulation (such storage size, port heights, heat exchange areas and mass flow of storage media) SOCO' simulation model can analyze the transferred energy of the storage and each heat exchanger. The parameters of heat exchangers and storages that have been used in the simulations are presented in the Appendix. At first in Run 1, all heat exchanger and storage sizes have been set to identical parameters. Only for mashing, the minimal temperature difference for heat exchange has been defined at 8 K for site 1 and 4 K for site 4 due to different mashing technology in use.

The results of Run 1 are presented in Table 7-13 and in Figure 7-25. With a storage size of 90 m³ the simulation shows that the integration scheme can cover 77 % of the energy demand of wort preheating, 54 % of the brew water energy demand and 87 % of the mash tun heating for brewery 1. When the same simulation is done for brewery 4, it results in covering 94 % of the energy demand in wort preheating, 86 % of the brew water energy demand and 84 % of the mash tun heating.

Table 7-13: Energy savings for each process in Run 1

process	Site 1A	Site 4A
mashing	86.9%	84.2%
brew water	53.7%	85.7%
wort preheating	76.9%	94.2%

Obviously the heat integration scheme is more effective for site 4, although there should be enough waste heat available at site 1 to achieve similar results. The reasons are analysed in the following: While the transferred energy of the vapour condenser is much larger at site 1, the remaining energy availability of site 1 is also significantly larger. It becomes clear that, at site 1, although wort preheating still requires energy, the potential of the vapour condenser cannot be fully tapped. The same occurs for brew water preparation and the energy use of the wort cooling energy.

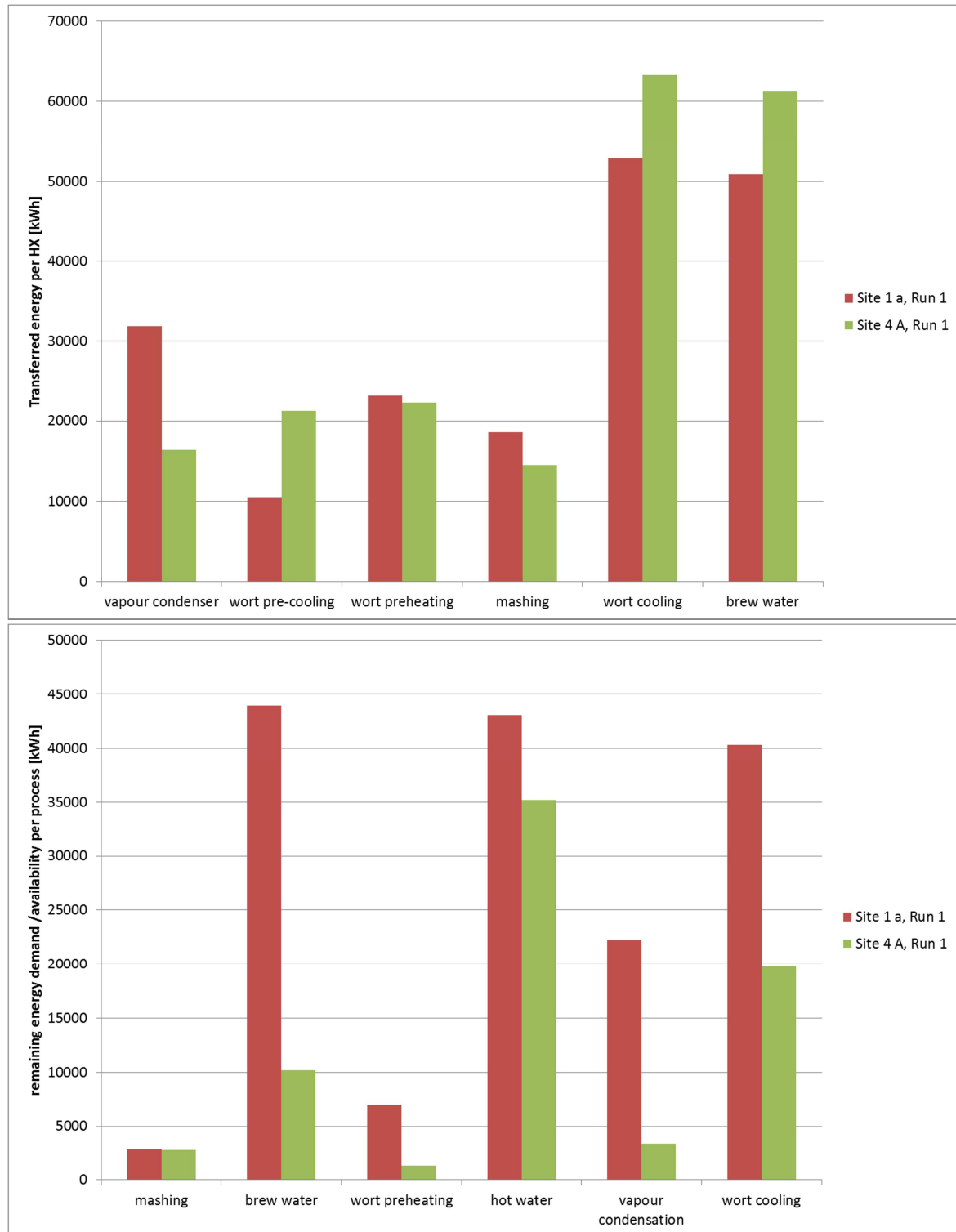


Figure 7-25: Heat exchanger performance and remaining energy demand for Run 1 at site 1 and site 4

By analysing the heat exchanger performances over time and the storage stratification results, the bottlenecks of the heat integration scheme can be easily identified. This is shown in the following figures presenting the performance of the vapour condenser of site 1 and site 4 in connection to the temperature stratification in the energy storage. Figure 7-26 shows the difference in temperature

profile for the two brewery cases studies on different heights (TSensor 0 - 4) in the storages. Additionally the simulated operation of the vapour condenser loading the storage is shown.

At site 1, it is not possible to load the storage with all energy available in vapour condensation due to the developing temperature profile in the storage at certain times. Several port heights have been analyzed, but the limit is basically only overcome when increasing storage sizing. The storage size of 90 m³ leads to loading the storage to such an extent that the temperature at the bottom of the storage increases significantly and reaches values well above 90 °C. Due to this fact the vapour condenser, which would potentially cool the vapours to 75 °C, is not able to operate at this full capacity. This is also shown in Figure 7-26.

Within the optimized process profile at site 1, the storage temperature at the bottom can be kept constant at around 70 °C and vapour condensation can fully integrated.

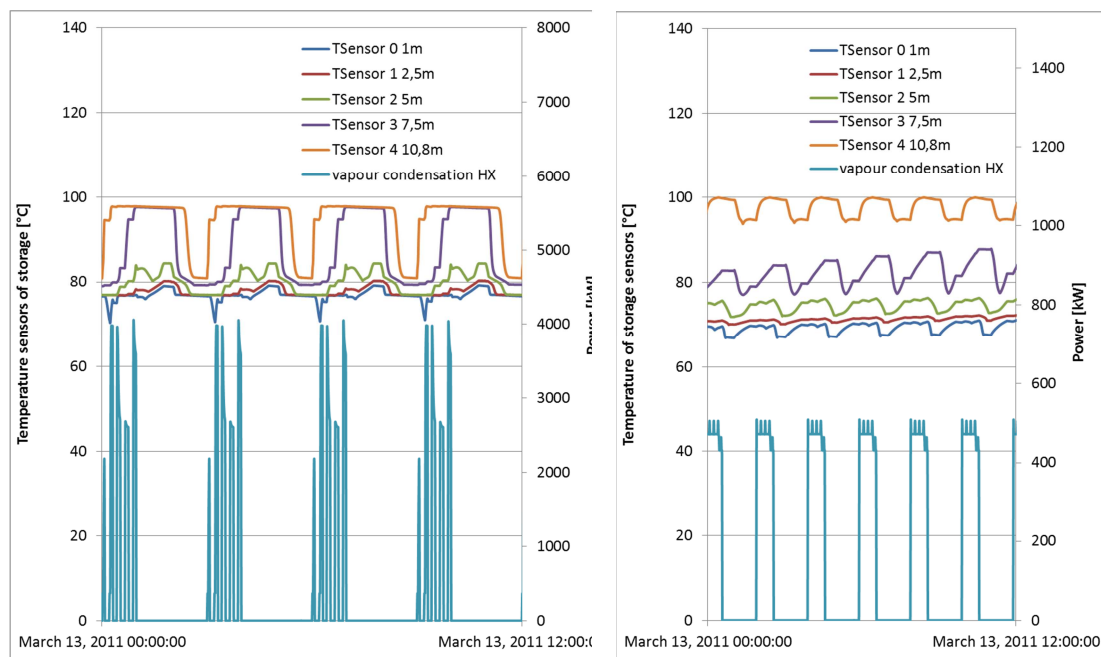


Figure 7-26: Temperature profile in the storages of brewery 1 (left) and brewery 4 while loading the storage with energy from vapour condensation

Based on the discussion above, it can be concluded from the results of SOCO that for improving the heat integration concept for site 1, a larger storage size is necessary or larger heat exchanger areas are required to enable the heat transfer at low temperature differences. In Run 2, therefore the storage size was increased to 150 m³ for site 1 and the heat exchange areas for the vapour condenser and the wort cooler were increased by a factor of 2 and 4 respectively.

Clearly, heat exchanger performance can be significantly increased and remaining energy demand is reduced substantially (see Figure 7-27). Brew water demand can now be covered by 89 % and wort preheating by 95 %.

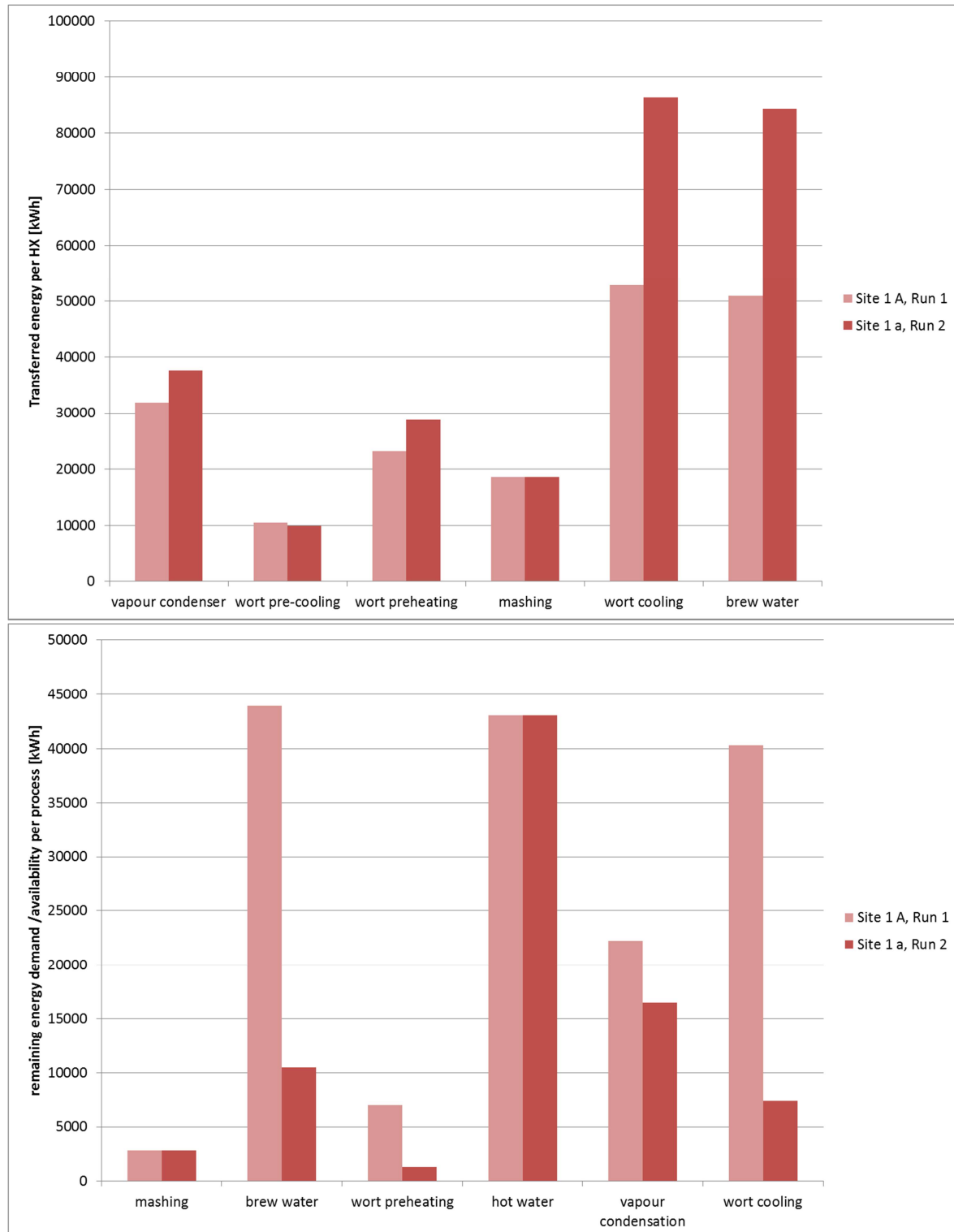


Figure 7-27: Heat exchanger performance and remaining energy demand for Run 1 and Run 2 at site 1

7.3.2.3 Effects on hot water management on the energy storage design

The same heat integration concept as depicted in Figure 7-24 is applied for Versions B of the case study with lower hot water demand and lower brew water temperature. While hot water demand is not yet included in the heat integration scheme, only the effects of the lower brew water

temperature are analysed. It becomes clear that for Site 1 the effects are minimal, while at site 4 brew water preparation can be covered over heat integration to 98 % with a brew water temperature at 75 °C instead of 85 % in Version A with higher brew water temperature at 80 °C.

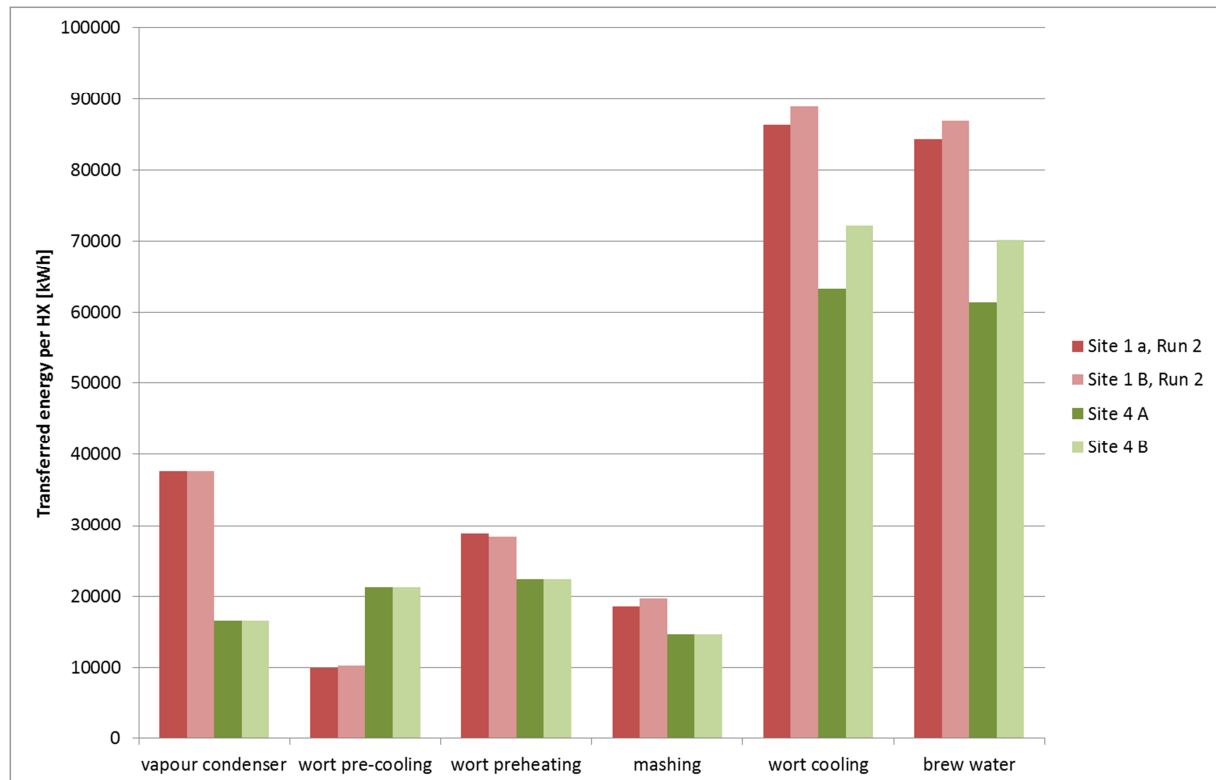


Figure 7-28: Heat exchanger performances for Versions A and B of site 1 and site 4

Finally hot water preparation is included into the heat integration scheme. This is shown here for Version C of site 4 with reduced hot water requirement at 75 °C. The waste heat of cooling compressors is additionally integrated which is in line with the HESN proposals of SOCO.

Two options are analysed:

- Scheme 1 - An energy storage tank loaded by wort cooling and waste heat of cooling compressors for heating brew water and hot water
- Scheme 2 - Preparation of hot water via the waste heat of cooling compressor into a separate hot water storage with varying level

Scheme 1 is depicted in Figure 7-29. The combined loading of the energy storage by wort cooling and the waste heat of cooling compressors however leads to instable temperature conditions in the storage, as shown in Figure 7-30. This phenomenon is heavily dependent on the specific demand profiles of the hot water requirement of each brewery. The heat transfer medium for the wort cooler is taken from the storage at the bottom to ensure that wort cooling can occur efficiently via this cold heat transfer medium. However, at site 4 at certain times when storage loading exceeds unloading, the temperature of the storage tank increases. Additionally the temperature differences over the unloading heat exchangers lead to the fact that the lower level of the storage cannot be cooled efficiently. At these times, wort cooling cannot be achieved to full extent and as a consequence the storage tank cannot be loaded by the full energy content of the wort cooler.

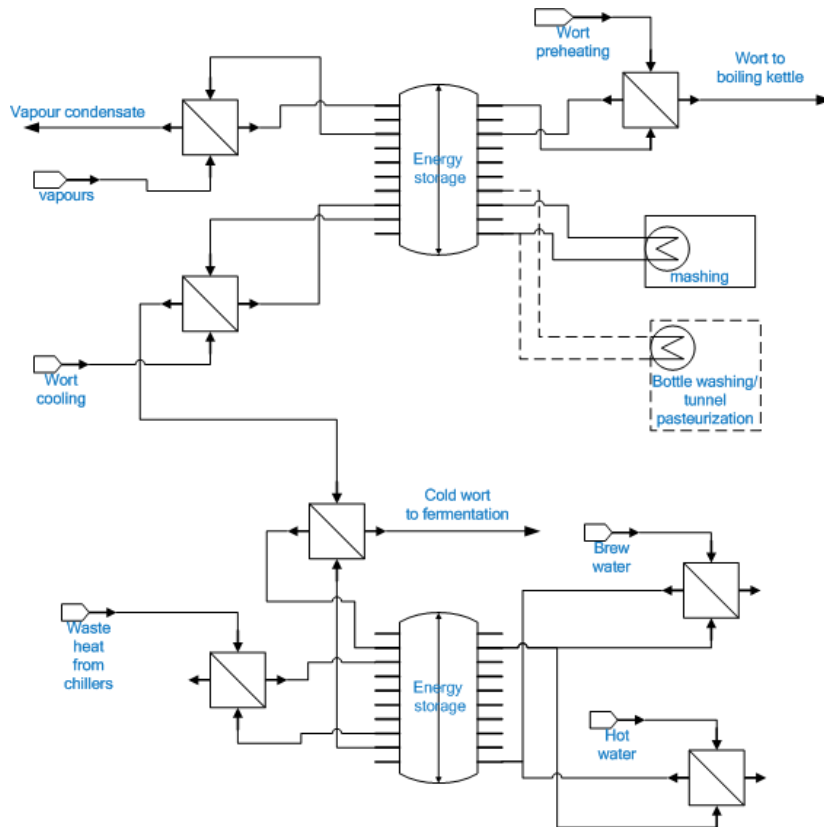


Figure 7-29: Scheme 1 for heat integration of chiller waste heat and hot water

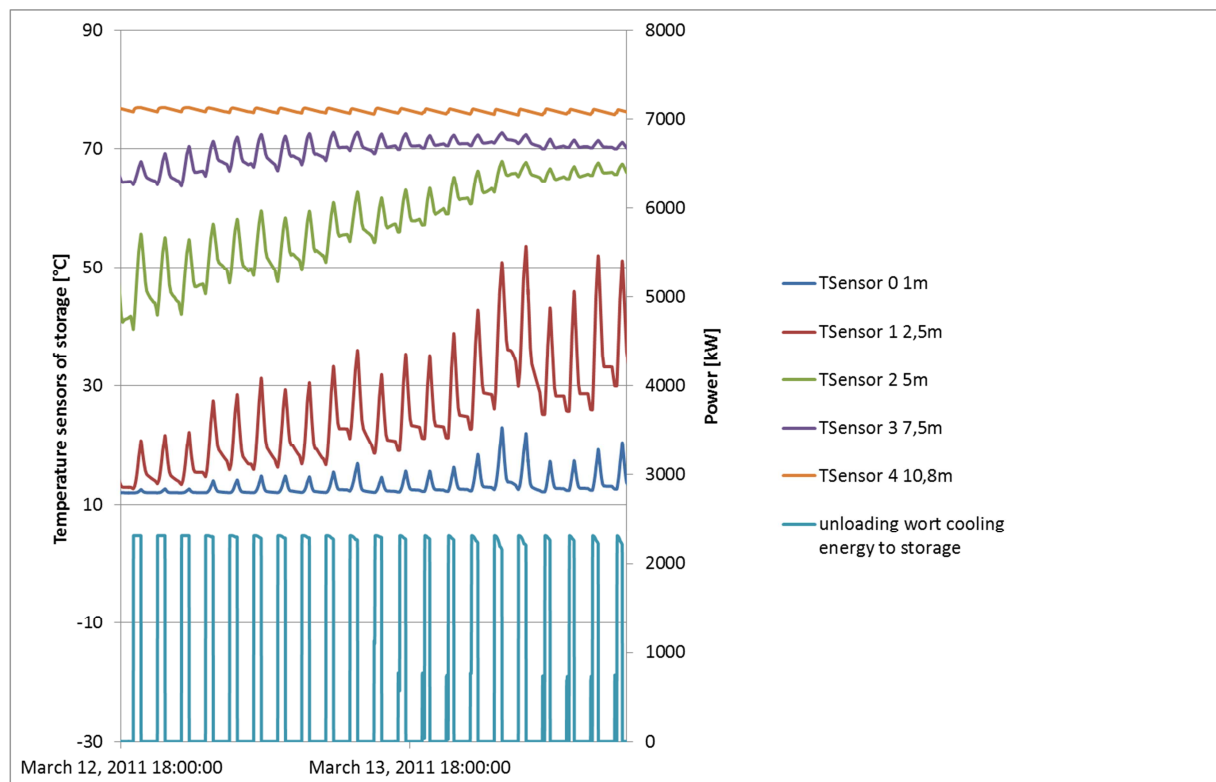


Figure 7-30: Temperature stratification results in energy storage for hot water, Site 4 Version C Heat Integration Scheme 1

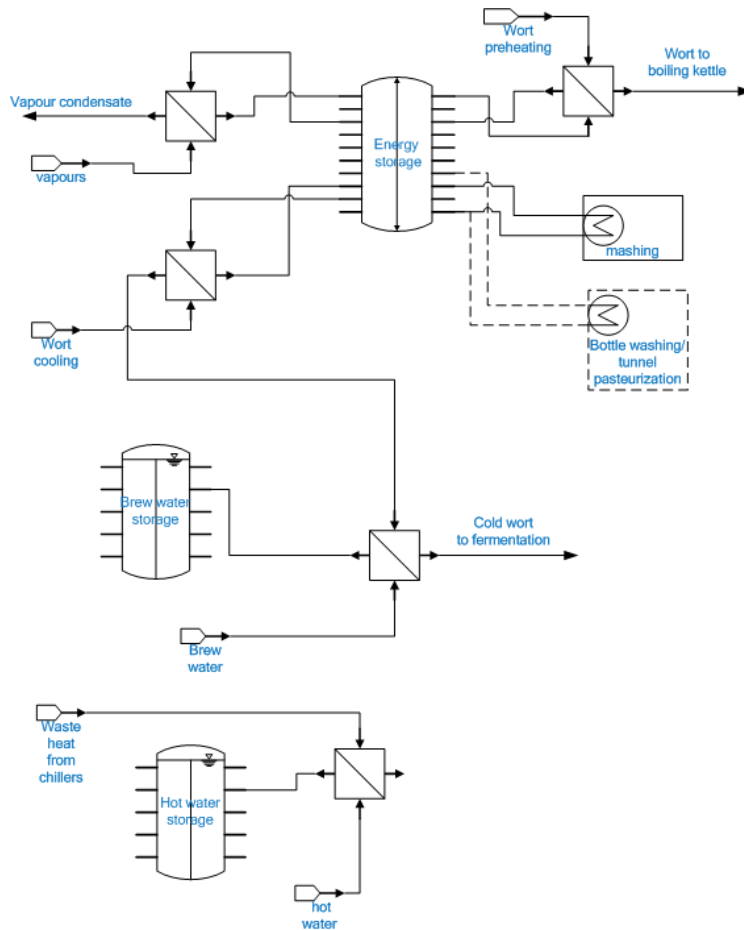


Figure 7-31: Scheme 2 for heat integration of chiller waste heat and hot water

Scheme 2 decouples the two heat sources for brew water and hot water preparation by heating two hot water flows independently. It also avoids additional ΔT over loading or unloading heat exchangers, but rather heats the hot water directly for later use. The simulation reveals that remaining energy demand can be lowered by 46.5 %. Table 7-14 summarizes the results. Comparing to the saving figures and the remaining energy demand of site 1 in Run 1, it can be effectively shown that SOCO allows analysing optimization strategies for heat integration concepts.

Table 7-14: Result in potential energy savings for mashing, wort preheating, brew water and hot water generation

	energy demand [kWh]	Remaining energy demand [kWh]	savings
mashing	17741	2807	84.2%
brew water	71526	1314	98.2%
wort preheating	23749	1382	94.2%
hot water	20939	2850	86.4%

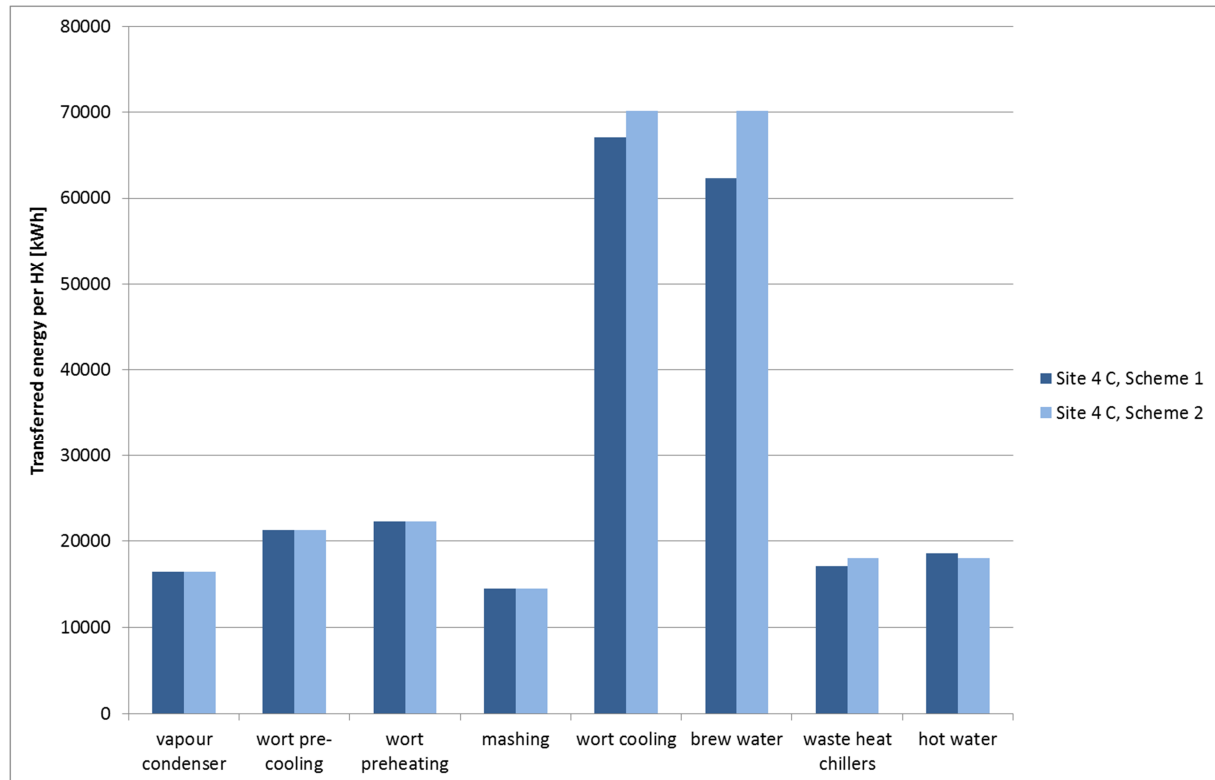


Figure 7-32: Heat exchanger performances of the heat integration concepts including chiller waste heat and hot water

Comparing the heat demand of site 1 for brewhouse and hot water requirement, as has been analysed in 7.2.2.2, which results to 36.2 MJ/hl to the integrated heat recovery concept for site 4, savings reach 68.6 %. The remaining energy demand of mashing, wort preheating and hot water as well as brew water preparation of site 4 results to 11.4 MJ/hl including minimized hot water demand at lower temperatures and waste heat recovery. It is important to note that about 4.5 MJ/hl are due to minimized hot water consumption and lowering the required temperature for hot water demand. These figures, however, compare brewing sites with very different evaporation rates. The reduction of energy demand for site 4 by the optimization measures results to 45.6 %. About half of these savings are due to optimization of the hot water consumption.

7.3.3 Solar heat integration and other renewable energy integration based on the result of SOCO

The in SOCO developed optimization algorithm suggests the settings of heat exchangers via a pinch-based approach. However, via several parameter definitions a HEN is created that is oriented on practical constraints (e.g. minimal heat exchanger size) and targets (e.g. maximum transferable energy over time). Therefore the remaining energy demand after heat integration might include more streams than the theoretical minimal energy requirement based on the hot and cold composite curves. When no technical or economical sensible match for heat recovery is available, certain low temperature streams might instead be heated with external energy sources, such as solar process heat, than being heated with waste heat.

The design for solar process heat plants is improved through the presented approach, as it helps in analyzing which processes might be best heated with waste heat and which processes could be

potentially heated with solar energy. In case study 1 we have seen that the practical HEN with a storage size of 90 m³ cannot cover all process demand. These processes are consequently candidates for solar process heating. Based on the energy transfer simulation of heat exchangers and storages over time, detailed load profiles for the processes can be exported from SOCO and re-imported in solar simulation tools for design studies on solar process heat plants.

For the here discussed brewery sites, site 1 and site 4, the remaining energy demand profiles for the brewhouse heat integration scheme as shown in Figure 7-24 (without consideration of hot water preparation over waste heat of chillers) are shown in Figure 7-33 and Figure 7-34. Results are shown for versions B with brew water preparation at 75 °C. For site 1 Run 2 with 150 m³ storage tank and larger heat exchange areas is considered.

While Figure 7-33 shows the actual variability, Figure 7-34 shows the weekly load curve as basis for new energy supply design. Clearly, site 4 requires minimal back-up by an additional energy supply system, while site 1 still shows strong demand peaks. Applying the same heat recovery concept, the remaining energy demand for the processes wort preheating, brew water heating and mashing could substantially be reduced by 52 % by different brewing technologies in site 4. Additionally storage size can be reduced by 40 % and heat exchanger surfaces by 50 %. This proves the importance of the holistic approach of technology selection and heat integration for minimal energy demand in the processing industry. Additionally, it shows that prior to designing energy supply systems, processing technologies should be sensibly chosen and optimized heat integration schemes should be conceived. With this approach energy consumption of the processing industry will be minimized.

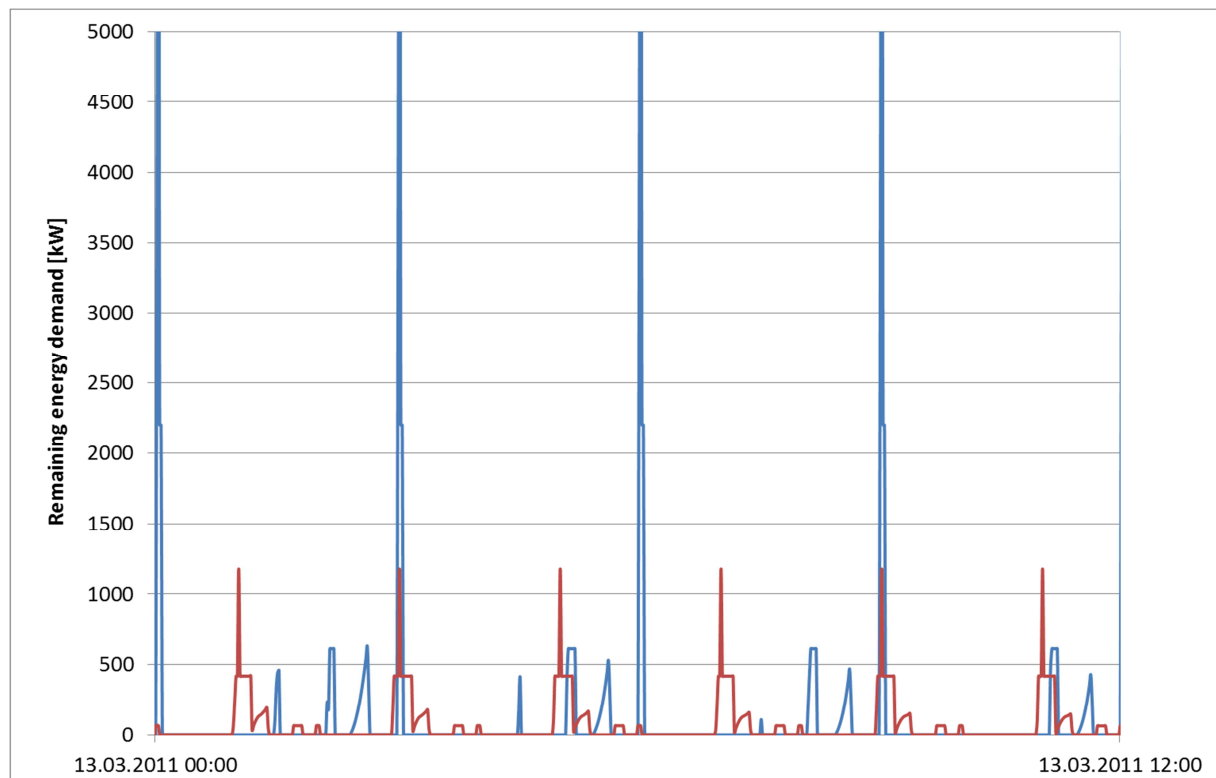


Figure 7-33: Variability of the remaining energy demand profile based on the heat integration concept (for brew water preparation, mashing and wort preheating)

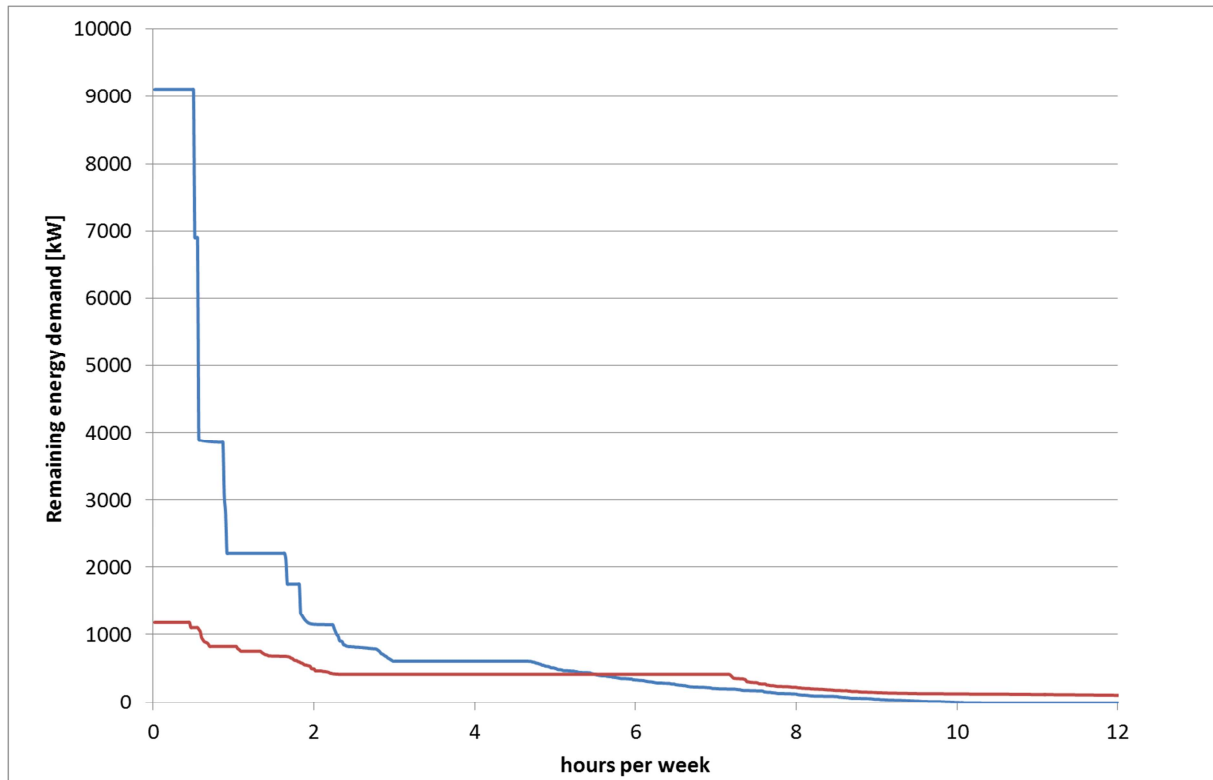


Figure 7-34: Weekly load profile of the remaining energy demand based on the heat integration concept (for brew water preparation, mashing and wort preheating)

7.3.4 Discussion of heat integration scenarios

While the choice of technologies does influence process demand profiles and waste heat availability profiles significantly, the application of SOCO to two different brewing sites has shown that similar trends for heat integration can be identified and that one integrated heat recovery concept can be recommended for both breweries. Although the initial HESN proposal by SOCO differs between the case studies, a closer evaluation taking into account necessary storage sizes reveals that in both breweries a heat recovery concept for the brewhouse is advisable not including packaging processes. This result, however, also stems from the fact that in both breweries only packaging into bottles has been assumed and similar operating schedules for the packaging plant have been defined.

One consistent result of an optimized heat integration concept for breweries is the recommendation to recover the energy contained in the hot wort in a 2 stage heat exchanger. The heat gained from the first stage is used for wort preheating. This fact, already published earlier [151] and also stated by other authors [157] has been re-confirmed in this work. Due to the similarity in heat capacity flow rate and temperatures, SOCO will suggest this heat exchange unless restricted by the temperature of the hot wort. This would be the case for site 5 where the temperature of the hot wort is too low to realise this heat recovery option. The energy gained from the 2nd stage of the wort cooler can then be used for brew water production as it is implemented in basically all large-scale breweries. It is important to note that brew water demand for mashing and sparging liquors can still be covered with only minimal external heating requirement.

SOCO further recommends covering the mashing process either by wort cooling energy as shown in this work or by vapour condensation [147]. At site 4 the HESN proposal generation recommended

the supply of the tunnel pasteurization process in favour over mashing, which is however due to the pinch temperature that lies exactly in between the process temperature levels of mashing. Other studies with SOCO for brewing sites with a slightly different layout and pinch temperature have confirmed that mashing is recommended for heat integration [147]. Heating the mash tun via an energy transfer medium charged by vapor condensation has already been suggested by Tokos et al. [196]. The company Krones markets the integration of mashing in a heat recovery system charged by wort cooling in their “Equitherm” system [81].

For conventional mash tuns retrofit will be necessary to enable heating the mash over a heat transfer medium at rather low temperatures. It has been successfully shown in this work that new mashing profiles can minimize the required additional heating plates (see 6.2.2).

While the choice whether vapour condensation or wort cooling (1st stage) is used for mashing might depend on the structure of each brewery, an integrated use of both of these heat streams to an energy storage can be recommended. This energy storage can then serve as energy supply for wort preheating and for the mashing process. The evaluation of SOCO confirms that this integrated concept is possible and temperature stratification can be ensured. However, here the demand profiles play a decisive role. In addition to lowering the heating rates for mashing, any measure that helps to smoothen the demand profile in breweries will be beneficial for realising the proposed heat recovery concept. The brewing profile with small batch sizes and high batch numbers per week (site 4) enables the use of much smaller equipment in terms of storage size and heat exchange area.

Wort cooling can cover brew water requirement in a 2nd wort cooling stage. However, the hot water demand of other production areas (CIP, packaging etc.) of breweries must not be neglected, as the overall hot water management is decisive for energy efficiency. Therefore the realisation of the above mentioned concept might lead to shifting the energy requirement to hot water production. Once hot water demand has been minimized, there is the potential to cover most of its requirement over waste heat of cooling compressors. Additionally low temperature heat supply, such as solar heat poses a promising option.

In the evaluation with the software tool SOCO some limits in the simulation appear. For the integration scheme evaluated in this work, the most relevant limits are the rough calculation of condensation in heat exchangers and the limited possibility of defining the regulation of storage medium flows.

8 CONCLUSIONS

This work shows the significant effects of technology choices on energy efficiency, heat integration and the overall thermal energy management in industry. The combined approach of process modelling that generates variable process profiles and heat integration analysis that allows planning of heat exchanger and storage networks based on these profiles, enables to design optimized technology sets in industry. Detailed models of those processes posing bottlenecks to efficient thermal energy supply can reveal new processing strategies. Such models naturally need to take into account quality criteria of the products and need to be verified by experiments.

The application of the Brewery Model shows that the choice of different technologies and of process profiles influences thermal energy demand and its required temperature level significantly. Hot water management is, again, proven to be a key for efficient brewhouse operations. The developed brewery modelling tool can predict industrial thermal energy demand variability to satisfactory extents. In addition to the comparison of specific demand figures, it allows a holistic view of the production site and most importantly the modelling of energy demand profiles. Energy demand profiles in brewing vary significantly based on the chosen technology set but are also influenced by production planning, heat exchanger surfaces and heat supply management. Thus, modelling of energy demand profiles will enhance detailed planning of heat recovery considerations and design of new energy supply equipment.

For realizing heat recovery concepts the varying process demand profiles as well as the varying waste heat availability profiles are decisive. Smoother demand profiles allow the realization of heat integration as well as the integration of low temperature heat supply (such as solar heat) with compact equipment.

The mashing process is an important candidate in considerations for heat recovery and low temperature heat supply. However, existing plants will require retrofitting of heat exchangers. This work has successfully shown that the variations of mashing temperature profiles can improve processing time, quality of the produced wort as well as enable the integration of low temperature heat in a more preferable way. From the experimental results we can conclude that a continuous process can be designed for mashing after a first amyloysis rest without negative effects on product quality. As the results of the thesis are based on a limited number of mashing experiments further experiments shall consolidate this conclusion. Additionally the alternating heating and cooling profiles for mashing showed that intensification of the mashing process is possible. The application of oscillatory flow reactors for mashing might further intensify the mashing process by increased dynamics due to the induced oscillations.

In most breweries a large peak in energy demand occurs when boiling, wort preheating and mashing the subsequent brew are performed at the same time. A reduction in energy intensity in these processes will therefore lead to the possibility of designing heat supply equipment at lower capacity avoiding losses in part load operation.

The evaluation of the new optimization approach within the software SOCO has shown a large potential of applying the software to thermal energy optimization in the food and drink industry. The software is able to deal with batch processes very well, simulating thermal energy systems over a user-defined time span (week, month or year). The heat exchanger proposal algorithm takes into

account the real operational process profile while calculating its criteria energy savings, power per heat exchanger and exergy losses. The proposed heat integration scheme for breweries suggests an integrated solution for making use of the energy in wort cooling and vapour condensation. Besides the common heat sinks such as wort preheating and brew water preparation the proposal seeks to deliver additional heat to heating of the mash tun. Due to the fact that mashing is currently being heated basically with welded steam tubes, retrofit is necessary for realizing this potential.

The simulations reveal that an optimized brewery process design including more process continuities enable smaller thermal storage tanks and more efficient heat transfer to the processes. This refers to the comparison of a “conventional brewery” with 6 % evaporation rate versus an “optimized brewhouse” scenario (low evaporation rate in boiling, new mashing technology, optimized water management) brewing more continuously with small batches. The energy demand variations show that such a brewery case generally leads to better technical and economic feasibility for low temperature heat integration.

The heat demand of a “conventional brewery” for of mashing, wort preheating and hot water as well as brew water preparation results to 36.2 MJ/hl. In comparison, the remaining energy demand of the same processes of an “optimized brewery” results to 11.4 MJ/hl including minimized hot water demand at lower temperatures and the proposed waste heat recovery concept by SOCO. Savings therefore reach 68.6 %. It is important to note that about 4.5 MJ/hl are due to minimized hot water consumption and lowering the required temperature for hot water demand. Neglecting the reduction of the hot water demand, savings reach 56 %. These figures, however, compare brewing sites with very different evaporation rates. The reduction of energy demand for the “optimized brewery” (by minimizing water demand and implementing the heat recovery concept) results to 45.6 %. About half of these savings are due to optimization of the hot water consumption.

The combined approach of process modelling and heat integration based on variable process profiles shows that by optimizing technology sets and production profiles in brewing a 80 % reduction in power demand peaks can be reached. Heat integration concepts can be effectively realised for this optimized site with 40 % less storage volume and up to 80 % smaller heat exchangers in comparison to conventional technologies.

The simulation algorithm of SOCO can evaluate the performance of energy storage very well. Based on the integrated algorithm of heat exchanger calculation and storage model, the effects of storage size, port heights, heat exchange area and maximum flow of storage medium can be pleasingly evaluated. The visualisation of temperature layers of the storage deliver interesting conclusions on the stratification reached with the given storage and heat exchange design.

This work shows the significant effects of technology choices on energy efficiency, heat integration and the overall thermal energy management in industry. The combined approach of process modelling - generating variable process profiles - and heat integration analysis - allowing planning of heat exchanger and storage networks based on these profiles - enables to design optimized technology sets in industry. Detailed models of those processes posing bottlenecks to efficient thermal energy supply can reveal new processing strategies. Such models naturally need to take into account quality criteria of the products and need to be verified by experiments. Process modelling tools similar to the brewery model are recommended for different industry sectors for the identification of bottlenecks for energy efficiency and low temperature heat supply. This might

Conclusions

stimulate new process developments for realising production sites with minimised greenhouse gas emissions.

9 APPENDIX A - BREWERY MODEL

In the following some screenshots of the Brewery Model are shown and the equations sets are given. Please note that EES uses “,” as decimal separator.

9.1 Screenshots

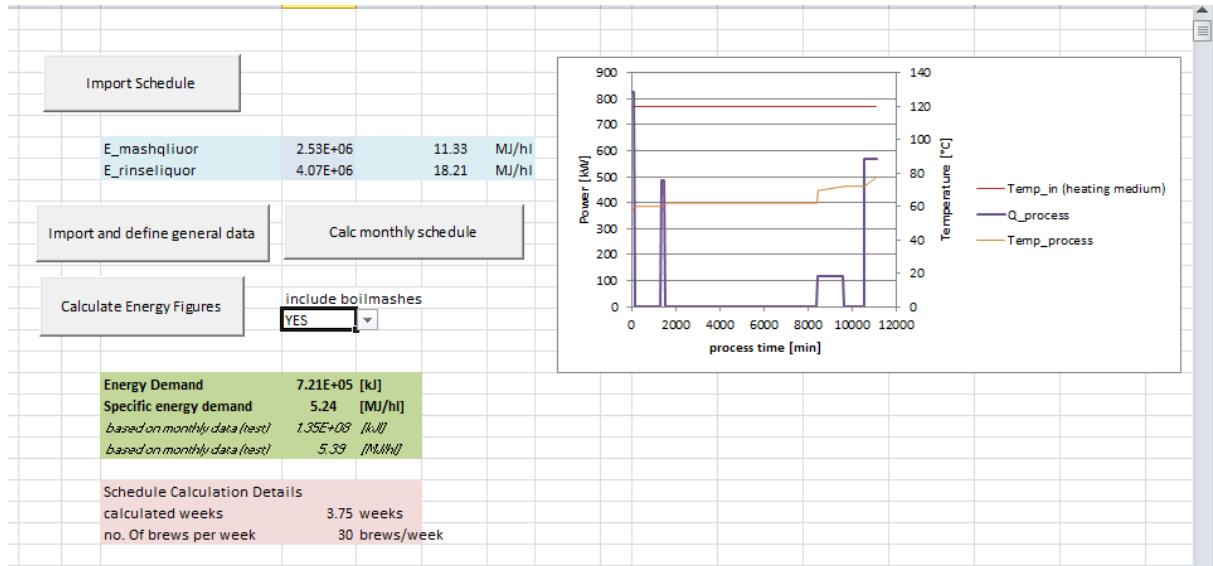
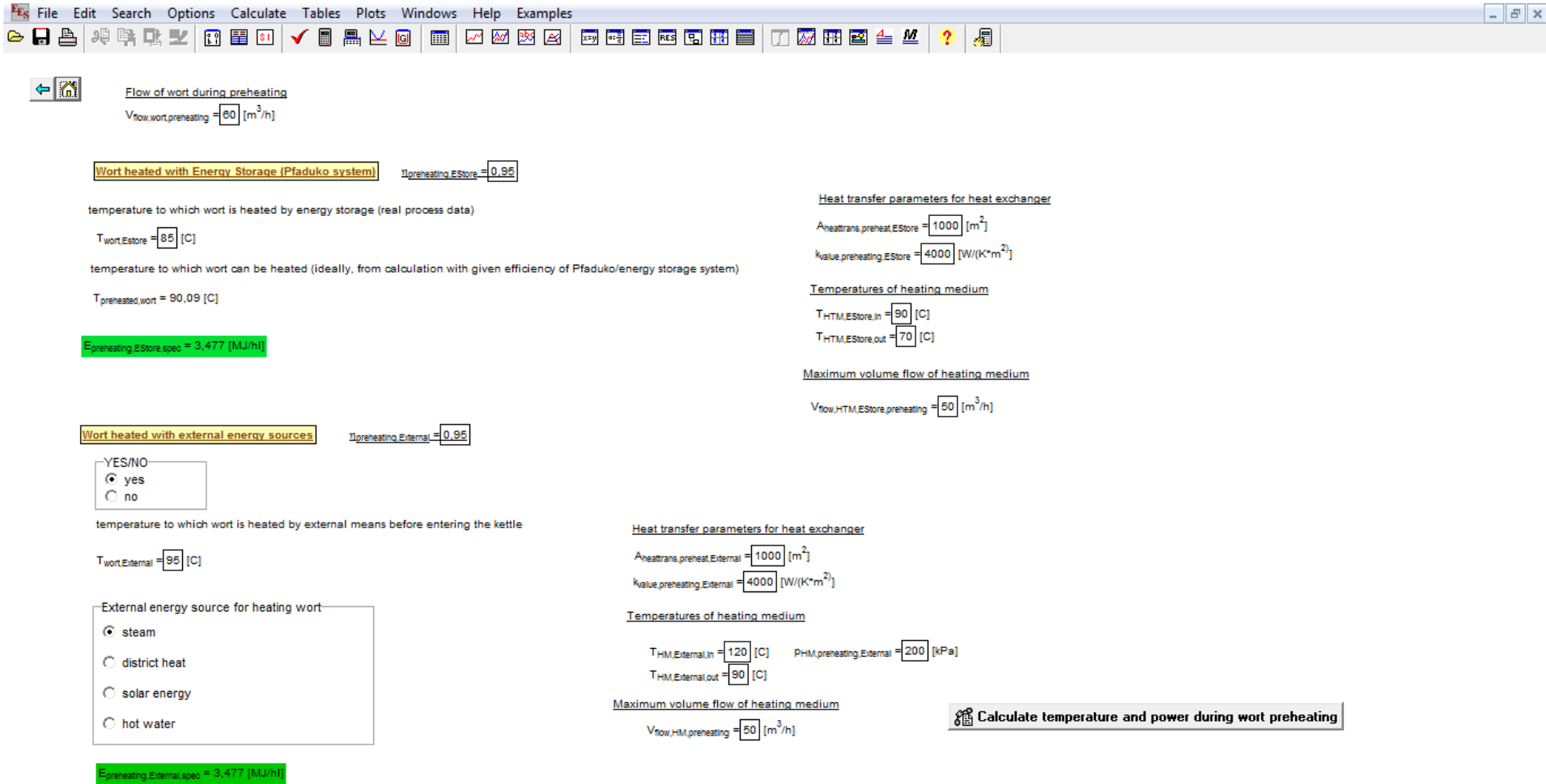


Figure 9-1: Screen of the Excel Tool for Visualisation of the demand profiles (linked to the Brewery Model)

Appendix



Flow of wort during preheating
 $V_{\text{flow, wort, preheating}} = 60 \text{ [m}^3/\text{h]}$

Wort heated with Energy Storage (Pfaduko system) $\eta_{\text{preheating, EStore}} = 0.95$

temperature to which wort is heated by energy storage (real process data)
 $T_{\text{wort, EStore}} = 85 \text{ [C]}$

temperature to which wort can be heated (ideally, from calculation with given efficiency of Pfaduko/energy storage system)
 $T_{\text{preheated, wort}} = 90.09 \text{ [C]}$

$E_{\text{preheating, EStore, spec}} = 3,477 \text{ [MJ/h]}$

Wort heated with external energy sources $\eta_{\text{preheating, External}} = 0.95$

YES/NO
 yes
 no

temperature to which wort is heated by external means before entering the kettle
 $T_{\text{wort, External}} = 95 \text{ [C]}$

External energy source for heating wort
 steam
 district heat
 solar energy
 hot water

$E_{\text{preheating, External, spec}} = 3,477 \text{ [MJ/h]}$

Heat transfer parameters for heat exchanger
 $A_{\text{heattrans, preheat, EStore}} = 1000 \text{ [m}^2]$
 $k_{\text{value, preheating, EStore}} = 4000 \text{ [W/(K}\cdot\text{m}^2)]$

Temperatures of heating medium
 $T_{\text{HTM, EStore, in}} = 90 \text{ [C]}$
 $T_{\text{HTM, EStore, out}} = 70 \text{ [C]}$

Maximum volume flow of heating medium
 $V_{\text{flow, HTM, EStore, preheating}} = 50 \text{ [m}^3/\text{h]}$

Heat transfer parameters for heat exchanger
 $A_{\text{heattrans, preheat, External}} = 1000 \text{ [m}^2]$
 $k_{\text{value, preheating, External}} = 4000 \text{ [W/(K}\cdot\text{m}^2)]$

Temperatures of heating medium
 $T_{\text{HM, External, in}} = 120 \text{ [C]}$ $P_{\text{HM, preheating, External}} = 200 \text{ [kPa]}$
 $T_{\text{HM, External, out}} = 90 \text{ [C]}$

Maximum volume flow of heating medium
 $V_{\text{flow, HM, preheating}} = 50 \text{ [m}^3/\text{h]}$

Calculate temperature and power during wort preheating

Figure 9-2: Technology Tab Wort Preheating

Appendix

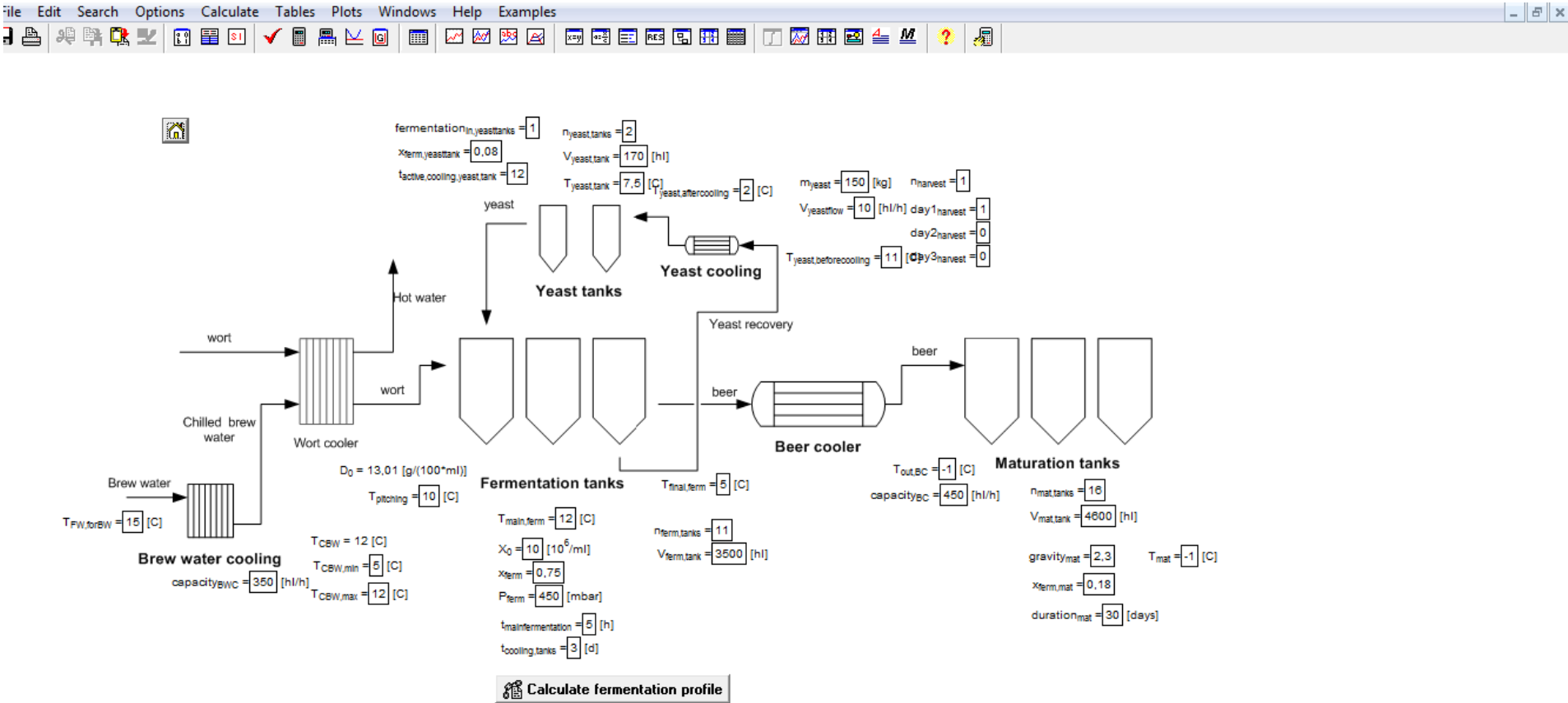


Figure 9-3: Section overview fermentation and filtration

9.2 Equation set of the Brewery model

9.2.1 Mass and energy balance

9.2.1.1 Brewhouse calculations

$T_{ref}=10$ [C]

$P[1]=101,3$ [kPa]

"Mashing"

$m_{mashliquor}=V_{mashliquor} \cdot \text{density}(\text{Water}; T=T_{mash}; P=P[1])$

$cp_{mash}=Cp(\text{Water}; T=T_{mash}; P=P[1])$

$m_{FW}=V_{FW} \cdot \text{density}(\text{Water}; T=T_{FW}; P=P[1])$

$cp_{FW}=Cp(\text{Water}; T=T_{FW}; P=P[1])$

$\rho_{BW}=\text{density}(\text{Water}; T=T_{BW}; P=P[1])$

$m_{BW}=V_{BW} \cdot \text{density}(\text{Water}; T=T_{BW}; P=P[1])$

$cp_{BW}=Cp(\text{Water}; T=T_{BW}; P=P[1])$

CALL WeakWortRecovery(weakwort_recovery;m_weakwort;perc_rec_weakwort:m_weakwort_rec_mash)

$m_{BW}+m_{FW}=m_{mashliquor}$

$m_{BW} \cdot cp_{BW} \cdot \text{convertTemp}(C;K;T_{BW})+m_{FW} \cdot cp_{FW} \cdot \text{convertTemp}(C;K;T_{FW})=m_{mashliquor} \cdot cp_{mash} \cdot \text{convertTemp}(C;K;T_{mash})$

$E_{BW_mashing}=m_{BW} \cdot cp_{BW} \cdot (T_{BW}-T_{ref})$

$E_{BW_mashing_spec}=E_{BW_mashing} \cdot \text{Convert}('kJ'; 'MJ') / (V_{AW_cold} \cdot \text{Convert}('m^3'; 'hl'))$

$E_{FW_mashing}=m_{FW} \cdot cp_{FW} \cdot (T_{FW}-T_{ref})$

$E_{FW_mashing_spec}=E_{FW_mashing} \cdot \text{Convert}('kJ'; 'MJ') / (V_{AW_cold} \cdot \text{Convert}('m^3'; 'hl'))$

$E_{weakwort_mashing}=m_{weakwort_rec_mash} \cdot cp_{weakwort} \cdot (T_{rinse}-T_{ref})$

$E_{weakwort_mashing_spec}=E_{weakwort_mashing} \cdot \text{Convert}('kJ'; 'MJ') / (V_{AW_cold} \cdot \text{Convert}('m^3'; 'hl'))$

$m_{mash_total}=m_{mashliquor}+m_{weakwort_rec_mash}$

$m_{weakwort_rec_mash} \cdot cp_{weakwort} \cdot \text{convertTemp}(C;K;T_{rinse})+m_{mashliquor} \cdot cp_{mash} \cdot \text{convertTemp}(C;K;T_{mash})=m_{mash_total} \cdot cp_{mash} \cdot \text{convertTemp}(C;K;T_{mash_total})$

$cp_{malt}=1,7$ [kJ/kgK]

$E_{malt_mashing}=m_{malt} \cdot cp_{malt} \cdot (T_{malt}-T_{ref})$

$E_{malt_mashing_spec}=E_{malt_mashing} \cdot \text{Convert}('kJ'; 'MJ') / (V_{AW_cold} \cdot \text{Convert}('m^3'; 'hl'))$

$m_{mashing}=m_{mash_total}+m_{malt}$

$cp_{mashing}=(m_{mash_total} \cdot cp_{mash}+m_{malt} \cdot cp_{malt})/m_{mashing}$

$m_{mashing}/\rho_{mashing}=m_{mash_total}/\text{density}(\text{Water}; T=T_{mash}; P=P[1])+m_{malt}/\rho_{malt}$

$V_{mashing}=m_{mashing}/\rho_{mashing}$

$m_{mashing} \cdot cp_{mashing} \cdot \text{convertTemp}(C;K;T_{mashing})=m_{mash_total} \cdot cp_{mash} \cdot \text{convertTemp}(C;K;T_{mash_total})+m_{malt} \cdot cp_{malt} \cdot \text{convertTemp}(C;K;T_{malt})$

"Infusion mashing"

$E_{mashing_infusion}=m_{mash_total} \cdot cp_{mash} \cdot (T_{mash_out}-T_{mash_total})+m_{malt} \cdot cp_{malt} \cdot (T_{mash_out}-T_{malt})$

$E_{mashing_infusion_real}=E_{mashing_infusion}/\eta_{mashtun}$

$cp_{mash_test}=(m_{mash_total} \cdot cp_{mash}+m_{malt} \cdot cp_{malt})/(m_{mash_total}+m_{malt})$

\$export ExportMash\$ T0_mash T_mashsteps[1..8] time_mashsteps[1..8] mashingtype tech_mashing n_steps_mash m_mash_total m_mashing_mainMash[1..8] T_mashsteps_afterBM2Mix[1..8] step_BM1_back step_BM2_back E_mainmash[1..8] cp_mashing heatsystem_mash k_value_mashtun A_heattransfer_mashtun

T_HTM_mashtun m_HTM_mashtun cp_HTM_mashtun p_HTM_mashtun type_HR_mash m_HTM_wortcooler
 T_HTM_in_WC T_HTM_out_WC p_HTM_wortcooler E_HTM_wortcooler k_value_HR_mashtun
 A_heattransfer_HR_mashtun HR_in_mashsteps[1..8] m_mashtun E_filling_mashtun t_filling_mashtun
 eta_mashtun

```
$export ExportBoilMash1$ TO_boilmash1 T_mashsteps_BM1[1..6] time_mashsteps_BM1[1..6] mashingtype
tech_mashing n_steps_mash_BM1 m_boilmash1 E_boilmash1[1..6] cp_mashing heatsystem_mash
k_value_mashtun_BM A_heattransfer_mashtun_BM T_HTM_mashtun_BM m_HTM_mashtun_BM
cp_HTM_mashtun_BM p_HTM_mashtun_BM type_HR_mash m_HTM_wortcooler T_HTM_in_WC
T_HTM_out_WC p_HTM_wortcooler E_HTM_wortcooler k_value_HR_mashtun A_heattransfer_HR_mashtun
HR_in_mashsteps[1..8] m_mashtun eta_boilmash1
```

```
$export ExportBoilMash2$ TO_boilmash2 T_mashsteps_BM2[1..6] time_mashsteps_BM2[1..6] mashingtype
tech_mashing n_steps_mash_BM2 m_boilmash2 E_boilmash2[1..6] cp_mashing heatsystem_mash
k_value_mashtun_BM A_heattransfer_mashtun_BM T_HTM_mashtun_BM m_HTM_mashtun_BM
cp_HTM_mashtun_BM p_HTM_mashtun_BM type_HR_mash m_HTM_wortcooler T_HTM_in_WC
T_HTM_out_WC p_HTM_wortcooler E_HTM_wortcooler k_value_HR_mashtun A_heattransfer_HR_mashtun
HR_in_mashsteps[1..8] m_mashtun eta_boilmash2
```

"Decoction mashing"

CALL

```
CheckV_mashing(V_mashing;V_boilmash[1..2];step_BM1_taken;step_BM1_back;step_BM2_taken;step_BM2_
back:V_mashing_mainMash[1..8];V_boilmash1[1..8];V_boilmash2[1..8])
```

```
Call Calculate_m_mashing_mainMash(V_mashing_mainMash[1..8]; roh_mashing:m_mashing_mainMash[1..8])
```

```
Call Calculate_m_mashing_mainMash(V_boilmash1[1..8]; roh_mashing:m_mashing_BoilMash1[1..8])
```

```
Call Calculate_m_mashing_mainMash(V_boilmash2[1..8]; roh_mashing:m_mashing_BoilMash2[1..8])
```

```
m_boilmash1=V_boilmash[1]*roh_mashing
```

```
m_boilmash2=V_boilmash[2]*roh_mashing
```

CALL

```
Calculate_E_boilmash_step(eta_boilmash1;V_boilmash[1];roh_mashing;cp_mashing;n_steps_mash_BM1;T_m
ashsteps_BM1[1..6];time_mashsteps_BM1[1..6];T_mashsteps[1..8];step_BM1_taken:E_boilmash1[1..6];E_boil
mash1_real[1..6];TO_boilmash1)
```

CALL

```
Calculate_E_boilmash_step(eta_boilmash2;V_boilmash[2];roh_mashing;cp_mashing;n_steps_mash_BM2;T_m
ashsteps_BM2[1..6];time_mashsteps_BM2[1..6];T_mashsteps[1..8];step_BM2_taken:E_boilmash2[1..6];E_boil
mash2_real[1..6];TO_boilmash2)
```

CALL

```
Calculate_T_boilmash_mix(V_mashing_mainMash[1..8];T_mashsteps[1..8];roh_mashing;cp_mashing;V_boilma
sh1[1..8];T_mashsteps_BM1[1..6];step_BM1_back;n_steps_mash_BM1:T_mashsteps_afterBM1Mix[1..8])
```

CALL

```
Calculate_T_boilmash_mix(V_mashing_mainMash[1..8];T_mashsteps_afterBM1Mix[1..8];roh_mashing;cp_mas
hing;V_boilmash2[1..8];T_mashsteps_BM2[1..6];step_BM2_back;n_steps_mash_BM2:T_mashsteps_afterBM2
Mix[1..8])
```

CALL

```
Calculate_E_mainmash_step(eta_mashtun;V_mashing_mainMash[1..8];roh_mashing;cp_mashing;n_steps_ma
sh;T_mashsteps[1..8];T_mashsteps_afterBM2Mix[1..8];time_mashsteps[1..8];TO_mash:E_mainmash[1..8];E_m
ainmash_real[1..8])
```

```
m_malt/m_mashliquor=m_boilmalt[1]/m_boilmash[1]
```

```
m_malt/m_mashliquor=m_boilmalt[2]/m_boilmash[2]
```

```
V_boilmash[1]=m_boilmash[1]/roh_BW+m_boilmalt[1]/roh_malt "total boil mash volume - water and malt"
```

```
V_boilmash[2]=m_boilmash[2]/roh_BW+m_boilmalt[2]/roh_malt "total boil mash volume - water and malt"
```

"Final Mashing energy demand"

CALL

CheckEnergyDemandMashing(mashing;E_mashing_infusion;E_mashing_infusion_real;E_mainmash[1..8];E_mainmash_real[1..8];E_boilmash1[1..6];E_boilmash1_real[1..6];E_boilmash2[1..6];E_boilmash2_real[1..6];E_mashing;E_mashing_real)

$$E_mashing_spec = E_mashing * Convert('kJ'; 'MJ') / (V_AW_cold * Convert('m^3'; 'hl'))$$

$$E_mashing_real_spec = E_mashing_real * Convert('kJ'; 'MJ') / (V_AW_cold * Convert('m^3'; 'hl'))$$

$$E_mash_to_lautering = m_mash_total * cp_mash * (T_mash_out - T_ref) + m_malt * cp_malt * (T_mash_out - T_ref)$$

$$E_mash_to_lautering_spec = E_mash_to_lautering * Convert('kJ'; 'MJ') / (V_AW_cold * Convert('m^3'; 'hl'))$$

"Lautering / Rinses"

$$m_rinse = V_rinse * density(Water; T=T_rinse; P=P[1])$$

$$cp_rinse = Cp(Water; T=T_rinse; P=P[1])$$

$$m_FW_rinse = V_FW_rinse * density(Water; T=T_FW; P=P[1])$$

$$m_BW_rinse = V_BW_rinse * density(Water; T=T_BW; P=P[1])$$

$$m_BW_rinse1 + m_FW_rinse = m_rinse$$

$$m_BW_rinse1 * cp_BW * convertTemp(C;K;T_BW) + m_FW_rinse * cp_FW * convertTemp(C;K;T_FW) = m_rinse * cp_rinse * convertTemp(C;K;T_rinse)$$

Call CheckBW_rinse(m_BW_rinse1;m_rinse;T_BW;T_rinse;cp_rinse:m_BW_rinse;dE_BW_rinse)

$$dE_BW_rinse_spec = dE_BW_rinse * Convert('kJ'; 'MJ') / (V_AW_cold * Convert('m^3'; 'hl'))$$

$$E_BW_rinse = m_BW_rinse * cp_BW * (T_BW - T_ref)$$

$$E_BW_rinse_spec = E_BW_rinse * Convert('kJ'; 'MJ') / (V_AW_cold * Convert('m^3'; 'hl'))$$

$$E_FW_rinse = m_FW_rinse * cp_FW * (T_FW - T_ref)$$

$$E_FW_rinse_spec = E_FW_rinse * Convert('kJ'; 'MJ') / (V_AW_cold * Convert('m^3'; 'hl'))$$

$$m_spgrain / m_malt = ratio_spgrain_malt$$

"Volume of grist in mash = 0,7-0,8hl/100 kg grist [120]"

$$roh_malt = 1330 [kg/m^3]$$

"extract conten weak wort 2% [120]"

$$m_extract_ww / m_weakwort = 0,02$$

"Density and heat capacity weak wort"

CALL WortDensity((0,02*100):p_vol_weakwort;roh_weakwort_cold;roh_weakwort)

CALL WortHeatCapacity ((0,02*100);T_ref;T_rinse;P[1];cp_malt:cp_weakwort)

$$m_spgrain + m_kettlefull + m_weakwort = m_mash_total + m_rinse + m_malt$$

$$m_malt + m_extract_ww / m_weakwort * m_weakwort_rec_mash =$$

$$m_extract + m_extract_ww + m_spgrain * p_w_spgrain$$

"energy values within spent grain and wort"

$$E_spgrain = m_spgrain * (1 - p_w_spgrain) * cp_rinse * (T_rinse - T_ref) + m_spgrain * p_w_spgrain * cp_malt * (T_rinse - T_ref)$$

$$E_spgrain_spec = E_spgrain * Convert('kJ'; 'MJ') / (V_AW_cold * Convert('m^3'; 'hl'))$$

$$E_weakwort = m_weakwort * cp_weakwort * (T_rinse - T_ref)$$

$$E_weakwort_spec = E_weakwort * Convert('kJ'; 'MJ') / (V_AW_cold * Convert('m^3'; 'hl'))$$

$$E_wort_to_kettle = m_kettlefull * cp_wort * (T_rinse - T_ref)$$

$$E_wort_to_kettle_spec = E_wort_to_kettle * Convert('kJ'; 'MJ') / (V_AW_cold * Convert('m^3'; 'hl'))$$

$$m_kettlefull = V_kettlefull * roh_wort_hot$$

$$m_weakwort = V_weakwort * roh_weakwort$$

"Wort density for kettlefull"

$$p_mass_kettlefull = m_extract / (m_kettlefull) * 100$$

CALL WortDensity(p_mass_kettlefull;p_vol_kettlefull;roh_wort_cold;roh_wort_hot)

"Wort preheating"

```
CALL WortHeatCapacity (p_mass_kettlefull;T_sat[2];T_rinse;P[1];cp_malt:cp_wort)
"overall energy requirement for heating wort to boiling temperature = E_preheating"
"calculate energy requirement of wort heater, with given outlet temperature of the user"
Call
Wortpreheating(eta_preheating_EStore;eta_preheating_External;preheating_EStore;m_kettlefull;cp_wort;T_s
at[2];T_rinse;T_wort_EStore;T_wort_External;boiling_system;t_wort_boiling[1];E_preheating_EStore;E_prehea
ting_EStore_real;E_preheating_External;E_preheating_External_real;E_preheating)
E_preheating_spec=E_preheating*Convert('kJ'; 'MJ')/(V_AW_cold*Convert('m^3';'hl'))
E_preheating_EStore_spec=E_preheating_EStore*Convert('kJ'; 'MJ')/(V_AW_cold*Convert('m^3';'hl'))
E_preheating_External_spec=E_preheating_External*Convert('kJ'; 'MJ')/(V_AW_cold*Convert('m^3';'hl'))
E_preheating_EStore_real_spec=E_preheating_EStore_real*Convert('kJ';
'MJ')/(V_AW_cold*Convert('m^3';'hl'))
E_preheating_Ext_real_spec=E_preheating_External_real*Convert('kJ'; 'MJ')/(V_AW_cold*Convert('m^3';'hl'))
$export ExportWortPreheating$ m_kettlefull V_flow_wort_preheating cp_wort roh_wort_hot T_rinse
T_wort_EStore T_wort_External V_flow_HTM_EStore_preheating T_HTM_EStore_in T_HTM_EStore_out
V_flow_HM_preheating type_HM_preheating T_HM_External_in T_HM_External_out
k_value_preheating_EStore A_heattrans_preheat_EStore k_value_preheating_External
A_heattrans_preheat_External preheating_EStore preheating_External p_HM_preheating_External
eta_preheating_EStore eta_preheating_External
E_wort_after_preheating=m_kettlefull*cp_wort*(T_sat[2]-T_ref)
E_wort_after_preheating_spec=E_wort_after_preheating*Convert('kJ'; 'MJ')/(V_AW_cold*Convert('m^3';'hl'))
```

"Wort boiling"

```
"Additions in wort pan"
yield_bitterness=0,32
acids_alpha_pellet=0,15
m_pellet_spec=BE/yield_bitterness/acids_alpha_pellet "g/hl"
m_hop_pellet=m_pellet_spec*(V_AW_cold*Convert('m^3';'hl'))*Convert('g';'kg')
roh_hop_pellet=560 [kg/m^3]
V_hop_pellet=m_hop_pellet/roh_hop_pellet
cp_hop=cp_malt
cp_lactic_acid_wort=Cp(Water; T=T_lactic_acid_wort; P=P[1])
m_lactic_acid_wort=pH_adjust_wort/0,1*30*Convert('ml';'l')*m_malt "30ml/kg of lactic acid (0,8%) for pH
adjustment of 0,1"
E_lactic_acid_wort=m_lactic_acid_wort*cp_lactic_acid_wort*(T_lactic_acid_wort-T_ref)
E_lactic_acid_wort_spec=E_lactic_acid_wort*Convert('kJ'; 'MJ')/(V_AW_cold*Convert('m^3';'hl'))
m_totalkettle=m_kettlefull+m_hop_pellet +m_lactic_acid_wort + m_VLT
m_VLT=V_VLT*density(Water; T=T_VLT; P=P[1])
cp_VLT=Cp(Water; T=T_VLT; P=P[1])
E_additions=m_hop_pellet*cp_hop*T_hop+m_lactic_acid_wort*cp_lactic_acid_wort*T_lactic_acid_wort+m_V
LT*cp_VLT*T_VLT
E_additions_spec=E_additions*Convert('kJ'; 'MJ')/(V_AW_cold*Convert('m^3';'hl'))
dE_additions_kettle=(m_hop_pellet*cp_hop +m_lactic_acid_wort*Cp(Water;
T=(T_lactic_acid_wort+T_sat[2])/2; P=P[1]) + m_VLT*Cp(Water; T=(T_VLT+T_sat[2])/2; P=P[1]))*T_sat[2] -
E_additions
dE_additions_kettle_spec=dE_additions_kettle*Convert('kJ'; 'MJ')/(V_AW_cold*Convert('m^3';'hl'))
"Wort density for total kettle"
p_mass_totalkettle=m_extract/(m_totalkettle)*100
```

```

CALL WortDensity(p_mass_totalkettle:p_vol_totalkettle;roh_totalwort_cold;roh_totalwort_hot)
V_totalkettle=m_totalkettle/roh_totalwort_hot
"Pressure at boiling start - state 2 = during boiling"
T_sat[2]=T_sat(Water;P=P[2])
"Pressure during boiling - state 3 = vapours after compression or after expansion"
T_sat[3]=T_sat(Water;P=P[3])
"for MVC, TVC, Pfaduko"
E_evaporation=m_vapors*h_vapors
E_evaporation_spec=E_evaporation*Convert('kJ'; 'MJ')/(V_AW_cold*Convert('m^3'; 'hl'))
h_vapors=Enthalpy(Water;T=T_sat[2]+0,5;P=P[2])-Enthalpy(Water;T=T_sat[2]-0,5;P=P[2])
CALL KettleVolumeForEvaporation(evap_incl_add; V_kettlefull;roh_wort_hot; V_totalkettle;roh_totalwort_hot:
V_kettle_evap;roh_wort_hot_evap)
m_vapors=V_kettle_evap*f_evap*density(Water; T=T_sat[3]-0,1; P=P[3])
V_vapors=V_kettle_evap*f_evap
f_evap_m=m_vapors/(V_kettle_evap*roh_wort_hot_evap)
m_AW=m_totalkettle-m_vapors "cast wort volume after boiling"
"Energy of wort after kettle"
E_wort_after_kettle=m_AW*cp_wort*(T_sat[2]-T_ref)
E_wort_after_kettle_spec=E_wort_after_kettle*Convert('kJ'; 'MJ')/(V_AW_cold*Convert('m^3'; 'hl'))
$export ExportBoil$ n_steps_boiling boiling_system V_totalkettle roh_totalwort_hot T_wort_External f_evap
cp_wort k_value_kettle A_heattransfer_kettle T_HTM_kettle T_HTM_kettle_out m_HTM_kettle p_HTM_kettle
sudhaustype m_vapors P[2] P[3] eff_isen eff_isen_tcv time_boilingsteps[1..10] p_wort_boiling[1..10]
t_wort_boiling[1..10] E_in_boilingsteps[1..10] HR_in_boilingsteps[1..10] m_kettle boiling_system boiler_type
addevap m_steam_add m_vapors_add p_steam_stripping P[5] E_addevap E_filling_kettle t_filling_kettle
T_air_kettle h_air_kettle phi_air_kettle d_kettle eta_kettle

```

"Whirlpool "

```

"Wort density in whirlpool"
p_mass_wort=m_extract/m_AW*100
CALL WortDensity(p_mass_wort:p_vol_wort;roh_AW_cold;roh_AW_hot)
row1=LookupRow('Lookup 1'; 1; p_mass_wort)
f_ausbeute_AW=Lookup('Lookup 1'; row1; 3)
m_AW_whirlpool=m_AW-m_hottrub
m_extract_AW_final=m_extract-m_extract_hottrub
m_extract_hottrub/m_hottrub = 0,005
" density for hottrub"
p_mass_trub=m_extract_hottrub/m_hottrub*100
CALL WortDensity(p_mass_trub:p_vol_trub;roh_trub_cold;roh_trub_hot)
V_hottrub=m_hottrub/roh_trub_hot
V_AW_whirlpool_cold=m_AW_whirlpool/roh_AW_whirlpool_cold
V_AW_whirlpool_hot=m_AW_whirlpool/roh_AW_whirlpool_hot
"Wort density for AW - AW_whirlpool after whirlpool"
p_mass_wort_whirlpool=m_extract_AW_final/m_AW_whirlpool*100
CALL
WortDensity(p_mass_wort_whirlpool:p_vol_wort_whirlpool;roh_AW_whirlpool_cold;roh_AW_whirlpool_hot)
CALL WortHeatCapacity (p_mass_wort_whirlpool;T_AWh_whirlpool;T_AWc;P[1];cp_malt:cp_AW_whirlpool)
"Whirlpool Losses"

```


CALL

SetT_to_Whirlpool(n_steps_boiling;T_AWh;p_wort_boiling[1..10];t_wort_boiling[1..10];addevap:T_to_whirlpool;T_AWh_whirlpool)

$$E_{\text{whirlpool_loss}} = cp_{\text{AW_whirlpool}} * m_{\text{AW_whirlpool}} * (T_{\text{to_whirlpool}} - T_{\text{AWh_whirlpool}})$$

$$E_{\text{whirlpool_loss_spec}} = E_{\text{whirlpool_loss}} * \text{Convert}('kJ'; 'MJ') / (V_{\text{AW_cold}} * \text{Convert}('m^3'; 'hl'))$$

$$E_{\text{wort_from_whirlpool}} = cp_{\text{AW_whirlpool}} * m_{\text{AW_whirlpool}} * (T_{\text{AWh_whirlpool}} - T_{\text{ref}})$$

$$E_{\text{wort_from_whirlpool_spec}} = E_{\text{wort_from_whirlpool}} * \text{Convert}('kJ'; 'MJ') / (V_{\text{AW_cold}} * \text{Convert}('m^3'; 'hl'))$$

"Evaporation after trub separation"

"Pressure at evaporation start - state 4 = before additional evaporation equipment"

$$T_{\text{sat}}[4] = T_{\text{sat}}(\text{Water}; P = P[4])$$

"Pressure during evaporation - state 5 = vapours after vacuum evaporation or after stripper"

$$T_{\text{sat}}[5] = T_{\text{sat}}(\text{Water}; P = P[5])$$

CALL

CalculateAdditionalEvaporation(cp_malt;p_mass_wort_whirlpool;T_AWh;addevap;perc_steam_stripping;p_steam_stripping;T_steam_stripping;m_AW_whirlpool; P[5]; T_sat[5]; P[4];T_sat[4]:T_AWh_addevap;m_vapors_add;m_steam_add;E_addevap)

$$E_{\text{addevap_real}} = E_{\text{addevap}} / \eta_{\text{kettle}}$$

$$E_{\text{addevap_spec}} = E_{\text{addevap}} * \text{Convert}('kJ'; 'MJ') / (V_{\text{AW_cold}} * \text{Convert}('m^3'; 'hl'))$$

$$E_{\text{addevap_real_spec}} = E_{\text{addevap_real}} * \text{Convert}('kJ'; 'MJ') / (V_{\text{AW_cold}} * \text{Convert}('m^3'; 'hl'))$$

$$m_{\text{AW_addevap}} = m_{\text{AW_whirlpool}} - m_{\text{vapors_add}} + m_{\text{steam_add}}$$

$$p_{\text{mass_wort_addevap}} = m_{\text{extract_AW_final}} / m_{\text{AW_addevap}} * 100$$

"heat capacity for evaporation step"

CALL WortHeatCapacity (p_mass_wort_addevap;T_AWh_addevap;T_ref;P[1];cp_malt:cp_AW_addevap)

"Energy of wort after final evaporation"

$$E_{\text{wort_after_addevap}} = m_{\text{AW_addevap}} * cp_{\text{AW_addevap}} * (T_{\text{AWh_addevap}} - T_{\text{ref}})$$

$$E_{\text{wort_after_addevap_spec}} = E_{\text{wort_after_addevap}} * \text{Convert}('kJ'; 'MJ') / (V_{\text{AW_cold}} * \text{Convert}('m^3'; 'hl'))$$

$$f_{\text{addevap_m}} = m_{\text{vapors_add}} / m_{\text{AW_whirlpool}}$$

"Density for volume based evaporation rate, based on density after whirlpool (correct extract, just different temperature, but not relevant for evaporation rate)"

$$V_{\text{vapors_add}} = m_{\text{vapors_add}} / \rho_{\text{h_AW_whirlpool_hot}}$$

$$f_{\text{addevap}} = V_{\text{vapors_add}} / V_{\text{AW_whirlpool_hot}}$$

$$t_{\text{startup_addevap}} = 0$$

T_vapourcond_addevap_rec=T_vapourcond_addevap "no difference between condensate temperature leaving the condenser and entering a recovery system"

CALL

Condensation(m_vapors_add;t_addevap;t_startup_addevap;P[5];T_subcooling_addevap;T_ref;T_vapourcond_addevap;T_vapourcond_addevap_rec;eta_HX_condensation_addevap:

dE_condensation_addevap;dE_condensation_addevap_rec;dE_subcooling_addevap;E_vapors_addevap;

E_condensate_addevap;E_condensate_addevap_real;

dE_subcooling_addevap_real;E_condensate_addevap_rec; dE_subcooling_addevap_rec)

$$E_{\text{vapors_addevap_spec}} = E_{\text{vapors_addevap}} * \text{Convert}('kJ'; 'MJ') / (V_{\text{AW_cold}} * \text{Convert}('m^3'; 'hl'))$$

$$dE_{\text{condensation_addevap_spec}} = dE_{\text{condensation_addevap}} * \text{Convert}('kJ'; 'MJ') / (V_{\text{AW_cold}} * \text{Convert}('m^3'; 'hl'))$$

$$dE_{\text{subcool_addevap_real_spec}} = dE_{\text{subcooling_addevap_real}} * \text{Convert}('kJ'; 'MJ') / (V_{\text{AW_cold}} * \text{Convert}('m^3'; 'hl'))$$

$$dE_{\text{cond_addevap_rec_spec}} = dE_{\text{condensation_addevap_rec}} * \text{Convert}('kJ'; 'MJ') / (V_{\text{AW_cold}} * \text{Convert}('m^3'; 'hl'))$$

CALL

HotWaterPreparation(eta_HX_subcooling_addevap;dE_subcooling_addevap_real;T_CW_addevap;T_WW_addevap;P[1]:m_WW_addevap) "warm water generation of vapor condensate"

CALL

HotWaterPreparation(eta_HX_condensation_addevap;dE_condensation_addevap;T_CW_addevap;T_HW_addevap;P[1]:m_HW_addevap) "Hot water generation of vapors"

"final wort properties before wort cooler"

$m_{AW_final} = m_{AW_addevap} + m_{dilutionwater}$

$V_{dilutionwater} = m_{dilutionwater} / \text{density}(\text{Water}; T = T_{dilution}; P = P[1])$

$V_{AW_final_cold} = m_{AW_final} / \rho_{AW_final_cold}$

$V_{AW_final_hot} = m_{AW_final} / \rho_{AW_final_hot}$

$V_{AW_cold} = V_{AW_final_cold}$

"Wort density for AW - AW_final after whirlpool"

$p_{mass_wort_final} = m_{extract_AW_final} / m_{AW_final} * 100$

CALL WortDensity(p_mass_wort_final;p_vol_wort_final;roh_AW_final_cold;roh_AW_final_hot)

row2=LookupRow('Lookup 1'; 1; p_mass_wort_final)

f_ausbeute_final=Lookup('Lookup 1'; row2; 3)

Ausbeute=f_ausbeute_final*V_AW_final_hot*10/m_malt

ausbeute_test=m_extract_AW_final/m_malt

contraction=density(Water; T=T_AWh_addevap; P=P[1])/density(Water; T=T_AWc; P=P[1])

CALL WortHeatCapacity (p_mass_wort_final;T_AWh;T_AWc;P[1];cp_malt;cp_AW_final)

"Wort cooler"

CALL

AWTemperaturWortCooler(dilution;cp_AW_final;cp_AW_addevap;m_AW_final;T_AWh_addevap;m_dilutionwater;P[1];T_dilution:T_AWh_inWC;m_AW_final_WC;cp_AW_inWC)

$E_{AW_hot} = m_{AW_final_WC} * cp_{AW_inWC} * (T_{AWh_inWC} - T_{ref})$

$E_{AW_hot_spec} = E_{AW_hot} * \text{Convert}('kJ'; 'MJ') / (V_{AW_cold} * \text{Convert}('m^3'; 'hl'))$

CALL

CalculateWortCooler(type_wortcooler;T_BW;T_ref;P[1];V_AW_cold;T_CBW;m_AW_final_WC;cp_AW_inWC;T_AWh_inWC;T_AWc;eta_wortcooler_1;T_CM_out;T_CM_in;T_AWc_1stage;eta_wortcooler_2;T_HTM_in;T_HTM_out:m_CM_wortcooler;m_BW_wortcooler;V_BW_wortcooler;E_BW_wortcooler;E_BW_wortcooler_spec;m_HTM_wortcooler;E_HTM_wortcooler;E_HTM_wortcooler_spec)

$T_{HTM_in} = T_{HTM_in_WC}$

$T_{HTM_out} = T_{HTM_out_WC}$

\$export exportWC\$ m_CM_wortcooler T_CM_out T_CM_in m_BW_wortcooler T_CBW T_BW m_HTM_wortcooler T_HTM_in_WC T_HTM_out_WC m_AW_final_WC T_AWh_inWC T_AWc T_AWc_1stage k_value_wortcooling A_heattransfer_wortcooling k_value_wortcooling2 A_heattransfer_wortcooling2 V_flow_AW V_flow_coldside V_flow_coldside_2 type_wortcooler roh_AW_final_cold cp_AW_final eta_wortcooler_1 eta_wortcooler_2

"Heat recovery from vapours and calculation of energy demand for wort boiling"

"Energy in vapours and vapour condensation"

CALL

Condensation(m_vapors;t_boiling;t_startup;P[3];T_subcooling;T_ref;T_vapourcond;T_vapourcond_rec;eta_pfa duko: dE_condensation1; dE_condensation_rec;dE_subcooling1;E_vapors; E_condensate;E_condensate_real; dE_subcooling_real;E_condensate_rec; dE_subcooling_rec)

$E_{vapors_spec} = E_{vapors} * \text{Convert}('kJ'; 'MJ') / (V_{AW_cold} * \text{Convert}('m^3'; 'hl'))$ "with boiling startup"

$E_{condensate_spec} = E_{condensate} * \text{Convert}('kJ'; 'MJ') / (V_{AW_cold} * \text{Convert}('m^3'; 'hl'))$ "without boiling startup, theoretic condensation temperature"

$E_{condensate_real_spec} = E_{condensate_real} * Convert('kJ'; 'MJ') / (V_{AW_cold} * Convert('m^3'; 'hl'))$ "without boiling startup, real condensate temperature"

$E_{condensate_rec_spec} = E_{condensate_rec} * Convert('kJ'; 'MJ') / (V_{AW_cold} * Convert('m^3'; 'hl'))$ "without boiling startup, condensate temperature entering recovery"

CALL HotWaterPreparation(eta_HX_subcooling; dE_subcooling_real; T_Wcold; T_Whot; P[1]:m_HW_ideal) "Hot water generation of vapor condensate"

CALL HotWaterPreparation(eta_HX_subcooling; dE_subcooling_rec; T_Wcold; T_Whot; P[1]:m_HW_rec) "Hot water generation of vapor condensate"

$dE_{subcooling_real_spec} = dE_{subcooling_real} * Convert('kJ'; 'MJ') / (V_{AW_cold} * Convert('m^3'; 'hl'))$

$dE_{subcooling_rec_spec} = dE_{subcooling_rec} * Convert('kJ'; 'MJ') / (V_{AW_cold} * Convert('m^3'; 'hl'))$

"3 types of energy demand - complete demand for preheating and boiling; process energy demand required within kettle; real energy demand in kettle over given process efficiency"

"PFADUKO with energy storage"

$dE_{condensation_rec} = m_{kettlefull} * cp_{wort} * (T_{preheated_wort} - T_{rinse})$ "Temperature to which wort can be preheated"

$ExternalEnergyPfaduko = E_{evaporation} + E_{preheating} - dE_{condensation_rec}$

$E_{Pfaduko_spec} = ExternalEnergyPfaduko * Convert('kJ'; 'MJ') / (V_{AW_cold} * Convert('m^3'; 'hl'))$

$ExternalEnergyPfaduko_kettle = E_{evaporation} + (E_{preheating} - E_{preheating_EStore} - E_{preheating_External})$

$E_{Pfaduko_kettle_spec} = ExternalEnergyPfaduko_kettle * Convert('kJ'; 'MJ') / (V_{AW_cold} * Convert('m^3'; 'hl'))$

$E_{Pfaduko_kettle_real} = ExternalEnergyPfaduko_kettle / eta_{kettle}$

$E_{Pfaduko_kettle_real_spec} = E_{Pfaduko_kettle_real} * Convert('kJ'; 'MJ') / (V_{AW_cold} * Convert('m^3'; 'hl'))$

$dE_{condensation_rec_spec} = dE_{condensation_rec} * Convert('kJ'; 'MJ') / (V_{AW_cold} * Convert('m^3'; 'hl'))$

"PFADUKO for hot water production"

$dE_{condensation1} * eta_{pfaduko} = m_{hotwater_pfaduko} * Cp(Water);$ $T = (T_{hotwater_pfaduko} + T_{FW}) / 2;$
 $P = P[1] * (T_{hotwater_pfaduko} - T_{FW})$

CALL SetHotwaterPfaduko(m_hotwater_pfaduko; sudhaus:m_HW_pfaduko)

$ExternalEnergyPfaduko_HW = E_{evaporation} + E_{preheating}$

$E_{Pfaduko_HW_spec} = ExternalEnergyPfaduko_HW * Convert('kJ'; 'MJ') / (V_{AW_cold} * Convert('m^3'; 'hl'))$

$ExternalEnergyPfaduko_HW_kettle = E_{evaporation} + (E_{preheating} - E_{preheating_EStore} - E_{preheating_External})$

$E_{Pfaduko_HW_kettle_spec} = ExternalEnergyPfaduko_HW_kettle * Convert('kJ'; 'MJ') / (V_{AW_cold} * Convert('m^3'; 'hl'))$

$E_{Pfaduko_HW_kettle_real} = ExternalEnergyPfaduko_HW_kettle / eta_{kettle}$

$E_{Pfaduko_HW_kettle_real_spec} = E_{Pfaduko_HW_kettle_real} * Convert('kJ'; 'MJ') / (V_{AW_cold} * Convert('m^3'; 'hl'))$

"Thermal vapour compression - TVC"

$eff_{isen_tvc} = 0,7$

CALL VaporCompression(P[2]; P[3]; eff_isen_tcv; h[6]; h[7]; h_poly_tcv; dh_poly_tcv; dh_isen_tcv)

$A_{compression_TCV} = m_{vapors} * 0,7 * (t_{boiling} - t_{startup}) / t_{boiling} * dh_{poly_tvc}$

$E_{steam_TVC} = A_{compression_TCV} / 1000$

$E_{steam_TVC_spec} = E_{steam_TVC} / (V_{AW_cold} * Convert('m^3'; 'hl'))$

$ExternalEnergyTVC = E_{evaporation} * (t_{startup} / t_{boiling}) + E_{preheating} + E_{steam_TVC}$

$E_{TVC_spec} = ExternalEnergyTVC * Convert('kJ'; 'MJ') / (V_{AW_cold} * Convert('m^3'; 'hl'))$

$ExternalEnergyTVC_kettle = E_{evaporation} * (t_{startup} / t_{boiling}) + (E_{preheating} - E_{preheating_EStore} - E_{preheating_External}) + E_{steam_TVC}$

$E_{TVC_kettle_spec} = ExternalEnergyTVC_kettle * Convert('kJ'; 'MJ') / (V_{AW_cold} * Convert('m^3'; 'hl'))$

$ExternalEnergyTVC_kettle_real = ExternalEnergyTVC_kettle / eta_{kettle}$

EETVC_kettle_real_spec=ExternalEnergyTVC_kettle_real*Convert('kJ'; 'MJ')/(V_AW_cold*Convert('m^3'; 'hl'))

"Mechanical vapour compression - MVC"

E_vapors_to_MVC=E_vapors*(t_boiling-t_startup)/t_boiling
 E_vapors_to_MVC_spec=E_vapors_to_MVC*Convert('kJ'; 'MJ')/(V_AW_cold*Convert('m^3'; 'hl'))
 eff_isen=0,7
 CALL VaporCompression(P[2];P[3];eff_isen:h[2];h[3];h_poly;dh_poly;dh_isen)
 A_compression=m_vapors*(t_boiling-t_startup)/t_boiling*dh_poly
 E_vapors_from_MVC=(E_vapors+m_vapors*dh_isen)*(t_boiling-t_startup)/t_boiling
 E_vapors_from_MVC_spec=E_vapors_from_MVC*Convert('kJ'; 'MJ')/(V_AW_cold*Convert('m^3'; 'hl'))
 E_compression_losses=A_compression-(E_vapors_from_MVC-E_vapors_to_MVC)
 E_compression_losses_spec=E_compression_losses*Convert('kJ'; 'MJ')/(V_AW_cold*Convert('m^3'; 'hl'))
 E_elec_MVC=A_compression/3600
 E_elec_MVC_spec=E_elec_MVC/(V_AW_cold*Convert('m^3'; 'hl'))
 E_MVC_spec=A_compression*Convert('kJ'; 'MJ')/(V_AW_cold*Convert('m^3'; 'hl'))
 ExternalEnergyMVC=E_evaporation*(t_startup/t_boiling)+E_preheating
 EEMVC_spec=ExternalEnergyMVC*Convert('kJ'; 'MJ')/(V_AW_cold*Convert('m^3'; 'hl'))
 ExternalEnergyMVC_kettle=E_evaporation*(t_startup/t_boiling)+(E_preheating-E_preheating_EStore-E_preheating_External)
 EEMVC_kettle_spec=ExternalEnergyMVC_kettle*Convert('kJ'; 'MJ')/(V_AW_cold*Convert('m^3'; 'hl'))
 ExternalEnergyMVC_kettle_real=ExternalEnergyMVC_kettle/eta_kettle
 EEMVC_kettle_real_spec=ExternalEnergyMVC_kettle_real*Convert('kJ'; 'MJ')/(V_AW_cold*Convert('m^3'; 'hl'))

"VacuumEvaporation"

CALL VacuumEvaporation(m_kettlefull; P[3]; T_sat[3]; P[2];T_sat[2]:T_cond_VE;m_vapors_VE;E_VE)
 ExternalEnergyVE=E_preheating+E_VE
 EEVE_spec=ExternalEnergyVE*Convert('kJ'; 'MJ')/(V_AW_cold*Convert('m^3'; 'hl'))
 ExternalEnergyVE_kettle=(E_preheating-E_preheating_EStore-E_preheating_External)+E_VE
 EEVE_kettle_spec=ExternalEnergyVE_kettle*Convert('kJ'; 'MJ')/(V_AW_cold*Convert('m^3'; 'hl'))
 ExternalEnergyVE_kettle_real=ExternalEnergyVE_kettle/eta_kettle
 EEVE_kettle_real_spec=ExternalEnergyVE_kettle_real*Convert('kJ'; 'MJ')/(V_AW_cold*Convert('m^3'; 'hl'))

CALL

CheckVaporRecovery(sudhaus;E_condensate_real_spec;E_HW_rec_spec;E_HW_pfaduko_spec;E_preheating_EStore_spec;E_vapors_to_MVC_spec;E_vapor_recovery_spec)

CALL

CheckEnergyDemand(sudhaus;Epfaduko_spec;Epfaduko_kettle_spec;Epfaduko_kettle_real_spec;Epfaduko_HW_spec;Epfaduko_HW_kettle_spec;Epfaduko_HW_kettle_real_spec;EEMVC_spec;EEMVC_kettle_spec;EMVC_kettle_real_spec;EETVC_spec;EETVC_kettle_spec;EETVC_kettle_real_spec;EEVE_spec;EEVE_kettle_spec;EEVE_kettle_real_spec;EE_wortboiling_spec;EE_kettle_spec;EE_kettle_real_spec)

E_total_brewhouse_spec=E_mashing_spec+E_preheating_External_spec+EE_kettle_spec+E_addevap_spec+E_CIP_brewhouse_spec "EE wort boiling sum of preheating and boiling energy requirement"

E_total_brewhouse_real_spec=E_mashing_real_spec+E_preheating_Ext_real_spec+EE_kettle_real_spec+E_addevap_real_spec+E_CIP_brewhouse_spec

V_wort_brewed=N_brews_week*(V_AW_cold*Convert('m^3'; 'hl'))*(weeks_year/12)

"Losses in batch operation"

"Size of vesselsl - acc. to Vey [207] "

```

d_mashtun^2*pi/4*h_mashtun=V_mashing*1,3 "20-40% additional volume"
d_mashtun=h_mashtun*f_DH_mashtun
d_mashtun=0,68*d_lautertun
d_kettle^2*pi/4*h_kettle=V_totalkettle*1,4 "25-50% additional volume "
d_kettle=h_kettle*f_DH_kettle
d_whirlpool^2*pi/4*h_whirlpool=V_AW_whirlpool_hot+V_hottrub "25-50% additional volume "
d_whirlpool=h_whirlpool*f_DH_whirlpool
"mass of vessels (calculated as cylinders - simplified)"
m_mashtun=(2*d_mashtun^2*pi/4+d_mashtun*h_mashtun)*s_mashtun*rho_('Stainless_AISI302';
T=(T_mash+T_cold_vessel)/2)
m_lautertun=(2*d_lautertun^2*pi/4+d_lautertun*h_lautertun)*s_lautertun*rho_('Stainless_AISI302';
T=(T_mash+T_cold_vessel)/2)
m_kettle=(2*d_kettle^2*pi/4+d_kettle*h_kettle)*s_kettle*rho_('Stainless_AISI302';
T=(T_mash+T_cold_vessel)/2)
m_whirlpool=(2*d_whirlpool^2*pi/4+d_whirlpool*h_whirlpool)*s_whirlpool*rho_('Stainless_AISI302';
T=(T_mash+T_cold_vessel)/2)
m_vessels=m_mashtun+m_lautertun+m_kettle+m_whirlpool
"surface area of vessels (calculated as cylinders - simplified)"
o_mashtun=(2*d_mashtun^2*pi/4+d_mashtun*h_mashtun)
o_lautertun=(2*d_lautertun^2*pi/4+d_lautertun*h_lautertun)
o_kettle=(2*d_kettle^2*pi/4+d_kettle*h_kettle)
o_whirlpool=(2*d_whirlpool^2*pi/4+d_whirlpool*h_whirlpool)
o_vessels=o_mashtun+o_lautertun+o_kettle+o_whirlpool
"cp-value of vessels"
cp_vessels=(m_mashtun*c_('Stainless_AISI302';
T=(T_mash+T_cold_vessel)/2)+m_lautertun*c_('Stainless_AISI302';
T=(T_rinse+T_cold_vessel)/2)+m_kettle*c_('Stainless_AISI302'; T=(T_sat[3]+T_cold_vessel)/2)+
m_whirlpool*c_('Stainless_AISI302'; T=(T_AWh+T_cold_vessel)/2))/(m_vessels)
"Average temperature of vessels immediately after operation"
T_avg_vessel*m_vessels*cp_vessels=m_mashtun*c_('Stainless_AISI302';
T=(T_mash+T_cold_vessel)/2)*T_mash_out+m_lautertun*c_('Stainless_AISI302';
T=(T_rinse+T_cold_vessel)/2)*T_rinse+m_kettle*c_('Stainless_AISI302';
T=(T_sat[3]+T_cold_vessel)/2)*T_sat[3]+ m_whirlpool*c_('Stainless_AISI302';
T=(T_AWh+T_cold_vessel)/2)*T_AWh
"1) Heat required to heat steel vessels after weekends"
E_loss_vessels_weekend=m_vessels*c_('Stainless_AISI302'; T=(T_avg_vessel+T_cold_vessel)/2)*(T_avg_vessel
-T_cold_vessel)
E_loss_vessels_weekend_spec=E_loss_vessels_weekend*Convert('kJ'; 'MJ')/(V_AW_cold*N_brews_week)
"2) Heat required to heat steel vessels after breaks between brews"
E_loss_mashtun_batch=o_mashtun*k_vessels*(T_mash_out-T_room)*dt*(1/1000)[J/kJ]
E_loss_lautertun_batch=o_lautertun*k_vessels*(T_rinse-T_room)*dt*(1/1000)[J/kJ]
E_loss_kettle_batch=o_kettle*k_vessels*(T_wort_boiling[n_steps_boiling]-T_room)*dt*(1/1000)[J/kJ]
E_loss_whirlpool_batch=o_whirlpool*k_vessels*(T_AWh-T_room)*dt*(1/1000)[J/kJ]
E_loss_vessels_batch=E_loss_mashtun_batch+E_loss_lautertun_batch+E_loss_kettle_batch+E_loss_whirlpool_
batch
k_vessels=1,1 [W/m^2*K]
dt=dt_brews*3600[s]
E_loss_vessels_batch=m_vessels*c_('Stainless_AISI302'; T=(T_avg_vessel+T_cold_vessel)/2)*(T_avg_vessel -
T_vessel_after_batch)

```

$E_{loss_vessels_batch_spec} = E_{loss_vessels_batch} * Convert('kJ'; 'MJ') / (V_{AW_cold})$

9.2.1.2 "Packaging calculations"

"Non-returnable bottles"

"Pasteurization"

$cp_glass_NRB = Cp('Glass_soda_lime'; T=30)$

Call

CheckandCalculatePast(Flash_NRB;Tunnel_NRB;Chamber_NRB;eta_FP_NRB;eta_TP_NRB;eta_CP_NRB;perc_recovery_TPast_NRB;T_beer_in_NRB;T_beer_out_NRB;T_past_NRB;V_beer_NRB;hours_flashpast_NRB;T_bot_in_TP_NRB;T_past_TP_NRB;V_bot_avg_TP_NRB;m_bot_avg_TP_NRB;cp_glass_NRB;hours_tpast_NRB;n_charge_NRB;n_pallet_charge_NRB;n_pack_pallet_NRB;V_pack_avg_NRB;m_pack_avg_NRB;T_pack_in_NRB;T_past_CP_NRB;time_past_CP_NRB;time_heating_CP_NRB;S_CP_NRB;U_CP_NRB;T_room_CP_NRB;Q_FP_NRB;E_FP_spec_NRB;E_FP_NRB;Q_TP_NRB;E_TP_spec_NRB;E_TP_NRB;Q_CP_NRB;E_CP_NRB;E_CP_spec_NRB)

\$export ExportTunnelPasteurisationNRB\$ Q_TP_NRB perc_Q_HX_TPast_NRB[1..3] T_bath_TPast_NRB[1..3] T_flow_to_HX_TPast_NRB[1..3] V_bath_TPast_NRB[1..3] cp_bath_medium_TPast_NRB T_bath_stop_TPast_NRB V_HTM_TPast_NRB_max T_HTM_TPast_NRB_in[1..3] T_HTM_TPast_NRB_out[1..3] A_heattransfer_TPast_NRB[1..3] k_value_TPast_NRB[1..3] type_HX_TPast_NRB n_HX_TPast_NRB h_cont_operation_TPast_NRB perc_norm_operation_TPast_NRB

"Cans"

"Pasteurization"

$cp_can = Cp(Aluminum; T=T_past_CAN)$

Call

CheckandCalculatePast(Flash_CAN;Tunnel_CAN;Chamber_CAN;eta_FP_CAN;eta_TP_CAN;eta_CP_CAN;perc_recovery_TPast_CAN;T_beer_in_CAN;T_beer_out_CAN;T_past_CAN;V_beer_CAN;hours_flashpast_CAN;T_bot_in_TP_CAN;T_past_TP_CAN;V_bot_avg_TP_CAN;m_bot_avg_TP_CAN;cp_can;hours_tpast_CAN;n_charge_CAN;n_pallet_charge_CAN;n_pack_pallet_CAN;V_pack_avg_CAN;m_pack_avg_CAN;T_pack_in_CAN;T_past_CP_CAN;time_past_CP_CAN;time_heating_CP_CAN;S_CP_CAN;U_CP_CAN;T_room_CP_CAN;Q_FP_CAN;E_FP_spec_CAN;E_FP_CAN;Q_TP_CAN;E_TP_spec_CAN;E_TP_CAN;Q_CP_CAN;E_CP_CAN;E_CP_spec_CAN)

\$export ExportTunnelPasteurisationCAN\$ Q_TP_CAN perc_Q_HX_TPast_CAN[1..3] T_bath_TPast_CAN[1..3] T_flow_to_HX_TPast_CAN[1..3] V_bath_TPast_CAN[1..3] cp_bath_medium_TPast_CAN T_bath_stop_TPast_CAN V_HTM_TPast_CAN_max T_HTM_TPast_CAN_in[1..3] T_HTM_TPast_CAN_out[1..3] A_heattransfer_TPast_CAN[1..3] k_value_TPast_CAN[1..3] type_HX_TPast_CAN n_HX_TPast_CAN h_cont_operation_TPast_CAN perc_norm_operation_TPast_CAN

"Returnable bottles"

"Bottlewasher"

Call

BottleWasher(eta_WM;P[1];T_bottle_in_WM;T_bottles_out_WM;V_baths_WM;T_bath_stop;T_bath_operation;n_startup;Q_operation_WM;hours_operation_WM;V_beer_returnable_month;E_Startup;E_operation;E_bottlewasher;E_bottlewasher_spec)

\$export ExportBottleWashing\$ Q_operation_WM eta_WM perc_Q_HX[1..3] T_bath[1..3] T_flow_to_HX[1..3] V_bath_WM[1..3] cp_bath_medium T_bath_stop V_HTM_WM_max T_HTM_WM_in[1..3] T_HTM_WM_out[1..3] A_heattransfer_WM[1..3] k_value_WM[1..3] type_HX_WM n_HX_WM h_cont_operation perc_normal_operation

"Pasteurization - Returnable Bottles - RB"

$cp_glass_RB = Cp('Glass_soda_lime'; T=30)$

Call

CheckandCalculatePast(Flash_RB;Tunnel_RB;Chamber_RB;eta_FP_RB;eta_TP_RB;eta_CP_RB;perc_recovery_TPast_RB;T_beer_in_RB;T_beer_out_RB;T_past_RB;V_beer_RB;hours_flashpast_RB;T_bottles_in_TP_RB;T_past_

TP_RB;
 V_bottle_avg_TP_RB;m_bottle_avg_TP_RB;cp_glass_RB;hours_tunnelpast_RB;n_charge_RB;n_pallet_charge_R
 B;n_pack_pallet_RB;V_pack_avg_RB;m_pack_avg_RB;T_pack_in_RB;T_past_CP_RB;time_past_CP_RB;time_he
 ating_CP_RB;S_CP_RB;U_CP_RB;T_room_CP_RB;Q_FP_RB;E_FP_spec_RB;E_FP_RB;Q_TP_RB;E_TP_spec_RB;E_
 TP_RB; Q_CP_RB;E_CP_RB;E_CP_spec_RB)
 \$export ExportTunnelPasteurisationRB\$ Q_TP_RB perc_Q_HX_TPast[1..3] T_bath_TPast[1..3]
 T_flow_to_HX_TPast[1..3] V_bath_TPast[1..3] cp_bath_medium_TPast T_bath_stop_TPast V_HTM_TPast_max
 T_HTM_TPast_in[1..3] T_HTM_TPast_out[1..3] A_heattransfer_TPast[1..3] k_value_TPast[1..3] type_HX_TPast
 n_HX_TPast h_cont_operation_TPast perc_normal_operation_TPast
 "Filler"
 Call
 BottleFilling_HWRinse(P[1];V_HW_rinse;T_HW_filler;T_FW_filler;perc_recovery;T_WW_filler;hours_HW_rinse;
 V_beer_filler;V_HW_filler;Q_HW_rinse;E_HW_rinse_spec;E_HW_rinse)

"Keg Packaging"

"Pasteurization"

Call

FlashPasteurization(eta_FP_keg;T_beer_in_keg;T_beer_out_keg;T_past_keg;V_beer_keg;hours_flashpast_keg;
 Q_FP_keg;E_FP_spec_keg;E_FP_keg)

"Keg washer and filler"

Call

KEGwashing_filling(eta_kegwasher;n_kegs_h;hours_kegwashing;m_keg;V_keg_avg;T_FW_keg;T_room;T_keg_i
 n;T_bath1;S_bath1;m_FW_bath1;m_spray_bath1;T_bath2;S_bath2;m_FW_bath2;m_spray_bath2;T_bath3;S_b
 ath3;m_FW_bath3;m_spray_bath3;T_bath4;S_bath4;m_FW_bath4;m_spray_bath4;time_sterilisation;
 m_HW_keg;T_HW_keg;m_FW_kegwasher;dE_HW_keg_spec;Q_kegwashing;E_kegwashing;E_kegwashing_spec
 ;Q_baths;Q_steam;Q_bath1;Q_bath2;Q_bath3;Q_bath4)

V_beer_packaged_NRB=V_beer_NRB*hours_flashpast_NRB+V_beer_NRB*hours_tpast_NRB+n_charge_NRB*n
 _pallet_charge_NRB*n_pack_pallet_NRB*V_pack_avg_NRB*Convert('ml'; 'hl') "hl/month"

V_beer_packaged_CAN=V_beer_CAN*hours_flashpast_CAN+V_beer_CAN*hours_tpast_CAN+n_charge_CAN*n
 _pallet_charge_CAN*n_pack_pallet_CAN*V_pack_avg_CAN*Convert('ml'; 'hl') "hl/month"

V_beer_packaged_RB=V_beer_RB*hours_flashpast_RB+V_beer_RB*hours_tunnelpast_RB "hl/month"

V_beer_packaged_keg=n_kegs_h*hours_kegwashing*V_keg_avg*Convert('l'; 'hl') "hl/month"

V_beer_packaged=V_beer_packaged_NRB+V_beer_packaged_CAN+V_beer_packaged_RB+V_beer_packaged_
 keg+V_beer_packaged_externally

Schwand_wort_to_packaging=(V_wort_brewed - V_beer_packaged)/V_wort_brewed

9.2.1.3 Hot water balance calculations

"hot water balance per week"

m_WW_addevap=V_WW_addevap*density(Water; T=T_WW_addevap; P=P[1]) "per brew"

m_HW_addevap=V_HW_addevap*density(Water; T=T_HW_addevap; P=P[1])

m_FW_kegwasher=V_FW_kegwasher*density(Water; T=T_FW_keg; P=P[1]) "per week"

m_HW_filler=V_HW_filler*density(Water; T=T_HW_filler; P=P[1])

m_HW_keg=V_HW_keg*density(Water; T=T_HW_keg; P=P[1])

m_HW_general_needs=V_HW_general_needs*density(Water; T=T_BW; P=P[1])

m_CIP_brewhouse=V_CIP_brewhouse*density(Water; T=T_CIP_brewhouse; P=P[1])

m_CIP_packaging=V_CIP_packaging*density(Water; T=T_CIP_packaging; P=P[1])

m_HW_externalheating+(m_BW_wortcooler+m_HW_rec+m_HW_pfaduko+m_HW_addevap+m_WW_addevap
)*N_brews_week+m_HW_steam_condensate=m_CIP_brewhouse+m_CIP_packaging+(m_BW+m_BW_rinse)*N
 _brews_week+m_HW_keg+m_HW_filler+m_HW_general_needs

m_HW_consumption_per_week=m_CIP_brewhouse+m_CIP_packaging+(m_BW+m_BW_rinse)*N_brews_week
 +m_HW_keg+m_HW_filler+m_HW_general_needs

$V_{HW_consumption_per_week} = m_{HW_consumption_per_week} / \text{density}(\text{Water}; T=T_{BW}; P=P[1])$
 $m_{HW_production_per_week} = (m_{BW_wortcooler} + m_{HW_rec} + m_{HW_pfaduko} + m_{HW_addevap} + m_{WW_addevap}) * N_{brews_week} + m_{HW_steam_condensate}$
 $V_{HW_production_per_week} = m_{HW_production_per_week} / \text{density}(\text{Water}; T=T_{BW}; P=P[1])$

9.2.1.4 Energy balance

$E_{HW_CIP_brewhouse} = m_{CIP_brewhouse} * Cp(\text{Water}; T=\text{average}(T_{CIP_brewhouse}; T_{ref}); P=P[1]) * (T_{CIP_brewhouse} - T_{ref})$
 $E_{HW_CIP_brewhouse_spec} = E_{HW_CIP_brewhouse} * \text{Convert}('kJ'; 'MJ') / (V_{AW_cold} * \text{Convert}('m^3'; 'hl') * n_{brews_week})$
 $E_{CIP_brewhouse} = (m_{CIP_brewhouse} * Cp(\text{Water}; T=T_{CIP_brewhouse}; P=P[1]) * (T_{CIP_brewhouse} - T_{FW}) + V_{CIP_brewhouse} * 0,14 * 3600)$ " per week; 0,14 kWh/m³and week"
 $E_{CIP_brewhouse_spec} = E_{CIP_brewhouse} * \text{Convert}('kJ'; 'MJ') / (V_{AW_cold} * \text{Convert}('m^3'; 'hl') * n_{brews_week})$
 $E_{HW_CIP_packaging} = m_{CIP_packaging} * Cp(\text{Water}; T=\text{average}(T_{CIP_packaging}; T_{ref}); P=P[1]) * (T_{CIP_packaging} - T_{ref})$
 $E_{HW_CIP_packaging_spec} = E_{HW_CIP_packaging} * \text{Convert}('kJ'; 'MJ') / (V_{beer_packaged} * \text{Convert}('m^3'; 'hl'))$
 $E_{CIP_packaging} = (m_{CIP_packaging} * Cp(\text{Water}; T=T_{CIP_packaging}; P=P[1]) * (T_{CIP_packaging} - T_{FW}) + V_{CIP_packaging} * 0,14 * 3600)$ " per week; 0,14 kWh/m³and week"
 $E_{CIP_packaging_spec} = E_{CIP_packaging} * \text{Convert}('kJ'; 'MJ') / (V_{beer_packaged} / 4,3)$ "per hl packaged beer"
 $E_{HW_general_needs} = m_{HW_general_needs} * Cp(\text{Water}; T=\text{average}(T_{HW_general_needs}; T_{ref}); P=P[1]) * (T_{HW_general_needs} - T_{ref})$
 $E_{HW_general_needs_spec} = E_{HW_general_needs} * \text{Convert}('kJ'; 'MJ') / (V_{AW_cold} * \text{Convert}('m^3'; 'hl') * n_{brews_week})$
 $E_{HW_rec} = m_{HW_rec} * Cp(\text{Water}; T=\text{average}(T_{Whot}; T_{ref}); P=P[1]) * (T_{Whot} - T_{ref})$
 $E_{HW_rec_spec} = E_{HW_rec} * \text{Convert}('kJ'; 'MJ') / (V_{AW_cold} * \text{Convert}('m^3'; 'hl'))$
 $E_{HW_pfaduko} = m_{HW_pfaduko} * Cp(\text{Water}; T=\text{average}(T_{hotwater_pfaduko}; T_{ref}); P=P[1]) * (T_{hotwater_pfaduko} - T_{ref})$
 $E_{HW_pfaduko_spec} = E_{HW_pfaduko} * \text{Convert}('kJ'; 'MJ') / (V_{AW_cold} * \text{Convert}('m^3'; 'hl'))$
 $E_{HW_steam_condensate} = m_{HW_steam_condensate} * Cp(\text{Water}; T=\text{average}(T_{HW_steam_condensate}; T_{ref}); P=P[1]) * (T_{HW_steam_condensate} - T_{ref})$
 $E_{HW_steam_condensate_spec} = E_{HW_steam_condensate} * \text{Convert}('kJ'; 'MJ') / (V_{AW_cold} * \text{Convert}('m^3'; 'hl') * n_{brews_week})$
 $E_{HW_keg} = m_{HW_keg} * Cp(\text{Water}; T=\text{average}(T_{HW_keg}; T_{ref}); P=P[1]) * (T_{HW_keg} - T_{ref})$
 $E_{HW_keg_spec} = E_{HW_keg} * \text{Convert}('kJ'; 'MJ') / (V_{AW_cold} * \text{Convert}('m^3'; 'hl') * n_{brews_week})$
 $E_{HW_filler} = m_{HW_filler} * Cp(\text{Water}; T=\text{average}(T_{HW_filler}; T_{ref}); P=P[1]) * (T_{HW_filler} - T_{ref})$
 $E_{HW_filler_spec} = E_{HW_filler} * \text{Convert}('kJ'; 'MJ') / (V_{beer_packaged} / 4,3)$ "per hl packaged beer"
 $E_{HW_addevap} = m_{HW_addevap} * Cp(\text{Water}; T=\text{average}(T_{HW_addevap}; T_{ref}); P=P[1]) * (T_{HW_addevap} - T_{ref})$
 $E_{HW_addevap_spec} = E_{HW_addevap} * \text{Convert}('kJ'; 'MJ') / (V_{AW_cold} * \text{Convert}('m^3'; 'hl'))$
 $E_{WW_addevap} = m_{WW_addevap} * Cp(\text{Water}; T=\text{average}(T_{WW_addevap}; T_{ref}); P=P[1]) * (T_{WW_addevap} - T_{ref})$
 $E_{WW_addevap_spec} = E_{WW_addevap} * \text{Convert}('kJ'; 'MJ') / (V_{AW_cold} * \text{Convert}('m^3'; 'hl'))$
 $E_{HW_externalheating} + (E_{BW_wortcooler} + E_{HW_rec} + E_{HW_pfaduko} + E_{HW_addevap} + E_{WW_addevap}) * N_{brews_week} + E_{HW_steam_condensate} = E_{HW_CIP_brewhouse} + E_{HW_CIP_packaging} + (E_{BW_mashing} + E_{BW_rinse}) * N_{brews_week} + E_{HW_keg} + E_{HW_filler} + E_{HW_general_needs}$
 $E_{HW_externalheating_spec} = E_{HW_externalheating} * \text{Convert}('kJ'; 'MJ') / (V_{AW_cold} * \text{Convert}('m^3'; 'hl') * n_{brews_week})$
 $V_{HW_externalheating} = m_{HW_externalheating} / \text{density}(\text{Water}; T=T_{BW}; P=P[1])$

Overall energy balance

$E_{\text{overall_spec}} = E_{\text{total_brewhouse_spec}} + E_{\text{total_packaging_spec}}$

$E_{\text{total_packaging_spec}} = E_{\text{FP_spec_NRB}} + E_{\text{TP_spec_NRB}} + E_{\text{CP_spec_NRB}} + E_{\text{FP_spec_CAN}} + E_{\text{TP_spec_CAN}} + E_{\text{CP_spec_CAN}} + E_{\text{FP_spec_RB}} + E_{\text{TP_spec_RB}} + E_{\text{bottleswasher_spec}} + E_{\text{HW_rinse_spec}} + E_{\text{FP_spec_keg}} + E_{\text{kegwashing_spec}} + dE_{\text{HW_keg_spec}} + E_{\text{CIP_packaging_spec}}$

9.2.1.5 Cooling

\$export exportfermentation\$ T_pitching T_main_ferm T_final_ferm D_0 x_ferm P_ferm X_0
t_mainfermentation_h t_cooling_tanks_h

$D_0 = p_{\text{mass_wort_final}}$

$t_{\text{mainfermentation_h}} = t_{\text{mainfermentation}} * 24$

$t_{\text{cooling_tanks_h}} = t_{\text{cooling_tanks}} * 2$

\$export exportcoolingdata\$ /N T_pitching T_main_ferm T_final_ferm D_0 x_ferm P_ferm X_0
t_mainfermentation_h t_cooling_tanks_h n_ferm_tanks V_ferm_tank capacity_BWC T_FW_forBW T_CBW
T_CBW_min T_CBW_max T_out_BC capacity_BC n_mat_tanks V_mat_tank T_mat gravity_mat x_ferm_mat
duration_mat n_harvest day1_harvest day2_harvest day3_harvest n_yeast_tanks V_yeast_tank T_yeast_tank
t_active_cooling_yeast_tank fermentation_in_yeasttanks x_ferm_yeasttank m_yeast V_yeastflow
T_yeast_beforecooling T_yeast_aftercooling

\$export ExportGeneralData\$ /U /N V_AW_cold m_AW_final f_evap V_mashliquor V_rinse startday_brewing
starttime_brewing weekdays_brewing N_brews_week t_brew dt_brews t_filling_mashtun time_mashing
t_lautering n_sparges t_filling_lautertun_BW t_sparge dt_sparges dt_boilmash1 dt_boilmash2
dt_startbrew_wortpreheating dt_startbrew_boiling t_filling_kettle t_boiling time_whirlpool t_addevap
dt_startbrew_wortcooling E_BW_mashing m_BW E_BW_rinse m_BW_rinse cp_BW T_BW T_ref

9.2.1.6 Calculation Procedures

"Procedures for wort physical properties"

Procedure WortDensity(p_mass;p_vol;roh_cold;roh_hot)

"Calculate Wort Density based on Plato table"

row0=LookupRow('Lookup 1'; 1;p_mass)

p_vol=Lookup('Lookup 1'; row0; 2)

$roh_cold = (p_vol/p_mass) * 1000$ [kg/m³]

$roh_hot = roh_cold * 0,96$

End

Procedure WortHeatCapacity (p_mass;T[1];T[2];P[1];cp_malt:cp_wort)

$cp_wort = Cp(\text{Water}; T = ((T[1] + T[2])/2); P = P[1]) * (1 - p_mass/100) + cp_malt * (p_mass/100)$

End

"Procedures for brewhouse-energy demand calculations"

Procedure

CheckV_mashing(V_mashing;V_boilmash[1..2];step_BM1_taken;step_BM1_back;step_BM2_taken;step_BM2_back;V_mashing_mainMash[1..8];V_boilmash1[1..8];V_boilmash2[1..8])

j:=1

repeat

If (j >= step_BM1_taken) And (j < step_BM1_back) Then

V_boilmash1[j]=V_boilmash[1]

Else

V_boilmash1[j]=0

EndIf

```

If (j >= step_BM2_taken) And (j < step_BM2_back) Then
V_boilmash2[j]=V_boilmash[2]
Else
V_boilmash2[j]=0
EndIf

V_mashing_mainMash[j]:=V_mashing-V_boilmash1[j]-V_boilmash2[j]
j=j+1
until (j>8)
end

Procedure
Calculate_E_boilmash_step(eta_boilmash;V_boilmash;roh_mashing;cp_mashing;n_steps_mash_BM;T_mashst
eps_BM[1..6];time_mashsteps_BM[1..6];T_mashsteps[1..8];step_BM_taken:E_boilmash[1..6];E_boilmash_real[
1..6];T_boilmash_0)

i:=1
T_boilmash_0=0
repeat
If i = step_BM_taken Then
T_boilmash_0=T_mashsteps[i]
EndIf
i=i+1
until (i>8)

j:=1
repeat
If j = 1 Then
E_boilmash[j]=V_boilmash*roh_mashing*cp_mashing*(T_mashsteps_BM[j]-T_boilmash_0)
Else
If j > n_steps_mash_BM Then
E_boilmash[j]=0
Else
E_boilmash[j]=V_boilmash*roh_mashing*cp_mashing*(T_mashsteps_BM[j]-T_mashsteps_BM[j-1])
EndIf
EndIf

E_boilmash_real[j]=E_boilmash[j]/eta_boilmash
j=j+1
until (j>6)
end

Procedure
Calculate_T_boilmash_mix(V_mashing_mainMash[1..8];T_mashsteps[1..8];roh_mashing;cp_mashing;V_boilma
sh[1..8];T_mashsteps_BM[1..6];step_BM_back;n_steps_mash_BM:T_mashsteps_afterBMMix[1..8])
i:=1
T_boilmash=0
repeat
If i = n_steps_mash_BM Then
T_boilmash = T_mashsteps_BM[i]
EndIf
i=i+1
until (i>6)

j:=1
repeat

```

```

If (j = step_BM_back-1) Then
T_mashsteps_afterBMMix[j]=(V_mashing_mainMash[j]*roh_mashing*cp_mashing*T_mashsteps[j]+V_boilmash[j]*roh_mashing*cp_mashing*T_boilmash)/(V_mashing_mainMash[j+1]*roh_mashing*cp_mashing)
Else
T_mashsteps_afterBMMix[j]=T_mashsteps[j]
EndIf
j=j+1
until (j>8)
end

```

Procedure

```

Calculate_E_mainmash_step(eta_mashtun;V_mashing_mainMash[1..8];roh_mashing;cp_mashing;n_steps_mashing;T_mashsteps[1..8];T_mashsteps_afterBM2Mix[1..8];time_mashsteps[1..8];T0_mash:E_mainmash[1..8];E_mainmash_real[1..8])

```

```

j:=1
repeat
If j = 1 Then
E_mainmash[j]=V_mashing_mainMash[j]*roh_mashing*cp_mashing*(T_mashsteps_afterBM2Mix[j]-T0_mash)
E_mainmash_real[j]=E_mainmash[j]/eta_mashtun
Else
E_mainmash[j]=V_mashing_mainMash[j]*roh_mashing*cp_mashing*(T_mashsteps[j]-T_mashsteps_afterBM2Mix[j-1])
E_mainmash_real[j]=E_mainmash[j]/eta_mashtun
EndIf
j=j+1
until (j>8)
end

```

Procedure CheckMainMash(heating_mashes_II;mash;boilmash:mash_main)

```

If heating_mashes_II=1 Then
mash_main=mash-boilmash
EndIf
If heating_mashes_II=0 Then
mash_main=mash
EndIf
End

```

Procedure

```

CheckEnergyDemandMashing(mashing;E_mashing_infusion;E_mashing_infusion_real;E_mainmash[1..8];E_mainmash_real[1..8];E_boilmash1[1..6];E_boilmash1_real[1..6];E_boilmash2[1..6];E_boilmash2_real[1..6];E_mashing;E_mashing_real)

```

```

If mashing=1 Then
E_mashing=E_mashing_infusion
E_mashing_real=E_mashing_infusion_real
EndIf
If mashing =2 Then
E_mashing=0
E_mashing_real=0
j:=1
repeat
E_mashing=E_mashing + E_mainmash[j]
E_mashing_real=E_mashing_real + E_mainmash_real[j]
j=j+1
until (j>8)

```

```

k:=1
repeat
  E_mashing=E_mashing+ E_boilmash1[k]+E_boilmash2[k]
  E_mashing_real=E_mashing_real + E_boilmash1_real[k]+E_boilmash2_real[k]
  k=k+1
until (k>6)
EndIf
End

```

```

Procedure Calculate_m_mashing_mainMash(V_mashing_mainMash[1..8];
roh_mashing:m_mashing_mainMash[1..8])
j:=1
repeat
m_mashing_mainMash[j]=V_mashing_mainMash[j]*roh_mashing
j=j+1
until (j>8)
end

```

```

Procedure
WeakWortRecovery(weakwort_recovery;m_weakwort;perc_rec_weakwort:m_weakwort_rec_mash)
If weakwort_recovery=1 Then
m_weakwort_rec_mash=m_weakwort*perc_rec_weakwort
EndIf
If weakwort_recovery=0 Then
m_weakwort_rec_mash=0
EndIf
If weakwort_recovery=2 Then
m_weakwort_rec_mash=0
EndIf
End

```

```

Procedure CheckBW_rinse(m_BW_rinse1;m_rinse;T_BW;T_rinse;cp_rinse:m_BW_rinse;dE_BW_rinse)
If T_BW<T_rinse Then
m_BW_rinse=m_rinse
dE_BW_rinse=m_BW_rinse*cp_rinse*(T_rinse-T_BW)
Else
m_BW_rinse=m_BW_rinse1
dE_BW_rinse=0
EndIf
end

```

```

Procedure
Wortpreheating(eta_preheating_EStore;eta_preheating_External;preheating_EStore;m_kettlefull;cp_wort;T_s
at[2];T_rinse;T_wort_EStore;T_wort_External;boiling_system;t_wort_boiling[1];E_preheating_EStore;E_prehea
ting_EStore_real;E_preheating_External;E_preheating_External_real;E_preheating)

```

```

If (boiling_system = 7) Or (boiling_system=8) Then "for Schoko and Varioboil overall pre-heating requirement
not linked to saturation temperature"
E_preheating=m_kettlefull*cp_wort*(t_wort_boiling[1]-T_rinse)
Else
E_preheating=m_kettlefull*cp_wort*(T_sat[2]-T_rinse)
EndIf

```

```

If preheating_EStore=1 Then
E_preheating_EStore=m_kettlefull*cp_wort*(T_wort_EStore-T_rinse)
E_preheating_External=m_kettlefull*cp_wort*(T_wort_External-T_wort_EStore)

```

```

EndIf
If preheating_EStore=0 Then
E_preheating_EStore=0
E_preheating_External=m_kettlefull*cp_wort*(T_wort_External-T_rinse)
EndIf

E_preheating_EStore_real=E_preheating_EStore/eta_preheating_EStore
E_preheating_External_real=E_preheating_External/eta_preheating_External
End

Procedure KettleVolumeForEvaporation(evap_incl_add; V_kettlefull;roh_wort_hot;
V_totalkettle;roh_totalwort_hot: V_kettle_evap;roh_wort_hot_evap)

If evap_incl_add=1 Then
V_kettle_evap=V_totalkettle
roh_wort_hot_evap=roh_totalwort_hot
Else
V_kettle_evap=V_kettlefull
roh_wort_hot_evap=roh_wort_hot
EndIf
End

Procedure
AWTemperaturWortCooler(dilution;cp_AW_final;cp_AW_addevap;m_AW_final;T_AWh;m_dilutionwater;P[1];
T_dilution:T_AWh_inWC;m_AW_final_WC;cp_AW_inWC)
If dilution=1 Then
T_AWh_inWC=(cp_AW_final*(m_AW_final-m_dilutionwater)*T_AWh+m_dilutionwater*Cp(Water;
T=T_dilution; P=P[1])*T_dilution)/(m_AW_final*cp_AW_final+m_dilutionwater*Cp(Water; T=T_dilution;
P=P[1]))
m_AW_final_WC= m_AW_final
cp_AW_inWC=cp_AW_final
Else
T_AWh_inWC=T_AWh
m_AW_final_WC= m_AW_final- m_dilutionwater
cp_AW_inWC=cp_AW_addevap
EndIf
End

Procedure Condensation(m_vapors;t_boiling;t_startup;P_vapourcond;T_subcooling;
T_ref;T_vapourcond;T_vapourcond_rec;eta_pfaduko: dE_condensation;dE_condensation_rec;dE_subcooling;
E_vapors; E_condensate;E_condensate_real; dE_subcooling_real;E_condensate_rec;dE_subcooling_rec)
"Calculate condensation and subcooling enthalpy for a condenser"
T_vapourcond_theory:=T_sat(Water;P=P_vapourcond)
m_vapors_used=m_vapors*(t_boiling-t_startup)/t_boiling
h_vapours=Enthalpy(Water;T=T_vapourcond_theory+1;P=P_vapourcond)
h_condensate=Enthalpy(Water;T=T_vapourcond;P=P_vapourcond)
E_vapors=m_vapors*(Enthalpy(Water;T=T_vapourcond_theory+1;P=P_vapourcond)-
Enthalpy(Water;T=T_ref;P=P_vapourcond))
dE_condensation:=m_vapors_used*(Enthalpy(Water;T=T_vapourcond_theory+1;P=P_vapourcond)-
Enthalpy(Water;T=T_vapourcond;P=P_vapourcond))
dE_condensation_rec= dE_condensation*eta_pfaduko
"with theoretical condensation temperature"
E_condensate=m_vapors_used*Cp(Water; T=((T_vapourcond_theory+T_ref)/2);
P=P_vapourcond)*(T_vapourcond_theory-T_ref)
dE_subcooling:=m_vapors_used*Cp(Water; T=((T_vapourcond_theory+T_subcooling)/2);
P=P_vapourcond)*(T_vapourcond_theory-T_subcooling)

```

"with real condensation temperature"

```
E_condensate_real=m_vapors_used*Cp(Water; T=((T_vapourcond+T_ref)/2);
P=P_vapourcond)*(T_vapourcond-T_ref)
dE_subcooling_real:=m_vapors_used*Cp(Water; T=((T_vapourcond+T_subcooling)/2);
P=P_vapourcond)*(T_vapourcond-T_subcooling)
```

"with temperature entering heat recovery system"

```
E_condensate_rec=m_vapors_used*Cp(Water; T=((T_vapourcond_rec+T_ref)/2);
P=P_vapourcond)*(T_vapourcond_rec-T_ref)
dE_subcooling_rec:=m_vapors_used*Cp(Water; T=((T_vapourcond_rec+T_subcooling)/2);
P=P_vapourcond)*(T_vapourcond_rec-T_subcooling)
End
```

Procedure SetVapourCondensationTemp(sudhaus;P_vapourcond:T_vapourcond)

"for Pfaduko system (sudhaus=1,4 or 5) - user specifies real condensate temperature"

```
T_vapourcond:=T_sat(Water;P=P_vapourcond)
```

End

Procedure HotWaterPreparation(eta;dE;T[1];T[2];P[1]:m_water)

"Calculate amount of water that can be heated with a given dE from T[1] to T[2]"

```
m_water:=dE*eta/(Cp(Water; T=((T[1]+T[2])/2); P=P[1])*(T[2]-T[1]))
```

End

Procedure VaporCompression(P[1];P[2];eff_isen:h[1];h[2];h_poly;dh_poly;dh_isen)

```
T_sat[1]:=T_sat(Water;P=P[1])
```

```
s[1]:=Entropy(Water;T=T_sat[1]+0,1;P=P[1])
```

```
h[1]:=Enthalpy(Water;T=T_sat[1]+0,1;P=P[1])
```

```
h[2]:=Enthalpy(Water;s=s[1];P=P[2]) "enthalpy for isentropic compression"
```

```
dh_isen:=(h[2] - h[1])
```

```
h_poly:= h[1] + 1 / (eff_isen / (h[2] - h[1])) "enthalpy for polytropic compression"
```

```
dh_poly:=h_poly-h[1]
```

End

Procedure

Pfaduko(m_vapors;m_kettlefull;cp_wort;T_sat[3];P[3];T_rinse:T_preheated_wort;dE_vapor_condensation)

"calculate temperature to which m_kettlefull can be preheated over Pfaduko"

```
dE_vapor_condensation:=m_vapors*(Enthalpy(Water;T=T_sat[3]+1;P=P[3])-
```

```
Enthalpy(Water;T=T_sat[3];P=P[3]))
```

```
T_preheated_wort:=T_rinse+dE_vapor_condensation/(m_kettlefull*cp_wort)
```

End

Procedure VacuumEvaporation(m_kettlefull; P[3]; T_sat[3]; P[2];T_sat[2]:T_cond_VE;m_vapors_VE;E_addevap)

"calculate vapours that evaporate in vacuum"

```
h_initial=Enthalpy(Water;T=T_initial-0,1;P=p_initial)
```

```
T_cond_VE=T_vacuum
```

```
y_VE=Quality(Water;T=T_vacuum;h=h_initial) "flash gas ratio"
```

```
m_vapors_VE=y_VE*m_wort
```

End

Procedure

SteamStripping(cp_AW_whirlpool;T_AWh;perc_steam_stripping;p_steam_stripping;T_steam_stripping;m_AW
_whirlpool; P[5]; T_sat[5]; P[4];T_sat[4]:T_wort_addevap;m_vapors_add;m_steam_add;E_addevap)

"calculate vapours that evaporate via steam stripping"

```
m_steam_add=m_AW_whirlpool*perc_steam_stripping
```

```
dE_evap_SS=m_steam_add*((Enthalpy(Water;T=T_steam_stripping+0,1;P=p_steam_stripping))-
```

```
(Enthalpy(Water;T=T_sat[5]-0,1;P=P[5]))) "energy of steam - energy of condensed steam in wort"
```

```
T_wort_addevap=T_sat[5]
```

```
m_vapors_add=dE_evap_SS/Enthalpy_vaporization(Water;T=T_sat[5])"pressure in state 4 and 5 identical, only
evaporation enthalpy"
```

```
"energy demand for steam stripping"
```

```
E_addevap=m_steam_add*(Enthalpy(Water;T=T_steam_stripping+0,1;P=p_steam_stripping))+m_AW_whirlpool*cp_AW_whirlpool*(T_sat[5]-T_AWh)
```

```
End
```

```
Procedure
```

```
CalculateAdditionalEvaporation(cp_malt;p_mass_wort_whirlpool;T_AWh;addevap;perc_steam_stripping;p_steam_stripping;T_steam_stripping;m_AW_whirlpool;P[5];T_sat[5];P[4];T_sat[4]:T_wort_addevap;m_vapors_add;m_steam_add;E_addevap)
```

```
CALL WortHeatCapacity (p_mass_wort_whirlpool;T_AWh;T_sat[5];P[5];cp_malt:cp_AW_whirlpool)
```

```
If addevap=2 Then
```

```
CALL VaccumEvaporation(m_AW_whirlpool;P[5];T_sat[5];P[4];T_sat[4]:T_wort_addevap;m_vapors_add;E_addevap)
```

```
m_steam_add=0
```

```
EndIf
```

```
If addevap=1 Then
```

```
CALL
```

```
SteamStripping(cp_AW_whirlpool;T_AWh;perc_steam_stripping;p_steam_stripping;T_steam_stripping;m_AW_whirlpool;P[5];T_sat[5];P[4];T_sat[4]:T_wort_addevap;m_vapors_add;m_steam_add;E_addevap)
```

```
EndIf
```

```
If addevap=0 Then
```

```
T_wort_addevap=T_AWh
```

```
m_vapors_add=0
```

```
m_steam_add=0
```

```
E_addevap=0
```

```
EndIf
```

```
end
```

```
Procedure
```

```
CheckVaporRecovery(sudhaus;E_condensate_real_spec;E_HW_rec_spec;E_HW_pfaduko_spec;E_preheating_EStore_spec;E_vapors_to_MVC_spec:E_vapor_recovery_spec)
```

```
If sudhaus=1 Then "Pfaduko"
```

```
E_vapor_recovery_spec=E_preheating_EStore_spec+E_HW_rec_spec
```

```
EndIf
```

```
If (sudhaus =2) Or (sudhaus =3) Then "MVC"
```

```
E_vapor_recovery_spec=(E_vapors_to_MVC_spec-E_condensate_real_spec)+E_HW_rec_spec
```

```
EndIf
```

```
If (sudhaus=4) Or (sudhaus=5) Then "pfaduko for HW"
```

```
E_vapor_recovery_spec=E_HW_pfaduko_spec+E_HW_rec_spec
```

```
EndIf
```

```
end
```

```
Procedure
```

```
CheckEnergyDemand(sudhaus;EEPfaduko_spec;EEPfaduko_kettle_spec;EEPfaduko_kettle_real_spec;EEPfaduko_o_HW_spec;EEPfaduko_HW_kettle_spec;EEPfaduko_HW_kettle_real_spec;EEMVC_spec;EEMVC_kettle_spec;EEMVC_kettle_real_spec;EETVC_spec;EETVC_kettle_spec;EETVC_kettle_real_spec;EEVE_spec;EEVE_kettle_spec;EEVE_kettle_real_spec;EE_wortboiling_spec;EE_kettle_spec;EE_kettle_real_spec)
```

```
If sudhaus=1 Then
```

```
EE_wortboiling_spec=EEPfaduko_spec
```

```
EE_kettle_spec=EEPfaduko_kettle_spec
```

```
EE_kettle_real_spec=EEPfaduko_kettle_real_spec
```

```
EndIf
```

```
If sudhaus =2 Then
```

```
EE_wortboiling_spec=EEMVC_spec
```

```

EE_kettle_spec=EEMVC_kettle_spec
EE_kettle_real_spec=EEMVC_kettle_real_spec
EndIf
If sudhaus =3 Then
EE_wortboiling_spec=EETVC_spec
EE_kettle_spec=EETVC_kettle_spec
EE_kettle_real_spec=EETVC_kettle_real_spec
EndIf
If sudhaus=4 Then
EE_wortboiling_spec=EEPfaduko_HW_spec
EE_kettle_spec=EEPfaduko_HW_kettle_spec
EE_kettle_real_spec=EEPfaduko_HW_kettle_real_spec
EndIf
If sudhaus=5 Then
EE_wortboiling_spec=EEPfaduko_HW_spec
EE_kettle_spec=EEPfaduko_HW_kettle_spec
EE_kettle_real_spec=EEPfaduko_HW_kettle_real_spec
EndIf
End

```

Procedure

```

SetT_to_Whirlpool(n_steps_boiling;T_AWh;p_wort_boiling[1..10];t_wort_boiling[1..10];addevap:T_to_whirlpool;T_AWh_whirlpool)
If addevap = 0 Then
T_to_whirlpool=T_sat(Water;P=p_wort_boiling[n_steps_boiling])
T_AWh_whirlpool=T_AWh
Else
T_to_whirlpool=T_sat(Water;P=p_wort_boiling[n_steps_boiling-2])
T_AWh_whirlpool=t_wort_boiling[n_steps_boiling-1]
EndIf
End

```

Procedure

```

CalculateWortCooler(type_wortcooler;T_BW;T_ref;P[1];V_AW_cold;T_CW;m_AW_final;cp_AW_final;T_AWh_inWC;T_AWc;eta_wortcooler_1;T_CM_out;T_CM_in;T_AWc_1stage;eta_wortcooler_2;T_HTM_in;T_HTM_out;m_CM_wortcooler;m_BW_wortcooler;V_BW_wortcooler;E_BW_wortcooler;E_BW_wortcooler_spec;m_HTM_wortcooler;E_HTM_wortcooler;E_HTM_wortcooler_spec)

```

```

If type_wortcooler = 1 Then "1stage"

```

```

m_BW_wortcooler=m_AW_final*cp_AW_final*(T_AWh_inWC-T_AWc)*eta_wortcooler_1/ (Cp(Water;
T=(T_BW+T_CW)/2; P=P[1])*(T_BW-T_CW))
E_BW_wortcooler=m_BW_wortcooler*Cp(Water; T=(T_BW+T_ref)/2; P=P[1])*(T_BW-T_ref)
E_BW_wortcooler_spec=E_BW_wortcooler*Convert('kJ'; 'MJ')/(V_AW_cold*Convert('m^3'; 'hl'))
V_BW_wortcooler=m_BW_wortcooler/density(Water; T=T_BW; P=P[1])
m_CM_wortcooler=0
m_HTM_wortcooler=0
E_HTM_wortcooler=0
E_HTM_wortcooler_spec=0
EndIf

```

```

If type_wortcooler = 2 Then "2stage with brew water production and cooling"

```

```

m_BW_wortcooler=m_AW_final*cp_AW_final*(T_AWh_inWC-T_AWc)*eta_wortcooler_1 / (Cp(Water;
T=(T_BW+T_CW)/2; P=P[1])*(T_BW-T_CW))
E_BW_wortcooler=m_BW_wortcooler*Cp(Water; T=(T_BW+T_ref)/2; P=P[1])*(T_BW-T_ref)
E_BW_wortcooler_spec=E_BW_wortcooler*Convert('kJ'; 'MJ')/(V_AW_cold*Convert('m^3'; 'hl'))
V_BW_wortcooler=m_BW_wortcooler/density(Water; T=T_BW; P=P[1])

```



```

m_CM_wortcooler=m_AW_final*cp_AW_final*(T_AWc_1stage-T_AWc)*eta_wortcooler_2/(Cp(Water;
T=(T_CM_out+T_CM_in)/2; P=P[1])*(T_CM_out-T_CM_in))
m_HTM_wortcooler=0
E_HTM_wortcooler=0
E_HTM_wortcooler_spec=0
EndIf

If type_wortcooler = 3 Then "2 stage with heatrecovery and cooling"
E_BW_wortcooler=0
E_BW_wortcooler_spec=0
m_BW_wortcooler=0
V_BW_wortcooler=m_BW_wortcooler/density(Water; T=T_BW; P=P[1])
m_CM_wortcooler=m_AW_final*cp_AW_final*(T_AWc_1stage-T_AWc)*eta_wortcooler_2/(Cp(Water;
T=(T_CM_out+T_CM_in)/2; P=P[1])*(T_CM_out-T_CM_in))
m_HTM_wortcooler=m_AW_final*cp_AW_final*(T_AWh_inWC-T_AWc_1stage)*eta_wortcooler_1/(Cp(Water;
T=(T_HTM_out+T_HTM_in)/2; P=P[1])*(T_HTM_out-T_HTM_in))
E_HTM_wortcooler=m_HTM_wortcooler*Cp(Water; T=(T_HTM_out+T_ref)/2; P=P[1])*(T_HTM_out-T_ref)
E_HTM_wortcooler_spec=E_HTM_wortcooler*Convert('kJ'; 'MJ')/(V_AW_cold*Convert('m^3'; 'hl'))
EndIf

If type_wortcooler = 4 Then "2 stage with heatrecovery and brew water production"
m_BW_wortcooler=m_AW_final*cp_AW_final*(T_AWc_1stage-T_AWc)*eta_wortcooler_2/(Cp(Water;
T=(T_BW+T_CW)/2; P=P[1])*(T_BW-T_CW))
E_BW_wortcooler=m_BW_wortcooler*Cp(Water; T=(T_BW+T_ref)/2; P=P[1])*(T_BW-T_ref)
E_BW_wortcooler_spec=E_BW_wortcooler*Convert('kJ'; 'MJ')/(V_AW_cold*Convert('m^3'; 'hl'))
V_BW_wortcooler=m_BW_wortcooler/density(Water; T=T_BW; P=P[1])
m_CM_wortcooler=0
m_HTM_wortcooler=m_AW_final*cp_AW_final*(T_AWh_inWC-T_AWc_1stage)*eta_wortcooler_1/(Cp(Water;
T=(T_HTM_out+T_HTM_in)/2; P=P[1])*(T_HTM_out-T_HTM_in))
E_HTM_wortcooler=m_HTM_wortcooler*Cp(Water; T=(T_HTM_out+T_ref)/2; P=P[1])*(T_HTM_out-T_ref)
E_HTM_wortcooler_spec=E_HTM_wortcooler*Convert('kJ'; 'MJ')/(V_AW_cold*Convert('m^3'; 'hl'))
EndIf

End

```

9.2.2 Variable energy demand calculations

In the following an example for the variable demand calculation is presented for the boiling process.

9.2.2.1 Macro file initialising the schedule calculation

```

Delete 'myBoilingSchedule.txt'
i=0
z=0
time_shift=0
m_process_last=0
m_vapors_current=0

repeat
Solve
SaveIntegral 'D:\Bettina\Diss\Brauereimodell\new model\BreweryModel\myBoilingSchedule.txt' /A
i=i+x
z=z+y

m_process_last=m_process_actual
m_vapors_current=m_vapors_current+m_vapors_step

```

```
if (start_time+ time_heatingup_real-end_time>0) then time_shift= time_shift+start_time+
time_heatingup_real-end_time
```

```
Until (i=n_steps)
```

9.2.2.2 Main programm for schedule calculation

```
$import 'exportboil.csv' n_steps_boiling boiling_system V_totalkettle roh_totalwort_hot T_wort_External
f_evap cp_wort k_value_kettle A_heattransfer_kettle T_HTM_kettle T_HTM_kettle_out m_HTM_kettle
p_HTM_kettle sudhaustype m_vapors p_kettle_start p_compression eff_isen_mvc eff_isen_tvc
time_boilingsteps[1..10] p_wort_boiling[1..10] t_wort_boiling[1..10] E_in_boilingsteps[1..10]
HR_in_boilingsteps[1..10] m_kettle boiling_system boiler_type addevap m_steam_add m_vapors_add
p_steam_stripping P[5] E_addevap filling_kettle t_filling_kettle T_air_kettle h_air_kettle phi_air_kettle d_kettle
eta_kettle
```

```
m_process_init=V_totalkettle*roh_totalwort_hot
cp_process=cp_wort
```

```
n_steps= n_steps_boiling
```

```
CALL
```

```
SetHeatingMedium(i;n_steps;m_HTM_kettle;p_HTM_kettle;T_HTM_kettle;T_HTM_kettle_out;A_heattransfer_
kettle;k_value_kettle;addevap;
m_steam_add;P[5];p_steam_stripping;time_boilingsteps[1..10];p_wort_boiling[1..10]:m_heating;p_heating;T_i
n;T_out;A;k;directSteamHeating)
T_air=T_air_kettle
h=h_air_kettle
d= d_kettle
phi_air=phi_air_kettle
```

```
$Include CalcAndSaveBoilingSchedule.emf
```

```
CALL Set_mprocess(i;m_process_init;m_process_last; filling_kettle;
t_filling_kettle;time_boilingsteps[1];t:m_process)
```

```
CALL SetTemperaturProfile
```

```
(n_steps;time_shift;i;T_wort_External;p_kettle_start;time_boilingsteps[1..10];p_wort_boiling[1..10];t_wort_bo
iling[1..10]:T_initial;p_initial;T_step;p_step;duration;last_duration;total_duration)
```

```
start_time=total_duration*60[s/min]+time_shift
```

```
end_time=start_time+duration*60[s/min]
```

```
CALL
```

```
Calculate_total_boiling_time(i;n_steps;time_boilingsteps[1..10];E_in_boilingsteps[1..10];p_initial;p_step;addev
ap;filling_kettle;p_wort_boiling[1..10]:boiling_time_total;boiling_time_left_vapours)
```

```
CALL CalcTimeforHeating(i;n_steps;A; m_steel; cp_steel;
```

```
cp_process;T_step;p_step;T_initial;p_initial;T_init_steel;T_in;T_out;k;m_process;m_process_fill;m_heating;p_h
eating;time_boilingsteps[1..10];E_in_boilingsteps[1..10];HR_in_boilingsteps[1..10];p_wort_boiling[1..10];
t_wort_boiling[1..10];sudhaustype;boiling_time_total;boiling_time_left_vapours;m_vapors;m_vapors_current;
p_compression;eff_isen_mvc;eff_isen_tvc;d;h;T_air;phi_air;addevap;m_steam_add;m_vapors_add;p_steam_st
ripping;E_addevap;boiler_type;directSteamHeating;eta_kettle:time_heatingup;share_HR;T_step_reached;Q_h
eattransfer_check;share_Qprocess)
```

```
CALL
```

```
CheckTimeforHeating(z;time_heatingup;start_time;end_time;T_step;T_initial;share_HR;T_step_reached;Q_hea
ttransfer_check;duration;total_duration;share_Qprocess:end_time_real;start_time_real;y;x;T_initial_real;T_ste
p_real;total_duration_real)
```

```
"Calculate vapour formation per time step"
```

```

h_process2=Enthalpy(Water;T=T_step;P=p_step)
h_process1=Enthalpy(Water;T=T_initial;p=p_initial) "h_process_previous_step"

```

```
Call
```

```
CalculateVaporsfromBoiling(i;n_steps;p_step;T_step;m_process;h_process1;p_initial;T_initial;boiling_time_tot
al;boiling_time_left_vapours;time_boilingsteps[1..10];E_in_boilingsteps[1..10];m_vapors;m_vapors_current;d;
h;T_air;phi_air;addevap;m_vapors_add:m_vapors_step)

```

```

T_vapors=T_sat(Water;P=p_step)+0,1[C]
T_vapors_cond=T_sat(Water;P=p_step)-0,1[C]
h_vapors2=Enthalpy(Water;T=T_vapors;P=p_step) "h_vapors in this step"
h_vapors1=h_process1 "before vapors in wort"
Q_vapors=m_vapors_step*(h_vapors2-h_vapors1)/(end_time_real-start_time_real)

```

```
Call
```

```
Calculate_EnergyinVaporsforHR(i;HR_in_boilingsteps[1..10];m_vapors_step;T_step;p_step;p_compression;eff_i
sen_mvc;eff_isen_tvcs;sudhaustype:E_vapors_HR;T_vapors_HR;T_vapor_HR_cond)

```

```
"Calculate heating power available from external heating medium"
```

```
h1=Enthalpy(Water;T=T_in;P=p_heating) "enthalpy of incoming heat transfer medium"
```

```
CALL CalcQ_HM(boiler_type;directSteamHeating;T_in;T_out;p_heating;p_step;T_step;m_heating:Q)

```

```
"Calculate heating power available from HR"
```

```
Q_HR=E_vapors_HR/(end_time_real-start_time_real)

```

```
Q=Q_HM+Q_HR

```

```
"Calculate process energy requirement"
```

```

m_process_actual=m_process-integral(m_vapors_step/(end_time_real-
start_time_real);t;start_time_real;end_time_real)+integral(m_process_add/(end_time_real-
start_time_real);t;start_time_real;end_time_real)

```

```
CALL
```

```
CalcQprocess(i;n_steps;m_process_actual;h_process2;h_process1;m_vapors_step;h_vapors2;h_vapors1;time_
heatingup;addevap;E_addevap;eta_kettle:Q_process)

```

```
"Calculate heat transfer "
```

```
dT = abs( ((T_in-Temp)+(T_out - Temp))/2 )
```

```
Call
```

```
CalcQ_testHM(boiler_type;directSteamHeating;k;A;dT;h1;h_process2;Q_process;m_steam_add:Q_testHM;m_
process_add)

```

```
dT_HR = ((T_vapors_HR-Temp)+(T_vapor_HR_cond - Temp))/2
```

```
Call Calc_Q_testHR(E_vapors_HR;k;A;dT_HR:Q_testHR)

```

```
Q_test=Q_testHM+Q_testHR

```

```
Call CheckQ(Q;Q_test;Q_process:Q_heattransfer)

```

```

h_process_actual=h_process1 + integral((Q_heattransfer-
Q_vapors)/(m_process_actual);t;start_time_real;end_time_real)

```

```
Temp=Temperature(Water;h=h_process_actual;p=p_step)

```

```
m_vapors_actual = integral(m_vapors_step/(end_time_real-start_time_real);t;start_time_real;end_time_real)

```

```
"share_HR_final=Q_HR/Q_heattransfer"
```

```
Q_thermal=Q_heattransfer-Q_HR

```

```
time_heatingup_real=(end_time_real-start_time_real)

```

```
$integraltable t:60, h_process_actual;Temp;Q_thermal;m_process_actual; m_vapors_actual;Q_HR

```

9.2.2.3 Subprogramms and procedure for boiling schedule

```

Procedure CheckQ(Q;Q_test;Q_process:Q_heattransfer)
Q_heattransfer=min(Q;Q_test;Q_process)
If Q_heattransfer<0 Then
Q_heattransfer=0
EndIf
end

```

```

Procedure CheckHeatingPhase(T_start;T_init:T_start_calc)
If (T_start>T_init+0,01[C]) or (T_start<T_init-0,01[C]) Then
T_start_calc=T_start
else
T_start_calc=T_start+0,01[C]
EndIf
end

```

```

Procedure SetToutforHR(T_out_defined;T_init;T_start:T_out)
if T_out_defined<(T_init+T_start)/2+2 then T_out:=(T_init+T_start)/2+2 else T_out:=T_out_defined
end

```

```

Procedure
CalcQprocess(i;n_steps;m_process_actual;h_process2;h_process1;m_vapors_step;h_vapors2;h_vapors1;time_
heatingup;addevap;E_addevap;eta_kettle:Q_process)
If (i>n_steps-2) And (addevap >0) Then "for additional evaporation (vacuum or steam stripping)"
Q_process=E_addevap/time_heatingup/eta_kettle
Else
If h_process2<h_process1 Then "flash; here enthalpy for vapour evaporation not considered, as this is
taken from cooling energy of wort"
Q_process=m_process_actual*(h_process2-h_process1)/time_heatingup/eta_kettle
Else
Q_process=(m_process_actual*(h_process2-h_process1)+m_vapors_step*(h_vapors2-
h_vapors1))/time_heatingup/eta_kettle
EndIf
EndIf
end

```

```

Procedure CalcSubcooledEvaporation(d;h;T_air;phi_air;T_step;p_step:m_vapors_step)
p_sat_water=P_sat(Water;T=T_air)
p_air=phi_air*P_sat_water
D_water_in_air=2,78e-5 [m^2/s]
MM_water=18 [g/mol]
R=8,314
m_vapors_step=- D_water_in_air*MM_water/(R*(T_step+273,15[C]))*p_step/h * ln((p_step -
p_sat_water)/(p_step-p_air))*(d^2*pi/4)
end

```

```

Procedure
CalculateVaporsfromBoiling(i;n_steps;p_step;T_step;m_process;h_process_previous_step;p_previous_step;T_i
nitial;boiling_time_total;boiling_time_left_vapours;time_boilingsteps[1..10];E_in_boilingsteps[1..10];m_vapors
;m_vapors_current;d;h;T_air;phi_air;addevap;m_vapors_add:m_vapors_step)
T_sat_step=T_sat(Water;P=p_step)

```

```

If (i=0) Then
T_average=average(T_step;T_initial)

```

```

If T_average < T_sat_step-0,1[C] Then "subcooled"
  Call CalcSubcooledEvaporation(d;h;T_air;phi_air;T_step;p_step:m_vapors_step)
Else
  If (p_previous_step=p_step) And (E_in_boilingsteps[i+1]>0) Then
    m_vapors_step = m_vapors*time_boilingsteps[i+1]/(boiling_time_total/60[s/min])
  Else
    Call CalcSubcooledEvaporation(d;h;T_air;phi_air;T_step;p_step:m_vapors_step)
  EndIf
EndIf

Else " i>0"

If (i>n_steps-2) and (addevap>0) Then "check if additional evaporation step (vacuum or steam stripping)"
m_vapors_step=m_vapors_add
Else

If (p_previous_step>p_step) Then
x_step=Quality(Water;P=p_step;h=h_process_previous_step)
  If x_step = -100 Then
    case=1
    m_vapors_step=0
  Else
    case=2
    m_vapors_step=m_process*x_step
  EndIf
Else

  If (p_previous_step=p_step) And (E_in_boilingsteps[i+1]>0) Then
    If T_step < T_sat_step-0,5[C] Then
      case=3
      Call CalcSubcooledEvaporation(d;h;T_air;phi_air;T_step;p_step:m_vapors_step)
    Else
      case=4
      m_vapors_step = (m_vapors-
m_vapors_current)*time_boilingsteps[i+1]/(boiling_time_left_vapours/60[s/min])
    EndIf
  Else
    case=5
    Call CalcSubcooledEvaporation(d;h;T_air;phi_air;T_step;p_step:m_vapors_step)
  EndIf
EndIf
ENDIF
EndIf

end

Procedure
Calculate_total_boiling_time(i;n_steps;time_boilingsteps[1..10];E_in_boilingsteps[1..10];p_previous_step;p_step;addevap;filling_kettle;p_wort_boiling[1..10]:boiling_time_total;boiling_time_left_vapours)
boiling_time_total=0
boiling_time_left_vapours=0
If (addevap>0) Then "If last step is additional evaporation equipment, this does not count to regular boiling time for vapour formation in kettle"
n_steps=n_steps-1
EndIf

```

```
j:=0
```

```
repeat
```

```
  boiling_time_total:=boiling_time_total+time_boilingsteps[j+1]*60[s/min]
```

```
  If j=0 Then
```

```
    If ((j>=i) And (E_in_boilingsteps[j+1]>0)) Then
```

```
      boiling_time_left_vapours:=boiling_time_left_vapours+time_boilingsteps[j+1]*60[s/min]
```

```
    Endif
```

```
  Else
```

```
    If ((j>=i) And (E_in_boilingsteps[j+1]>0)) Or ((j>i) And (p_wort_boiling[j]>p_wort_boiling[j+1])) Then
```

```
      boiling_time_left_vapours:=boiling_time_left_vapours+time_boilingsteps[j+1]*60[s/min]
```

```
    Endif
```

```
  Endif
```

```
  j=j+1
```

```
until (j>=n_steps)
```

```
end
```

```
Procedure VaporCompression(P[1];P[2];eff_isen:h[1];h[2];h_poly;dh_poly;dh_isen)
```

```
T_sat[1]:=T_sat(Water;P=P[1])
```

```
s[1]:=Entropy(Water;T=T_sat[1]+0,1[C];P=P[1])
```

```
h[1]:=Enthalpy(Water;T=T_sat[1]+0,1[C];P=P[1])
```

```
h[2]:=Enthalpy(Water;s=s[1];P=P[2]) "enthalpy for isentropic compression"
```

```
dh_isen:=(h[2] - h[1])
```

```
h_poly:= h[1] + 1 / (eff_isen / (h[2] - h[1])) "enthalpy for polytropic compression"
```

```
dh_poly:=h_poly-h[1]
```

```
End
```

```
Procedure
```

```
Calculate_EnergyinVaporsforHR(i;HR_in_boilingsteps[1..10];m_vapors_step;T_step;p_step;p_compression;eff_i  
sen_mvc;eff_isen_tvc;sudhaustype:E_vapors_step_HR;T_vapors_HR;T_vapor_HR_cond)
```

```
If HR_in_boilingsteps[i+1]>0 Then "when HR from vapours active"
```

```
if sudhaustype = 2 Then eff_isen:=eff_isen_mvc Else eff_isen:=eff_isen_tvc
```

```
"Calculate vapour compression and available energy - from last time step"
```

```
CALL VaporCompression(p_step;p_compression;eff_isen:h_step;h_compression;h_poly;dh_poly;dh_isen)
```

```
h_vapors=h_step
```

```
E_vapors_step=m_vapors_step*h_vapors
```

```
A_compression=m_vapors_step*dh_poly
```

```
T_vapors_HR=Temperature(Steam;P=p_compression;h=h_compression)
```

```
T_vapor_HR_cond=T_sat(Water;P=p_compression)
```

```
h_vapors_cond=Enthalpy(Water;T=T_vapor_HR_cond-0,1[C];p=p_compression)
```

```
E_vapors_step_compression=E_vapors_step+m_vapors_step*dh_isen
```

```
E_vapors_step_HR=(E_vapors_step_compression-m_vapors_step*h_vapors_cond)
```

```
E_compression_losses=A_compression-(E_vapors_step_compression-E_vapors_step)
```

```
E_elec_MVC=A_compression/3600
```

```
Else "when HR from vapours inactive"
```

```
E_vapors_step_HR=0
```

```
T_vapors_HR=0
```

```
T_vapor_HR_cond=0
```

```
Endif
```

```
end
```

```
Procedure Set_p_initial(i;p_wort_boiling[1..10];p_initial)
```

```
p_initial=p_wort_boiling[i]
```

```
end
```

```

Procedure Set_time_heatingup(i;time_boilingsteps[1..10]:time_heatingup)
time_heatingup=time_boilingsteps[i+1]*60[s/min]
end

```

```

Procedure Calc_Q_testHR(E_vapors_HR;k;A;dT_HR:Q_testHR)
If E_vapors_HR>0 Then
Q_testHR=k*A*dT_HR/1000[W/kW]
Else
Q_testHR=0
EndIf
m_process_add=0
end

```

```

Procedure
CalcQ_testHM(boiler_type;directSteamHeating;k;A;dT;h1;h_process2;Q_process;m_steam_add:Q_testHM;m_
process_add)
If (boiler_type=4) Then "boiler_type=4 signifies direct steam injection"
m_heating_inject=Q_process/(h1-h_process2) "amount of vapour injection necessary, based on enthalpy of
heating medium minus enthalpy of wort in this step = enthalpy of condensate, as vapour condenses in wort"
m_process_add=m_heating_inject "condensed vapour in wort"
Q_testHM=Q_process
EndIf
If (directSteamHeating=1) Then " directSteamHeating=1 signifies final wort treatment step is steam
stripping(no matter what other heating system is generally applied)"
m_heating_inject=m_steam_add "amount of vapour injection necessary, based on enthalpy of heating medium
minus enthalpy of wort in this step = enthalpy of condensate, as vapour condenses in wort"
m_process_add=m_steam_add "condensed vapour in wort"
Q_testHM=Q_process
Else
Q_testHM=k*A*dT/1000[W/kW]
m_process_add=0
EndIf
end

```

```

Procedure CalcQ_HM(boiler_type;directSteamHeating;T_in;T_out;p_heating;p_step;T_step;m_heating:Q)
If (directSteamHeating=1) Or (boiler_type = 4) Then " directSteamHeating=1 signifies final wort treatment step
is steam stripping(no matter what other heating system is generally applied)"
h1=Enthalpy(Water;T=T_in;P=p_heating)
h2=Enthalpy(Water;T=T_step;P=p_step)
Else
h1=Enthalpy(Water;T=T_in;P=p_heating)
h2=Enthalpy(Water;T=T_out;P=p_heating)
EndIf
Q=m_heating*(h1-h2)
end

```

```

subprogram CalcTimeHeating_HR(i;n_steps;A; m_steel; cp_steel;
cp_process;T_step;p_step;T_initial;p_initial;T_init_steel;T_in;T_out;k;m_process;m_process_fill;m_heating;p_h
eating;time_boilingsteps[1..10];E_in_boilingsteps[1..10];HR_in_boilingsteps[1..10];p_wort_boiling[1..10];
t_wort_boiling[1..10];sudhaustype;boiling_time_total;boiling_time_left_vapours;m_vapors;m_vapors_current;
p_compression;eff_isen_mvc;eff_isen_tvc;d;h;T_air;phi_air;addevap;
m_steam_add;m_vapors_add;p_steam_stripping;E_addevap;boiler_type;directSteamHeating;eta_kettle:time_
heatingup;share_HR;Temp;Q_heattransfer)

```

Call Set_time_heatingup(i;time_boilingsteps[1..10]:time_heatingup)

"Calculate vapour formation per time step"

h_process2=Enthalpy(Water;T=T_step;P=p_step)

h_process1=Enthalpy(Water;T=T_initial;p=p_initial)

Call

CalculateVaporsfromBoiling(i;n_steps;p_step;T_step;m_process;h_process1;p_initial;T_initial;boiling_time_total;boiling_time_left_vapours;time_boilingsteps[1..10];E_in_boilingsteps[1..10];m_vapors;m_vapors_current;d;h;T_air;phi_air;addevap;m_vapors_add:m_vapors_step)

T_vapors=T_sat(Water;P=p_step)+0,01[C]

T_vapors_cond=T_sat(Water;P=p_step)-0,01[C]

h_vapors2=Enthalpy(Water;T=T_vapors;P=p_step)

h_vapors1=h_process1

h_process2_test=Enthalpy(Water;x=0;P=p_step)

h_vapors2_test=Enthalpy(Water;x=1;P=p_step)

Call

Calculate_EnergyinVaporsforHR(i;HR_in_boilingsteps[1..10];m_vapors_step;T_step;p_step;p_compression;eff_isen_mvc;eff_isen_tvcs;sudhaustype:E_vapors_HR;T_vapors_HR;T_vapor_HR_cond)

"Calculate heating power available from external heating medium"

CALL CalcQ_HM(boiler_type;directSteamHeating;T_in;T_out;p_heating;p_step;T_step;m_heating:Q)

"Calculate heating power available from HR"

Q_HR=E_vapors_HR/time_heatingup

Q=Q_HM+Q_HR

"Calculate process energy requirement"

m_process_actual=m_process-integral(m_vapors_step/time_heatingup;t;1;time_heatingup)

CALL

CalcQprocess(i;n_steps;m_process_actual;h_process2;h_process1;m_vapors_step;h_vapors2;h_vapors1;time_heatingup;addevap;E_addevap;eta_kettle:Q_process)

"Calculate heat transfer; regular + HR"

dT = abs(((T_in-T_step)+(T_out - T_initial))/2)

h1=Enthalpy(Water;T=T_in;P=p_heating)

CALL

CalcQ_testHM(boiler_type;directSteamHeating;k;A;dT;h1;h_process2;Q_process;m_steam_add:Q_testHM;m_process_add)

dT_HR = ((T_vapors_HR-T_step)+(T_vapor_HR_cond - T_initial))/2

Call Calc_Q_testHR(E_vapors_HR;k;A;dT_HR:Q_testHR)

Q_test=Q_testHM+Q_testHR

Call CheckQ(Q;Q_test;Q_process:Q_heattransfer)

h_process_actual=h_process1 + integral(Q_heattransfer/(m_process_actual);t;1;time_heatingup)

Temp=Temperature(Water;h=h_process_actual;p=p_step)

share_HR=0

end


```

subprogram CalcTimeforHeating_ExternalHM(i;n_steps;A; m_steel; cp_steel;
cp_process;T_step;p_step;T_initial;p_initial;T_init_steel;T_in;T_out;k;m_process;m_process_fill;m_heating;p_h
eating;p_wort_boiling[1..10];
t_wort_boiling[1..10];time_boilingsteps[1..10];E_in_boilingsteps[1..10];boiling_time_total;boiling_time_left_va
pours;m_vapors;m_vapors_current;p_compression;eff_isen_mvc;eff_isen_tvc;d;h;T_air;phi_air
;addevap;m_steam_add;m_vapors_add;p_steam_stripping;E_addevap;boiler_type;directSteamHeating;eta_ke
ttle : time_heatingup;Q_heattransfer;Temp;Q_process)
.....similar subprogramm as CalcTimeHeating_HR however without consideration of heat recovery...
end

```

```

Procedure CalcTimeforHeating(i;n_steps;A; m_steel; cp_steel;
cp_process;T_step;p_step;T_initial;p_initial;T_init_steel;T_in;T_out;k;m_process;m_process_fill;m_heating;p_h
eating;time_boilingsteps[1..10];E_in_boilingsteps[1..10];HR_in_boilingsteps[1..10];p_wort_boiling[1..10];
t_wort_boiling[1..10];sudhaustype;boiling_time_total;boiling_time_left_vapours;m_vapors;m_vapors_current;
p_compression;eff_isen_mvc;eff_isen_tvc;d;h;T_air;phi_air;addevap;
m_steam_add;m_vapors_add;p_steam_stripping;E_addevap;boiler_type;directSteamHeating;eta_kettle:time_
heatingup;share_HR;T_step_reached;Q_heattransfer;share_Qprocess)

```

```

If (sudhaustype <2) or (sudhaustype >3) Then "2 = MVC; 3=TVC"
CALL CalcTimeforHeating_ExternalHM(i;n_steps;A; m_steel; cp_steel;
cp_process;T_step;p_step;T_initial;p_initial;T_init_steel;T_in;T_out;k;m_process;m_process_fill;m_heating;p_h
eating;p_wort_boiling[1..10];
t_wort_boiling[1..10];time_boilingsteps[1..10];E_in_boilingsteps[1..10];boiling_time_total;boiling_time_left_va
pours;m_vapors;m_vapors_current;p_compression;eff_isen_mvc;eff_isen_tvc;d;h;T_air;phi_air;addevap;
m_steam_add;m_vapors_add;p_steam_stripping;E_addevap;boiler_type;directSteamHeating;eta_kettle :
time_heatingup;Q_heattransfer;T_step_reached;Qprocess)
share_HR=0
share_Qprocess=Q_heattransfer/Qprocess
EndIf

```

```

If (sudhaustype =2) or (sudhaustype =3) Then "2 = MVC; 3=TVC"
CALL CalcTimeHeating_HR(i;n_steps;A; m_steel; cp_steel;
cp_process;T_step;p_step;T_initial;p_initial;T_init_steel;T_in;T_out;k;m_process;m_process_fill;m_heating;p_h
eating;time_boilingsteps[1..10];E_in_boilingsteps[1..10];HR_in_boilingsteps[1..10];p_wort_boiling[1..10];
t_wort_boiling[1..10];sudhaustype;boiling_time_total;boiling_time_left_vapours;m_vapors;m_vapors_current;
p_compression;eff_isen_mvc;eff_isen_tvc;d;h;T_air;phi_air;addevap;m_steam_add;m_vapors_add;p_steam_st
ripping;E_addevap;boiler_type;directSteamHeating;eta_kettle:time_heatingup;share_HR;T_step_reached;Q_h
eattransfer)

```

```
EndIf
```

```
end
```

```

Procedure SetTemperaturProfile
(n_steps;time_shift;k;T_wort_External;p_kettle_start;time_boilingsteps[1..10];p_wort_boiling[1..10];T_wort_b
oiling[1..10];T_initial;p_initial;T_step;p_step;duration;last_duration;total_duration)

```

```

If k=0 Then
T_initial=T_wort_External
p_initial=p_kettle_start
total_duration=0
last_duration=0
Else

```

```
p_initial=p_wort_boiling[k]
```

```
T_sat_initial=T_sat(Water;P=p_initial)
T_given_initial=T_wort_boiling[k]
If T_given_initial<=T_sat_initial-0,1[C] Then T_initial := T_given_initial Else T_initial :=T_sat_initial-0,1[C]
```

```
total_duration=0
j:=1
repeat
  total_duration:=total_duration+time_boilingsteps[j]
  j=j+1
until (j>=k+1)
last_duration=time_boilingsteps[k]
```

```
EndIf
```

```
p_step=p_wort_boiling[k+1]
T_sat_step=T_sat(Water;P=p_step)
T_given=T_wort_boiling[k+1]
If T_given<=T_sat_step-0,1[C] Then T_step := T_given Else T_step :=T_sat_step-0,1[C]
duration=time_boilingsteps[k+1]
end
```

Procedure

```
CheckTimeforHeating(z;time_heatingup;start_time;end_time;T_step;T_initial;share_HR;T_step_reached;Q_heating;duration;total_duration;share_Qprocess:end_time_real;start_time_real;y;x;T_initial_real;T_step_real;total_duration_real)
```

"Checks whether steps without HR where heating time was calculated have the correct heating time as specified by user; if not correction of user-data is done by adding more substeps"

"For steps with HR, the reached temperature at the end of the step is checked, if the target has not been reached the time is prolonged"

```
If (T_step_reached>T_step) or (T_step_reached=T_step) Then
```

```
If ((start_time+ time_heatingup)< end_time) Then
```

```
case=1
start_time_real=start_time
end_time_real=end_time
total_duration_real=total_duration
duration_real=duration
T_initial_real=T_initial
T_step_real=T_step
x=1 "variable for counting number of integration steps"
y=0 "variable for counting substep in one step"
EndIf
```

```
If ((start_time+ time_heatingup)>= end_time) Then
```

```
case=2
start_time_real=start_time
end_time_real=start_time+ time_heatingup
total_duration_real=total_duration+(start_time+ time_heatingup-end_time)/60[s/min]
duration_real=duration+(start_time+ time_heatingup-end_time)/60[s/min]
T_initial_real=T_initial
T_step_real=T_step
x=1 "variable for counting number of integration steps"
y=0
EndIf
```

```

Else "If T_step has not been reached"
case=3
start_time_real=start_time
If T_step_reached >T_initial Then
end_time_real=start_time+ time_heatingup*(T_step-T_initial)/(T_step_reached-T_initial)
Else
end_time_real=start_time+ time_heatingup/share_Qprocess
EndIf
total_duration_real=total_duration+(end_time_real-start_time_real)/60[s/min]
duration_real=(end_time_real-start_time_real)/60[s/min]
T_initial_real=T_initial
T_step_real=T_step
x=1 "variable for counting number of integration steps"
y=0 "variable for counting substep in one step"

EndIf
end

```

```

Procedure CheckQprocess(Q_test;Q;Q_process;T_out;T_in;m_heating;cp:Q_process_corr;T_out_corr)
If Q_process>0 Then
Q_process_corr=min(Q_test;Q)
Else
Q_process_corr=0
EndIf
T_out_corr=T_in-Q_process_corr/(m_heating*cp)
end

```

```

Procedure Set_mprocess(i;m_process_init;m_process_last; filling_kettle;
t_filling_kettle;time_boilingsteps[1];t:m_process)
If i =0 Then
If filling_kettle = 0 Then
m_process=m_process_init
Else
m_process_start=m_process_init/t_filling_kettle*(t_filling_kettle-time_boilingsteps[1])
dm= (m_process_init - m_process_start)/(time_boilingsteps[1]*60)
m_process = m_process_start +dm*(t+1)
EndIf
Else
m_process=m_process_last
EndIf
end

```

```

Procedure
SetHeatingMedium(i;n_steps;m_HTM_kettle;p_HTM_kettle;T_HTM_kettle;T_HTM_kettle_out;A_heattransfer_
kettle;k_value_kettle;addevap;
m_steam_add;P[5];p_steam_stripping;time_boilingsteps[1..10];p_wort_boiling[1..10];m_heating;p_heating;T_i
n;T_out;A;k;directSteamHeating)
"set correct heating medium in case of steam stripping as last boiling step"
If (addevap=1) And (i>n_steps-2) Then
directSteamHeating=1
m_heating=m_steam_add/time_boilingsteps[i]
p_heating=p_steam_stripping
T_in=T_sat(Water;P=p_steam_stripping)+0,1
T_out=T_sat(Water;P=p_wort_boiling[i]+0,1) "should be equivalent to P[5]"

```

```

A=A_heattransfer_kettle
k= k_value_kettle
Else
directSteamHeating=0
m_heating=m_HTM_kettle
p_heating=p_HTM_kettle
T_in=T_HTM_kettle
T_out=T_HTM_kettle_out
A=A_heattransfer_kettle
k= k_value_kettle
EndIf
end

```

9.2.3 Biochemical fermentation model

```

T[1]=T_ferm
P[1]=P_ferm
roh_C=Density(CarbonDioxide;T=T[1];P=101,3)
C_p_g=C_p*roh_C "g/l"
"linear relationships between CO2 produced, sugars assimilated and ethanol produced"
S=S_0-Y_S*C_p
E=Y_E_g*C_p" in g/l"
D=D_0-Y_D*C_p
roh_E=Density(Ethanol;T=T[1];P=P[1])
E_ml=((E*Convert(g; kg))/roh_E)*Convert(m^3; ml) "in ml/l"

"main model"
C_p=integral(v_max*S/(K_s+S)*(1/(1+K_i*E^2))*(C_p+C_0*X_0); t; 0; t_total) "C_p in l/l; E and S in g/l"
test_s=S/(K_s+S)
test_e=(1/(1+K_i*E^2))
test_v=v_max*S/(K_s+S)*(1/(1+K_i*E^2))
"dependence of v_max depending on operating conditions"
v_max=(a_T*T_n+a_p*P_n+a_x*X_n+a_TP*T_n*P_n+a_TX*T_n*X_n+a_PX*P_n*X_n+a_0)
T_n=(2*T_ferm-(T_max+T_min))/(T_max-T_min)
P_n=(2*P_ferm-(P_max+P_min))/(P_max-P_min)
X_n=(2*X_0-(X_0_max+X_0_min))/(X_0_max-X_0_min)

"Operating conditions"
ExportFerm$='D:\Bettina\Diss\Brauereimodell\new model\BreweryModel\exportfermentation.csv'
$import 'D:\Bettina\Diss\Brauereimodell\new model\BreweryModel\exportfermentation.csv' T_pitching
T_main_ferm T_final D_0_1 x_ferm P_ferm X_0 t_main t_cooling_tanks
t_total=t_main+t_cooling_tanks
D_0=D_0_1 "g sucrose/100g wort; Plato"
Call WortDensity(D_0:D_0_v)
S_0=D_0_v*10*x_ferm "g/l, initial sugar concentration"
E_0=0 "ml/100ml, initial ethanol concentration"

$include fermentation_Tprofile.emf

Call SetT_ferm(t;T_pitching;T_main_ferm;T_final;t_main;t_cooling_tanks:T_ferm)
T_max=16
T_min=10
P_max=800
P_min=50
X_0_max=20

```

X_0_min=5

"Constants"

"yield coefficients"

Y_S=3,394 "yield coefficient on CO2 based on sugars, g/l"

Y_E=0,251 "yield coefficient on CO2 based on ethanol, ml/100ml"

Y_E_g=Y_E*Convert(ml;l)*roh_E*Convert(l;100ml) "yield coefficient on CO2 based on ethanol, g/l"

Y_D=0,341 "yield coefficient on CO2 based on density, Plato //original value = 0,471"

"kinetic model constants"

K_s = 4,045 "Monod constant accounting for substrate saturation effect, g/l"

K_i = 0,0023 "accounting for ethanol inhibition effect, l²/g²"

C_0=0,278 "vmax*C_0*X_0 represents initial CO2 production rate, l"

"constants for operating conditions dependence"

a_T=0,0260

a_P=-0,0032

a_X=0,0019

a_0=0,0712

a_TP=-0,0005

a_TX=-0,0020

a_PX=0,0001

\$integrate t:1, C_p;C_p_g;D;S;E;E_ml;T_ferm

Procedures:

Procedure WortDensity(p_mass:p_vol)

"Calculate Wort Density based on Lookup1 table"

row0=LookupRow('Lookup 1'; 1;p_mass)

p_vol=Lookup('Lookup 1'; row0; 2)

End

Procedure SetT_ferm(t;T_pitching;T_ferm_main;T_final;t_main;t_cooling:T_ferm)

If t<=24 Then "lag phase; constant temperature, 24 hours"

T_ferm=T_pitching

EndIf

If (t>24) And (t<=36) Then

T_ferm = T_pitching+(T_ferm_main-T_pitching)/(12)*(t-24) "temperature increase to fermentation temperature; 1,5d=36h"

EndIf

If (t>36) And (t<=t_main) Then "main fermentation at specified temperature"

T_ferm=T_ferm_main

EndIf

If t>t_main Then

T_ferm=T_ferm_main-(T_ferm_main-T_final)/(t_cooling)*(t-t_main) "cooling in vessel"

EndIf

End

9.3 Biochemical mashing models

9.3.1 Biochemical mashing model – Model A

"Mashing model A"

MAIN PROGRAMM

"constants"

$R=8,3143[\text{J}/(\text{mol}\cdot\text{K})]$ "gas constant"

"input parameters"

$M_{\text{malt}}=3000[\text{g}] \cdot 10^3$

$\rho_{\text{malt_in_mash}}=1330 [\text{kg}/\text{m}^3]$

$V_{\text{malt}}=M_{\text{malt}}/\rho_{\text{malt_in_mash}}$ "volume of malt in wet mash (14,5-12)"

$V_{\text{sol}}=12[\text{l}] \cdot 10^3$ "volume of liquid phase in the mash = volume of Brew water added to mash"

CALL SetTemperaturProfile

(t;T0;T1;time1;T2;time2;T3;time3;T4;time4;T5;time5;T6;time6;T7;time7;Temp;duration;last_duration;total_duration)

final_end_time=(time1+time2+time3+time4+time5+time6+time7)

start_time=total_duration

end_time=start_time+duration

"initial conditions"

$\alpha_{\text{malt_inital}}=x [\text{g}/\text{l}] \cdot 10^{(-3)}$

$\alpha_{\text{sol_inital}}=0[\text{g}/\text{l}] \cdot 10^{(-3)}$

$\beta_{\text{malt_inital}}=x [\text{g}/\text{l}] \cdot 10^{(-3)}$

$\beta_{\text{sol_inital}}=0[\text{g}/\text{l}] \cdot 10^{(-3)}$

$\text{starch_inital}=x[\text{g}/\text{l}]$

$\text{glucose_inital}=x[\text{g}/\text{l}]$

$\text{maltose_inital}=x[\text{g}/\text{l}]$

$\text{maltotriose_inital}=x[\text{g}/\text{l}]$

$\text{dextrin_inital}=x[\text{g}/\text{l}]$

$\text{saccharose_inital}=x[\text{g}/\text{l}]$

$\text{fructose_inital}=x[\text{g}/\text{l}]$

$\text{limitdextrin_inital}=x[\text{g}/\text{l}]$

"Enzymatic activity of alpha and beta amylase"

"Denaturation coefficients"

$E_{\alpha_denat}=2 \cdot 4,185[\text{J}/\text{mol}] \cdot 10^{(4)}$

"Activation energy, initial unit cal/mol"

$k_{\alpha_0}=2,16[1/\text{min}] \cdot 10^{(11)}$

"Frequency factor"

$E_{\beta_denat}=4,5 \cdot 4,185[\text{J}/\text{mol}] \cdot 10^{(4)}$

"Activation energy, initial unit cal/mol"

$k_{\beta_0}=2,35[1/\text{min}] \cdot 10^{(28)}$

"Frequency factor"

"Dissolution"

$H_{\alpha}=5,1[\text{l}/(\text{g}\cdot\text{min})] \cdot 10^{(-5)}$

$H_{\beta}=5,1[\text{l}/(\text{g}\cdot\text{min})] \cdot 10^{(-5)}$

"Hydrolysis"

$A_{\text{mlt}_0}=3[\text{l}/(\text{g}\cdot\text{min})] \cdot 10^{(13)}$

$A_{\text{dex}_0}=2[\text{l}/(\text{g}\cdot\text{min})] \cdot 10^{(14)}$

$E_{\alpha_mlt}=2 \cdot 4,185[\text{J}/\text{mol}] \cdot 10^{(4)}$

$E_{\alpha_dex}=2 \cdot 4,185[\text{J}/\text{mol}] \cdot 10^{(4)}$

$B_{\text{gl}_0}=9[\text{l}/(\text{g}\cdot\text{min})] \cdot 10^{(12)}$

$B_{\text{mal}_0}=12[1/\text{min}] \cdot 10^{(25)}$

$K_m=40[\text{g}/\text{l}]$

$C=0,67[1/\text{min}] \cdot 10^{(-2)}$

$B_{\text{mlt}_0}=5[\text{l}/(\text{g}\cdot\text{min})] \cdot 10^{(12)}$

$B_{\text{ldex}_0}=2[\text{l}/(\text{g}\cdot\text{min})] \cdot 10^{(13)}$

$E_{\beta_mal}=3,5 \cdot 4,185[\text{J}/\text{mol}] \cdot 10^{(4)}$

$E_{\beta_gl}=2 \cdot 4,185[\text{J}/\text{mol}] \cdot 10^{(4)}$

$E_{\beta_mlt} = 2 \cdot 4,185 [J/mol] \cdot 10^4$
 $E_{\beta_ldex} = 2 \cdot 4,185 [J/mol] \cdot 10^4$

"Equations"

"alpha-amylase - dissolution and denaturation"

$\alpha_malt = \alpha_malt_inital + \int_0^{final_end_time} (-H_{\alpha} \cdot M_{malt} / V_{malt} \cdot (\alpha_malt - \alpha_{sol})) dt$
 $\alpha_{sol} = \alpha_{sol_inital} + \int_0^{final_end_time} (H_{\alpha} \cdot M_{malt} / V_{malt} \cdot (\alpha_{malt} - \alpha_{sol}) - k_{\alpha} \cdot \alpha_{sol}) dt$
 $k_{\alpha} = k_{\alpha_0} \cdot \exp(-E_{\alpha_denat} / (R \cdot Temp))$

"beta-amylase - dissolution and denaturation"

$\beta_malt = \beta_malt_inital + \int_0^{final_end_time} (-H_{\beta} \cdot M_{malt} / V_{malt} \cdot (\beta_malt - \beta_{sol})) dt$
 $\beta_{sol} = (\beta_{sol_inital} + \int_0^{final_end_time} (H_{\beta} \cdot M_{malt} / V_{malt} \cdot (\beta_{malt} - \beta_{sol}) - k_{\beta} \cdot \beta_{sol}) dt)$
 $k_{\beta} = k_{\beta_0} \cdot \exp(-E_{\beta_denat} / (R \cdot Temp))$

"starch"

$starch = starch_inital + \int_0^{final_end_time} (-\alpha_{sol} \cdot starch \cdot (0,964 \cdot A_{mlt} + A_{dex})) dt$

"glucose"

$glucose = glucose_inital + \int_0^{final_end_time} (B_{gl} \cdot \beta_{sol} \cdot dextrin) dt$

"maltose"

$maltose = maltose_inital + \int_0^{final_end_time} (B_{mal} \cdot \beta_{sol} \cdot dextrin / (K_m + dextrin)) dt$

"maltotriose"

$maltotriose = maltotriose_inital + \int_0^{final_end_time} (A_{mlt} \cdot \alpha_{sol} \cdot starch + B_{mlt} \cdot \beta_{sol} \cdot dextrin) dt$

"dextrins"

$dextrin = dextrin_inital + \int_0^{final_end_time} (A_{dex} \cdot \alpha_{sol} \cdot starch - \beta_{sol} \cdot dextrin \cdot (0,9 \cdot B_{gl} + 0,947 \cdot B_{mal} / (K_m + dextrin) + 0,964 \cdot B_{mlt} + B_{ldex})) dt$

"limitdextrins"

$limitdextrin = limitdextrin_inital + \int_0^{final_end_time} (B_{ldex} \cdot \beta_{sol} \cdot dextrin) dt$

total_extract = glucose + maltose + maltotriose + saccharose + fructose + dextrin + limitdextrin

total_extract_ferm = glucose + maltose + maltotriose + saccharose + fructose

"arrhemius relationships"

$A_{mlt} = A_{mlt_0} \cdot \exp(-E_{\alpha_mlt} / (R \cdot (Temp)))$

$A_{dex} = A_{dex_0} \cdot \exp(-E_{\alpha_dex} / (R \cdot (Temp)))$

$B_{mal} = B_{mal_0} \cdot \exp(-E_{\beta_mal} / (R \cdot (Temp)))$

$B_{gl} = B_{gl_0} \cdot \exp(-E_{\beta_gl} / (R \cdot (Temp)))$

$B_{mlt} = B_{mlt_0} \cdot \exp(-E_{\beta_mlt} / (R \cdot (Temp)))$

$B_{ldex} = B_{ldex_0} \cdot \exp(-E_{\beta_ldex} / (R \cdot (Temp)))$

\$integrale table t:1,

$\alpha_malt; \alpha_{sol}; \beta_malt; \beta_{sol}; starch; glucose; maltose; maltotriose; dextrin; limitdextrin; saccharose; fructose; k_{\alpha}; k_{\beta}; total_extract_ferm; total_extract; Temp$

Procedures:

Procedure SetTemperaturProfile

(t;T0;T1;time1;T2;time2;T3;time3;T4;time4;T5;time5;T6;time6;T7;time7:Temp;duration;last_duration;total_duration)

$$Temp = (273,15 + T_{initial}) + \frac{T_{step} - T_{initial}}{duration * 60} * (t - total_{duration} * 60)$$

End

9.3.2 Biochemical mashing model – Model B

"Mashing model B"

"constants"

$$R = 8,3143 \left[\frac{J}{mol \cdot K} \right]$$

"input parameters"

$$M_{malt} = 3000[g] * 10^3$$

$$V_{sol} = 12[l] * 10^3 \text{ "volume of liquid phase in the mash = volume of Brew water added to mash"}$$

$$approx_{mash,gravity} = M_{malt} * \frac{0,75}{V_{malt} * 10 \left[\frac{100ml}{l} \right]} \text{ "g extract/l wort"}$$

"bei 15,5g/100ml wort acc. to Plato wort density approx. 1058 kg/m³"

CALL SetTemperaturProfile

(t;T0;T1;time1;T2;time2;T3;time3;T4;time4;T5;time5;T6;time6;T7;time7:Temp;duration;last_duration;total_duration)

$$final_end_time = (time1 + time2 + time3 + time4 + time5 + time6 + time7) * 60$$

$$start_time = total_duration * 60$$

$$end_time = start_time + duration * 60$$

"initial conditions"

$$alpha_malt_inital = x[U/kg]$$

$$alpha_sol_inital_0 = x[U/kg]$$

$$beta_malt_inital = x[U/kg]$$

$$beta_sol_inital_0 = x[U/kg]$$

$$starch_inital = x[g/l] / roh_wort$$

$$glucose_inital = x[g/l] / roh_wort$$

$$maltose_inital = x[g/l] / roh_wort$$

$$maltotriose_inital = x[g/l] / roh_wort$$

$$dextrin_inital = x[g/l] / roh_wort$$

$$saccharose_inital = x[g/l] / roh_wort$$

$$fructose_inital = x[g/l] / roh_wort$$

$$limitdextrin_inital = x[g/l] / roh_wort$$

$$a_alpha_inital = 1$$

$$a_beta_inital = 1$$

$$alpha_sol_inital = alpha_sol_inital_0 / a_alpha_inital$$

$$beta_sol_inital = beta_sol_inital_0 / a_beta_inital$$

"Enzymatic activity of alpha and beta amy

"Gelatinization"

$$kg1 = 5,7 [1/s] * 10^{(31)} \text{ "below gelatinization temp"}$$

$$E_g1 = 220,6 [J/mol] * 10^{(3)}$$

$$kg2 = 3,1 [1/s] * 10^{(14)} \text{ "above gelatinization temp"}$$

$$E_g2 = 108,3 [J/mol] * 10^{(3)}$$

"Denaturation coefficients"

$$E_alpha_denat = 224,2 [J/mol] * 10^{(3)}$$

$$k_alpha_0 = 6,9 [1/s] * 10^{(30)}$$

"Activation energy, initial unit cal/mol"

"Frequency factor"

$$E_beta_denat = 410,7 [J/mol] * 10^{(3)}$$

$$k_beta_0 = 7,6 [1/s] * 10^{(60)}$$

"Activation energy, initial unit cal/mol"

"Frequency factor"

"Hydrolysis"

$k_{gl}=0,023 \text{ [kg/(U*s)]}$

$k_{mlt}=0,117 \text{ [kg/(U*s)]}$

$k_{dex}=0,317 \text{ [kg/(U*s)]}$

$k_{\alpha_mal}=0,389 \text{ [kg/(U*s)]}$

$k_{\beta_mal}=0,137 \text{ [kg/(U*s)]}$

"from dextrans"

$k1_{gl}=2,9 \text{ [kg/(U*s)]*10}^{-8}$

$k1_{mlt}=1,5 \text{ [kg/(U*s)]*10}^{-8}$

$k1_{\alpha_mal}=1,2 \text{ [kg/(U*s)]*10}^{-7}$

$k1_{\beta_mal}=8,4 \text{ [kg/(U*s)]*10}^{-8}$

"Equations"

"Gelatinization"

CALL GelatinizationRate(T_gelatinisation;kg1;kg2;E_g1;E_g2;R;Temp;starch_s:r_g)

$starch_s=starch_initial - \text{integral}(r_g;t;0;final_end_time)$

"alpha-amylase - T-dependent activity and denaturation"

CALL Activity_Alpha(Temp:a_alpha)

$r_act_alpha=k_alpha*\alpha_sol$

$\alpha_sol=(\alpha_sol_initial - \text{integral}(r_act_alpha;t;0;final_end_time))*(a_alpha)$

$k_alpha=k_alpha_0*\exp(-E_alpha_denat/(R*Temp))$

"beta-amylase - T-dependent activity and denaturation"

CALL Activity_Beta(Temp:a_beta)

$r_act_beta=k_beta*\beta_sol$

$\beta_sol=(\beta_sol_initial - \text{integral}(r_act_beta;t;0;final_end_time))*(a_beta)$

$k_beta=k_beta_0*\exp(-E_beta_denat/(R*Temp))$

"starch"

$starch = \text{integral}(r_g-r_gl-r_mal-r_mlt-r_dex;t;0;final_end_time) \text{ "gelatinized starch"}$

"glucose"

$r_gl=k_gl*\alpha_sol*starch$

$r_gl1=k1_gl*\alpha_sol*dextrin$

$glucose=glucose_initial+\text{integral}(r_gl+r_gl1;t;0;final_end_time)$

"maltose"

$r_mal=k_alpha_mal*\alpha_sol*starch+k_beta_mal*\beta_sol*starch$

$r_mal1=k1_alpha_mal*\alpha_sol*dextrin+k1_beta_mal*\beta_sol*dextrin$

$maltose=maltose_initial+\text{integral}(r_mal+r_mal1;t;0;final_end_time)$

"maltotriose"

$r_mlt=k_mlt*\alpha_sol*starch$

$r_mlt1=k1_mlt*\alpha_sol*dextrin$

$maltotriose=maltotriose_initial+\text{integral}(r_mlt+r_mlt1;t;0;final_end_time)$

"dextrans"

$r_dex=k_dex*\alpha_sol*starch$

$dextrin=dextrin_initial+\text{integral}(r_dex-r_mlt1-r_mal1-r_gl1;t;0;final_end_time)$

"limitdextrans"

$total_extract=glucose+maltose+maltotriose+saccharose+fructose+dextrin+limitdextrin$

$total_extract_ferm=glucose+maltose+maltotriose+saccharose+fructose$

$starch_print=starch_s*roh_wort \text{ "[g/kg * kg/l = g/l]"}$

$glucose_print=glucose*roh_wort$

$maltose_print=maltose*roh_wort$

$maltotriose_print=maltotriose*roh_wort$

$dextrin_print=dextrin*roh_wort$

```

limitdextrin_print=limitdextrin*roh_wort
saccharose_print=saccharose*roh_wort
fructose_print=fructose*roh_wort
total_extract_print=total_extract*roh_wort
total_extract_ferm_print=total_extract_ferm*roh_wort

```

```

$integraltable t:1,
alpha_malt_inital;alpha_sol;beta_malt_inital;beta_sol;starch_print;glucose_print;maltose_print;maltotriose_pr
int;dextrin_print;limitdextrin_print;saccharose_print;fructose_print;a_alpha;a_beta;k_alpha;k_beta;total_extrac
t_ferm_print;total_extract_print;Temp

```

Procedures:

Procedure SetTemperaturProfile

```

(t;T0;T1;time1;T2;time2;T3;time3;T4;time4;T5;time5;T6;time6;T7;time7;Temp;duration;last_duration;total_dur
ation)

```

$$Temp = (273,15 + T_{initial}) + \frac{T_{step} - T_{initial}}{duration * 60} * (t - total_{duration} * 60)$$

End

"acc. to model B: alpha- and beta amylase and inital hydrocarbons can be considered as immidiately dissolved in liquid phase --> no dissultion calculated"
"gelatinization not instantanuus"

Procedure GelatinizationRate(T_gelatinisation;kg1;kg2;E_g1;E_g2;R;Temp;starch_s:r_g)

```

If Temp <(273 [K]+T_gelatinisation) Then

```

```

r_g=kg1*exp(-E_g1/(R*Temp))*starch_s

```

```

Else

```

```

r_g=kg2*exp(-E_g2/(R*Temp))*starch_s

```

```

EndIf

```

```

End

```

Procedure Activity_Alpha(Temp:a_alpha)

```

If Temp < 312 Then

```

```

a_alpha=1

```

```

EndIf

```

```

If (Temp >=312) and (Temp<336) Then

```

```

a_alpha=-0,0011229*Temp^3+1,091*Temp^2-352,89*Temp+38003,3

```

```

EndIf

```

```

If (Temp >=336) and (Temp<347) Then

```

```

a_alpha=0,0055023*Temp^3-5,663*Temp^2+1941,9*Temp-221864

```

```

EndIf

```

```

If Temp >= 347 Then

```

```

a_alpha=0

```

```

EndIf

```

```

End

```

Procedure Activity_Beta(Temp:a_beta)

```

If Temp < 312 Then

```

```

a_beta=1

```

```

EndIf

```

```

If (Temp >=312) and (Temp<336) Then

```

```

a_beta=0,049*Temp-13,9

```

```

EndIf

```

```

If (Temp >=336) and (Temp<342) Then

```

```

a_beta=-0,374*Temp+128,3
EndIf
If Temp >= 342 Then
a_beta=0
EndIf
End

```

```

Procedure Checkalpha_sol(alpha_sol:alpha_sol_check)
If alpha_sol < 0 Then
alpha_sol_check = 0
Else
alpha_sol_check = alpha_sol
EndIf
end

```

9.3.3 Biochemical mashing model – Model C

"input parameters acc. to laboratory tests"

$M_{\text{malt}}=1,5[\text{g}] \cdot 10^3$

$V_{\text{sol}}=6[\text{l}]$ "volume of liquid phase in the mash = volume of Brew water added to mash"

"initial conditions acc. to malt analyses"

$\alpha_{\text{malt_inital}}=xy[\text{g/l}] \cdot 10^{-3}$

$\alpha_{\text{sol_inital}}=\alpha_{\text{malt_inital}}$

$\beta_{\text{malt_inital}}=xy[\text{g/l}] \cdot 10^{-3}$

$\beta_{\text{sol_inital}}=\beta_{\text{malt_inital}}$

$\text{starch_inital}=130,61 [\text{g/l}]$

$\text{glucose_inital}=6,23 [\text{g/l}]$

$\text{maltose_inital}=1,45[\text{g/l}]$

$\text{maltotriose_inital}=0,83[\text{g/l}]$

$\text{dextrin_inital}=29,16 [\text{g/l}]$

$\text{saccharose_inital}=7,68 [\text{g/l}]$

$\text{fructose_inital}=1,04 [\text{g/l}]$

$\text{limitdextrin_inital}=0 [\text{g/l}]$

"Changes with respect to Model A:"

- 1) Immediate dissolution of enzymes

$\alpha_{\text{sol}}=\alpha_{\text{sol_inital}}+\text{integral}(-k_{\alpha} \cdot \alpha_{\text{sol}};t;0;\text{final_end_time})$

$\beta_{\text{sol}}=(\beta_{\text{sol_inital}}+\text{integral}(-k_{\beta} \cdot \beta_{\text{sol}};t;0;\text{final_end_time}))$

- 2) Slightly lower activation energy for β -denaturation

$E_{\beta\text{denat}}=4,488 \cdot 4,185[\text{J/mol}] \cdot 10^4$

- 3) slightly higher value for glucose formation

$B_{\text{gl}_0}=12,5[\text{l}/(\text{g} \cdot \text{min})] \cdot 10^{12}$

10 APPENDIX B – SOCO

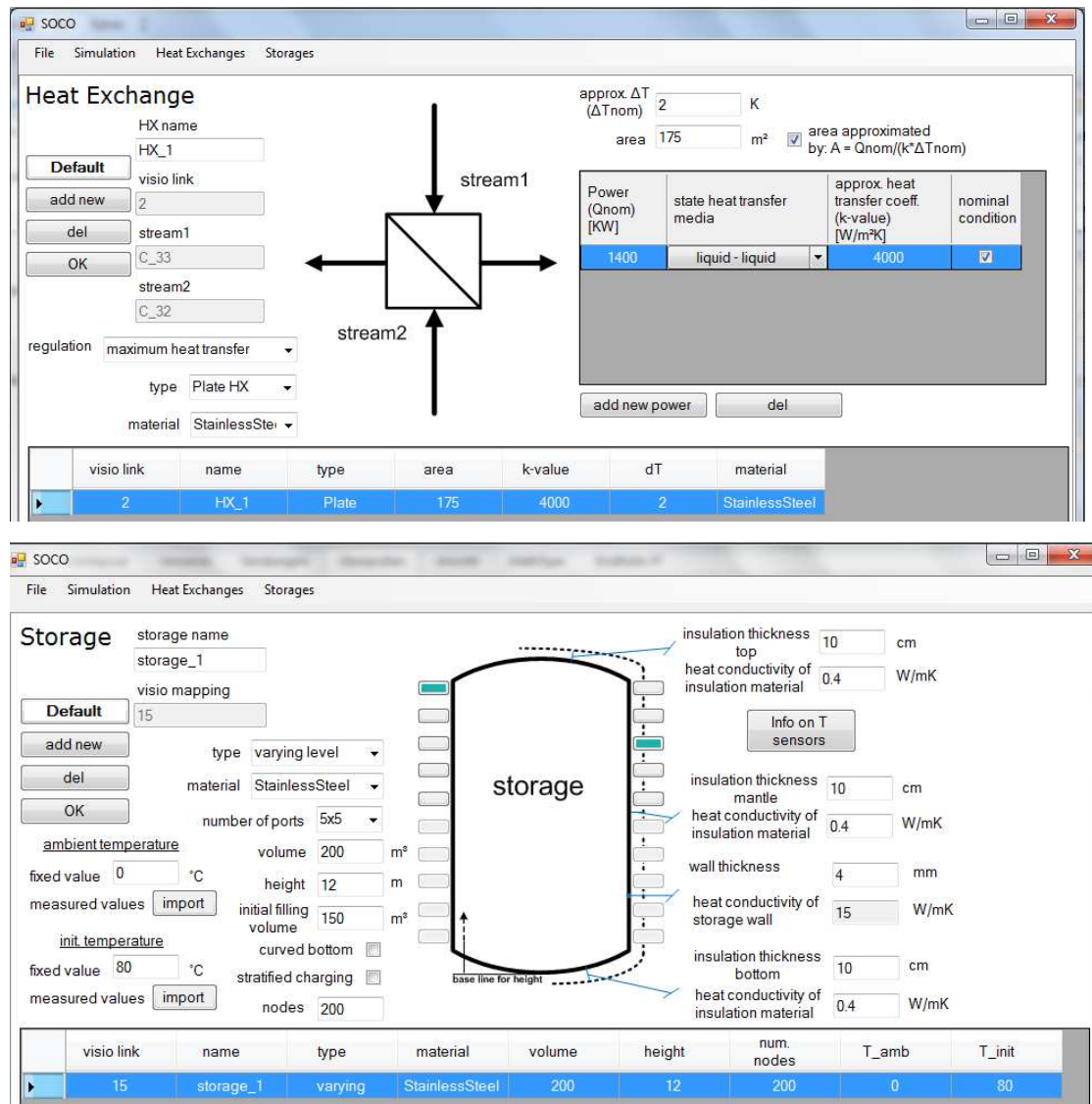


Figure 10-1: Screenshots of data entry mask for storage and HX definition

Table 10-1: Stream data overview for brewery site 1 and site 4

	Brewery Site 1					
	Time-Average Data			Peak data		
	T _{in} [°C]	T _{out} [°C]	C _p [kJ/K]	T _{in} [°C]	T _{out} [°C]	C _p [kJ/K]
Brew Water for Mashing and Sparging a)	10,00	80,00	4,85E+01	10,00	80,00	1,30E+02
Brew Water for Mashing and Sparging b&c)	10,00	75,00	5,23E+01	10,00	75,00	1,40E+02
Mashing	65,89	66,17	2,43E+03	56,90	75,53	4,39E+03
Wort Preheating	75,00	95,00	9,66E+01	75,00	95,00	9,80E+01
Boiling	100,6	101,10	6,15E+03	94,50	106,90	7,83E+04
Bottle Washing	78,30	79,70	4,00E+02	49,00	80,00	2,99E+03
Flash Pasteurisation	68,00	72,00	5,60E+01	68,00	72,00	5,60E+01

Tunnel Pasteurisation	58,90	59,90	2,58E+02	39,00	60,00	1,40E+03
Hot Water a)	10,00	80,00	1,00E+01	10,00	80,00	7,43E+01
Hot Water b)	10,00	80,00	5,14E+00	10,00	80,00	3,82E+01
Hot Water c)	10,00	75,00	5,14E+00	10,00	75,00	3,82E+01
Vapour Condensation	99,90	75,00	1,78E+02	99,90	75,00	2,22E+02
Wort Cooling	88,00	10,00	7,09E+01	88,00	10,00	7,12E+01
Waste Heat Cooling Compressors	75,00	40,00	7,29E+00	75,00	40,00	2,42E+01
Brewery Site 4						
	Time-Average Data			Peak data		
	Tin [°C]	Tout [°C]	Cp [kJ/K]	Tin [°C]	Tout [°C]	Cp [kJ/K]
Brew Water for Mashing and Sparging a)	10,00	80,00	1,88E+01	10,00	80,00	4,04E+01
Brew Water for Mashing and Sparging b&c)	10,00	75,00	2,02E+01	10,00	75,00	4,35E+01
Mashing	64,60	65,00	9,99E+02	56,10	75,00	4,39E+03
Wort Preheating	75,00	95,00	6,24E+01	75,00	95,00	6,47E+01
Boiling	100,70	101,10	1,46E+03	94,50	102,30	6,22E+03
Bottle Washing	78,30	79,70	4,00E+02	49,00	80,00	2,99E+03
Flash Pasteurisation	68,00	72,00	5,60E+01	68,00	72,00	5,60E+01
Tunnel Pasteurisation						
Hot Water a)	10,00	80,00	8,19E+00	10,00	80,00	2,87E+01
Hot Water b)	10,00	80,00	5,13E+00	10,00	80,00	1,80E+01
Hot Water c)	10,00	75,00	5,13E+00	10,00	75,00	1,80E+01
Vapour Condensation	103,60	75,00	2,06E+01	103,60	75,00	2,38E+01
Wort Cooling	97,00	10,00	3,56E+01	97,00	10,00	3,56E+01
Waste Heat Cooling Compressors	75,00	40,00	4,37E+00	75,00	40,00	1,45E+01

HX and Storage Proposal Simulation

Detailed simulation settings

stream name	Criteria settings	HX settings	Storage settings
<input checked="" type="checkbox"/> mashing	Energy <input type="text" value="0.3"/>	Min. Power <input type="text" value="5"/> kW	Min. volume <input type="text" value="0.5"/> m ³
<input checked="" type="checkbox"/> wort preheating	Power <input type="text" value="0.1"/>	Min. Energy transfer (based on total energy requirement) <input type="text" value="0.5"/> %	Max. volume <input type="text" value="200"/> m ³
<input checked="" type="checkbox"/> wort boiling	Exergy <input type="text" value="0.6"/>	Load in HX should not exceed average load by <input type="text" value="100"/> times	Possible Storage mode <input type="text"/>
<input checked="" type="checkbox"/> vapours	Sum <input type="text" value="1"/>	k-value <input type="text" value="4000"/> W/m ² K	Temperature levels of +/- <input type="text" value="5"/> K <small>will be integrated in one storage</small>
<input checked="" type="checkbox"/> wort cooling	Pinch delta T <input type="text" value="2"/> K	dT <input type="text" value="3"/> K	Minimum mass flow for creation of new storage <input type="text" value="0.3"/> %
<input checked="" type="checkbox"/> waste heat co..			
<input checked="" type="checkbox"/> BottleWashing			

After separating streams for HX Proposal in Above/Below Pinch Region only streams with > % energetic value of the initial stream will be considered in proposal generation

After HX generation, remaining streams with > % energetic value of the initial stream will be considered in proposal generation

Figure 10-2: Settings for the HESN algorithm in SOCO

Table 10-2: Heat exchanger parameters for simulations of the heat integration concept

Heat exchange data	Area	approximate k-value	dT _{min}
	[m ²]	[W/m ² K]	[K]
Vapour Condenser	312.5	4000	2
Vapour Condenser, Run 2	625	4000	2
Wort pre-cooler	125	4000	2
Wort cooler	250	4000	2
Wort cooler, Run 2	1000	4000	2
Wort preheating	400	2500	2
Mashing, Site 1	150	2500	8
Mashing, Site 4	150	2500	4



Figure 10-3: Storage parameters for simulations of the heat integration concept

11 APPENDIX C – NEW MASHING TECHNOLOGY

11.1 Experimental results

Table 11-1: Malt analysis

Malt sample Best Pilsner Malt 2012187313001	value	unit
Water content	4.6	%
Extract Malt	79	% lftr.
Extract Malt (DS)	82.8	% wfr.
α -amylase	52.8	ASBC, wfr.
Diastatic Power	316	WK
Gelatinization temperature	63.9	°C
Starch content	54	%

Table 11-2: Experimental results of extract and sugar analysis

TEST1	total extract		Sucrose		Glucose		Maltose	
	°P [g/100ml]	StdAW	[g/l]	StdAW	[g/l]	StdAW	[g/l]	StdAW
	10.06	0.58	7.42	0.21	6.22	0.09	42.19	1.07
	13.73	0.16	8.24	0.53	9.43	0.25	64.59	0.93
	15.47	0.10	7.25	0.53	10.86	0.20	76.91	0.26
	16.95	0.02	6.76	0.41	11.77	0.07	86.63	1.94
	17.30	0.10	6.45	0.21	11.74	0.23	85.94	0.00
	17.45	0.03	7.49	0.91	11.39	0.64	86.96	2.06
	17.43	0.03	6.79	0.36	11.59	0.08	85.33	0.85
	17.50	0.03	6.75	0.06	11.87	0.18	89.05	0.22
Test2	total extract		Sucrose		Glucose		Maltose	
	°P [g/100ml]		[g/l]	StdAW	[g/l]	StdAW	[g/l]	StdAW
	11.30	0.00	7.96	0.10	8.02	0.46	49.69	1.90
	14.05	0.11	7.09	1.71	10.98	0.82	66.16	0.26
	15.73	0.23	8.91	2.25	11.27	0.40	76.17	2.78
	17.06	0.25	8.17	2.11	12.26	0.27	89.18	0.48
	17.31	0.00	7.37	0.00	12.26	0.00	91.52	0.00
	17.43	0.06	6.79	0.70	12.38	0.05	91.49	1.12
	17.40	0.00	6.41	0.48	12.07	0.11	88.86	3.50
	17.79	0.07	7.15	0.46	12.24	0.29	90.06	2.31

Test3	total extract		Sucrose		Glucose		Maltose	
	°P [g/100ml]		[g/l]	StdAW	[g/l]	StdAW	[g/l]	StdAW
	9.4	0.0	17.7	10.5	6.2	0.5	42.9	13.7
	14.4	0.2	0.0	0.0	0.0	0.0	64.5	6.9
	15.4	0.4	0.0	0.0	10.7	0.2	75.0	1.7
	16.9	0.0	0.0	0.0	0.0	0.0	80.9	7.5
	17.4	0.1	0.0	0.0	12.2	0.6	86.8	3.3
	17.5	0.0	0.0	0.0	0.0	0.0	89.3	1.0
	17.4	0.0	6.6	0.3	12.0	0.6	90.7	1.1
TEST4	total extract		Sucrose		Glucose		Maltose	
	°P [g/100ml]		[g/l]	StdAW	[g/l]	StdAW	[g/l]	StdAW
	10.03	0.45	8.81	1.30	6.56	0.22	45.38	3.35
	13.81	0.02					67.34	0.69
	15.39	0.45			11.44	0.19	83.67	0.74
	16.83	0.03					93.24	0.94
	17.42	0.02			12.74	0.25	96.80	0.47
	17.69	0.02					96.70	0.81
	17.71	0.01	6.18	0.46	12.98	0.11	95.08	0.65
TEST9	total extract		Sucrose		Glucose		Maltose	
	°P [g/100ml]		[g/l]	StdAW	[g/l]	StdAW	[g/l]	StdAW
	10.01	0.61	8.77	0.23	5.81	0.10	45.08	1.95
	13.67	0.12					65.28	0.05
	15.67	0.02			10.97	0.00	78.91	1.41
	16.60	0.14					89.20	2.34
	17.42	0.06			12.55	0.22	94.35	0.59
	17.41	0.09					95.82	1.70
	17.59	0.04	6.41	0.60	12.94	0.02	93.70	0.60
TEST6	total extract		Sucrose		Glucose		Maltose	
	°P [g/100ml]		[g/l]	StdAW	[g/l]	StdAW	[g/l]	StdAW
	10.08	0.93	9.20	0.94	6.11	0.48	43.96	4.90
	14.14	0.03					69.71	0.80
	15.68	0.09			11.03	0.12	82.15	1.06
	17.04	0.04					92.00	0.89
	17.49	0.07			12.46	0.11	96.39	1.32
	17.59	0.08					96.39	0.81
	17.72	0.04	6.46	0.17	12.26	0.03	94.91	1.48

TEST8	total extract		Sucrose		Glucose		Maltose	
	°P		[g/l]	StdAW	[g/l]	StdAW	[g/l]	StdAW
	[g/100ml]		[g/l]		[g/l]		[g/l]	
	9.6	0.3	8.6	0.1	6.0	0.5	44.1	2.5
	14.1	0.2					68.3	2.3
	15.1	0.1			10.7	0.1	76.7	2.5
	16.0	0.1					85.3	1.9
	16.4	0.0			11.1	0.9	88.2	0.3
	17.1	0.1					96.1	2.3
	17.4	0.0			12.9	0.2	97.1	2.0
Test1 HG	total extract		Sucrose		Glucose		Maltose	
	°P		[g/l]	StdAW	[g/l]	StdAW	[g/l]	StdAW
	[g/100ml]		[g/l]		[g/l]		[g/l]	
	10.05	1.48	9.45	0.28	7.69	1.48	39.31	6.34
	16.48	0.17					75.84	0.16
	18.66	0.16			15.02	0.28	90.70	1.41
	21.46	0.02					116.69	0.43
	21.69	0.08			16.48	0.13	110.20	1.77
	21.82	0.03					111.78	0.68
	21.83	0.12					109.54	2.90
Test4 HG	total extract		Sucrose		Glucose		Maltose	
	°P		[g/l]	StdAW	[g/l]	StdAW	[g/l]	StdAW
	[g/100ml]		[g/l]		[g/l]		[g/l]	
	11.72	0.65	9.72	1.18	8.13	0.74	48.34	1.57
	16.69	0.18					78.57	0.95
	18.47	0.25			14.05	0.56	91.64	5.03
	20.38	0.20					109.93	0.04
	21.30	0.41			17.13	0.07	117.51	1.75
	21.92	0.15					118.91	1.62
	21.93	0.12	6.49	0.51	17.50	0.37	112.80	1.41

Table 11-3: Experimental results of FAN, β -glucan and pH of final test samples

	FAN	β-glucan	pH
	g/l	mg/l	
Test 1	312.5	260.5	5.92
Test 2	325.4	282.4	5.95
Test 3	309.0	245.2	5.95

Test 4	328.3	245.8	5.94
Test 9	not analysed		5.99
Test 6	325.3	231.8	5.99
Test 8	322.9	249.4	5.92
Test 1 HG	328.35	417.3	5.82
Test 4 HG	299.15	433.4	5.83

12 APPENDIX D –NOMENCLATURE, REFERENCES

12.1 Nomenclature

Due to the large number of variables used throughout the calculations of the Brewery Model, at first general abbreviations and indices are declared which are the basis for the logic of the variable naming. Then selected combinations are presented of those variables for which equations have been given in the main text.

general terms	
AW	cast wort
A	heat transfer area [m ²]
C _p	Heat capacity flow rate of process streams [kJ/kg.K]
D	diffusion coefficient [m/s]
dE (Brewery Model)	energy difference [kJ]
dE (SOCO)	Difference between energy availability and energy demand [kWh/timestep]
E	Energy [kJ]
E _{spec}	specific energy demand [MJ/hl]
EER	Energy efficiency ratio for cooling compressors (COP)
FET	final thermal energy demand
h	specific enthalpy [kJ/kg]
HEN	Heat Exchanger Network
HESN	Heat exchanger and storage network
HR	Heat Recovery
k-value	Heat transfer coefficient [W/m ² .K]
m	mass [kg]
MEDTtech	minimal thermal energy demand per technology
MJ/hl	Thermal energy intensity (GJ/m ³)
MM	molar mass [g/mol]
n	number
η	efficiency
η	viscosity [mPas]
p _{mass}	extract content as percentage by mass [g/100g]
p _{vol}	extract content as percentage by volume [g/100ml]
perc	percentage
Q	power [kW]
Q _{cold}	cooling demand [kW]
QHx	Power of heat exchange [kW]
Q _{process}	Thermal power required for process heating [kW]
R	ideal gas constant [J/mol.K]
ρ	density [kg/m ³]
S	surface area [m ²]
s	specific entropy [kJ/kg]
T	temperature [°C]
t	time

U	U-value [W/m ² K]
UPH	useful process heat
USH	useful supply heat
V	volume [m ³]
x_ferm	fermentation rate
y	flash gas ratio at given temperature and pressure
ΔT_HX	Minimal temperature difference required in respective heat exchanger [K]
indices and abbreviations	
addevap	additional evaporation after trub separation
AWc	cold cast wort
AWh	hot cast wort
bath	bath of washing medium in bottle or keg washer
BC	beer cooler
boilmash	boilmash seperated from main mash tun
BW	hot brew water required for mash liquor
BW	brew water
BWC	brew water cooler
CIP	cleaning in place
CP, pal	chamber pasteurization (pasteurizers for pallets)
CW	chilled / cold water entering the wort cooler
CW	chilled water
evap	Evaporation
evaporation	evaporation in the wort kettle
FP	flash pasteurization
FW	cold brew water (e.g. required for mash liquor)
h	Hours
hottrub	hot trub separated during whirlpool operation
HTM, HM	heat transfer medium
HW	hot water
HX	heat exchanger
i	Index for each time step
in	Incoming
isen	Isentropic
j....n	Indices for each process step
kettlefull	wort withdrawn from wort separation to kettle
mash	Mashliquor
mash_total	total mash liquor (mash liquor and weak wort recovery)
mashing	mashing process / complete mash
mat	Maturation
min	Minutes
MVC	mechanical vapour compression
out	Outgoing
pack (Gebinde)	packaged unit (bottle, keg, can)

pal	pasteurizer for pallets
past	pasteurization
pfaduko	vapour condenser
poly	Polytropic
rec	recovered from vapour condensate
ref	Reference
rinse	sparges/rinses in wort separation
room	surrounding atmosphere in which process unit is placed
s	Seconds
sat	Saturation
sm	storage medium
spgrain	spent grain
SS	steam stripping
steam,SS	steam used in steam stripping
steam_add	steam added in steam stripping
step	process step; change of temperature and/or pressure within a specified time
step	process step
steril	Sterilisation
TP	tunnel pasteurization
TVC	thermal vapour compression
vaporcond	vapour condensation
vapors	vapours from wort evaporation
vapours_add	vapours from additional evaporation step
VE	vaccum evaporation
w	Water
WC	wort cooler
weakwort / ww	weak wort withdrawn for recovery in mashing
WM	bottle washing machine
WW	Warm water
YC	yeast cooling

selected combinations	
capacity_BC	capacity of beer cooler [hl/h]
capacity_BWC	capacity of brew water cooler [hl/h]
dE_storable	Amount of energy available at respective time step [kWh/timestep]
dTmin	Minimal temperature difference required in heat exchange
E_BW_mashing	energy content of hot brew water required for the mashing process [kJ]
E_cs	Energy content of cold stream [kWh/timestep]
E_ferm	fermented extract per time step [kg/l.s]
E_hs	Energy content of hot stream [kWh/timestep]
E_HX_hs	amount of energy required from the hot stream [kWh/timestep]
E_HX_hs_direct	amount of energy required from the hot stream for direct heat exchange [kWh/timestep]
E_HX_hs_indirect	amount of energy required from the hot stream for indirect heat exchange over storage [kWh/timestep]

E_mash_to_lautering	energy content of mash withdrawn to wort separation [kJ]
E_operation	energy demand for bottle washing during continuous operation [kJ]
E_preheating_Estore	energy for wort preheating coming from the energy storage [kJ]
E_preheating_External	energy for wort preheating from "external" energy supply (not from heat recovery), e.g. boiler [kJ]
E_startup	energy demand at start up for bottle washing [kJ]
E _{mainmashj}	Energy demand in mash step j [kJ]
h_air	height of air above kettle [m]
m_AW	mass of wort leaving the wort kettle [kg]
m_AW_addevap	mass of wort after the additional evaporation step [kg]
m_AW_final	mass of wort entering the wort cooler [kg]
m_AW_whirlpool	mass of wort after hot trub separation [kg]
m_pack_avg	average weight of empty unit for packaging [kg]
m_sm	Mass flow of heat storage medium [kg/timestep]
m_spray_bath	mass of cleaning medium/water being sprayed onto kegs and being recycled to the bath [kg]
m _{extract,ww}	Mass of extract in weak wort [kg]
m _{process}	Mass of process medium [kg]
m _{spgrain}	Mass of spent grain [kg]
m _{weakwort,rec,mash}	Mass of weak wort which is recovered to the mash [kg]
n_brews_week	number of brews per week
n_charge	number of charges pasteurized in a pallet pasteurizer
n_pack_per_pallet	number of packaged units per pallet
n_pallet_charge	number of pallets per charge
n_startup	number of start-ups per week
p_vapourcond	pressure in vapour condenser
p_w_spgrain	extract content of spent grains
perc_recovery_TP	percentage of thermal energy recovered in tunnel pasteurization over recycle of water/wash medium flows
p _{water_spgrain}	Water content of spent grain [kg/kg]
Q_cold_BC	cold demand for beer cooler [kW]
Q_cold_BWC	cold demand for brew water cooler [kW]
Q_ferm	cold demand for fermentation tanks [kW]
q_ferm	specific heat of reaction of fermentation [kJ/kg]
Q_operation_WM	thermal power required for the bottle washer during continuous operation [kW]
state 1	room atmosphere
state 2	atmosphere in kettle (wort boiling)
state 3	physical state of vapours in heat recovery system (e.g. compression, condensation)
state 4	physical state of wort before additional evaporation
state 5	physical state of wort and vapours after additional evaporation (e.g. after pressure release in vacuum evaporation)
T_bath_operation	temperature of washing baths during operation [°C]
T_bath_stop	temperature of washing baths after breaks [°C]
T_beer_in	temperature of beer entering the process/heat exchanger [°C]
T_beer_in	temperature of beer entering HX [°C]
T_beer_out	temperature of beer leaving the process/heat exchanger [°C]

T_beer_out	temperature of beer after HX [°C]
T_cs_in	Temperature of cold stream entering a heat exchanger unloading the storage [K]
T_hs_in	Temperature of hot stream entering a heat exchanger loading the storage [K]
T_HTM_in	temperature of heat transfer medium before HX [°C]
T_HTM_out	temperature of heat transfer medium after HX [°C]
T_mash_out	final temperature of mashing; temperature at which mash is withdrawn from mashtun [°C]
T_mat	maturation temperature [°C]
T_sm_in	temperature of the storage medium entering the heat exchanger (leaving the storage) [K]
T_sm_out	temperature of the storage medium leaving the heat exchanger (entering the storage) [K]
T_vapourcond	temperature of condensate leaving the vapour condenser [°C]
T_vapourcond, theory	theoretic condensation temperature acc. to given pressure [°C]
t _{end}	End time
T _{in}	Start temperature of process streams
T _{initial}	Initial temperature [°C]
T _{mashstep[j]}	Final temperature in mash step j [°C]
T _{mashstep_afterBMMix[j]}	Temperature in mash step j (after a boilermash has been possibly added to the mash) [°C]
T _{out}	End temperature of process streams [°C]
t _{start}	Start time
V_beer	volume flow of beer [hl/h]
V_mat_tank	volume of maturation tank [hl]
V_pack_avg	volume of packaged unit [ml]
V_tank	volume of fermentation tank [hl]
V _{mashing_mainmash[j]}	Volume of main mash in mash step j [m ³]

Fermentation model	
C _p	produced carbon dioxide [l/l]
S	fermentable sugar concentration [g/l]
E	ethanol concentration [ml/100ml]
D ₀	initial wort density expressed over the extract content [g/100g]
X ₀	initial yeast concentration, in millions of cells per millilitre (×10 ⁶ ml ⁻¹)
Y _D	yield coefficient of density decrease versus CO ₂ production (Plato)
Y _E	yield coefficient of ethanol versus CO ₂ production (ml (100 ml) ⁻¹)
Y _S	yield coefficient of sugar consumption versus CO ₂ production (g l ⁻¹)
C ₀	initial CO ₂ production rate coefficient [10 ⁻⁶ ml]
K ₁	product inhibition coefficient[l ² /g ²]
K _s	substrate limitation coefficient[g/l]
p	pressure in fermentation tank [kPa]
aT...a ₀	biochemical model parameters
D	wort density expressed over the extract content [g/100g]
S ₀	initial fermentable sugar concentration [g/l]
X ₀	initial yeast concentration, in millions of cells per millilitre (×10 ⁶ ml ⁻¹)

Mashing models	
Act	enzyme activity [U/kg] or [g/l]
Act_max	maximum enzyme activity [U/kg] or [g/l]
Act_rel	relative enzyme activity [%]
alpha_malt_initial	initial α - amylase present in malt [g/l] (Model A) or [U/kg] (Model B)
alpha_sol_initial	initial α - amylase present in mash [g/l] (Model A) or [U/kg] (Model B)
beta_malt_initial	initial β - amylase present in malt [g/l] (Model A) or [U/kg] (Model B)
beta_sol_initial	initial β - amylase present in mash [g/l] (Model A) or [U/kg] (Model B)
dextrin_inital	initial dextrin concentration in mash (solute from malt) [g/l]
E_alpha_denat	activation energy for denaturation of α - amylase [J/mol]
E_beta_denat	activation energy for denaturation of β - amylase [J/mol]
end_time	end time of actual mashing step
fructose_inital	initial fructose concentration in mash (solute from malt) [g/l]
glucose_inital	initial glucose concentration in mash (solute from malt) [g/l]
k_alpha_0	frequency factor for denaturation of α - amylase [1/min]
k_beta_0	frequency factor for denaturation of β - amylase [1/min]
limitdextrin_inital	initial limitdextrin concentration in mash (solute from malt) [g/l]
m_malt	mass of malt added to the mash liquor [kg]
maltose_inital	initial maltose concentration in mash (solute from malt) [g/l]
maltotriose_inital	initial maltotriose concentration in mash (solute from malt) [g/l]
ρ _malt_in_mash	density of malt in mash [kg/m ³]
saccharose_inital	initial sucrose concentration in mash (solute from malt) [g/l]
starch_inital	initial starch concentration in mash (solute from malt) [g/l]
start_time	start time of actual mashing step
t	time (integral variable)
T0 - T7	temperature of mashing steps [°C]
time1 - time7	time per mashing step [s]
V_sol	volume of liquid phase in the mash [m ³]
Model A specific constants	
H_alpha, H_beta	dissolution coefficients for α - and β - amylase [l/(g*min)]
A_dex_0	kinetic constant for dextrin formation by α - amylase [l/(g*min)]
A_mlt_0	kinetic constant for maltotriose formation by α - amylase [l/(g*min)]
B_gl_0	kinetic constant for glucose formation by β - amylase [l/(g*min)]
B_ldex_0	kinetic constant for limitdextrin formation by β - amylase [l/(g*min)]
B_mal_0	kinetic constant for maltose formation by β - amylase [l/(g*min)]
B_mlt_0	kinetic constant for maltotriose formation by β - amylase [l/(g*min)]
E_alpha_dex	activation energy for dextrin production by α - amylase [J/mol]
E_alpha_mlt	activation energy for maltotriose production by α - amylase [J/mol]
E_beta_gl	activation energy for glucose production by β - amylase [J/mol]
E_beta_ldex	activation energy for limitdextrin production by β - amylase [J/mol]
E_beta_mal	activation energy for maltose production by β - amylase [J/mol]
E_beta_mlt	activation energy for maltotriose production by β - amylase [J/mol]
K_m = 40[g/l]	michaelis constant for production of maltose by α - amylase (g/l)
Model B specific constants	

a_alpha	specific enzyme activity
a_beta	specific enzyme activity
E_g1	activation energy for gelatinization $T < T_{gelatinization}$ [J/mol]
E_g2	activation energy for gelatinization $T > T_{gelatinization}$ [J/mol]
k_alpha_mal	kinetic constant for maltose hydrolysis from gelatinized starch by α - amylase [kg/(U*s)]
k_beta_mal	kinetic constant for maltose hydrolysis from gelatinized starch by β - amylase [kg/(U*s)]
k_dex	kinetic constant for dextrin hydrolysis from gelatinized starch [kg/(U*s)]
k_gl	kinetic constant for glucose hydrolysis from gelatinized starch [kg/(U*s)]
k_mlt	kinetic constant for maltotriose hydrolysis from gelatinized starch [kg/(U*s)]
k1_alpha_mal	kinetic constant for maltose hydrolysis from dextrans by α - amylase [kg/(U*s)]
k1_beta_mal	kinetic constant for maltose hydrolysis from dextrans by β - amylase [kg/(U*s)]
k1_gl	kinetic constant for glucose hydrolysis from dextrans [kg/(U*s)]
k1_mlt	kinetic constant for maltotriose hydrolysis from dextrin [kg/(U*s)]
kg1	pre-exponential factor for gelatinization $T < T_{gelatinization}$ [1/s]
kg2	pre-exponential factor for gelatinization $T > T_{gelatinization}$ [1/s]
r_act_alpha; r_act_beta	reaction rate for global enzyme activity [U/kg s]
T_gelatinization	gelatinization temperature [°C]

Experimental results and OBR design	
TE	total extract [g/l]
E	Extract compound n [g/l]
ST	starch degradation [g/l]
FAN	free amino nitrogen
V1 - V8	test run 1 - 8
T_hs,in	temperature of incoming heat supply medium [°C]
T_hs,out	temperature of outgoing heat supply medium [°C]
T_mash,start	start temperature of mash before heating [°C]
T_mash,end	final temperature of mash after heating [°C]
T_mash(t)	temperature of mash at the time t [°C]
mdot_hs	mass flow of heat supply medium [kg/s]
cp_hs	heat capacity of heat supply medium [kJ/kg.K]
m_mash	mass of mash in mash tun [kg]
cp_mash	heat capacity of mash [kJ/kg.K]
α_{hs}	heat transfer coefficient at the heat supply side [W/m ² .K]
λ_w	heat conductivity of the wall [W/m.K]
λ_f	heat conductivity of the fouling layer [W/m.K]
s_w	wall thickness [m]
s_f	thickness of the fouling layer [m]
α_{pm}	heat transfer coefficient at the process medium side [W/m ² .K]
Re_net	Reynolds number based on net flow
Re_o	Reynolds number based on oscillatory flow
St	Strouhal number
ψ	velocity ratio
u	flow velocity [m/s]

d	tube diameter [m]
η	dynamic viscosity [Pa.s]
x	oscillation amplitude [m]
ω	angular frequency [Hz]
L	baffle spacing [m]
S	baffle orifice open area [m ²]
Q	production volume [m ³ /s]

12.2 List of figures

Figure 4-1: Hot and cold composite curve	8
Figure 4-2: Grand composite curve [15].....	9
Figure 4-3: Pinch design method [130]	10
Figure 4-4 : Hot and cold composite curves (TAM approach) and storage composite curve [116].....	14
Figure 4-5: Limiting supply temperature profiles [116]	15
Figure 4-6: Schematic of the heat recovery loop [26].....	16
Figure 4-7: Superstructure of the mathematical model [134]	18
Figure 4-8: Conceptual structure of an indirect network (2 hot streams, 1 cold stream and one heat transfer medium) [54]	19
Figure 4-9: Possible configurations of heat exchange units: serial absorption (a), parallel absorption (b), serial rejection (c), parallel rejection (d), heat storage (e) [54].....	19
Figure 4-10: Algorithm for heat exchanger network design with batch processes [149].....	20
Figure 4-11: Process and utility grand composite curves [137]	22
Figure 4-12: Site targets for solar capture and storage in one time slice [204].....	23
Figure 4-13: Process scheme for heat storage design for solar thermal system [154].....	23
Figure 4-14: Generation of the minimal capture temperature curve [154].....	24
Figure 4-15: Intersecting the captured solar energy curve with the minimal capture temperature curve [154].....	24
Figure 4-16: The PI tower - steps towards an intensified process (steps acc. to [173])	28
Figure 4-17: Mash tuns (schematic figure and real plant) supplied by steam (source: AEE INTEC)	35
Figure 4-18: Heating plates on the inside of the mash tuns for low temperature heat supply (source: AEE INTEC and GEA Brewery Systems GmbH)	36
Figure 4-19: Basic scheme of a membrane distillation unit heated by solar thermal energy over an energy storage tank [46]	40
Figure 4-20: Flow characteristics in stirred tanks versus plug flow reactors [202].....	41
Figure 4-21: Amylose (left) and Amylopectin (right).....	44
Figure 4-22: Relative activity of amylases activity as a function of temperature acc. to [145]	49
Figure 4-23: Polynoms describing the specific activity of amylases during mashing acc. to [44].....	50
Figure 4-24: Comparison of the hydrolysis schemes a) Marc and Engasser, 1983 [136] b) Brandam et al., 2003 [44].....	51
Figure 4-25: Example of a decoction procedure with 2 decoction mashes	54
Figure 4-26: Temperature profiles in temperature programmed infusion mashes.....	55
Figure 4-27: Profile of wort collection and rinses during lautering [125]	56
Figure 5-1: Start page of the Brewery Model.....	68

Figure 5-2: Overview of the Brewery Model.....	68
Figure 5-3: Brewhouse section of the Brewery Model	70
Figure 5-4: Technology tab for mashing.....	71
Figure 5-5: Technology tab for wort boiling.....	74
Figure 5-6: Flowsheet of cooling processes in breweries	76
Figure 5-7: Section overview for returnable bottle washing	77
Figure 5-8: Input of brewing operating schedule in the Brewery Model.....	79
Figure 5-9: Hot water management analysis within the Brewery Model	80
Figure 5-10: Summary of energy demand figures within the Brewery Model.....	81
Figure 5-11: Calculation procedure for energy variability in mashing.....	90
Figure 5-12: Visualisation of an energy demand profile for the mashing process	92
Figure 5-13: Temperature sensitivity of the implemented kinetic mashing models (top: Model A, bottom: Model B).....	94
Figure 5-14: Relative enzyme activity over time modelled for an industrial temperature programmed mashing	95
Figure 5-15: Run 1: Starch degradation modelled in Model A and B with same enzyme activity ratios	96
Figure 5-16: Run 2: Starch degradation modelled in Model A and B with same enzyme activity ratios	97
Figure 5-17: Reduction of wort gravity over fermentation time for various fermentation temperatures (initial wort gravity 12° Plato)	99
Figure 5-18: Formation of ethanol and CO ₂ based on the biochemical model (initial gravity of 12°Plato; pitching temperature of 9°C and main fermentation temperature of 12°C)	100
Figure 5-19: Reduction of wort gravity as a function of initial wort gravity acc. to the biochemical model (initial yeast cells 10 x 10 ⁶ cells/ml; saturated oxygen)	100
Figure 5-20: Electricity demand for cold production from 3 breweries (Brewery 1 data from 2008, Brewery 2 data from 2010 and Brewery 3 data from 2009) in comparison with the average ambient temperature per months in 2008 at the site of Brewery 1.....	101
Figure 5-21: Influence of evaporation (T1) and condensation temperature on the EER of a single-stage cooling compressor	102
Figure 5-22: Effect of ambient temperature of the cold demand of one brewery (measured data) .	103
Figure 5-23: Demand profile of cooling requirement for the fermentation tanks	104
Figure 5-24: Modelled profile of cooling demand over several weeks in a 1 Mio. hl brewery	105
Figure 5-25: GCC of the food packaging line including all streams (left) , and GCC excluding several heat recovery options (right) at $\Delta T_{\min}=5^{\circ}\text{C}$. [116]	109
Figure 5-26: CCs after introducing solar heat as a hot utility stream (selected and sized with the GCCs from Figure 5-25); $\Delta T_{\min}=5^{\circ}\text{C}$. [116].....	110
Figure 5-27: Solve-ability matrix of SOCO simulation algorithm.....	112
Figure 5-28: Detailed settings for the heat exchange and storage proposal algorithm	116
Figure 5-29: Algorithmic steps of the heat integration proposal.....	117
Figure 5-30: Presentation of one proposed heat exchanger in SOCO (example)	117
Figure 5-31: Presentation of heat exchange performance results in SOCO (example)	118
Figure 5-32: Holistic methodology for developing intensified food production systems for low temperature heat supply.....	119

Figure 6-1: Model results for temperature profiles 1-8 simulated with Model A (a-d).....	126
Figure 6-2: Model results for temperature profiles 1-8 simulated with Model B (a-d).....	127
Figure 6-3: Experimental set-up.....	130
Figure 6-4: Sucrose concentration during the course of mashing.....	131
Figure 6-5: Sugar analysis of maltotriose and higher oligomers.....	132
Figure 6-6: Evolution of total extract, maltose and glucose during mashing - comparison of the standard temperature profile (Test 1) to Test 2.....	133
Figure 6-7: Evolution of total extract, maltose and glucose during mashing - comparison of the standard temperature profile (Test 1) to Test 3.....	133
Figure 6-8: Evolution of total extract, maltose and glucose during mashing - comparison of the standard temperature profile (Test 1) to Test 4 and Test 9.....	134
Figure 6-9: Evolution of total extract, maltose and glucose during mashing - comparison of the standard temperature profile (Test 1) to Test 6 and Test 8.....	134
Figure 6-10: Evolution of total extract, maltose and glucose during mashing - comparison of the standard temperature profile (Test 1) to Test 4 at higher gravity.....	135
Figure 6-11: FAN and β -glucan analysis for the test runs.....	136
Figure 6-12: Comparison of experimental test result to starch hydrolysis models.....	138
Figure 6-13: Comparison of experimental data to Model A (top) and to the adapted Model A (bottom).....	139
Figure 6-14: Results of the adapted Model A for Test 1 and Test 2.....	140
Figure 6-15: Relative enzyme activity modelled by the adapted Model A for Test 1.....	140
Figure 6-16: Exemplary data for heat transfer coefficients and stirrer power for a high viscosity process medium in a batch stirred tank with heating jackets.....	141
Figure 6-17: Visualisation of flow behaviour in plug flow reactors [154].....	142
Figure 6-18: Visualisation of fluid flow in an oscillatory baffled reactor [154].....	147
Figure 6-19: Increase in heat and mass transfer in oscillating reactors [155, 192].....	147
Figure 6-20: Strouhal number for different oscillation amplitudes.....	150
Figure 6-21: Design diagramm for OBR design for a mash with coarse grist (viscosity 130 mPas)....	154
Figure 6-22: Design diagramm for OBR design for a mash with fine grist (viscosity 20 mPas).....	155
Figure 6-23: Scheme for mashing with an oscillatory reactor.....	160
Figure 7-1: Benchmark comparison for a brewery (production capacity \sim 1 Mio. hl).....	162
Figure 7-2: Measured thermal energy demand of the brewhouse over 4 hours.....	164
Figure 7-3: Sankey of energy flows in the brewhouse of brewery S, used for model verification....	166
Figure 7-4: Calculated versus measured energy demand profile.....	168
Figure 7-5: Calculated versus measured cooling load profile.....	169
Figure 7-6: Specific energy demand for key brewing processes on different temperature levels....	173
Figure 7-7: Specific energy demand for key brewing processes and hot water preparation on different temperature levels.....	174
Figure 7-8: Sankey diagramm of brewhouse energy flows of site 1.....	180
Figure 7-9: Sankey diagramm of brewhouse energy flows of site 4.....	181
Figure 7-10: Sankey diagramm of brewhouse energy flows of site 5.....	182
Figure 7-11: Energy demand variability for the brewery case studies 1 and 4.....	183
Figure 7-12: Energy demand profiles of the five breweries with different technology sets.....	184

Figure 7-13: Comparison of specific energy demand of wort preheating and boiling for two vapour recovery options for brewery 3: mechanical vapour compression versus vapour condensation for wort preheating	185
Figure 7-14: Specific energy demand for Hot Water Preparation at different evaporation rates for site 4 and site 5	187
Figure 7-15: Specific energy demand for Brewing Processes and Hot Water Preparation at different evaporation rates for site 4 and site 5	188
Figure 7-16: Specific energy demand for hot water preparation at site 5 with different efficiency of brew water recovery	188
Figure 7-17: Influence of hot water temperature on the energy demand for hot water preparation for site 4 and site 5.....	189
Figure 7-18: Results of the fermentation model for site 2 and site 4 (5 days mainfermentation at 12°C)	190
Figure 7-19: Minimal specific thermal energy demand in selected brewhouse processes for varying addition of dilution water (above: site 4; below: site 5)	192
Figure 7-20: Minimal specific thermal energy demand for selected processes with increasing malt input and constant brew water input (above: site 4; below: site 5).....	193
Figure 7-21: Minimal specific thermal energy demand for selected processes with increasing malt input and corresponding increase in dilution water (above: site 4; below: site 5).....	194
Figure 7-22: Hot and cold composite curves of the brewery site 1 (above a; below c).....	198
Figure 7-23: Hot and cold composite curves of the brewery site 4 (above a; below c).....	199
Figure 7-24: Scheme of the heat exchanger network proposed by SOCO.....	203
Figure 7-25: Heat exchanger performance and remaining energy demand for Run 1 at site 1 and site 4	205
Figure 7-26: Temperature profile in the storages of brewery 1 (left) and brewery 4 while loading the storage with energy from vapour condensation.....	206
Figure 7-27: Heat exchanger performance and remaining energy demand for Run 1 and Run 2 at site 1.....	207
Figure 7-28: Heat exchanger performances for Versions A and B of site 1 and site 4.....	208
Figure 7-29: Scheme 1 for heat integration of chiller waste heat and hot water.....	209
Figure 7-30: Temperature stratification results in energy storage for hot water, Site 4 Version C Heat Integration Scheme 1	209
Figure 7-31: Scheme 2 for heat integration of chiller waste heat and hot water.....	210
Figure 7-32: Heat exchanger performances of the heat integration concepts including chiller waste heat and hot water.....	211
Figure 7-33: Variability of the remaining energy demand profile based on the heat integration concept (for brew water preparation, mashing and wort preheating)	212
Figure 7-34: Weekly load profile of the remaining energy demand based on the heat integration concept (for brew water preparation, mashing and wort preheating)	213
Figure 9-1: Screen of the Excel Tool for Visualisation of the demand profiles (linked to the Brewery Model)	218
Figure 9-2: Technology Tab Wort Preheating	219
Figure 9-3: Section overview fermentation and filtration	220
Figure 10-1: Screenshots of data entry mask for storage and HX definition	261

Figure 10-2: Settings for the HESN algorithm in SOCO	262
Figure 10-3: Storage parameters for simulations of the heat integration concept	263

12.3 List of tables

Table 4-1: Selected intensification examples for heat transfer applied in or researched for operations in the food industry	30
Table 4-2: Intensification examples for heat transfer in the food industry	31
Table 4-3: Figure 12: Increase in heat transfer efficiency from batch stirred tanks to intensified heat exchangers ([a] own data, [b] own calculations based on comparison with batch stirred tank (base data [189]), [c] estimated based on tubular heat exchanger)	37
Table 4-4: Intensification approaches of selected process steps in brewing.....	62
Table 4-5: Specific energy consumption figures of breweries	63
Table 5-1: Technology, heat supply and heat recovery options in the brewery model for mashing...	69
Table 5-2: Technology, heat supply and heat recovery options in the brewery model for wort boiling	73
Table 5-3: Technology, heat supply and heat recovery options in the brewery model for thermal brewhouse operations	75
Table 5-4: Example of process steps in mashing.....	91
Table 5-5: Input parameters for modelling starch degradation with similar enzyme activity ratios....	96
Table 6-1: Initial starch composition for modelling mashing temperature profiles	123
Table 6-2: Selected Temperature profiles applied to analyse the effects of temperature profiles on sugar composition with the kinetic mashing model	124
Table 6-3: Model results for mashing programs with low temperature heating gradients	125
Table 6-4: Results of extract and selected fermentable sugars in the final wort after mashing	132
Table 6-5: Malt composition assessment.....	137
Table 6-6: Parameter adaptation for Model A.....	138
Table 6-7: Parameters for calculating heat transfer coefficient in a hot water heated mash tun (welded tubes).....	144
Table 6-8: Heat transfer in a conventional hot water heated mash tun.....	144
Table 6-9: Heat transfer in mash tuns via welded tubes heated with low temperature heating medium for different mashing programs.....	145
Table 6-10: Parameters for calculating heat transfer coefficient in a low temperature heated mash tun (internal heating plates).....	146
Table 6-11: Heat transfer in mash tuns via internal heating plates heated with low temperature heating medium for different mashing programs.....	146
Table 6-12: Examples of OBR implementation in research studies	148
Table 6-13: Summary of design examples for OBRs for mashing	156
Table 6-14: OBR design for 200 hl/h production.....	158
Table 7-1: Calculated energy flows in the brewhouse S for model verification	164
Table 7-2: Description of breweries	170
Table 7-3: Assumed process efficiency in key brewing processes	172
Table 7-4: Specific hot water consumption and recovery figures.....	176
Table 7-5: Specific energy demand figures ($MEDT_{Tech}$) in the brewhouse	176

Table 7-6: Specific energy demand figures including process efficiencies (UPH) in the brewhouse..	177
Table 7-7: Waste heat in selected processes in the brewhouse	177
Table 7-8: Specific energy demand figures in packaging	178
Table 7-9: Cooling demand for fermentation at the different production sites.....	191
Table 7-10: Overview of case study versions simulated with SOCO	196
Table 7-11: Heat exchanger and storage network proposal by SOCO for Brewery Site 1	200
Table 7-12: Heat exchanger and storage network proposal by SOCO for Brewery Site 4	201
Table 7-13: Energy savings for each process in Run 1.....	204
Table 7-14: Result in potential energy savings for mashing, wort preheating, brew water and hot water generation.....	210
Table 10-1: Stream data overview for brewery site 1 and site 4	261
Table 10-2: Heat exchanger parameters for simulations of the heat integration concept	263
Table 11-1: Malt analysis.....	264
Table 11-2: Experimental results of extract and sugar analysis.....	264
Table 11-3: Experimental results of FAN, β -glucan and pH of final test samples	266

12.4 Literature references

1. Alpha Amylase Assay Procedure (Ceralpha Method), Megazyme International, Ireland, (2012).
2. The British Brewing Industry - 30 Years of Environmental Improvement 1976-2006, British Beer & Pub Association, London, (2006); [cited 2014 February 15]; Available from: www.ibd.org.uk/cms/file/338.
3. Data & Trends of the European Food and Drink Industry 2012, Food and Drink Europe, Brussels, Belgium, (2013); [cited 2013 15.11.]; Available from: http://www.fooddrinkeurope.eu/uploads/publications_documents/Data_Trends_%28inter-active%29.pdf.
4. Energy efficiency index (ODEX) in the EU-27, European Environment Agency, (2011); [cited 2014 March]; Available from: <http://www.eea.europa.eu/data-and-maps/figures/energy-efficiency-index-odex-in-5>
5. Energy Saver Tool, Campden BRI, Surrey, UK; [cited 2014 February 18]; Available from: <http://www.campdenbri.co.uk/services/brewing-energy-saver.php>.
6. Equitherm, Kronos AG; [cited 2013 November 30]; Available from: <http://www.kronos.com/en/products/magazine-egitherm.php>.
7. Global Brewery Survey, Campden BRI and KWA, (2012); Available from: <http://www.campdenbri.co.uk/global-brewery-survey.php>.
8. Guide to energy efficiency opportunities in the Canadian brewing industry, Natural Resources Canada, C.I.P.f.E. Conservation, Ottawa, Canada, (2012).
9. Handbook of Process Integration, Woodhead Publishing Limited, Cambridge, 2013.
10. Industrial Energy Efficiency Accelerator - Guide to the brewing sector, The Carbon Trust, London, (2011).
11. Meura 2001 Hybrid, Meura S.A., Belgium, (2011); [cited 2014 March, 12]; Available from: http://www.meura.com/uploads/pdf/MEURA%202001%20Hybrid_Technical%20Leaflet.pdf.
12. The MEURABREW: the brewhouse of the future!, Meura S.A., (2008); [cited 2012 March]; Available from: <http://www.meura.com/uploads/pdf/Meurabrew%20Paper.pdf>.
13. Neuentwicklungen für Spezialitätsbrauereien, *Brauindustrie* **1**, 28-30 (2010).

14. PDX™ Sonic Beverages, Soft Drinks & Sugar Dissolution, Pursuit Dynamics plc, Cambridgeshire, (2010); [cited 2012 March]; Available from: www.pdx.biz.
15. Pinch Analyses - For the Efficient Use of Energy, Water and Hydrogen, Canment Energy Technology Center - Varennes, N.R. Canada, Quebec, Canada, (2003). DOI: 0-662-34964-4.
16. Reference Document on Best Available Techniques in Food, Drink and Milk Industries, European Commission, Seville, Spain, (2006); [cited 2014 February]; Available from: http://ftp.jrc.es/pub/eippcb/doc/fdm_bref_0806.pdf.
17. Adonyi, R., et al., Incorporating heat integration in batch process scheduling, *Applied Thermal Engineering* **23**, 1743–1762 (2003).
18. Anderson, N.G., Continuous Operations, in *Practical Process Research and Development*. Elsevier Inc., 2012, p. 397-414.
19. Andrews, J.M.H., The Brewhouse, in *Brewing-New technology*, C.W. Bamforth, Editor. Woodhead Publishing Limited: Cambridge, England, 2006, p. 208-227.
20. Andrews, J.M.H., et al., Some recent engineering advances in brewing and distilling, *Journal of the Institute of brewing* **117**, 23-32 (2011).
21. Antoni, D., R. Meyer-Pittroff, and W. Ruß, SchoKo-Verfahren und Wärmehaushalt der Brauerei, *Brauwelt* **12-13**, 356-358 (2005).
22. Anxionnaz, Z., et al., Heat exchanger/reactors (HEX reactors): Concepts, technologies: State-of-the-art, *Chemical Engineering and Processing: Process Intensification* **47**, 2029-2050 (2008).
23. ASBC Methods of Analysis, Alpha Amylase - Fixed Color and Variable Time Method (International Method) American Society of Brewing Chemists, St. Paul, Michigan, (2014).
24. Askounis, D.T. and J. Psarras, Information system for monitoring and targeting (M&T) of energy consumption in breweries, *Energy* **23**, 413-419 (1998).
25. Atkins, M.J., M.R.W. Walmsley, and A.S. Morrison, Integration of solar thermal for improved energy efficiency in low-temperature-pinch industrial processes, *Energy* **35**, 1867–1873 (2010).
26. Atkins, M.J., M.R.W. Walmsley, and J.R. Neale, The challenge of integrating non-continuous processes – milk powder plant case study, *Journal of Cleaner Production* **18**, 927-934 (2010).
27. Atkins, M.J., M.R.W. Walmsley, and J.R. Neale, Process integration between individual plants at a large dairy factory by the application of heat recovery loops and transient stream analysis, *Journal of Cleaner Production* **34**, 21-28 (2012).
28. Awad, T.S., et al., Applications of ultrasound in analysis, processing and quality control of food: A review, *Food Research International* **48**, 410-427 (2012).
29. Baars, A., T. Biwanski, and A. Delgado, Subjet Würzekochung - physikalische Phänomene und Technologie während Aufheiz- und Kochphase, *Brauwelt* **28**, 830-834 (2006).
30. Bagajewicz, M. and H. Rodera, Energy savings in the total site Heat integration across many plants, *Computers and Chemical Engineering* **24**, 1237-1242 (2000).
31. Bagajewicz, M. and H. Rodera, Multiple Plant Heat Integration in a Total Site, *AIChE Journal* **48**, 2255-2270 (2002).
32. Bai, J., et al., Research on Energy Consumption Analysis of Beer Brewing Process, International Conference on Electronic & Mechanical Engineering and Information Technology, (2011).
33. Baird, M.H.I. and P. Stonestreet, Energy dissipation in oscillatory flow within a baffled tube, *Chemical Engineering Research and Design* **73**, 503-511 (1995).
34. Bamforth, C.W., Beer: An Ancient Yet Modern Biotechnology, *Chem. Educator* **5**, 102–112 (2000).
35. Bamforth, C.W., Beer: Tap into the art and science of Brewing, Oxford University Press, Inc., New York, 2003.
36. Bamforth, C.W., Continuous Improvement?, *Brewers' Guardian*, May/June 2010, 22-24 (2010).

37. Bamforth, C.W., Current perspectives on the role of enzymes in brewing, *Journal of Cereal Science* **50**, 353-357 (2009).
38. Barton, S., C. Bullock, and D. Weir, The effects of ultrasound on the activities of some glycosidase enzymes of industrial importance, *Enzyme and Microbial Technology* **18**, 190-194 (1996).
39. Besselink, T., et al., A stochastic model for predicting dextrose equivalent and saccharide composition during hydrolysis of starch by alpha-amylase, *Biotechnology and Bioengineering* **100**, 684-97 (2008).
40. Binkert, J. and D. Haertl, Neues Würzekochsystem mittels Expansionsverdampfung, *Brauwelt* **37**, 1494-1503 (2001).
41. Binkert, J., D. Haertl, and Bamberg, Praxiserfahrungen mit dem SchoKo-Verfahren, *Brauwelt* **27/28**, 953-956 (2002).
42. Blevins, R.D., Flow-Induced Vibration (2nd reprint), Krieger Publishing Company, New York, 2006.
43. Bramsiepe, C., et al., Low-cost small scale processing technologies for production applications in various environments—Mass produced factories, *Chemical Engineering and Processing: Process Intensification* **51**, 32-52 (2012).
44. Brandam, C., et al., An original kinetic model for the enzymatic hydrolysis of starch during mashing, *Biochemical Engineering Journal* **13**, 43-52 (2003).
45. Brau-UnionÖsterreich, Facts & Objectives Energy, (2013); [cited 2014 January]; Available from: <http://nachhaltigkeit.brauunion.at/brewing/blog.html>.
46. Brunner, C., U. Herzog, and B. Muster, Darstellung des Potentials zur Effizienzsteigerung und zum erhöhten Einsatz Solarer Prozesswärme durch den Einsatz neuer Technologien für die betrachteten Prozess, Projekt Solar Foods, AEE INTEC, Förderprogramm Energie der Zukunft, Gleisdorf, (2012).
47. Brunner, C., et al., EINSTEIN - Expertensystem spürt systematisch Energie-Einsparpotentiale auf, *Energy 2.0- Zukunft Energie, Kompendium 2011*, 270-272 (2010).
48. Brunner, C., et al., Industrial Process Indicators and Heat Integration in Industries, International Energy Agency, IEA Task 33, J. Research, Graz, Austria, (2008).
49. Buckow, R., et al., Stability and catalytic activity of alpha-amylase from barley malt at different pressure-temperature conditions, *Biotechnol Bioeng* **97**, 1-11 (2007).
50. Chaturvedi, N.D. and S. Bandyopadhyay, Indirect thermal integration for batch processes, *Applied Thermal Engineering* **62**, 229-238 (2014).
51. Chaturvedi, N.D. and S. Bandyopadhyay, Minimization of storage requirement in a batch process using pinch analysis, **31**, 670-674 (2012).
52. Chemat, F., H. Zill e, and M.K. Khan, Applications of ultrasound in food technology: Processing, preservation and extraction, *Ultrason Sonochem* **18**, 813-35 (2011).
53. Chen, C.-L. and Y.-J. Ciou, Design of Indirect Heat Recovery Systems with Variable-Temperature Storage for Batch Plants, *Ind. Eng. Chem. Res.* **48**, 4375–4387 (2009).
54. Chen, C.-L. and Y.J. Ciou, Design and Optimization of Indirect Energy Storage Systems for Batch Process Plants, *Ind. Eng. Chem. Res.* **47**, 4817-4829 (2008).
55. Coors, G., M. Krottenthaler, and W. Back, Auswirkungen einer Würzevorkühlung beim Ausschlagen, *Brauwelt* **42/43**, 1696-1699 (2000).
56. de Andrés-Toro B., J.M.G.-S., J.A. Lopez-Orozco, C. Fernandez-Conde, J.M. Peinado, F. Garcia-Ochoa A kinetic model for beer production under industrial operational conditions, *Mathematics and Computers in Simulation* **48**, 105-424 (1998).
57. Defernez, M., et al., Modelling beer fermentation variability, *Journal of Food Engineering* **83**, 167-172 (2007).
58. Denk, V., et al., Manual of Good Practice, Wort Boiling and Clarification, European Brewery Convention, F.H. Carl, Nürnberg, (2000).

59. Dennis E. Briggs, C.A.B., Peter A. Brookes and Roger Stevens, *Brewing - Science and Practice*, Woodhead Publishing Limited, Cambridge, 2004.
60. Deuter, P., P. Gattermeyer, and M. Lubbe, Continuous Brewing Process, Kronen AG, Patent No. US 2010/0291261, (2010).
61. Dhole, V.R. and B. Linnhoff, Total site targets for fuel, co-generation, emissions, and cooling, *Computers & Chemical Engineering* **17**, 101-109 (1993).
62. Dickel, T., Untersuchungen zu enzymatischen Abbauprodukten beim Maischen im Hinblick auf die Entwicklung eines Prozessführungssystems, Dissertation, Technische Universität München, Munich, (2003).
63. Donoghue, C., et al., The Environmental Performance of the European Brewing Sector, KWA, Campden BRI, (2012); [cited 2014 March]; Available from: http://www.brewersofeurope.org/docs/publications/2012/envi_report_2012_web.pdf.
64. Drioli, E., A.I. Stankiewicz, and F. Macedonio, Membrane engineering in process intensification—An overview, *Journal of Membrane Science* **380**, 1-8 (2011).
65. Dumbliauskaite, M., H. Becker, and F. Marechal. Utility Optimization in a Brewery Process Based on Energy Integration Methodology. in *Proceedings of ECOs - International Conference on Efficiency, Cost, Optimization, Simulation and Environmental Impact of Energy*. Lausanne, 2010, p. 91-98.
66. Durand, G.A., et al., Simulation-based Dynamic Optimization under Uncertainty of an Industrial Biological Process, **29**, 808-812 (2011).
67. Durand, G.A., et al., Dynamic optimization of the mashing process, *Food Control* **20**, 1127-1140 (2009).
68. Evans, D.E., et al., Refining the Prediction of Potential Malt Fermentability by Including an Assessment of Limit Dextrinase Thermostability and Additional Measures of Malt Modification, Using Two Different Methods for Multivariate Model Development, *Journal of the Institute of Brewing* **116** 86–96 (2010).
69. Evans, D.E., C. Li, and J.K. Eglinton, Improving the predictability and consistency of malt fermentability performance, Proceedings of the Institute of Brewing and Distilling, Asia Pacific Section Conference, (2008).
70. Evans, D.E., et al. Potential to modify the wort fermentability of the E α -amylase, β -amylase and limit dextrinase diastatic power enzymes. in *Conference Proceedings, A Joint Meeting for the 11th Australian Barley Technical Symposium & the 53rd Australian Cereal Chemistry Conference*. Glenelg, 2003, p. 166-171.
71. Fadare, D.A., et al., Energy and exergy analyses of malt drink production in Nigeria, *Energy* **35**, 5336-5346 (2010).
72. Feilner, R., Kontrollierte Reduktion, *Brauindustrie* **4**, 14-17 (2011).
73. Fernández, I., et al., A review: energy recovery in batch processes, *Renew. Sust. Energy Rev.* **16**, 2260-2277 (2012).
74. Ferrouillat, S., P. Tochon, and H. Peerhossaini, Micromixing enhancement by turbulence: Application to multifunctional heat exchangers, *Chemical Engineering and Processing: Process Intensification* **45**, 633-640 (2006).
75. Ferrouillat, S., et al., Open loop thermal control of exothermal chemical reactions in multifunctional heat exchangers, *International Journal of Heat and Mass Transfer* **49**, 2479-2490 (2006).
76. Foo, D.C.Y., Y.H. Chew, and C.T. Lee, Minimum units targeting and network evolution for batch heat exchanger network, *Applied Thermal Engineering* **28**, 2089–2099 (2008).
77. Gaddis, E.S., N3 Wärmeübertragung und Leistungsaufnahme in Rührkesseln, in *VDI-Wärmeatlas*, V. e.V., Editor. Springer-Verlag: Berlin Heidelberg, 2013, p. 1621-1654.
78. Gahbauer, H., Green Brewery Project [Personal Communication], Leoben (2008).
79. Gaidhani, H.K., B. McNeil, and X. Ni, Fermentation of Pullulan Using an Oscillatory Baffled Fermenter, *Chemical Engineering Research and Design* **83**, 640-645 (2005).

80. Galitsky, C., et al., Energy Efficiency Improvement and Cost Saving Opportunities for Breweries, E.O. LAWRENCE and B.N. LABORATORY, Berkeley, (2003).
81. Gattermeyer, P. and C. Kappeler, Ersatz von Einzelaggregaten bis hin zu Komplettlösungen, *Brauindustrie* **10**, 42-45 (2012).
82. Glatzl, W., Verification and Evaluation of the Heat Integration Tool SOCO, Master Thesis, Fachhochschule Burgenland GmbH, Pinkafeld, (2014).
83. Gorak, A. and A. Stankiewicz, Research Agenda for Process Intensification - Towards a Sustainable World of 2050, Institute of Sustainable Process Technology, Amersfoort, The Netherlands, (2011).
84. Gorak, A. and A. Stankiewicz, Research Agenda for Process Intensification - Towards a Sustainable World of 2050, (2011).
85. Górak, A. and A. Stankiewicz, Editorial, *Chemical Engineering and Processing: Process Intensification* **51**, 1 (2012).
86. Gremouti, I.D., Integration of batch processes for energy savings and debottlenecking, Master Thesis, University of Manchester Institute of Science and Technology (UMIST), U.K., (1991).
87. Hackenseller, T. and T.M. Bühler, Efficient use of energy in the brewhouse, Huppmann GmbH, Germany, (2008).
88. Hackensellner, T. and B. Kantelberg, Zeitgemäße Würzekochung, *Brauindustrie* **9**, 18-22 (2001).
89. Hall, R.D., G. Harris, and I.C. MacWilliam, *J. Inst. Brewing* **62**, 232 (1956).
90. Hans Michael Eßlinger, L.N., Beer, Wiley-VCH Verlag GmbH & Co. KGaA, Weinheim, Germany, 2012, vol. 5.
91. Harvey, A., Email Correspondence on Limits for Strouhal number [Personal Communication], Newcastle (2014).
92. Hellwig, T. and E. Thöne, OMNIUM: Ein Verfahren zur Abwärmenutzung, *BWK* **46**, 393-397 (1994).
93. Hepworth, N., et al., The Use of Laboratory-Scale Fermentations as a Tool for Modelling Beer Fermentations, *Food and Bioproducts Processing* **81**, 50-56 (2003).
94. Herrmann, J., Entwicklung von Messmethoden zur Untersuchung der rheologischen Eigenschaften der Maische, Dissertation, Technische Universität München, München, (2002).
95. Hertel, M., The rectification wort boiling system, *TCE Magazine*, 38-39 (2009).
96. Hertel, M., et al., Die Würzekochung Ausdampfvorgänge korrekt betrachtet - Teil 1, *Brauwelt* **1-2**, 22-26 (2007).
97. Hertel, M., et al., Die Würzekochung Ausdampfvorgänge korrekt betrachtet - Teil 4, *Brauwelt* **29-30**, 810-814 (2007).
98. Hertel, M. and K. Sommer, Wort Boiling by Batch Rectification-Possibilities for Reducing Required Evaporation, *MBAA Technical Quarterly* **46**, (2009).
99. Hohmann, E.C., Optimum networks for heat exchange, PhD Thesis, University of Southern California, Los Angeles, USA, (1971).
100. Holtekjølen, A.K., et al., Contents of starch and non-starch polysaccharides in barley varieties of different origin, *Food Chemistry* **94**, 348-358 (2006).
101. Hough, J.S., et al., Malting and Brewing Science II. Hopped Wort and Beer, Chapman and Hall, London, 1982.
102. Icier, F., Ohmic Heating of Fluid Foods, in *Novel Thermal and Non-Thermal Technologies for Fluid Foods*. Elsevier Inc., 2012, p. 305-367.
103. Jakób, A., et al., Inactivation kinetics of food enzymes during ohmic heating, *Food Chemistry* **123**, 369-376 (2010).
104. Jentsch, M., Sudhaustechnologie Stand 2005, *Brauindustrie* **10**, 10-16 (2005).

105. Jones, P.S., Targeting and design of heat exchanger networks under multiple base case operation, PhD Thesis, University of Manchester Institute of Science and Technology (UMIST), U.K., (1991).
106. Kantelberg, B., Schwächen und Stärken moderner Würzekochanlagen - Teil 1, *Brauindustrie* **11**, 30-35 (2012).
107. Kantelberg, B., Schwächen und Stärken moderner Würzekochanlagen - Teil 2, *Brauindustrie* **12**, 22-27 (2012).
108. Kemp, I.C., Pinch Analysis and Process Integration, Butterworth-Heinemann, Oxford, UK, ed. 2, 2007.
109. Kemp, I.C. and A.W. Deakin, The cascade analysis for energy and process integration of batch processes. I-III. , *Chemical Engineering Research and Design* **67**, 495–525.
110. Kessler, M., Analytische Erfassung und Interpretation der Stärkedegradation im Gersten- und Malzkorn und die Aussagekraft für den Brauprozess, Dissertation, Technical University Munich, Munich, (2006).
111. Kettunen, A., et al., A Model for the Prediction of beta-Glucanase Activity and beta-Glucan Concentration during Mashing, *Journal of Food Engineering* **29**, 185-200 (1996).
112. Klemeš, J.J., et al., Targeting and design methodology for reduction of fuel, power and CO₂ on total sites, *Applied Thermal Engineering* **17**, 993-1003 (1997).
113. Klemeš, J.J. and Z. Kravanja, Forty years of Heat Integration: Pinch Analysis (PA) and Mathematical Programming (MP), *Current Opinion in Chemical Engineering* **2**, 461-474 (2013).
114. Koljonen, T., et al., A model for predictions of fermentable sugar concentrations during mashing, *Journal of Food Engineering* **26**, 329-350 (1995).
115. Krummenacher, P., Contribution to the heat integration of batch processes (with or without heat storage), École Polytechnique fédérale de Lausanne, Lausanne, Switzerland, (2002).
116. Krummenacher, P. and D. Favrat, Indirect and Mixed Direct-Indirect Heat Integration of Batch Processes Based on Pinch Analysis, *Int.J. Applied Thermodynamics*, **4**, 135-143 (2001).
117. Krummenacher, P. and D. Favrat, "Intégration énergétique de procédés industriels par la méthode du pincement étendue aux procédés discontinus" (in french), EPFL-DGM-LENI, Lausanne, Switzerland, (1995).
118. Krummenacher, P. and B. Muster-Slawitsch, Methodologies and software tools for integrating solar heat into industrial processes 13th International Conference on Sustainable Energy technologies SET2014- E10049 (2014).
119. Kühbeck, F., et al., Effects of Mashing Parameters on Mash β -Glucan, FAN and Soluble Extract Levels, *J. Inst. Brew.* **111**, 316–327 (2005).
120. Kunze, W., Technology of malting and brewing (in German), Versuchs- und Lehranstalt für Brauerei in Berlin, Berlin, Germany, ed. 9th, 2007.
121. Kwiatkowska, B., et al., Stimulation of bioprocesses by ultrasound, *Biotechnol Adv* **29**, 768-80 (2011).
122. Ledwig, J., M. Hilser, and L. Scheller, Stillstand ist Rückstand, *Brauindustrie* **9**, 34-36 (2008).
123. Lee, C.T., A.M. Buswell, and A.P.J. Middelberg, The influence of mixing on lysozyme renaturation during refolding in an oscillatory flow and a stirred-tank reactor, *Chemical Engineering Science* **57**, 1679 – 1684 (2002).
124. Lees, M., et al. A Utilities Consumption Model for Real-Time Load Identification in a Brewery. in *IEEE International Conference on Industrial Technology*. 2009, p. 1-6.
125. Leiper, K.A. and M. Miedl, Brewery Technology, in *Handbook of Brewing, 2nd edition*, F. Priest and G. Stewart, Editors. Taylor & Francis Group: Boca Raton, 2006.
126. Lewis, M.L. and C.W. Bamforth, Essays in Brewing Science, Springer Science and Business Media, USA, 2006.
127. Li, Y., et al., Factors predicting malt extract within a single barley cultivar, *Journal of Cereal Science* **48**, 531-538 (2008).

128. Linnhoff, B., Thermodynamic analysis in the design of process networks, The University of Leeds, Leeds, UK, (1979).
129. Linnhoff, B., G.J. Ashton, and E.D.A. Obeng, Process integration of batch processes, *ICHEME Symposium Series* **109**, 221-237 (1988).
130. Linnhoff, B. and E. Hindmarsh, The pinch design method for heat exchanger networks, *Chemical Engineering Science* **38**, 745-763 (1983).
131. Lutze, P., R. Gani, and J.M. Woodley, Process intensification: A perspective on process synthesis, *Chemical Engineering and Processing: Process Intensification* **49**, 547-558 (2010).
132. M.G.E. Wolters, J.W.C., Prediction of Degradability of Starch by Gelatinization Enthalpy as Measured by Differential Scanning Calorimetry, *Starch/Stärke* **48**, 14-18 (1992).
133. Ma, Y., et al., Comparative Enzyme Kinetics of Two Allelic Forms of Barley (*Hordeum vulgare* L.) Beta -amylase, *Journal of Cereal Science* **31**, 335-344 (2000).
134. Majozi, T., Minimization of energy use in multipurpose batch plants using heat storage, *Journal of Cleaner Production* **17**, 945-950 (2009).
135. Mao, W., et al., Mathematical simulation of liquid food pasteurization using far infrared radiation heating equipment, *Journal of Food Engineering* **107**, 127-133 (2011).
136. Marc, A. and J.M. Engasser, A kinetic model of starch hydrolysis by alpha and beta amylase during mashing, *Biotechnology and Bioengineering* **25**, 481-496 (1983).
137. Marechal, F., Improving process performances using pinch analysis, in *UNESCO Encyclopedia of Life Support Systems*, C. Frangopoulos and G. Tsatsaronis, Editors. EOLSS Publishers Co Ltd: <http://www.eolss.net/>.
138. Marra, F., L. Zhang, and J.G. Lyng, Radio frequency treatment of foods: Review of recent advances, *Journal of Food Engineering* **91**, 497-508 (2009).
139. Masngut, N. and A.P. Harvey, Intensification of Biobutanol Production in Batch Oscillatory Baffled Bioreactor, *Procedia Engineering* **42**, 1079-1087 (2012).
140. Mauthner, F., et al., Manufacture of Malt and Beer with Low Temperature Solar Process Heat, *Energy Procedia* **48**, 1188-1193 (2014).
141. Mezger, Diss - Betrachtung moderner Würzekochsysteme bezüglich ihres Einflusses auf technologisch und physiologisch bedeutende Würzeinhaltsstof, (2006).
142. Mignon, D. and J. Hermia, Using BATCHES for modeling and optimizing the brewhouses of an industrial brewery, *Comput. Chem. Eng.* **17**, 51-56 (1993).
143. Moser, C., Optimierte Einbindung von Energiespeichern in industrielle Prozesse, Master Thesis, Graz University of Technology, Graz, (2012).
144. Mujumdar, A.S., Principles, Classification, and Selection of Dryers, in *Handbook of Drying*, M. A.S., Editor. Taylor & Francis Group: New York, 2006.
145. Muller, R., A mathematical model of the formation of fermentable sugars from starch hydrolysis during high-temperature mashing, *Enzyme and Microbial Technology* **27**, 337-344 (2000).
146. Muslin, E.H., et al., Overexpression, purification, and characterization of a barley alpha-glucosidase secreted by *Pichia pastoris*, *Protein expression and purification* **18**, 20-26 (2000).
147. Muster-Slawitsch, B., C. Brunner, and J. Fluch, Application of an advanced Pinch Methodology for the food and drink production *WIREs Energy Environment* **3**, (2014).
148. Muster-Slawitsch, B., et al., Process modelling and technology evaluation in brewing, *Chemical Engineering and Processing: Process Intensification* **84**, 98-108 (2014).
149. Muster-Slawitsch, B., et al. Methodology for Batch Heat Integration and Storage System Design for Ideal Integration of Solar Process Heat. in *Chemical Engineering Transactions*. Prague: AIDIC Servizi S.r.l., 2011.
150. Muster-Slawitsch, B., et al., eds. Integration Guideline. IEA Task 49/IV, 2014.
151. Muster-Slawitsch, B., et al., The green brewery concept – Energy efficiency and the use of renewable energy sources in breweries, *Applied Thermal Engineering* **31**, 2123-2134 (2011).

152. Nassar, N.N. and A.K. Mehrotra, Design of a laboratory experiment on heat transfer in an agitated vessel, *Education for Chemical Engineers* **6**, e83-e89 (2011).
153. Nedovi, N., et al., Beer Production Using Immobilized Cells, in *Applications of Cell Immobilisation Biotechnology*, V. Nedovi and R. Willaert, Editors. Springer: The Netherlands, 2005, p. 259-273.
154. Nemet, A. and J.J. Klemeš. Optimising the Temperature of Heat Storage to Serve Processes with Varying Supply and Demand - Captured Solar Energy Curve. in *Chemical Engineering Transactions*. Prague: AIDIC Servizi S.r.l., 2011.
155. Ni, X., et al., Mixing Through Oscillations and Pulsations—A Guide to Achieving Process Enhancements in the Chemical and Process Industries, *Chemical Engineering Research and Design* **81**, 373-383 (2003).
156. O'Rourke, T., The function of wort boiling, *The Brewer International*, 17-19 (2002).
157. O'Rourke, T., The process of wort boiling, *The Brewer International*, 26-28 (2002).
158. Olajire, A.A., The brewing industry and environmental challenges, *Journal of Cleaner Production*, (2012).
159. Oonsivilai, R. and A. Oonsivilai, Temperature Profile in Fermenting Process using Differential Evolution, *Recent advances in Energy and Environment*, 315-319 (2011).
160. Özkan, L., et al., Towards Perfect Reactors: Gaining full control of chemical transformations at molecular level, *Chemical Engineering and Processing: Process Intensification* **51**, 109-116 (2012).
161. Palmer, G.H., Barley and Malt, in *Handbook of Brewing*, F. Priest and G.G. Stewart, Editors. Taylor and Francis Group: Boca Raton, 2006, p. 19.
162. Palmer, G.H., *Cereal Science and Technology*., *Aberdeen University Press*, (1989).
163. Patist, A. and D. Bates, Ultrasonic innovations in the food industry: From the laboratory to commercial production, *Innovative Food Science & Emerging Technologies* **9**, 147-154 (2008).
164. Pereira, R.N. and A.A. Vicente, Environmental impact of novel thermal and non-thermal technologies in food processing, *Food Research International* **43**, 1936-1943 (2010).
165. Perry, S.J., J. Klemeš, and I. Butalov, Integrating waste and renewable energy to reduce the carbon footprint of locally integrated energy sectors, *Energy* **33**, 1489– 1497 (2008).
166. Phan, A.N. and A. Harvey, Development and evaluation of novel designs of continuous mesoscale oscillatory baffled reactors, *Chemical Engineering Journal* **159**, 212-219 (2010).
167. Phan, A.N., A.P. Harvey, and M. Rawcliffe, Continuous screening of base-catalysed biodiesel production using New designs of mesoscale oscillatory baffled reactors, *Fuel Processing Technology* **92**, 1560-1567 (2011).
168. Ponce-Ortega, J.M., M.M. Al-Thubaiti, and M.M. El-Halwagi, Process intensification: New understanding and systematic approach, *Chemical Engineering and Processing: Process Intensification* **53**, 63-75 (2012).
169. Pourali, O., M. Amidpour, and D. Rashtchian, Time decomposition in batch process integration, *Chemical Engineering and Processing* **45**, 14–21 (2006).
170. Quijera, J.A. and J. Labidi, Pinch and exergy based thermosolar integration in a dairy process, *Applied Thermal Engineering* **50**, 464-474 (2013).
171. Ratnayake, W.S., C. Otani, and D.S. Jackson, DSC enthalpic transitions during starch gelatinisation in excess water, dilute sodium chloride and dilute sucrose solutions, *Journal of the Science of Food and Agriculture* **89**, 2156-2164 (2009).
172. Reay, D., The role of process intensification in cutting greenhouse gas emissions, *Applied Thermal Engineering* **28**, 2011-2019 (2008).
173. Reay, D., C. Ramshaw, and A. Harvey, *Process Intensification: Engineering for efficiency, sustainability and flexibility*, Butterworth-Heinemann, 2013.
174. Reis, N., et al., The intensification of gas–liquid flows with a periodic, constricted oscillatory-meso tube, *Chemical Engineering Science* **62**, 7454-7462 (2007).

175. Reis, N., A.A. Vicente, and J.A. Teixeira, Liquid backmixing in oscillatory flow through a periodically constricted meso-tube, *Chemical Engineering and Processing: Process Intensification* **49**, 793-803 (2010).
176. Rivera, A., et al., Operational change as a profitable cleaner production tool for a brewery, *Journal of Cleaner Production* **17**, 137-142 (2009).
177. Rötzel, W. and B. Spang, C3 Typische Werte von Wärmedurchgangskoeffizienten, in *VDI-Wärmeatlas*, VDI, Editor. Springer-Verlag: Berlin Heidelberg, 2013.
178. Santos, M.M.M. and P. Riis, Optimized McCleary method for measurement of total beta-amylase in barley and its applicability, *Journal of the Institute of Brewing* **102**, 271-275 (1996).
179. Scheffold, T., Nachhaltige Energieversorgung einer mittelständischen Brauerei, *Brauindustrie* **3**, 42-45 (2012).
180. Scheller, L., Telephone Conference on Heat transfer coefficient in mash tuns [Personal Communication], Kitzingen (2011).
181. Schmitt, B., Integration of solar heating plants for supply of process heat in industrial companies, University of Kassel, Shaker Verlag, Aachen, Germany, (2014).
182. Schnitzer, H., C. Brunner, and G. Gwehenberger, Minimizing greenhouse gas emissions through the application of solar thermal energy in industrial processes, *Journal of Cleaner Production* **15**, 1271-1286 (2007).
183. Schweiger, H., et al., Guide for EINSTEIN thermal energy audits, Barcelona, Spain, (2012).
184. Shewale, S.D. and A.B. Pandit, Enzymatic production of glucose from different qualities of grain sorghum and application of ultrasound to enhance the yield, *Carbohydr Res* **344**, 52-60 (2009); published online EpubJan 5.
185. Smith, K.B. and M.R. Mackley, An Experimental Investigation into the Scale-up of Oscillatory Flow Mixing in Baffled Tubes, *Chemical Engineering Research and Design* **84**, 1001-1011 (2006).
186. Solano, J.P., et al., Numerical study of the flow pattern and heat transfer enhancement in oscillatory baffled reactors with helical coil inserts, *Chemical Engineering Research and Design* **90**, 732-742 (2012).
187. Stancl, J. and R. Zitny, Milk fouling at direct ohmic heating, *Journal of Food Engineering* **99**, 437-444 (2010).
188. Stankiewicz, A., Energy Matters, *Chemical Engineering Research and Design* **84**, 511-521 (2006).
189. Stephens, G.G. and M.R. Mackley, Heat transfer performance for batch oscillatory flow mixing, *Experimental Thermal and Fluid Science* **25**, 583-594 (2002).
190. Stevnebo, A., S. Sahlström, and B. Svihus, Starch structure and degree of starch hydrolysis of small and large starch granules from barley varieties with varying amylose content, *Animal Feed Science and Technology* **130**, 23-38 (2006).
191. Stoltze, S., et al., Waste-heat recovery in batch processes using heat storage, *J. Energy Resour. Technol.* **117**, 142-149 (1995).
192. Stonestreet, P. and A.P. Harvey, A Mixing-Based Design Methodology for Continuous Oscillatory Flow Reactors, *Chemical Engineering Research and Design* **80**, 31-44 (2002).
193. Sturm, B., et al., The feasibility of the sustainable energy supply from bio wastes for a small scale brewery – A case study, *Applied Thermal Engineering* **39**, 45-52 (2012).
194. Sturm, B., et al., Opportunities and barriers for efficient energy use in a medium-sized brewery, *Applied Thermal Engineering* **53**, 397-404 (2013).
195. T., G., A process integration primer — implementing agreement on process integration, SINTEF Energy Research, I.E. Agency, Trondheim, Norway, (2000).
196. Tokos, H., Z.N. Pintarič, and P. Glavič, Energy saving opportunities in heat integrated beverage plant retrofit, *Applied Thermal Engineering* **30**, 36-44 (2010).

197. Trambouze, P. and J.P. Euzen, Les réacteurs chimiques de la conception à la mise en oeuvre, Editions Technip, Paris, 2002.
198. Trelea, I.C., et al., Predictive modelling of brewing fermentation: from knowledge-based to black-box models, *Mathematics and Computers in Simulation* **56**, 405-424 (2001).
199. Tse, K.L., et al., Assessment of the Effects of Agitation on Mashing for Beer Production in a Small Scale Vessel, *Food and Bioproducts Processing* **81**, 3-12 (2003).
200. Uhlenbruck, S., R. Vogel, and K. Lucas, Heat Integration of Batch Processes, *Chemical Engineering Technology* **23**, 226-229 (2000).
201. Umesh Hebbar, H. and N.K. Rastogi, Microwave Heating of Fluid Foods, 369-409 (2012).
202. Van Gerven, T. and A. Stankiewicz, Structure, Energy, Synergy, Times - The Fundamentals of Process Intensification, *Ind. Eng. Chem. Res.* **48**, 2465–2474 (2009).
203. Varbanov, P. and J. Klemeš, Integration and Management of Renewables into Total Sites with Variable Supply and Demand, *Computers and Chemical Engineering and Processing in press*, in press (2010).
204. Varbanov, P.S. and J.J. Klemeš, Total sites integrating renewables with extended heat transfer and recovery, *Heat Transfer Engineering* **31**, 733-741 (2010).
205. Verheyen, W. and N. Zhang, Design of flexible heat exchanger network for multi-period operation, *chemical Engineering Science* **61**, 7730-7753 (2006).
206. Versteegh, C.W. and H.J. Visscher, Process for continuous boiling of wort, Heineken Technical Services B.V, Patent No. US 6,017,568, (2000).
207. Vey, S., Anlagenplanung in Brauereien und Getränkeabfüllbetrieben unter Verwenden von Standardsoftware, PhD, Technical University Munich, Munich, (2000).
208. Walmsley, M.R.W., M.J. Atkins, and T.G. Walmsley, Application of Heat Recovery Loops to semi-continuous processes, in *Handbook of Process Integration*, J.J. Klemeš, Editor. Woodhead Publishing Limited: Cambridge, 2013.
209. Walmsley, M.R.W., et al., Methods for improving heat exchanger area distribution and storage temperature selection in heat recovery loops, *Energy* **55**, 15-22 (2013).
210. Wang, Y., et al., Synthesis of heat exchanger networks featuring batch streams, *Applied Energy* **114**, 30-44 (2014).
211. Wee S.-L., T.c.-T., Bhatia S., , Membrane separation process—Pervaporation through zeolite membrane, *Separation and Purification Technology* **63**, 500-516 (2008).
212. Werner, A., et al., Green Brewery - Final Report, Klima und Energiefonds, Vienna, (2008).
213. Willaert, R.G. and G.V. Baron, Applying sustainable technology for saving primary energy in the brewhouse during beer brewing, *Clean Technologies and Environmental Policy* **7**, 15-32 (2004).
214. Windisch, W., W. Dietrich, and A. Beyer, Stärkeverflüssigende Funktion der Malzdiastase, *Wochenschrift Brau.* **40**, 49-70 (1923).
215. Xhagolli, L. and J. Marku, Efficient use of energy and resource through conservation and recovery in breweries, *Materials Protection* **55**, 181-188 (2014).
216. Zhao, X.G., et al., Heat integration for batch processes - Part 2: Heat exchanger network design, *Trans IChemE* **76**, Part A (1998).
217. Zhu, J., et al., Study on supramolecular structural changes of ultrasonic treated potato starch granules, *Food Hydrocolloids* **29**, 116-122 (2012).
218. Ziada, S. and H. Gelbe, O2 Schwingungen in Wärmeübertrager-Rohrbündeln, in *VDI-Wärmeatlas*, VDI, Editor. Springer-Verlag: Berlin Heidelberg, 2013, p. 1723-1760.